

**Hydrosilylation and Hydroboration Catalyzed by
Imido-Hydride Complexes of Molybdenum(IV)**

Oleg G. Shirobokov

Dipl. Chem.

PhD in Chemistry

Thesis submitted to the Faculty of Graduate Studies

in the partial fulfillment of the requirements

for the Ph.D. degree in chemistry

Chemistry Department

Faculty of Mathematics and Science

Brock University

St. Catharines, Ontario

April 2011

© Oleg G. Shirobokov, 2011

Dedicated to my parents,
my brother
and
my wife

Manuscripts based on this work

1. Shirobokov, O. G.; Kuzmina, L. G.; Nikonov, G. I. Nonhydride mechanism of metal catalyzed hydrosilylation *J. Am. Chem. Soc.* **2011**.
2. Shirobokov, O. G.; Gorelsky, S. I.; Simionescu, R.; Kuzmina, L. G.; Nikonov, G. I., The unexpected mechanism of carbonyl hydrosilylation catalyzed by $(\text{Cp})(\text{ArN}=\text{Mo(H)(PMe}_3))$. *Chem. Commun.* **2010**, 46 (41), 7831-7833.
3. Shirobokov, O. G.; Nikonov, G. I. $(\text{Tp})(\text{ArN})\text{Mo(H)(PMe}_3)$: an efficient catalyst for carbonyl and nitrile hydroboration (*Transcript in progress*).
4. Khalimon, A.; Shirobokov, O. G.; Simionescu, R.; Kuzmina, L. G.; Nikonov, G. I. Mechanistic studies of hydrosilylation catalyzed by $(\text{ArN})\text{Mo(H)(Cl)(PMe}_3)$ (*Transcript in progress*).

Abstract

This thesis describes the synthesis, structural studies, stoichiometric and catalytic reactivity of novel Mo(IV) imido hydride complexes (Cp)(ArN)Mo(H)(PMe₃) (**1**) and (Tp)(ArN)Mo(H)(PMe₃) (**2**). Both **1** and **2** catalyze hydrosilylation of a variety of carbonyls. Detailed kinetic and DFT studies found that **1** reacts by an unexpected associative mechanism, which does not involve Si-H addition either to the imido group or the metal. Despite **1** being a d² complex, its reaction with PhSiH₃ proceeds via a σ -bond metathesis mechanism giving the silyl derivative (Cp)(ArN)Mo(SiH₂Ph)(PMe₃). In the presence of BPh₃ reaction of **1** with PhSiH₃ results in formation of (Cp)(ArN)Mo(SiH₂Ph)(H)₂ and (Cp)(ArN)Mo(SiH₂Ph)₂(H), the first examples of Mo(VI) silyl hydrides.

A 1:1:1 reaction between **2**, PhSiD₃ and carbonyl substrate established that hydrosilylation is not accompanied by deuterium incorporation into the hydride position of the catalyst, thus ruling out the conventional mechanism based on carbonyl insertion carbonyl. As **2** is nonreactive to both the silane and ketone, the only mechanistic alternative we are left with is that the metal center activates the carbonyl as a Lewis acid. The analogous nonhydride mechanism was observed for the catalysis by (ArN)Mo(H)(Cl)(PMe₃), (Ph₃P)₂(I)(O)Re(H)(OSiMe₂Ph) and (PPh₃CuH)₆.

Complex **2** also catalyzes hydroboration of carbonyls and nitriles. We report the first case of metal-catalyzed hydroboration of nitriles as well as hydroboration of carbonyls at very mild conditions. Conversion of carbonyl functions can be performed with high selectivities in the presence of nitrile groups.

This thesis also reports the first case of the H/H exchange between H₂ and Si-H of silanes mediated by Lewis acids such as Mo(IV), Re(V), Cu(I), Zn(II) complexes, B(C₆F₅)₃ and BPh₃.

Acknowledgements

First of all, I would like to acknowledge my supervisor Professor Georgii Nikonov for offering me great projects to work on and for his guidance and assistance throughout my four-year PhD study at Brock University. His exceptional scientific intuition guided my research in the right direction. Only due to Professor Nikonov, I obtained a lot of great results and gained an outstanding research experience in the heart of organometallic chemistry.

I would like to thank my graduate committee members Professor Martin Lemaire and Professor Jeffery Atkinson for keeping track of my research and their helpful suggestions. I express my gratitude to NMR technologist Razvan Simionescu for his collaboration and being a great assistance in running numerous and sometimes nontrivial NMR experiments; Prof. Ludmila Kuzmina (Institute of General and Inorganic Chemistry RAS, Moscow, Russia) for providing us with X-ray data; Dr. Serge Gorelsky (University of Ottawa) for the computational studies; the glassblowing technicians John Vandenhoff and Jordan Vandenhoff for their quick and professional help in fixing the glassware.

I am grateful to the current and the former Nikonov's group members: Dr. Andrey Khalimon, Dr. Somying Leelasubcharoen, Dmitry Gutsulyak, Eric Peterson, Nick McLeod, Phillip Farha, and Sun-Hwa. I also would like to thank my friends from other labs: Sergey Vshivenko, Kseniya Revunova, Tom Metcalf, Piotrek Lupa, Kristina Whitbread, Lory Van Belle, Aleš Machara, Brandon Djukic, David R. Adams, Graeme Piercy, Jacqueline Gilmet, Roland Asha, Raymond Akong, Joshua Zaifman, Pat

Cassolato, Samuel Mula, Shufen Xu. Thank you guys for being my friends and colleagues, I really enjoyed your company!

A special gratitude I would like express to the number of people, who gave me a great opportunity to work as a Teaching Assistant (Laboratory Demonstrator and Tutorial Instructor) during my graduate studies at Brock University to enforce my teaching potential and communicational skills: Professor Heather Gordon, Dr. Sergio Paone, and Dr. Paul Zelisko. I gained valuable experience working independently, further developing my organizational skills a chemistry instructor. I also would like to thank Fran Brown I was lucky to work with for sharing her life-time experience! I am sure I have acquired some of it! Thank you all, I really enjoyed working with you!

I would like to thank the people I worked with at Moscow State University, in particular: my former supervisor Professor Ilya Nifant'ev for bringing up my research potential and developing great skills in synthetic organic chemistry; Dr. Igor Kashulin, Dr. Eugeny Kanshin and Vladimir Bagrov for being my best friends and colleagues.

I owe my gratitude to my high-school teachers: Solodilova Valentina Gavrilovna, who sparked my neverending interest in chemistry literally at a first chemistry lesson; Ostroukhova Irina Vladimirovna for polishing my chemistry knowledge, preparing me for the university studies and assisting me in participation in different level chemistry Olympiad contests; Valent'ev Alexander Federovich, the most talented mathematics instructor, for giving me start in life.

Finally, I am extremely grateful to my parents, my brother and my wife for their warm support and understandings throughout the years of my education...

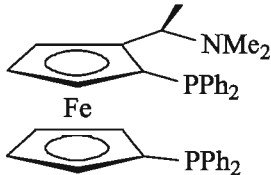
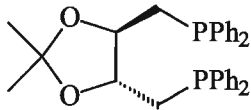
Table of Contents

MANUSCRIPTS BASED ON THIS WORK.....	I
ABSTRACT.....	II
ACKNOWLEDGEMENTS.....	IV
TABLE OF CONTENTS	VI
ABBREVIATIONS	IX
LIST OF FIGURES	XIII
LIST OF SCHEMES.....	XXII
LIST OF TABLES	XXX
I INTRODUCTION	1
II HISTORICAL	2
II. 1 HYDROSILYLATION OF CARBONYLS: EARLY STUDIES.....	2
II. 2 RH-CATALYZED HYDROSILYLATION OF CARBONYLS.....	3
II. 3 TITANOCENE-CATALYZED HYDROSILYLATION OF CARBONYLS	11
II. 4. HYDROSILYLATION OF CARBONYLS CATALYZED BY ZINC COMPLEXES	14
II. 5. OXO-RHENIUM COMPLEXES: MECHANISTIC STUDIES OF CATALYTIC HYDROSILYLATION OF CARBONYLS.....	18
II.5.1. Neutral dioxo-rhenium(V) complexes.....	18
II.5.2. Neutral monooxo-rhenium(V) complexes.....	23
II.5.3. Cationic monooxo-rhenium(V) complexes: hydrosilylation of carbonyls.....	24
II.5.4. Cationic monooxorhenium(V) complexes: hydrolytic oxidation of silanes.....	27
II.5.5. Rhenium(I)-catalyzed hydrosilylation.....	28
II. 6. OXO-MOLYBDENUM(VI) COMPLEXES	29
II. 7. IMIDO MOLYBDENUM (IV) COMPLEXES.....	31
II. 8. HYDROSILYLATION CATALYZED BY $\text{CuH}(\text{PPh}_3)$	33
II. 9. HYDROSILYLATION OF CARBONYLS CATALYZED BY NI-COMPLEXES	36
II. 10. HYDROSILYLATION CATALYZED BY $\text{B}(\text{C}_6\text{F}_5)_3$	38
II. 11. CATALYTIC HYDROBORATION OF CARBONYLS AND NITRILES	46
II. 12. METAL-FREE ACTIVATION OF MOLECULAR HYDROGEN	50

III	RESULTS AND DISCUSSIONS	57
III. 1	HYDROSILYLATION CATALYZED BY (Cp)(ArN)Mo(H)(PMe ₃).....	59
III.1.1	Phosphine exchange between (Cp)(ArN)Mo(H)(PMe ₃) and PMe ₃	60
III.1.2	Reaction of (Cp)(ArN)Mo(H)(PMe ₃) with benzaldehyde	61
III.1.3	Reactions of (Cp)(ArN)Mo(H)(PMe ₃) with ketones.....	67
III.1.4	Reactions of (Cp)(ArN)Mo(H)(PMe ₃) with alcohols	67
III.1.5	Phosphine exchange between (Cp)(ArN)Mo(OCH ₂ Ph)(PMe ₃) and PMe ₃	68
III.1.6	Reaction between (Cp)(ArN)Mo(OCH ₂ Ph)(PMe ₃) and PhSiH ₃	68
III.1.7	Reaction of (Cp)(ArN)Mo(H)(PMe ₃) with PhSiH ₃	71
III.1.8	Stoichiometric reaction between (Cp)(ArN)Mo(H)(PMe ₃), PhCHO and PhSiD ₃	74
III. 2	HYDROSILYLATION CATALYZED BY (Tp)(ArN)Mo(H)(PMe ₃).....	75
III.2.1	Hydrosilylation catalyzed by (Tp)(ArN)Mo(H)(PMe ₃)	77
III.2.2	Dissociation of the Tp ligand.....	77
III.2.3	Phosphine exchange between (Tp)(ArN)Mo(H)(PMe ₃) and free PMe ₃	78
III.2.4	Reaction between (Tp)(ArN)Mo(H)(PMe ₃) and carbonyls.....	78
III.2.5	Reaction between (Tp)(ArN)Mo(H)(PMe ₃) and PhSiH ₃	82
III.2.6	Reaction between (Tp)(ArN)Mo(OCH ₂ Ph)(PMe ₃) and PhSiH ₃	82
III.2.7	Reaction between (Tp)(ArN)Mo(H)(PMe ₃), PhSiD ₃ and cyclohexanone and the mechanism of hydrosilylation.....	83
III.2.8	Reactions of (Tp)(ArN)Mo(H)(PMe ₃) with alcohols	84
III.2.9	Reaction of (Tp)(ArN)Mo(H)(PMe ₃) with benzonitrile	84
III. 3	HYDROSILYLATION CATALYZED BY (PPh ₃)CuH.....	86
III. 4	HYDROSILYLATION CATALYZED BY OXO-RE(V) COMPLEXES.....	94
III. 5	HYDROSILYLATION CATALYZED BY ZN(II)	101
III. 6	HYDROSILYLATION CATALYZED BY (ArN)Mo(H)(Cl)(PMe ₃) ₃	105
III.6.1	Reactions (ArN)Mo(H)(Cl)(PMe ₃) ₃ with benzaldehyde.....	105
III.6.2	Reaction between (ArN)Mo(OCH ₂ Ph)(Cl)(PMe ₃) ₃ and PhSiH ₃ : kinetic studies.....	109
III.6.3	Reactivity of (ArN)Mo(OCH ₂ Ph)(Cl)(PMe ₃) ₃ with aldehydes	110
III.6.4	Reactivity of (ArN)Mo(H)(Cl)(PMe ₃) ₃ with ketones.....	112
III.6.5	Reaction of (ArN)Mo(H)(Cl)(PMe ₃) ₃ with PhSiH ₃	114
III.6.6	Reaction between (ArN)Mo(H)(Cl)(PMe ₃) ₃ , PhSiD ₃ and PhCHO	115
III.6.7	Reactions between (ArN)Mo(H)(Cl)(PMe ₃) ₃ , PhSiD ₃ and cyclohexanone.....	116
III.6.8	Reactions between (ArN)Mo(H)(Cl)(PMe ₃) ₃ , PhSiD ₃ and acetophenone.....	118
III.6.9	Catalysis by (ArN)Mo(H)(Cl)(PMe ₃) ₃	119

III.6.10	Silyl derivatives of $(ArN)Mo(H)(Cl)(PMe_3)_3$: preparation and reactivity.....	120
III. 7	HYDROBORATION CATALYZED BY $(Tp)(ArN)Mo(H)(PMe_3)_3$	122
III.7.1	Catalytic hydroboration of carbonyls	123
III.7.2	Catalytic hydroboration of nitriles	124
III.7.3	Hydroboration of amides.....	126
III.7.4	Hydroboration of alkynes	126
III.7.5	Competitive hydroboration.....	126
III.7.6	Mechanistic considerations	128
III. 8	$H_2/PhSiH_3$ EXCHANGE MEDIATED BY METAL COMPLEXES AND BORANES	134
III.8.1	Metal complexes	134
III.8.2	Boranes	135
IV	CONCLUSIONS AND FUTURE WORK	137
V	EXPERIMENTAL.....	140
V. 1.	HYDROSILYLATION CATALYZED BY $(Cp)(ArN)Mo(H)(PMe_3)_3$	141
V. 2.	HYDROSILYLATION CATALYZED BY $(Tp)(ArN)Mo(H)(PMe_3)_3$	178
V. 3.	HYDROSILYLATION CATALYZED BY $(PPh_3)CuH$	209
V. 4.	HYDROSILYLATION CATALYZED BY OXO-RE(V) COMPLEXES.....	211
V. 5.	HYDROSILYLATION CATALYZED BY $Zn(II)$ COMPLEXES.....	213
V. 6.	HYDROSILYLATION CATALYZED BY $(ArN)Mo(H)(Cl)(PMe_3)_3$	213
V. 7.	HYDROBORATION CATALYZED BY $(Tp)(ArN)Mo(H)(PMe_3)_3$	235
V. 8.	SILYL IMIDO MOLYBDENUM(IV) COMPLEXES	258
V. 9.	$H_2/Si-H$ EXCHANGE MEDIATED BY METAL COMPLEXES AND BORANES	261
VI	APPENDIX	265
VII	REFERENCES.....	280

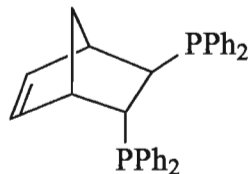
Abbreviations

Å	Angström
Acac	acetylacetonate
Ar	2,6-diisopropylphenyl, unless stated otherwise
Atm	atmosphere (1 atm = 1 bar, 760 mm Hg, 101.3 kPa, 14.696 psi)
B	broad (NMR)
Bn	benzyl
BPPFA	
Cat	catechol
cat.	catalyst
COD	cyclooctadiene
Cp	η^5 -C ₅ H ₅ , unless specified
Cp*	η^5 -C ₅ Me ₅ , unless specified
Cy	cyclohexyl
Cy=O	cyclohexanone
D	doublet (NMR)
DFT	density functional theory
DIOP	
DME	1,2-dimethoxyethane
DMF	dimethylformamide

DMSO	dimethyl sulphoxide
Dppe	1,2-Bis(diphenylphosphino)ethane
ebpe	<i>N,N'</i> -ethylenebis(1-phenylethylamine)
eq.	equivalents
ESI-MS	electrospray ionization mass-spectroscopy
Et	ethyl
exc.	excess
H	hour
Hal	halogen
HOMO	highest occupied molecular orbital
Hoz	2-(2'-hydroxyphenyl)-2-oxazoline
Hz	Hertz, cycles per second
<i>hν</i>	light
<i>i</i> -Pr	isopropyl
IR	infrared
<i>J</i>	coupling constant (NMR)
<i>K</i>	reaction rate constant
KIE	kinetic isotope effect
<i>L_n</i>	ligands
LUMO	lowest unoccupied molecular orbital
M	central metal atom in a complex
M	multiplet (NMR)
<i>m</i> -	<i>meta</i> -
Me	methyl

Mes	mesityl (2,4,6-Me ₃ C ₆ H ₂)
<i>n</i> -Bu	<i>n</i> -butyl
NMR	nuclear magnetic resonance

Norphos



o- *ortho*-

OTf CF₃SO₃⁻, triflate

P pentet (NMR)

p- *para*-

Ph phenyl

PhMe toluene

PinBH pinacolborane

PMHS Polymethylhydrosiloxane,
Me₃Si-[OSi(H)(Me)]_n-SiMe₃

Pr propyl

Py pyridine

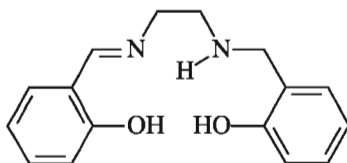
Q quartet (NMR)

RT RT

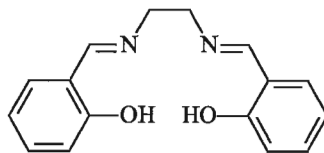
S singlet (NMR)

S₂CNEt₂ diethyldithiocarbamate

salalen



salen



Sat

satellite (NMR)

Sept

septet (NMR)

Sia₂BH

$[(\text{CH}_3)_2\text{CH-CH}(\text{CH}_3)\text{-}]_2\text{BH}$

Solv

solvent

T

triplet (NMR)

TBAF

tetrabutylammonium fluoride

t-Bu

tert-butyl

tert-, *t*-

tertiary

Tex₂BH

$[(\text{CH}_3)_2\text{CH-C}(\text{CH}_3)_2\text{-}]_2\text{BH}$

THF

tetrahydrofuran

TMEDA

tetramethylethylenediamine

TMS

trimethylsilyl

Tol

tolyl

Tp

trispyrazolylborate

UV

ultraviolet

VT

variable temperature

Vt

virtual triplet (NMR)

Δ

heat

ΔH^\ddagger

activation enthalpy

ΔS^\ddagger

activation entropy

δ

chemical shift

List of Figures

Figure III-1. ORTEP plot of the molecular structure of (Cp)(ArN)Mo(OCH ₂ Ph)(PMe ₃) (one of two independent molecules is shown). Anisotropic displacement ellipsoids are plotted at 50% probability.	63
Figure III-2. ORTEP plot of the molecular structure of (Tp)(ArN)Mo(H)(PMe ₃) (All hydrogen atoms except BH and MoH are omitted for clarity. One of two independent molecules is shown). Anisotropic displacement parameters are plotted at 50% probability.	75
Figure III-3. Dependence of the rate constant k_{eff} on PMe ₃ concentration (eq.) for the reaction of (Tp)(ArN)Mo(H)(PMe ₃) with PhCHO (1eq.).....	79
Figure III-4. Stoichiometric reaction between CuH(PPh ₃), PhCHO and PhMe ₂ SiD (29% conversion).....	90
Figure III-5. Stoichiometric reaction between CuH(PPh ₃), PhCHO and PhMe ₂ SiD (95% conversion).....	91
Figure III-6. The end of reaction between CuH(PPh ₃), PhCHO and PhMe ₂ SiD. ² H NMR spectrum (top), and ¹ H NMR spectrum (bottom).....	92
Figure III-7. Hydrosilylation of PhCHO with PhMe ₂ SiD in the presence of catalytic amounts (~5 mol%) of CuH(PPh ₃).	93
Figure III-8. ¹ H NMR spectrum of (PPh ₃) ₂ (I)(O)Re(H)(OSiMe ₂ Ph) in CDCl ₃	98
Figure III-9. Reaction between PhCHO, PhMe ₂ SiD and (PPh ₃) ₂ (I)(O)Re(H)(OSiMe ₂ Ph) in CDCl ₃ (77% conversion).....	99
Figure III-10. Reaction between PhCHO, PhMe ₂ SiD and (PPh ₃) ₂ (I)(O)Re(H)(OSiMe ₂ Ph) in CDCl ₃ (100% conversion).....	100
Figure III-11. A mixture of PhCHO and PMHS in the presence of zinc 2-ethylhexanoate and NaBD ₄	102
Figure III-12. ¹ H spectrum of the reaction mixture of PhCHO, PMHS, zinc 2-ethylhexanoate and NaBD ₄ in <i>tert</i> -butyl methyl ether.	103
Figure III-13. ² H spectrum of the reaction mixture of PhCHO, PMHS, zinc 2-ethylhexanoate and NaBD ₄ in <i>tert</i> -butyl methyl ether.	103

Figure III-14. ^1H - ^{13}C HSQC spectrum of the reaction mixture containing two isomers of $(\text{ArN})\text{Mo}(\text{H})(\eta^2\text{-PhCHO})(\text{Cl})(\text{PMe}_3)_2$	106
Figure III-15. Formation of free benzaldehyde when complex $(\text{ArN})\text{Mo}(\text{OCH}_2\text{Ph})(\text{Cl})(\text{PMe}_3)_3$ reacts with <i>t</i> -BuCHO. ^1H NMR spectrum.....	110
Figure III-16. ORTEP plot for the molecular structure of $(\text{ArN})(\text{CyO})\text{Mo}(\text{Cl})(\text{PMe}_3)_3$. Anisotropic displacement parameters are plotted at 50% probability.	113
Figure III-17. A. ^1H NMR spectrum of $(\text{Tp})(\text{ArN})\text{Mo}(\text{H})(\text{PMe}_3)$. B. ^1H NMR spectrum of $(\text{Tp})(\text{ArN})\text{Mo}(\text{H})(\text{PMe}_3)$ in the presence of catecholborane.	129
Figure III-18. A. ^{11}B NMR spectrum of CatBH. B. ^{11}B NMR spectrum of CatBH in the presence of $(\text{Tp})(\text{ArN})\text{Mo}(\text{H})(\text{PMe}_3)$	130
Figure III-19. ^{11}B NMR spectrum of PinBH (28.6 ppm, doublet, $^1J_{\text{B-H}} = 174.1$ Hz) and PinBD (28.6 ppm, singlet) mixture.	131
Figure V-1. $C(\text{PhCHO})/\text{time}$ plot for hydrosilylation of benzaldehyde with phenylsilane in the presence of different catalytic species.	143
Figure V-2. Eyring plot for phosphine exchange between $(\text{Cp})(\text{ArN})\text{Mo}(\text{H})(\text{PMe}_3)$ and free PMe_3	144
Figure V-3. $(1/C)/\text{time}$ plot for the reaction of $(\text{Cp})(\text{ArN})\text{Mo}(\text{H})(\text{PMe}_3)$ with PhCHO (1eq.) in the presence of PMe_3 (10 eq.) at 26.0 °C.....	146
Figure V-4. $(1/C)/\text{time}$ plot for the reaction of $(\text{Cp})(\text{ArN})\text{Mo}(\text{H})(\text{PMe}_3)$ with PhCHO (1eq.) in the presence of PMe_3 (10 eq.) at 40.0 °C.....	146
Figure V-5. $(1/C)/\text{time}$ plot for the reaction of $(\text{Cp})(\text{ArN})\text{Mo}(\text{H})(\text{PMe}_3)$ with PhCHO (1eq.) in the presence of PMe_3 (10 eq.) at +50.0 °C.....	147
Figure V-6. $(1/C)/\text{time}$ plot for the reaction of $(\text{Cp})(\text{ArN})\text{Mo}(\text{H})(\text{PMe}_3)$ with PhCHO (1eq.) in the presence of PMe_3 (10 eq.) at 60.0 °C.....	147
Figure V-7. Eyring plot for the reaction of $(\text{Cp})(\text{ArN})\text{Mo}(\text{H})(\text{PMe}_3)$ with PhCHO (1eq.) in the presence of PMe_3 (10 eq.)	148
Figure V-8. $k_{\text{eff}}/\text{PMe}_3(\text{eq.})$ plot for the reaction between $(\text{Cp})(\text{ArN})\text{Mo}(\text{H})(\text{PMe}_3)$ and PhCHO.....	148
Figure V-9. $\ln(C)/\text{time}$ plot for the reaction of $(\text{Cp})(\text{ArN})\text{Mo}(\text{OCH}_2\text{Ph})(\text{PMe}_3)$ with PhSiH_3 (10 eq.) at 16.0 °C	151

Figure V-10. $\ln(C)/\text{time}$ plot for the reaction of $(\text{Cp})(\text{ArN})\text{Mo}(\text{OCH}_2\text{Ph})(\text{PMe}_3)$ with PhSiH_3 (10 eq.) at 26.0°C	151
Figure V-11. $\ln(C)/\text{time}$ plot for the reaction of $(\text{Cp})(\text{ArN})\text{Mo}(\text{OCH}_2\text{Ph})(\text{PMe}_3)$ with PhSiH_3 (10 eq.) at 36.0°C	152
Figure V-12. $\ln(C)/\text{time}$ plot for the reaction of $(\text{Cp})(\text{ArN})\text{Mo}(\text{OCH}_2\text{Ph})(\text{PMe}_3)$ with PhSiH_3 (10 eq.) at 46.0°C	152
Figure V-13. Eyring plot for the reaction of $(\text{Cp})(\text{ArN})\text{Mo}(\text{OCH}_2\text{Ph})(\text{PMe}_3)$ with PhSiH_3 (10 eq.).....	153
Figure V-14. $\ln(C)/\text{time}$ plot the reaction of $(\text{Cp})(\text{ArN})\text{Mo}(\text{OCH}_2\text{Ph})(\text{PMe}_3)$ with PhSiD_3 (10 eq.) 16.0°C	154
Figure V-15. $\ln(C)/\text{time}$ plot the reaction of $(\text{Cp})(\text{ArN})\text{Mo}(\text{OCH}_2\text{Ph})(\text{PMe}_3)$ with PhSiD_3 (10 eq.) at 26.0°C	154
Figure V-16. $\ln(C)/\text{time}$ plot the reaction of $(\text{Cp})(\text{ArN})\text{Mo}(\text{OCH}_2\text{Ph})(\text{PMe}_3)$ with PhSiD_3 (10 eq.) at 36.0°C	155
Figure V-17. $\ln(C)/\text{time}$ plot the reaction of $(\text{Cp})(\text{ArN})\text{Mo}(\text{OCH}_2\text{Ph})(\text{PMe}_3)$ with PhSiD_3 (10 eq.) at 46.0°C	156
Figure V-18. Eyring plot for the reaction of $(\text{Cp})(\text{ArN})\text{Mo}(\text{OCH}_2\text{Ph})(\text{PMe}_3)$ with PhSiD_3 (10 eq.).....	156
Figure V-19. $\ln(C)/\text{time}$ plot for the reaction of $(\text{Cp})(\text{ArN})\text{Mo}(\text{H})(\text{PMe}_3)$ with PhSiH_3 (5 eq.) in the presence of 0, 10, and 20 eq. of PMe_3	158
Figure V-20. $\ln(C)/\text{time}$ plot for the reaction of $(\text{Cp})(\text{ArN})\text{Mo}(\text{H})(\text{PMe}_3)$ with PhSiH_3 (10 eq.) at 25.0°C	159
Figure V-21. $\ln(C)/\text{time}$ plot for the reaction of $(\text{Cp})(\text{ArN})\text{Mo}(\text{H})(\text{PMe}_3)$ with PhSiH_3 (10 eq.) at 35.0°C	159
Figure V-22. $\ln(C)/\text{time}$ plot for the reaction of $(\text{Cp})(\text{ArN})\text{Mo}(\text{H})(\text{PMe}_3)$ with PhSiH_3 (10 eq.) at 45.0°C	160
Figure V-23. $\ln(C)/\text{time}$ plot for the reaction of $(\text{Cp})(\text{ArN})\text{Mo}(\text{H})(\text{PMe}_3)$ with PhSiH_3 (10 eq.) at 55.0°C	160
Figure V-24. Eyring plot for the reaction of $(\text{Cp})(\text{ArN})\text{Mo}(\text{H})(\text{PMe}_3)$ with PhSiH_3 (10 eq.).....	161

Figure V-25. Ln(C)/time plot for reaction between (Cp)(ArN)Mo(H)(PMe ₃) and PhSiD ₃ (5 eq) at 25.0 °C.	162
Figure V-26. Relative integral intensity vs. time plot for concurrent formation of (Cp)(ArN)Mo(D)(PMe ₃) and (Cp)(ArN)Mo(SiD ₂ Ph)(PMe ₃) from (Cp)(ArN)Mo(H)(PMe ₃) and PhSiD ₃ (5 eq.) at 25 °C.	163
Figure V-27. Ln(C)/time plot for the reaction of (Cp)(ArN)Mo(H)(PMe ₃) with PhSiD ₃ (5 eq) at 25 °C.	163
Figure V-28. Ln(C)/time plot for reaction between (Cp)(ArN)Mo(OCH ₂ Ph)(PMe ₃) and PhCHO (10 eq.) at 26.0 °C.	164
Figure V-29. Ln(C)/time plot for reaction between (Cp)(ArN)Mo(OCH ₂ Ph)(PMe ₃) and PhCHO (10 eq.) at 40.0 °C.	165
Figure V-30. Ln(C)/time plot for the reaction between (Cp)(ArN)Mo(OCH ₂ Ph)(PMe ₃) and PhCHO (10 eq.) at 55.0 °C.	165
Figure V-31. Eyring plot for the reaction of (Cp)(ArN)Mo(OCH ₂ Ph)(PMe ₃) with PhCHO (10 eq.)	166
Figure V-32. Ln(C)/time plot for the reaction of (Cp)(ArN)Mo(OCH ₂ Ph)(PhCHO) with PhSiH ₃ (12 eq.)	167
Figure V-33. ²⁹ Si INEPT+ NMR spectrum of a reaction mixture containing (Cp)(ArN)Mo(H)(SiH ₂ Ph)(H) (A), (Cp)(ArN)Mo(H) ₂ (SiH ₂ Ph) (B) and PhSiD ₃	168
Figure V-34. ²⁹ Si INEPT+ NMR spectrum of (Cp)(ArN)Mo(SiH ₂ Ph) ₂ (H), C.	169
Figure V-35. Computed reaction pathways for the formation of (Cp)(MeN)Mo(OCH ₃)(PMe ₃)	173
Figure V-36. Computed reaction pathways for the addition of SiH ₄ to (Cp)(MeN)Mo(OCH ₃)(PMe ₃).	173
Figure V-37. Energy profile for the addition of SiH ₄ to CH ₂ =O mediated by (Cp)(MeN)Mo(H)(PMe ₃) (at 298 K).	174
Figure V-38. Computed reaction pathways for the formation of (Cp)(MeN)Mo(H) ₂ (SiH ₃) (at 298 K).	174
Figure V-39. Computed reaction pathway for the formation of (Cp)(MeN)Mo(SiH ₃)(PMe ₃) (at 298 K).	175

Figure V-40. Energy profile for the reactions of SiH_4 with $\text{Cp}(\text{MeN})\text{Mo}(\text{PMe}_3)(\text{H})$ (at 298 K)	175
Figure V-41. The lowest unoccupied molecular orbital (LUMO) of $(\text{Cp})(\text{MeN})\text{Mo}(\text{H})(\text{PMe}_3)$	176
Figure V-42. ^1H - ^1H EXSY NMR spectrum of $(\text{Tp})(\text{ArN})\text{Mo}(\text{H})(\text{PMe}_3)$ at 22.0 °C ($d_8 = 0.300$ s).	184
Figure V-43. ^1H - ^1H EXSY NMR spectrum of $(\text{Tp})(\text{ArN})\text{Mo}(\text{H})(\text{PMe}_3)$ at -50.0 °C ($d_8 = 0.300$ s).	185
Figure V-44. $\ln[1-I(d_8)/I(\text{EQ})]/d_8$ plot for Pz-ring dissociation in $(\text{Tp})(\text{ArN})\text{Mo}(\text{H})(\text{PMe}_3)$ at 17.0 °C.....	186
Figure V-45. $\ln[1-I(d_8)/I(\text{EQ})]/d_8$ plot for Pz-ring dissociation in $(\text{Tp})(\text{ArN})\text{Mo}(\text{H})(\text{PMe}_3)$ at 22.0 °C.....	186
Figure V-46. $\ln[1-I(d_8)/I(\text{EQ})]/d_8$ plot for Pz-ring dissociation in $(\text{Tp})(\text{ArN})\text{Mo}(\text{H})(\text{PMe}_3)$ at 27.0 °C.....	187
Figure V-47. $\ln[1-I(d_8)/I(\text{EQ})]/d_8$ plot for Pz-ring dissociation in $(\text{Tp})(\text{ArN})\text{Mo}(\text{H})(\text{PMe}_3)$ at 32.0 °C.....	187
Figure V-48. Eyring plot for pyrazolyl ligand dissociation in $(\text{Tp})(\text{ArN})\text{Mo}(\text{H})(\text{PMe}_3)$	188
Figure V-49. $(1/C)/\text{time}$ plot for the reaction of $(\text{Tp})(\text{ArN})\text{Mo}(\text{H})(\text{PMe}_3)$ with PhCHO (1eq.).....	189
Figure V-50. $(1/C)/\text{time}$ plot for the reaction of $(\text{Tp})(\text{ArN})\text{Mo}(\text{H})(\text{PMe}_3)$ with PhCHO (1eq.) in the presence of 5 eq. of PMe_3	190
Figure V-51. $(1/C)/\text{time}$ plot for the reaction of $(\text{Tp})(\text{ArN})\text{Mo}(\text{H})(\text{PMe}_3)$ with PhCHO (1eq.) in the presence of 10 eq. of PMe_3	190
Figure V-52. $(1/C)/\text{time}$ plot for the reaction of $(\text{Tp})(\text{ArN})\text{Mo}(\text{H})(\text{PMe}_3)$ with PhCHO (1eq.) in the presence of 20 eq. of PMe_3	191
Figure V-53. $(1/C)/\text{time}$ plot for the reaction of $(\text{Tp})(\text{ArN})\text{Mo}(\text{H})(\text{PMe}_3)$ with PhCHO (1eq.) in the presence of 10 eq. of PMe_3 at 36.0 °C.	191
Figure V-54. $(1/C)/\text{time}$ plot for the reaction of $(\text{Tp})(\text{ArN})\text{Mo}(\text{H})(\text{PMe}_3)$ with PhCHO (1eq.) in the presence of 10 eq. of PMe_3 at 46.0 °C.	192

Figure V-55. (1/C)/time plot for the reaction of (Tp)(ArN)Mo(H)(PMe ₃) with PhCHO (1eq.) in the presence of 10 eq. of PMe ₃ at 55.6 °C.	192
Figure V-56. Eyring plot for the reaction of (Tp)(ArN)Mo(H)(PMe ₃) with PhCHO (1eq.) in the presence of 10 eq. of PMe ₃	193
Figure V-57. ln(C)/time plot for the reaction of (Tp)(ArN)Mo(H)(PMe ₃) with PhSiD ₃ (5 eq.) at 60.0 °C.....	194
Figure V-58. ln(C)/time plot for the reaction between (Tp)(ArN)Mo(OCH ₂ Ph)(PMe ₃) and PhSiH ₃ (10 eq.) at 17.0 °C.....	195
Figure V-59. ln(C)/time plot for the reaction between (Tp)(ArN)Mo(OCH ₂ Ph)(PMe ₃) and PhSiH ₃ (10 eq.) at 22.0 °C.....	196
Figure V-60. ln(C)/time plot for the reaction between (Tp)(ArN)Mo(OCH ₂ Ph)(PMe ₃) and PhSiH ₃ (10 eq.) at 27.0 °C.....	196
Figure V-61. ln(C)/time plot for the reaction between (Tp)(ArN)Mo(OCH ₂ Ph)(PMe ₃) and PhSiH ₃ (10 eq.) at 32.0 °C.....	197
Figure V-62. Eyring plot for the reaction of (Tp)(ArN)Mo(OCH ₂ Ph)(PMe ₃) with PhSiH ₃ (10 eq.).....	197
Figure V-63. ln(C)/time plot for reaction between (Tp)(ArN)Mo(OCH ₂ Ph)(PMe ₃) and PhSiD ₃ (10 eq.) at 17.0 °C.	198
Figure V-64. ln(C)/time plot for reaction between (Tp)(ArN)Mo(OCH ₂ Ph)(PMe ₃) and PhSiD ₃ (10 eq.) at 22.0 °C.	199
Figure V-65. ln(C)/time plot for reaction between (Tp)(ArN)Mo(OCH ₂ Ph)(PMe ₃) and PhSiD ₃ (10 eq.) at 27.0 °C.	199
Figure V-66. ln(C)/time plot for reaction between (Tp)(ArN)Mo(OCH ₂ Ph)(PMe ₃) and PhSiD ₃ (10 eq.) at 32.0 °C.	200
Figure V-67. Eyring plot for the reaction of (Tp)(ArN)Mo(OCH ₂ Ph)(PMe ₃) with PhSiD ₃ (10 eq.).....	200
Figure V-68. (1/C)/time plot for the reactions (Tp)(ArN)Mo(H)(PMe ₃)+cyclohexanol+PhSiD ₃ (1:1:1) (green), (Tp)(ArN)Mo(H)(PMe ₃)+2cyclohexanol+PhSiD ₃ (1:2:1) (red), and (Tp)(ArN)Mo(H)(PMe ₃)+cyclohexanol+2PhSiD ₃ (1:1:2) (blue).	202

Figure V-69. ^{31}P ^{31}P EXSY NMR spectrum of $(\text{ArN})\text{Mo}(\text{OCy})(\text{Cl})(\text{PMe}_3)_3$ in the presence of PMe_3 in C_6D_6 with the mixing time of 0.500 s showing fast exchange between all bound and free phosphines (Bruker 600 MHz NMR machine).	215
Figure V-70. Selective ge-1D EXSY experiment of the sample containing $(\text{ArN})\text{Mo}(\text{OCy})(\text{Cl})(\text{PMe}_3)_3$: irradiation of the area of <i>trans</i> - PMe_3 groups at 1.356 ppm with the mixing time of 1.000 s (Bruker 600 MHz NMR machine).	216
Figure V-71. Selective ge-1D EXSY experiment of the sample containing $(\text{ArN})\text{Mo}(\text{OCy})(\text{Cl})(\text{PMe}_3)_3$: irradiation of the area of <i>cis</i> - PMe_3 groups at 1.402 ppm with the mixing time of 1.000 s (Bruker 600 MHz NMR machine).	216
Figure V-72. $\text{Ln}(\text{C})$ vs. time plot for the reaction of $(\text{ArN})\text{Mo}(\text{H})(\text{PhCHO})(\text{Cl})(\text{PMe}_3)_2$ with PhCHO (10 eq.) at 10.0 °C.	217
Figure V-73. $\text{Ln}(\text{C})$ vs. time plot for the reaction of $(\text{ArN})\text{Mo}(\text{H})(\text{PhCHO})(\text{Cl})(\text{PMe}_3)_2$ with PhCHO (10 eq.) at 18.0 °C.	218
Figure V-74. $\text{Ln}(\text{C})$ vs. time plot for the reaction of $(\text{ArN})\text{Mo}(\text{H})(\text{PhCHO})(\text{Cl})(\text{PMe}_3)_2$ with PhCHO (10 eq.) at 23.4 °C.	218
Figure V-75. $\text{Ln}(\text{C})$ vs. time plot for the reaction of $(\text{ArN})\text{Mo}(\text{H})(\text{PhCHO})(\text{Cl})(\text{PMe}_3)_2$ with PhCHO (10 eq.) at 34.0 °C.	219
Figure V-76. Eyring plot for the reaction of $(\text{ArN})\text{Mo}(\text{H})(\text{PhCHO})(\text{Cl})(\text{PMe}_3)_2$ with PhCHO (10 eq.)	219
Figure V-77. $\text{Ln}(\text{C})$ vs. time plot for the reaction $(\text{ArN})\text{Mo}(\text{H})(\text{PhCHO})(\text{Cl})(\text{PMe}_3)_2$ with PhCHO (5, 10, 15, and 20 eq.)	220
Figure V-78. Selective ge-1D EXSY NMR experiment of the sample containing $(\text{ArN})\text{Mo}(\text{H})(\text{PhCHO})(\text{Cl})(\text{PMe}_3)_2$: irradiation of the C-H proton of coordinated aldehyde at the frequency of 5.763 ppm with mixing time of 0.300 s (600 MHz machine).	221
Figure V-79. Selective ge-1D EXSY NMR experiment of the sample containing $(\text{ArN})\text{Mo}(\text{H})(\text{PhCHO})(\text{Cl})(\text{PMe}_3)_2$: irradiation of the C-H proton of coordinated aldehyde of its minor isomer at the frequency of 5.417 ppm with mixing time of 0.300 s (600 MHz machine).	222

Figure V-80. Selective ge-1D EXSY NMR experiment of the sample containing (ArN)Mo(H)(PhCHO)(Cl)(PMe ₃) ₂ : irradiation of the C-H proton of free benzaldehyde at the frequency of 9.638 ppm with the mixing time of 0.300 s (600 MHz machine).	223
Figure V-81. Selective ge-1D EXSY NMR experiment of the sample containing (ArN)Mo(H)(PhCHO)(Cl)(PMe ₃) ₂ : irradiation of the PMe ₃ protons at the frequency of 1.572 ppm with the mixing time of 1.000 s (600 MHz machine).	224
Figure V-82. Selective ge-1D EXSY NMR experiment of the sample containing (ArN)Mo(H)(PhCHO)(Cl)(PMe ₃) ₂ : irradiation of the PMe ₃ protons at the frequency of 1.290 ppm with the mixing time of 1.000 s (600 MHz machine).	224
Figure V-83. Ln(1-R) vs. mixing time (d8, s) plot for the exchange of two enantiomers of (ArN)Mo(OCH ₂ Ph)(PhCHO)(Cl)(PMe ₃) at 18.1 °C.....	225
Figure V-84. Ln(1-R) vs. mixing time (d8) plot for the exchange of two enantiomers of (ArN)Mo(OCH ₂ Ph)(PhCHO)(Cl)(PMe ₃) at 22.0 °C.....	226
Figure V-85. Ln(1-R) vs. mixing time (d8) plot for the exchange of two enantiomers of (ArN)Mo(OCH ₂ Ph)(PhCHO)(Cl)(PMe ₃) at 26.0 °C.....	226
Figure V-86. Ln(1-R) vs. mixing time (d8) plot for the exchange of two enantiomers of (ArN)Mo(OCH ₂ Ph)(PhCHO)(Cl)(PMe ₃) at 30.0 °C.....	227
Figure V-87. Eyring plot for the exchange of two enantiomers of (ArN)Mo(OCH ₂ Ph)(PhCHO)(Cl)(PMe ₃).	227
Figure V-88. Selective ge-1D EXSY NMR experiment of the sample containing (ArN)Mo(OCH ₂ Ph)(PhCHO)(Cl)(PMe ₃): irradiation of the PMe ₃ protons at the frequency of 0.913 ppm with the mixing time of 1.000 s (600 MHz machine).	228
Figure V-89. Selective ge-1D EXSY NMR experiment of the sample containing (ArN)Mo(OCH ₂ Ph)(PhCHO)(Cl)(PMe ₃): irradiation of free PhCHO protons at the frequency of 9.766 ppm with the mixing time of 1.000 s (600 MHz machine).....	229
Figure V-90. Selective ge-1D EXSY NMR experiment of the sample containing (ArN)Mo(OCH ₂ Ph)(PhCHO)(Cl)(PMe ₃): irradiation of free PhCHO protons at the frequency of 5.505 ppm with the mixing time of 1.000 s (600 MHz machine).....	229
Figure V-91. Ln(C) vs. time plot for the reaction of (ArN)Mo(OCH ₂ Ph)(Cl)(PMe ₃) ₃ with PhSiH ₃ (5 eq.) in the presence of PMe ₃ (30 eq.) at 10.0 °C.....	230

Figure V-92. Ln(C) vs. time plot for the reaction of (ArN)Mo(OCH ₂ Ph)(Cl)(PMe ₃) ₃ with PhSiD ₃ (5 eq.) in the presence of PMe ₃ (30 eq.) at 10.0 °C.....	231
Figure V-93. Eyring plot for H/H exchange between H ₂ and PhSiH ₃ in the presence of (ArN)Mo(SiH ₂ Ph)(Cl)(PMe ₃) ₂	261
Figure VI-1. ¹ H NMR spectrum of PhSiD ₃ and ZnCl ₂ in Et ₂ O under H ₂ atmosphere.	268
Figure VI-2. ¹ H NMR spectrum of PhSiD ₃ and CuH(PPh ₃) in C ₆ D ₆ under H ₂ atmosphere.	269
Figure VI-3. ¹ H NMR spectrum of (ArN)Mo(H)(Cl)(PMe ₃) ₃ and PhSiD ₃ under H ₂ atmosphere.	270
Figure VI-4. ¹ H NMR spectrum of (Cp)(ArN)Mo(H)(PMe ₃) and PhSiD ₃ under H ₂ atmosphere.	271
Figure VI-5. ¹ H NMR spectrum of (Tp)(ArN)Mo(H)(PMe ₃) and PhSiD ₃ under H ₂ atmosphere (30 min, RT).	272
Figure VI-6. ¹ H NMR spectrum of (Tp)(ArN)Mo(H)(PMe ₃) and PhSiD ₃ under H ₂ atmosphere (3 days, RT).	273
Figure VI-7. ¹ H NMR spectrum of PhSiD ₃ in C ₆ D ₆ under the hydrogen atmosphere (control experiment)	274
Figure VI-8. ¹ H NMR spectrum of PhSiD ₃ and BPh ₃ in C ₆ D ₆ under the hydrogen atmosphere	275
Figure VI-9. ¹ H NMR spectrum of PhSiD ₃ and B(C ₆ F ₅) ₃ in C ₆ D ₆ under the hydrogen atmosphere	276
Figure VI-10. ¹ H NMR spectrum of PhMeSiD ₂ and B(C ₆ F ₅) ₃ in C ₆ D ₆ under the hydrogen atmosphere.....	277
Figure VI-11. ¹ H NMR spectrum of PhMe ₂ SiD and B(C ₆ F ₅) ₃ in C ₆ D ₆ under the hydrogen atmosphere.....	278
Figure VI-12. ¹ H NMR spectrum of PhSiD ₃ , Et ₃ SiH and BPh ₃ in C ₆ D ₆ (after 1 month at RT).	279

List of Schemes

Scheme II-1. Hydrosilylation of 1-octene catalyzed by diacetyl peroxide.	2
Scheme II-2. Ojima's mechanism of hydrosilylation of carbonyls catalyzed by RhCl(PPh ₃) ₃	4
Scheme II-3. Ojima's mechanism of hydrosilylation of α,β -unsaturated carbonyls catalyzed by (Ph ₃ P) ₃ RhCl	5
Scheme II-4. Proposed modes of the hydride shift promoted by the other molecule of silane. ^{23d}	6
Scheme II-5. Regiospecific hydrosilylation of α,β -unsaturated carbonyls by different silanes.....	6
Scheme II-6. Chan's mechanism of hydrosilylation of carbonyls by mono- and polyhydrosilanes.....	7
Scheme II-7. Chan's mechanism of hydrosilylation of α,β -unsaturated carbonyls by mono- and polyhydrosilanes.	8
Scheme II-8. Chan's proposed transition states for hydrosilylation of 3,5-dimethyl-2-cyclohexene-1-one by PhMe ₂ SiH.....	9
Scheme II-9. Proposed mechanistic pathways for Rh-catalyzed hydrosilylation of ketones based on DFT computational studies of Hofmann and Gade. ³⁴	10
Scheme II-10. Nakano's mechanism of hydrosilylation of ketones catalyzed by Cp ₂ TiPh ₂	11
Scheme II-11. Generation of catalytically active Ti-H species from titanium(IV) alkoxide and triethoxy silane.....	12
Scheme II-12. Preparation of the chiral Ti(III) hydride complex.....	13
Scheme II-13. Unfavourable and favourable transition states when acetophenone approaches the titanium complex.	13
Scheme II-14. Proposed catalytic cycle of hydrosilylation of carbonyls by Ti-H catalyst.	14
Scheme II-15. Mimoun's mechanism of hydrosilylation of ketones catalyzed by zinc hydride species.	15

Scheme II-16. Mimoun's alternative mechanism of hydrosilylation catalyzed by zinc hydride species.	16
Scheme II-17. Proposed mechanism of hydrosilylation of carbonyls catalyzed by dialkylzinc complexes.....	17
Scheme II-18. Product of reaction between benzaldehyde and $\text{ZnEt}_2^*(S,S)$ -ebpe, and its X-ray structure ⁵¹	18
Scheme II-19. Hydrosilylation catalyzed by $(\text{Ph}_3\text{P})_2\text{Re}(\text{O})_2\text{I}$	18
Scheme II-20. Proposed mechanism of hydrosilylation of carbonyls by $(\text{Ph}_3\text{P})_2\text{Re}(\text{O})_2\text{I}$	19
Scheme II-21. Concerted [2+2] addition mechanism of $(\text{Ph}_3\text{P})_2(\text{I})\text{Re}(\text{H})(\text{OSiR}_3)(\text{O})$ formation supported by DFT calculations.	20
Scheme II-22. An alternative mechanism of Lewis base activation of silane by oxo ligand.	20
Scheme II-23. Proposed mechanism of reaction between $(\text{Ph}_3\text{P})_2\text{Re}(\text{H})(\text{OSiMePh}_2)(\text{O})(\text{I})$ and <i>p</i> -anisaldehyde.	22
Scheme II-24. Reaction of ¹⁸ O-labeled <i>p</i> -anisaldehyde with siloxyrhenium complex.	22
Scheme II-25. Proposed mechanism of hydrosilylation of carbonyls by $\text{ReOCl}_3(\text{PPh}_3)_2$	24
Scheme II-26. An alternative mechanism of carbonyl hydrosilylation by oxo-rhenium complexes proposed by Abu-Omar.	25
Scheme II-27. Cationic monooxo-rhenium(V) <i>salen</i> complexes.	26
Scheme II-28. Hydrolytic oxidation of silanes catalyzed by $[\text{Re}(\text{O})(\text{hoz})_2][\text{B}(\text{C}_6\text{F}_5)_4]$	27
Scheme II-29. ¹⁸ O-labeling experiments to study the mechanism of silane hydrolysis catalyzed by cationic oxorhenium(V) complex.	27
Scheme II-30. Berke's mechanism of hydrosilylation of carbonyls catalyzed by $[\text{Re}(\text{CH}_3\text{CN})_3\text{Br}_2(\text{NO})]$	28
Scheme II-31. Possible mechanism of hydrosilylation of carbonyls catalyzed by MoO_2Cl_2 suggested on the basis of DFT calculations.	30

Scheme II-32. Proposed catalytic cycle of hydrosilylation of benzaldehyde by PhSiH_3 catalyzed by $(\text{ArN})\text{Mo}(\text{H})(\text{Cl})(\text{PMe}_3)_3$	32
Scheme II-33. Proposed mechanism of dehydrogenative silylation of ethanol.	33
Scheme II-34. Hydrosilylation of carbonyls catalyzed by $\text{CuH}(\text{PPh}_3)$	34
Scheme II-35. Proposed mechanism of hydrosilylation of carbonyls catalyzed by $\text{CuH}(\text{PPh}_3)$	35
Scheme II-36. Mindiola's Ni(II)-catalysts for carbonyl hydrosilylation.	36
Scheme II-37. Mindiola's mechanism of carbonyl hydrosilylation catalyzed by $[(\text{PN}^{\text{iPr}_3})\text{Ni}(\mu_2\text{-Br})]_2$	37
Scheme II-38. Guan's mechanism of carbonyl hydrosilylation by nickel PCP-pincer complexes. ^{7b}	38
Scheme II-39. Mechanism of hydrosilylation of carbonyls catalyzed by $\text{B}(\text{C}_6\text{F}_5)_3$	39
Scheme II-40. H/D exchange between Et_3SiD and Ph_3SiH promoted by $\text{B}(\text{C}_6\text{F}_5)_3$	40
Scheme II-41. The proposed nucleophilic attack of LUMO of the $\text{R}_3\text{Si-H-B}(\text{C}_6\text{F}_5)_3$ adduct by carbonyl.....	40
Scheme II-42. Preparations of ketone-silyl cation adduct.	41
Scheme II-43. Hydrosilylation of thiocarbonyls catalyzed by $\text{B}(\text{C}_6\text{F}_5)_3$	42
Scheme II-44. Proposed mechanism of reduction of carbonyl groups ($\text{C}=\text{O}$) to methylenes ($-\text{CH}_2-$) with PMHS mediated by $\text{B}(\text{C}_6\text{F}_5)_3$	43
Scheme II-45. Mechanism of hydrosilylation of alcohols catalyzed by $\text{B}(\text{C}_6\text{F}_5)_3$	43
Scheme II-46. Proposed mechanism of hydrosilylation of imines catalyzed by $\text{B}(\text{C}_6\text{F}_5)_3$	44
Scheme II-47. Proposed mechanism for the hydride transfer step in hydrosilylation of carbonyls and imines by the silicon-stereogenic silane.	45
Scheme II-48. Synthesis of $[2,5\text{-Ph}_2\text{-3,4-Tol}_2(\eta^5\text{-C}_4\text{COBpin})\text{Ru}(\text{CO})_2\text{H}]$	47
Scheme II-49. Stoichiometric reaction between $[2,5\text{-Ph}_2\text{-3,4-Tol}_2(\eta^5\text{-C}_4\text{COBpin})\text{Ru}(\text{CO})_2\text{H}]$ and benzaldehyde.....	47
Scheme II-50. Clark-Casey's mechanism of carbonyl hydroboration catalyzed by $[2,5\text{-Ph}_2\text{-3,4-Tol}_2(\eta^5\text{-C}_4\text{COBpin})\text{Ru}(\text{CO})_2\text{H}]$	48
Scheme II-51. H/D-exchange in the $\text{D}_2\text{—KOH/H}_2\text{O}$ and $\text{D}_2\text{—KNH}_2/\text{NH}_3$ systems. ...	50

Scheme II-52. Hydrogenation of benzophenone by H_2 in the presence of <i>t</i> -BuOK.....	51
Scheme II-53. Walling-Bollyky mechanism of base-catalyzed hydrogenation of benzophenone.....	51
Scheme II-54. Berkessel's mechanism of base-catalyzed hydrogenation of ketones and base-catalyzed isotope exchange. ¹²⁵	52
Scheme II-55. DeWitt's scheme of hydrogenation of olefins catalyzed by trialkylboranes.....	53
Scheme II-56. Hydrogenation of benzene ring in the presence of HF-TaF ₅	54
Scheme II-57. Reaction between N^5, N^{10} -methenyl tetrahydromethanopterin and H_2 catalyzed by enzyme isolated from <i>Methanobacterium thermoautotrophicum</i>	54
Scheme II-58. Possible transition states for the H-H bond cleavage by imidazolidinium cation and a base (bifunctional catalysis). ¹³⁵	55
Scheme II-59. Reaction between <i>p</i> -(C ₆ H ₂ Me ₃) ₂ P-C ₆ F ₄ -B(C ₆ F ₅) ₂ and H_2	55
Scheme II-60. Hydrogenation of nitroarenes to aminoarenes in the presence of fullerene (C ₆₀ /C ₆₀ ⁻ mixture). ^{137a}	56
Scheme III-1. Proposed catalytic cycle of hydrosilylation of benzaldehyde by phenylsilane catalyzed by (ArN)Mo(H)(Cl)(PMe ₃) ₃ . ^{5a}	58
Scheme III-2. Preparation of (Cp)(ArN)Mo(H)(PMe ₃) and (Tp)(ArN)Mo(H)(PMe ₃) from (ArN)Mo(H)(Cl)(PMe ₃) ₃	58
Scheme III-3. Hydrosilylation of benzaldehyde with phenylsilane in the presence of (Cp)(ArN)Mo(H)(PMe ₃).....	59
Scheme III-4. Phosphine exchange between (Cp)(ArN)Mo(H)(PMe ₃) and PMe ₃	60
Scheme III-5. Reaction between (Cp)(ArN)Mo(H)(PMe ₃) and benzaldehyde.....	61
Scheme III-6. Calculated mechanism of the reaction between (Cp)(MeN)Mo(H)(PMe ₃) and CH ₂ =O.....	62
Scheme III-7. Proposed mechanism for the reaction between (Cp)(ArN)Mo(H)(PMe ₃) and excess benzaldehyde.....	65
Scheme III-8. Proposed mechanism for the reaction between (Cp)(ArN)Mo(OCH ₂ Ph)(PMe ₃) and benzaldehyde.....	65

Scheme III-9. Reaction between (Cp)(ArN)Mo(OCH ₂ Ph)(PMe ₃) and <i>o</i> -bromobenzaldehyde.	66
Scheme III-10. Proposed mechanism for the reaction between (Cp)(ArN)Mo(OCH ₂ Ph)(PMe ₃) and <i>o</i> -bromobenzaldehyde.	67
Scheme III-11. Phosphine exchange between (Cp)(ArN)Mo(OCH ₂ Ph)(PMe ₃) and PMe ₃	68
Scheme III-12. Reaction between (Cp)(ArN)Mo(OCH ₂ Ph)(PMe ₃) and PhSiH ₃	69
Scheme III-13. Proposed pathways for the reaction between (Cp)(ArN)Mo(OCH ₂ Ph)(PMe ₃) and PhSiH ₃	70
Scheme III-14. Calculated mechanism of carbonyl hydrosilylation.	70
Scheme III-15. Computed reaction pathways for formation of (Cp)(MeN)MoH ₂ (SiH ₃) (at 298 K).	71
Scheme III-16. Reaction of (Cp)(ArN)Mo(H)(PMe ₃) with PhSiH ₃ (>2 eq.) in the presence of BPh ₃	72
Scheme III-17. Reaction between (Cp)(ArN)Mo(H)(PMe ₃) and PhSiH ₃	73
Scheme III-18. Computed reaction pathway for formation of (Cp)(MeN)Mo(SiH ₃)(PMe ₃) (at 298 K)	73
Scheme III-19. Stoichiometric reaction between (Cp)(ArN)Mo(H)(PMe ₃), PhCHO and PhSiD ₃	74
Scheme III-20. Reaction between (Tp)(ArN)Mo(H)(PMe ₃) and PhCHO.	78
Scheme III-21. Proposed mechanism for the reaction between (Tp)(ArN)Mo(H)(PMe ₃) and PhCHO.	80
Scheme III-22. Reaction between (Tp)(ArN)Mo(H)(PMe ₃) and PhCHO (excess).	80
Scheme III-23. Reaction between (Tp)(ArN)Mo(OCH ₂ Ph)(η^2 -PhCHO) and <i>p</i> -bromobenzaldehyde.	81
Scheme III-24. Reaction between (Tp)(ArN)Mo(H)(PMe ₃) and acetophenone.	81
Scheme III-25. Reaction between (Tp)(ArN)Mo(H)(PMe ₃) and (+)camphor.	81
Scheme III-26. Reaction between (Tp)(ArN)Mo(H)(PMe ₃) and PhSiD ₃ (5 eq.).	82
Scheme III-27. Proposed mechanism for the reaction between (Tp)(ArN)Mo(OCH ₂ Ph)(PMe ₃) and PhSiH ₃	83

Scheme III-28. Reaction between $(\text{Tp})(\text{ArN})\text{Mo}(\text{H})(\text{PMe}_3)$, PhSiD_3 and cyclohexanone.	84
Scheme III-29. Reaction of $(\text{Tp})(\text{ArN})\text{Mo}(\text{H})(\text{PMe}_3)$ with benzonitrile.	85
Scheme III-30. Reaction of $(\text{Tp})(\text{ArN})\text{Mo}(-\text{N}=\text{CHPh})(\text{PMe}_3)$ with benzaldehyde.	85
Scheme III-31. Lipshutz mechanism of hydrosilylation of carbonyls catalyzed by $\text{CuH}(\text{PPh}_3)$	87
Scheme III-32. Reaction between $(\text{PPh}_3)\text{CuH}$ and PhCHO to give $(\text{PPh}_3)\text{CuOCH}_2\text{Ph}$ followed by the reaction with PhMe_2SiH	87
Scheme III-33. Toste mechanism of carbonyl hydrosilylation catalyzed by $(\text{PPh}_3)_2(\text{I})\text{Re}(\text{O})_2$	94
Scheme III-34. 1:1:1 reaction between $(\text{PPh}_3)_2(\text{I})(\text{O})\text{Re}(\text{H})(\text{OSiMe}_2\text{Ph})$, PhMe_2SiD and PhCHO	95
Scheme III-35. Preparation of $(\text{PPh}_3)_2\text{Re}(\text{H})\text{OCl}_2$ and $(\text{PCy}_3)_2\text{Re}(\text{D})\text{OCl}_2$	96
Scheme III-36. Reaction between $(\text{PPh}_3)_2\text{Re}(\text{H})\text{OCl}_2$ and benzaldehyde (1 eq.) in the presence of Et_3SiD (1 eq.).	96
Scheme III-37. Reaction between $(\text{PCy}_3)_2\text{Re}(\text{D})\text{OCl}_2$ and propanal (1 eq.) in the presence of Et_3SiH (1 eq.).	97
Scheme III-38. H/D exchange between $(\text{PCy}_3)_2\text{Re}(\text{D})\text{OCl}_2$ and Et_3SiH	97
Scheme III-39. Mimoun's mechanism of hydrosilylation of ketones catalyzed by zinc hydride species.	101
Scheme III-40. Proposed catalytic cycle of hydrosilylation of benzaldehyde by PhSiH_3 catalyzed by $(\text{ArN})\text{Mo}(\text{H})(\text{Cl})(\text{PMe}_3)_3$	105
Scheme III-41. Exchange between two isomers of $(\text{ArN})\text{Mo}(\text{H})(\eta^2\text{-PhCHO})(\text{Cl})(\text{PMe}_3)_2$	107
Scheme III-42. Formation of $(\text{ArN})\text{Mo}(\text{OCH}_2\text{Ph})(\eta^2\text{-PhCHO})(\text{Cl})(\text{PMe}_3)$	107
Scheme III-43. Exchange of diastereotopic protons in $(\text{ArN})\text{Mo}(\text{OCH}_2\text{Ph})(\eta^2\text{-PhCHO})(\text{Cl})(\text{PMe}_3)$	108
Scheme III-44. Proposed mechanism for the reaction between $(\text{ArN})\text{Mo}(\text{OCH}_2\text{Ph})(\text{Cl})(\text{PMe}_3)_3$ and PhSiH_3	109

Scheme III-45. Reversible formation of $(\text{ArN})\text{Mo}(\eta^2\text{-PhCHO})(\text{OCH}_2\text{Ph})(\text{Cl})(\text{PMe}_3)$ from $(\text{ArN})\text{Mo}(\text{OCH}_2\text{Ph})(\text{Cl})(\text{PMe}_3)_3$.	110
Scheme III-46. Reaction of $(\text{ArN})\text{Mo}(\text{H})(\text{Cl})(\text{PMe}_3)_3$ with acetophenone and cyclohexanone.	112
Scheme III-47. Proposed mechanism of formation of ketoxy derivatives of $(\text{ArN})\text{Mo}(\text{H})(\text{Cl})(\text{PMe}_3)_3$.	114
Scheme III-48. Stoichiometric reaction between $(\text{ArN})\text{Mo}(\text{H})(\text{Cl})(\text{PMe}_3)_3$, PhSiD_3 and benzaldehyde.	116
Scheme III-49. Stoichiometric reaction between $(\text{ArN})\text{Mo}(\text{H})(\text{Cl})(\text{PMe}_3)_3$, PhSiD_3 and cyclohexanone.	117
Scheme III-50. Hydrosilylation of cyclohexanone with PhSiD_3 mediated by $(\text{ArN})\text{Mo}(\text{H})(\text{Cl})(\text{PMe}_3)_3$. Two concurrent mechanisms are shown.	117
Scheme III-51. Stoichiometric reaction between $(\text{ArN})\text{Mo}(\text{H})(\text{Cl})(\text{PMe}_3)_3$, PhSiD_3 and acetophenone.	118
Scheme III-52. Reaction of $(\text{ArN})\text{Mo}(\text{H})(\text{Cl})(\text{PMe}_3)_3$ with PhSiH_3 and BPh_3 .	120
Scheme III-53. Preparation of $(\text{ArN})\text{Mo}(\text{SiH}_2\text{Ph})(\text{Cl})(\text{PMe}_3)_3$ from $(\text{ArN})\text{Mo}(\text{OCy})(\text{Cl})(\text{PMe}_3)_3$.	121
Scheme III-54. Dehydrogenative borylation of N-benzylbenzamide.	126
Scheme III-55. Catalytic hydroboration of phenylacetylene with catecholborane.	126
Scheme III-56. Reaction of $(\text{Tp})(\text{ArN})\text{Mo}(\text{H})(\text{PMe}_3)$ with acrylonitrile.	127
Scheme III-57. Hydroboration of ethyl 4-cyanobenzoate.	128
Scheme III-58. Exchange between $(\text{Tp})(\text{ArN})\text{Mo}(\text{H})(\text{PMe}_3)$ and CatBH .	128
Scheme III-59. Reaction between $(\text{Tp})(\text{ArN})\text{Mo}(\text{D})(\text{PMe}_3)$ and PinBH .	130
Scheme III-60. Reaction of carbonyl with a mixture of $(\text{Tp})(\text{ArN})\text{Mo}(\text{H})(\text{PMe}_3)$ and CatBH .	131
Scheme III-61. Reactions of the molybdenum alkoxy complexes with CatBH and PinBH .	132
Scheme III-62. Proposed mechanism of carbonyl hydroboration catalyzed by $(\text{Tp})(\text{ArN})\text{Mo}(\text{H})(\text{PMe}_3)$.	132

Scheme III-63. H/Si-H exchange between H_2 and $(ArN)Mo(SiH_2Ph)(Cl)(PMe_3)_2$ observed by EXSY NMR.....	134
Scheme III-64. Possible activation of the H/D exchange between silane and dihydrogen.....	136
Scheme III-65. H/D exchange between catecholborane and triethylsilane- <i>d</i> 1.....	136
Scheme III-66. H/D exchange between $PhSiD_3$ and Et_3SiH	136

List of Tables

Table III-1. Hydrosilylation of carbonyls with PhSiH_3 catalyzed by $(\text{Cp})(\text{ArN})\text{Mo}(\text{H})(\text{PMe}_3)$	59
Table III-2. Selected bond distances (\AA) and angles ($^\circ$) for $(\text{Cp})(\text{ArN})\text{Mo}(\text{OCH}_2\text{Ph})(\text{PMe}_3)$	63
Table III-3. Rate constants and kinetic isotope effect for the reaction between $(\text{Cp})(\text{ArN})\text{Mo}(\text{OCH}_2\text{Ph})(\text{PMe}_3)$ and $\text{PhSiH}_3/\text{PhSiD}_3$ (10 eq.)	71
Table III-4. Selected bond distances (\AA) and angles ($^\circ$) for $(\text{Tp})(\text{ArN})\text{Mo}(\text{Cl})(\text{PMe}_3)$	76
Table III-5. Hydrosilylation of various substrates catalyzed by $(\text{Tp})(\text{ArN})\text{Mo}(\text{H})(\text{PMe}_3)$	77
Table III-6. Kinetic isotope effect for the reaction of $(\text{Tp})(\text{ArN})\text{Mo}(\text{OCH}_2\text{Ph})(\text{PMe}_3)$ with $\text{PhSiH}_3/\text{PhSiD}_3$	82
Table III-7. Selected bond distances (\AA) and angles ($^\circ$) for $(\text{ArN})(\text{CyO})\text{Mo}(\text{Cl})(\text{PMe}_3)_3$	113
Table III-8. Change in the hydride intensity for $(\text{ArN})\text{Mo}(\text{H})(\text{Cl})(\text{PMe}_3)_3$ in the presence of PhSiD_3 (4.2 eq.).....	115
Table III-9. Hydrosilylation of organic substrates using $(\text{ArN})\text{Mo}(\text{H})(\text{Cl})(\text{PMe}_3)_3$ as catalyst	119
Table III-10. Hydroboration of carbonyls with catecholborane catalyzed by $(\text{Tp})(\text{ArN})\text{Mo}(\text{H})(\text{PMe}_3)$	123
Table III-11. Hydroboration of carbonyls with pinacolborane catalyzed by $(\text{Tp})(\text{ArN})\text{Mo}(\text{H})(\text{PMe}_3)$	124
Table III-12. Hydroboration of nitriles with catecholborane catalyzed by $(\text{Tp})(\text{ArN})\text{Mo}(\text{H})(\text{PMe}_3)$	125
Table III-13. Competitive hydroboration of carbonyls and nitriles by catecholborane catalyzed by $(\text{Tp})(\text{ArN})\text{Mo}(\text{H})(\text{PMe}_3)$	127
Table V-1. Hydrosilylation of carbonyls with PhSiH_3 catalyzed by $(\text{Cp})(\text{ArN})\text{Mo}(\text{H})(\text{PMe}_3)$	170

Table V-2. Hydrosilylation of PhCHO with PhSiH ₃	170
Table V-3. Hydrosilylation of PhCHO with PhSiH ₃ (and PhSiD ₃) catalyzed by (Cp)(ArN)Mo(H)(PMe ₃): reaction rate constants of individual steps and activation parameters	171
Table V-4. Hydrosilylation of various organic substrates catalyzed by (Tp)(ArN)Mo(H)(PMe ₃) (5 mol%).	207
Table V-5. Hydrosilylation of PhCHO with PhSiH ₃ (and PhSiD ₃) catalyzed by (Tp)(ArN)Mo(H)(PMe ₃): reaction rate constants of individual steps and activation parameters.	208
Table V-6. Hydrosilylation of organic substrates using (ArN)Mo(H)(Cl)(PMe ₃) ₃ as a catalyst	234
Table V-7. Characteristic signals in the ¹ H and ¹¹ B NMR spectra for pinacolborane, (Tp)(ArN)Mo(H)(PMe ₃) and their mixture.....	236
Table V-8. Chemical shifts of the B-H signal (¹ H NMR) for catecholborane and its mixture with various carbonyls and benzonitrile.	241
Table V-9. Rate constants for H/H exchange between H ₂ and PhSiH ₃ in the presence of (ArN)Mo(SiH ₂ Ph)(Cl)(PMe ₃) ₂	261
Table VI-1. Crystal structure determination parameters for (Cp)(ArN)Mo(OCH ₂ Ph)(PMe ₃).	265
Table VI-2. Crystal structure determination parameters for (Tp)(ArN)Mo(H)(PMe ₃).	266
Table VI-3. Crystal structure determination parameters for (ArN)(CyO)Mo(Cl)(PMe ₃) ₃	267

I Introduction

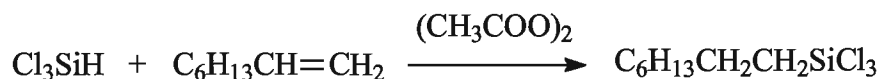
Metal-catalyzed hydrosilylation of carbonyls is a convenient reduction method and produces protected alcohols in one step at mild conditions.¹ It is considered a greener alternative to metal hydride reduction of carbonyls. Most industrial applications of hydrosilylation are catalyzed by late transition metals, which are toxic and expensive. Much current effort is aimed at replacing heavy late transition metal complexes for less expensive and more environmentally benign early metals, such as Ti², Zr³, and Mo^{4,5}, or first d-series metals^{6,7}, particularly Fe⁸ and Cu⁹. The mechanistic proposals offered for these metal catalysts share a common theme: the formation of a metal hydride intermediate upon the addition of silane followed by carbonyl insertion into the Mo-H bond to give an alkoxide (the hydride mechanism).^{7b} Indeed, some metal hydride complexes have been obtained or observed under the hydrosilylation conditions and proved to turn over.^{5, 7b, 10} But are they the actual catalysts and what is the true role of the hydride ligand? Understanding how catalysis works is important for the rational design of new catalysts. Unfortunately, mechanistic data on hydrosilylation catalysis are scarce, and further investigations are required.

Metal-catalyzed hydroboration is a useful addition to non-catalytic hydroboration of unsaturated organic compounds, and proceeds with different chemo-, regio- and stereoselectivities.¹¹ Despite the fact that metal-catalyzed hydroboration of olefins and alkynes is well-established and thoroughly studied, hydroboration of carbonyls and nitriles is still untouched. The use of transition metals for carbonyl and nitrile hydroboration may provide milder conditions, and thus, better selectivities and higher yields. Hydroboration of nitriles may produce N,N-bisborylated amines¹², a relatively new class of compounds that may find applications in organic synthesis.

II Historical

II. 1 Hydrosilylation of carbonyls: early studies

Hydrosilylation is an addition reaction of hydrosilanes R_3SiH to organic compounds with multiple bonds, such as carbonyls, alkenes, alkynes and nitriles.¹¹ The history of hydrosilylation begins in 1947 with Sommer's report of the reaction between trichlorosilane and 1-octene in the presence of diacetyl peroxide (Scheme II-1).¹³



Scheme II-1. Hydrosilylation of 1-octene catalyzed by diacetyl peroxide.

It is interesting to note that until 1957, reactions of hydrosilanes with carbonyl compounds had not yet been reported. Calas and Duffaut found that trichlorosilane and triphenylsilane could easily be added across the carbonyl group of ketones and aldehydes under the photoinduced conditions (UV radiation).¹⁴ For instance, a photochemical reaction between acetone and trichlorosilane afforded formation of isopropyl trichlorosilyl ether. Acetophenone and benzophenone, in contrast, did not react with the silane under the UV radiation. Soon after 1958, Gilman and Wittenberg found that triphenylsilane, diphenylsilane and phenylsilane react with benzophenone to produce the corresponding silyl ethers at high temperatures and in the absence of any added catalyst.¹⁵ Calas then studied the influence of different electronic factors on the addition of hydrosilanes to carbonyls.¹⁶ It was found that when hydrosilylation was promoted by UV radiation, the yields of alkoxysilanes were very sensitive to the presence of electron-withdrawing substituents in carbonyls.^{16b, 17} For example, reaction of acetophenone with trichlorosilane gave the product in 95% yield after one hour of UV radiation. α -Chloroacetophenone in the same reaction did not react (0% yield) even after 40 hours of radiation. In contrast, the influence of steric factors on hydrosilylation was not found to be very significant. n - C_6H_{11} -CO- CH_3 , t -Bu-CO- CH_3 and t -Bu-CO-Bu- t were all hydrosilylated within one hour in >93% yields. All observations were consistent with the radical mechanism of hydrosilylation induced by UV radiation.¹⁷

In the 1960s, Calas *et al.* discovered that hydrosilylation of carbonyls could also be mediated by ZnCl_2 .¹⁸ This new method became a milder alternative to the temperature- and UV-induced hydrosilylation and worked on a broader range of substrates. However, in case of aldehydes, the products often disproportionate to disilyl ether and dialkyl ether.

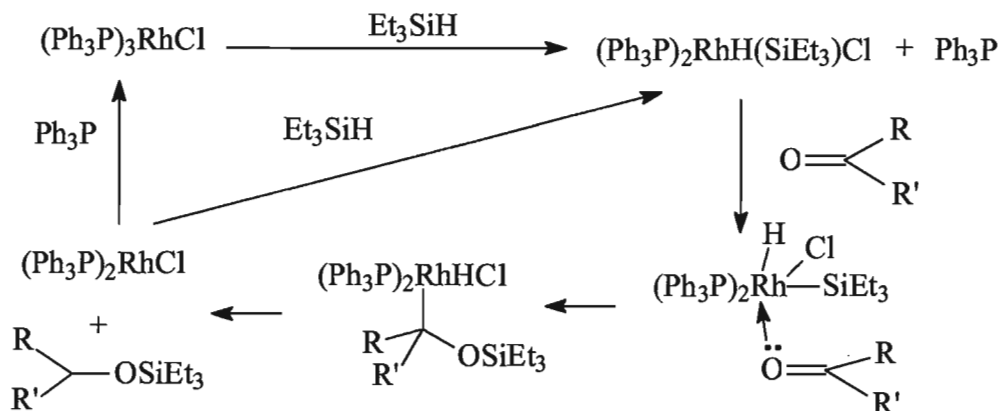
Calas emphasized the influence of different types of silane substituents on hydrosilylation reactions.¹⁷ Two mechanisms for the Si-H bond cleavage have been considered, homolytic and heterolytic. Homolytic cleavage of the Si-H bond ($\text{Si}\cdot + \cdot\text{H}$) takes place in the photoinduced hydrosilylation. It is facilitated by substituents such as Cl and Ph, which can stabilize the radicals by π -conjugation. Accordingly, trichlorosilane and triphenylsilane demonstrated the best results in the *photoinduced* hydrosilylation reactions. In contrast, donor alkyl substituents in trialkylsilanes make the Si-H bond more electron-rich and the hydride more nucleophilic ($\text{Si}^{\delta+}-\text{H}^{\delta-}$) and thereby promoting the addition of silanes across the carbonyl group ($\text{O}^{\delta-}=\text{C}^{\delta+}$). In the latter process, ZnCl_2 helps the addition reaction by polarizing the C=O further by Lewis acid coordination (Lewis acid-catalyzed hydrosilylation).

II. 2 Rh-catalyzed hydrosilylation of carbonyls

In 1972, Ojima reported hydrosilylation of carbonyls catalyzed by the chlorotris(triphenyl-phosphine)rhodium complex (Wilkinson's catalyst).¹⁹ Hydrosilylation was observed as a clean reaction and under mild conditions. When the hydrosilylation proceeded slowly (for certain substrates), Ojima noticed formation of a yellow precipitate, which re-dissolved as the reaction temperature rose. The yellow precipitate was isolated from the reaction mixture and identified as $(\text{Ph}_3\text{P})_2\text{Rh}(\text{H})(\text{SiEt}_3)(\text{Cl})$. This product resulted from oxidative addition of the silane to $\text{RhCl}(\text{PPh}_3)_3$, which had previously been observed by Wilkinson²⁰ and Haszeldine²¹. This hydrosilylrhodium(III) complex was reported to catalyze hydrosilylation of carbonyls as well.²²

Following these observations, a mechanism of hydrosilylation catalyzed by $\text{RhCl}(\text{PPh}_3)_3$ was proposed (Scheme II-2).^{22b, 23} It involves the oxidative addition of silane to rhodium catalyst to form a hydridosilylrhodium complex followed by the silicon

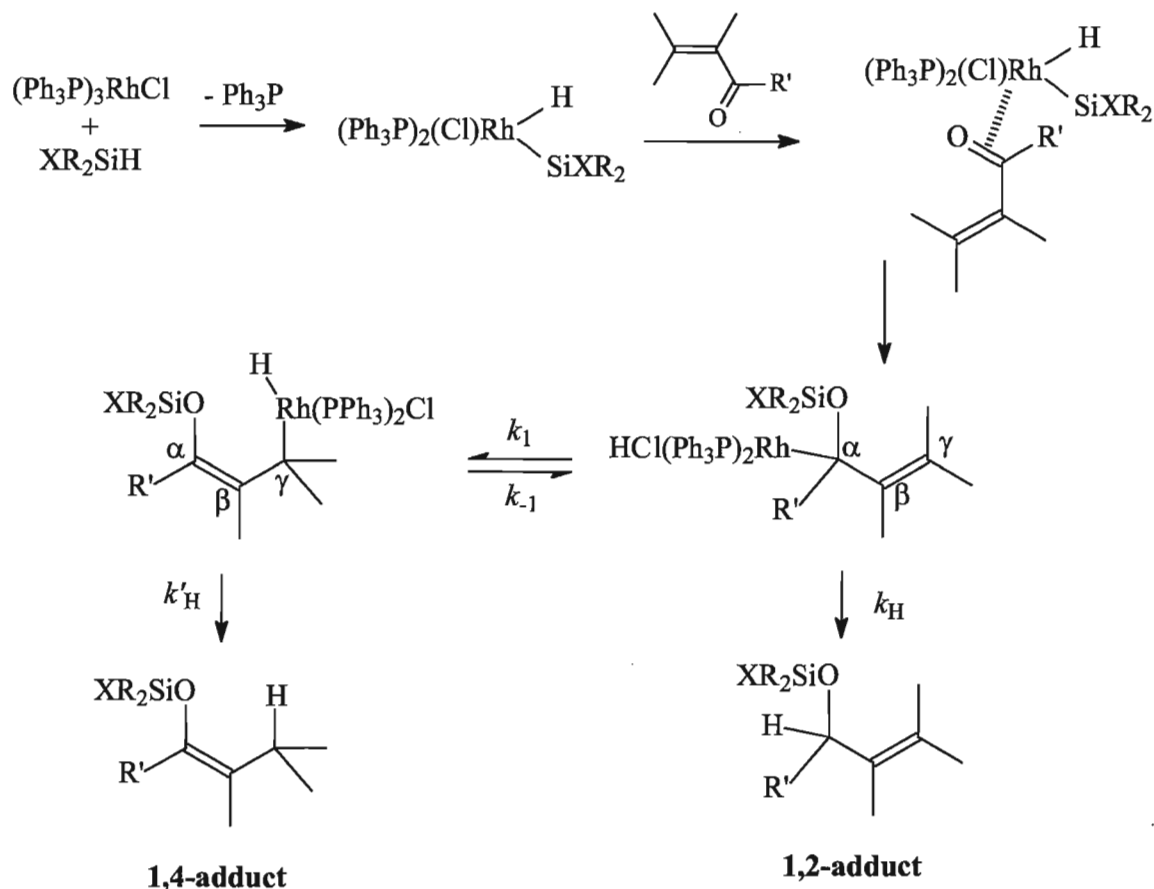
migration from rhodium to the carbonyl oxygen to give (α -siloxyalkyl)rhodium hydride as a key intermediate. Kagan's spin-trapping experiments also support this mechanism.²⁴



Scheme II-2. Ojima's mechanism of hydrosilylation of carbonyls catalyzed by $\text{RhCl}(\text{PPh}_3)_3$.

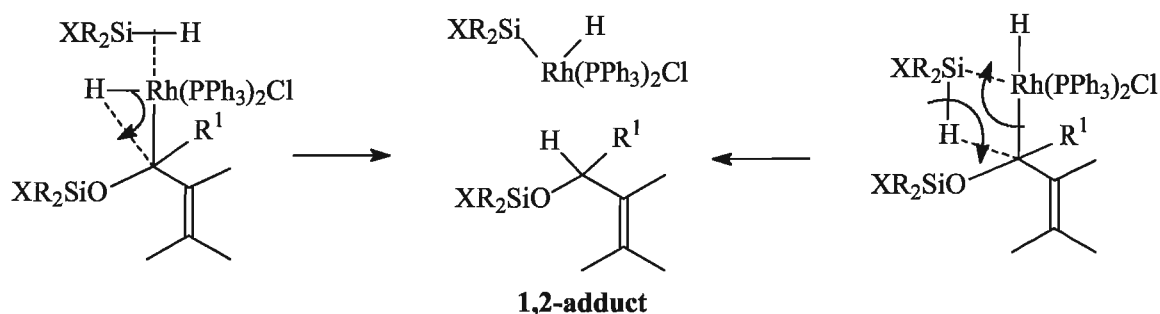
Wilkinson's catalyst and hydridosilylrhodium complex were found to catalyze hydrosilylation of α,β -unsaturated carbonyls compounds with high regioselectivity.^{22c} Hydrosilylation with monohydrosilanes afforded enol silyl ethers (1,4-addition), while polyhydrosilanes gave α,β -unsaturated silylated alcohols (1,2-addition).^{23d, 25}

To study the regioselective hydrosilylation, spin-labeling experiments have been performed.^{23d} Geranial, as a typical substrate, was hydrosilylated with Et_3SiD and Ph_2SiD_2 in the presence of Wilkinson catalyst. The silylated products were exposed to methanolysis to the corresponding alcohols. It was indicated that Et_3SiD resulted in exclusive formation of citronellal-3- d_1 , while Ph_2SiD_2 afforded geraniol-1- d_1 . Ojima proposed formation of an (α -siloxyallyl)rhodium hydride as a key intermediate (Scheme II-3). The latter can be isomerized to (γ -siloxyallyl)rhodium hydride complex. Each isomer gives the corresponding product by β -C-H reductive elimination.



Scheme II-3. Ojima's mechanism of hydrosilylation of α,β -unsaturated carbonyls catalyzed by $(\text{Ph}_3\text{P})_3\text{RhCl}$

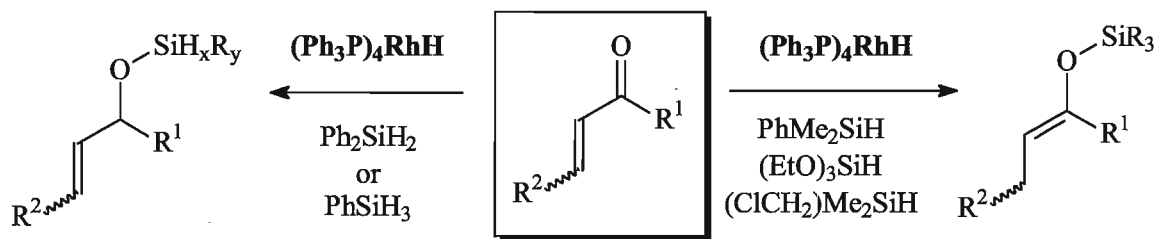
EPR spectra of the reaction mixture of β -ionone, diphenylsilane, $(\text{Rh}_3\text{P})_3\text{RhCl}$, and nitrosoderene obtained 15 min and 30 min after the reagents were mixed, strongly indicate the formation of both proposed isomers and the equilibrium between them.^{23d} Ojima emphasized that the ratio of two isomers may be influenced by several factors, such as the bulkiness of the α -siloxy group and the electronic effects of the silyl group. For instance, strong steric repulsion between the siloxy group and the rhodium moiety favours formation of the γ -adduct (1,4-addition intermediate). Electronic influence of the silyl group on the allylic system may affect the ease of isomerization. In addition, Ojima proposed that another molecule of hydrosilane may participate in accelerating the hydride shift from rhodium and promote the formation of the 1,2-adduct (Scheme II-4).^{23d}



Scheme II-4. Proposed modes of the hydride shift promoted by the other molecule of silane.^{23d}

Ojima finally concluded that polyhydrosilanes are not bulky enough, in comparison to monohydrosilanes, to cause isomerization of the α -adduct to the γ -adduct. Furthermore, polyhydrosilanes participation in promoting the hydride shift and their potential ease of oxidative addition were considered to be more expectable. For monohydrosilanes, all the factors favour the formation of the γ -adduct.

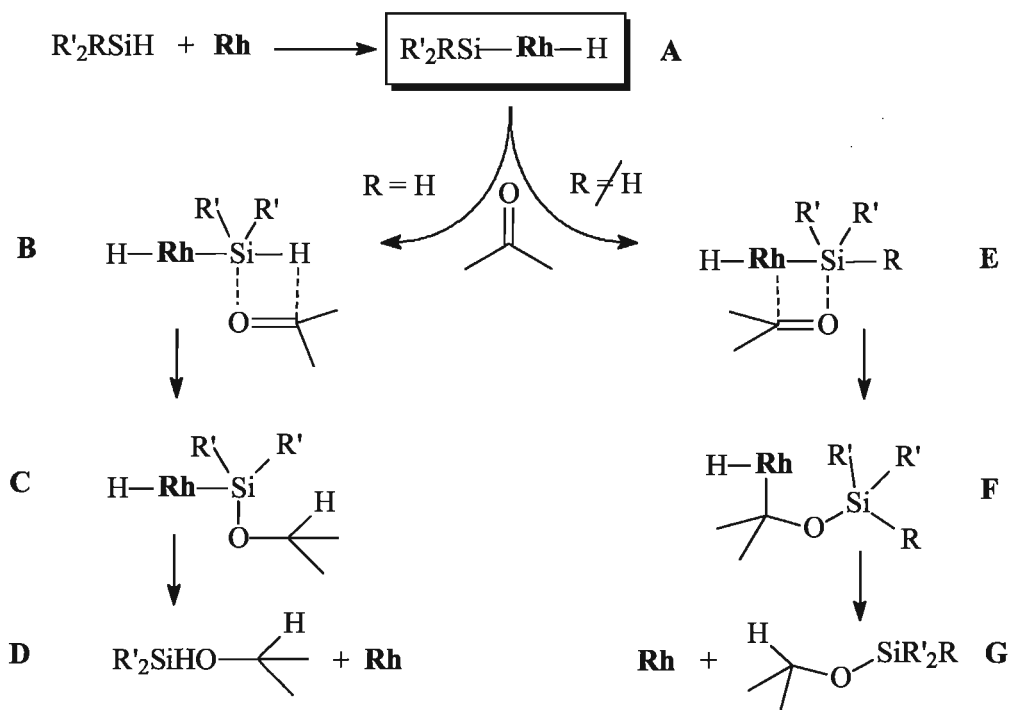
In 1995, Chan and Zheng reported highly regiocontrolled hydrosilylation of α,β -unsaturated carbonyl compounds catalyzed by $(\text{Ph}_3\text{P})_4\text{RhH}$ and proposed a new mechanism of hydrosilylation based on the observed regioselectivities and kinetic isotope effects.²⁶ It was found that depending on the silane used, it is possible to perform either regioselective 1,2- (di- and trihydrosilanes, R_xSiH_n , $n = 2$ or 3) or 1,4-hydrosilylation (monohydrosilanes, R_3SiH) (Scheme II-5).



Scheme II-5. Regiospecific hydrosilylation of α,β -unsaturated carbonyls by different silanes.

Chan performed a series of kinetic investigations of the hydrosilylation of acetophenone using a mixture of deuterated and protiosilanes.²⁶ It was found that kinetic

isotope effect $k_H/k_D = 2$ corresponds to the hydrosilylation with polyhydrosilanes, and $k_H/k_D = 1$ for monohydrosilanes. In contrast to Ojima's mechanism, Chan proposed that after the formation of a silylhydride complex **A** (Scheme II-6), the carbonyl group coordinates the silicon atom. Then, depending on the silane used, either a hydride of the Si-H group migrates to the carbon atom of the carbonyl group (**B**→**C**), or the carbonyl inserts into the Rh-Si bond via a four-membered transition state **E** to form the organorhodium complex **F**.

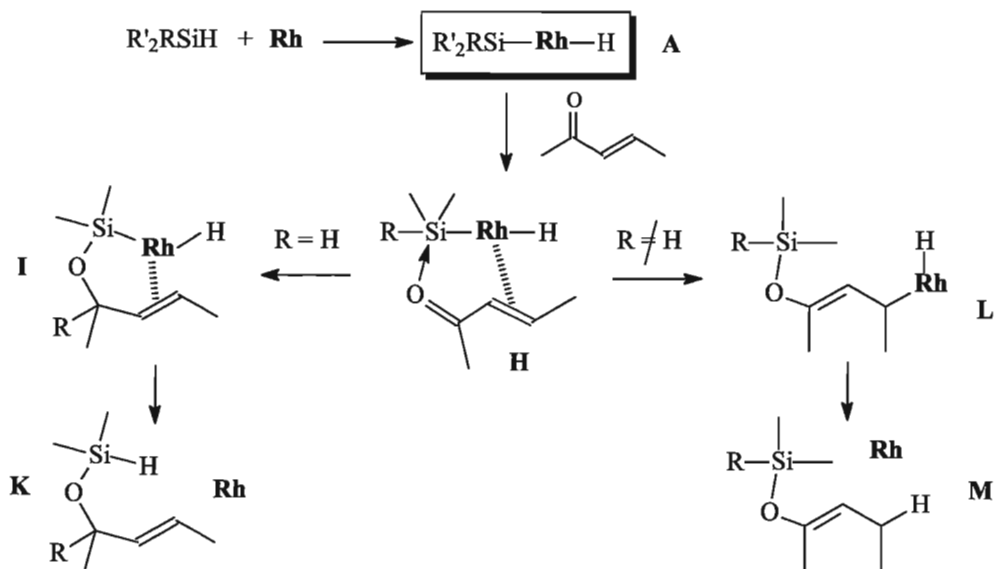


Scheme II-6. Chan's mechanism of hydrosilylation of carbonyls by mono- and polyhydrosilanes.

Given the absence of a significant isotope effect in the hydrosilylation by monohydrosilanes, Chan concluded that neither the formation of the silylhydrido complex **A** nor the reductive elimination **F**→**G** can be the rate-determining step. Observation of a primary isotope effect in the hydrosilylation by polyhydrosilanes may suggest that the hydride transfer step **B**→**C** is the rate-determining.²⁶

For the hydrosilylation of α,β -unsaturated carbonyls a mechanism was proposed by Chan (including a key step of the hydride migration from the silicon to the carbon atom

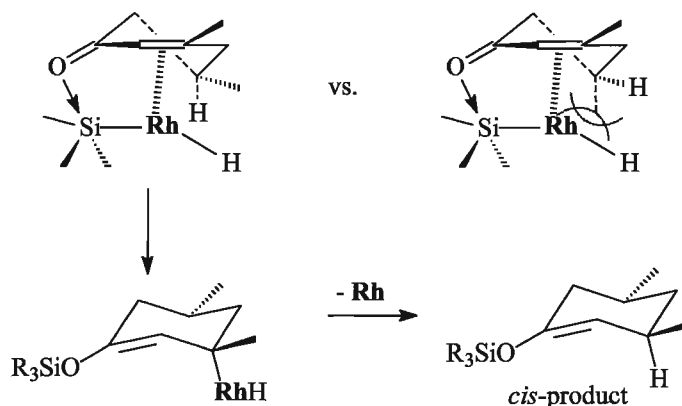
for polyhydrosilanes) (Scheme II-7). It was suggested that α,β -unsaturated carbonyl substrate and the silylhydrido complex **A** first forms the complex **H**, where the carbonyl group is σ -coordinated to the silicon atom, and the C=C double bond is π -coordinated to the metal centre (Scheme II-7).



Scheme II-7. Chan's mechanism of hydrosilylation of α,β -unsaturated carbonyls by mono- and polyhydrosilanes.

Complex **H** can undergo a reductive elimination to the enol silyl ether **L** (for monohydrosilanes), or the hydride from the Si atom can migrate to the carbonyl carbon to form **I** (for polyhydrosilanes). Each way was proposed to be exclusive for the certain type of silane.²⁶ The kinetic isotope effect for hydrosilylation of 4,4-dimethyl-2-cyclohexene-1-one by $PhMe_2SiH/PhMe_2SiD$ or by Ph_2SiH_2/Ph_2SiD_2 was found to be $k_H/k_D = 1$ in both cases. This suggested that the rate-determining step could be, most likely, the formation of the intermediate **H** (Scheme II-7) that does not involve the Si-(H/D) or the Rh-(H/D) bond cleavage. It was mentioned²⁶ that coordination of ketone to the silylhydridorhodium complex as a rate-determining step had been shown earlier by Kolb and Hetflejs in kinetic studies of hydrosilylation of *tert*-butyl phenyl ketone using a $[Rh(1,5-COD)((-)-DIOP)]ClO_4$ -catalyst.²⁷

Existence of π -coordination between the double bond and the rhodium centre could explain the observed stereoselectivity in reduction of 3,5-dimethyl-2-cyclohexene-1-one. Hydrosilylation by PhMe_2SiH gave selectively the *cis*-product (*cis/trans* = 92:8). Of two proposed transition states, one could be disfavoured due to the steric repulsions between the metal centre and the methyl group (Scheme II-8).²⁶

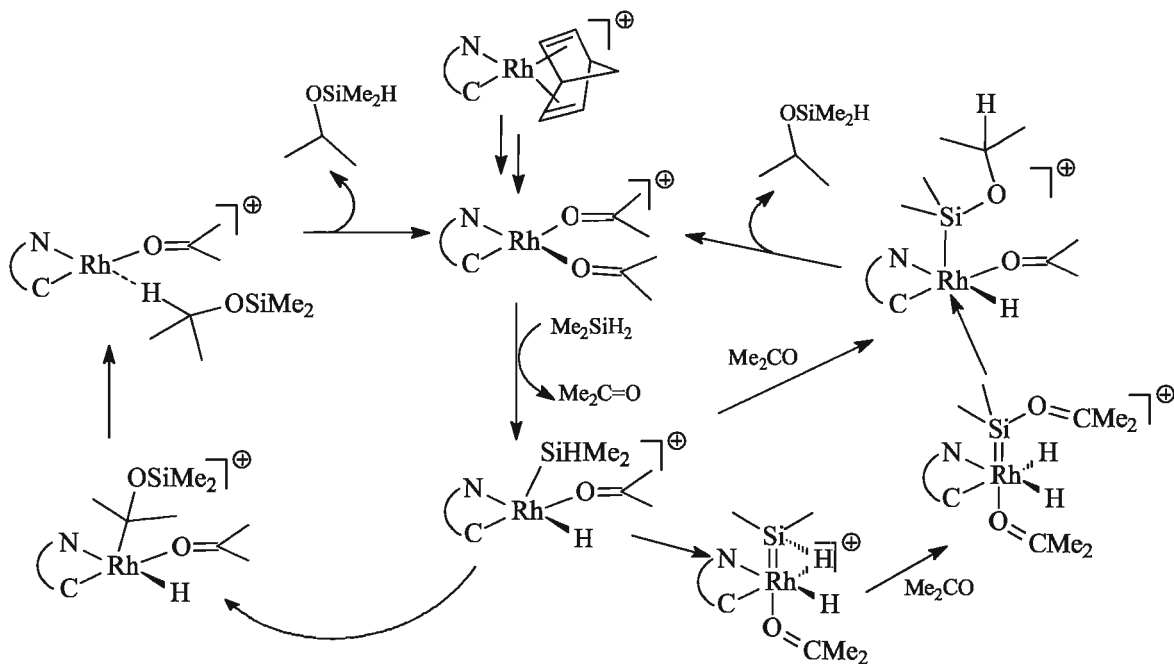


Scheme II-8. Chan's proposed transition states for hydrosilylation of 3,5-dimethyl-2-cyclohexene-1-one by PhMe_2SiH .

Maitlis *et al.* studied hydrosilylation of alkenes by triethylsilane mediated by $[(\text{Cp}^*\text{Rh})_2\text{Cl}_4]$, and observed the formation of Rh(V) complex, $[\text{Cp}^*\text{Rh}(\text{H})_2(\text{SiEt}_2)_2]$, resulting from double oxidative addition of silane to rhodium.²⁸ The complex was isolated and fully characterized (^1H , ^{13}C , ^{29}Si , ^{103}Rh NMR, X-ray, and neutron diffraction).²⁹ The isolated rhodium(V) complex was considered to be a possible part of a catalytic cycle.³⁰

Further studies performed by Goikhman and Milstein revealed the possibility of α -hydrogen elimination in the reaction between $[\text{Rh}(\text{iPr}_3\text{P})_2(\text{OTf})]$ and Ph_2SiH_2 .³¹ The reaction first provided formation of $[\text{Rh}(\text{iPr}_3\text{P})_2(\text{OTf})(\text{H})(\text{SiHPh}_2)]$, which then decomposed to $[\text{Rh}(\text{iPr}_3\text{P})_2(\text{OTf})(\text{H})_2]$ and silylene. The latter was not observed directly but was trapped by the starting Rh complex. A pathway for catalytic hydrosilylation of alkenes by $[\text{Rh}(\text{iPr}_3\text{P})_2(\text{OTf})]$ was proposed to involve formation of silylene intermediates.³¹ Formation of *iridium* silylene complexes has been previously observed by Tilley *et al.*³²

Hofmann and Gade reported enantioselective hydrosilylation of ketones catalyzed by a cationic Rh(I) complex with chiral oxazoline-N-heterocyclic carbene chelate ligand.³³ Kinetic studies of the hydrosilylation catalysis were found to be incompatible with the mechanisms reported by Ojima and Chan. They also emphasized that neither the Ojima nor Chan mechanisms could explain the significant enhancement of reaction rate when dihydrosilanes were used instead of monohydrosilanes. The Ojima and the Chan mechanisms also did not explain the *inverse* kinetic isotope effect observed in hydrosilylation catalysis. Hofmann and Gade have recently published the detailed DFT studies of the Rh-catalyzed hydrosilylation of ketones.³⁴ Three catalytic pathways have been suggested. They stated that the proposed catalytic pathway, which involves the formation of silylene intermediates, has the lowest activation barrier for the step of hydride migration from rhodium to the ketone bound to the silylene ligand, and is more accessible (Scheme II-9).³⁴ Chan's mechanism was found to have the highest barrier and was disfavoured. Therefore, it appears that Rh catalyzed hydrosilylation by primary and secondary silanes proceed by the silylene mechanism.

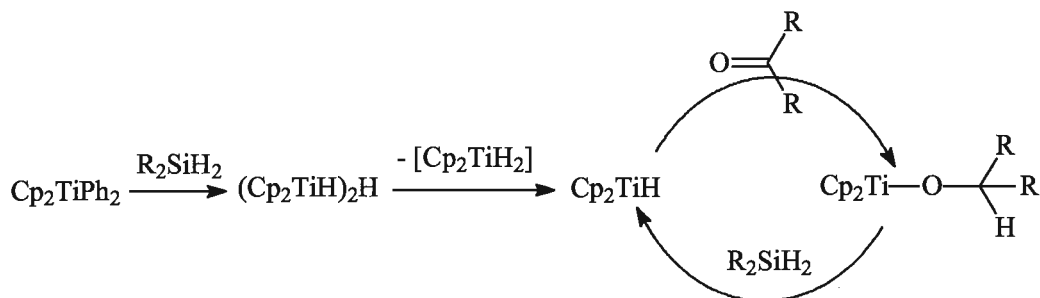


Scheme II-9. Proposed mechanistic pathways for Rh-catalyzed hydrosilylation of ketones based on DFT computational studies of Hofmann and Gade.³⁴

II. 3 Titanocene-catalyzed hydrosilylation of carbonyls

In 1980, Sato discovered that the reaction of Grignard reagents (RMgX , $\text{R} = \text{Alk, Ar}$) with carbonyls in the presence of catalytic amounts of Cp_2TiCl_2 suppresses the regular 1,2-addition of RMgX to the carbonyl group, but instead provides the carbonyl reduction to the corresponding alcohols.³⁵ Titanium(III) complex Cp_2TiH was suggested as a key participant in the catalytic cycle, which reacts with carbonyls to give titanium alkoxide complexes $\text{Cp}_2\text{Ti-OR}$. The latter reacts with RMgX to give the magnesium salt of the corresponding alcohol (product) and $\text{Cp}_2\text{Ti-R}$.

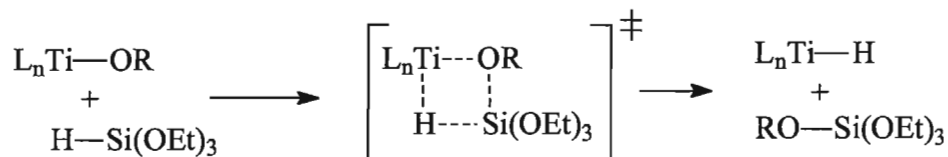
Nakano, in 1988 found that Cp_2TiPh_2 catalyzes hydrosilylation of carbonyls by PhSiH_3 , Ph_2SiH_2 and PhMeSiH_2 .³⁶ To propose the possible pathway of the hydrosilylation catalysis, he referred to Harrod's work, where Cp_2TiMe_2 and Cp_2TiBz_2 were known to react with silanes to give Ti-H species.³⁷ However, Cp_2TiPh_2 was not found to react with silanes. Nevertheless, Nakano proposed that the Ti-H species, such as $(\text{Cp}_2\text{TiH})_2\text{H}^{38}$ and Cp_2TiH , are being formed during the catalysis and react with carbonyls to give the titanium alkoxy-complex.³⁶ Reaction of the latter with silane closes the catalytic cycle, providing the product of hydrosilylation and regenerating the proposed Ti-H catalyst (Scheme II-10).



Scheme II-10. Nakano's mechanism of hydrosilylation of ketones catalyzed by Cp_2TiPh_2 .

Buchwald (1991) reported hydrosilylation of esters to the corresponding alcohols catalyzed by Cp_2TiCl_2 .^{2a} Two equivalents of $n\text{-BuLi}$ were used to generate the active catalytic species under the inert atmosphere. One year later he announced the second-generation catalytic system, $\text{Ti}(\text{OPr-}i)_4$ and $(\text{EtO})_3\text{SiH}$, which is air-stable, self-activating

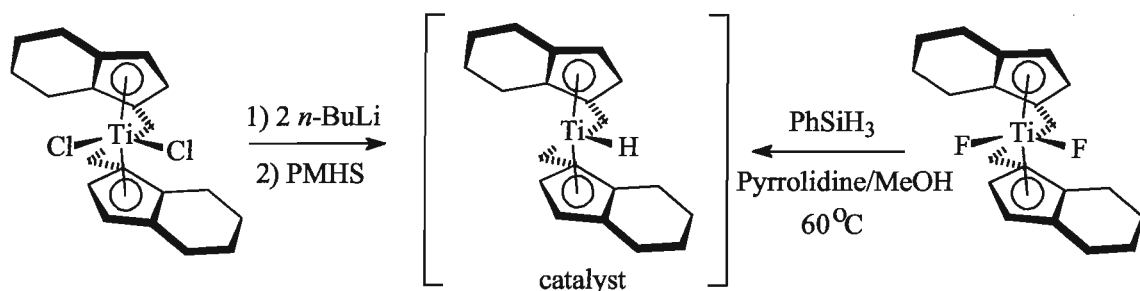
and needs no solvent.^{2b} He emphasized that production of an active catalytic species may be achieved by a simple reaction of titanium alkoxide with silanes, which proceeds via σ -bond metathesis³⁹ (Scheme II-11).



Scheme II-11. Generation of catalytically active Ti-H species from titanium(IV) alkoxide and triethoxy silane.

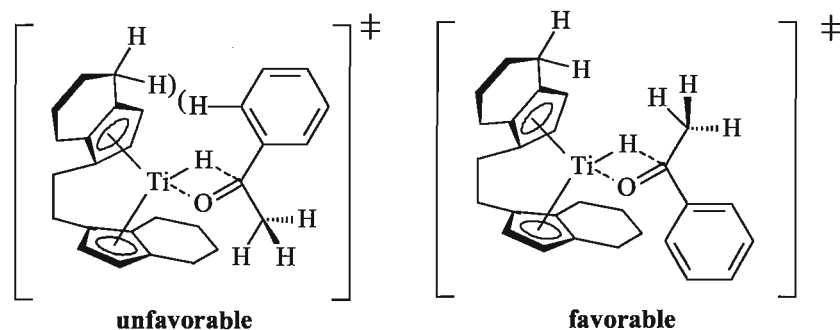
However, Buchwald was not sure what the active catalyst really was in this system. He considered the possibility of a simple Lewis acid-catalyzed hydrosilylation. But the results showed that hydrosilylation of esters were not affected by the presence of Lewis bases in the system (pyridine, THF, PMe_3). A radical mechanism was also unlikely, since heating the mixture of $\text{Ti}(\text{OPr-}i)_4$, $(\text{EtO})_3\text{SiH}$ and benzyl bromide at 45 °C for 2 hours did not result in the formation of dibenzyl; and no rearrangement product was found in ester hydrosilylation. It was finally concluded that catalysis is initiated by the formation of titanium hydride species, which directly react with esters followed by reaction with silane.^{2b}

In 1994, Buchwald reported the first efficient method of enantioselective hydrosilylation of ketones by an early transition metal catalyst with a chiral ligand.^{2d} Treatment of ethylenebis(tetrahydroindenyl)titanium dichloride⁴⁰ with 2 eq. of *n*-BuLi and 5 eq. of PMHS provides formation of an active catalyst, which was postulated to be a titanium(III) hydride complex. It could also be prepared from the TiF_2 -derivative and phenylsilane (Scheme II-12).^{2g}



Scheme II-12. Preparation of the chiral Ti(III) hydride complex.

Hydrosilylation was typically carried out in benzene in the presence of 4.5 mol% of catalyst at RT during 0.8-4.5 days.^{2d} PMHS was used as the hydrosilylating agent. The highest *ee* (>95%) were achieved for aromatic ketones and non-aromatic ketones with conjugated carbonyl groups. Saturated ketones, in contrast, resulted in products with very low *ee* (~12-24%). To explain this phenomenon, Buchwald suggested a transition state to explain how the ketone approaches the catalyst. Of two possible transition states, only one significantly minimizes interactions between the benzene ring and the tetrahydroindenyl ligand and thus should be favourable (Scheme II-13).

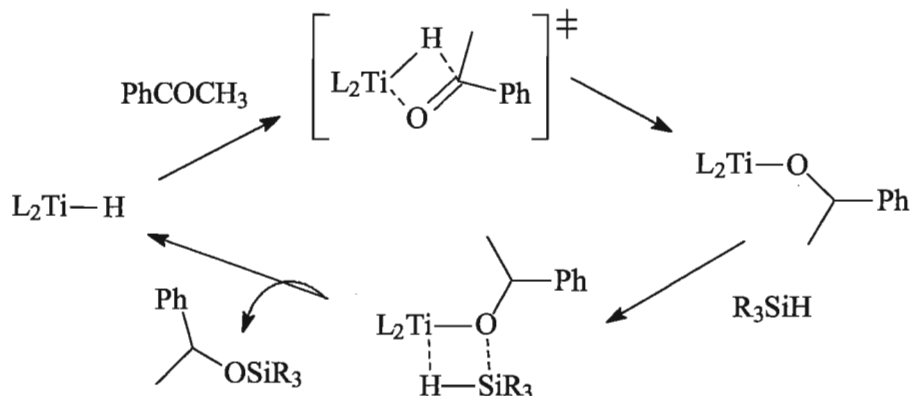


Scheme II-13. Unfavourable and favourable transition states when acetophenone approaches the titanium complex.

Approach of the carbonyl compound to the titanium centre, which results in the formation of an alkoxide, is the enantioselectivity-determining step.^{2g} Enantioselectivity of products was explained by how selectively the reaction proceeds through only one transition state. For the rigid structures, such as aromatic or conjugated ketones, the C—C=O bond rotation requires additional energy and is less likely, thus, two transition states will have different energies, and the one with the smallest energy will be favourable and

will determine the enantioselectivity of the reaction. In contrast, saturated carbonyls are very flexible, and this minimizes the energy between possible transition states, which results in poor enantioselectivities.

The catalytic cycle has been proposed to go through the formation of the corresponding alkoxide followed by reaction with silane via the σ -bond metathesis mechanism of the Ti-O and Si-H bonds (Scheme II-14).^{2g}



Scheme II-14. Proposed catalytic cycle of hydrosilylation of carbonyls by Ti-H catalyst.

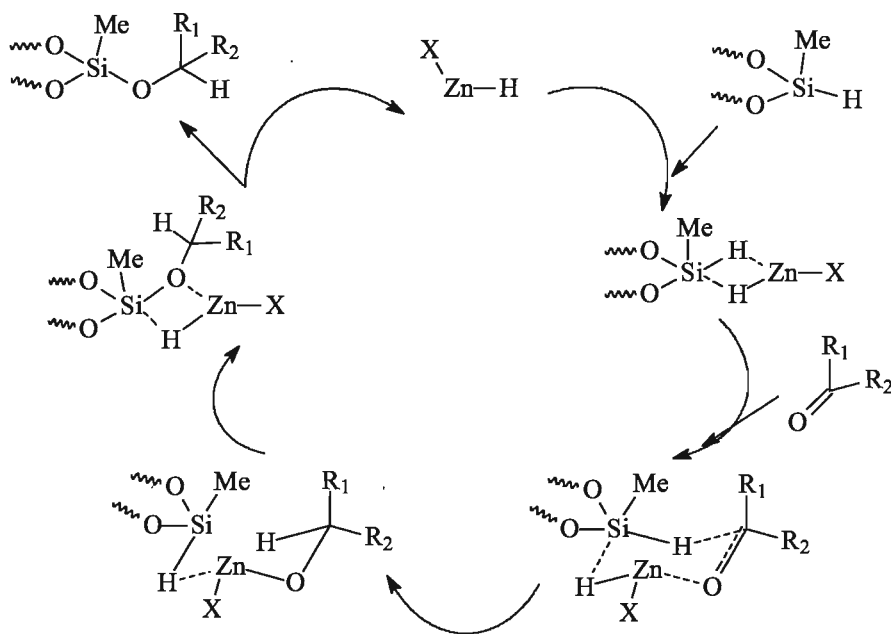
II. 4. Hydrosilylation of carbonyls catalyzed by zinc complexes

Mimoun developed a very efficient, environmentally benign, safe and industrially important method of hydrosilylation of aldehydes and ketones by PMHS catalyzed by various zinc catalysts.⁴¹ Zinc compounds such as $ZnCl_2$, $Zn(RCOO)_2$, $ZnEt_2$, $Zn(BH_4)_2$ and ZnH_2 were previously reported to be inactive to catalyze hydrosilylation.⁴¹ The active catalyst species, however, were generated by addition of stoichiometric amounts of $NaBH_4$ or $LiAlH_4$ to $Zn(2\text{-ethylhexanoate})_2$ as well as by addition of ethylenediamine or TMEDA to $ZnEt_2$. Complexes of other metals such as $Co(2\text{-ethylhexanoate})_2$, $Cd(propionate)_2$, $Mn(stearate)_2$, $Fe(2\text{-ethylhexanoate})_2$, $Zr(OPr-i)_4$, $Cu(2\text{-ethylhexanoate})_2$, $Sn(2\text{-ethylhexanoate})_2$ have also been tested, but they were found to be less efficient compared to the zinc catalysts.

Mimoun emphasized the key role of transition metal complexes *to coordinate carbonyl compounds* in hydrosilylation reactions. Thus, Müller *et al.* obtained the benzaldehyde-coordinated zinc complex $[ZnCl_2(PhCHO)]_2$ and characterized it by X-

ray.⁴² $\text{Ti}(\text{OPh})_4$ can form a 1:1 complex with acetone.⁴³ Titanium alkoxides were mentioned to catalyze transesterification of esters.⁴⁴ Specifically, the ability of zinc to coordinate carbonyls would explain the reactivity of $\text{Zn}(\text{BH}_4)_2$ to reduce esters, while NaBH_4 was not active in the same reactions.⁴⁵

Zinc hydride complexes have been proposed to be the key catalytic species in hydrosilylation reactions, and they were assumed to be generated *in situ* by reactions of zinc carboxylates with NaBH_4 .⁴¹ The active catalytic species have not been characterized. Several model zinc hydrido complexes such as $[\text{HZnOC}_2\text{H}_4\text{NMe}_2]_2$,⁴⁶ $[\text{PhZnH}\cdot\text{Py}]$,⁴⁷ $[\text{HZnN}(\text{Me})\text{C}_2\text{H}_4\text{NMe}_2]_2$ ⁴⁸ and $(\text{PhZnH})_2\cdot\text{TMEDA}$ ⁴⁷ have been separately prepared and tested to catalyze hydrosilylation reaction. Neither of these complexes was as effective as the species generated *in situ* by the reaction between $\text{Zn}(\text{2-ethylhexanoate})_2$ and NaBH_4 .⁴¹ This was attributed to the oligomeric nature of the former reagents that prevents association with the Si-H bonds.⁴¹ A mechanism of hydrosilylation of carbonyls mediated by zinc hydride complexes has been proposed (Scheme II-15).⁴¹



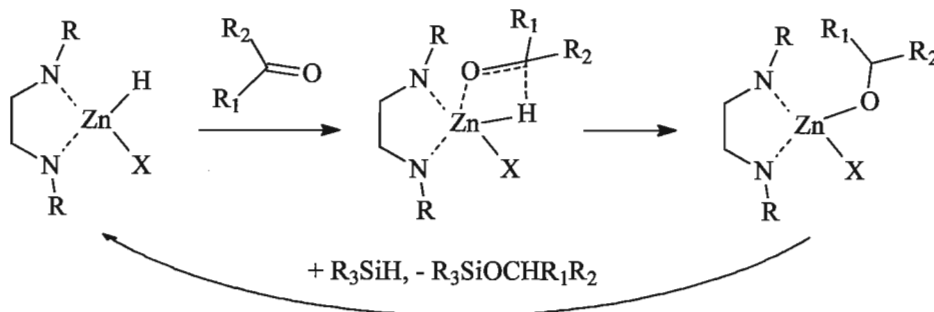
Scheme II-15. Mimoun's mechanism of hydrosilylation of ketones catalyzed by zinc hydride species.

Provided that alkali metal hydrides may form adducts with silanes⁴⁹, Mimoun suggested formation of a four-membered silane-zinc adduct in the proposed catalytic

cycle (Scheme II-15). In his opinion, the Si-H bond of the silane is activated in the resulting pentavalent dihydrosilicate intermediate. This intermediate has been compared to LiAlH_4 .⁴¹ When LiAlH_4 is used for reduction of carbonyls, Li^+ activates the carbonyl group as a Lewis acid whereas Al-H acts as a hydride donor.⁵⁰ In reductions by $\text{Zn}(\text{BH}_4)_2$, zinc activates the carbonyl group, and B-H is used to donate the hydride⁴⁵. Similarly, the zinc atom may activate the C=O group, and the pentavalent dihydrosilicate transfers one of its two hydrides to the carbon atom of C=O group. The Si-H hydride may be transferred to the carbonyl group in a *concerted* way via the six-membered transition state (as for LiAlH_4 ⁵⁰). The resulting zinc alkoxide would react with the Si-H species through heterolytic splitting of the Zn-O and Si-H bonds to regenerate the zinc hydride and polysiloxane (product), in the same way as proposed by Buchwald in titanium chemistry^{2g}.

A while later, enantioselective reduction of ketones by PMHS catalyzed by chiral zinc catalysts was published by Mimoun in collaboration with Floriani.⁵¹ Two more mechanisms of hydrosilylation (in addition to the one discussed above⁴¹, Scheme II-15) were suggested to interpret the enantioselective reduction of ketones.

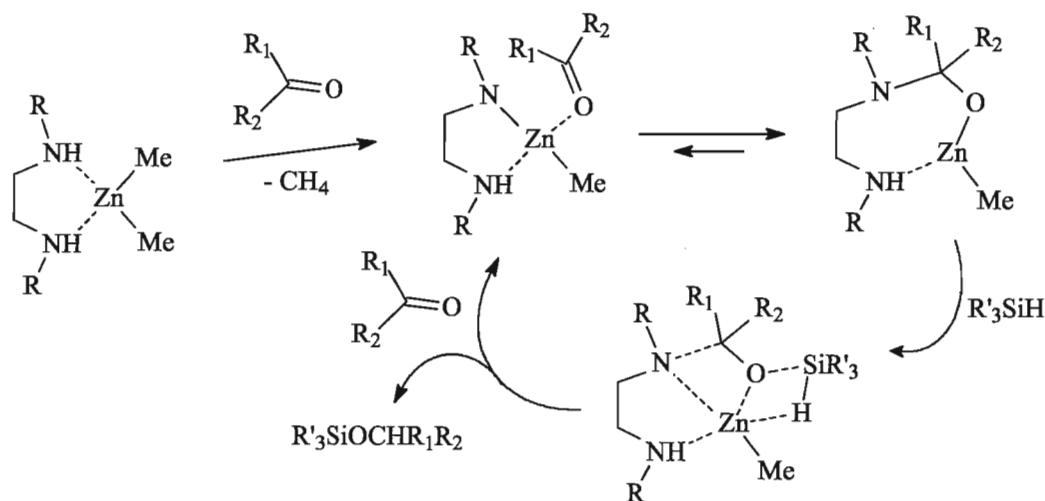
The first mechanism relates to the zinc hydride species and describes the carbonyl insertion across the Zn-H bond to form an alkoxy complex. The latter may react with the silane via the heterolytic splitting of Zn-O and Si-H bonds to give the initial zinc hydrido complex and the hydrosilylation product (Scheme II-16).



Scheme II-16. Mimoun's alternative mechanism of hydrosilylation catalyzed by zinc hydride species.

It has been demonstrated that complex $[\text{Zn}(\text{H})(\text{OCH}_2\text{CH}_2\text{NMe}_2)]_2$ reacts with benzaldehyde giving a zinc alkoxy complex with the proposed structure of $[\text{Zn}(\text{OCH}_2\text{PhH})(-\text{OCH}_2\text{CH}_2\text{NMe}_2)]_2$.⁵¹ When the alkoxy complex was treated with $(\text{EtO})_3\text{SiH}$, the obtained ^1H NMR spectrum reflected the formation of the initial zinc hydride complex.⁵¹ This experiment suggested the potentially possible sequence of steps for catalytic hydrosilylation of carbonyls by zinc hydrides (Scheme II-16).

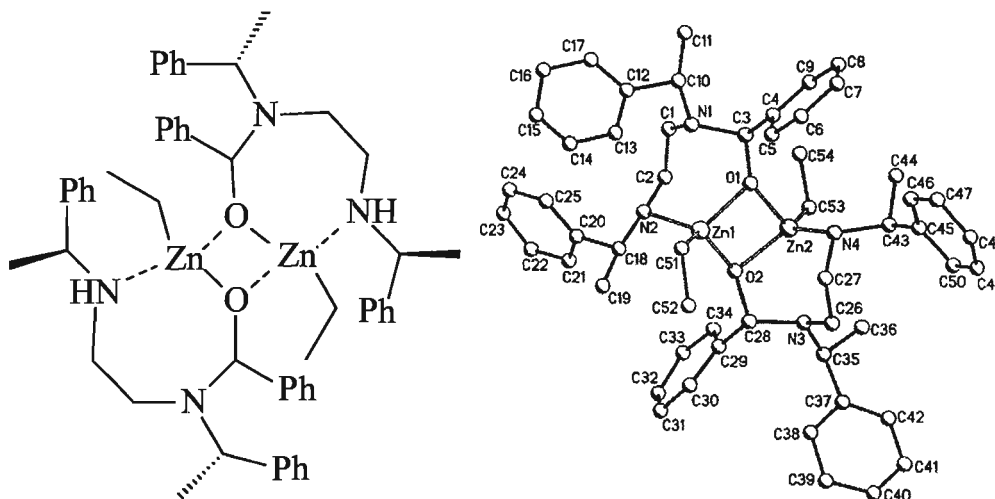
The second mechanism corresponds to catalytic hydrosilylation of carbonyls by dialkylzinc compounds (Scheme II-17). The diamine ligands were presumed to directly participate in the carbonyl activation.



Scheme II-17. Proposed mechanism of hydrosilylation of carbonyls catalyzed by dialkylzinc complexes

The mechanism displayed in Scheme II-17 is based on the result provided by the reaction between $\text{ZnEt}_2^*(S,S)\text{-ebpe}$ and benzaldehyde (or acetophenone). The product of the reaction was isolated and its structure was elucidated by X-ray analysis (Scheme II-18).

Transition states for all three proposed mechanisms (Scheme II-15, Scheme II-16, Scheme II-17) have been evaluated by semiempirical PM3 calculations.⁵¹

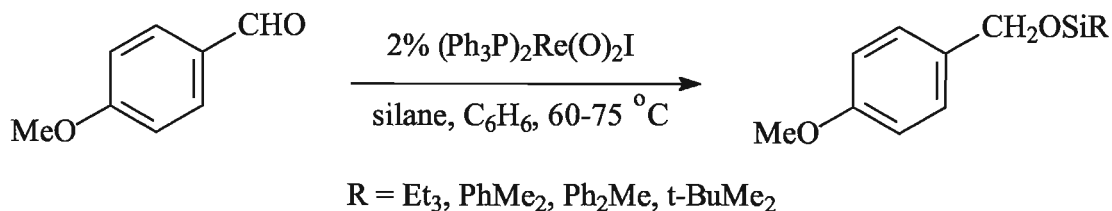


Scheme II-18. Product of reaction between benzaldehyde and $\text{ZnEt}_2^*(S,S)\text{-ebpe}$, and its X-ray structure⁵¹.

II. 5. Oxo-rhenium complexes: mechanistic studies of catalytic hydrosilylation of carbonyls

II.5.1. Neutral dioxo-rhenium(V) complexes

High-valent rhenium oxo complexes have found many applications in catalytic oxidation and oxygen transfer reactions.⁵² Applications of electron-deficient metal complexes in catalytic reductions, such as hydrogenation, hydrosilylation and hydroformylation, are very unusual and extremely rare.⁵³ Recently, Toste *et al.* found that rhenium(V) dioxo complexes may serve as catalysts for the hydrosilylation of carbonyls⁵⁴ and imines⁵⁵. In particular, iododioxo(bistriphenylphosphine)rhenium(V) was found to be an unexpectedly active catalyst for hydrosilylation of a wide range of ketones (aromatic and aliphatic) and aldehydes (aliphatic, aromatic, heteroaromatic) (Scheme II-19).⁵⁴

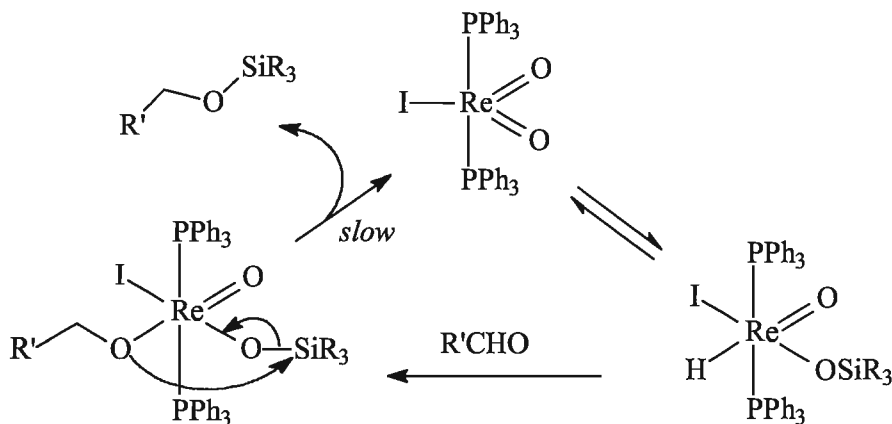


Scheme II-19. Hydrosilylation catalyzed by $(\text{Ph}_3\text{P})_2\text{Re}(\text{O})_2\text{I}$

Rhenium(V) dioxo complexes were of particular interest in the study of reactions undergoing the [2+2]-type addition between Re=O and Si-H bonds. Toste believes that the reactivity of the Re=O bond would be enhanced by the presence of the second oxo ligand.⁵⁴ The latter, a *spectator* group, could play a central role in stabilizing the critical intermediate.⁵⁶

The proposed mechanism involves a [2+2]-addition of silane to the Re=O bond to produce a metal hydride (Scheme II-20). This is followed by the reaction of the metal hydride with aldehyde and the subsequent formation of an alkoxy complex. Transfer of the silyl group to the alkoxy ligand produces the silyl ether and regenerates the initial dioxorhenium complex.

The reaction of $(\text{Ph}_3\text{P})_2\text{Re}(\text{O})_2\text{I}$ with excess of Et_3SiH was studied separately. It resulted in the production of the hydrido silyloxy complex $(\text{Ph}_3\text{P})_2(\text{I})\text{Re}(\text{H})(\text{OSiEt}_3)(\text{O})$. The structure of this Re-H complex was supported by NMR data. Addition of *p*-nitrobenzaldehyde to $(\text{Ph}_3\text{P})_2(\text{I})\text{Re}(\text{H})(\text{OSiEt}_3)(\text{O})$ afforded the silyl ether.



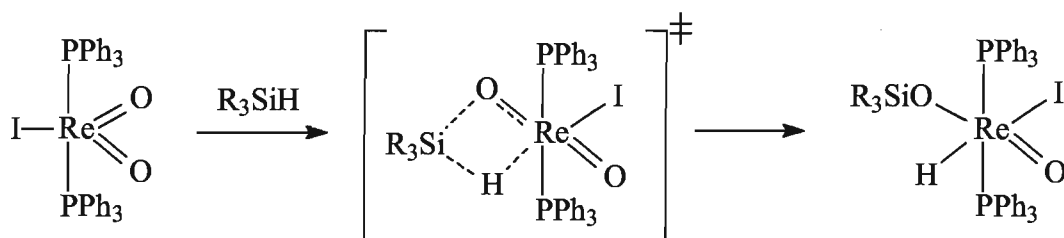
Scheme II-20. Proposed mechanism of hydrosilylation of carbonyls by $(\text{Ph}_3\text{P})_2\text{Re}(\text{O})_2\text{I}$.

A possibility of [3+2]-type addition⁵⁷ of silane to $\text{O}=\text{Re}=\text{O}$ was also considered.⁵³⁻⁵⁴

Toste's first report⁵⁴ intrigued many chemists, and a number of publications appeared describing other hydrosilylation reactions catalyzed by metal-oxo complexes involving various types of electron-deficient $\text{Re}=\text{O}$ and $\text{Mo}=\text{O}$ complexes.^{4a, b, 58}

Four years later, Toste *et al.* published a more extensive investigation of the hydrosilylation mechanism catalyzed by $(\text{Ph}_3\text{P})_2\text{Re}(\text{O})_2(\text{I})$.^{10a} Treatment of

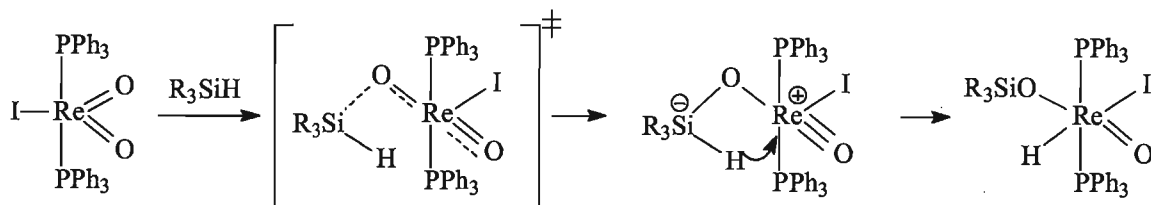
$(\text{Ph}_3\text{P})_2\text{Re}(\text{O})_2(\text{I})$ with excess of PhMe_2SiH afforded the silyloxy hydride complex $(\text{Ph}_3\text{P})_2(\text{I})\text{Re}(\text{H})(\text{OSiMe}_2\text{Ph})(\text{O})$, which was isolated and characterized. They also reported that this complex was present in the reaction mixture during the catalysis. The latter observation supported the idea that complex $(\text{Ph}_3\text{P})_2(\text{I})\text{Re}(\text{H})(\text{OSiMe}_2\text{Ph})(\text{O})$ could be an intermediate in the catalytic cycle. Kinetic investigations of the formation of complex $(\text{Ph}_3\text{P})_2(\text{I})\text{Re}(\text{H})(\text{OSiMe}_2\text{Ph})(\text{O})$ revealed the first-order dependence on concentration of silane. Computational studies for this reaction published by Lin and Wu suggested that the concerted [2+2]-addition mechanism for this reaction is most favourable among other different possible mechanisms (Scheme II-21).⁵⁹



Scheme II-21. Concerted [2+2] addition mechanism of $(\text{Ph}_3\text{P})_2(\text{I})\text{Re}(\text{H})(\text{OSiR}_3)(\text{O})$ formation supported by DFT calculations.

DFT studies proposed that this mechanism must include a phosphine dissociative step. However, kinetic studies demonstrated no dependence of the reaction rate on the concentration of phosphine, indicating that the mechanism should be associative.

Toste suggested another stepwise mechanism for the activation of silane by the Lewis basic oxo ligands followed by the hydride transfer to the metal centre (Scheme II-22)^{10a}. However, this alternative pathway was not examined in the DFT calculations by Lin and Wu⁵⁹.



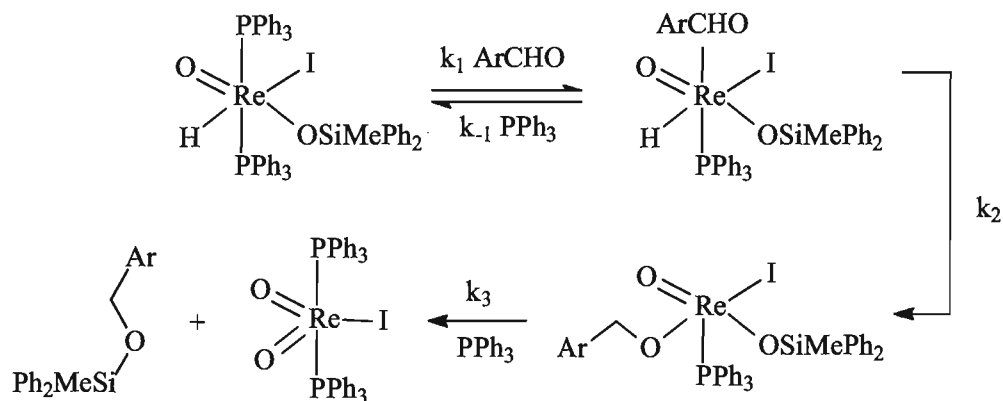
Scheme II-22. An alternative mechanism of Lewis base activation of silane by oxo ligand.

The kinetic isotope effect (KIE) for the formation of $(\text{Ph}_3\text{P})_2(\text{I})\text{Re}(\text{H})(\text{OSiMe}_2\text{Ph})(\text{O})$ was found to be 0.78. An inverse KIE could arise if the rate-determining step is the reversible formation of a zwitter-ion intermediate, which does not include the participation of Si-H (or Si-D) bond. The hydride transfer is suggested to be a fast (not rate-determining) step (Scheme II-22).

Reaction between $\text{Re}=\text{O}$ and Si-H was found to be irreversible. Ph_2MeSiH was never observed to exchange with $(\text{Ph}_3\text{P})_2(\text{I})\text{Re}(\text{H})(\text{OSiMe}_2\text{Ph})(\text{O})$. However, experiments with Ph_2MeSiD demonstrated the H/D exchange between silane protons and Re-H. In addition, H/D exchange was revealed in a mixture of $(\text{Ph}_3\text{P})_2\text{Re}(\text{D})(\text{OSiMe}_2\text{Ph})(\text{O})(\text{I})$ and $(\text{Ph}_3\text{P})_2(\text{I})\text{Re}(\text{H})(\text{OSiMe}_2\text{Ph})(\text{O})$ in the absence of other reagents.

Toste emphasized that the second oxo ligand provides the thermodynamic driving force for the addition of silane across the primary oxo ligand.^{10a} It is known that oxo ligands may stabilize the metal centre due to its π -donation.^{56, 60} This is essential for the intermediates: while the one oxo ligand reacts with silane and loses the ability to stabilize the cationic metal centre, the π -stabilization is supported by the other oxo ligand.

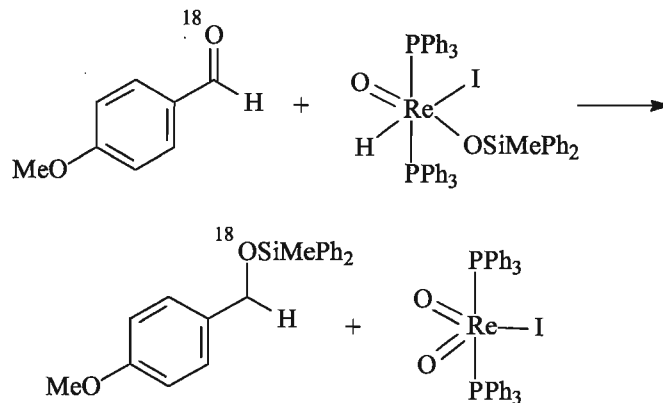
To understand the mechanism of reaction of $(\text{Ph}_3\text{P})_2\text{Re}(\text{H})(\text{OSiMe}_2\text{Ph})(\text{O})(\text{I})$ with *p*-anisaldehyde, Toste *et al.* carried out a number of kinetic experiments. They found the first-order dependence of the reaction rate on the concentration of both substrates, and also found that the reaction is inhibited by the presence of free triphenylphosphine in the reaction mixture. In addition, some amount of free phosphine was formed during the reaction indicating a dissociative mechanism. In conclusion, they proposed that the reaction begins with phosphine dissociation followed by reaction with the aldehyde (Scheme II-23).



Scheme II-23. Proposed mechanism of reaction between $(\text{Ph}_3\text{P})_2\text{Re}(\text{H})(\text{OSiMePh}_2)(\text{O})(\text{I})$ and *p*-anisaldehyde.

Nevertheless, the specific intermediates illustrated in Scheme II-23 *were not observed*.

The experiments with the ^{18}O -labeled *p*-anisaldehyde showed that ^{18}O atom is not incorporated into the Re-complex (Scheme II-24).



Scheme II-24. Reaction of ^{18}O -labeled *p*-anisaldehyde with siloxyrhenium complex.

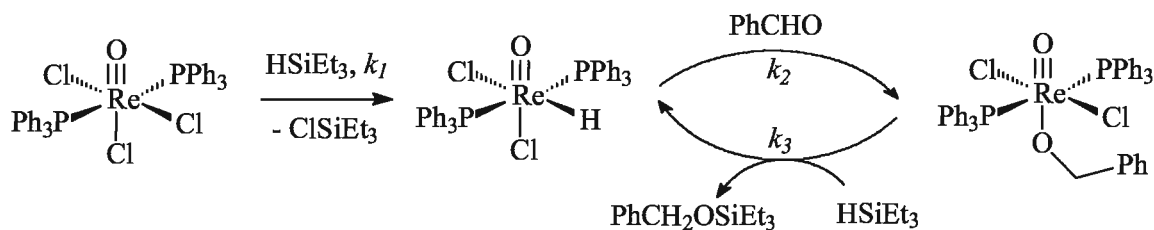
Kinetic studies of catalytic reactions provided some information about the catalyst resting states. NMR data for the hydrosilylation of *p*-anisaldehyde by PhMe_2SiH showed the presence of $(\text{Ph}_3\text{P})_2(\text{I})\text{Re}(\text{H})(\text{OSiMe}_2\text{Ph})(\text{O})$ as a major component in the catalytic reaction mixture and trace amounts of $(\text{Ph}_3\text{P})_2\text{Re}(\text{O})_2(\text{I})$. This led to the conclusion that the hydrido siloxyrhenium complex is a catalyst resting state. Other experiments with

Ph_2MeSiH revealed, in contrast, a steady concentration of $(\text{Ph}_3\text{P})_2\text{Re}(\text{O})_2(\text{I})$, and this (starting) complex was concluded to be the catalyst resting state.

II.5.2. Neutral monooxo-rhenium(V) complexes

Proposed mechanisms of hydrosilylation are often very speculative and are not reliable. Since the discovery of catalytic hydrosilylation by $\text{Re}(\text{V})$ dioxo complexes⁵⁴, many questions remained unanswered concerning the mechanism of hydrosilylation. In particular, the role of the second oxo ligand in stabilization of an intermediate has not been elucidated, and its stabilization effect has only been hypothesized. Royo *et al.* found that complex $(\text{Ph}_3\text{P})_2\text{Re}(\text{O})\text{Cl}_3$, which has only one oxo ligand, is still rather reactive.^{4a}

Abu-Omar *et al.* carried out studies on the hydrosilylation mechanism of monooxo-rhenium complexes specifically taking into consideration complexes of $\text{ReXCl}_3(\text{PR}_3)_2$ ($\text{X} = \text{O}$, NAr , and $\text{R} = \text{Ph}$, Cy)^{10b}. Under catalytic conditions of hydrosilylation of benzaldehyde by $\text{ReOCl}_3(\text{PPh}_3)_2$, two major intermediates have been observed in ^{31}P NMR spectra, $\text{ReOCl}_2(\text{H})(\text{PPh}_3)_2$ and $\text{ReOCl}_2(\text{OCH}_2\text{Ph})(\text{PPh}_3)_2$. Complexes $\text{ReOCl}_3(\text{PPh}_3)_2$, $\text{ReOCl}_3(\text{PCy}_3)_2$ and $\text{Re}(\text{NMes})\text{Cl}_3(\text{PPh}_3)_2$, when individually treated with excess of silane (Et_3SiH), gave monohydride dichloride derivatives in excellent yields. Kinetic investigations of individual steps were carried out using $\text{ReOCl}_2(\text{H})(\text{PPh}_3)_2$ as a model catalyst. When $\text{ReOCl}_2(\text{H})(\text{PPh}_3)_2$ is treated with benzaldehyde, it forms the alkoxide complex, $\text{ReOCl}_2(\text{OCH}_2\text{Ph})(\text{PPh}_3)_2$. The reaction rate was first order in PhCHO . It was found that the insertion of benzaldehyde was inhibited by the presence of free triphenylphosphine. Consequently, the reaction of Re-H with benzaldehyde required dissociation of one of the phosphine ligands, and the excessive amounts of PPh_3 only inhibited dissociation. The kinetic isotope effect was found to be negligible: $k[\text{ReOCl}_2(\text{H})(\text{PPh}_3)_2]/k[\text{ReOCl}_2(\text{D})(\text{PPh}_3)_2] = 1.1$. The resulting alkoxy-complex $\text{ReOCl}_2(\text{OCH}_2\text{Ph})(\text{PPh}_3)_2$ was then reacted with Et_3SiH to give the initial $\text{ReOCl}_2(\text{H})(\text{PPh}_3)_2$ and $\text{Et}_3\text{SiOCH}_2\text{Ph}$. Abu-Omar emphasized that the kinetic studies of individual steps were consistent with the catalytic cycle shown in Scheme II-25.



Scheme II-25. Proposed mechanism of hydrosilylation of carbonyls by $\text{ReOCl}_3(\text{PPh}_3)_2$

Abu-Omar *et al.* have determined the rate constants for each individual step in the proposed catalytic cycle (Scheme II-25), and tried to simulate the overall rate of catalysis. The estimated rate was found to be much lower than the one experimentally observed. Therefore, the mechanism of hydrosilylation could be different and could involve other catalytic species.

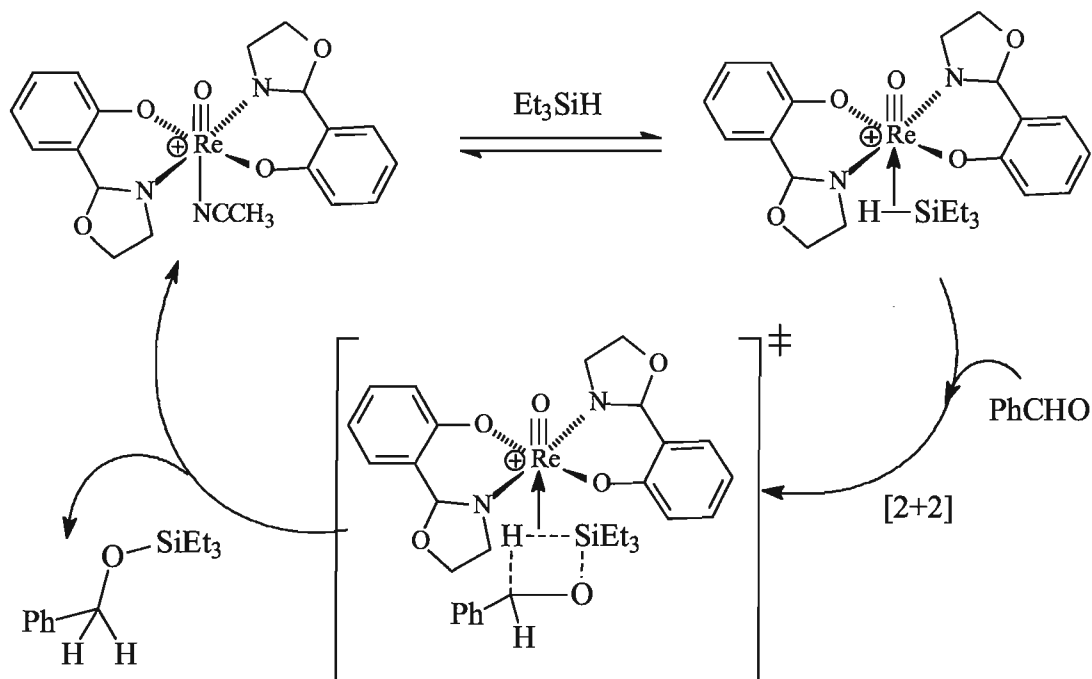
The imido derivative $\text{Re}(=\text{NMes})\text{Cl}_3(\text{PPh}_3)_2$ was found to be much more reactive than $\text{ReOCl}_3(\text{PPh}_3)_2$. The rhenium imido hydride complex was not observed in the catalytic mixture until the end of the catalysis. It also did not react with benzaldehyde to form a benzyloxy complex. Thus, in Abu-Omar's opinion it could not be an active form of the catalyst^{10b}.

As a result, the mechanism of hydrosilylation of carbonyls catalyzed by $\text{ReXC}_3(\text{PR}_3)_2$ ($\text{X} = \text{O}, \text{NAr}$, and $\text{R} = \text{Ph}, \text{Cy}$) remained unresolved. There were several alternative ways of catalysis discussed, but neither one was supported by the experimental data^{10b}.

II.5.3. Cationic monooxo-rhenium(V) complexes: hydrosilylation of carbonyls

Abu-Omar *et al.* carried out the study of hydrosilylation mediated by cationic monooxorhenium(V) complexes, in particular by $[\text{Re}(\text{O})(\text{hoz})_2][\text{B}(\text{C}_6\text{F}_5)_4]^{61}$. This catalyst was found to be very active (with a catalyst load of just 0.1%) catalyzing hydrosilylation of ketones and aldehydes at ambient temperature. Hydrosilylation catalysis was performed even without the use of solvent, wherein the catalyst precipitated at the end of reaction^{61b}.

Abu-Omar *et al.* proposed a new alternative mechanism of hydrosilylation of carbonyls catalyzed by $[\text{Re}(\text{O})(\text{hoz})_2][\text{B}(\text{C}_6\text{F}_5)_4]^{61\text{b}}$. They suggested that the mechanism involves the Si-H bond activation by the cationic Re centre via formation of a η^2 -adduct, followed by a [2+2]-type reaction with the carbonyl (Scheme II-26).

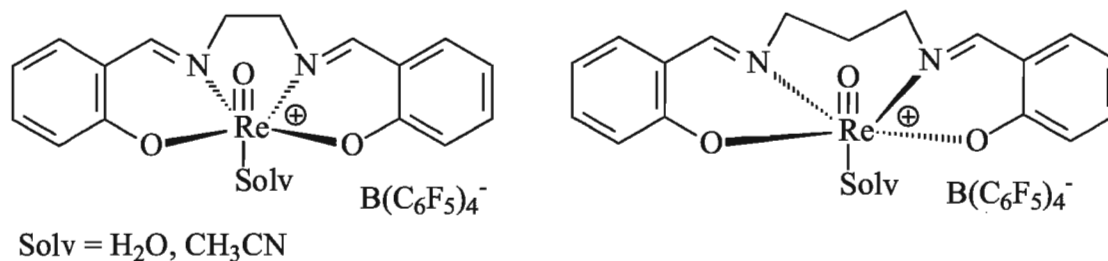


Scheme II-26. An alternative mechanism of carbonyl hydrosilylation by oxo-rhenium complexes proposed by Abu-Omar.

Formation of the η^2 -adduct was postulated to be the rate-determining step. Abu-Omar also referred to the kinetic isotope effect results found for the hydrosilylation of benzaldehyde by triethylsilane: $k(\text{Et}_3\text{SiH})/k(\text{Et}_3\text{SiD}) = 1.3$ and $k(\text{PhCHO})/k(\text{PhCDO}) = 1.0$. In his opinion, it correlates with the proposed mechanism (Scheme II-26).

Concerning the role of the second oxo-ligand, these authors did not provide any conclusions^{61b}. They only mentioned that the cationic complex $[\text{Re}(\text{O})(\text{hoz})_2][\text{B}(\text{C}_6\text{F}_5)_4]$ was an order of magnitude more reactive than Toste's complex $(\text{Ph}_3\text{P})_2\text{Re}(\text{O})_2(\text{I})$. There was no evidence that the high reactivity was caused by the cationic nature of the metal centre in $[\text{Re}(\text{O})(\text{hoz})_2][\text{B}(\text{C}_6\text{F}_5)_4]$ or by any other electronic factor.

Abu-Omar *et al.* continued investigations of hydrosilylation of carbonyls catalysis by cationic monooxo-rhenium complexes, and one year later, in 2006, they published synthesis and catalytic studies of the Re(V) *salen* complexes (Scheme II-27)^{58a, 62}.



Scheme II-27. Cationic monooxo-rhenium(V) *salen* complexes.

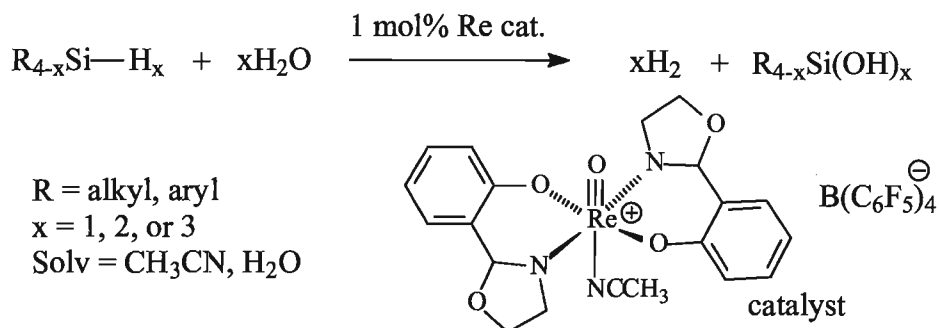
Preliminary studies showed that an equilibrium exists between the butanone and the Re(V) complex: the ketone could reversely substitute the solvent (acetonitrile) with the formation of a new ketone-coordinated species, which was observed by ¹H NMR. In addition, a peak, *presumably* corresponding to the Re-silane adduct, has been detected by ESI-MS. (The use of the Electrospray Ionization Tandem Mass-Spectroscopy for catalyst screenings was first introduced by Chen in 2003⁶³) However, the presumed silane adduct has never been observed by NMR spectroscopy, even at low temperatures (-80 °C).

Kinetic investigations of the hydrosilylation of benzaldehyde by PhMe₂SiH revealed the first-order dependence of the reaction rate on the concentration of the catalyst and the inhibition by PhCHO⁶². On the basis of these results, it was concluded that the mechanism based on the initiation of catalysis by carbonyl insertion is less possible. Therefore, the most probable mechanism would first involve the formation of a σ-complex between Re and Si-H bond followed by nucleophilic attack of carbonyl at silicon as indicated in the Scheme II-26. Abu-Omar *et al.* emphasized that the key prerequisite for the formation of silane adduct would be the back-donation from rhenium(V) d_{xy} orbital to the σ* orbital of Si-H⁶².

Activation of catalysis via a Re-(Si-H) σ-complex was also postulated for other similar cationic Re(V) catalysts⁶⁴.

II.5.4. Cationic monooxorhenium(V) complexes: hydrolytic oxidation of silanes

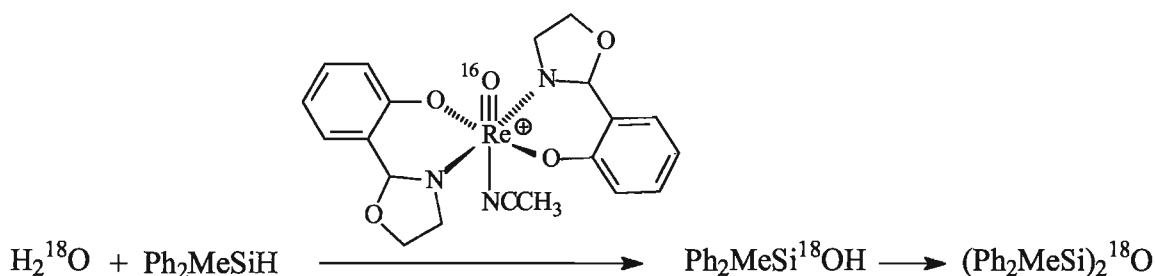
The cationic monooxorhenium(V) complex $[\text{Re}(\text{O})(\text{hoz})_2][\text{B}(\text{C}_6\text{F}_5)_4]$ was found to catalyze hydrolytic oxidation of silanes producing molecular hydrogen^{61a}. This process was taken into consideration as a potential way of production of molecular hydrogen directly from water and silanes (Scheme II-28).



Scheme II-28. Hydrolytic oxidation of silanes catalyzed by $[\text{Re}(\text{O})(\text{hoz})_2][\text{B}(\text{C}_6\text{F}_5)_4]$.

Isotope-labeling experiments with D_2O and Et_3SiH (and also with H_2O and Et_3SiD) demonstrated the highly selective (~94-98%) production of H-D, indicating that one proton originates from water and another one from the silane.

Abu-Omar *et al.* also performed the ^{18}O labeling experiments with H_2^{18}O to better understand the mechanism of this reaction (Scheme II-29).



Scheme II-29. ^{18}O -labeling experiments to study the mechanism of silane hydrolysis catalyzed by cationic oxorhenium(V) complex.

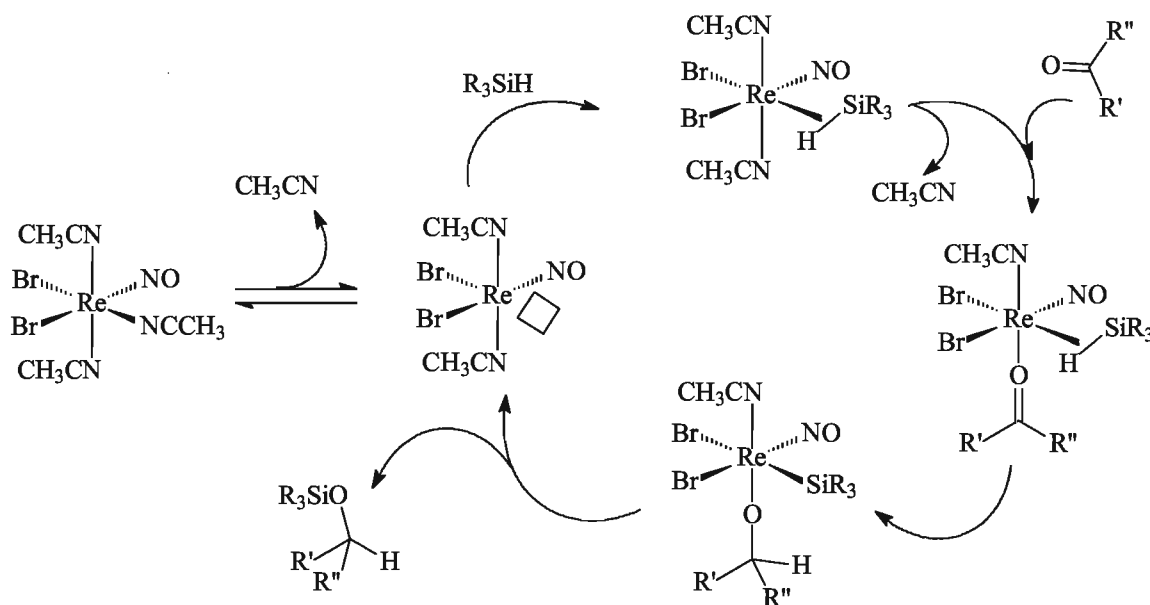
At the end of the catalysis, all the ^{18}O atoms were specifically incorporated into the bis(silyl) ether product. This result was similar to the Toste's hydrosilylation experiments

with the ^{18}O -labeled *p*-anisaldehyde (Scheme II-24)^{10a}, where ^{18}O carbonyl atoms were never incorporated into the $\text{Re}=\text{O}$ groups.

Unfortunately, no other relevant mechanistic investigations concerning the mechanism of hydrolytic oxidation of silane and hydrogen production have been performed^{61a}.

II.5.5. Rhenium(I)-catalyzed hydrosilylation

Recently, Berke *et al.* reported a highly efficient system for hydrosilylation of carbonyls based on phosphine-free rhenium(I) complex $[\text{Re}(\text{CH}_3\text{CN})_3\text{Br}_2(\text{NO})]$.⁶⁵ The catalytic system required relatively low catalyst loadings (0.2-1.0 mol%) and provided excellent yields of silyl ethers. Berke proposed a new mechanism of hydrosilylation of carbonyls (Scheme II-30) and rationalized it according to his observations.⁶⁵



Scheme II-30. Berke's mechanism of hydrosilylation of carbonyls catalyzed by $[\text{Re}(\text{CH}_3\text{CN})_3\text{Br}_2(\text{NO})]$.

Catalysis was proposed to begin with dissociation of the acetonitrile ligand. Dissociation of a bound acetonitrile was directly observed in ^1H NMR by the appearance of the singlet of free acetonitrile. In addition, the catalysis carried out in coordinating solvents, such as acetonitrile or THF provided only moderate yields. Formation of the η^2 -

Si-H adduct was concluded from a ^1H NOE experiment, where a very broad (>100 Hz) NOE signal was observed and assigned to the rhenium-coordinated Si-H bond. However, attempts to isolate the η^2 -Si-H adduct were unsuccessful. A possibility of oxidative addition of silane was considered as well. However, there was no evidence that oxidative addition took place. It is believed that coordination of carbonyl proceeds through the dissociation of another acetonitrile ligand, followed by the consecutive hydride transfer from the silane to the carbonyl group. The resulting silyl alkoxy complex undergoes reductive elimination of silyl ether (product) and regenerates the initial Re(I) complex.⁶⁵

II. 6. Oxo-molybdenum(VI) complexes

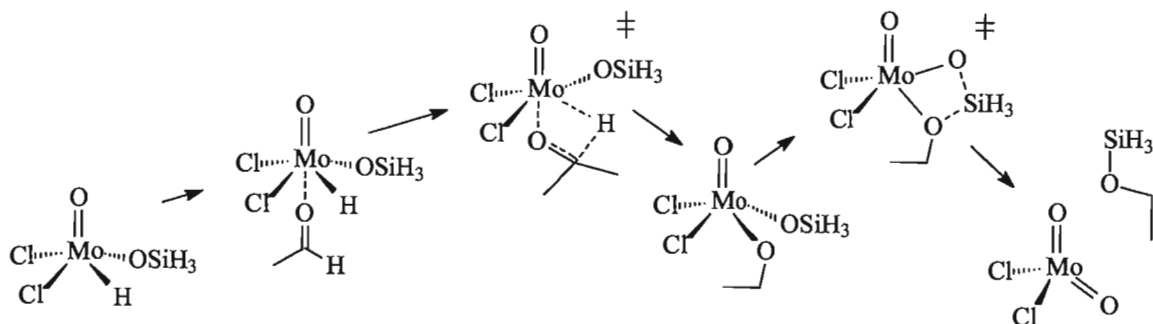
Royo *et al.* found that dioxo-molybdenum(VI) complex MoO_2Cl_2 is a highly effective catalyst for hydrosilylation of carbonyls⁶⁶. In the early studies, they screened different types (aromatic and aliphatic) of ketones and aldehydes. During the catalysis, no intermediates were observed by ^1H NMR. Stoichiometric reaction of MoO_2Cl_2 with PhMe_2SiH led to complex decomposition mixtures. It was mentioned that decomposition may be caused by the formation of unstable intermediates due to a [2+2]-addition reaction of silane to the $\text{Mo}=\text{O}$ bond. Addition of chlorosilanes to the $\text{Mo}=\text{O}$ bond of MoO_2Cl_2 with formation of $\text{Cl}_2\text{Mo}(\text{Hal})(\text{OSiR}_3)$ had been known in the literature before⁶⁷.

Shortly thereafter, Royo *et al.* examined the hydrosilylation activity of a number of oxo-molybdenum(VI) complexes including MoO_2Cl_2 , $\text{MoO}_2\text{Cl}_2(\text{CH}_3\text{CN})$, $\text{MoO}_2\text{Cl}_2(t\text{-BuCN})$, CpMoO_2Cl , $\text{MoO}_2(\text{mes})_2$, $\text{MoO}_2(\text{acac})_2$, $\text{MoO}_2(\text{S}_2\text{CNEt}_2)_2$, and $(\text{R}_3\text{Sn})_2\text{MoO}_4$ ($\text{R} = \text{n-Bu}$, t-Bu , Me)^{4b}. They found that MoO_2Cl_2 was the most active catalyst in this series. The best results of hydrosilylation catalysis (reaction time, yields, conversion of organic substrates) were obtained when acetonitrile was used as a solvent. Hydrosilylation worked well with PhMe_2SiH and Et_3SiH . Hydrosilylation of aldehydes proceeded at ambient temperature, but ketones required heating at 80°C .

Because the hydrosilylation mediated by MoO_2Cl_2 did not show formation of any active catalytic species in the reaction mixture, other Mo-complexes were tested. In particular, $\text{MoO}_2\text{Cl}_2(t\text{-BuCN})$ was chosen as a good candidate to study the catalysis

because of the ease to observe the single peak of the *t*-Bu group. No other components were detected in the reaction mixture by NMR during the catalysis. Nevertheless, stoichiometric reaction between $\text{MoO}_2\text{Cl}_2(t\text{-BuCN})$ and PhMe_2SiH led to a new product, $[\text{MoO}(\text{OSiMe}_2\text{Ph})\text{Cl}_2]_2$, which was individually prepared and fully characterized^{4b}. This compound also catalyzed the hydrosilylation of carbonyls.

Several possible mechanisms of hydrosilylation catalysis by MoO_2Cl_2 were studied by DFT calculations by Costa *et al.*⁶⁸ [2+2]-Addition of Si-H to the Mo=O bond with the formation of $\text{MoH}(\text{O})(\text{OSiR}_3)\text{Cl}_2$ was found to be the most favourable first step. Then, the most possible pathway has been proposed; a weak coordination of aldehyde through the oxygen atom to $\text{MoH}(\text{O})(\text{OSiR}_3)\text{Cl}_2$ may result in the formation of an alkoxide species, which can then react with the siloxy ligand to give the silyl ether (Scheme II-31).



Scheme II-31. Possible mechanism of hydrosilylation of carbonyls catalyzed by MoO_2Cl_2 suggested on the basis of DFT calculations.

A radical mechanism has been considered to be involved in the MoO_2Cl_2 -based hydrosilylation catalysis, since the radical scavengers significantly slowed down catalysis.⁶⁸

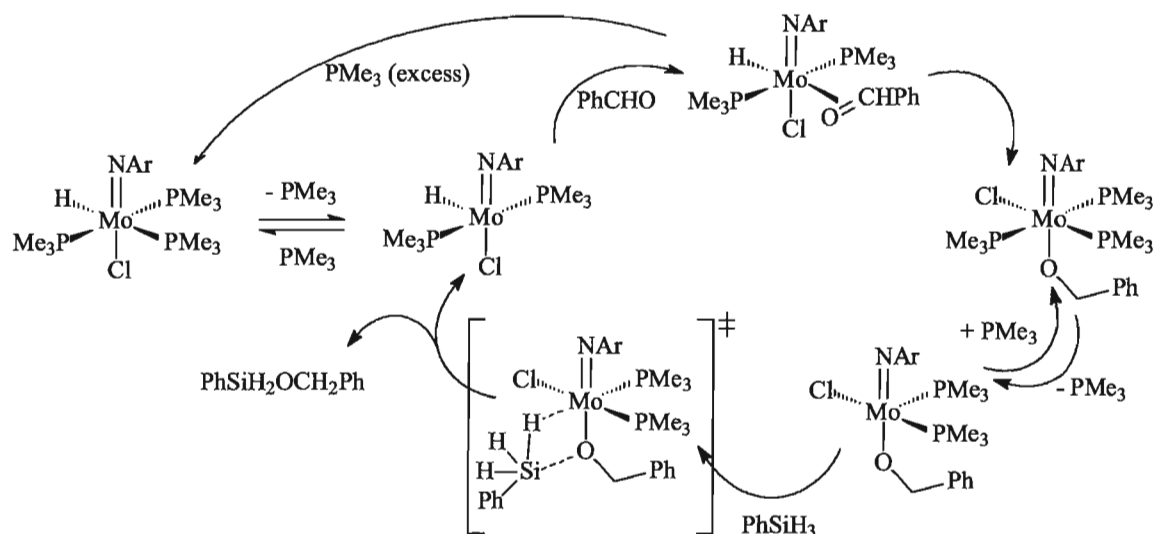
In conclusions, DFT calculations provided some useful ideas on how the hydrosilylation mechanism may work. However, there was no experimental proof of the proposed mechanism because of the inability to observe/detect the formation of any of the intermediate species in the reaction mixture during the catalysis^{4b, 66, 68}. Later, several other dioxo-molybdenum(VI) complexes were prepared, and their catalytic activity was examined⁶⁹. However, further mechanistic studies on the hydrosilylation catalysis were not performed.

Abu-Omar *et al.* prepared several molybdenum(VI) dioxo salalen complexes and studied their activity in hydrosilylation.^{4c} They did not believe that the mechanism proposed by Royo^{4b, 68} (Scheme II-31) takes place in their system. Based on their study^{4c}, Abu-Omar *et al.* showed that the dioxo functionality is not a prerequisite for the hydrosilylation catalysis. The most important factor is the presence of an open coordination site or a labile ligand. Because the dioxo molybdenum(VI) salalen complexes were saturated, an induction period in catalysis was observed. This observation led to the conclusion that Mo(VI) is not the real catalytic species. It was proposed that presumably Mo^{IV}(O)(salalen-Bu-*t*₂) was the true catalyst. The monooxo-molybdenum(IV) complex was not fully characterized by NMR, mass-spectroscopy and elemental analyses. Abu-Omar also considered the possibility of a radical mechanism of hydrosilylation previously mentioned by Royo^{4b}.

II. 7. Imido molybdenum (IV) complexes

Abu-Omar studied hydrosilylation catalysis by oxo-Re(V), imido-Re(V) and oxo-Mo(VI) complexes.^{6, 10b} He mentioned a class of imido Mo(IV) complexes known to catalyze hydrogenation of olefins⁷⁰. However, imido Mo(IV) complexes have not been investigated in his group as hydrosilylation catalysts.

Application of imido Mo(IV) complexes in hydrosilylation of carbonyls was first studied by Nikonov *et al.*^{5a} The imido-hydrido complex (ArN)Mo(H)(Cl)(PMe₃)₃ was prepared and fully characterized. It was found to catalyze the hydrosilylation of a variety of carbonyls to the corresponding silyl-protected alcohols, the dehydrogenative silylation of alcohols, and also the selective hydrosilylation of nitriles to the monosilylated imines. Thorough mechanistic investigation of catalysis was based on kinetic studies of individual steps of the hydrosilylation of benzaldehyde by phenylsilane (Scheme II-32).

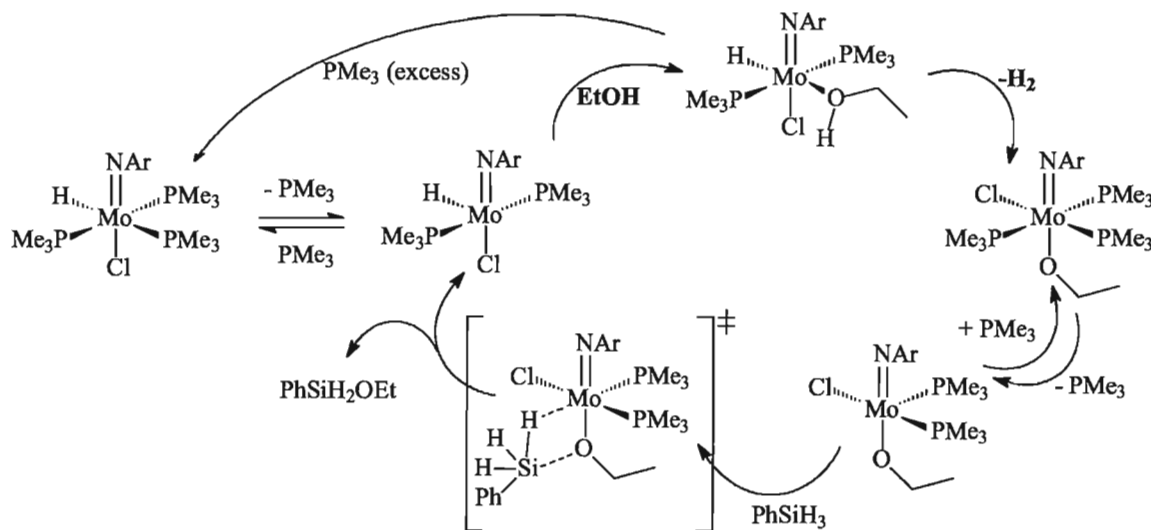


Scheme II-32. Proposed catalytic cycle of hydrosilylation of benzaldehyde by PhSiH_3 catalyzed by $(\text{ArN})\text{Mo}(\text{H})(\text{Cl})(\text{PMe}_3)_3$.

Complex $(\text{ArN})\text{Mo}(\text{H})(\text{Cl})(\text{PMe}_3)_3$ does not react with phenylsilane in contrast to the reported $\text{Re}(\text{V})=\text{O}^{10\text{a}, 54}$ and $\text{Mo}(\text{VI})=\text{O}^{4\text{b}, 66, 68}$ species. However, it undergoes a *slow* H/D exchange with PhSiD_3 . Kinetic studies showed that the reaction with benzaldehyde proceeds via dissociation of the *trans*-to-the-hydride phosphine ligand with *fast* formation of the η^2 -coordinated benzaldehyde hydrido complex $(\text{ArN})\text{Mo}(\text{H})(\text{PhCHO})(\text{Cl})(\text{PMe}_3)_2$. The latter *slowly* re-arranges into the benzyloxy triphosphine complex $(\text{ArN})\text{Mo}(\text{OCH}_2\text{Ph})(\text{Cl})(\text{PMe}_3)_3$. The next reaction with silane requires phosphine dissociation and finally results in the formation of silyl ether and regeneration of the initial complex (Scheme II-32). Each intermediate of the proposed cycle has been characterized by NMR spectroscopy.

Remarkably, the proposed catalytic cycle (Scheme II-32) looks very similar to that one proposed by Abu-Omar *et al.* for the hydrido oxo rhenium(V) complex $(\text{PPh}_3)_2\text{Re}(\text{H})(\text{O})(\text{Cl})_2$ in the reaction of hydrosilylation of benzaldehyde with triethylsilane.⁶ Both mechanisms include similar key steps, such as phosphine dissociation, coordination of aldehyde, hydride transfer to form a benzyloxy complex, and reaction with the silane proceeding via the proposed heterolytic splitting of Si-H and Mo-O (Re-O) bonds.

In-depth kinetic investigations of dehydrogenative silylation of alcohols by $(\text{ArN})\text{Mo}(\text{H})(\text{Cl})(\text{PMe}_3)_3$ suggested a mechanism in which the phosphine ligand dissociation is followed by the coordination of ethanol through the oxygen atom, which acidifies the $-\text{OH}$ proton enough for its transfer to the hydride to generate molecular hydrogen (Scheme II-33).^{5a}



Scheme II-33. Proposed mechanism of dehydrogenative silylation of ethanol.

The results of this work^{5a} have been contrasted to the earlier proposed mechanisms of catalytic alcoholysis of silanes reported by Crabtree⁷¹, Brookhart⁷² and Kubas⁷³. Therein, the silicon atom was suggested to be activated by the metal centre to become accessible for attack by an external nucleophile. It was also emphasized that the observed kinetics for the silane alcoholysis by $(\text{ArN})\text{Mo}(\text{H})(\text{Cl})(\text{PMe}_3)_3$ was inconsistent with direct proton transfer to the metal hydride, which is observed for systems with dihydrogen bonding ($\text{M}-\text{H}\cdots\text{H}-\text{O}$).⁷⁴

II. 8. Hydrosilylation catalyzed by $\text{CuH}(\text{PPh}_3)$

The first report of hydrosilylation catalysis by $\text{Cu}(\text{I})$ reagents was made by Brunner and Miehling in 1984⁷⁵. They found that $t\text{-BuOCu}$ and PhCOOCu in the presence of optically active phosphine ligands ((-)-DIOP, (+)-Norphos, (-)-BPPFA) catalyze

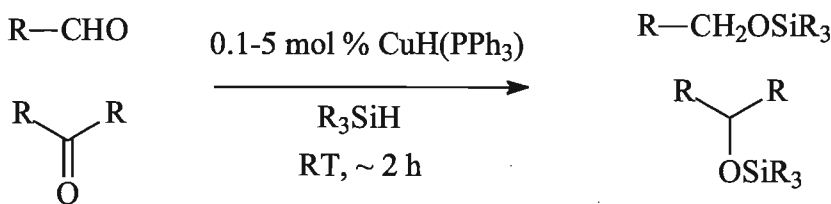
hydrosilylation of acetophenone with diphenylsilane quantitatively yielding the corresponding silyl ether with *ee* 10-40%.

Hexameric triphenylphosphine complex of copper(I) hydride $[\text{CuH}(\text{PPh}_3)]_6$ (or simply $\text{CuH}(\text{PPh}_3)$) is known as Stryker's reagent⁷⁶. It is a mild selective reducing agent, and is used in many stoichiometric reactions with conjugated enones and enoates^{9b, 76a} as well as a catalyst for conjugate reductions of various substrates^{76b, 77} and hydrosilylation.⁷⁸

Stryker's reagent can be prepared according to a classic procedure from CuCl , PPh_3 , *t*-BuOK, and H_2 ⁷⁹. Mixing of the first three reagents in toluene provides formation of copper(I) *tert*-butoxide, which then reacts with the molecular hydrogen to give $\text{CuH}(\text{PPh}_3)$ and *t*-BuOH. An alternative one-pot synthesis of Stryker's reagent from copper(II) acetate has been developed.⁸⁰

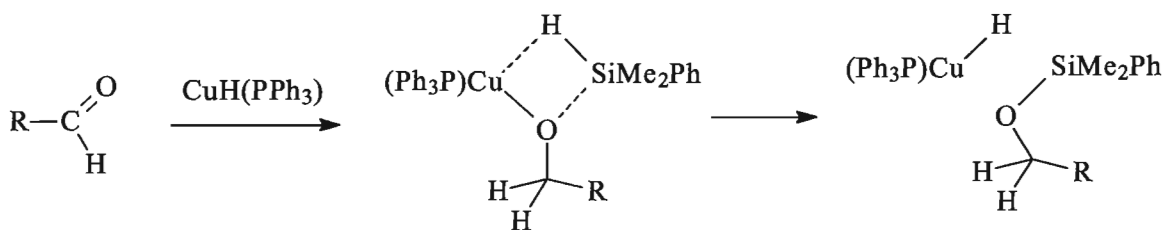
Recent studies emphasize the possibility for PhMe_2SiH ⁸¹, polymethylhydrosiloxane (PMHS)^{77c, 82}, and tetramethyldisiloxane (TMDS)⁸³ to generate a copper(I) hydride *in situ* from copper(I) alkoxides and copper(I) halides. However, the direct formation of Cu-H was not observed by NMR experiments.^{81, 84} Bu_3SnH has been demonstrated to generate copper(I) hydride stoichiometrically from a copper(I) iodide.⁸⁵

High catalytic activity of $\text{CuH}(\text{PPh}_3)$ in hydrosilylation of ketones and aldehydes was first reported by Lipshutz in 2001⁷⁸ (Scheme II-34).



Scheme II-34. Hydrosilylation of carbonyls catalyzed by $\text{CuH}(\text{PPh}_3)$.

Treatment of carbonyls with PhMe_2SiH in the presence of 0.1-5 mol % of $\text{CuH}(\text{PPh}_3)$ at temperatures from 0 °C to RT provided fast and quantitative formation of silyl ethers. The mechanism is believed to proceed via formation of an intermediate copper(I) alkoxide, which undergoes heterolytic splitting with the silane yielding the product of hydrosilylation and regenerating the initial copper(I) hydride (Scheme II-35)^{78, 86}.



Scheme II-35. Proposed mechanism of hydrosilylation of carbonyls catalyzed by $\text{CuH}(\text{PPh}_3)$.

A stoichiometric reaction of $\text{CuH}(\text{PPh}_3)$ with carbonyls to give copper(I) alkoxides has not been observed. The assumption of the possible formation of an intermediate alkoxide was derived from the fact that copper(I) hydride was sufficiently reactive to catalyze the hydrogenation of aldehydes^{77a}. Therefore, the first step was proposed to be reductive and proceed via formation of an intermediate alkoxide.⁷⁸ The last step was presumed to involve heterolytic splitting of H-Si on the Cu-O bond.⁸¹

The influence of the hydride on the catalytic activity of Cu(I) is essential. The combination of $\text{CuCl}/\text{PhMe}_2\text{SiH}$ showed no detectable catalytic activity until the catalytic system was heated in dimethylimidazole to (presumably) regenerate CuH ⁸⁷.

Bulkier silanes, such as Ph_3SiH , Ph_2MeSiH and $(t\text{-Bu})\text{Ph}_2\text{SiH}$, were found to be less reactive than PMHS in hydrosilylation, and their use in catalysis required heating at 40–50 °C. However, the overall conversion of carbonyl substrates (yields >90%) was not affected, and lower yields were not observed.⁷⁸

Aldehydes have been reported to be one hundred times more active than ketones. It was also demonstrated that aldehydes may be selectively hydrosilylated in the presence of ketones⁷⁸.

Various types of carbonyls have been tested in catalytic hydrosilylation by $\text{CuH}(\text{PPh}_3)$: aliphatic and aromatic. Aromatic carbonyls were found to be more reactive than aliphatic analogues. Donor substituents in the benzene ring facilitate the hydrosilylation of aromatic carbonyls. Chemoselectivity of catalysis was checked with carbonyls containing non-conjugated C=C double bonds, and/or -OMe, -OTs, -OBn, -NO₂, -Br groups. The latter were inert during the catalysis.

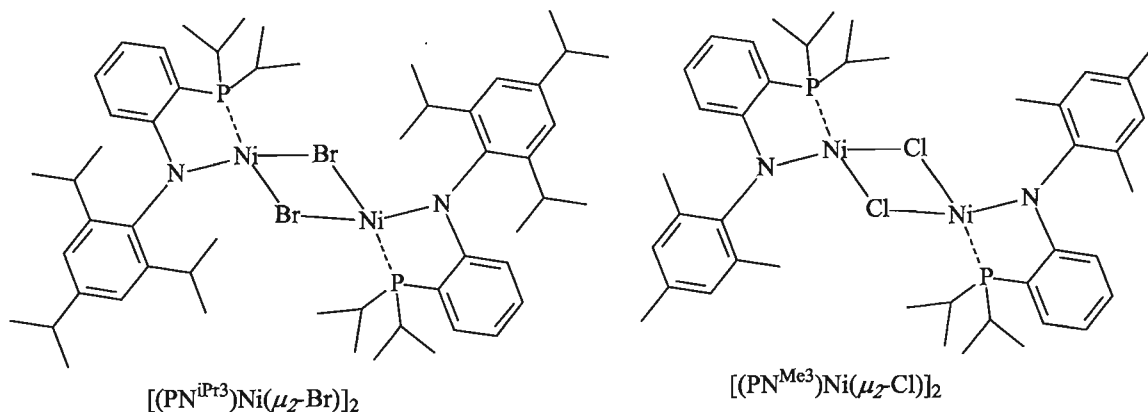
Further investigations of catalytic activity of $\text{CuH}(\text{PPh}_3)$ led to the development of methods of asymmetric hydrosilylation^{84b, 88} and hydrogenation^{9b} of carbonyls, and conjugate reductions of α,β -unsaturated carbonyls.^{53b, 59, 65} This was typically achieved by the replacement of triphenylphosphine by other chiral phosphine ligands.

Detailed investigations of the mechanism of hydrosilylation of carbonyls by $\text{CuH}(\text{PPh}_3)$ have never been reported.

Furthermore, there is no information about hydrosilylation of nitriles, esters, amides by Stryker's reagent in the literature to date.

II. 9. Hydrosilylation of carbonyls catalyzed by Ni-complexes

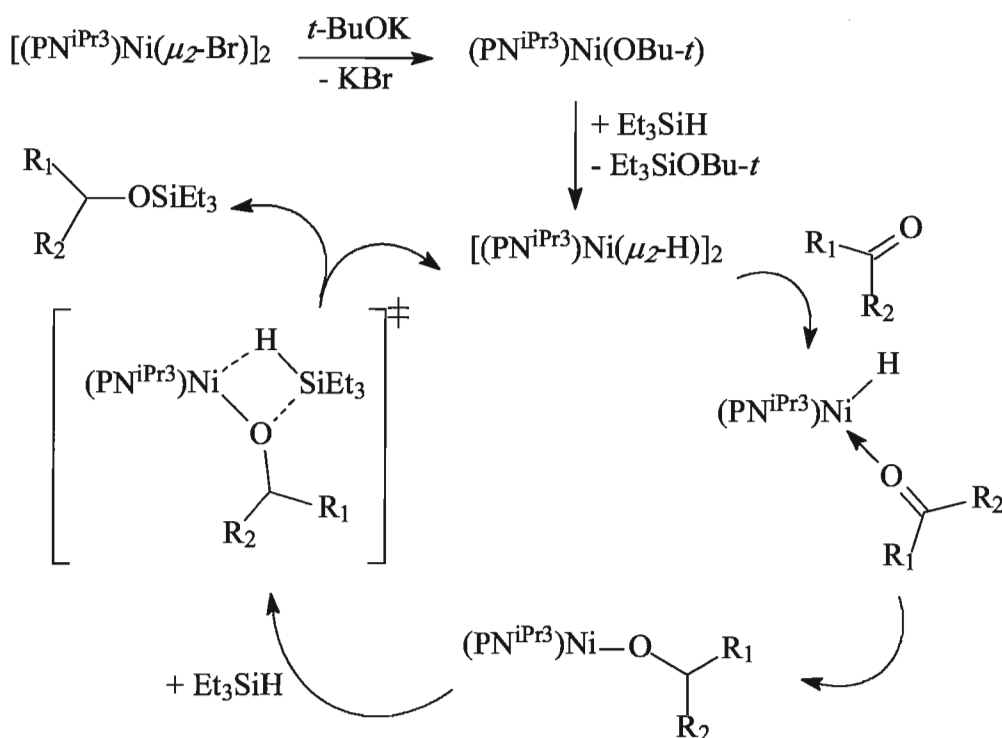
Mindiola *et al.* suggested a mechanism of hydrosilylation of carbonyls catalyzed by $[(\text{PN}^{\text{iPr}_3})\text{Ni}(\mu_2\text{-Br})]_2$ (PN^{iPr_3} = N-(2-(diisopropylphosphino)-4-methylphenyl)-2,4,6-triisopropylanilide) and $[(\text{PN}^{\text{Me}_3})\text{Ni}(\mu_2\text{-Cl})]_2$ (PN^{Me_3} = N-(2-(diisopropylphosphino)-4-methylphenyl)-2,4,6-trimethylanilide) (Scheme II-36).^{7c}



Scheme II-36. Mindiola's Ni(II)-catalysts for carbonyl hydrosilylation.

Complexes $[(\text{PN}^{\text{iPr}_3})\text{Ni}(\mu_2\text{-Br})]_2$ and $[(\text{PN}^{\text{Me}_3})\text{Ni}(\mu_2\text{-Cl})]_2$ do not individually react with Et_3SiH . They also do not express catalytic activity in hydrosilylation catalysis unless *t*-BuOK is added to the reaction mixture. It was presumed that addition of *t*-BuOK is required to generate a nickel *tert*-butoxy intermediate $\text{XNi-OBu-}t$ followed by the reaction with Et_3SiH to give an *active* nickel hydride complex $[(\text{PN}^{\text{iPr}_3})\text{Ni}(\mu_2\text{-H})]_2$. Formation of a hydride complex was observed in ^1H NMR spectrum by the appearance of

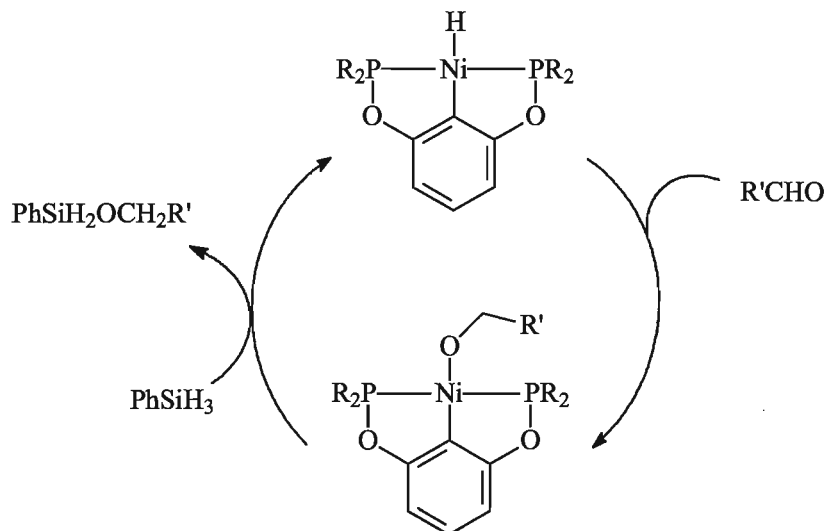
a doublet ($J_{\text{H-P}} = 18 \text{ Hz}$) at -20.66 ppm assigned to Ni-H. However, all attempts to isolate or individually prepare complex $[(\text{PN}^{\text{iPr}_3})\text{Ni}(\mu_2\text{-H})]_2$ were unsuccessful.^{7c} Coordination of a carbonyl compound is followed by its insertion to form an alkoxy complex. Reaction with triethylsilane was proposed to proceed via a σ -bond metathesis mechanism to regenerate the hydrido complex and to provide the hydrosilylation product. A catalytic cycle (Scheme II-37) has been proposed on the basis of studying stoichiometric/individual reactions of substrates (Et_3SiH , benzaldehyde, $t\text{-BuOK}$) with $[(\text{PN}^{\text{iPr}_3})\text{Ni}(\mu_2\text{-Br})]_2$, $[(\text{PN}^{\text{Me}_3})\text{Ni}(\mu_2\text{-Cl})]_2$ and other model nickel(II) complexes.^{7c} No theoretical or physico-chemical investigations have been performed.



Scheme II-37. Mindiola's mechanism of carbonyl hydrosilylation catalyzed by $[(\text{PN}^{\text{iPr}_3})\text{Ni}(\mu_2\text{-Br})]_2$.

Guan *et al.* reported hydrosilylation of aldehydes and ketones by nickel PCP-pincer complex and proposed a similar mechanism of catalysis (Scheme II-38).^{7b} Insertion of carbonyl into Ni-H bond to form an alkoxy derivative was best observed for benzaldehyde. Ketones (benzophenone, acetophenone) did not afford formation of alkoxy

complexes. Cleavage of the Ni-O bond by silane regenerates the nickel hydride species (Scheme II-38).



Scheme II-38. Guan's mechanism of carbonyl hydrosilylation by nickel PCP-pincer complexes.^{7b}

II. 10. Hydrosilylation catalyzed by $B(C_6F_5)_3$

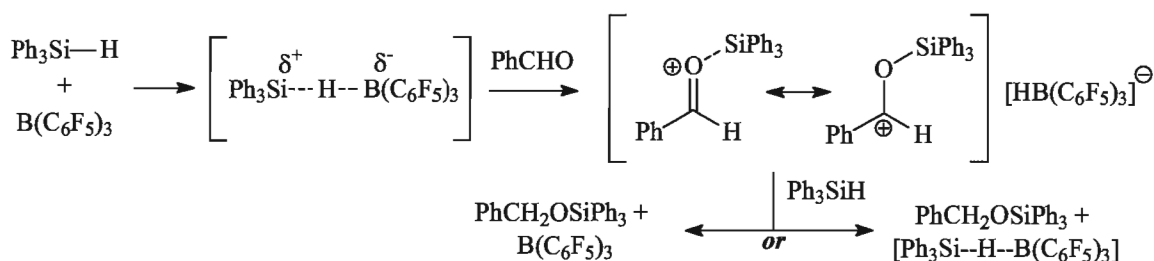
In 1996, Piers *et al.* reported that tris(pentafluorophenyl)borane may serve as a mild and very efficient catalyst for hydrosilylation of carbonyls.⁸⁹ $B(C_6F_5)_3$ (1-4 mol%) catalyzes the hydrosilylation of aromatic and aliphatic aldehydes, ketones and esters by Ph_3SiH at RT. Aldehydes and ketones have been reduced to the corresponding silyl ethers, and esters to the acetal products. Several years later, extensive mechanistic studies were performed to determine the mechanism of this reaction.⁹⁰

Tris(pentafluorophenyl)borane is a very strong Lewis acid and thus was expected to activate carbonyls to promote the hydrosilylation reaction. Even though there had not been supporting data in the literature that the hydrosilylation of carbonyls may be initiated by Lewis acid activation of carbonyls⁹⁰, the equilibrium between $B(C_6F_5)_3$ and carbonyls had been studied⁸⁹. Stable borane-carbonyl adducts are very rare, and only a few of them were prepared, isolated and characterized.⁹¹ Similar type of adducts, such as $R-OH \cdots B(C_6F_5)_3$ and $H_2O \cdots B(C_6F_5)_3$ are known.⁹² Even nitriles may bind to $B(C_6F_5)_3$ relatively strongly.⁹³

$\text{BF}_3 \cdot \text{Et}_2\text{O}$ promotes reduction of carbonyls with organosilanes to boron trifluoro etherates⁹⁴. Despite the fact that a stoichiometric amount of $\text{BF}_3 \cdot \text{Et}_2\text{O}$ is required, the reaction is induced by the Lewis acidic activation of carbonyl groups. Alcohols and ketones can be reduced to hydrocarbons by the action of gaseous BF_3 and R_3SiH in CH_2Cl_2 , and this process likewise was promoted by activation of the carbonyl group by BF_3 .⁹⁵ Catalytic amounts of ZnCl_2 or AlCl_3 (Lewis acids) may induce hydrosilylation of ketones to silyl ethers but in low yields and with a competitive formation of symmetrical dialkylethers.⁹⁴

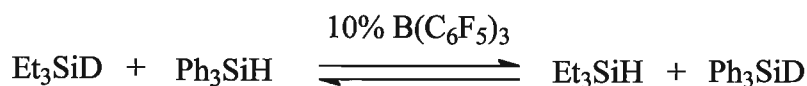
Tris(pentafluorophenyl)borane was chosen as a good alternative to $\text{BF}_3 \cdot \text{Et}_2\text{O}$ as it is air-stable and water-tolerant Lewis acid reagent⁹⁶. Piers *et al.* showed that the key point in the hydrosilylation of the carbonyl by $\text{B}(\text{C}_6\text{F}_5)_3$ is the unexpected activation of the Si-H bond rather than activation of carbonyls group. Kinetic studies demonstrate that the rate of hydrosilylation catalysis by $\text{B}(\text{C}_6\text{F}_5)_3$ has an inverse proportional dependence on the concentration of carbonyl in the reaction mixture. In other words, large amounts of ketone *inhibits* catalysis. The trend of reactivity of carbonyl substrates was found to be opposite of the expected one: ethyl benzoate \gg acetophenone $>$ benzaldehyde. Carbonyls may reversely bind with their nucleophilic oxygen to $\text{B}(\text{C}_6\text{F}_5)_3$ (Lewis acid) in solution, but the order of coordination is the opposite: benzaldehyde $>$ acetophenone \gg ethyl benzoate (since the most basic oxygen binds strongly to the electrophilic boron). These observations led to the conclusion that formation of a carbonyl-boron adduct is not preferable and it does not promote hydrosilylation; conversely, it inhibits the catalysis. The activation of carbonyl group by $\text{B}(\text{C}_6\text{F}_5)_3$ is not a catalytic step.

A mechanism involving activation of the Si-H bond by $\text{B}(\text{C}_6\text{F}_5)_3$ to generate a silyl cation was proposed (Scheme II-39).



Scheme II-39. Mechanism of hydrosilylation of carbonyls catalyzed by $\text{B}(\text{C}_6\text{F}_5)_3$.

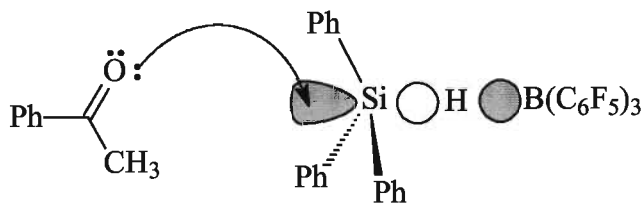
To show the possibility of hydride abstraction from silanes by borane, several NMR experiments were carried out. First of all, addition of $\text{B}(\text{C}_6\text{F}_5)_3$ to a solution of Et_3SiH in C_6D_6 caused the loss of the Si-H coupling to the CH_2 protons, resulting in a broad Si-H peak. This phenomenon resembles the known behaviour of -OH protons of alcohols in ^1H NMR spectra when small amounts of water are added. It was hypothesised that $\text{B}(\text{C}_6\text{F}_5)_3$ may act similarly causing a very fast exchange of the silyl protons, which results in signal broadening. When a 1:1 mixture of Et_3SiD and Ph_3SiH was treated with 10% $\text{B}(\text{C}_6\text{F}_5)_3$, only H/D scrambling between both silanes is observed (Scheme II-40).



Scheme II-40. H/D exchange between Et_3SiD and Ph_3SiH promoted by $\text{B}(\text{C}_6\text{F}_5)_3$.

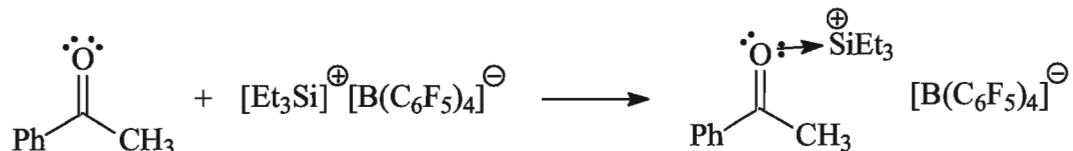
Formation of a borane-silane adduct was further supported by computational studies (AM1). Kinetic investigations of hydrosilylation of acetophenone by Et_3SiH (and Et_3SiD) in the presence of $\text{B}(\text{C}_6\text{F}_5)_3$ revealed the primary kinetic isotope effect ($k_{\text{H}}/k_{\text{D}} = 1.40$), indicating that hydride abstraction from silane by borane is the rate-determining step in catalysis.

Because the most basic carbonyls were observed to be the most active substrates in hydrosilylation mediated by $\text{B}(\text{C}_6\text{F}_5)_3$, it is believed that carbonyls attack, via their nucleophilic oxygen atom, the silyl cation of the silane-borane adduct. Computational studies found that the LUMO of the Si-H-B bond lies aside and *trans* to the Si-H bond, and this orbital was considered to be a site of nucleophilic attack of carbonyls (Scheme II-41).



Scheme II-41. The proposed nucleophilic attack of LUMO of the $\text{R}_3\text{Si-H-B}(\text{C}_6\text{F}_5)_3$ adduct by carbonyl.

To simulate the formation of a hypothetical ketone-silyl cation adduct, Piers *et al.* prepared $[\text{Et}_3\text{Si}^+][\text{B}(\text{C}_6\text{F}_5)_4^-]$ from Et_3SiH and $[\text{Ph}_3\text{C}^+][\text{B}(\text{C}_6\text{F}_5)_4^-]$ ⁹⁷, and treated acetophenone with this reagent. They were able to prepare and fully characterize the relatively unstable adduct (Scheme II-42) by NMR. The carbon atom of the carbonyl group shifted downfield from 196.8 ppm to 217.8 ppm, indicating the increased carbocationic character.



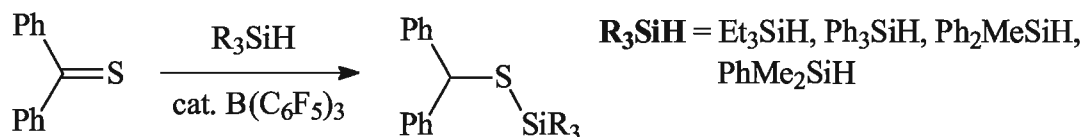
Scheme II-42. Preparations of ketone-silyl cation adduct.

This experiment showed the possibility for the formation of such species (adducts) in catalysis involving carbonyls and boron-mediated silyl cations. Interestingly, similar stable adducts of alkenes and silyl cations had been previously known.⁹⁸

When the carbonyl-silyl adduct is formed, what could be the source of hydride for the carbonyl atom? That was a question that required some additional investigations. Piers considered two possible ways: the hydride may come from another silane giving a product of hydrosilylation and a new silyl cation, or $[\text{HB}(\text{C}_6\text{F}_5)_3]$ could offer its hydride converting into $\text{B}(\text{C}_6\text{F}_5)_3$. To examine the possibility for silane to be a source of a hydride, Piers treated the $[\text{acetophenone-SiEt}_3][\text{HB}(\text{C}_6\text{F}_5)_3]$ adduct (Scheme II-42) with excess triethylsilane. He obtained a mixture of products including ethylbenzene, the expected silyl ether and hexaethyldisiloxane, where ethylbenzene was a major component of the mixture. While the presence of triethylsilyl ether could possibly indicate that the silane could be a source of hydride for this species, the product distribution was very different from that obtained in $\text{B}(\text{C}_6\text{F}_5)_3$ -catalyzed hydrosilylation. For example, ethylbenzene and hexaethyldisiloxane were never products of $\text{B}(\text{C}_6\text{F}_5)_3$ -catalyzed hydrosilylation⁸⁹⁻⁹⁰. It was concluded that silanes cannot be the donors of hydride, but, specifically $[\text{HB}(\text{C}_6\text{F}_5)_3]$ offers the required hydride to complete the hydrosilylation reaction.

The following experiment was carried out to demonstrate that the silane cannot be a source of hydride. A mixture of acetophenone, Ph_3SiD and $(p\text{-Tol})_3\text{SiH}$ was treated with $\text{B}(\text{C}_6\text{F}_5)_3$. As a result, only two products formed exclusively, $\text{PhCD}(\text{OSiPh}_3)\text{CH}_3$ and $\text{PhCH}(\text{OSi}(p\text{-Tol})_3)\text{CH}_3$. If silane were a source of hydride, that would lead to formation of all four possible products. This experiment indicates that it is not the case.

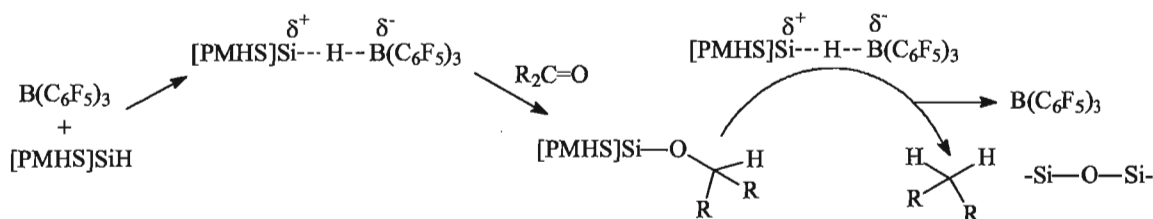
Rosenberg *et al.* studied $\text{B}(\text{C}_6\text{F}_5)_3$ -catalyzed hydrosilylation of thiobenzophenone with a variety of silanes to produce silyl thioether compounds under mild conditions and low catalyst loadings (from 0.006 to 4 mol%).⁹⁹ They pointed out that since thiocarbonyls are less basic than ketones, then, according to Piers mechanism⁸⁹⁻⁹⁰, they are good candidates to use in hydrosilylation reactions catalyzed by $\text{B}(\text{C}_6\text{F}_5)_3$ (Scheme II-43).



Scheme II-43. Hydrosilylation of thiocarbonyls catalyzed by $\text{B}(\text{C}_6\text{F}_5)_3$.

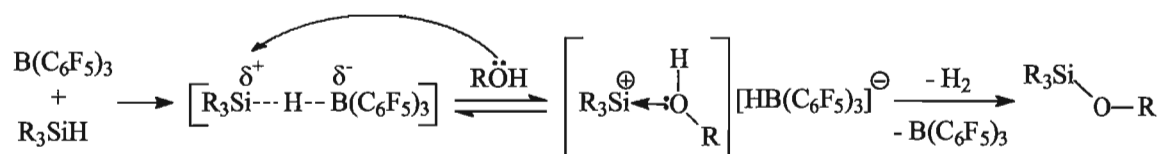
It was suggested that lowered basicity of the thioketone groups may explain their high reactivity. However, the observed activities do not support directly the mechanism based on activation of the Si-H group by boranes. Hydrosilylation of benzophenone was found to proceed with comparable or even higher rates than the hydrosilylation of thiobenzophenone.⁹⁹ Later studies of the hydrosilylation of thiosubstrates by Rosenberg *et al.* did not reveal any contradictions with the Piers mechanism.¹⁰⁰

Polymethylhydrosiloxane (PMHS)/ $\text{B}(\text{C}_6\text{F}_5)_3$ combination may be used in direct and rapid conversion of aromatic and aliphatic carbonyl compounds to the corresponding alkanes in high yields¹⁰¹. Though this system does not provide hydrosilylation, it is worth being mentioned here because the mechanism presumably includes a Si-H bond activation step. This method can provide selective reduction of carbonyl group in the presence of ester group within the same molecule.¹⁰¹ The mechanism has not been studied in details, and the proposed scheme remains speculative (Scheme II-44).



Scheme II-44. Proposed mechanism of reduction of carbonyl groups (C=O) to methylenes (-CH₂-) with PMHS mediated by B(C₆F₅)₃

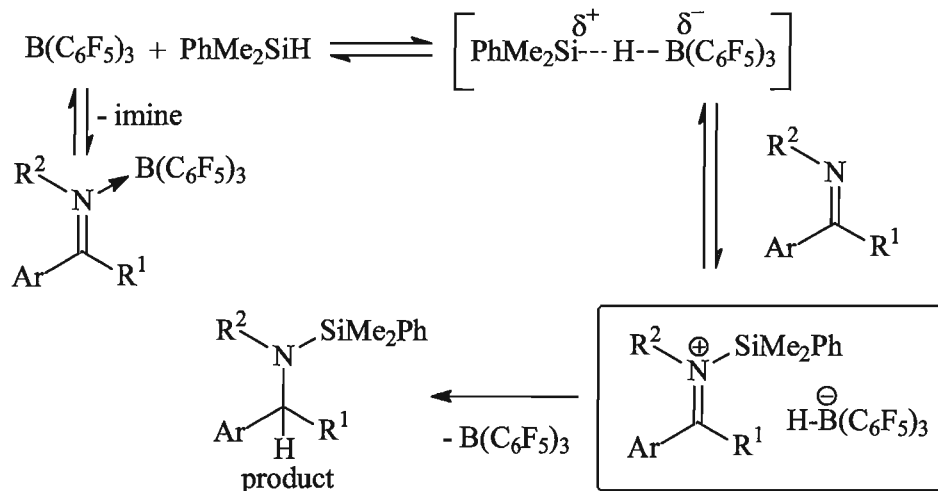
Blackwell *et al.* focused primarily on the development of a general method of synthesis of silyl ethers from alcohols catalyzed by B(C₆F₅)₃ and have not studied dehydrogenative silylation of alcohols in detail.^{92b} Nevertheless, observations and kinetic data suggest that it proceeds through an analogous mechanism, where activation of silane by B(C₆F₅)₃ is involved in the primary step of catalysis (Scheme II-45)^{92b}.



Scheme II-45. Mechanism of hydrosilylation of alcohols catalyzed by B(C₆F₅)₃

Other catalyst (B(C₆F₅)₃) derivatives, such as (perfluoroaryl)borane-functionalized carbosilane dendrimers, have been obtained and tested in hydrosilylation catalysis.¹⁰²

Piers *et al.* also reported that B(C₆F₅)₃ catalyzes hydrosilylation of a broad range of imines¹⁰³. They specified that the silyl-borane adduct [R₃Si-H-B(C₆F₅)₃] may react with imine to form the silyliminium-hydroborate ionic pair, which may either give the product or react with another equivalent of silane. The mechanism via a borane-imine complex was excluded.



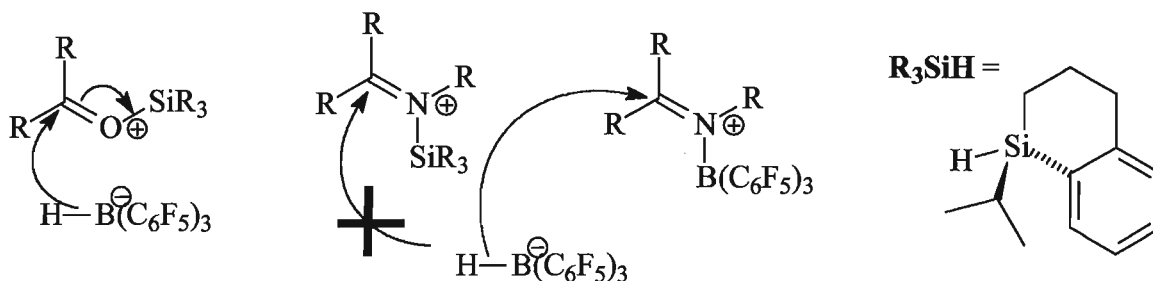
Scheme II-46. Proposed mechanism of hydrosilylation of imines catalyzed by $\text{B(C}_6\text{F}_5)_3$.

The less basic imines, bearing electron-withdrawing groups R^2 , were hydrosilylated more efficiently than their more basic analogues. In cases where imines coordinated to borane very strongly, the catalysis was inhibited. This fact shows that the imine-borane complex is not a participant in the catalytic cycle, and its dissociation is necessary for the hydrosilylation to occur.

Piers obtained the silyliminium-hydroborate ionic complex¹⁰³ shown in Scheme II-46 by mixing $\text{Ph}_2\text{C}=\text{NBn}$, PhMe_2SiH , and $\text{B(C}_6\text{F}_5)_3$ in the 1:1:1 ratio in C_6D_6 . Mixing reagents resulted in formation of a kind of liquid clathrate not soluble in benzene. Full NMR characterizations of the ionic complex thus obtained were performed. The formation of $\text{N-SiMe}_2\text{Ph}$ complex rather than $\text{N-B(C}_6\text{F}_5)_3$ complex suggest that the silyl cation is the catalytically active species. However, in order to verify the mechanism, experiments with a stereogenic silane were needed. Two years later, Piers *et al.* prepared more silyliminium-hydroborate ionic complexes in solution and in solid states and studied them in detail.¹⁰⁴

Oestreich was intrigued by the necessity to “complete” the mechanistic investigations of hydrosilylation catalysis with the use of chiral silanes, and decided to apply the chiral silanes with stereogenic silicon center.¹⁰⁵ When silicon-stereogenic silanes were applied, significant differences in the hydrosilylation catalysis of ketones and imines were found.¹⁰⁶ According to the mechanism reported by Piers, the use of a silicon-stereogenic

silane in the $\text{B}(\text{C}_6\text{F}_5)_3$ -catalyzed hydrosilylation must provide not only the inversion of the Si-atom configuration but also the enantioselectivity in the product formation. The results obtained for the catalytic hydrosilylation of ketones were indeed consistent with Piers mechanism. However, the hydrosilylation of imines proceeded without stereinduction (*ee* 0%)! This result was rationalized that the hydride-transfer step is possible when $[\text{HB}(\text{C}_6\text{F}_5)_3]^-$ attacks specifically the imine-borane complex rather than the imine-silyl complex. The latter is less hindered and, thus, less reactive (Scheme II-47).¹⁰⁶



Scheme II-47. Proposed mechanism for the hydride transfer step in hydrosilylation of carbonyls and imines by the silicon-stereogenic silane.

II. 11. Catalytic hydroboration of carbonyls and nitriles

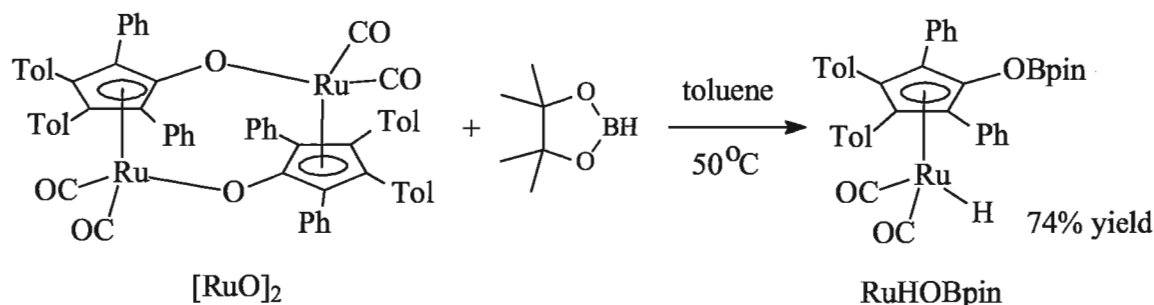
Hydroboration of carbonyl compounds by diborane (B_2H_6) was first reported by Brown in 1939.¹⁰⁷ The reaction produced alkoxyborane derivatives, which were hydrolyzed to corresponding alcohols and boric acid. Two decades later, Brown found that nitriles can be easily converted to amines by reaction with B_2H_6 .¹⁰⁸

Catalytic hydroboration was discovered by Männig and Nöth in 1985.¹⁰⁹ They reported that hydroboration of alkenes and alkynes by CatBH in the presence of Wilkinson catalyst proceeds very fast at ambient temperatures, while the same reaction without the catalyst required heating at 70-100 °C. Since then, catalytic hydroborations of alkenes, alkynes and dienes have been extensively studied.¹⁰⁹⁻¹¹⁰ Catalytic methods of hydroboration offered selective conversion of alkene group in the presence of carbonyl group, while in non-catalyzed hydroboration diborane reacts with both the carbonyl group and the olefin moiety.¹⁰⁹

Many commercially available hydroborating reagents, such as catecholborane, dimesitylborane, or 9-BBN, are known to react with the carbonyl group without the presence of a catalyst.¹⁰⁹ Possibly for this reason, catalytic hydroboration of carbonyl compound have not received a lot of attention so far.

In 2009, Clark *et al.* reported the first example of hydroboration of aldehydes, ketones and imines by pinacolborane (PinBH) catalyzed by Shvo reagent $[2,3,4,5-Ph_4(\eta^5-C_4COH)Ru(CO)_2H]$ (RuHOH).¹¹¹ This reagent had been previously studied by Shvo to catalyze hydrogenation of carbonyls, alkenes, alkynes,¹¹² as well as disproportionation of aldehydes to esters¹¹³ and in reduction of ketones to alcohols with formic acid¹¹⁴. Casey *et al.* provided a very detailed mechanistic insight into hydrogenation of carbonyls and imines with Shvo reagent.¹¹⁵

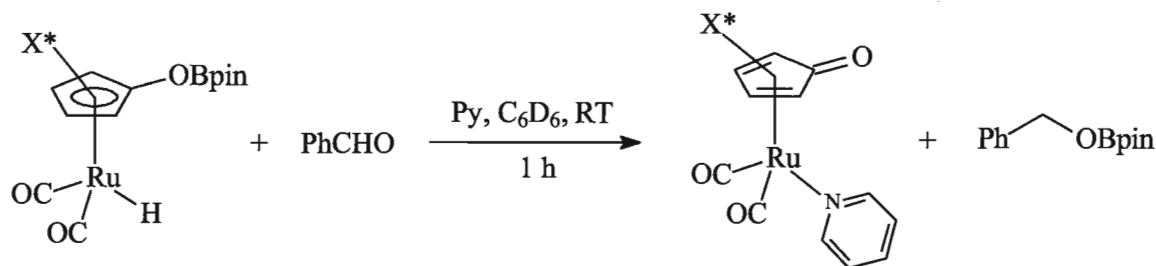
Clark *et al.* prepared a borylated analogue of Shvo catalyst, $[2,5-Ph_2-3,4-Tol_2(\eta^5-C_4COBpin)Ru(CO)_2H]$ (RuHOBpin), by the reaction of ruthenium dimer $[2,3,4,5-Ph_4(\eta^5-C_4CO-)Ru(CO)_2]_2$ (or $(RuO)_2$) with pinacolborane (Scheme II-48).¹¹¹



Scheme II-48. Synthesis of $[2,5\text{-Ph}_2\text{-3,4-Tol}_2(\eta^5\text{-C}_4\text{COBpin})\text{Ru}(\text{CO})_2\text{H}]$.

Casey's group previously showed a critical role of the acidic proton of the -OH group of Shvo catalyst (RuHOH) in carbonyl and imine hydrogenation.^{115a} It was believed that the empty p -orbital of the boron atom of the borylated analogue (RuHOBpin) would behave similarly to the -OH proton of Shvo catalyst and express catalytic activity in hydroboration of carbonyls and imines.¹¹¹ For instance, the silylated derivative RuHOSiEt_3 did not express any reactivity toward carbonyls, because the silicon atom does not possess a reactive (empty) p -orbital.^{115a}

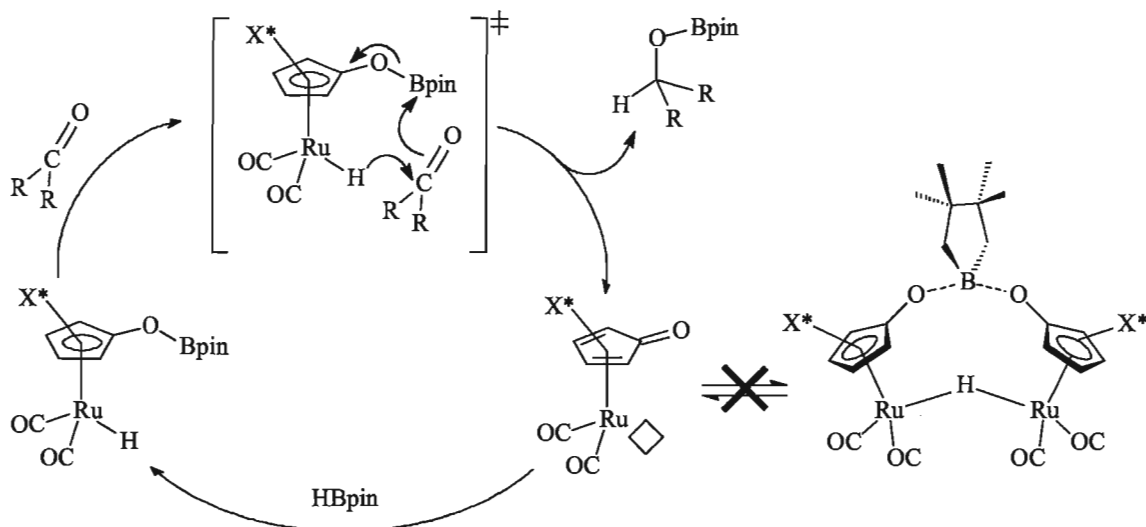
Stoichiometric (1:1) reaction between RuHOBpin and benzaldehyde in the presence of pyridine afforded boryl ether (product) and RuO^*Py in one hour at RT (Scheme II-49).¹¹¹ By this experiment, it has been demonstrated that the boryl group in RuHOBpin is sufficiently acidic to provide catalytic hydroboration of carbonyls.



Scheme II-49. Stoichiometric reaction between $[2,5\text{-Ph}_2\text{-3,4-Tol}_2(\eta^5\text{-C}_4\text{COBpin})\text{Ru}(\text{CO})_2\text{H}]$ and benzaldehyde.

Catalytic hydroboration of benzaldehyde by pinacolborane in the presence of 2% $(\text{RuO})_2$ has been successfully performed both in NMR and preparative scale experiments.

The mechanism of hydroboration of carbonyls was proposed to be analogous to the mechanism of hydrogenation of carbonyls by Shvo catalyst (Scheme II-50).¹¹¹



Scheme II-50. Clark-Casey's mechanism of carbonyl hydroboration catalyzed by [2,5-Ph₂-3,4-Tol₂(η^5 -C₄COBpin)Ru(CO)₂H].

Catalytic hydroboration of carbonyls by Shvo catalyst required several hours of heating at 50 °C in benzene, while hydrogenation of carbonyls mediated by Shvo catalyst proceeded under harsher conditions: either at temperatures >90 °C or at high pressure of hydrogen (35 atm, 60 °C).¹¹¹ It has been emphasized that the borylated derivative of Shvo catalyst cannot form a complex with the bridging hydride (Scheme II-50) probably due to the bulkiness of the pinacol group. In case of hydrogenation catalysis, the analogous structure with a bridging hydride does occur, and its slow dissociation *significantly* limits the overall rate of catalysis.¹¹¹ The formation of a bridging *catecholboryl* derivative was observed and characterized by ¹H and ¹¹B NMR.¹¹⁶

Competition experiments of hydroboration of benzaldehyde with different *para*-substituted benzaldehyde have been performed to examine the influence of electronic effects of substituents on the catalysis rate. Electron-donating substituents (-OCH₃, -CH₃) were found to suppress the catalysis, whereas electron-withdrawing groups (-Cl, -NO₂) promoted faster catalysis.¹¹¹

To identify the reversibility of hydroboration catalysis, 4-methoxybenzaldehyde (1.0 eq.) was mixed with pinacolborane (1.2 eq.) in the presence of $(\text{RuO})_2$ (4 mol%) and the reaction was monitored by ^1H NMR. When all the amount of aldehyde was consumed, 4-nitrobenzaldehyde (1.0 eq.) was added to the reaction mixture. Then, the reaction mixture was heated at 50 °C during two hours, and the only reaction observed was the hydroboration of 4-nitrobenzaldehyde by the unreacted pinacolborane (0.2 eq.). When the same reaction mixture was left for 24 hours of heating at 50 °C, significant amounts of hydroborated 4-nitrobenzaldehyde and the regenerated 4-methoxybenzaldehyde were observed.¹¹¹ Thus, this experiment demonstrated the reversibility of hydroboration catalysis.

Catalytic hydroboration of acetophenone was very slow and provided only 50% conversion after 3 days of heating at 70 °C (4% cat.). 4-Nitroacetophenone showed better results, and 95% conversion was observed after 4.5 days of heating at 70 °C (4% cat.).¹¹¹

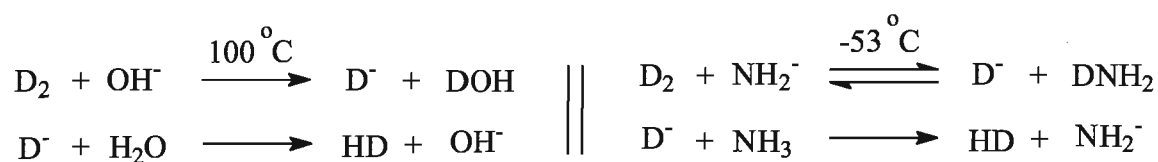
Casey and Clark also reported catalytic hydroboration of imines (N-benzilidenaniline and its *para*-substituted derivatives).¹¹¹ Catalysis proceeded very slowly and required up to 5 days of heating at 70 °C (4 mol% cat.) with overall yields of 74-86%. Hydroboration products were subjected to hydrolysis by silica gel chromatography to give the corresponding amines.¹¹¹

Catalytic hydroboration of nitriles has not been reported in the literature to date.

II. 12. Metal-free activation of molecular hydrogen

In the 1930s, Wirtz and Bonhoeffer studied the H/D-exchange reactions between D₂ and NH₃, D₂ and HCl, H₂ and D₂O (in the presence of strong bases).¹¹⁷ The H/D exchange between D₂ (gas) and KNH₂/NH₃(l.), and between D₂ and KOH/H₂O was later mentioned by Abe in 1941¹¹⁸ and by Wilmarth in 1950¹¹⁹.

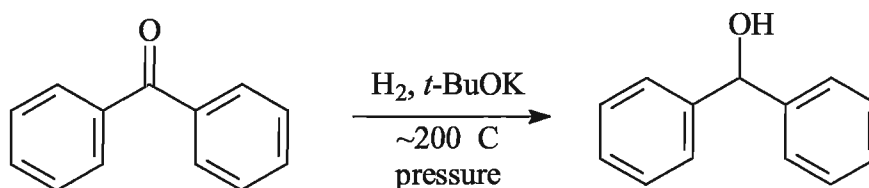
In 1953, Wilmarth *et al.* published kinetic studies of H/D exchange for the D₂—KOH/H₂O¹²⁰ and D₂—KNH₂/NH₃¹²¹ systems. They proposed that the deuterium gas first reacts with the base (OH⁻ or NH₂⁻), playing the role of an acid (Scheme II-51). According to kinetic investigations, the first step was considered to be rate-determining.



Scheme II-51. H/D-exchange in the D₂—KOH/H₂O and D₂—KNH₂/NH₃ systems.

In 1948, Ipatieff reported the effect of hydrogen on the action of AlCl₃ on *n*-pentane.¹²² When *n*-pentane was heated with AlCl₃ in the presence of H₂, no reaction was observed. The same reaction under the nitrogen atmosphere caused self-destructive alkylation. In the presence of promoters, such as water or hydrogen chloride, heating *n*-pentane with AlCl₃ afforded *iso*-pentane in excellent yields. The influence of molecular hydrogen on the system of *n*-heptane (and higher alkanes)/AlCl₃ was totally different. Heating *n*-heptane with AlCl₃ under the hydrogen atmosphere did not prevent the autodestructive alkylation. The additional presence of HCl in the reaction mixture did not cause any isomerization, but instead, the autodestructive hydrogenation was observed. The mechanism of the observed processes remains uncertain.¹²²

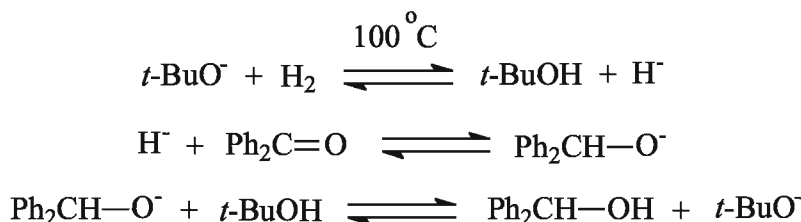
The first example of transition-metal-free hydrogenation of ketones was reported in 1961 by Walling and Bollyky.¹²³ They found that benzophenone can be reduced to benzhydrol in 40-60% yield in the presence of *t*-BuOK at high temperature (~170-230 °C) and high pressure of H₂ (88.5-174.2 atm) (Scheme II-52).



Scheme II-52. Hydrogenation of benzophenone by H_2 in the presence of $t\text{-BuOK}$.

Interestingly, Walling and Bollyky mentioned that a large number of reactions of oxidation of organic molecules at elevated temperatures are accompanied by evolution of molecular hydrogen. They also referred to the activation of molecular hydrogen by aqueous solutions of potassium hydroxide previously observed by Wirtz^{117a}, Willmarth¹²⁰ and Miller¹²⁴.

The mechanism of base-catalyzed hydrogenation of benzophenone was proposed to proceed as follows (Scheme II-53).^{123b}



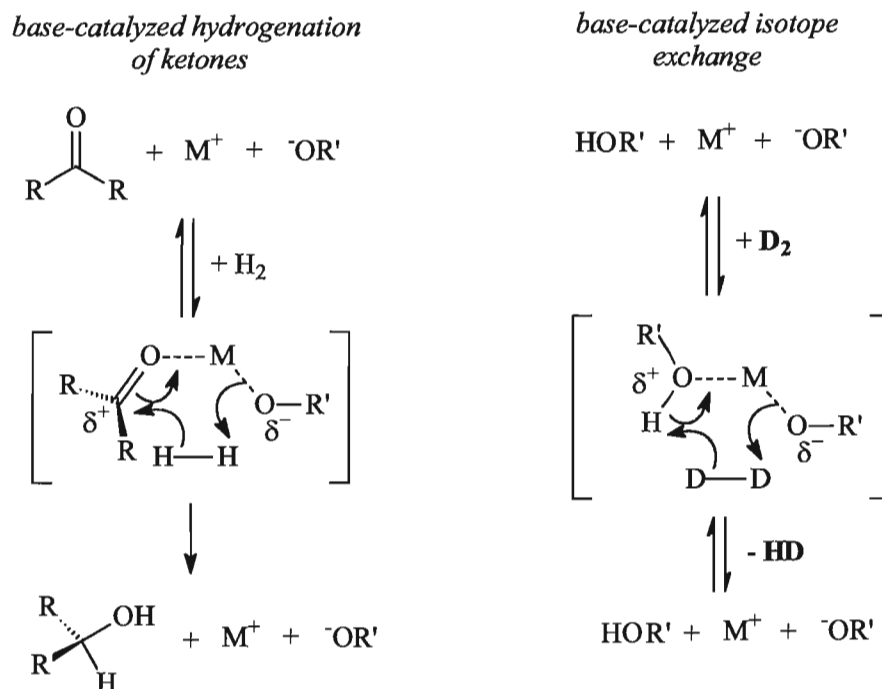
Scheme II-53. Walling-Bollyky mechanism of base-catalyzed hydrogenation of benzophenone.

Hydrogenation of acetone and cyclohexanone was not successful because of the extensive aldol condensations.^{123b} Nitrobenzene produced aniline in 34% yield.^{123b}

Acid-catalyzed hydrogenation was also mentioned as being possible. Walling and Bollyky reported that hydrogenation of cyclohexene in the presence of 15.8% AlBr_3 in cyclohexane at 150 °C and 82 atm removed all the unsaturation, providing a mixture of 4% of methylcyclopentane and a large amount of higher-boiling (black, tarry) products.^{123b} The same reaction in CHCl_3 in the presence of AlCl_3 afforded only traces of saturated hydrocarbons and the unchanged starting materials.

Berkessel *et al.* performed mechanistic investigation of Walling-Bollyky hydrogenation of non-enolizable ketones in order to further improve the hydrogenation

technique.¹²⁵ They reported that hydrogenation is irreversible and is first order in ketone, base, and molecular hydrogen. They discovered that the rate of hydrogenation also depends on the nature of the alkali ion and that it decreases in the following order: $\text{Cs}^+ > \text{Rb}^+ \approx \text{K}^+ \gg \text{Na}^+ \gg \text{Li}^+$. Several issues that could cause the influence of alkali ions have been discussed.¹²⁵ When D_2 was used, the resulting alcohols were *partially* deuterated. The latter was explained by the very fast exchange between the gas phase and solution, resulting in formation of a large amount of H-D. The rate of reaction did not depend significantly on whether H-D or H_2 was used, and H-H fission could not be the rate-determining step. The mechanism of base-catalyzed hydrogenation of ketones and base-catalyzed isotope exchange was proposed (Scheme II-54).¹²⁵ The six-membered cyclic transition state was supported by computational studies.¹²⁵

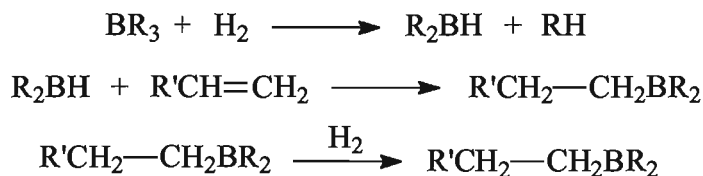


Scheme II-54. Berkessel's mechanism of base-catalyzed hydrogenation of ketones and base-catalyzed isotope exchange.¹²⁵

Berkessel emphasized that the proposed mechanism strongly resembles Noyori mechanism of Ru-catalyzed transfer hydrogenation.¹²⁶ The main reason of the poor

efficiency of the base-catalyzed hydrogenation can be the poor “population” of the appropriate (active) pre-orientation of the substrate (ketone) and the reactive base.¹²⁵

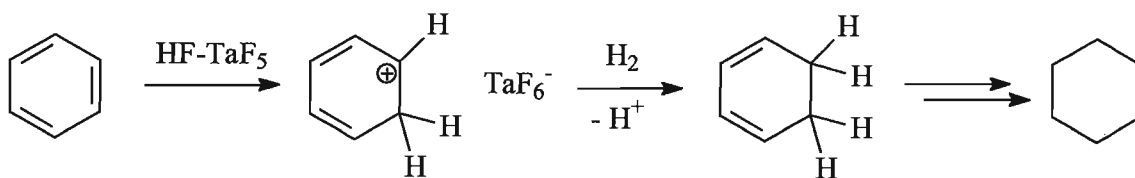
In 1958 Köster *et al.* discovered that the boron-carbon bond in trialkylboranes can undergo hydrogenolysis with formation of dialkylboranes and saturated hydrocarbons.¹²⁷ Later, in 1961, DeWitt *et al.* reported a highly efficient method of hydrogenation of alkenes catalyzed by trialkylboranes.¹²⁸ They found that cyclohexene or caprylene may be quantitatively hydrogenated in the presence of 3.8 mol% of *n*-Bu₃B at 220 °C and 68 H₂ atm. Hydrogenation of olefins catalyzed by trialkylboranes and tetraalkyldiboranes at harsh conditions (*T* > 200 °) became known.¹²⁸⁻¹²⁹ DeWitt specified that hydrogenation mediated by trialkylboranes starts with hydrogenolysis of the B-R bond followed by the insertion of hydridoborane into the olefin C=C bond. The resulting –CH-CBR₂ species undergo hydrogenolysis to yield the saturated hydrocarbon (product) and some form of hydridoborane (Scheme II-55).^{128, 129e}



Scheme II-55. DeWitt’s scheme of hydrogenation of olefins catalyzed by trialkylboranes.

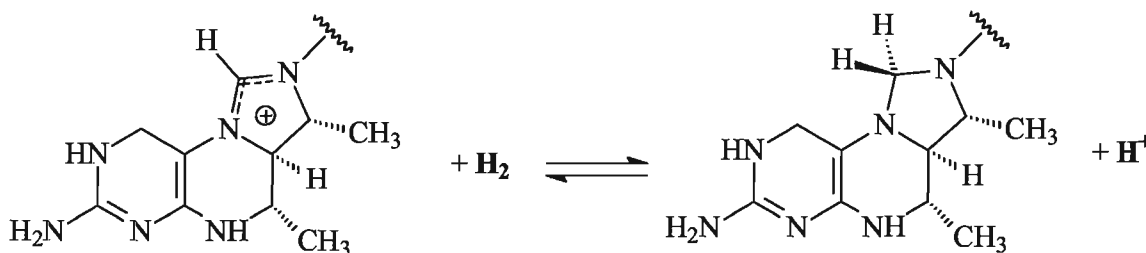
Haenel *et al.* reported that hydrogenation of olefins can also be effectively performed in the presence of *n*-Pr₂BI, I₂, NaBH₄/I₂ and by BI₃.^{129c}

Siskin *et al.*, in 1974, reported the first hydrogenation of aromatic (benzene) ring in the presence of strong Lewis acids, such as HF-TaF₅, HF-SbF₅ and HBr-AlBr₃.¹³⁰ Although the mechanism was not totally understood^{130a}, Wrister *et al.*, in 1975, published more detailed mechanistic insights and proposed that hydrogenation goes via protonation of the aromatic ring followed by hydride transfer directly from H₂ (Scheme II-56).¹³¹



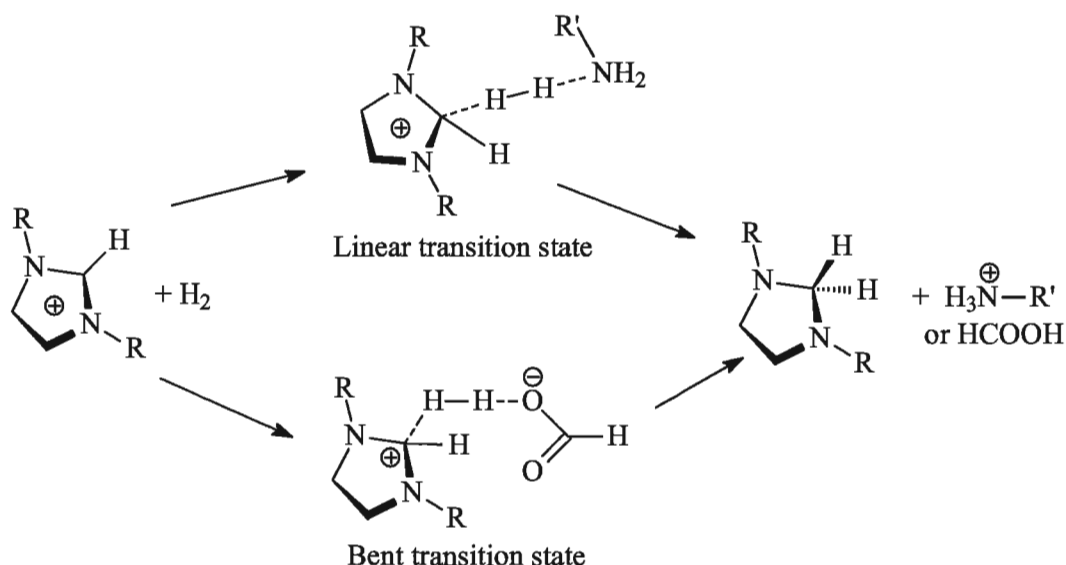
Scheme II-56. Hydrogenation of benzene ring in the presence of HF-TaF₅.

Enzymatic activation of molecular hydrogen is known. Thauer *et al.* found that *Methanobacterium thermoautotrophicum* contains a metal-free enzyme, which consists of polypeptide chain only and can utilize H₂ without the aid of metal clusters.¹³² The enzyme catalyzes the reaction of *N*⁵,*N*¹⁰-methenyl tetrahydromethanopterin with H₂ (Scheme II-57).



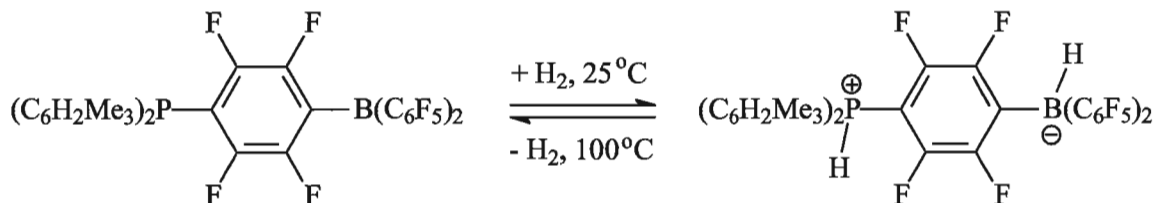
Scheme II-57. Reaction between *N*⁵,*N*¹⁰-methenyl tetrahydromethanopterin and H₂ catalyzed by enzyme isolated from *Methanobacterium thermoautotrophicum*.

These findings were followed by computational investigations of the hydrogen activation step by Teles and Berkessel.¹³³ High-level *ab initio* calculation indicated that molecular hydrogen bond can be cleaved by 1,3-dimethylimidazolidin-2-yl cation in the presence of base (NH₃ or HCOO⁻).¹³⁴ These theoretical studies concluded that *bifunctional catalysis* must take place in order to break the H-H bond. Berkessel suggested several transition states on how the H-H bond can be cleaved.¹³⁵ Computational investigations support transition states in which molecular hydrogen is cooperatively activated by a Lewis base and a Brønsted base. Experimental evidence shows that two bound hydrogen atoms of the H₂ can rapidly exchange with each other and the solvent. Although, it is still unclear which of these transition states take place, the heterolysis of H-H bond *requires* the joined action of both the acid and the base (bifunctional catalysis) (Scheme II-58).¹³⁵



Scheme II-58. Possible transition states for the $H-H$ bond cleavage by imidazolidinium cation and a base (bifunctional catalysis).¹³⁵

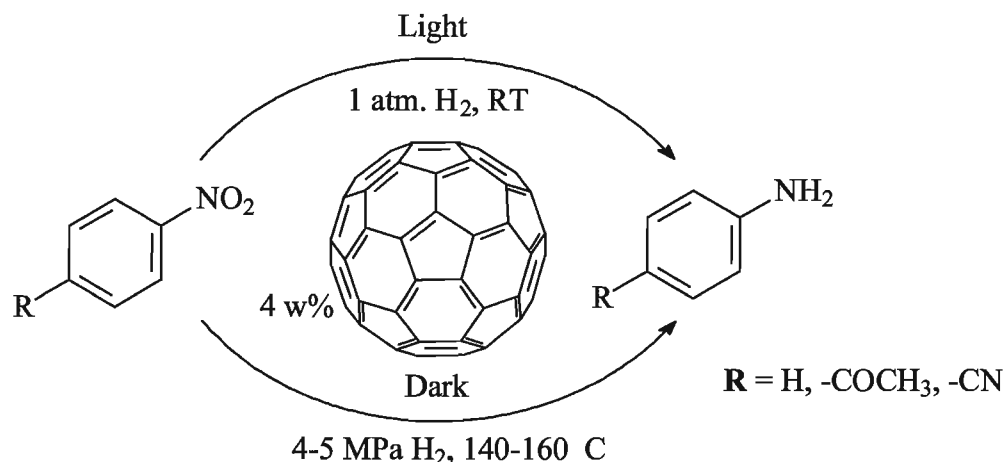
In 2006, Stephan *et al.* reported that the compound $p-(C_6H_2Me_3)_2P-C_6F_4-B(C_6F_5)_2$ reacts with 1 atm of H_2 at 25 °C with formation of $p-(C_6H_2Me_3)_2PH^{(+)}-C_6F_4-BH^{(-)}(C_6F_5)_2$.¹³⁶ Remarkably, the resulting compound reversely releases H_2 when heated to 100 °C (Scheme II-59).



Scheme II-59. Reaction between $p-(C_6H_2Me_3)_2P-C_6F_4-B(C_6F_5)_2$ and H_2 .

Such types of compounds were called Frustrated Lewis pairs.

Xu and Li recently reported that fullerenes C_{60} and C_{70} can activate molecular hydrogen and catalyze hydrogenation of aromatic nitro compounds to aromatic amino derivatives with high yields.¹³⁷ Hydrogenation was very selective, and such groups as ketone and nitrile remained unchanged (Scheme II-60). The mechanism of hydrogenation of nitroarenes in the presence of fullerene has not yet been proposed.^{137a}



Scheme II-60. Hydrogenation of nitroarenes to aminoarenes in the presence of fullerene (C₆₀/C₆₀⁻ mixture).^{137a}

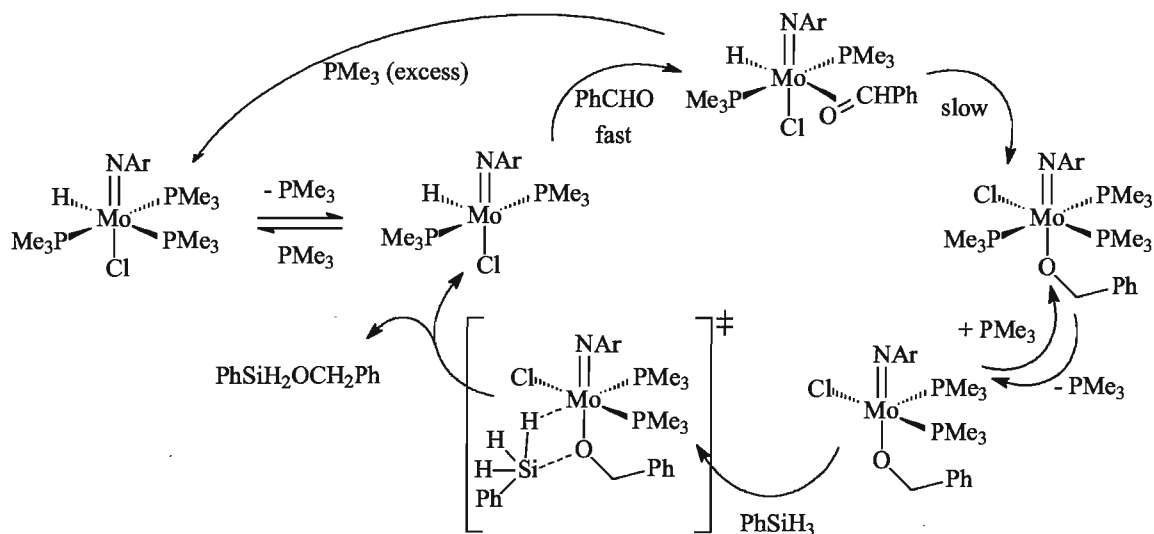
In 2010, Piers *et al.* reported the direct activation of molecular hydrogen exclusively by boron-based Lewis acid in the absence of Lewis base.¹³⁸ Perfluoropentaphenylborole was found to rapidly react with hydrogen to produce boracyclopent-3-ene products. Non-fluorinated pentaphenylborole was also found to react with H₂ in the same fashion, though much slower.¹³⁸ The significant driving force of this reaction was the disruption of anti-aromaticity of the initial borole.

III Results and Discussions

Hydrosilylation is an important industrial process of reduction of unsaturated organic compounds. It has several unique advantages over other reduction methods. Hydrosilylation can be performed under *very mild* conditions, and it offers production of protected alcohols from carbonyls *in one step*, whereas the use of aluminum- or borohydrides requires at least two steps: the reduction and protection. Industrial hydrosilylation usually employs late transition metals, which are toxic and expensive.¹ Therefore, the development of methods of hydrosilylation using cheap and less-toxic early transition metals is an important goal.¹³⁹

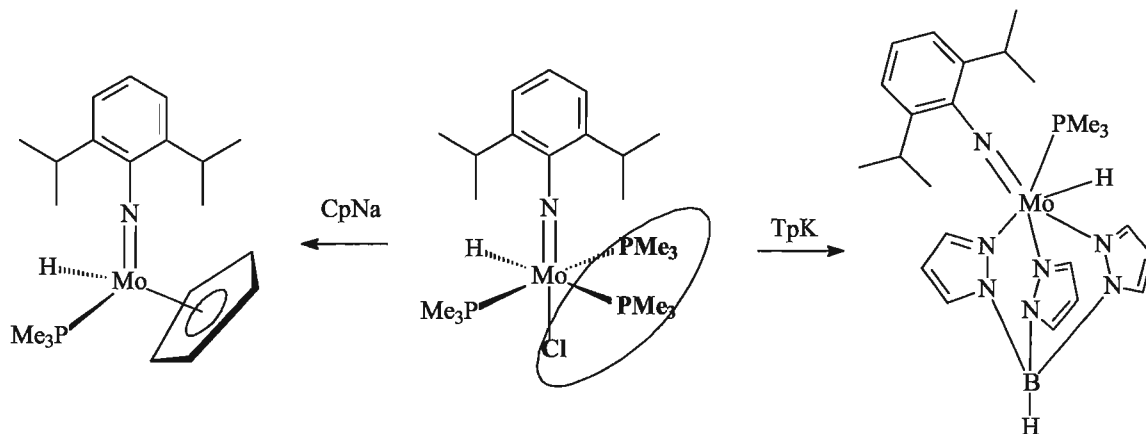
Hydrosilylation is poorly understood mechanistically. Literature data does not provide detailed investigations of the hydrosilylation catalysis: most of the mechanisms of hydrosilylation are very speculative. In this regard, we devote the current research to the investigation of mechanisms of hydrosilylation catalyzed by Mo(IV) complexes. Molybdenum is not only a cheap and non-toxic early transition metal but it also the only second transition series metal that occurs in biological structures.¹⁴⁰

Our group has recently found that complex $(\text{ArN})\text{Mo}(\text{H})(\text{Cl})(\text{PMe}_3)_3$ catalyzes hydrosilylation of aldehydes and ketones.^{5a} Detailed kinetic and mechanistic studies of the hydrosilylation of benzaldehyde with phenylsilane demonstrated that the catalysis begins with dissociation of a phosphine ligand (*trans*-H-Mo-PMe₃) followed by the fast formation of the *trans*- η^2 -benzaldehyde complex and its slow re-arrangement into the benzyloxy triphosphine complex (Scheme III-1).



Scheme III-1. Proposed catalytic cycle of hydrosilylation of benzaldehyde by phenylsilane catalyzed by $(\text{ArN})\text{Mo}(\text{H})(\text{Cl})(\text{PMe}_3)_3$.^{5a}

The *fac* ligand set (Cl , 2 PMe_3) is isolobal to the Cp^- and Tp^- ligands. Therefore, we have chosen to prepare a series of new catalysts, $(\text{Cp})(\text{ArN})\text{Mo}(\text{H})(\text{PMe}_3)_3$ and $(\text{Tp})(\text{ArN})\text{Mo}(\text{H})(\text{PMe}_3)_3$ (Scheme III-2), and to investigate their catalytic behaviour in hydrosilylation of both ketones and aldehydes. We also decided to study the hydrosilylation of ketones catalyzed by $(\text{ArN})\text{Mo}(\text{H})(\text{Cl})(\text{PMe}_3)_3$.



Scheme III-2. Preparation of $(\text{Cp})(\text{ArN})\text{Mo}(\text{H})(\text{PMe}_3)_3$ and $(\text{Tp})(\text{ArN})\text{Mo}(\text{H})(\text{PMe}_3)_3$ from $(\text{ArN})\text{Mo}(\text{H})(\text{Cl})(\text{PMe}_3)_3$.

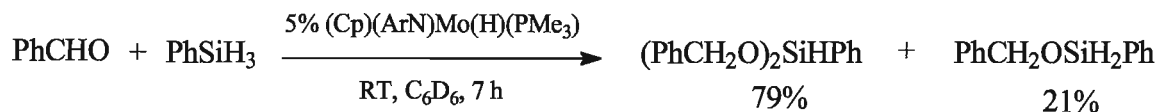
III. 1 Hydrosilylation catalyzed by (Cp)(ArN)Mo(H)(PMe₃)

The complex (Cp)(ArN)Mo(H)(PMe₃) was prepared by the reaction of (ArN)Mo(H)(Cl)(PMe₃)₃ with CpNa in THF (Scheme III-2) and characterized by NMR and IR spectroscopy. Compared to (ArN)Mo(H)(Cl)(PMe₃)₃, complex (Cp)(ArN)Mo(H)(PMe₃) is a more sluggish catalyst of hydrosilylation (Table III-1), which most likely reflects the fact that the PMe₃ ligand that dissociates from (Cp)(ArN)Mo(H)(PMe₃) to give a catalytically potent species is now “part of” the Cp ligand (Scheme III-2).

Table III-1. Hydrosilylation of carbonyls with PhSiH₃ catalyzed by (Cp)(ArN)Mo(H)(PMe₃).

<i>Substrate</i>	<i>Conversion of org. substrate</i>	<i>Product(s)</i>	<i>Conditions</i>	<i>Yield, %</i>
PhC(O)H	100%	PhCH ₂ OSiH ₂ Ph, (PhCH ₂ O) ₂ SiHPh	0.5 day, RT	21, 79
PhC(O)Me	0%	-	5 days, 50 °C	0, 0
Cyclohexanone	54%	CyOSiH ₂ Ph, (CyO) ₂ SiHPh	5 days, 50 °C	36, 18

The goal of the current research is to study the mechanism of hydrosilylation mediated by complex (Cp)(ArN)Mo(H)(PMe₃), choosing benzaldehyde and phenylsilane as model substrates (Scheme III-3).

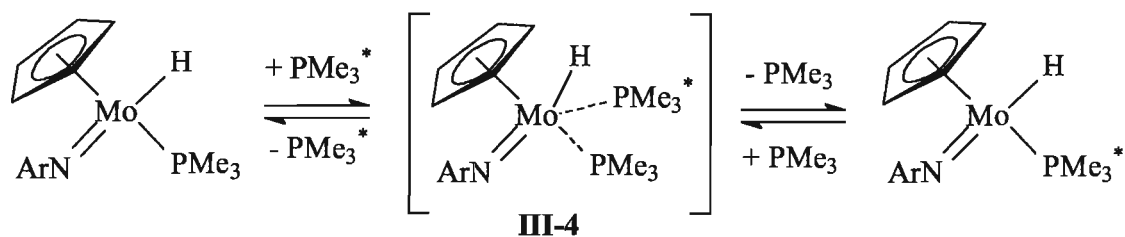


Scheme III-3. Hydrosilylation of benzaldehyde with phenylsilane in the presence of (Cp)(ArN)Mo(H)(PMe₃).

Complex (Cp)(ArN)Mo(H)(PMe₃) was found to react with both benzaldehyde and phenylsilane giving some derivatives. Below we provide the detailed kinetic investigation for each individual reaction, and discuss their mechanistic features.

III.1.1 Phosphine exchange between (Cp)(ArN)Mo(H)(PMe₃) and PMe₃

The possibility of phosphine dissociation from complex (Cp)(ArN)Mo(H)(PMe₃) requires special attention. First of all, we previously observed that the *trans*-PMe₃ ligand in complex (ArN)Mo(H)(Cl)(PMe₃)₃ undergoes dissociation to provide a vacancy on the metal center for further reactions with substrates.^{5a} In the latter compound, the phosphine experiences strong *trans*-influence of the hydride ligand, which promotes the dissociation.¹¹ We did not observe the dissociation of phosphine from complex (Cp)(ArN)Mo(H)(PMe₃); however, the phosphine ligand was found to be in a very fast exchange with free phosphine added to the solution. We studied this exchange by the Selective *ge*-1D EXSY (SELNOGP) NMR experiments and determined exchange rate constants at four temperatures: $(2.89 \pm 0.04) \cdot 10^1 \text{ s}^{-1}$ (12 °C), $(4.29 \pm 0.07) \cdot 10^1 \text{ s}^{-1}$ (22.0 °C), $(6.22 \pm 0.12) \cdot 10^1 \text{ s}^{-1}$ (32 °C) and $(8.56 \pm 0.15) \cdot 10^1 \text{ s}^{-1}$ (42.0 °C). The enthalpy and entropy of activation, $\Delta H^\ddagger = 24.7 \pm 0.4 \text{ kJ/mol}$ and $\Delta S^\ddagger = - (130 \pm 1) \text{ J/(K}\cdot\text{mol)}$, determined from the Eyring plot, suggest that the phosphine exchange is an *associative* reaction (Scheme III-4).



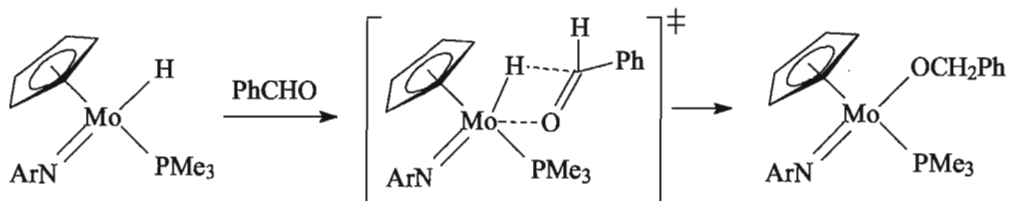
Scheme III-4. Phosphine exchange between (Cp)(ArN)Mo(H)(PMe₃) and PMe₃.

The associative mechanism is very surprising, given the fact that complex (Cp)(ArN)Mo(H)(PMe₃) is formally a saturated, 18e compound, if one considers M-imido bond as having triple character.¹⁴¹ To shed more light on this process, DFT

calculations ^a were carried out by Dr. Serge Gorelski from the University of Ottawa. Calculations found that the structure **III-4**, which is a minimum of the electron energy surface but a maximum of the free energy surface (due to the entropic factor). Therefore, the DFT calculations are consistent with our kinetic studies.

III.1.2 Reaction of (Cp)(ArN)Mo(H)(PMe₃) with benzaldehyde

Complex (Cp)(ArN)Mo(H)(PMe₃) slowly reacts with benzaldehyde with the formation of the alkoxy-derivative (Cp)(ArN)Mo(OCH₂Ph)(PMe₃) (Scheme III-5).

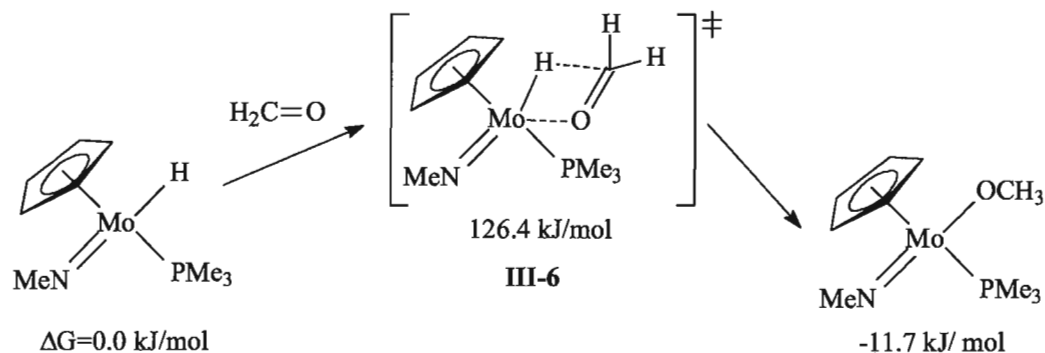


Scheme III-5. Reaction between (Cp)(ArN)Mo(H)(PMe₃) and benzaldehyde.

The reaction of complex (Cp)(ArN)Mo(H)(PMe₃) with 1 eq. of benzaldehyde was monitored by ¹H NMR. The kinetic data were linearized in the 1/C(PhCHO) vs time coordinates (See Chapter V for details), suggesting second-order kinetics. The rate constants were determined at four temperatures: $k(26\text{ }^{\circ}\text{C}) = (3.6 \pm 0.1) \cdot 10^{-3} \text{ M}^{-1} \cdot \text{s}^{-1}$, $k(40\text{ }^{\circ}\text{C}) = (1.25 \pm 0.17) \cdot 10^{-2} \text{ M}^{-1} \cdot \text{s}^{-1}$, $k(50\text{ }^{\circ}\text{C}) = (2.44 \pm 0.17) \cdot 10^{-2} \text{ M}^{-1} \cdot \text{s}^{-1}$, $k(60\text{ }^{\circ}\text{C}) = (4.17 \pm 0.05) \cdot 10^{-2} \text{ M}^{-1} \cdot \text{s}^{-1}$. The activation parameters, $\Delta H^{\ddagger} = 57.6 \pm 3.6 \text{ kJ/mol}$ and $\Delta S^{\ddagger} = -(99.7 \pm 11.4) \text{ J/(K} \cdot \text{mol)}$, extracted from Eyring plot, suggest that the reaction proceeds via an associative mechanism. We additionally demonstrated that the reaction rate constant does not depend on phosphine concentration, and thus, the dissociative mechanism is unlikely for this system.

^a Details of the DFT calculations will be further provided.

DFT studies of a model system ($\text{CH}_2=\text{O}$ for carbonyl, SiH_4 for silane, and $(\text{Cp})(\text{MeN})\text{Mo}(\text{H})(\text{PMe}_3)$ for complex) found that the reaction proceeds via the transition state **III-6** (associative mechanism) (Scheme III-6).



Scheme III-6. Calculated mechanism of the reaction between $(\text{Cp})(\text{MeN})\text{Mo}(\text{H})(\text{PMe}_3)$ and $\text{CH}_2=\text{O}$.

Complex $(\text{Cp})(\text{ArN})\text{Mo}(\text{OCH}_2\text{Ph})(\text{PMe}_3)$ has been individually synthesized and characterized by NMR and X-ray diffraction analysis (see Chapter VI, Table VI-1 for the crystal structure determination parameters).

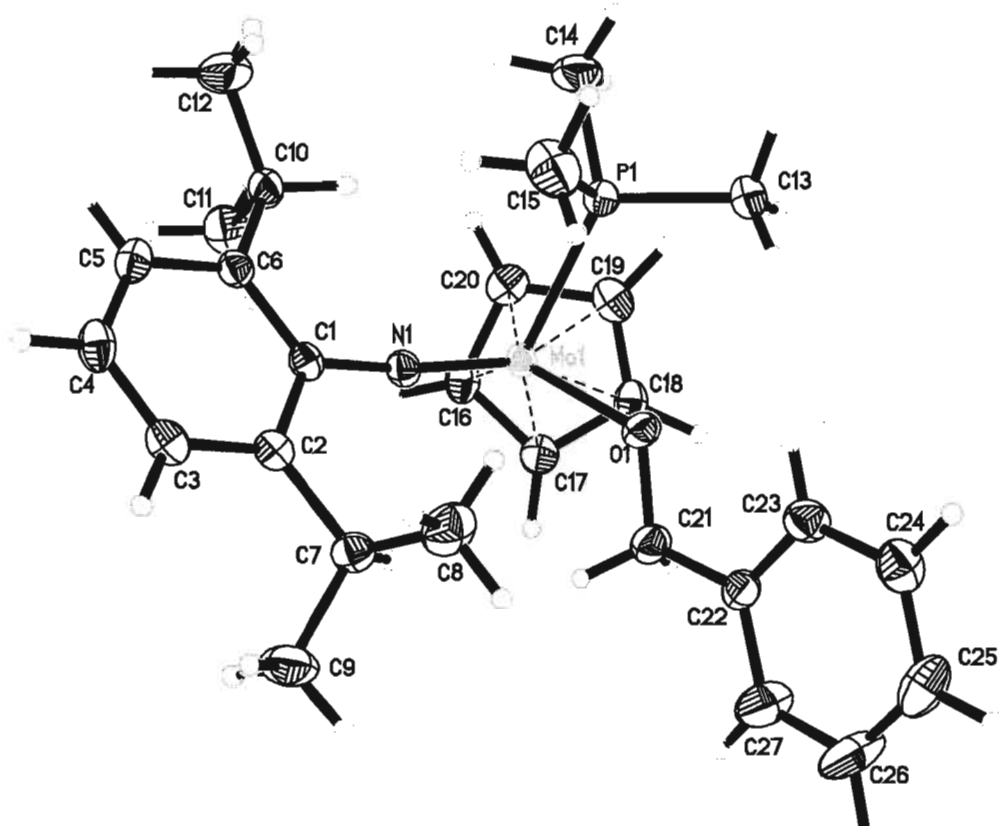


Figure III-1. ORTEP plot of the molecular structure of (Cp)(ArN)Mo(OCH₂Ph)(PMe₃) (one of two independent molecules is shown). Anisotropic displacement ellipsoids are plotted at 50% probability.

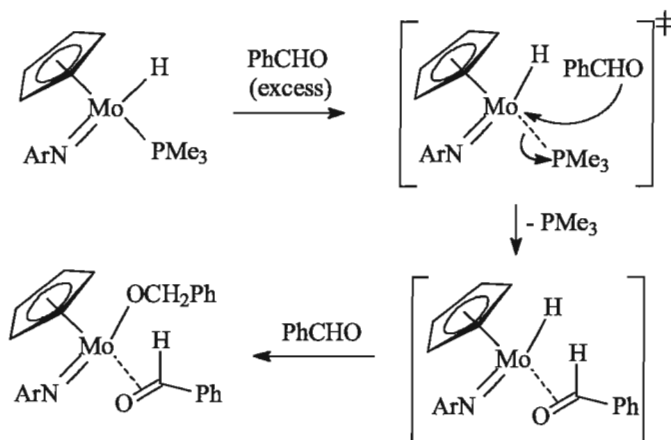
Table III-2. Selected bond distances (Å) and angles (°) for (Cp)(ArN)Mo(OCH₂Ph)(PMe₃)

<i>distances, Å</i>		<i>angles, °</i>	
Mo1-N1	1.7652(14)	C1-N1-Mo1	173.38(12)
Mo1-O1	2.0485(11)	O1-Mo1-P1	80.26(4)

Mo1-P1	2.4336(5)	N1-Mo1-O1	105.58(6)
Mo1-C16	2.2085(17)	N1-Mo1-P1	98.95(5)
Mo1-C17	2.3147(17)	C21-O1-Mo1	118.93(10)
Mo1-C18	2.4603(18)	O1-Mo1-C18	83.40(6)
Mo1-C19	2.4287(18)	O1-Mo1-C17	98.41(6)
Mo1-C20	2.2665(17)	O1-Mo1-C19	101.50(6)
		N1-Mo1-C18	156.35(6)
		N1-Mo1-C19	152.41(7)

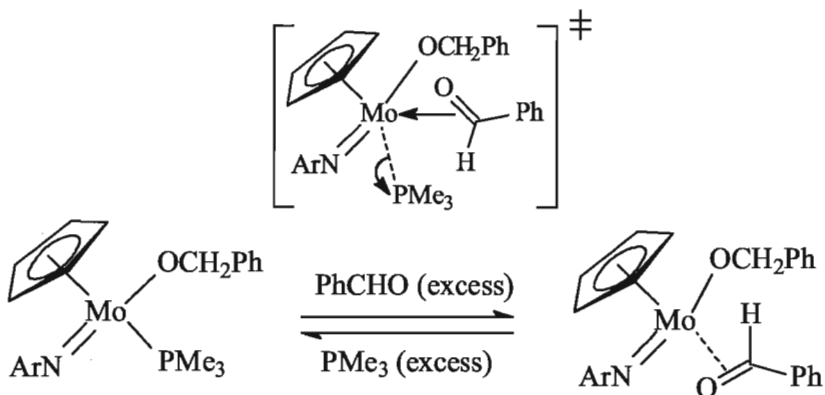
Complex (Cp)(ArN)Mo(OCH₂Ph)(PMe₃) (Figure III-1) adopts a pseudo-octahedral geometry, if the Cp-ligand is considered as occupying three coordination sites, one axial and two equatorial positions. The atoms C19 and C18 of the Cp ring are located *trans*- to the imido group and are characterized by relatively longer Mo1-C19 and Mo1-C18 distances than the Mo1-C16, Mo1-C17, and Mo1-C20 bonds (Table III-2). This may be a result of the strong *trans*-influence of the imido group.¹⁴² The C1-N1-Mo1 linkage is almost linear, 173.38(12)°, which can indicate that the imido group is a six electron donor to the molybdenum stabilizing its 18e⁻ valence shell.¹⁴¹

The treatment of (Cp)(ArN)Mo(H)(PMe₃) with excess benzaldehyde (20 eq.) provides formation of an η^2 -aldehyde complex (Cp)(ArN)Mo(OCH₂Ph)(η^2 -PhCHO) as the sole product within one hour at RT. The complex was obtained as a mixture of two isomers. The upfield shifted PhCHO signals at 5.58 and 6.08 ppm (for two isomers) indicate the η^2 -coordination mode of the aldehyde.¹⁴³ Alternatively, complex (Cp)(ArN)Mo(OCH₂Ph)(η^2 -PhCHO) can be prepared, but at a much slower rate (one day at RT), by the treatment of (Cp)(ArN)Mo(OCH₂Ph)(PMe₃) with 20 eq. of benzaldehyde. This observation suggests that formation of the benzaldehyde η^2 -complex from (Cp)(ArN)Mo(H)(PMe₃) does not proceed via the benzyloxy-phosphine complex (Cp)(ArN)Mo(OCH₂Ph)(PMe₃). Possibly, the benzaldehyde associatively substitutes the labile phosphine ligand to form a [(Cp)(ArN)Mo(H)(PhCHO)] intermediate, followed by a reaction with the second equivalent of benzaldehyde (Scheme III-7).



Scheme III-7. Proposed mechanism for the reaction between $(\text{Cp})(\text{ArN})\text{Mo}(\text{H})(\text{PMe}_3)$ and excess benzaldehyde.

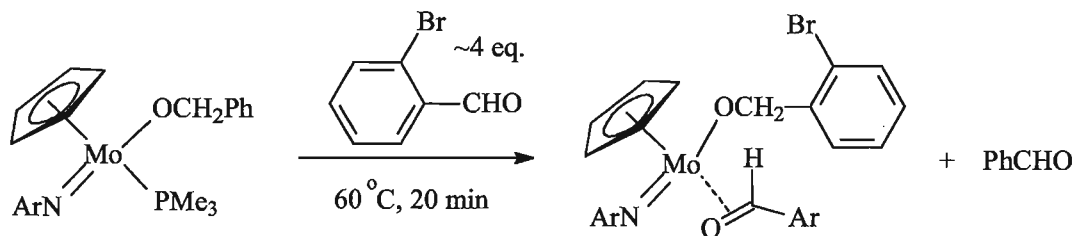
Kinetic parameters for the reaction between $(\text{Cp})(\text{ArN})\text{Mo}(\text{OCH}_2\text{Ph})(\text{PMe}_3)$ and benzaldehyde (10 eq.) have been determined at three temperatures: $k(26.0\text{ }^\circ\text{C}) = (3.66 \pm 0.03) \cdot 10^{-5}\text{ s}^{-1}$, $k(40.0\text{ }^\circ\text{C}) = (2.31 \pm 0.05) \cdot 10^{-4}\text{ s}^{-1}$, and $k(55.0\text{ }^\circ\text{C}) = (1.08 \pm 0.03) \cdot 10^{-3}\text{ s}^{-1}$. The activation parameters suggest that the reaction most likely proceeds via an associative mechanism: $\Delta H^\ddagger = (92.5 \pm 4.3)\text{ kJ/mol}$, $\Delta S^\ddagger = -(20.3 \pm 13.6)\text{ J/(K}\cdot\text{mol)}$ (Scheme III-8).



Scheme III-8. Proposed mechanism for the reaction between $(\text{Cp})(\text{ArN})\text{Mo}(\text{OCH}_2\text{Ph})(\text{PMe}_3)$ and benzaldehyde.

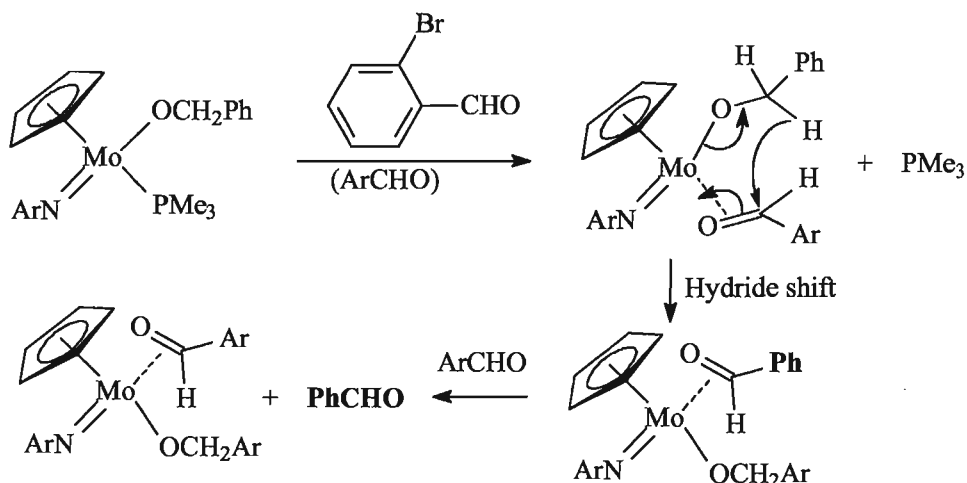
Excess of phosphine cleanly substitutes the η^2 -coordinated benzaldehyde in $(\text{Cp})(\text{ArN})\text{Mo}(\text{OCH}_2\text{Ph})(\eta^2\text{-PhCHO})$ to regenerate the alkoxy phosphine complex $(\text{Cp})(\text{ArN})\text{Mo}(\text{OCH}_2\text{Ph})(\text{PMe}_3)$ (Scheme III-8).

To check if the reaction between $(\text{Cp})(\text{ArN})\text{Mo}(\text{H})(\text{PMe}_3)$ and benzaldehyde is reversible, the benzyloxy complex was treated with excess *o*-bromobenzaldehyde. No reaction was observed at RT, but heating at 60 °C resulted in the formation of free benzaldehyde in the reaction mixture (detected by ^1H NMR) (Scheme III-9).



Scheme III-9. Reaction between $(\text{Cp})(\text{ArN})\text{Mo}(\text{OCH}_2\text{Ph})(\text{PMe}_3)$ and *o*-bromobenzaldehyde.

We believe that this reaction may be initiated by the substitution of the phosphine ligand by *o*-bromobenzaldehyde followed by intramolecular interligand hydride shift from the methylene group to the η^2 -coordinated *o*-bromobenzaldehyde.¹⁴⁴ The η^2 -benzaldehyde thus formed may be then released by a substitution reaction with excess *o*-bromobenzaldehyde (Scheme III-10).



Scheme III-10. Proposed mechanism for the reaction between $(\text{Cp})(\text{ArN})\text{Mo}(\text{OCH}_2\text{Ph})(\text{PMe}_3)$ and *o*-bromobenzaldehyde.

As long as this reaction requires heating, we conclude that the catalytic hydrosilylation at RT involves irreversible addition of benzaldehyde to $(\text{Cp})(\text{ArN})\text{Mo}(\text{H})(\text{PMe}_3)$ to give $(\text{Cp})(\text{ArN})\text{Mo}(\text{OCH}_2\text{Ph})(\text{PMe}_3)$.

III.1.3 Reactions of $(\text{Cp})(\text{ArN})\text{Mo}(\text{H})(\text{PMe}_3)$ with ketones

Complex $(\text{Cp})(\text{ArN})\text{Mo}(\text{H})(\text{PMe}_3)$ was stable in the presence of excess acetone (up to 5 eq.) and did not react. Heating the reaction mixture resulted in decomposition of the hydride complex. The complex was stable in the presence of a large excess of acetophenone (up to 5-10 eq.) and did not react even under heating at 50 °C for several days. The hydrosilylation of either acetophenone or acetone was not observed.

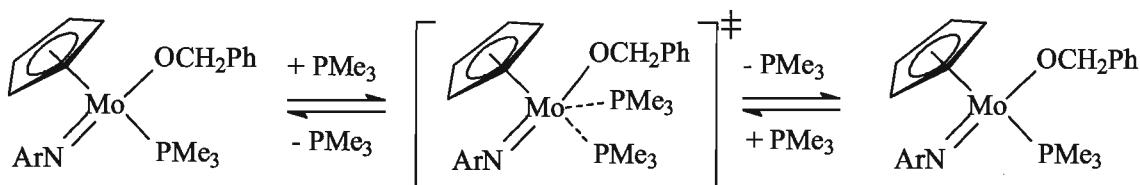
III.1.4 Reactions of $(\text{Cp})(\text{ArN})\text{Mo}(\text{H})(\text{PMe}_3)$ with alcohols

The hydride complex $(\text{Cp})(\text{ArN})\text{Mo}(\text{H})(\text{PMe}_3)$ is relatively stable when dissolved in pure ethanol or *iso*-propanol. However, heating the alcohol solutions at 50 °C results in decomposition of the complex. Experiments with *iso*-propanol- d_8 did not reveal any H/D exchange between the Mo-H and O-D groups.

III.1.5 Phosphine exchange between

(Cp)(ArN)Mo(OCH₂Ph)(PMe₃) and PMe₃

Benzyloxy-phosphine complex (Cp)(ArN)Mo(OCH₂Ph)(PMe₃), like (Cp)(ArN)Mo(H)(PMe₃), exchanges the bound phosphine with free phosphine in solutions (Scheme III-11).

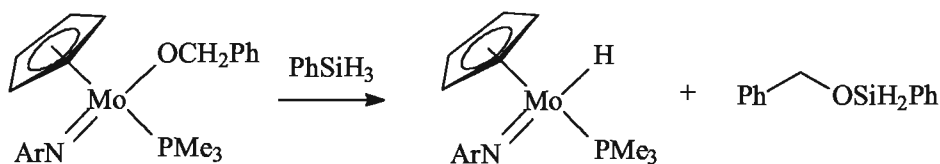


Scheme III-11. Phosphine exchange between (Cp)(ArN)Mo(OCH₂Ph)(PMe₃) and PMe₃.

The exchange has been studied using ³¹P-³¹P EXSY NMR spectroscopy at 40, 50, 60 and 70 °C. With the mixing time of 0.300 s, cross-peaks were observed between the free and bound phosphine, indicating their exchange. At a mixing time of 0.003 s, there were no cross-peaks. The cross-peaks have been integrated by means of TOP SPIN Bruker NMR software. Exchange rates have been calculated using EXSY Calc MestRe software: $k(40\text{ °C}) = 0.655\text{ s}^{-1}$, $k(50\text{ °C}) = 0.805\text{ s}^{-1}$, $k(60\text{ °C}) = 0.965\text{ s}^{-1}$ and $k(70\text{ °C}) = 1.230\text{ s}^{-1}$. The thermodynamic parameters of activation have been extracted from the Eyring plot: $\Delta H^\ddagger = 15.8 \pm 1.0\text{ kJ/mol}$ and $\Delta S^\ddagger = -199 \pm 3\text{ J/(K}\cdot\text{mol)}$. The negative entropy of activation indicates an associative mechanism of the reaction (Scheme III-11).

III.1.6 Reaction between (Cp)(ArN)Mo(OCH₂Ph)(PMe₃) and PhSiH₃

The benzyloxy-phosphine complex (Cp)(ArN)Mo(OCH₂Ph)(PMe₃) cleanly reacts with PhSiH₃, giving the hydrosilylation products PhCH₂OSiH₂Ph and (PhCH₂O)₂SiHPh and regenerating the starting hydrido phosphine complex (Cp)(ArN)Mo(H)(PMe₃).

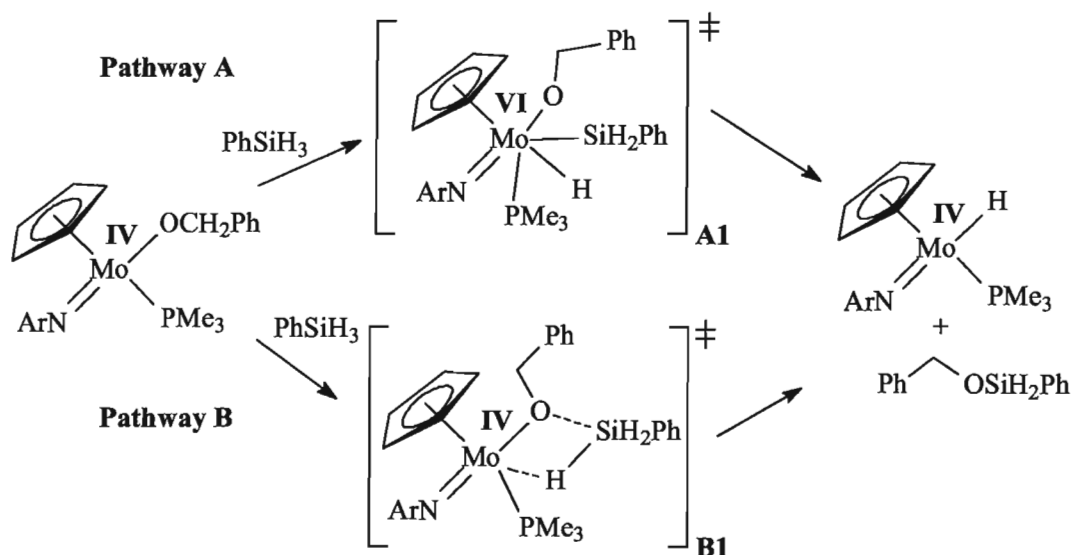


Scheme III-12. Reaction between (Cp)(ArN)Mo(OCH₂Ph)(PMe₃) and PhSiH₃.

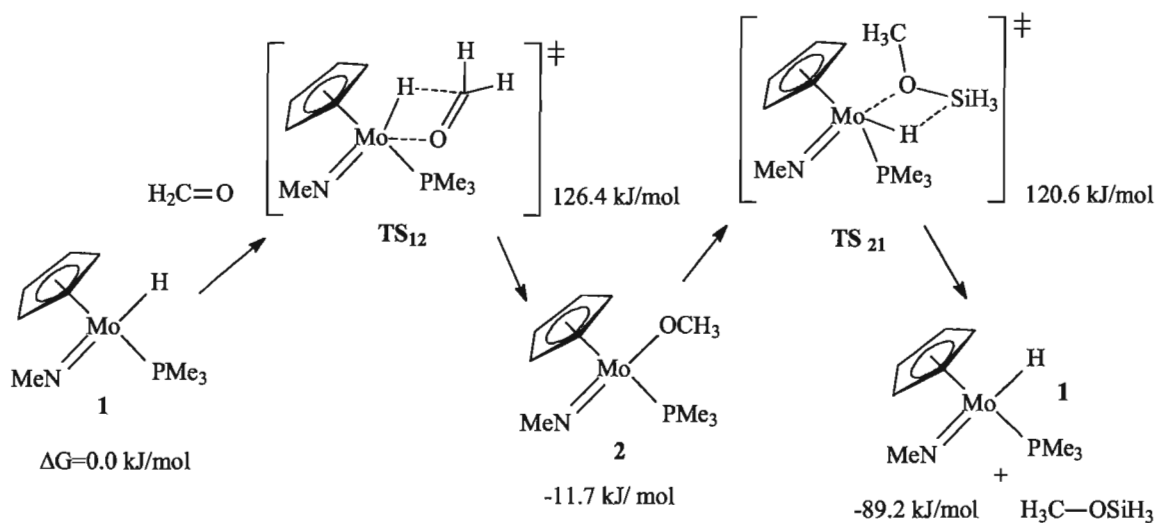
Kinetic studies may indicate that the reaction proceeds via an associative mechanism: $\Delta H^\ddagger = 58.9 \pm 4.9$ kJ/mol, $\Delta S^\ddagger = -111 \pm 16$ J/(K·mol). We envisioned that the possible associative reaction could proceed either via the oxidative addition of silane (Pathway A) or via the heterolytic splitting of the Si-H bond on the Mo-O bond (Pathway B) (Scheme III-13).

The oxidative addition of silane (Pathway A, Scheme III-13) is disfavoured because of the steric strain in the intermediate A1. Alternatively, the alkoxy and the imido groups may be considered as the potential sites for a silane attack as shown in Pathway B. The Mo-O bond is more preferable on the premises of charge concentration and steric accessibility. Therefore, we suggested that the complex (Cp)(ArN)Mo(OCH₂Ph)(PMe₃) reacts with silane according to Pathway B (Scheme III-13).

DFT studies of a model system (CH₂=O for carbonyl, SiH₄ for silane, and (Cp)(MeN)Mo(H)(PMe₃) for complex) allowed us to determine the most preferable pathway of hydrosilylation (Scheme III-14). It was found that carbonyl inserts into the Mo-H bond of **1** via the transition state TS₁₂ with the formation of the alkoxy complex **2**. The latter reacts with silane via a very late transition state TS₂₁ to give the initial complex **1** and silyl ether.



Scheme III-13. Proposed pathways for the reaction between $(\text{Cp})(\text{ArN})\text{Mo}(\text{OCH}_2\text{Ph})(\text{PMe}_3)$ and PhSiH_3 .



Scheme III-14. Calculated mechanism of carbonyl hydrosilylation.

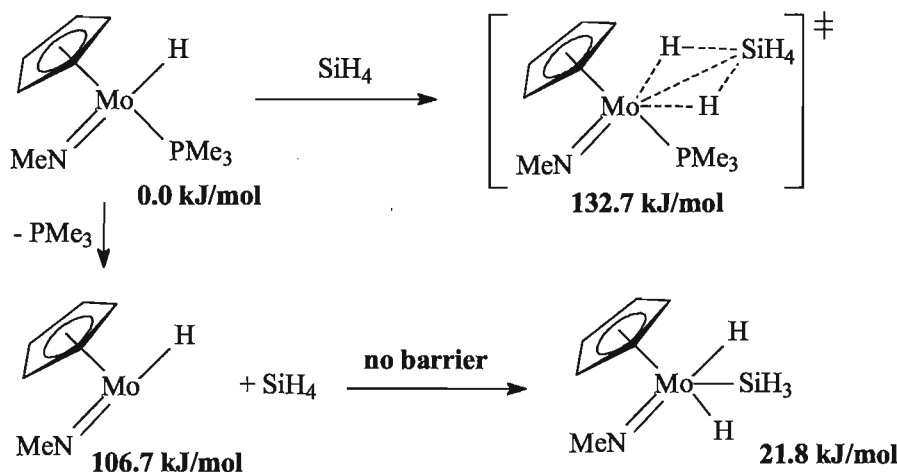
Further kinetic studies with the deuterated silane PhSiD_3 revealed that the kinetic isotope effect for the reaction between $(\text{Cp})(\text{ArN})\text{Mo}(\text{OCH}_2\text{Ph})(\text{PMe}_3)$ and PhSiH_3 or PhSiD_3 changes dramatically at different temperatures (Table III-3). Such small values of the KIE and its temperature behaviour indicate that the cleavage of the Si—H bond is not the only contribution to the activation energy barrier. The calculated KIE at 25 °C is 1.0.

Table III-3. Rate constants and kinetic isotope effect for the reaction between (Cp)(ArN)Mo(OCH₂Ph)(PMe₃) and PhSiH₃/PhSiD₃ (10 eq.)

T, °C	k_H (PhSiH ₃), s ⁻¹	k_D (PhSiD ₃), s ⁻¹	KIE, k_H/k_D
16.0	$(1.97 \pm 0.02) \cdot 10^{-4}$	$(2.7 \pm 0.02) \cdot 10^{-4}$	0.73
26.0	$(5.85 \pm 0.03) \cdot 10^{-4}$	$(7.40 \pm 0.02) \cdot 10^{-4}$	0.79
36.0	$(1.22 \pm 0.01) \cdot 10^{-3}$	$(1.09 \pm 0.01) \cdot 10^{-3}$	1.12
46.0	$(2.21 \pm 0.16) \cdot 10^{-3}$	$(1.60 \pm 0.03) \cdot 10^{-3}$	1.38

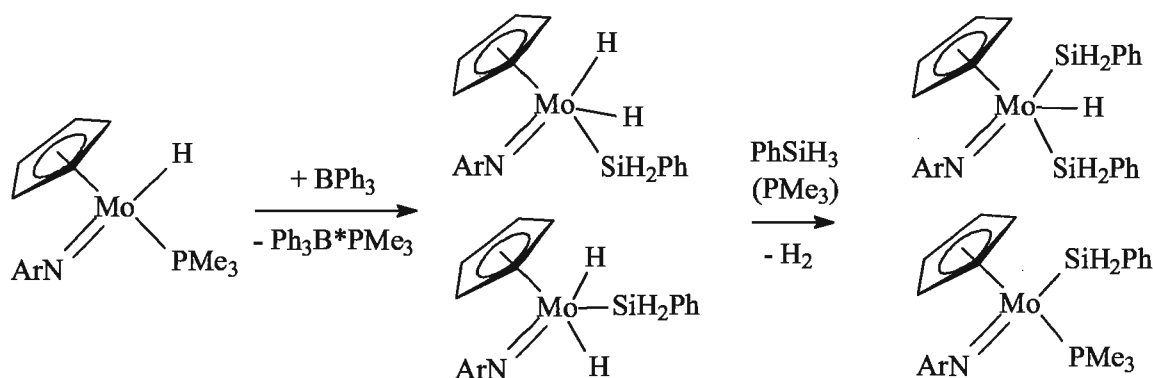
III.1.7 Reaction of (Cp)(ArN)Mo(H)(PMe₃) with PhSiH₃

In the experiments with the deuterated silane PhSiD₃, we found that complex (Cp)(ArN)Mo(H)(PMe₃) exchanges its hydride for deuterium. We were unable to obtain the activation parameters of the exchange because it is too slow and concurrent with the dehydrogenative addition of silane to give the silyl derivative (Cp)(ArN)Mo(SiH₂Ph)(PMe₃) (see below). A DFT study suggests that the reaction possibly goes via phosphine dissociation followed by oxidative addition of the silane with the formation of a dihydride silyl species (Scheme III-15).



Scheme III-15. Computed reaction pathways for formation of (Cp)(MeN)MoH₂(SiH₃) (at 298 K).

Formation of an isomeric mixture of dihydride silyl species $(\text{Cp})(\text{ArN})\text{Mo}(\text{H})_2(\text{SiH}_2\text{Ph})$ and $(\text{Cp})(\text{ArN})\text{Mo}(\text{H})(\text{SiH}_2\text{Ph})(\text{H})$ (1:5) was indeed observed when the reaction of $(\text{Cp})(\text{ArN})\text{Mo}(\text{H})(\text{PMe}_3)$ with PhSiH_3 was carried out in the presence of BPh_3 . These intermediate species further release molecular hydrogen and react with the second equivalent of PhSiH_3 to give finally the bis(silyl) hydride molybdenum(VI) complex $(\text{Cp})(\text{ArN})\text{Mo}(\text{SiH}_2\text{Ph})_2(\text{H})$ and $(\text{Cp})(\text{ArN})\text{Mo}(\text{SiH}_2\text{Ph})(\text{PMe}_3)$ in the 8:1 ratio (Scheme III-16).

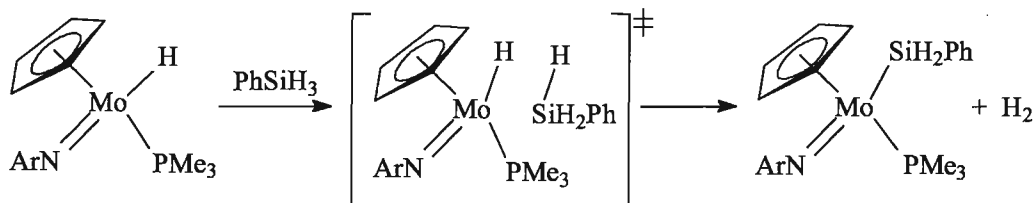


Scheme III-16. Reaction of $(\text{Cp})(\text{ArN})\text{Mo}(\text{H})(\text{PMe}_3)$ with PhSiH_3 (>2 eq.) in the presence of BPh_3 .

The absence of significant Si-H coupling constant ($J < 10$ Hz) in the observed silyl di- and mono-hydride complexes may indicate that they have no significant Si-HMo interactions, and they are, therefore, the derivatives of Mo(VI). An example of Mo(VI) hydride (Cp^*MoH_5) has been reported,¹⁴⁵ but to the best of our knowledge silyl hydride derivatives of Mo(VI) are not known.

In the absence of BPh_3 , complex $(\text{Cp})(\text{ArN})\text{Mo}(\text{H})(\text{PMe}_3)$ slowly reacts with phenylsilane to give the silyl phosphine derivative $(\text{Cp})(\text{ArN})\text{Mo}(\text{SiH}_2\text{Ph})(\text{PMe}_3)$. Kinetic studies show that this reaction proceeds with a small entropy of activation, which is indicative of the absence of a well-defined rate-limiting step: $\Delta H^\ddagger = 66.1 \pm 3$ kJ/mol, $\Delta S^\ddagger = -110 \pm 10$ J/(K·mol). The reaction was also carried out in the presence of different amounts of free PMe_3 . We observed no dependence of the reaction rate constant on the phosphine concentration, suggesting the absence of PMe_3 dissociation. The kinetic isotope effect was found to be 1.0. These results suggest that the reaction could proceed

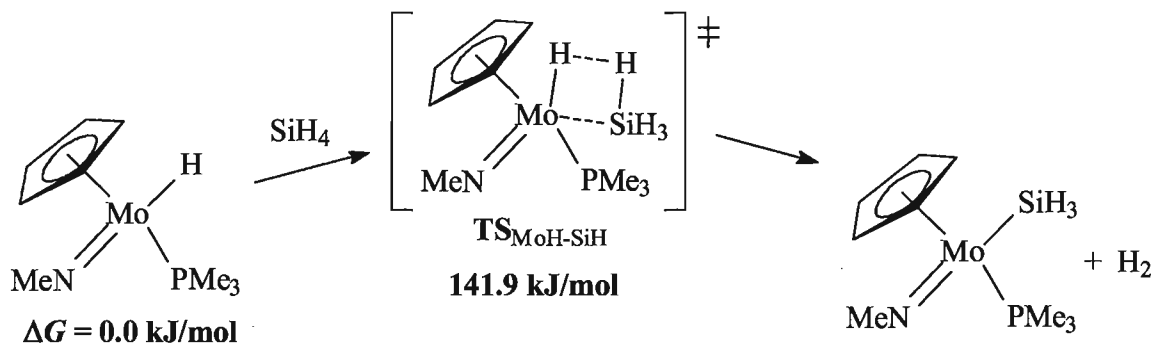
via a σ -bond metathesis mechanism^{61b, 146} to avoid the formation of an unfavourable Mo(VI) species (Scheme III-17).



Scheme III-17. Reaction between $(\text{Cp})(\text{ArN})\text{Mo}(\text{H})(\text{PMe}_3)$ and PhSiH_3 .

The σ -bond metathesis mechanism was originally discovered and elaborated for early transition metals in the d^0 configuration¹⁴⁷, and there are also a few well-documented examples for late transition metals.¹⁴⁸ DFT calculations of the transition state $\text{TS}_{\text{MoH-SiH}}$ (Scheme III-18) showed that the Si—H (1.614 Å) and the H—H (2.149 Å) distances are characteristic for σ -bond metathesis.¹⁴⁹ Calculations also suggested that there is no formation of a silyl σ -complex, possibly due to the weak antibonding character of the LUMO $\pi^*(\text{Mo-N})$ orbital of $(\text{Cp})(\text{ArN})\text{Mo}(\text{H})(\text{PMe}_3)$.

Although the σ -bond metathesis mechanism has been reported for some *late* metal systems, this is only the second case of a σ -bond metathesis mechanism for an *early* transition metal complex with d^n ($n \geq 2$) configuration.¹⁵⁰

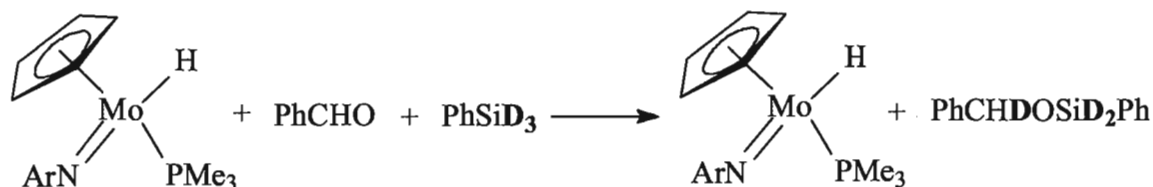


Scheme III-18. Computed reaction pathway for formation of $(\text{Cp})(\text{MeN})\text{Mo}(\text{SiH}_3)(\text{PMe}_3)$ (at 298 K)

Complex $(\text{Cp})(\text{ArN})\text{Mo}(\text{SiH}_2\text{Ph})(\text{PMe}_3)$ does not react with benzaldehyde at ambient and elevated temperatures and is not active as a hydrosilylation catalyst.

III.1.8 Stoichiometric reaction between (Cp)(ArN)Mo(H)(PMe₃), PhCHO and PhSiD₃

When complex (Cp)(ArN)Mo(H)(PMe₃) is mixed with stoichiometric (1:1:1) amounts of benzaldehyde and PhSiD₃, the hydrosilylation proceeds rapidly (< 5 min) to give a mixture of PhCHDOSiD₂Ph and the initial catalyst (Cp)(ArN)Mo(H)(PMe₃) (Scheme III-19).



Scheme III-19. Stoichiometric reaction between (Cp)(ArN)Mo(H)(PMe₃), PhCHO and PhSiD₃.

The 100% retention of the hydride at the Mo centre indicates that under the stoichiometric conditions, there is no significant insertion of benzaldehyde into the Mo—H bond to form the alkoxy complex. Otherwise, the reaction would have provided the deuterated derivative of the molybdenum hydride complex, i.e. (Cp)(ArN)Mo(D)(PMe₃). This experiment demonstrated the existence of an alternative mechanism of hydrosilylation catalysis, where the molybdenum hydride complex possibly activates the substrates as a Lewis acid without the direct involvement of the Mo—H bond. All mechanisms of metal catalyzed hydrosilylation discussed so far involved the formation of a metal hydride complex and its reaction with substrates, with the hydride shift to substrate being the key reduction step, so called *hydride mechanism*.¹⁵¹ The hydrosilylation of carbonyls in which the M—H bond plays the role of a spectator ligand has never been reported in the literature.

III. 2 Hydrosilylation catalyzed by (Tp)(ArN)Mo(H)(PMe₃)

To underpin the ligand effect on the course and mechanism of hydrosilylation, we decided to study the catalyst (Tp)(ArN)Mo(H)(PMe₃), an isolobal analogue of complex Cp(ArN)Mo(H)(PMe₃). The new compound (Tp)(ArN)Mo(H)(PMe₃) was prepared by the reaction of (ArN)Mo(H)(Cl)(PMe₃) with KTp in 74% yield. It was studied by spectroscopic methods and its molecular structure was characterized by X-ray diffraction analysis (See chapter VI, Table VI-2 for the crystal structure determination parameters).

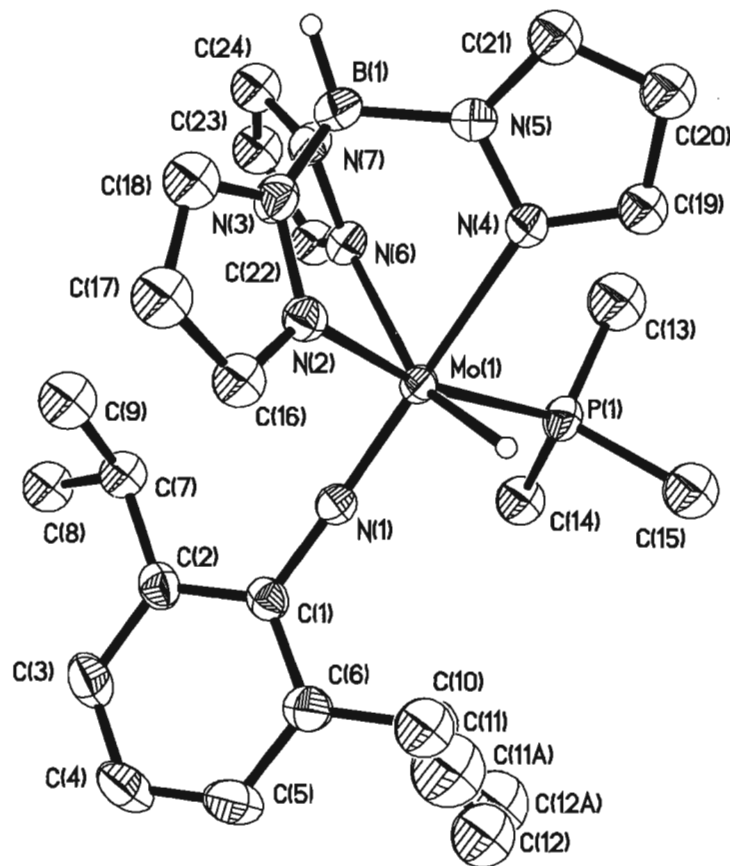


Figure III-2. ORTEP plot of the molecular structure of (Tp)(ArN)Mo(H)(PMe₃) (All hydrogen atoms except BH and MoH are omitted for clarity. One of two independent molecules is shown). Anisotropic displacement parameters are plotted at 50% probability.

Table III-4. Selected bond distances (Å) and angles (°) for (Tp)(ArN)Mo(Cl)(PMe₃).

<i>distances, Å</i>		<i>angles, °</i>	
Mo1-H1	1.66(3)	N1-Mo1-N2	95.69(8)
Mo1-P1	2.4322(6)	N1-Mo1-N6	106.95(8)
Mo1-N1	1.7544(19)	N1-Mo1-N4	172.62(8)
Mo1-N2	2.2003(19)	N1-Mo1-H1	97.2(11)
Mo1-N6	2.230(2)	N2-Mo1-H1	88.6(11)
Mo1-N4	2.311(2)	N6-Mo1-H1	155.5(11)
		N4-Mo1-H1	77.9(11)
		P1-Mo1-H1	86.7(11)
		C1-N1-Mo1	170.51(17)

The molecular structure of (Tp)(ArN)Mo(H)(PMe₃) adopts an octahedral geometry, with one of the pyrazolyl group lying *trans*- to the imido-group, and two other pyrazolyl groups with the hydride and PMe₃ in the equatorial position (Figure III-2). The linkage C1-N1-Mo1 is almost linear (170.51(17) °) (Table III-4), which can indicate that the imido group is a six electron donor to the molybdenum stabilizing its 18e⁻ valence shell.¹⁴¹ The bonds Mo1-N2, Mo1-N6 and Mo1-N4 have different lengths, and the *trans*- to the imido group Mo1-N4 distance is the longest, possibly due to the strongest *trans*-influence of the imido group.

III.2.1 Hydrosilylation catalyzed by (Tp)(ArN)Mo(H)(PMe₃)

We found that complex (Tp)(ArN)Mo(H)(PMe₃) catalyzes the hydrosilylation of a variety of aldehydes and ketones (Table III-5).^b The best results were observed when PhSiH₃ was used as a hydrosilylating agent. The hydrosilylation with PhMeSiH₂ required elevated temperatures and extended reaction time. The hydrosilylation with PhMe₂SiH, (EtO)₃SiH and Et₃SiH was not observed, possibly due to the high steric congestion.

Table III-5. Hydrosilylation of various substrates catalyzed by (Tp)(ArN)Mo(H)(PMe₃).

Substrate	Silane	Product	Reaction conditions	Yield, according to ¹ H-NMR
PhCHO	PhSiH ₃	PhCH ₂ OSiH ₂ Ph (PhCH ₂ O) ₂ SiHPh	0.5 d, RT	38% 62%
PhCOCH ₃	PhSiH ₃	PhSiH ₂ OCH(Me)Ph PhSiH(OCH(Me)Ph) ₂	1.5 d, RT	85% 15%
Cyclohexanone	PhSiH ₃	CyOSiH ₂ Ph (CyO) ₂ SiHPh	53 min, RT	85% 15%
PhCHO	PhMeSiH ₂	PhCH ₂ OSiHMePh	1.5 d, 50 °C	30%
PhCOCH ₃	PhMeSiH ₂	PhMeSiHOCH(Me)Ph	2.5 d, 50 °C	100%
Cyclohexanone	PhMeSiH ₂	CyOSiHMePh (CyO) ₂ SiMePh	1 d, RT	96% 4%
Cyclohexanone	PhMe ₂ SiH	CyOSiMe ₂ Ph	1.5 d, 50 °C	11%

III.2.2 Dissociation of the Tp ligand

The possibility of the dissociation of Tp ligand may play an important role in catalysis and requires special attention. We found (by EXSY NMR) that the pyrazolyl groups of the Tp ligand are in a very fast exchange: $k(17.0\text{ °C}) = 0.618\text{ s}^{-1}$, $k(22.0\text{ °C}) = 1.138\text{ s}^{-1}$, $k(27.0\text{ °C}) = 2.077\text{ s}^{-1}$, $k(32.0\text{ °C}) = 3.407\text{ s}^{-1}$, $\Delta H^\ddagger = 81.8 \pm 2.1\text{ kJ/mol}$, $\Delta S^\ddagger = 32.4 \pm 7.0\text{ J/(K}\cdot\text{mol)}$. We assume that this exchange may be caused by dissociation of the

^b Also see Table V-4 for more detailed information.

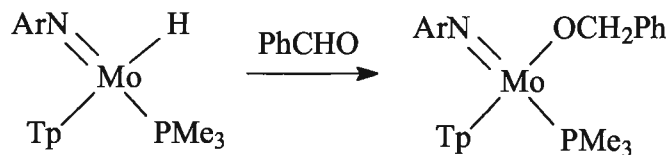
pyrazolyl group lying *trans* to the imido ligand, because of its largest (Pz)N—Mo bond length (*i.e.* the weakest bond) of all three (Pz)N—Mo bonds.

III.2.3 Phosphine exchange between (Tp)(ArN)Mo(H)(PMe₃) and free PMe₃

Unlike (Cp)(ArN)Mo(H)(PMe₃), complex (Tp)(ArN)Mo(H)(PMe₃) does not exchange the bound phosphine ligand with free PMe₃. Heating the solution containing molybdenum hydride complex did not result in the appearance of free PMe₃ in ¹H NMR.^c The solution containing a mixture of (Tp)(ArN)Mo(H)(PMe₃) and free PMe₃ was studied by EXSY NMR at different temperatures, and the phosphine exchange was not observed.

III.2.4 Reaction between (Tp)(ArN)Mo(H)(PMe₃) and carbonyls

Complex (Tp)(ArN)Mo(H)(PMe₃) reacts with benzaldehyde with formation of an alkoxy complex (Tp)(ArN)Mo(OCH₂Ph)(PMe₃) (Scheme III-20).



Scheme III-20. Reaction between (Tp)(ArN)Mo(H)(PMe₃) and PhCHO.

We determined the reaction rate constants and the activation parameters: $k(26\text{ }^{\circ}\text{C}) = (8.75 \pm 0.10) \cdot 10^{-4} \text{ M}^{-1} \cdot \text{s}^{-1}$, $k(36.0\text{ }^{\circ}\text{C}) = (1.005 \pm 0.003) \cdot 10^{-2} \text{ M}^{-1} \cdot \text{s}^{-1}$, $k(46.0\text{ }^{\circ}\text{C}) = (1.50 \pm 0.03) \cdot 10^{-2} \text{ M}^{-1} \cdot \text{s}^{-1}$, $k(55.6\text{ }^{\circ}\text{C}) = (1.18 \pm 0.02) \cdot 10^{-1} \text{ M}^{-1} \cdot \text{s}^{-1}$, $\Delta H^{\ddagger} = 103 \pm 7 \text{ kJ/mol}$, $\Delta S^{\ddagger} = 45.3 \pm 53.5 \text{ J/(K} \cdot \text{mol)}$. The large uncertainty in determination of the entropy of activation

^c Previously, we observed some amounts of free PMe₃ by ¹H and ³¹P NMR in the solutions of (ArN)Mo(H)(Cl)(PMe₃) and (ArN)(CyO)Mo(Cl)(PMe₃) formed as a result of dissociation.

does not allow us to differentiate between a dissociative mechanism (e.g. dissociation of the pyrazolyl ligand) and an associative step (e.g. via addition of carbonyl).

We have found that the reaction rate does not depend on the PMe_3 concentration (Figure III-3). We may conclude that dissociation of the phosphine in the reaction between $(\text{Tp})(\text{ArN})\text{Mo}(\text{H})(\text{PMe}_3)$ and PhCHO does not take place.

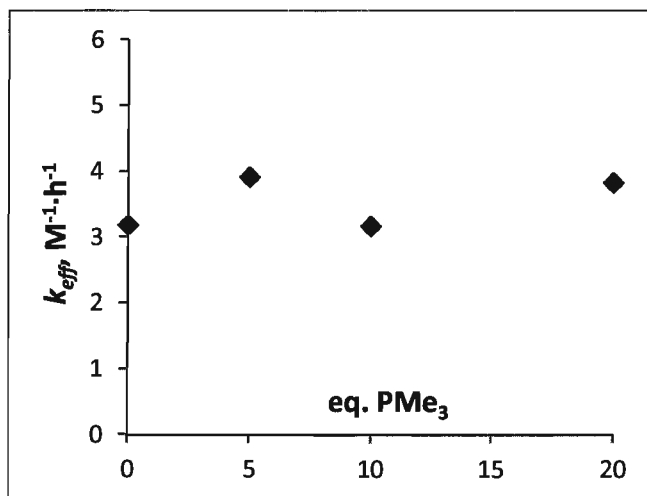
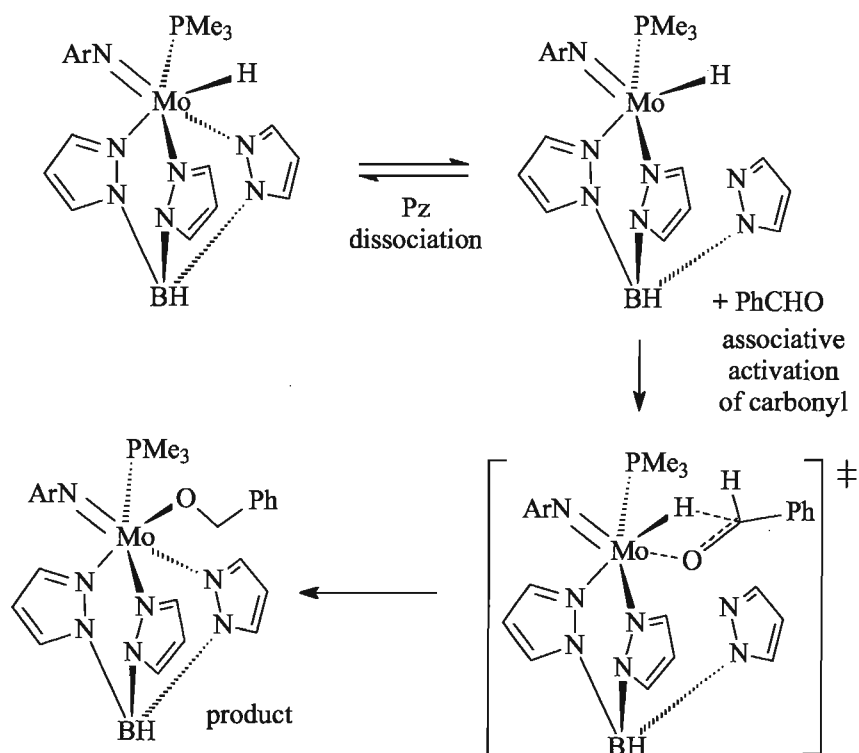


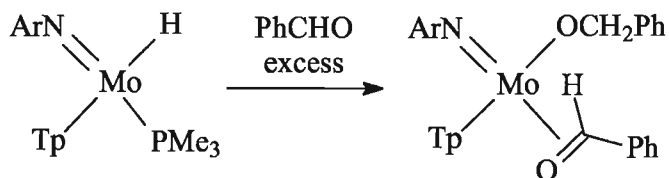
Figure III-3. Dependence of the rate constant k_{eff} on PMe_3 concentration (eq.) for the reaction of $(\text{Tp})(\text{ArN})\text{Mo}(\text{H})(\text{PMe}_3)$ with PhCHO (1 eq.).

Given the above data, we suggest that the reaction between $(\text{Tp})(\text{ArN})\text{Mo}(\text{H})(\text{PMe}_3)$ and PhCHO proceeds via dissociation of the pyrazolyl ligand, providing an “open” site for the associative activation of carbonyl^{5b} (Scheme III-21).



Scheme III-21. Proposed mechanism for the reaction between $(\text{Tp})(\text{ArN})\text{Mo}(\text{H})(\text{PMe}_3)$ and PhCHO .

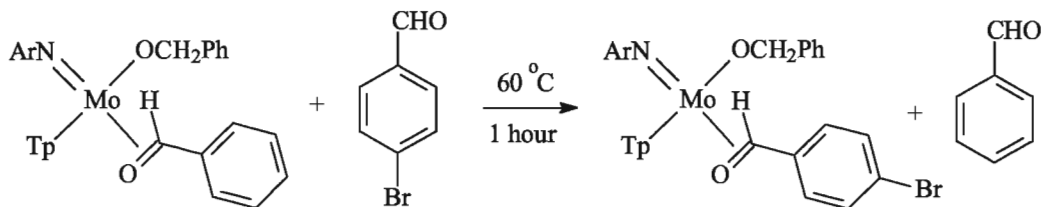
In the presence of excess benzaldehyde (>2 eq.), the complex $(\text{Tp})(\text{ArN})\text{Mo}(\text{H})(\text{PMe}_3)$ slowly yields the carbonyl adduct $(\text{Tp})(\text{ArN})\text{Mo}(\text{OCH}_2\text{Ph})(\eta^2\text{-PhCHO})$, characterized by an upfield shift of the $\eta^2\text{-PhCHO}$ signal at 5.38 ppm (Scheme III-22). The formation of only one isomer was observed, possibly because of steric demands of the bulky Tp ligand.^d



Scheme III-22. Reaction between $(\text{Tp})(\text{ArN})\text{Mo}(\text{H})(\text{PMe}_3)$ and PhCHO (excess).

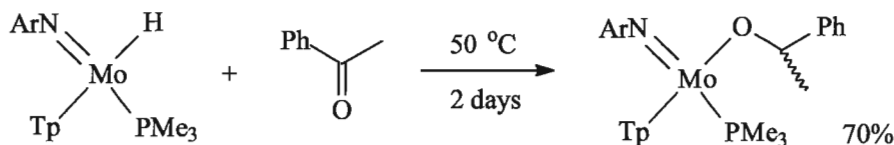
^d In case of $(\text{Cp})(\text{ArN})\text{Mo}(\text{OCH}_2\text{Ph})(\eta^2\text{-PhCHO})$, we observed two diastereomers.

When $(\text{Tp})(\text{ArN})\text{Mo}(\text{OCH}_2\text{Ph})(\eta^2\text{-PhCHO})$ is treated with *p*-bromobenzaldehyde, we observed full substitution of the η^2 -coordinated benzaldehyde by *p*-bromobenzaldehyde (Scheme II-22). Unlike the related system $(\text{Cp})(\text{ArN})\text{Mo}(\text{OCH}_2\text{Ph})(\eta^2\text{-PhCHO})$, the hydride transfer from the alkoxy ligand to the carbonyl does not take place.



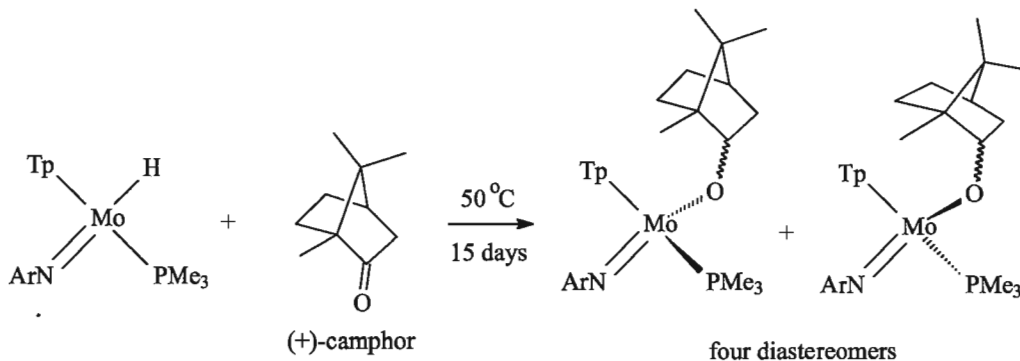
Scheme III-23. Reaction between $(\text{Tp})(\text{ArN})\text{Mo}(\text{OCH}_2\text{Ph})(\eta^2\text{-PhCHO})$ and *p*-bromobenzaldehyde.

Complex $(\text{Tp})(\text{ArN})\text{Mo}(\text{H})(\text{PMe}_3)$ reacts with ketones very slowly, and the reactions require intensive heating over several days. Thus, a reaction with acetophenone provided the formation of $(\text{Tp})(\text{ArN})\text{Mo}(\text{OC}(\text{CH}_3)\text{Ph})(\text{PMe}_3)$, obtained as a mixture of two diastereomers in 1.3:1 ratio, after two days at 50 °C (Scheme III-24).



Scheme III-24. Reaction between $(\text{Tp})(\text{ArN})\text{Mo}(\text{H})(\text{PMe}_3)$ and acetophenone.

A reaction of $(\text{Tp})(\text{ArN})\text{Mo}(\text{H})(\text{PMe}_3)$ with (+)camphor proceeded without enantioselectivity and yielded all four possible diastereomers (Scheme III-25).

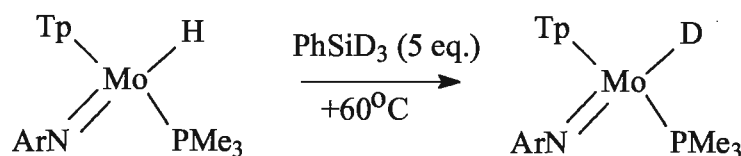


Scheme III-25. Reaction between $(\text{Tp})(\text{ArN})\text{Mo}(\text{H})(\text{PMe}_3)$ and (+)camphor.

A reaction with acetone did not afford the expected alkoxy complex. Instead, heating a mixture of (Tp)(ArN)Mo(H)(PMe₃) with acetone gave only products of acetone condensation.

III.2.5 Reaction between (Tp)(ArN)Mo(H)(PMe₃) and PhSiH₃

The molybdenum hydride Tp-complex does not react with phenylsilane to give any derivative. The H/D scrambling between (Tp)(ArN)Mo(H)(PMe₃) and PhSiD₃ was, however, observed but only at elevated temperatures: $k_{\text{H/D}}(60.0\text{ }^{\circ}\text{C}) = (1.20 \pm 0.23) \cdot 10^{-4} \text{ s}^{-1}$ (Scheme III-26).



Scheme III-26. Reaction between (Tp)(ArN)Mo(H)(PMe₃) and PhSiD₃ (5 eq.).

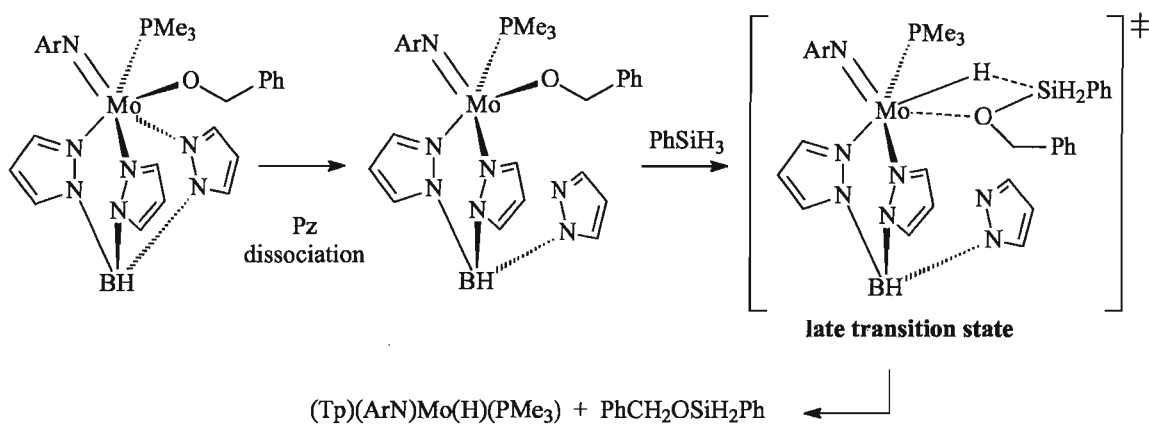
III.2.6 Reaction between (Tp)(ArN)Mo(OCH₂Ph)(PMe₃) and PhSiH₃

Like its Cp-analogue, the alkoxy complex (Tp)(ArN)Mo(OCH₂Ph)(PMe₃) cleanly reacts with phenylsilane to give (Tp)(ArN)Mo(H)(PMe₃) and the silyl ether. Kinetics of this reaction has been studied at four different temperatures (Table III-6).

Table III-6. Kinetic isotope effect for the reaction of (Tp)(ArN)Mo(OCH₂Ph)(PMe₃) with PhSiH₃/PhSiD₃

Temperature, °C	$k_{\text{PhSiH}_3}, \text{s}^{-1}$	$k_{\text{PhSiD}_3}, \text{s}^{-1}$	KIE
17.0	$(1.13 \pm 0.02) \cdot 10^{-4}$	$(2.10 \pm 0.02) \cdot 10^{-4} \text{ s}^{-1}$	0.54
22.0	$(2.35 \pm 0.02) \cdot 10^{-4}$	$(2.92 \pm 0.02) \cdot 10^{-4} \text{ s}^{-1}$	0.85
27.0	$(4.37 \pm 0.04) \cdot 10^{-4}$	$(6.60 \pm 0.04) \cdot 10^{-4}$	0.65
32.0	$(8.67 \pm 0.01) \cdot 10^{-4}$	$(1.08 \pm 0.01) \cdot 10^{-3}$	0.80

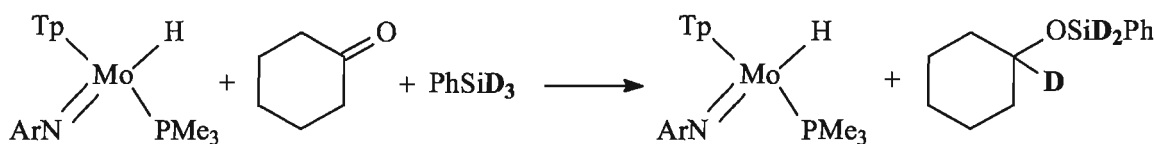
The corresponding activation parameters are: $\Delta H_{\text{PhSiH}_3}^\ddagger = 96.6 \pm 1.8 \text{ kJ/mol}$, $\Delta S_{\text{PhSiH}_3}^\ddagger = 12.5 \pm 6.2 \text{ J/(K}\cdot\text{mol)}$. Previously, we demonstrated that the heterolytic splitting of Si-H bond on the Mo-O bond in $(\text{Cp})(\text{ArN})\text{Mo}(\text{OCH}_2\text{Ph})(\text{PMe}_3)$ is an associative reaction characterized by large negative entropy of activation ($-111 \pm 16 \text{ J/(K}\cdot\text{mol)}$). A small positive entropy of activation found for $(\text{Tp})(\text{ArN})\text{Mo}(\text{OCH}_2\text{Ph})(\text{PMe}_3)$ may indicate the possibility of dissociation of one of the pyrazolyl substituents. Here we assume that the reaction proceeds in two sequential steps: the dissociation of the pyrazolyl ligand (to reduce the bulkiness and provide more space for the reaction) and heterolytic splitting of the Si-H bond on the Mo-O bond. The last step should proceed via a late transition state according to the observed inverse kinetic isotope effect (Table III-6 and Scheme III-27).



Scheme III-27. Proposed mechanism for the reaction between $(\text{Tp})(\text{ArN})\text{Mo}(\text{OCH}_2\text{Ph})(\text{PMe}_3)$ and PhSiH_3 .

III.2.7 Reaction between $(\text{Tp})(\text{ArN})\text{Mo}(\text{H})(\text{PMe}_3)$, PhSiD_3 and cyclohexanone and the mechanism of hydrosilylation

When PhSiD_3 and cyclohexanone are mixed in the presence of a stoichiometric amount of $(\text{Tp})(\text{ArN})\text{Mo}(\text{H})(\text{PMe}_3)$ (100% catalyst load), the reaction produces the silyl ether of cyclohexanol and the initial catalyst with full retention of the hydride ligand (Scheme III-28). The same was observed when the reaction was performed under the actual catalysis conditions, i.e. in the presence of 5 mol% of $(\text{Tp})(\text{ArN})\text{Mo}(\text{H})(\text{PMe}_3)$. The fact that the Mo-D bond was not formed in any detectable amount indicates that the catalytic reaction proceeds without hydride transfer from molybdenum to the carbonyl.



Scheme III-28. Reaction between (Tp)(ArN)Mo(H)(PMe₃), PhSiD₃ and cyclohexanone.

We also found that variation of concentration of the cyclohexanone significantly changes the reaction rate. Variation of concentration of the silane did not show any significant response in the reaction rate. This may indicate that the activation of carbonyl is the rate-determining step in this process. The experimental data do not allow us, however, to propose any detailed mechanism of activation of substrates. Nevertheless, three notions can be made: 1) the substrates are activated by a Lewis acidic metal centre, 2) the molybdenum hydride ligand does not react with the substrates, and 3) the activation of carbonyl has an effect on the reaction rate.

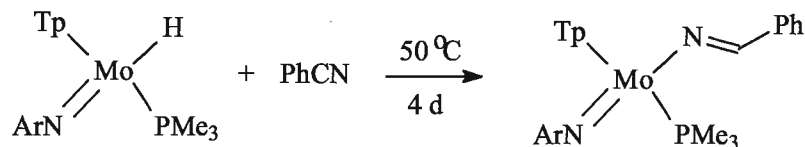
III.2.8 Reactions of (Tp)(ArN)Mo(H)(PMe₃) with alcohols

The complex (Tp)(ArN)Mo(H)(PMe₃) quickly reacts with methanol with the formation of the methoxy derivative (Tp)(ArN)Mo(OCH₃)(PMe₃) and H₂. Ethanol and *iso*-propanol do not react with (Tp)(ArN)Mo(H)(PMe₃), probably because of the insufficient acidity of the O-H proton. The complex is stable when dissolved in ethanol or isopropanol during several days at RT. However, the experiments with isopropanol-*d*₈ revealed a slow H/D exchange between the Mo-*H* and O-*D* positions. We were able to prepare the fully deuterated derivative of the hydride complex (Tp)(ArN)Mo(D)(PMe₃) by dissolving the hydride complex in neat isopropanol-*d*₈ and evaporating the solvent when the hydride was fully substituted by deuterium.

III.2.9 Reaction of (Tp)(ArN)Mo(H)(PMe₃) with benzonitrile

The molybdenum hydride complex (Tp)(ArN)Mo(H)(PMe₃) cleanly reacts with benzonitrile, producing the vinylidenamido derivative (Tp)(ArN)Mo(-N=CHPh)(PMe₃)

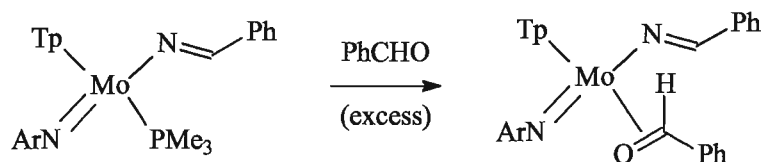
(Scheme III-29). The product was isolated in 97% yield and characterized by NMR, IR and elemental analysis.



Scheme III-29. Reaction of (Tp)(ArN)Mo(H)(PMe₃) with benzonitrile.

Complex (Tp)(ArN)Mo(-N=CHPh)(PMe₃) did not react with PhSiH₃ under heating at 50 °C. Neither was there any reaction when BPh₃ was added to pull off the phosphine ligand.

However, the excess of benzaldehyde (~5 eq.) substitutes the phosphine ligand and gives the η^2 -benzaldehyde adduct.



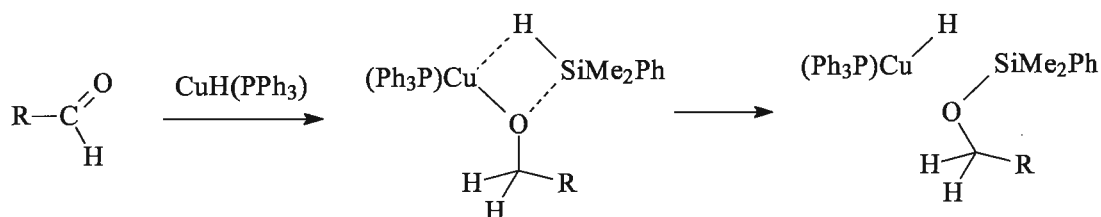
Scheme III-30. Reaction of (Tp)(ArN)Mo(-N=CHPh)(PMe₃) with benzaldehyde.

The formulation of (Tp)(ArN)Mo(-N=CHPh)(η^2 -PhCHO) as a η^2 -aldehyde complex is evidenced from the observation of an upfield shifted -CHO proton at 5.37 ppm in the ¹H NMR spectrum.

III. 3 Hydrosilylation catalyzed by (PPh₃)CuH

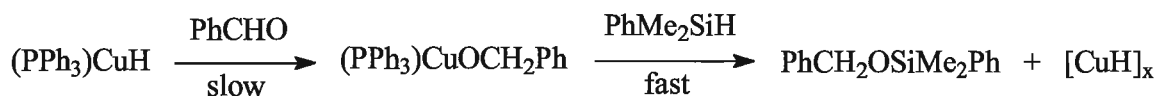
As previously discussed, we unexpectedly found that carbonyl hydrosilylation may be catalyzed by (Cp)(ArN)Mo(H)(PMe₃) and (Tp)(ArN)Mo(H)(PMe₃) without a direct participation of the hydride ligand. The latter merely played the role of a spectator group and did not react with either carbonyl or silane. Electrophilic activation of hydrosilylation catalysis by metal hydrides has never been mentioned in the literature. It is generally believed that hydrosilylation of carbonyls catalyzed by transition metal complexes proceeds via a sequence of steps involving the reactions of a metal hydride with substrates, with the key M-H functionality being either part of the pre-catalyst or being formed *in situ* upon the reaction with silane. For instance, Sato³⁵, Nakano³⁶, Buchwald^{2b}, Mimoun⁴¹, Toste^{10a}, Abu-Omar^{10b}, Berke⁶⁵, Lipshutz⁷⁸, Mindiola^{7c}, and Guan^{7b} described hydrosilylation catalysis as a reaction of a metal hydride with carbonyl to form an alkoxy complex followed by the reaction with silane to regenerate the initial metal hydride complex and yield the product of hydrosilylation. We decided to investigate if other transition metal complexes may also catalyze hydrosilylation without the direct reaction of the metal hydride with substrates.

The copper hydride complex CuH(PPh₃), known as the Stryker reagent, catalyzes hydrosilylation of carbonyls.⁷⁸ The mechanism of hydrosilylation was proposed by Lipshutz *et al.*⁷⁸ It was suggested that the copper hydride reacts with carbonyl to form an alkoxy complex followed by a metathesis reaction with silane (Scheme III-31) to give the initial catalyst and the hydrosilylation product. Formation of an intermediate copper alkoxy complex was proposed but it was not observed.



Scheme III-31. Lipshutz mechanism of hydrosilylation of carbonyls catalyzed by $\text{CuH}(\text{PPh}_3)$.

First of all, we decided to find out if the formation of the proposed alkoxide intermediate could be achieved in the individual reaction between $(\text{PPh}_3)\text{CuH}$ and benzaldehyde. The Stryker's reagent has been freshly prepared by the reaction of CuCl with $t\text{-BuOK}$ and PhMe_2SiH in the presence of triphenylphosphine in 47% yield.^e The Cu-H peak was clearly observed at 3.62 ppm as a broad singlet. The reaction of $(\text{PPh}_3)\text{CuH}$ with benzaldehyde afforded formation of the alkoxy complex $(\text{PPh}_3)\text{CuOCH}_2\text{Ph}$ in 65% NMR yield with a relatively large amount of a black precipitate (presumably metallic copper). The methylene protons of the alkoxy complex, $\text{Cu-OCH}_2\text{Ph}$, were observed at 5.23 ppm and their identity was proved by ^{13}C DEPT(135), ^1H - ^{13}C HSQC and ^1H - ^{13}C HMBC NMR experiments. When an equimolar amount of PhMe_2SiH was added to the resulting solution, the formation of silyl ether, $\text{PhCH}_2\text{OSiMe}_2\text{Ph}$, was observed immediately by ^1H NMR (Scheme III-32).



Scheme III-32. Reaction between $(\text{PPh}_3)\text{CuH}$ and PhCHO to give $(\text{PPh}_3)\text{CuOCH}_2\text{Ph}$ followed by the reaction with PhMe_2SiH .

^e In the original procedure, a suspension of CuCl , $t\text{-BuOK}$ and PPh_3 in toluene was treated with molecular hydrogen (H_2).

The copper hydride was regenerated as a mixture of $[\text{CuH}]_x$ species characterized by the CuH signals at 2.55, 3.14, and 3.63 ppm.

Therefore, we have demonstrated that the Stryker's reagent may individually react with benzaldehyde with the formation of the alkoxy complex $(\text{PPh}_3)\text{CuOCH}_2\text{Ph}$, which previously was not reported in the literature. The alkoxy complex was individually treated with silane to give a mixture of oligomeric $[\text{CuH}]_x$ species and the hydrosilylation product $\text{PhCH}_2\text{OSiMe}_2\text{Ph}$. Based on these observations alone, it could be proposed that indeed the hydrosilylation of benzaldehyde catalyzed by $(\text{PPh}_3)\text{CuH}$ could proceed via the Lipshutz mechanism (Scheme III-31).

We decided then to study the hydrosilylation catalysis with the deuterated silane PhMe_2SiD in order to verify the proposed hydride mechanism.

When mixed with PhMe_2SiD , complex $(\text{PPh}_3)\text{CuH}$ does not show any evidence of H/D scrambling or any other reaction even after several days at RT. When $(\text{PPh}_3)\text{CuH}$ was mixed with equimolar amounts of PhCHO and PhMe_2SiD , the formation of $\text{PhCHDOSiMe}_2\text{Ph}$ as a sole product was observed within one hour at RT. The reaction was monitored by ^1H NMR (Figure III-4, Figure III-5). At the end of the reaction, we observed the signal of CuH at 3.62 ppm integrated as one and the peak at 4.69 ppm due to the hydrosilylation product $\text{PhCHDOSiMe}_2\text{Ph}$. The ^2H NMR spectrum of the resulting mixture showed no incorporation of deuterium into the Stryker's reagent but presented only the peak at 4.74 ppm corresponding to $\text{PhCHDOSiMe}_2\text{Ph}$ (Figure III-6). Finally, the hydrosilylation of PhCHO by PhMe_2SiD was carried out in the presence of 1.3 mol% of $(\text{PPh}_3)\text{CuH}$. When the reaction was 97% complete, we were still able to observe the CuH signal at 3.61 ppm (Figure III-7). We therefore conclude that the hydride mechanism of hydrosilylation catalysis proposed by Lipshutz (Scheme III-31) does not occur.

Our experiments employing the deuterated silane have provided evidence that the copper hydride CuH does not react with either of the substrates during the catalysis. We tentatively postulate that the latter were just activated at the Lewis acidic metal center. However, we think that the presence of hydride is critical for catalysis due to its very small size it provides a coordination space for the substrate (especially in such a bulky molecule as $[(\text{PPh}_3)\text{CuH}]_6$).

Hydrosilylation of other substrates

Unfortunately, copper catalyzed hydrosilylation of acetophenone, cyclohexanone and benzonitrile by either PhMe_2SiH or PhSiH_3 was not observed. Attempts to promote the catalysis by heating resulted in the catalyst decomposition (possibly due to disproportionation of Cu(I) into Cu(0) and Cu(II)).

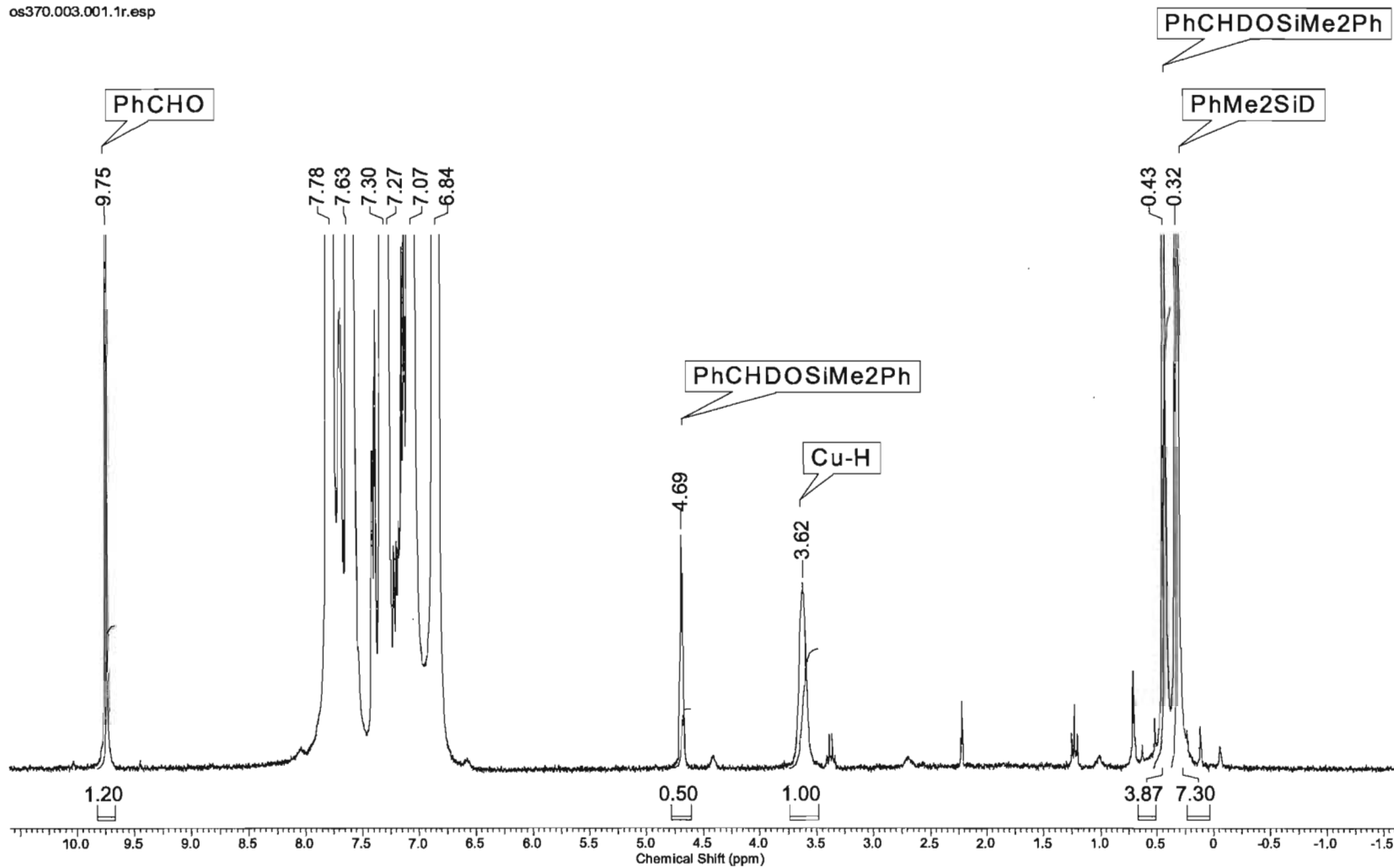


Figure III-4. Stoichiometric reaction between $\text{CuH}(\text{PPh}_3)$, PhCHO and PhMe_2SiD (29% conversion)

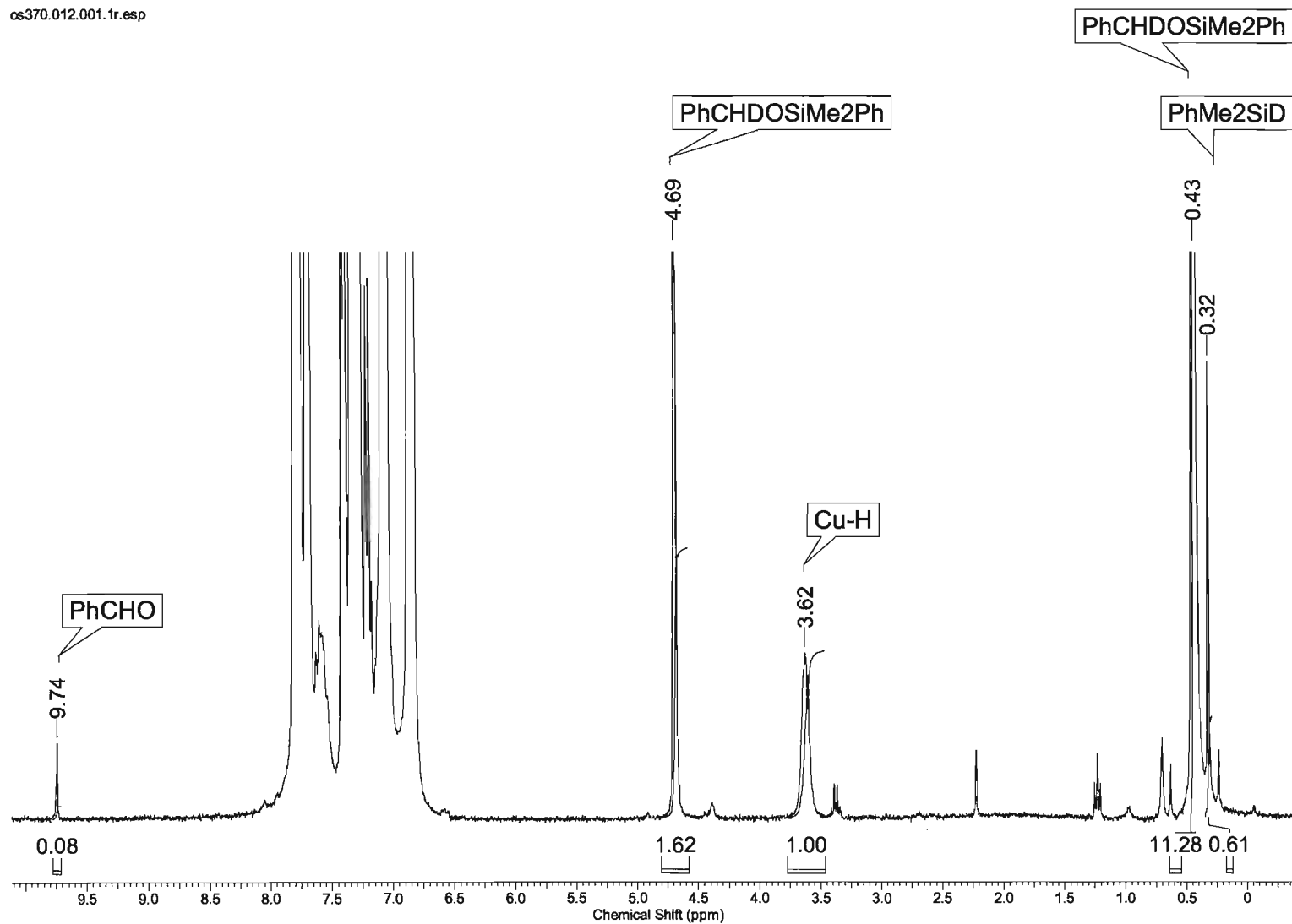
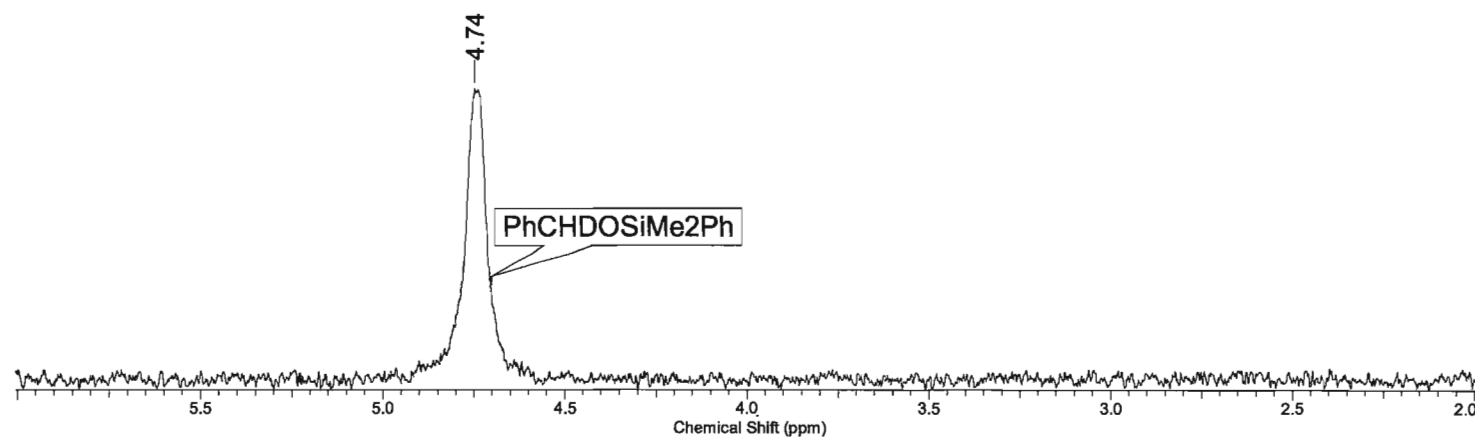


Figure III-5. Stoichiometric reaction between CuH(PPh₃), PhCHO and PhMe₂SiD (95% conversion)

OS-CuH.002.001.1r.esp



OS-CuH.001.001.1r.esp

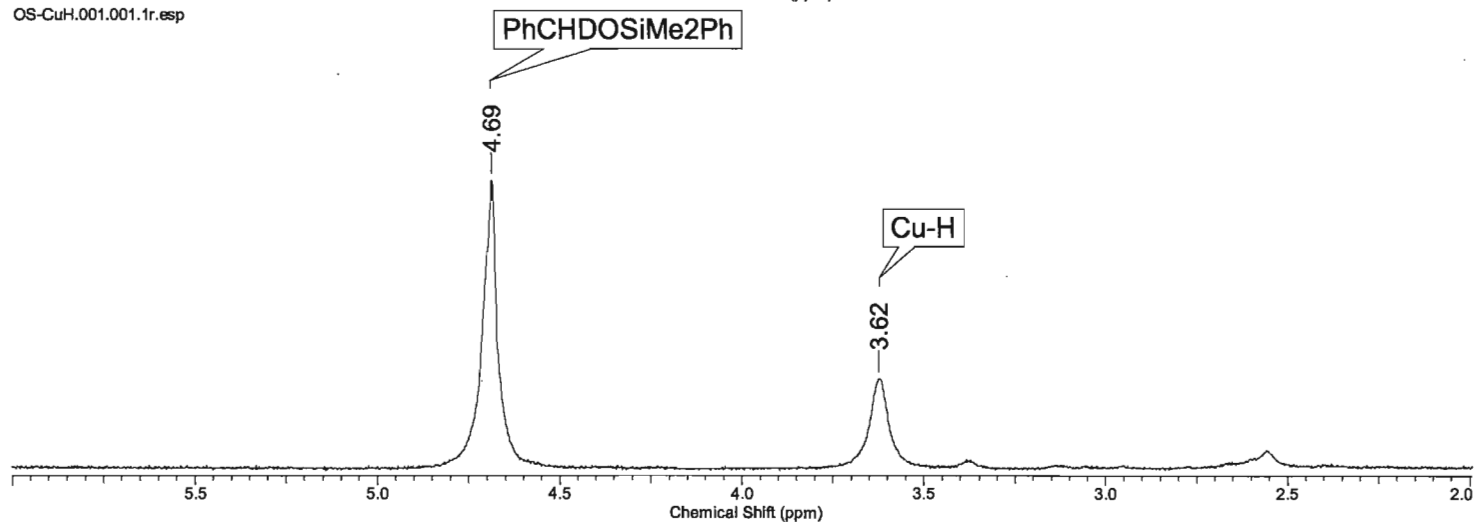


Figure III-6. The end of reaction between $\text{CuH}(\text{PPh}_3)$, PhCHO and PhMe_2SiD .
 ^2H NMR spectrum (top), and ^1H NMR spectrum (bottom)

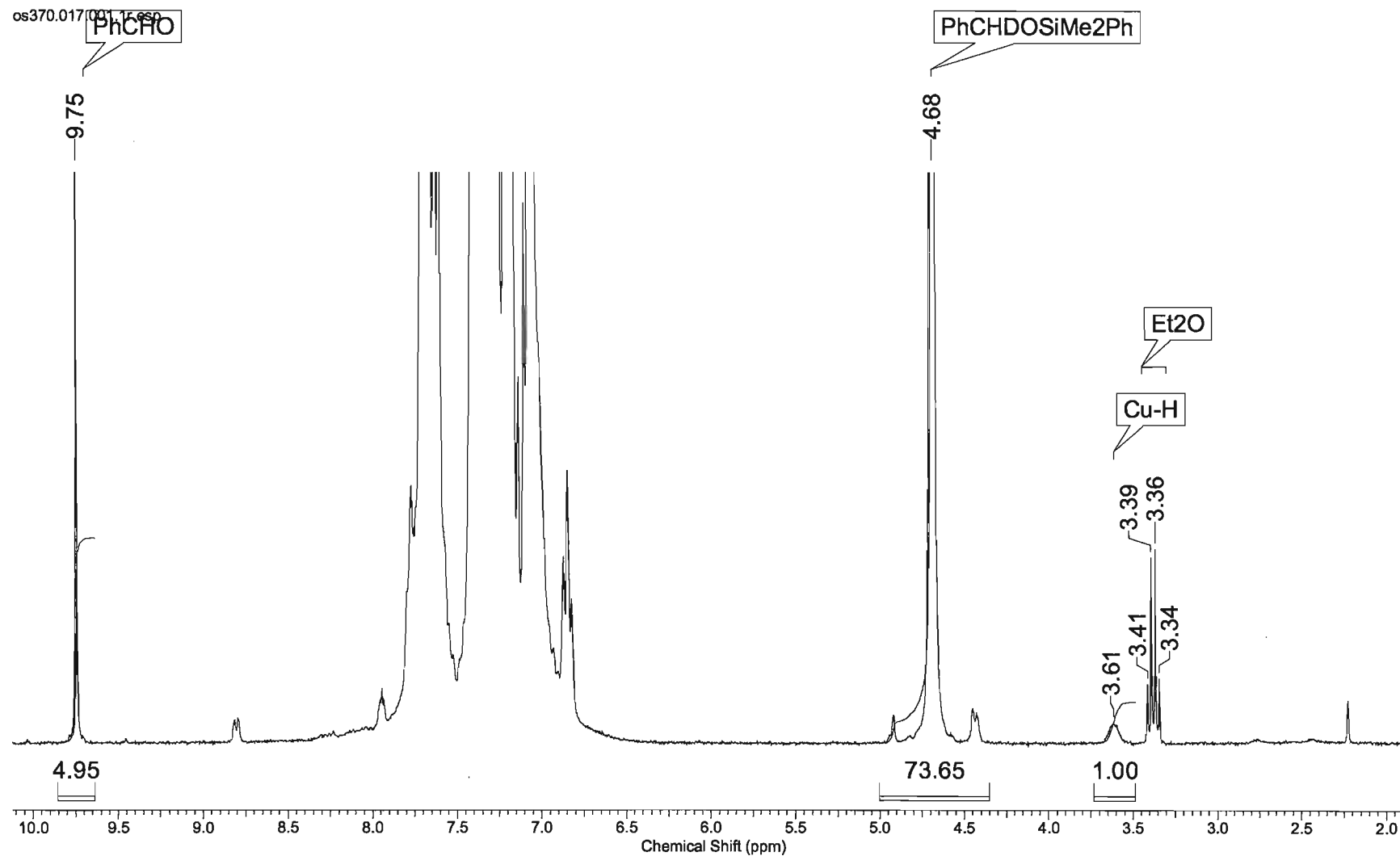
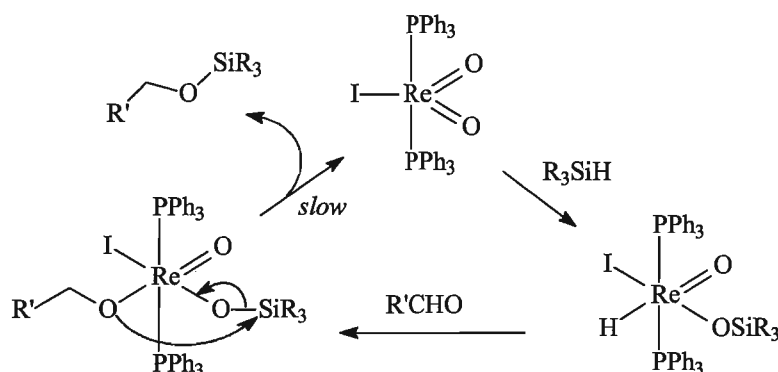


Figure III-7. Hydrosilylation of PhCHO with PhMe₂SiD in the presence of catalytic amounts (~5 mol%) of CuH(PPh₃).

III. 4 Hydrosilylation catalyzed by oxo-Re(V) complexes

We successfully demonstrated that the hydrosilylation of carbonyls catalyzed by $(\text{PPh}_3)_3\text{CuH}$ does not proceed via formation of a copper alkoxy complex in contrast to what was proposed by Lipshutz *et al.*⁷⁸ We decided then to extend our knowledge of the hydrosilylation catalysis to other catalytic systems, specifically on the high-valent oxo-Re complexes reported by Toste *et al.*^{10a} and Abu-Omar *et al.*^{10b}.

Toste *et al.* reported that complex $(\text{PPh}_3)_2(\text{I})\text{Re}(\text{O})_2$ catalyzes the hydrosilylation of carbonyls and proposed a new reaction mechanism based on Si-H addition to the oxo-group to give a hydride catalyst (Scheme III-33).

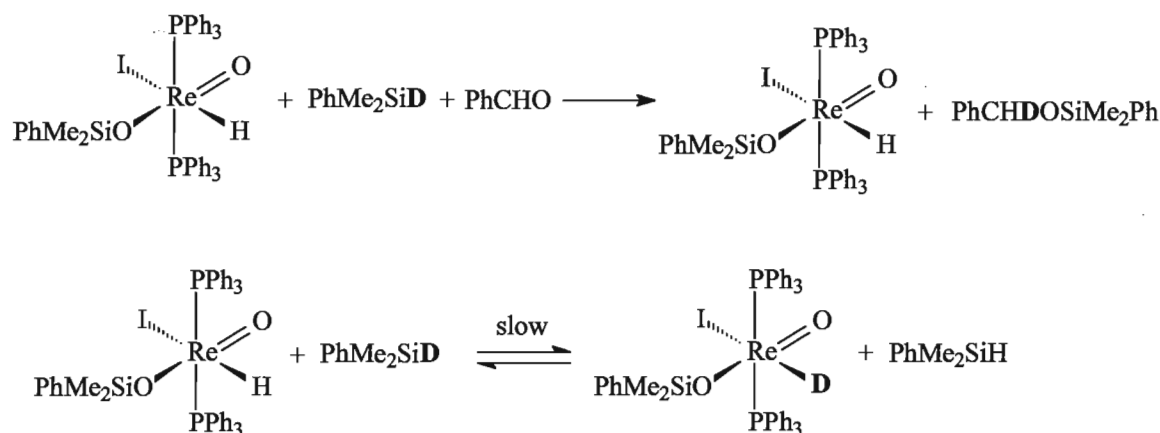


Scheme III-33. Toste mechanism of carbonyl hydrosilylation catalyzed by $(\text{PPh}_3)_2(\text{I})\text{Re}(\text{O})_2$.

We decided to find out if carbonyl insertion into the Re-H bond actually takes place in this catalysis.

The complex $(\text{PPh}_3)_2(\text{I})(\text{O})\text{Re}(\text{H})(\text{OSiMe}_2\text{Ph})$ was prepared according to Toste's procedure.^{10a} It is characterized by the Re-H triplet ($J = 14$ Hz) at 6.37 ppm in the ^1H NMR spectrum taken in CD_2Cl_2 (Figure III-8). When the complex was mixed with PhCHO (1.5 eq.) and PhMe_2SiD (1.5 eq.), the formation of $\text{PhCHDOSiMe}_2\text{Ph}$ was observed (Figure III-9). At the end of catalysis (approximately after one hour at RT), the rhenium hydride was present in the reaction mixture (Figure III-10). According to integration, 81% of hydride was retained at the Re centre, and 19% was replaced by

deuterium. The H/D scrambling could be the cumulative result of a slow Re-H/Si-D exchange previously observed by Toste *et al.* and the competitive hydrosilylation by the hydride mechanism.^{10a} The evidence that the hydride was not fully substituted by deuterium indicates that complex $(\text{PPh}_3)_2(\text{I})(\text{O})\text{Re}(\text{H})(\text{OSiMe}_2\text{Ph})$ can catalyze the hydrosilylation of carbonyls without the involvement of the hydride (Scheme III-34). Toste and co-workers carried out a thorough mechanistic investigation of the hydrosilylation catalysis^{10a} but did not attempt to model the overall catalytic cycle by the proposed sequence of stoichiometric reactions..

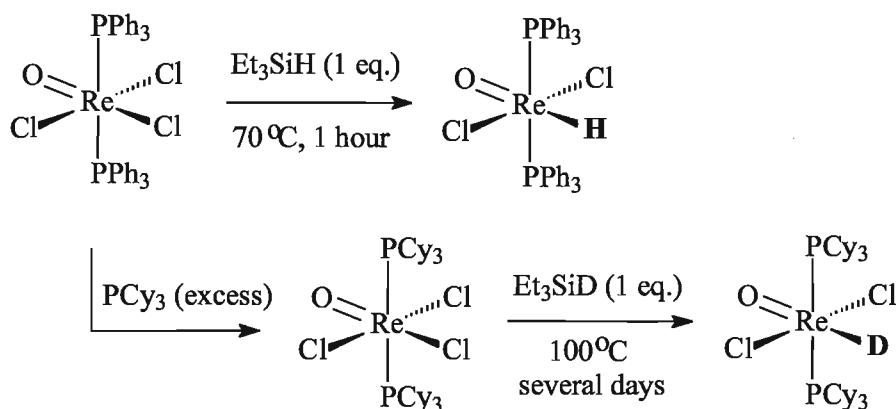


Scheme III-34. 1:1:1 reaction between $(\text{PPh}_3)_2(\text{I})(\text{O})\text{Re}(\text{H})(\text{OSiMe}_2\text{Ph})$, PhMe_2SiD and PhCHO .

Abu-Omar *et al.* worked on a similar Re system, $(\text{PPh}_3)_2\text{ReOCl}_3$, and showed that it can catalyze the hydrosilylation of aldehydes, albeit at much slower rate than Toste's system.^{10b} Their mechanistic studies demonstrated that the complex $(\text{PPh}_3)_2\text{ReOCl}_3$ is a pre-catalyst and must be activated by a reaction with silane. The observable product of this reaction was the hydride $(\text{PPh}_3)_2\text{Re}(\text{H})\text{OCl}_2$. Despite the obvious similarity between $(\text{PPh}_3)_2\text{Re}(\text{H})\text{OCl}_2$ and the Toste's hydride $(\text{PPh}_3)_2(\text{I})(\text{O})\text{Re}(\text{H})(\text{OSiMe}_2\text{Ph})$, mechanistic studies by Abu-Omar *et al.* do not support the idea that catalysis by $(\text{PPh}_3)_2\text{Re}(\text{H})(=\text{O})\text{Cl}_2$ is the dominant reaction pathway. Although complex $(\text{PPh}_3)_2\text{Re}(\text{H})\text{OCl}_2$ forms the alkoxy complex $(\text{PPh}_3)_2\text{Re}(\text{OCH}_2\text{Ph})(=\text{O})\text{Cl}_2$ in a stoichiometric reaction with benzaldehyde, kinetic modeling of the rate of catalysis shows a significantly slower process than the actual catalysis. Abu-Omar *et al.* suggested an alternative mechanism of hydrosilylation

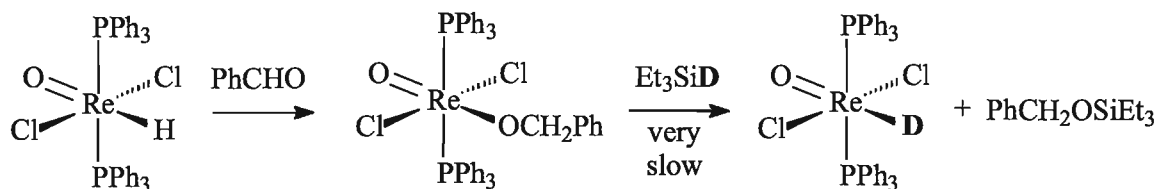
of carbonyls, based on intermediate formation of a η^2 -silane complex $(\text{PPh}_3)_2\text{Re}(\eta^2\text{-HSiR}_3)(=\text{O})\text{Cl}_2$ and nucleophilic abstraction of the silylium ion by the carbonyl (ionic hydrosilylation).

We decided to investigate if complex $(\text{PPh}_3)_2\text{Re}(\text{H})\text{OCl}_2$ can catalyze hydrosilylation without the formation of an alkoxy complex. The rhenium(V) hydride complex $(\text{PPh}_3)_2\text{Re}(\text{H})\text{OCl}_2$ was prepared according to the published protocol.^{10b} We also prepared the deuterated analogue $(\text{PCy}_3)_2\text{Re}(\text{D})\text{OCl}_2$ (Scheme III-35).



Scheme III-35. Preparation of $(\text{PPh}_3)_2\text{Re}(\text{H})\text{OCl}_2$ and $(\text{PCy}_3)_2\text{Re}(\text{D})\text{OCl}_2$.

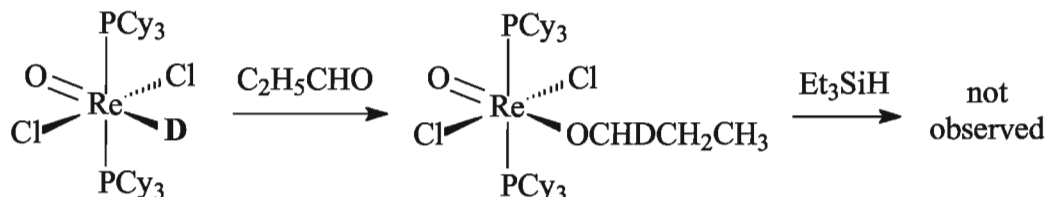
When complex $(\text{PPh}_3)_2\text{Re}(\text{H})\text{OCl}_2$ was mixed with Et_3SiD (1 eq.) and PhCHO (1 eq.), the formation of the alkoxy complex $(\text{PPh}_3)_2\text{Re}(\text{OCH}_2\text{Ph})\text{OCl}_2$ was observed by ^1H and ^{31}P NMR. The silyl ether, $\text{PhCH}_2\text{OSiEt}_3$, was also present in the reaction mixture in minor amounts. The reaction was very slow. After approximately one week at RT, the reaction mixture mostly consisted of the alkoxy complex $(\text{PPh}_3)_2\text{Re}(\text{OCH}_x\text{D}_y\text{Ph})\text{OCl}_2$ and the silyl ether, with even deuterium scrambling on all positions.



Scheme III-36. Reaction between $(\text{PPh}_3)_2\text{Re}(\text{H})\text{OCl}_2$ and benzaldehyde (1 eq.) in the presence of Et_3SiD (1 eq.).

Therefore our results do not allow us to differentiate between the hydride and possible nonhydride mechanisms.

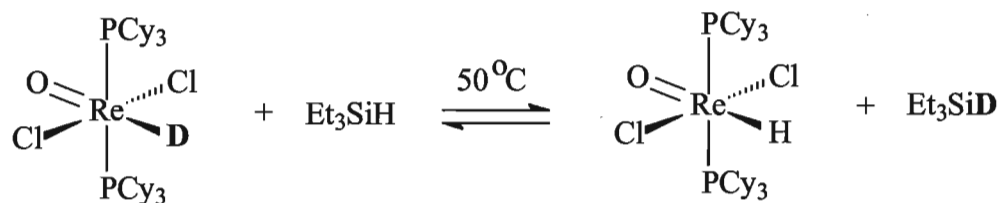
A similar result was obtained when $(\text{PCy}_3)_2\text{Re}(\text{D})\text{OCl}_2$ was used as the catalyst. When it was added to a mixture of propional (1 eq.) and Et_3SiH (1 eq.), the only reaction observed was a slow formation of the alkoxy complex $(\text{PCy}_3)_2\text{Re}(\text{OCHDCH}_2\text{CH}_3)\text{OCl}_2$.



Scheme III-37. Reaction between $(\text{PCy}_3)_2\text{Re}(\text{D})\text{OCl}_2$ and propanal (1 eq.) in the presence of Et_3SiH (1 eq.)

Activation of substrates without carbonyl insertion across the Re-D bond was not observed. We conclude that the only likely mechanism of carbonyl hydrosilylation catalyzed by $(\text{PCy}_3)_2\text{Re}(\text{H})\text{OCl}_2$ and $(\text{PPh}_3)_2\text{Re}(\text{H})\text{OCl}_2$ involves the formation of an alkoxy complex followed by the reaction with silane to give the silyl ether and the initial catalyst.^{10b}

In addition, we found that complex $(\text{PCy}_3)_2\text{Re}(\text{D})\text{OCl}_2$ may undergo a slow H/D exchange with Et_3SiH at elevated temperatures, which was not previously reported by Abu-Omar *et al.* (Scheme III-38).



Scheme III-38. H/D exchange between $(\text{PCy}_3)_2\text{Re}(\text{D})\text{OCl}_2$ and Et_3SiH .

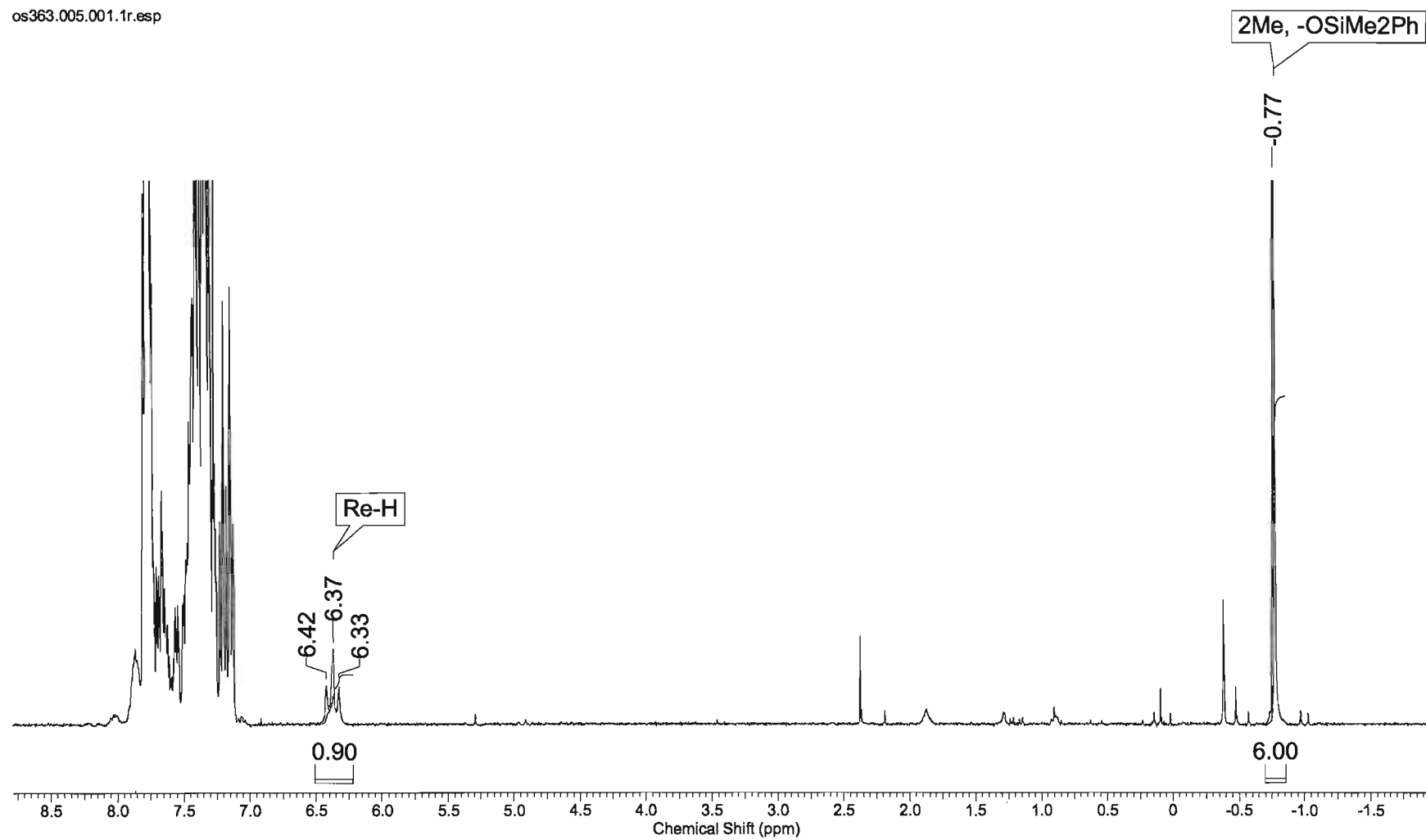


Figure III-8. ¹H NMR spectrum of (PPh₃)₂(I)(O)Re(H)(OSiMe₂Ph) in CDCl₃

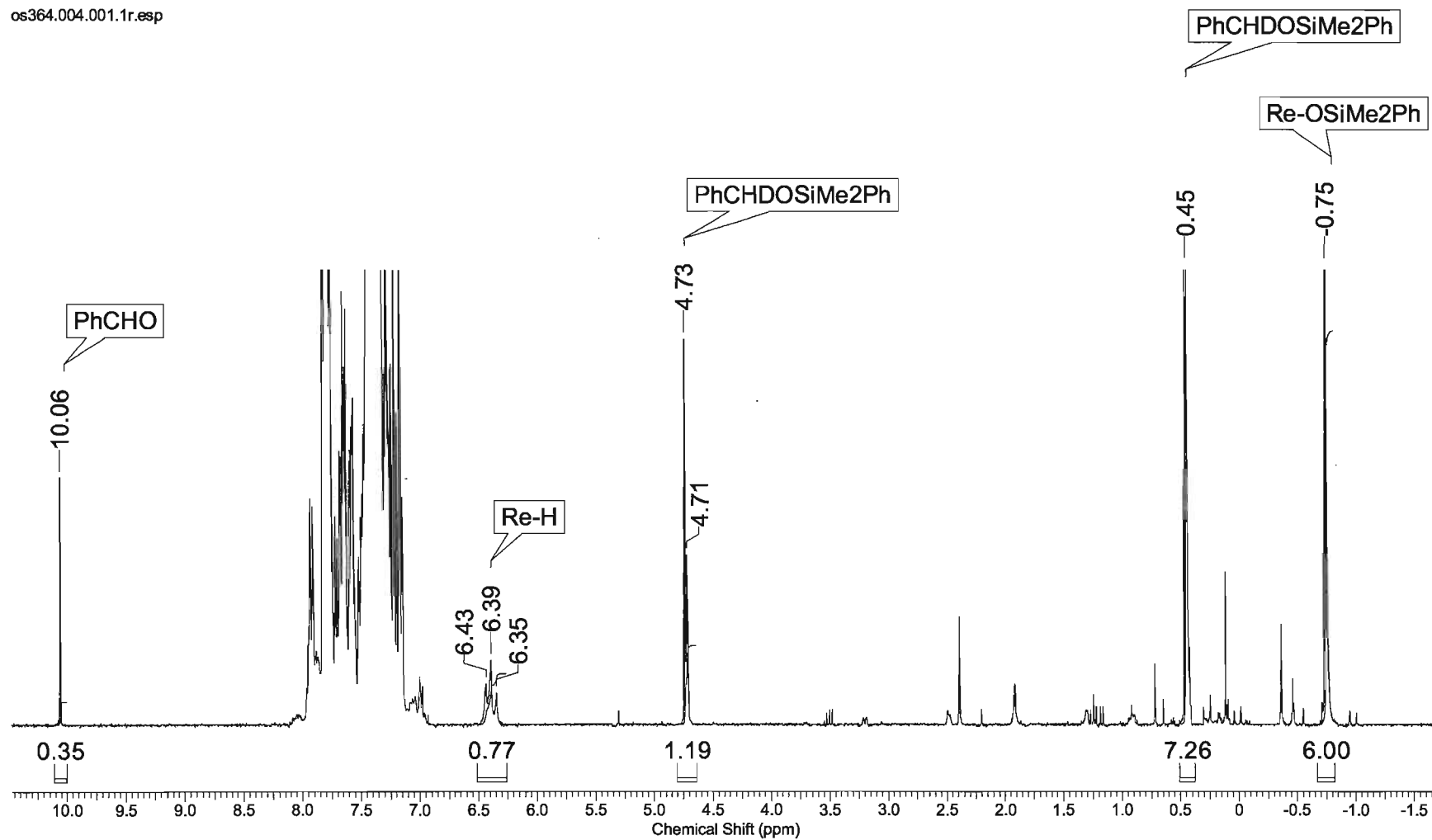


Figure III-9. Reaction between PhCHO, PhMe₂SiD and (PPh₃)₂(I)(O)Re(H)(OSiMe₂Ph) in CDCl₃ (77% conversion)

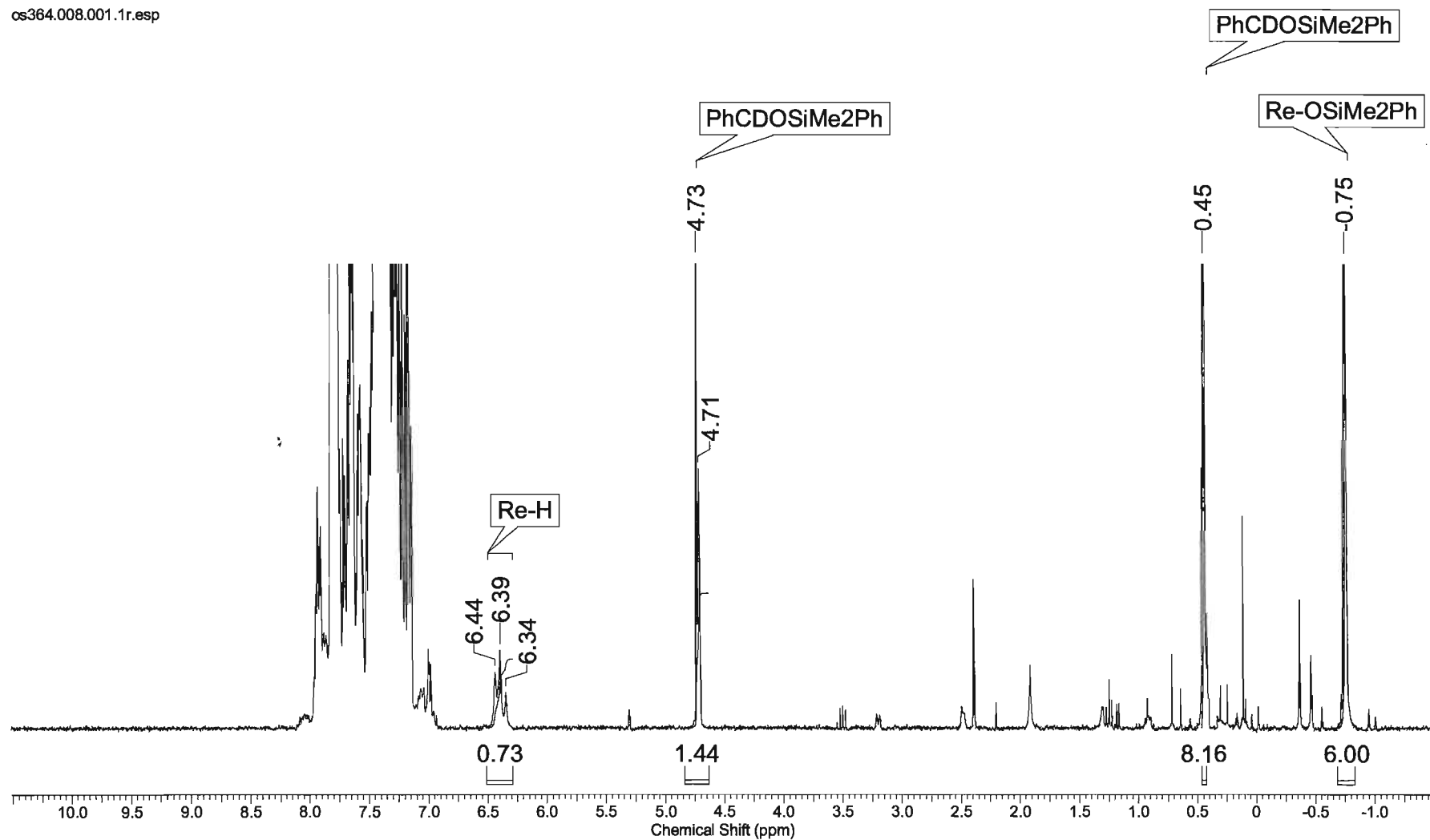
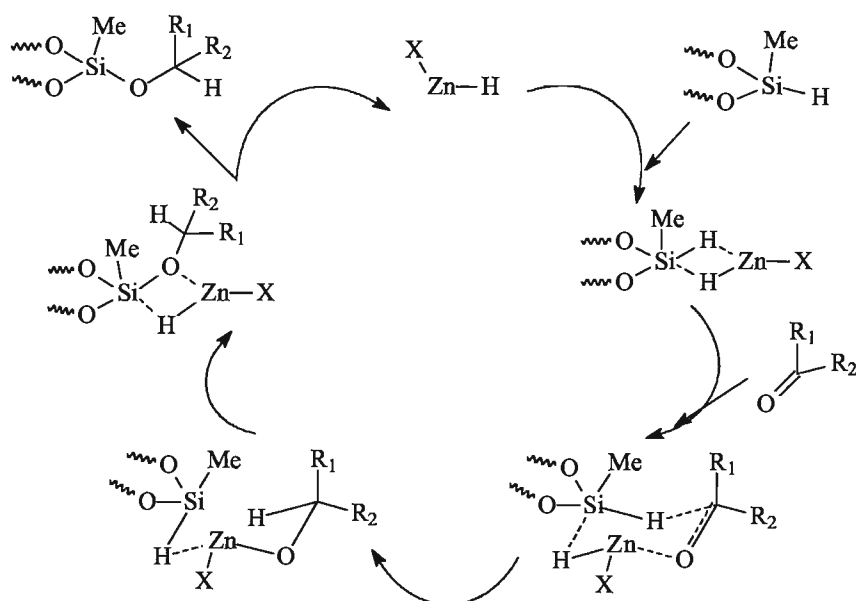


Figure III-10. Reaction between PhCHO, PhMe₂SiD and (PPh₃)₂(I)(O)Re(H)(OSiMe₂Ph) in CDCl₃ (100% conversion)

III. 5 Hydrosilylation catalyzed by Zn(II)

Our attention was then drawn to Zn(II) as a possible catalyst of carbonyl hydrosilylation. Mimoun previously reported that a mixture of zinc 2-ethylhexanoate and NaBH₄ mediates the hydrosilylation of a variety of aldehydes and ketones.⁴¹ The proposed catalytic cycle involves the *in situ* generation of zinc(II) hydride species followed by the formation of a putative pentavalent dihydrosilicate intermediate, and hydride transfer to the carbonyl group via a concerted six-membered transition state to form a zinc alkoxy complex (Scheme III-39).



Scheme III-39. Mimoun's mechanism of hydrosilylation of ketones catalyzed by zinc hydride species.

All intermediates in the catalytic cycle were are merely hypothetical and were never observed or characterized. We decided to extend our mechanistic studies with the isotopically labeled reagents to this system in order to obtain more information about the mechanism of hydrosilylation catalyzed by Zn(II) species.

The active catalyst species were prepared according to the Mimoun's protocol⁴¹ by mixing the zinc 2-ethylhexanoate and NaBD₄ in *tert*-butyl methyl ether as a solvent. Benzaldehyde and PMHS were added to the resulting solution (Figure III-11).

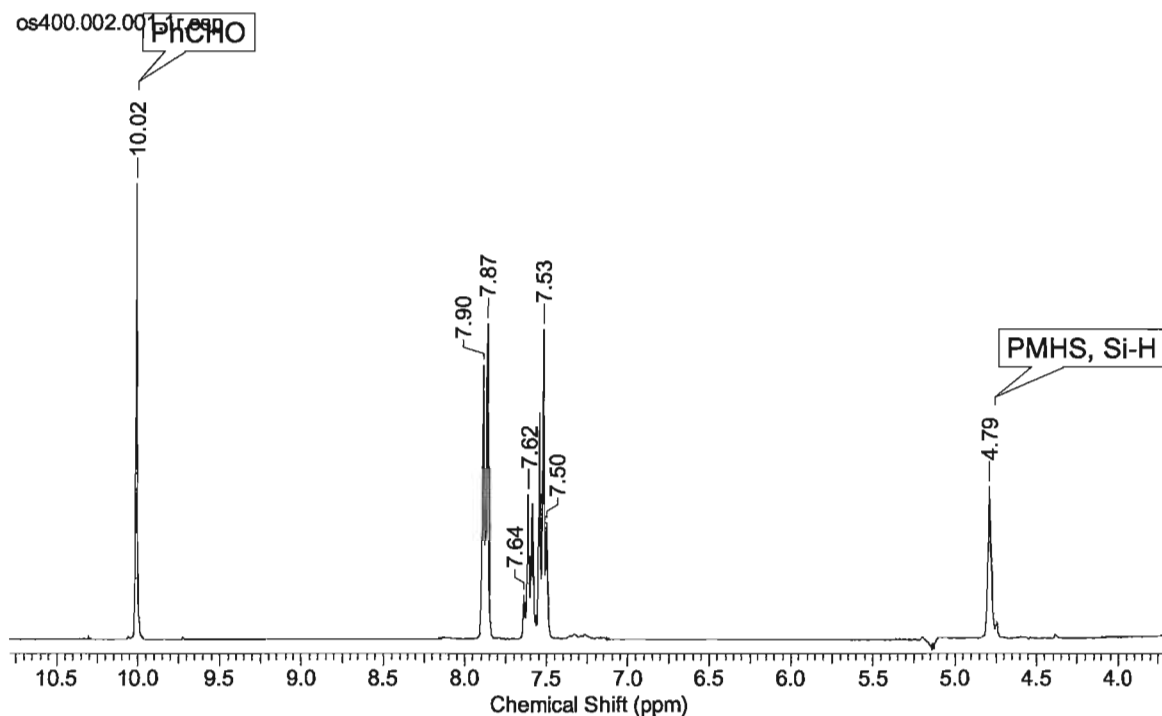


Figure III-11. A mixture of PhCHO and PMHS in the presence of zinc 2-ethylhexanoate and NaBD₄.

Heating the reaction mixture at 70 °C for several days resulted in the formation of new products identified by peaks at 3.78-3.85 and 4.90-4.97 ppm in ¹H NMR (Figure III-12). The ²H NMR spectrum also showed the presence of signals at 3.82 and 4.79-4.98 ppm (Figure III-13). Establishing the nature of the products was not our primary goal, as we aimed to check the possibility of H/D scrambling between the reagents and the products. We believe that the signals at 4.90-4.97 ppm correspond to the products of hydrosilylation, PhCH_xD_yOPMHS.^f Signals at 3.78-3.85 ppm correspond to some unidentified side-products. Hydrosilylation catalyzed by zinc salts may result in the formation of a large number of carbonyl condensation products, as previously reported by Calas.^{16a}

^f The silyl benzyl ether PhCH₂OPMHS was characterized in our studies by the -CH₂- signal at ~4.9 ppm.

os400.005.001.1r.esp

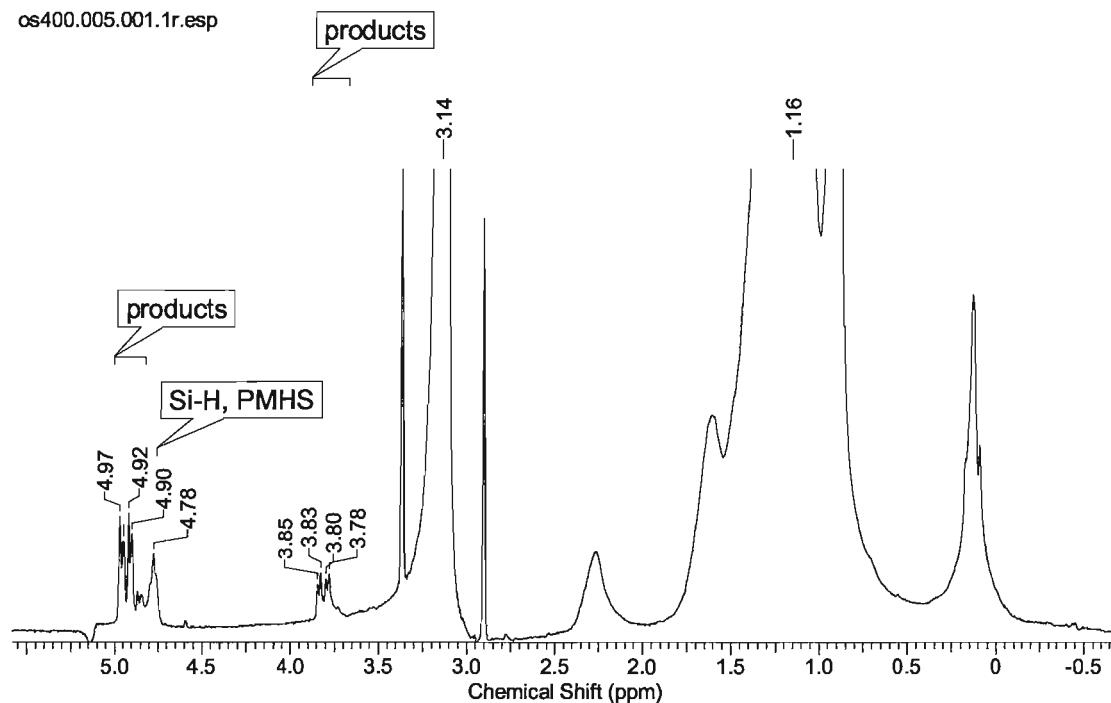


Figure III-12. ^1H spectrum of the reaction mixture of PhCHO, PMHS, zinc 2-ethylhexanoate and NaBD_4 in *tert*-butyl methyl ether.

os-400.002.001.1r.esp

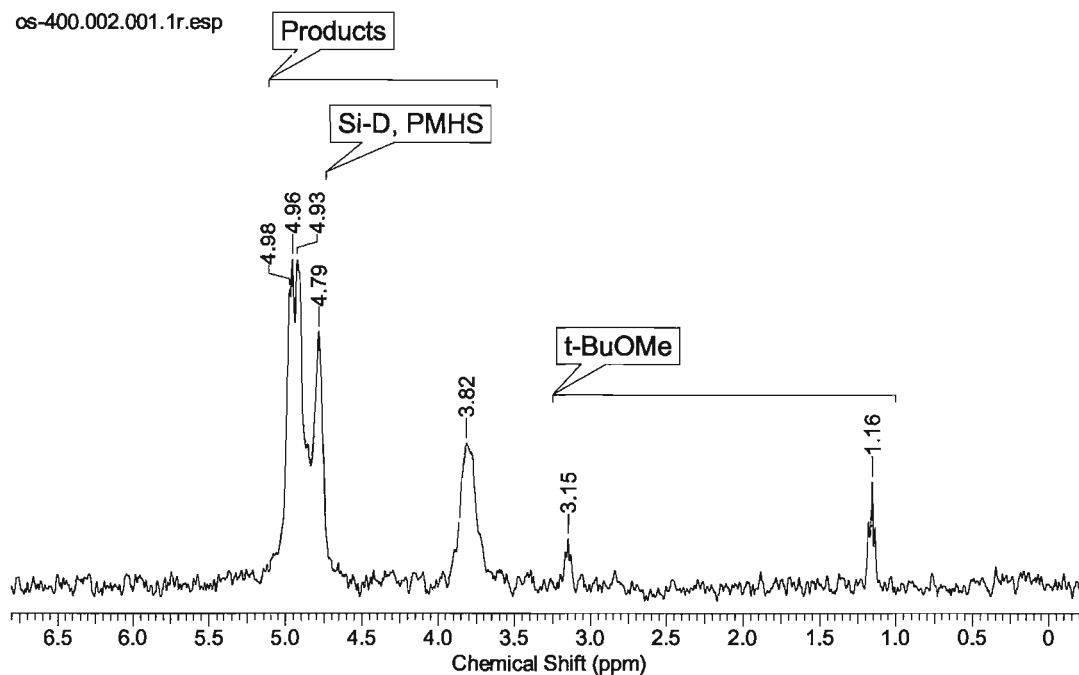


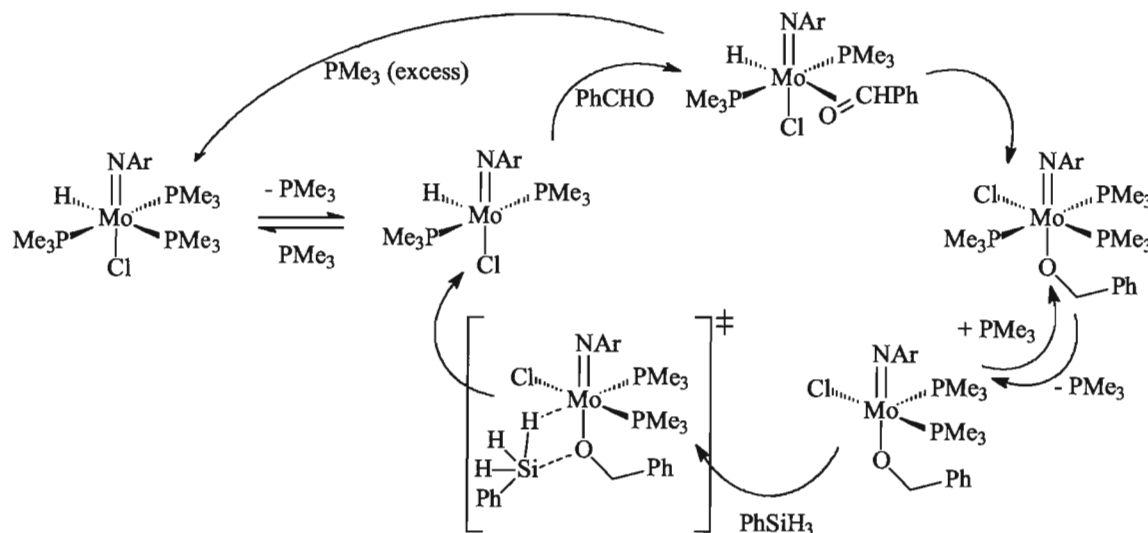
Figure III-13. ^2H spectrum of the reaction mixture of PhCHO, PMHS, zinc 2-ethylhexanoate and NaBD_4 in *tert*-butyl methyl ether.

PMHS also exchanged its Si-*H* protons with the deuterium atoms of NaBD₄: see the corresponding signals at 4.78 ppm in ¹H NMR (Figure III-12) and 4.79 ppm in ²H NMR (Figure III-13).

Our studies provided evidence that deuterium incorporates into the products, consistent with Scheme III-39. However, the use of labeled reagents did not elucidate the mechanism of zinc(II) catalyzed carbonyl hydrosilylation as significant H/D scrambling was observed.

III. 6 Hydrosilylation catalyzed by (ArN)Mo(H)(Cl)(PMe₃)₃

The hydrosilylation of benzaldehyde catalyzed by (ArN)Mo(H)(Cl)(PMe₃)₃ was previously studied by Andrey Khalimon and Eric Peterson from our group.^{5a} It was shown that benzaldehyde replaces the phosphine ligand *trans* to the hydride to give the η^2 -coordinate benzaldehyde derivative (ArN)Mo(H)(η^2 -PhCHO)(Cl)(PMe₃)₂ followed by its slow re-arrangement into the benzyloxy triphosphine complex (ArN)Mo(OCH₂Ph)(Cl)(PMe₃)₃ and then, by the reaction with silane (Scheme III-40).



Scheme III-40. Proposed catalytic cycle of hydrosilylation of benzaldehyde by PhSiH₃ catalyzed by (ArN)Mo(H)(Cl)(PMe₃)₃.

Given the possibility of new reaction pathways discussed in this Thesis, we decided to revisit the investigation of this system.

III.6.1 Reactions (ArN)Mo(H)(Cl)(PMe₃)₃ with benzaldehyde

As previously reported, complex (ArN)Mo(H)(Cl)(PMe₃)₃ reacts with a stoichiometric amount of benzaldehyde to give two isomers of (ArN)Mo(H)(η^2 -PhCHO)(Cl)(PMe₃)₂,^{5a} formed in the 5:1 mol ratio. These isomers give rise to characteristic ¹H NMR signals at 5.41 ppm (d, *J*_{H-P} = 13.3 Hz, C-H, CHO, PhCHO, minor isomer) and 5.77 ppm (vt, *J*_{H-P} = 2.7 Hz, C-H, CHO, PhCHO, major isomer). The C-H

identity of the signal at 5.41 ppm was verified by a correlation with the characteristic carbon signal at 87.5 ppm in the ^1H - ^{13}C HSQC NMR spectrum (Figure III-14).

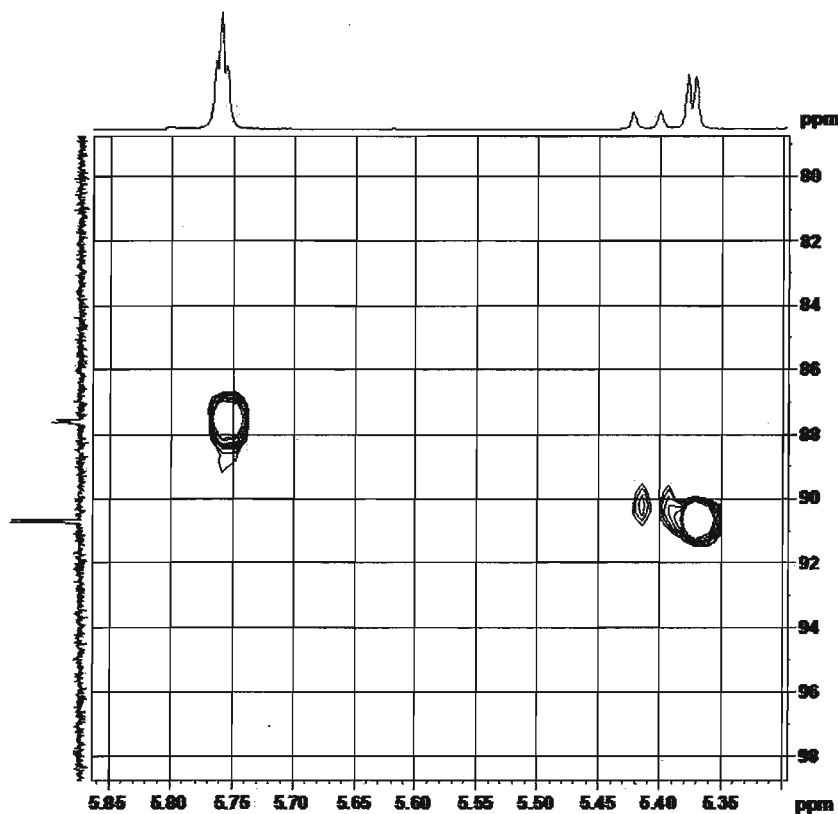
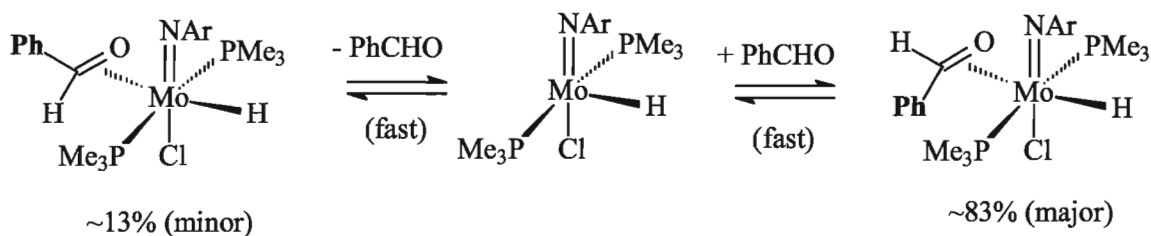


Figure III-14. ^1H - ^{13}C HSQC spectrum of the reaction mixture containing two isomers of $(\text{ArN})\text{Mo}(\text{H})(\eta^2\text{-PhCHO})(\text{Cl})(\text{PMe}_3)_2$.

The two isomers presumably correspond to two different orientations of the η^2 -coordinated benzaldehyde: “up” and “down” isomers. In addition, we found by Selective ge-1D EXSY NMR experiments that two isomers are in a very fast exchange, and they exchange the η^2 -coordinated benzaldehyde with free PhCHO (Figure V-78, Figure V-79, Figure V-80).

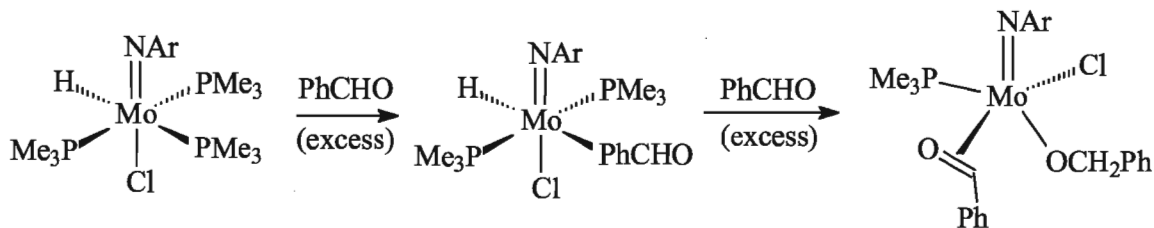


Scheme III-41. Exchange between two isomers of $(\text{ArN})\text{Mo}(\text{H})(\eta^2\text{-PhCHO})(\text{Cl})(\text{PMe}_3)_2$.

We propose that the “down” isomer is thermodynamically more stable and is the major isomer. Position of the benzene ring of PhCHO opposite to the imido group minimizes steric repulsions within the molecule.

Two PMe_3 ligands are also in a fast exchange (Figure V-81, Figure V-82). However, they do not exchange with the external phosphine on the EXSY NMR time scale. It is likely that dissociation of aldehyde forms a five-coordinate intermediate in which the exchange of phosphines may take place.

Complex $(\text{ArN})\text{Mo}(\text{H})(\eta^2\text{-PhCHO})(\text{Cl})(\text{PMe}_3)_2$ is not stable and either decomposes (in the absence of the external phosphine) or re-arranges into the triphosphine benzyloxy complex $(\text{ArN})\text{Mo}(\text{OCH}_2\text{Ph})(\text{Cl})(\text{PMe}_3)_3$. Additionally, we found that in the presence of the large excess of external aldehyde (~ 10 eq.) complex $(\text{ArN})\text{Mo}(\text{H})(\eta^2\text{-PhCHO})(\text{Cl})(\text{PMe}_3)_2$ gives $(\text{ArN})\text{Mo}(\text{OCH}_2\text{Ph})(\eta^2\text{-PhCHO})(\text{Cl})(\text{PMe}_3)$ (Scheme III-42).



Scheme III-42. Formation of $(\text{ArN})\text{Mo}(\text{OCH}_2\text{Ph})(\eta^2\text{-PhCHO})(\text{Cl})(\text{PMe}_3)$.

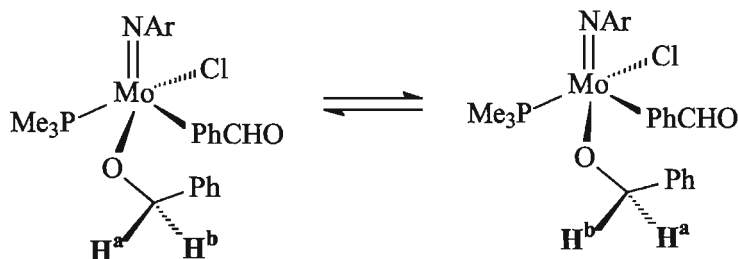
We determined the rate constants of the re-arrangement of $(\text{ArN})\text{Mo}(\text{H})(\eta^2\text{-PhCHO})(\text{Cl})(\text{PMe}_3)_2$ into $(\text{ArN})\text{Mo}(\text{OCH}_2\text{Ph})(\eta^2\text{-PhCHO})(\text{Cl})(\text{PMe}_3)$ in the presence of 10 eq. PhCHO at four temperatures: $k(10.0\text{ }^\circ\text{C}) = (3.77 \pm 0.02) \cdot 10^{-5} \text{ s}^{-1}$, $k(18.0\text{ }^\circ\text{C}) = (1.57 \pm 0.03) \cdot 10^{-4} \text{ s}^{-1}$, $k(23.4\text{ }^\circ\text{C}) = (3.02 \pm 0.02) \cdot 10^{-4} \text{ s}^{-1}$, and $k(34.0\text{ }^\circ\text{C}) = (3.12 \pm 0.05) \cdot 10^{-3} \text{ s}^{-1}$. Activation parameters were extracted from the Eyring plot (Figure

V-76): $\Delta H^\ddagger = 131 \pm 11$ kJ/mol, $\Delta S^\ddagger = 133 \pm 38$ J/(K·mol). The large positive value of the entropy of activation suggests that the rate-determining step is dissociative. We believe that the reaction begins with hydride transfer to the coordinated benzaldehyde to give the benzyloxy group followed by dissociation of a phosphine ligand and coordination of the external benzaldehyde.

We determined that conversion of $(\text{ArN})\text{Mo}(\text{H})(\eta^2\text{-PhCHO})(\text{Cl})(\text{PMe}_3)_2$ into $(\text{ArN})\text{Mo}(\text{OCH}_2\text{Ph})(\eta^2\text{-PhCHO})(\text{Cl})(\text{PMe}_3)$ does not depend on the concentration of the external aldehyde (see Figure V-77). The reaction rate did not change when 5, 10 or 15 eq. of PhCHO were used. However, the different amounts of free PhCHO affected the ratio of the two major products, $(\text{ArN})\text{Mo}(\text{OCH}_2\text{Ph})(\text{Cl})(\text{PMe}_3)_3$ and $(\text{ArN})\text{Mo}(\text{OCH}_2\text{Ph})(\eta^2\text{-PhCHO})(\text{Cl})(\text{PMe}_3)$.

Complex $(\text{ArN})\text{Mo}(\text{OCH}_2\text{Ph})(\eta^2\text{-PhCHO})(\text{Cl})(\text{PMe}_3)$ exchanges the coordinated benzaldehyde with free PhCHO (Figure V-89, Figure V-90). However, no exchange between the phosphine ligand and the free PMe_3 was observed (Figure V-88).

The dissociation of coordinated benzaldehyde results in exchange between the diastereotopic protons of the benzyloxy group (Scheme III-43), which was followed by NMR.

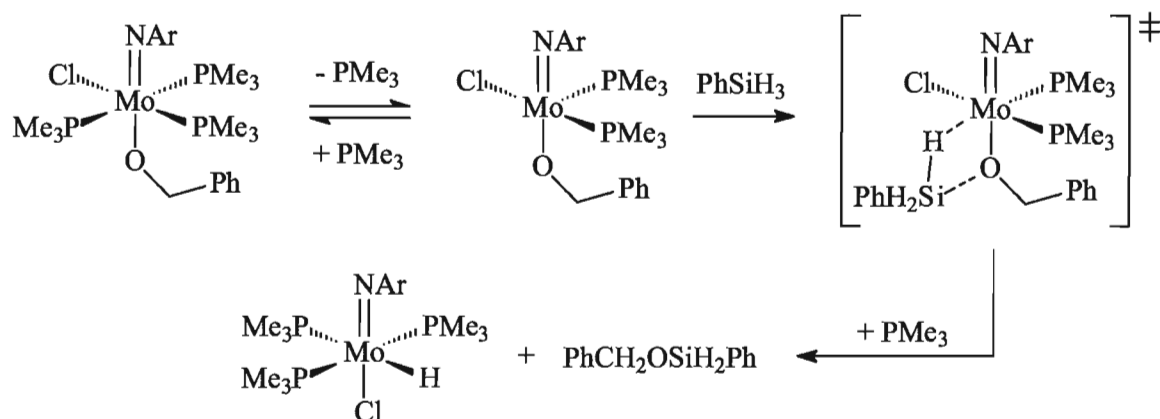


Scheme III-43. Exchange of diastereotopic protons in $(\text{ArN})\text{Mo}(\text{OCH}_2\text{Ph})(\eta^2\text{-PhCHO})(\text{Cl})(\text{PMe}_3)$.

The rate constants were measured at four different temperatures: $k(18.1\text{ }^\circ\text{C}) = (5.60 \pm 0.08) \cdot 10^{-1} \text{ s}^{-1}$, $k(22.0\text{ }^\circ\text{C}) = (1.378 \pm 0.007) \text{ s}^{-1}$, $k(26.0\text{ }^\circ\text{C}) = (2.61 \pm 0.05) \text{ s}^{-1}$, and $k(30.0\text{ }^\circ\text{C}) = (5.01 \pm 0.04) \text{ s}^{-1}$. The activation parameters suggest that the mechanism of the exchange is dissociative: $\Delta H^\ddagger = 131 \pm 8$ kJ/mol, $\Delta S^\ddagger = 200 \pm 27$ J/(K·mol).

III.6.2 Reaction between $(\text{ArN})\text{Mo}(\text{OCH}_2\text{Ph})(\text{Cl})(\text{PMe}_3)_3$ and PhSiH_3 : kinetic studies

Previous studies in our group showed that the reaction between $(\text{ArN})\text{Mo}(\text{OCH}_2\text{Ph})(\text{Cl})(\text{PMe}_3)_3$ and PhSiH_3 regenerates the initial hydride $(\text{ArN})\text{Mo}(\text{H})(\text{Cl})(\text{PMe}_3)_3$ and gives the silyl ether $\text{PhCH}_2\text{OSiH}_2\text{Ph}$ (Scheme III-40). When PhSiD_3 is used, the reaction provides the exclusive formation of $(\text{ArN})\text{Mo}(\text{D})(\text{Cl})(\text{PMe}_3)_3$. The reaction rate constants were found under the pseudo-first order conditions (5 eq. of silane, 30 eq. of PMe_3)^g at 10 °C: $k(\text{PhSiH}_3) = (4.98 \pm 0.02) \cdot 10^{-4} \text{ s}^{-1}$, $k_D(\text{PhSiD}_3) = (5.20 \pm 0.02) \cdot 10^{-4} \text{ s}^{-1}$. The negligible kinetic isotope effect $\text{KIE} = 0.96$ may indicate that the reaction transition state does not involve a significant activation of silane Si-H bond. Most likely the reaction proceeds via a heterolytic splitting of silane on the Mo-O bond rather than via the formation of a silane σ -complex and/or the oxidative addition of silane to give a Mo(VI) species (the latter case would provide a primary KIE). The reaction rate constant is inversely proportional to the PMe_3 concentration, which suggests the pre-dissociation of phosphine as depicted in Scheme III-44.

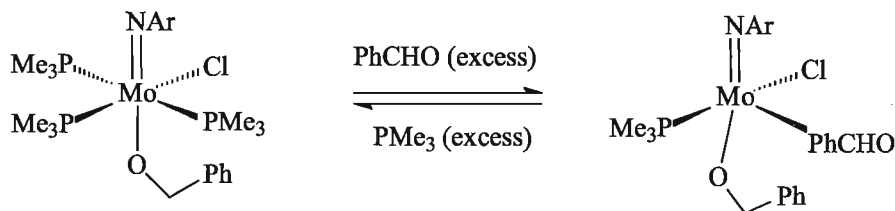


Scheme III-44. Proposed mechanism for the reaction between $(\text{ArN})\text{Mo}(\text{OCH}_2\text{Ph})(\text{Cl})(\text{PMe}_3)_3$ and PhSiH_3 .

^g A large excess of PMe_3 in the reaction mixture was necessary to provide the clean formation of $(\text{ArN})\text{Mo}(\text{H})(\text{Cl})(\text{PMe}_3)_3$.

III.6.3 Reactivity of $(\text{ArN})\text{Mo}(\text{OCH}_2\text{Ph})(\text{Cl})(\text{PMe}_3)_3$ with aldehydes

Our recent results show that under actual catalytic conditions (e.g 10 times excess of benzaldehyde) the complex $(\text{ArN})\text{Mo}(\text{OCH}_2\text{Ph})(\text{Cl})(\text{PMe}_3)_3$ can be converted into the benzyloxy benzaldehyde complex $(\text{ArN})\text{Mo}(\eta^2\text{-PhCHO})(\text{OCH}_2\text{Ph})(\text{Cl})(\text{PMe}_3)$. The reaction is reversible. Evaporation of the excessive amount of benzaldehyde and addition of 10 eq. of PMe_3 regenerates the initial benzyloxy triphosphine complex (Scheme III-45).



Scheme III-45. Reversible formation of $(\text{ArN})\text{Mo}(\eta^2\text{-PhCHO})(\text{OCH}_2\text{Ph})(\text{Cl})(\text{PMe}_3)$ from $(\text{ArN})\text{Mo}(\text{OCH}_2\text{Ph})(\text{Cl})(\text{PMe}_3)_3$.

We found that, when treated with pivalaldehyde (1.3 eq.), the complex $(\text{ArN})\text{Mo}(\text{OCH}_2\text{Ph})(\text{Cl})(\text{PMe}_3)_3$ regenerates the free benzaldehyde (Figure III-15).

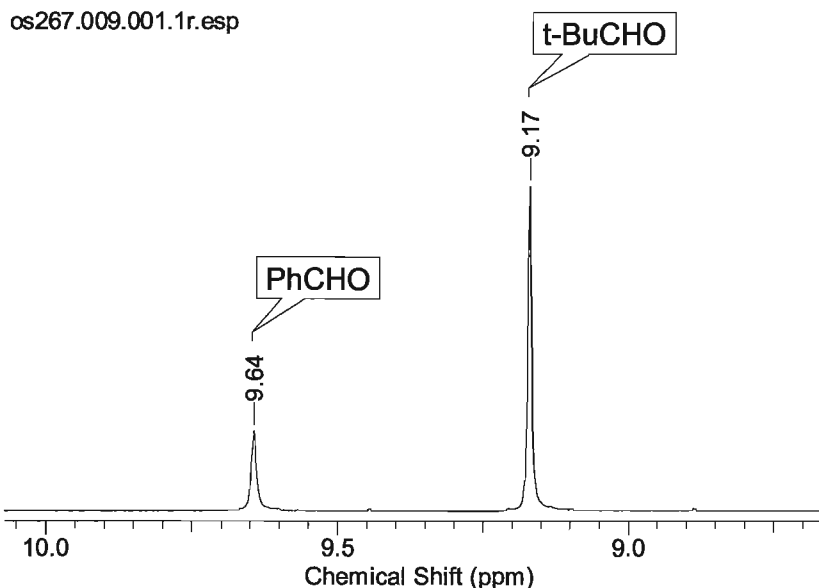
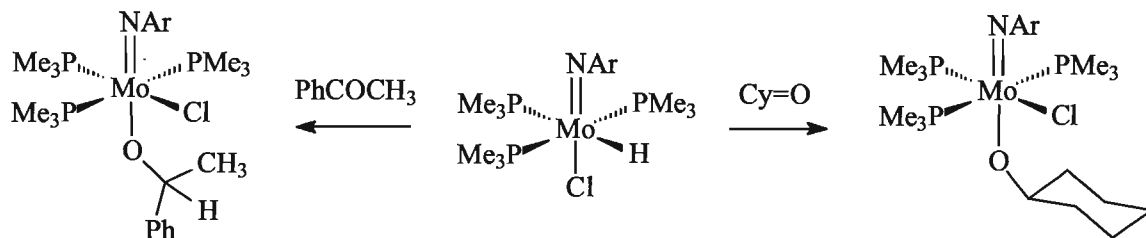


Figure III-15. Formation of free benzaldehyde when complex $(\text{ArN})\text{Mo}(\text{OCH}_2\text{Ph})(\text{Cl})(\text{PMe}_3)_3$ reacts with $t\text{-BuCHO}$. ^1H NMR spectrum.

This reaction is likely initiated by phosphine dissociation and coordination of the external aldehyde to the metal centre followed by hydride transfer from the methylene group of the alkoxy ligand to the carbonyl group. We failed to determine the exact products from this reaction due to complexity of the NMR spectra.

III.6.4 Reactivity of $(\text{ArN})\text{Mo}(\text{H})(\text{Cl})(\text{PMe}_3)_3$ with ketones

We also investigated the reactivity of complex $(\text{ArN})\text{Mo}(\text{H})(\text{Cl})(\text{PMe}_3)_3$ toward ketones. Cyclohexanone and benzophenone, similarly to benzaldehyde, react with $(\text{ArN})\text{Mo}(\text{H})(\text{Cl})(\text{PMe}_3)_3$ and give the ketyoxy derivatives, $(\text{ArN})\text{Mo}(\text{OCy})(\text{Cl})(\text{PMe}_3)_3$ and $(\text{ArN})\text{Mo}(\text{OC}(\text{Me})\text{Ph})(\text{Cl})(\text{PMe}_3)_3$, respectively (Scheme III-46).



Scheme III-46. Reaction of $(\text{ArN})\text{Mo}(\text{H})(\text{Cl})(\text{PMe}_3)_3$ with acetophenone and cyclohexanone.

The complex $(\text{ArN})\text{Mo}(\text{OCy})(\text{Cl})(\text{PMe}_3)_3$ was isolated in 51% yield and characterized by NMR and X-ray diffraction analysis (Table VI-3, Chapter VI). The molecular structure of $(\text{ArN})\text{Mo}(\text{OCy})(\text{Cl})(\text{PMe}_3)_3$ shows that the Mo atom is in the octahedral environment (Scheme III-15). The cyclohexoxy ligand is laying *trans*- to the imido group (O1-Mo1-N1 angle is $175.99(11)^\circ$, Table III-7). That geometry minimizes the steric repulsion in the molecule and is consistent with the strong *trans*-influence of the imido group.¹⁴²

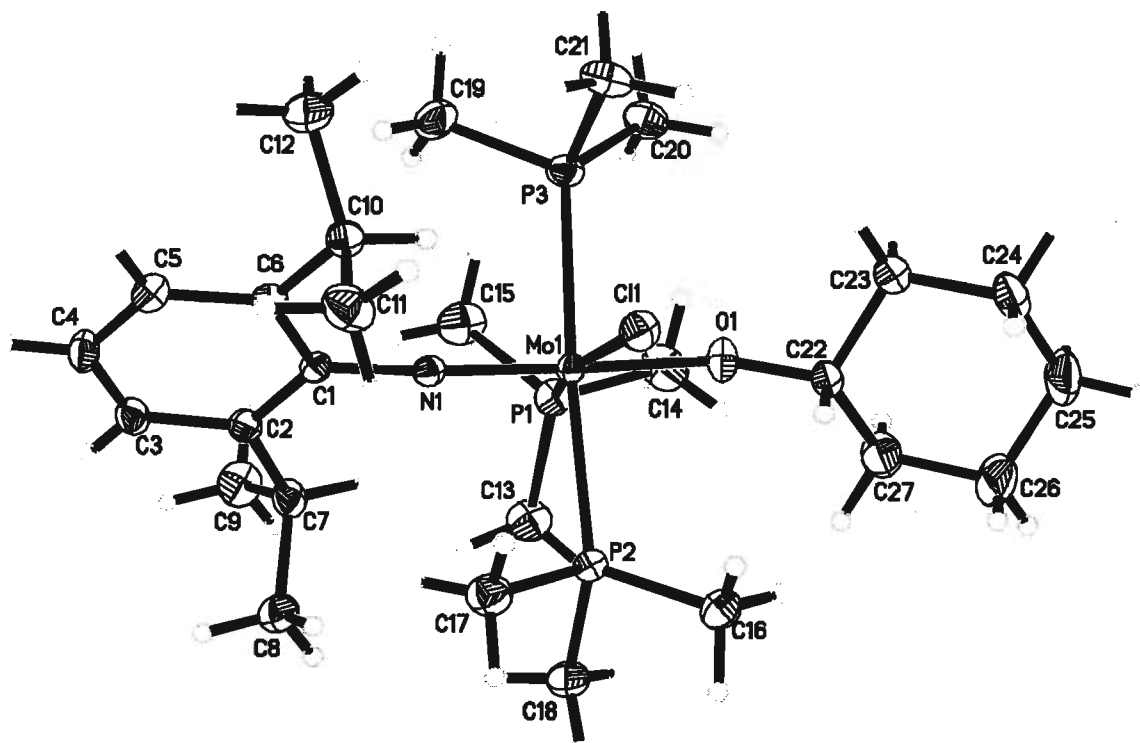
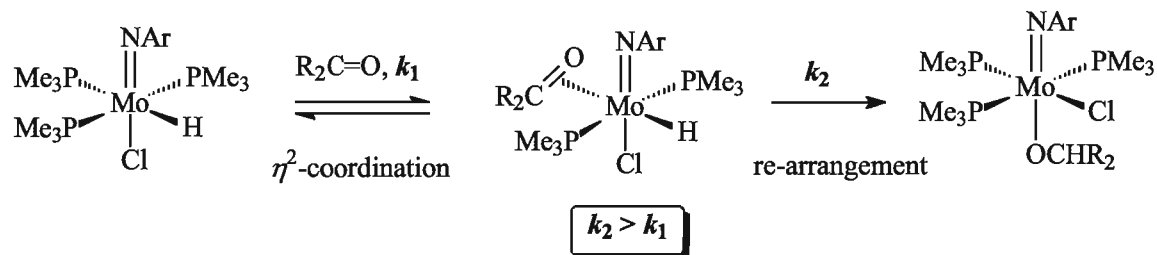


Figure III-16. ORTEP plot for the molecular structure of $(\text{ArN})(\text{CyO})\text{Mo}(\text{Cl})(\text{PMe}_3)_3$. Anisotropic displacement parameters are plotted at 50% probability.

Table III-7. Selected bond distances (\AA) and angles ($^\circ$) for $(\text{ArN})(\text{CyO})\text{Mo}(\text{Cl})(\text{PMe}_3)_3$

<i>distances, \AA</i>		<i>angles, $^\circ$</i>	
Mo1-N1	1.786(3)	Mo1-N1-C1	176.4(2)
Mo1-O1	1.984(2)	N1-Mo1-O1	175.99(11)
Mo1-Cl1	2.5462(8)	P1-Mo1-Cl1	166.80(3)
Mo1-P1	2.4762(9)	P2-Mo1-P3	168.64(3)
Mo1-P2	2.5524(9)	N1-Mo1-Cl1	98.02(8)
Mo1-P3	2.5072(9)	N1-Mo1-P2	90.88(8)

We were unable to observe the possible η^2 -ketone intermediate in this reaction. This fact suggests that the re-arrangement of such a η^2 -ketone complex into the alkoxy derivatives proceeds faster than its formation.



Scheme III-47. Proposed mechanism of formation of ketoxy derivatives of $(\text{ArN})\text{Mo}(\text{H})(\text{Cl})(\text{PMe}_3)_3$.

The complex $(\text{ArN})\text{Mo}(\text{OCy})(\text{Cl})(\text{PMe}_3)_3$ undergoes phosphine dissociation, which was observed directly in ^1H NMR spectrum by the appearance of a signal at 0.90 ppm and in the ^{31}P NMR by the peak at 61 ppm. All the bound phosphine ligands are in a very fast exchange with the free PMe_3 , as evidenced by the 2D ^{31}P - ^{31}P EXSY NMR (Figure V-69) and by Selective ge-1D EXSY NMR (Figure V-70, Figure V-71). Judging by the peak intensities in the 2D EXSY spectrum, the *cis*-phosphines dissociate more easily than the *trans*-phosphine ligand, consistent with the stronger phosphine trans-effect as compare with chloride trans-effect.

The cyclohexoxy complex $(\text{ArN})\text{Mo}(\text{OCy})(\text{Cl})(\text{PMe}_3)_3$ is stable in the presence of a large excess of cyclohexanone (>20 eq.). We did not observe further formation of a η^2 -cyclohexanone adduct, similar to the aldehyde complex $(\text{ArN})\text{Mo}(\text{OCH}_2\text{Ph})(\eta^2\text{-PhCHO})(\text{Cl})(\text{PMe}_3)$. Attempts to force ketone coordination by addition of an equivalent of BPh_3 led to decomposition of $(\text{ArN})\text{Mo}(\text{OCy})(\text{Cl})(\text{PMe}_3)_3$ into a mixture of unidentifiable products and $(\text{ArN})\text{Mo}(\text{Cl})_2(\text{PMe}_3)_3$.

III.6.5 Reaction of $(\text{ArN})\text{Mo}(\text{H})(\text{Cl})(\text{PMe}_3)_3$ with PhSiH_3

Previous experiments with labelled silane PhSiD_3 revealed the exchange between Mo-H of $(\text{ArN})\text{Mo}(\text{H})(\text{Cl})(\text{PMe}_3)_3$ and the Si-H protons of silane. In the presence of

PhSiD₃, the Mo-*H* group is fully substituted by deuterium within one day at RT (Table III-8).

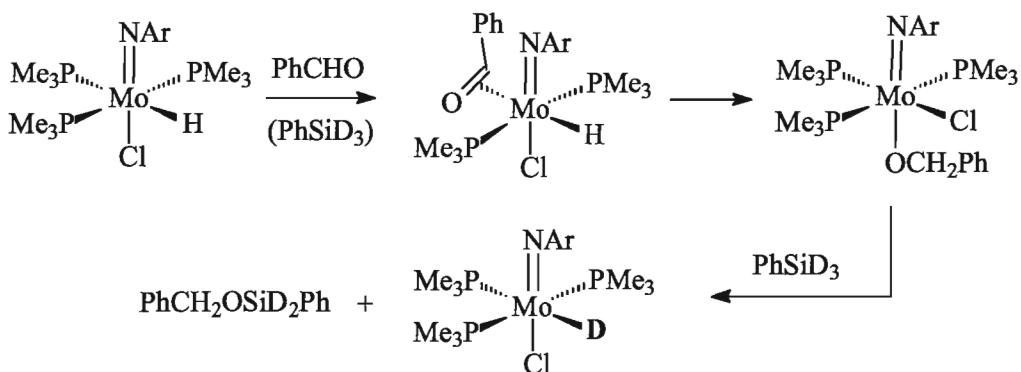
Table III-8. Change in the hydride intensity for (ArN)Mo(H)(Cl)(PMe₃)₃ in the presence of PhSiD₃ (4.2 eq.).

<i>Time</i>	<i>Mo-H, %</i>
10 min	~91%
6 hours	~45%
26 hours	~1%

When reacted with PhSiH₃ for more than one day at RT, the hydride (ArN)Mo(H)(Cl)(PMe₃)₃ slowly decomposes into a mixture of unidentifiable products. This reaction is accompanied by silane redistribution into Ph₂SiH₂, Ph₃SiH and SiH₄.

III.6.6 Reaction between (ArN)Mo(H)(Cl)(PMe₃)₃, PhSiD₃ and PhCHO

Mixing (ArN)Mo(H)(Cl)(PMe₃)₃, PhSiD₃ and PhCHO in the 1:1:1 mol ratio results in quick formation of (ArN)Mo(H)(η^2 -PhCHO)(Cl)(PMe₃)₂ followed by its slow rearrangement into the benzyloxy complex and the reaction with the silane (Scheme III-48). The reaction produced a large amount of (ArN)Mo(D)(Cl)(PMe₃)₃ as a result of the hydride insertion into the carbonyl group, consistent with our previously suggested mechanism.

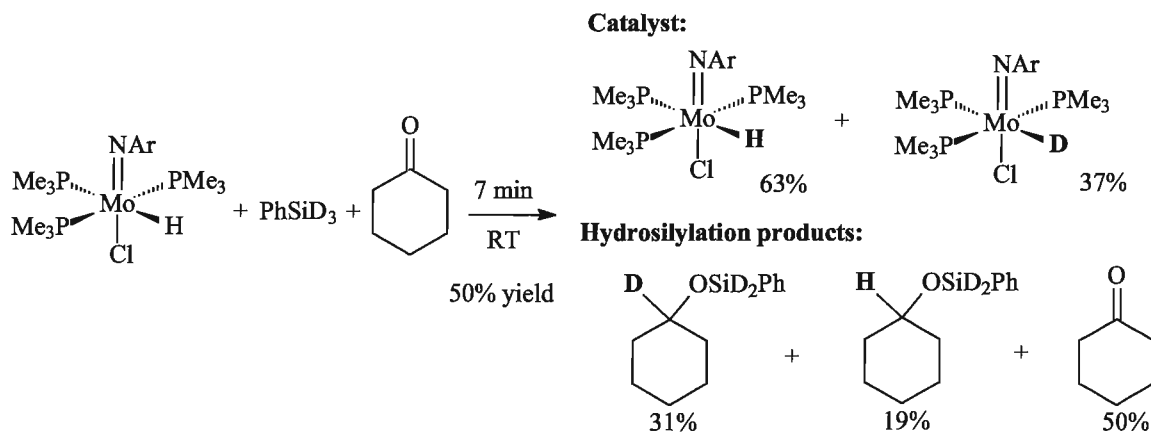


Scheme III-48. Stoichiometric reaction between $(\text{ArN})\text{Mo}(\text{H})(\text{Cl})(\text{PMe}_3)_3$, PhSiD_3 and benzaldehyde.

We did not observe the activation of substrates without the hydride migration to the carbonyl group in this system. The ability of benzaldehyde to form easily the η^2 -adduct dominates this reaction.

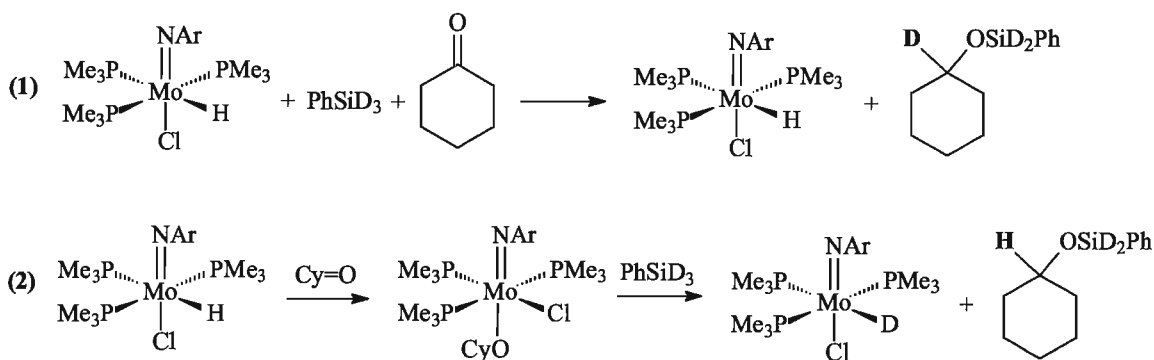
III.6.7 Reactions between $(\text{ArN})\text{Mo}(\text{H})(\text{Cl})(\text{PMe}_3)_3$, PhSiD_3 and cyclohexanone

The reaction between $(\text{ArN})\text{Mo}(\text{H})(\text{Cl})(\text{PMe}_3)_3$, cyclohexanone (1 eq.) and PhSiD_3 (1 eq.) at 50% conversion (approximately 7 minutes) provided the following distribution of the components: $(\text{ArN})\text{Mo}(\text{H})(\text{Cl})(\text{PMe}_3)_3$ (63%), $(\text{ArN})\text{Mo}(\text{D})(\text{Cl})(\text{PMe}_3)_3$ (37%), $\text{Cy}(\text{H})\text{OSiD}_2\text{Ph}$ (19%) and $\text{Cy}(\text{D})\text{OSiD}_2\text{Ph}$ (31%) (Scheme III-49). In approximately one hour, the conversion of cyclohexanone was complete, and the catalyst was present as a mixture of $(\text{ArN})\text{Mo}(\text{H})(\text{Cl})(\text{PMe}_3)_3$ (44%) and $(\text{ArN})\text{Mo}(\text{D})(\text{Cl})(\text{PMe}_3)_3$ (66%).



Scheme III-49. Stoichiometric reaction between $(\text{ArN})\text{Mo}(\text{H})(\text{Cl})(\text{PMe}_3)_3$, PhSiD_3 and cyclohexanone.

This experiment suggests the hydrosilylation of cyclohexanone may proceed via two independent mechanisms. On one hand, a fast hydride transfer from the catalyst to cyclohexanone gives the alkoxy complex $(\text{ArN})\text{Mo}(\text{OCy})(\text{Cl})(\text{PMe}_3)_3$, which further reacts with PhSiD_3 to give CyOSiD_2Ph and $(\text{ArN})\text{Mo}(\text{D})(\text{Cl})(\text{PMe}_3)_3$. On the other hand, the substrates do not react with the hydride ligand and are merely activated by the Lewis acidic metal center to give CyOSiD_2Ph and $(\text{ArN})\text{Mo}(\text{H})(\text{Cl})(\text{PMe}_3)_3$ (Scheme III-50).

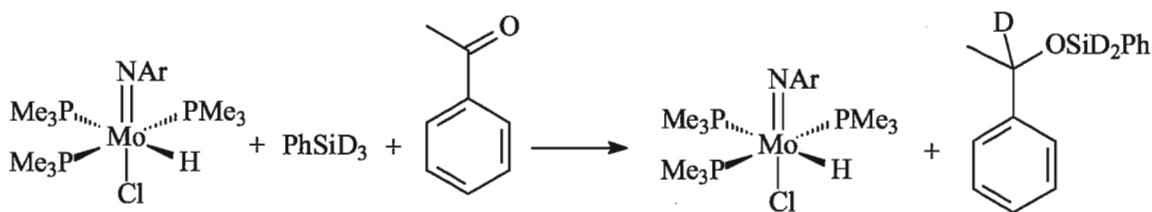


Scheme III-50. Hydrosilylation of cyclohexanone with PhSiD_3 mediated by $(\text{ArN})\text{Mo}(\text{H})(\text{Cl})(\text{PMe}_3)_3$. Two concurrent mechanisms are shown.

III.6.8 Reactions between (ArN)Mo(H)(Cl)(PMe₃)₃, PhSiD₃ and acetophenone

When (ArN)Mo(H)(Cl)(PMe₃)₃ was added to a solution of acetophenone (1 eq.) and PhSiD₃ (1 eq.), the reaction was 50% complete in 3.5 hours at RT. The reaction mixture consisted of (ArN)Mo(H)(Cl)(PMe₃)₃, PhCD(CH₃)OSiD₂Ph and acetophenone. No Mo-bound deuteride was observed in the ¹H NMR spectrum. The reaction mixture was left overnight at RT. The next day, all acetophenone was converted into PhCD(CH₃)OSiD₂Ph, and the catalyst was present as a mixture of (ArN)Mo(H)(Cl)(PMe₃)₃ (80%) and (ArN)Mo(D)(Cl)(PMe₃)₃ (20%).

Since the insertion of acetophenone across the Mo-H bond requires elevated temperatures and is not observed at ambient temperatures, the hydride/ketoxide mechanism can be ruled out. The partial substitution of hydride by deuterium was caused by the slow H/D scrambling between the Mo-H and PhSiD₃ positions. We have previously established that the H/D exchange between (ArN)Mo(H)(Cl)(PMe₃)₃ and PhSiD₃ (1:1 ratio) results in the 30% substitution of Mo-H by deuterium after one day at RT. As a result, we conclude that the hydrosilylation of acetophenone catalyzed by (ArN)Mo(H)(Cl)(PMe₃)₃ proceeds exclusively via the activation of the substrate by the Lewis acidic metal center without the involvement of the Mo-H bond (Scheme III-51).



Scheme III-51. Stoichiometric reaction between (ArN)Mo(H)(Cl)(PMe₃)₃, PhSiD₃ and acetophenone.

We believe the conventional hydride mechanism is suppressed by increased steric hindrance.

III.6.9 Catalysis by (ArN)Mo(H)(Cl)(PMe₃)₃.

The hydrosilylation of aldehydes with PhSiH₃ catalysed by (ArN)Mo(H)(Cl)(PMe₃)₃ was previously established in our group.^{5a} In the present work, we examined other substrates. In particular, we discovered hydrosilylation of cyclohexanone with PhSiH₃, and the hydrosilylation of benzaldehyde, acetophenone and cyclohexanone with polymethylhydrosiloxane (PMHS) (Table III-9). The latter reducing reagent is highly attractive due to its low cost. The best results were observed for the hydrosilylation of ketones with PMHS (100% conversion of substrate).

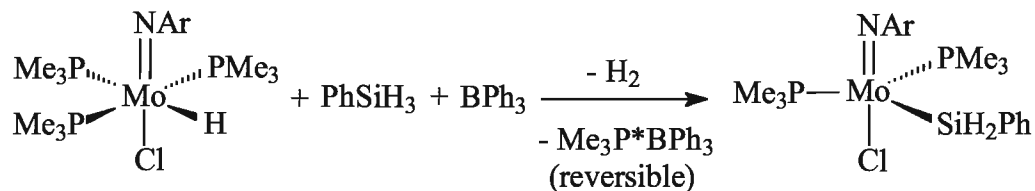
The use of PMHS in hydrosilylation is very advantageous because it is a safe and inexpensive polymer co-product in the silicone industry. In contrast to other reducing hydride agents, PMHS is air- and water-stable, and soluble in most organic solvents.

Table III-9. Hydrosilylation of organic substrates using (ArN)Mo(H)(Cl)(PMe₃)₃ as catalyst

Substrate	Silane	Product	Reaction conditions	Yield, according to ¹ H-NMR	Catalyst mol%
Cy=O	PhSiH ₃	CyOSiH ₂ Ph (CyO) ₂ SiHPh	35 min, RT	79% 21%	5
Cy=O	PhSiH ₃	CyOSiH ₂ Ph (CyO) ₂ SiHPh	3 h, RT	60% 40%	5
PhCHO	PMHS	(PhCH ₂ O) _x (PMHS)	2 days, 50 °C	~50%	6
PhCOCH ₃	PMHS	(Ph(Me)CHO) _x (PMHS)	2 days, 50 °C	100%	6
Cy=O	PMHS	(CyO) _x (PMHS)	3 hours, RT	100%	6

III.6.10 Silyl derivatives of (ArN)Mo(H)(Cl)(PMe₃)₃: preparation and reactivity

Although the reaction (ArN)Mo(H)(Cl)(PMe₃)₃ with PhSiH₃ described above does not yield any silyl product, the reaction goes in a different direction in the presence of borane. Thus, when complex (ArN)Mo(H)(Cl)(PMe₃)₃ is mixed with equimolar amounts of PhSiH₃ and BPh₃, the dehydrogenative silylation is observed, (Scheme III-52).



Scheme III-52. Reaction of (ArN)Mo(H)(Cl)(PMe₃)₃ with PhSiH₃ and BPh₃.

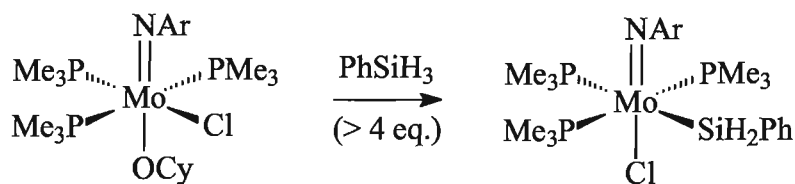
This reaction proceeds only in an open vial under the inert atmosphere of the glovebox. Under these conditions, the molecular hydrogen evolved can freely escape from the reaction mixture. In a sealed NMR tube, H₂ reversely adds with (ArN)Mo(SiH₂Ph)(Cl)(PMe₃)₂ regenerating the initial hydride complex.

The silyl complex (ArN)Mo(SiH₂Ph)(Cl)(PMe₃)₂ is a unique example of an unsaturated molybdenum(IV) complex (16 electrons in the valence electron shell of Mo). It was fully characterized by NMR. We expected it to be highly reactive towards organic compounds and briefly examined its reactivity.

In the presence of PMe₃, (ArN)Mo(SiH₂Ph)(Cl)(PMe₃)₂ forms the triphosphine derivative (ArN)Mo(SiH₂Ph)(Cl)(PMe₃)₃. Addition of one equivalent of BPh₃ reverses the reaction.

We found that the triphosphine silyl complex (ArN)Mo(SiH₂Ph)(Cl)(PMe₃)₃ can be alternatively generated from (ArN)Mo(OCy)(Cl)(PMe₃)₃ by a reaction with excess PhSiH₃ (Scheme III-53). When an equimolar amount of PhSiH₃ is used, the reaction produces a mixture of (ArN)Mo(SiH₂Ph)(Cl)(PMe₃)₃ and (ArN)Mo(H)(Cl)(PMe₃)₃.

In order to obtain the hydride complex as the sole product by this reaction, the cyclohexoxy complex must be reacted with PhSiH₃ in the presence of a large excess of PMe₃ (>10 eq.).



Scheme III-53. Preparation of $(\text{ArN})\text{Mo}(\text{SiH}_2\text{Ph})(\text{Cl})(\text{PMe}_3)_3$ from $(\text{ArN})\text{Mo}(\text{OCy})(\text{Cl})(\text{PMe}_3)_3$.

Both $(\text{ArN})\text{Mo}(\text{SiH}_2\text{Ph})(\text{Cl})(\text{PMe}_3)_2$ and $(\text{ArN})\text{Mo}(\text{SiH}_2\text{Ph})(\text{Cl})(\text{PMe}_3)_3$ are relatively unstable compounds. They can be prepared in microscale amount in a separate vial in the glovebox or generated *in situ* in an NMR tube. Attempts to prepare these complexes in a large-scale amount were unsuccessful due to their instability.

III. 7 Hydroboration catalyzed by (Tp)(ArN)Mo(H)(PMe₃)

As demonstrated above, the complexes (Cp)(ArN)Mo(H)(PMe₃) and (Tp)(ArN)Mo(H)(PMe₃) catalyze the hydrosilylation of carbonyls. The mechanistic studies suggested that at least in some cases the hydrosilylation may proceed via the conventional hydride mechanism, in which one of the key steps is the reaction with silane occurring in the Si-H heterolytic fashion. We reckoned that the more Lewis acidic boranes will facilitate this step, which may at least in some systems have a beneficial effect on the course of catalysis. To our surprise, a literature survey showed that catalytic hydroboration of carbonyls and related substrates, such as nitriles, has never been reported.

To test this hypothesis, we reacted the alkoxy complexes (Cp)(ArN)Mo(OCH₂Ph)(PMe₃) and (Tp)(ArN)Mo(OCH₂Ph)(PMe₃) with one equivalent of catecholborane. Rewardingly, the reactions cleanly generated the corresponding hydride complexes and provided the boryl ether PhCH₂OBCat. Similarly, when the complex (Tp)(ArN)Mo(η^1 -N=CHPh)(PMe₃) was treated with two equivalents of catecholborane, the molybdenum hydride complex was cleanly regenerated, and the reaction yielded PhCH₂N(BCat)₂ in ~100% NMR yield.^h We rationalized that the hydroboration of carbonyls and nitriles could be catalyzed by (Cp)(ArN)Mo(H)(PMe₃) and (Tp)(ArN)Mo(H)(PMe₃) by means of hydride mechanism.

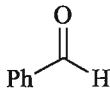
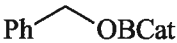
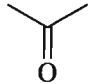
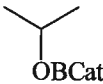
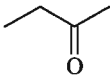
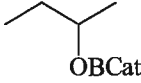
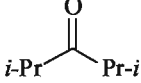
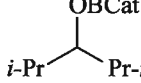
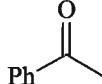
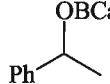
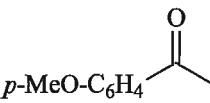
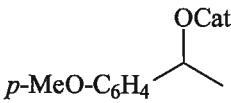
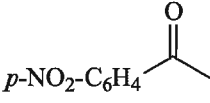
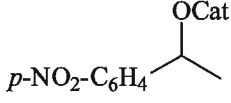
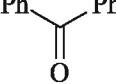
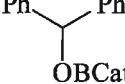
Complex (Cp)(ArN)Mo(H)(PMe₃) quickly decomposes in the presence of catecholborane, and, unfortunately, the hydroboration is not observed. However, the complex (Tp)(ArN)Mo(H)(PMe₃) indeed catalyzes the hydroboration of both carbonyls and nitriles and is perfectly stable in the presence of catecholborane. Below are given some results of our catalytic studies.

^h Addition of an equivalent of CatBH to (Tp)(ArN)Mo(-N=CHPh)(PMe₃) provides only 50% conversion. The partially reduced product PhCH=N-BCat has never been observed.

III.7.1 Catalytic hydroboration of carbonyls

Hydroboration of carbonyls by catecholborane in the presence of 1 mol% of (Tp)(ArN)Mo(H)(PMe₃) in benzene at ambient temperature was observed as an “immediate” reaction in most cases (Table III-10).ⁱ

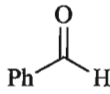
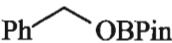
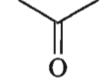
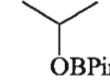
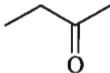
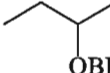
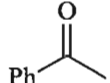
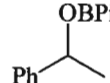
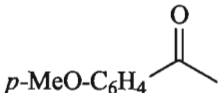
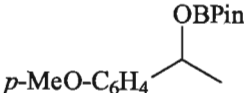
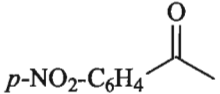
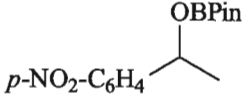
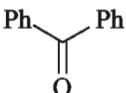
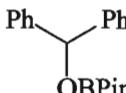
Table III-10. Hydroboration of carbonyls with catecholborane catalyzed by (Tp)(ArN)Mo(H)(PMe₃).

Substrate	Product	Conditions	NMR yield, %	Catalyst load, mol%
		RT, < 5 min	100	1
		RT, < 5 min	100	1
		RT, < 5 min	100	1
Cy=O	CyOBCat	RT, < 5 min	100	1
		RT, 1 d	76	10
		RT, < 5 min	100	1
		RT, < 5 min	100	1
		RT, < 5 min	~45	1
		RT, 5 hr	100	1

ⁱ Uncatalyzed hydroboration of benzaldehyde and cyclohexanone by catecholborane took approximately ~40 min. Other substrates did not react with CatBH in benzene under the mentioned conditions.

The hydroboration by pinacolborane was slower but still clean, with ~ 100% conversions for most substrates (Table III-11). We noticed that the hydroboration of *p*-nitroacetophenone provided low yields (Table III-10, Table III-11) due to catalyst decomposition presumably caused by the presence of the nitro group.

Table III-11. Hydroboration of carbonyls with pinacolborane catalyzed by (Tp)(ArN)Mo(H)(PMe₃).

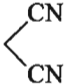

Substrate	Product	Conditions	NMR yield, %	Catalyst load, mol%
		RT, 2.5 hrs	100	5
		RT, < 1hr	100	5
		RT, < 1hr	100	5
Cy=O	CyOBPin	RT, < 1hr	100	5
		RT, 0.5 d	100	2
		RT, 0.5 d	100	5
		RT, 0.5 d	~50%	5
		RT, 1 hr	100	5

III.7.2 Catalytic hydroboration of nitriles

Given the fact that catalytic hydroboration of carbonyls proceeds very easily, we decided to study the hydroboration of more challenging substrates, such as nitriles. We found that the complex (Tp)(ArN)Mo(H)(PMe₃) catalyzes the hydroboration of aromatic

and aliphatic nitriles with catecholborane under relatively mild conditions (Table III-12). The catalysis provides the exclusive formation of N,N-bis(borylamines) in high yields (by NMR).

Table III-12. Hydroboration of nitriles with catecholborane catalyzed by (Tp)(ArN)Mo(H)(PMe₃).

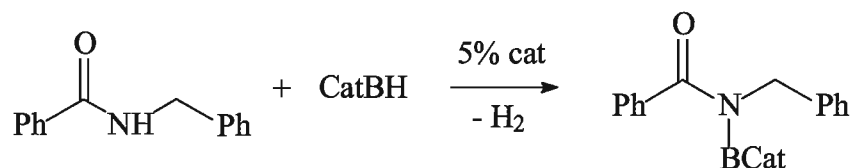
Substrate	Product	Conditions	NMR yield	Catalyst load, mol%
PhCN	PhCH ₂ N(BCat) ₂	0.5 d, RT	100%	5
CH ₃ CN	CH ₃ CH ₂ N(BCat) ₂	0.5 d, 60 °C	100%	5
(CH ₃) ₂ CHCN	(CH ₃) ₂ CHCH ₂ N(BCat) ₂	0.5 d, 60 °C	100%	5
(CH ₃) ₃ CCN	(CH ₃) ₃ CCH ₂ N(BCat) ₂	0.5 d, 60 °C	100%	5
		14 d, RT	20%	20

A 1:1:1 reaction between the benzonitrile, catecholborane and (Tp)(ArN)Mo(H)(PMe₃) was studied by low temperature (VT) NMR in attempts to intercept any possible intermediates or half-products especially the monoborylated nitrile PhCH=NBCat. However, only PhCH₂N(BCat)₂ was seen in spectra.

Pinacolborane was found to be inactive in the hydroboration of nitriles, possibly because of its lower Lewis acidity.

III.7.3 Hydroboration of amides

Primary amides, such as acetamide and benzamide, were not well soluble in benzene, and we could not identify the products of hydroboration.^j Secondary amides reacted with catecholborane via dehydrogenative borylation (Scheme III-54).



Scheme III-54. Dehydrogenative borylation of N-benzylbenzamide.

Hydroboration of tertiary amides was not observed.

III.7.4 Hydroboration of alkynes

Catalytic hydroboration of phenylacetylene by catecholborane results in the formation of *trans*-vinyl product, although competitive polymerization was also observed.



Scheme III-55. Catalytic hydroboration of phenylacetylene with catecholborane.

3-Hexyne (non-terminal alkyne) did not react with catecholborane in the presence of the catalyst over the extended period of time up to one month at RT.

III.7.5 Competitive hydroboration

In order to underpin any potential chemoselectivity of catalytic hydroboration, competitive experiments were undertaken.

Carbonyls vs nitriles

^j Solvents other than benzene or toluene (CDCl_3 , CD_2Cl_2 , $\text{THF}-d_8$, $\text{acetone}-d_6$) could not be used because of the catalyst instability.

We found that carbonyls may be reduced in the presence of nitriles in high yields and chemoselectivities, keeping the nitrile groups unreacted (Table III-13).

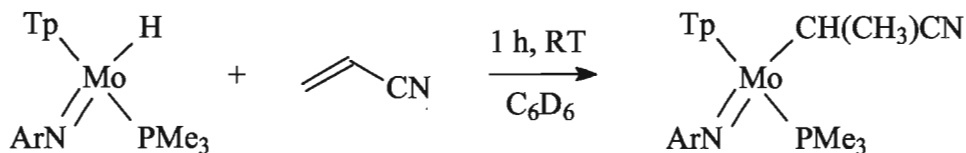
Table III-13. Competitive hydroboration of carbonyls and nitriles by catecholborane catalyzed by (Tp)(ArN)Mo(H)(PMe₃).

Entry	Substrates	Products
1	PhCHO, PhCN	PhCH ₂ OBCat, PhCN
2	<i>p</i> -NCC ₆ H ₄ COCH ₃	<i>p</i> -NCC ₆ H ₄ CH(OBCat)CH ₃
3	PhCOCH ₃ , PhCN	PhCH(OBCat)CH ₃ , PhCN
4	PhCOCH ₃ , (CH ₃) ₂ CHCN	PhCH(OBCat)CH ₃ , (CH ₃) ₂ CHCN

Though the hydroboration was almost 100% selective, we noticed that the reactions required longer time to proceed than the same reactions without the presence of nitrile groups. The mechanistic considerations are discussed in the subsequent paragraphs.

Alkenes vs nitriles

Catalytic hydroboration of acrylonitrile was not observed. However, we found that (Tp)(ArN)Mo(H)(PMe₃) cleanly reacts with acrylonitrile giving the derivative (Tp)(ArN)Mo(CHMeCN)(PMe₃) (Scheme III-56). The product was fully characterized by NMR.



Scheme III-56. Reaction of (Tp)(ArN)Mo(H)(PMe₃) with acrylonitrile.

The reaction is regio- and chemo-specific. Acrylonitrile is an α,β-conjugated system, thus, the hydride transfer proceeds to the terminal (β-) carbon atom, as expected.

The hydroboration of 3-pentenitrile resulted in slow polymerization of the substrate. Additionally, treatment of a mixture of acetonitrile and styrene with

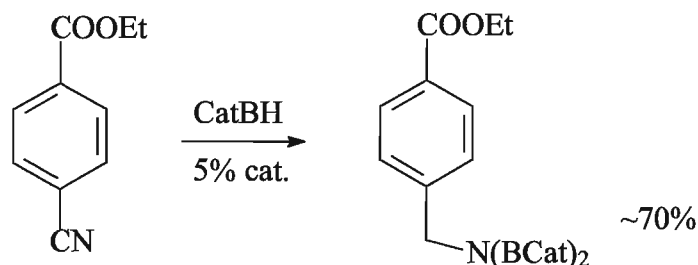
catecholborane in the presence of the catalyst also resulted in slow alkene polymerization and partial hydroboration of the nitrile.

Nitriles vs alkynes

The hydroboration of 1-hexynenitrile resulted in reduction of both the nitrile group and the triple bond. Overall, the reaction was slow and took up to two weeks to proceed. A significant polymerization of the substrate was also observed.

Nitriles vs esters

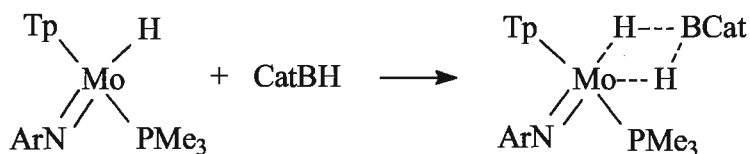
The hydroboration of ethyl 4-cyanobenzoate provided the reduction of the nitrile group with ~70% selectivity (Scheme III-57). The other products related to the reduction of the ester group.



Scheme III-57. Hydroboration of ethyl 4-cyanobenzoate.

III.7.6 Mechanistic considerations

In the presence of catecholborane, the complex $(\text{Tp})(\text{ArN})\text{Mo}(\text{H})(\text{PMe}_3)$ exchanges its hydride with the B-H protons (Scheme III-58).



Scheme III-58. Exchange between $(\text{Tp})(\text{ArN})\text{Mo}(\text{H})(\text{PMe}_3)$ and CatBH .

The ^1H NMR spectrum of a solution containing catecholborane and $(\text{Tp})(\text{ArN})\text{Mo}(\text{H})(\text{PMe}_3)$ showed the coalescence of the Mo-H doublet (3.66 ppm) with the B-H quartet into one broad singlet at 4.06 ppm at room temperature (Figure III-17). The ^{11}B NMR spectrum showed the loss of B-H coupling (Figure III-18).

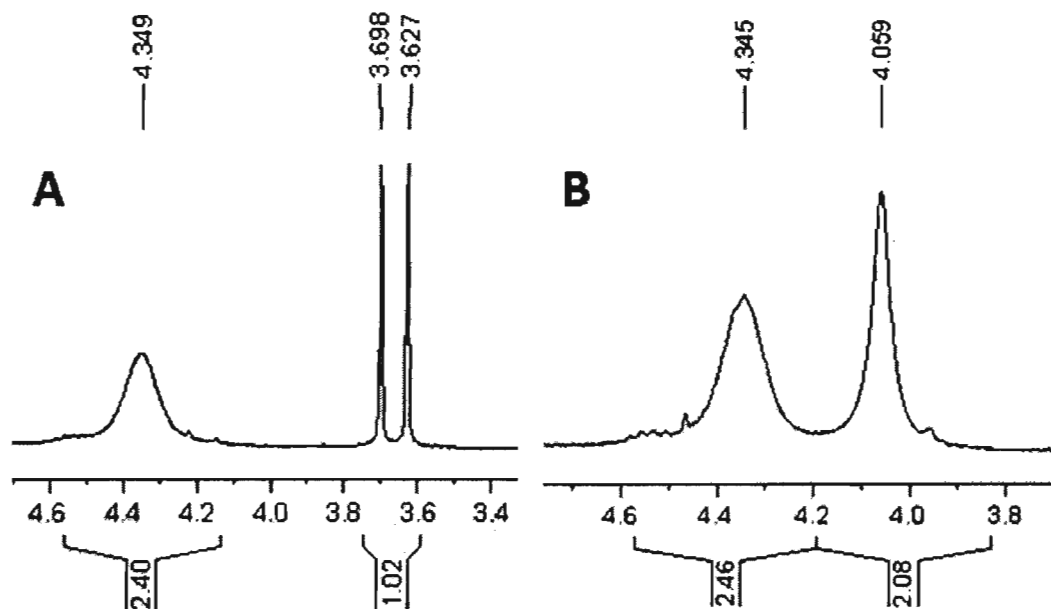


Figure III-17. A. ^1H NMR spectrum of $(\text{Tp})(\text{ArN})\text{Mo}(\text{H})(\text{PMe}_3)$. B. ^1H NMR spectrum of $(\text{Tp})(\text{ArN})\text{Mo}(\text{H})(\text{PMe}_3)$ in the presence of catecholborane.

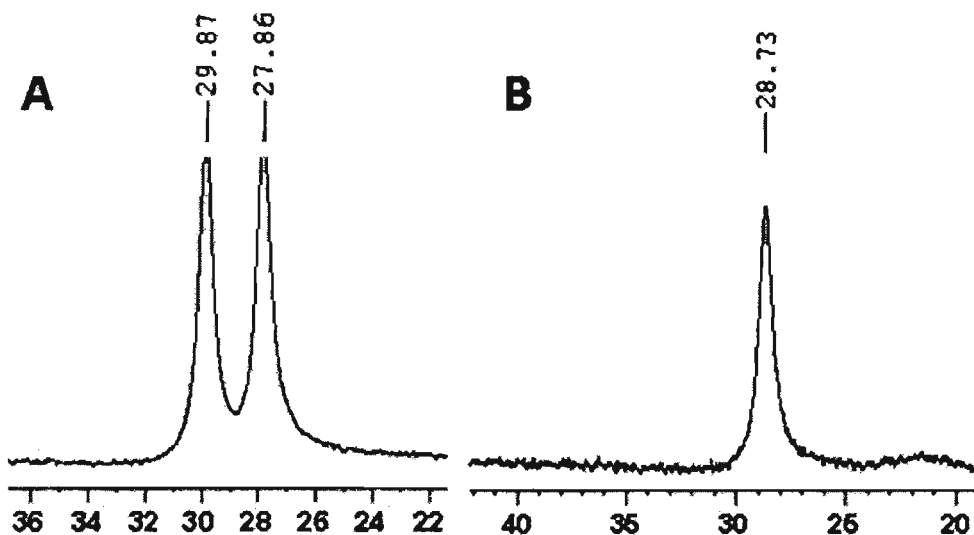
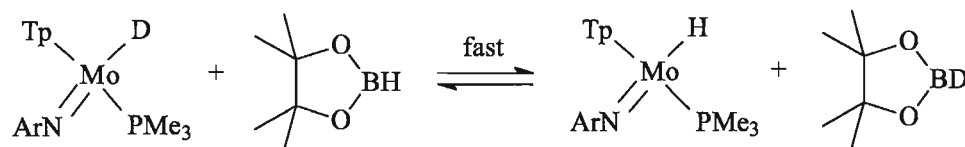


Figure III-18. A. ^{11}B NMR spectrum of CatBH. B. ^{11}B NMR spectrum of CatBH in the presence of $(\text{Tp})(\text{ArN})\text{Mo}(\text{H})(\text{PMe}_3)$.

Addition of PinBH to $(\text{Tp})(\text{ArN})\text{Mo}(\text{H})(\text{PMe}_3)$ does not result in any visible changes in the ^1H and ^{11}B NMR spectra. However, when the deuterated derivative of the molybdenum hydride complex was mixed with PinBH (1 eq), a fast H/D scrambling occurred (Scheme III-59).



Scheme III-59. Reaction between $(\text{Tp})(\text{ArN})\text{Mo}(\text{D})(\text{PMe}_3)$ and PinBH.

The ^{11}B NMR spectrum showed the presence of both PinBH and PinBD in the reaction mixture (Figure III-19).

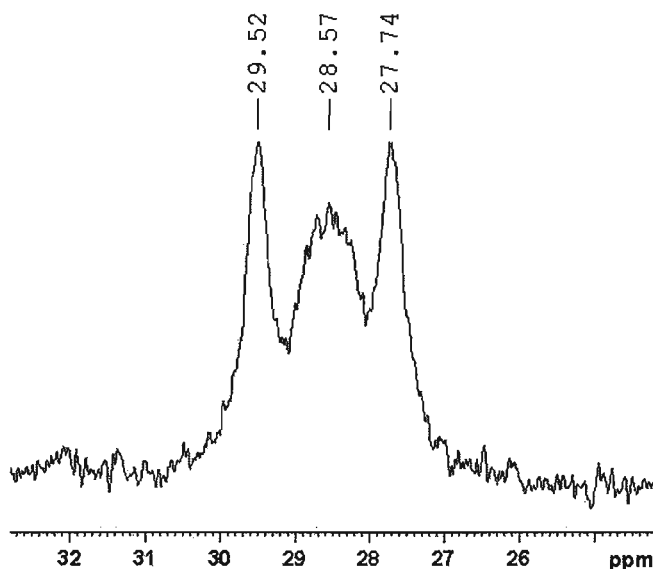
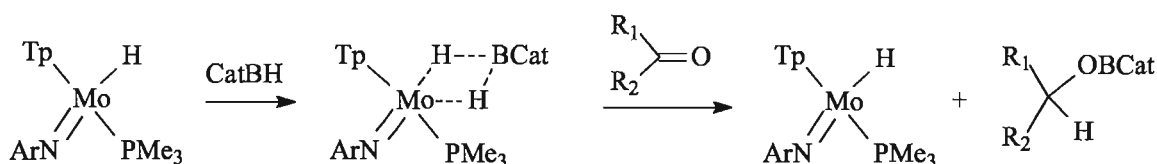


Figure III-19. ^{11}B NMR spectrum of PinBH (28.6 ppm, doublet, $^1J_{\text{B-H}} = 174.1$ Hz) and PinBD (28.6 ppm, singlet) mixture.

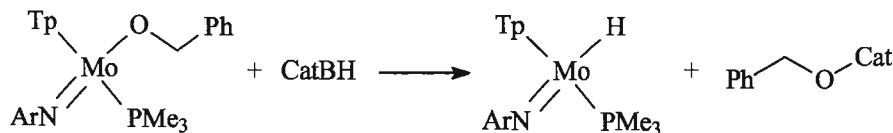
Addition of an equivalent of a carbonyl to a mixture of $(\text{Tp})(\text{ArN})\text{Mo}(\text{H})(\text{PMe}_3)$ and CatBH (or PinBH) provides formation of the corresponding boryl ether and $(\text{Tp})(\text{ArN})\text{Mo}(\text{H})(\text{PMe}_3)$ (Scheme III-60).

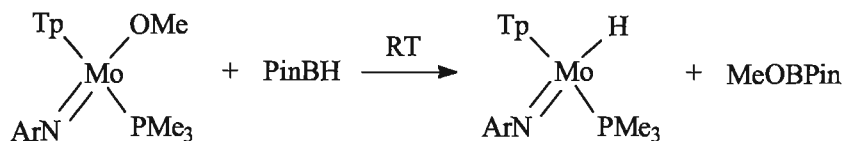


Scheme III-60. Reaction of carbonyl with a mixture of $(\text{Tp})(\text{ArN})\text{Mo}(\text{H})(\text{PMe}_3)$ and CatBH.

The same result is obtained when $(\text{Tp})(\text{ArN})\text{Mo}(\text{H})(\text{PMe}_3)$ is mixed with 1 equivalent of carbonyl followed by the addition of CatBH (or PinBH).

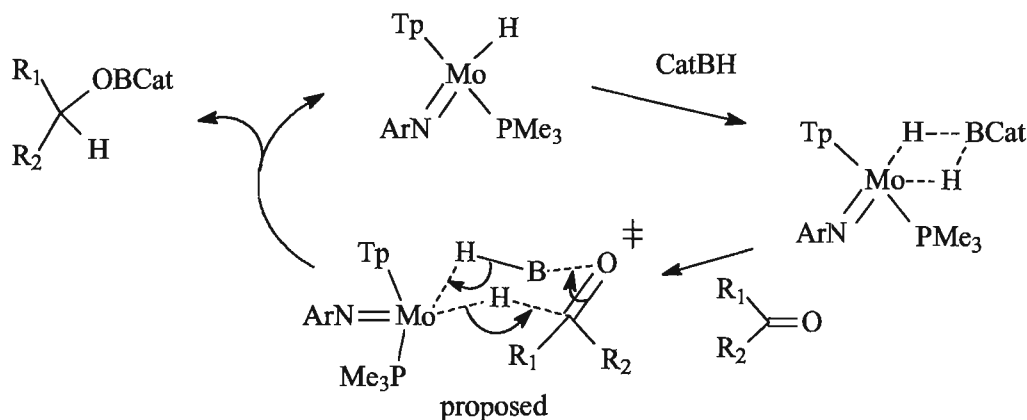
Similarly, alkoxy derivatives of $(\text{Tp})(\text{ArN})\text{Mo}(\text{H})(\text{PMe}_3)$ produce boryl ethers when reacting with CatBH or PinBH (Scheme III-61).





Scheme III-61. Reactions of the molybdenum alkoxy complexes with CatBH and PinBH.

However, there is no experimental evidence that carbonyls may react quickly with $(\text{Tp})(\text{ArN})\text{Mo}(\text{H})(\text{PMe}_3)$ at *ambient temperatures* to produce the alkoxy derivatives. Also, when catalytic reactions were monitored by NMR, only $(\text{Tp})(\text{ArN})\text{Mo}(\text{H})(\text{PMe}_3)$ was present in the reaction mixture. A mechanism that involves the formation of alkoxy derivatives can be ruled out. The catalysis most likely proceeds via a nonhydride mechanism, akin to what has been discussed in the previous sections for catalytic hydrosilylation. The activation of substrates does not appear to involve hydride transfer to the carbonyl group. As one of the options, we suggested the mechanism may include the formation of a molybdenum borate complex followed by its reaction with a carbonyl in a concerted way, via a six-membered transition state (Scheme III-62).



Scheme III-62. Proposed mechanism of carbonyl hydroboration catalyzed by $(\text{Tp})(\text{ArN})\text{Mo}(\text{H})(\text{PMe}_3)$.

However, we were unable to probe experimentally the existence of a concerted mechanism. The reaction of $(\text{Tp})(\text{ArN})\text{Mo}(\text{D})(\text{PMe}_3)$ with PinBH resulted in an “immediate” H/D scrambling, which made it impossible to keep track of the original Mo-H hydride in the further reaction with the carbonyl.

The hydroboration of nitriles appears to follow the hydride mechanism. A catalytic reaction between the benzonitrile and catecholborane showed quick conversion of the initial hydride complex to the methylenamide derivative $(\text{Tp})(\text{ArN})\text{Mo}(-\text{N}=\text{CHPh})(\text{PMe}_3)$, which was observed in the reaction mixture throughout the whole catalysis. Complex $(\text{Tp})(\text{ArN})\text{Mo}(-\text{N}=\text{CHPh})(\text{PMe}_3)$ was individually prepared and characterized. We demonstrated that this complex reacts with two equivalents of CatBH resulting in full regeneration of the starting hydride complex and clean formation of $\text{PhCH}_2\text{N}(\text{BCat})_2$.

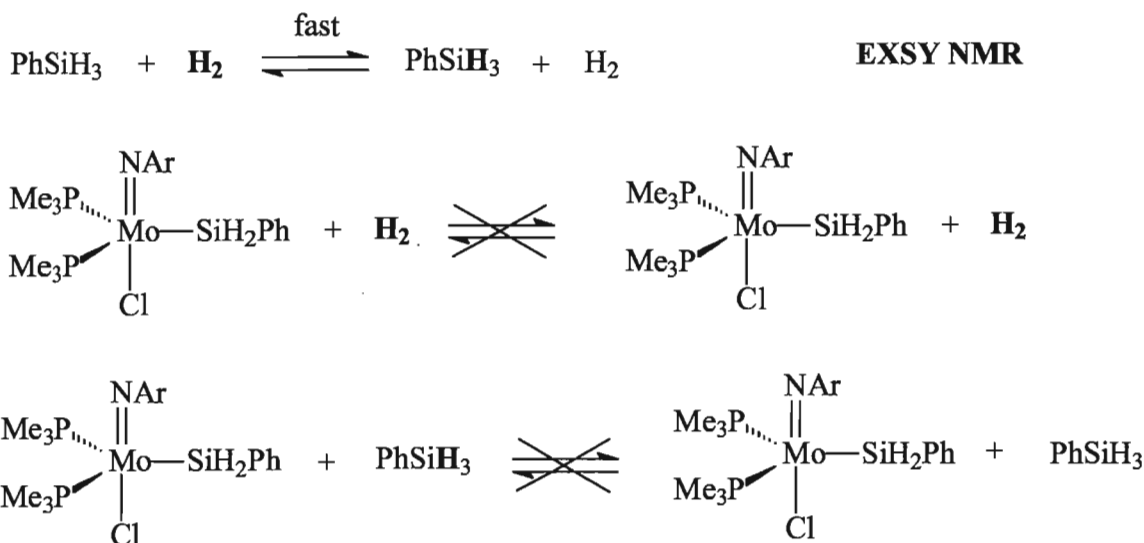
It is interesting to note that the carbonyl hydroboration is inhibited to some extent by the presence of nitriles. We found that the molybdenum hydride complex was converted to the methylenamide derivative in the catalytic mixture containing benzonitrile, acetophenone and catecholborane. A conclusion can be made that the hydroboration of acetophenone can still proceed via the Lewis acid activation of substrates by the metal centre of the methylenamide derivative. The latter is expected to be less active in carbonyl hydroboration due to its increased bulkiness and the diminished electrophilic properties of the molybdenum because of donation of the lone pair of the methyleneamide nitrogen atom to molybdenum.

III. 8 H₂/PhSiH₃ exchange mediated by metal complexes and boranes

III.8.1 Metal complexes

Metal catalyzed H/D exchange reactions can be used in the production of isotopically labeled organic compounds, which is a prospective area of research.¹⁵²

We found that a reaction between (ArN)Mo(H)(Cl)(PMe₃)₃ and PhSiH₃ in the presence of BPh₃ is reversible and leads to the formation of the molybdenum silyl complex (ArN)Mo(SiH₂Ph)(Cl)(PMe₃)₂ and molecular hydrogen H₂. Surprisingly, low-temperature (VT) EXSY NMR studies revealed a very fast proton exchange between H₂ and PhSiH₃ in the presence of (ArN)Mo(SiH₂Ph)(Cl)(PMe₃)₂. The corresponding peaks of H₂ and the silane in ¹H NMR were broad as a result of the exchange.



Scheme III-63. H/Si-H exchange between H₂ and (ArN)Mo(SiH₂Ph)(Cl)(PMe₃)₂ observed by EXSY NMR.

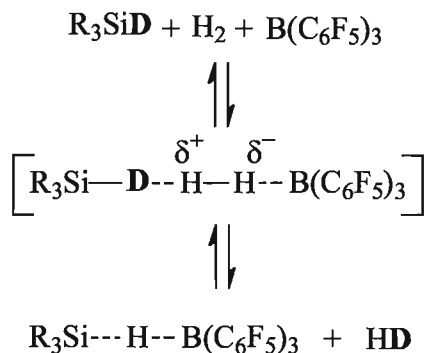
The activation parameters extracted from kinetic measurements indicate the exchange proceeds via an associative mechanism: $\Delta H^\ddagger = 10.7 \text{ J/mol}$, $\Delta S^\ddagger = -197.8 \text{ J/(K}\cdot\text{mol)}$. Although, the detailed mechanistic picture is still unclear, the H/H exchange does not involve the hydrogenation of the Mo-Si bond, i.e. via the silane re-generation/ addition to the complex. EXSY NMR experiments showed that the proton exchange involves only H₂ and the free silane. We studied this reaction in the presence of external phenylsilane,

under conditions when there was no observable exchange in EXSY NMR between the protons of the silane and the silyl ligand.

The silane/hydrogen exchange appears to be a general phenomenon. The solutions of various deuterium-labeled silanes were studied in the presence of catalytic amounts of metal complexes under the hydrogen atmosphere. The H/D exchange was observed by the appearance of *H-D* and *Si-H* characteristic peaks in ^1H NMR spectra. The following metal complexes were tested and demonstrated to mediate $\text{H}_2/\text{Si-D}$ exchange: ZnCl_2 (Figure VI-1), $(\text{PPh}_3)\text{CuH}$ (Figure VI-2), $(\text{ArN})\text{Mo}(\text{H})(\text{Cl})(\text{PMe}_3)$ (Figure VI-3), $(\text{Cp})(\text{ArN})\text{Mo}(\text{H})(\text{PMe}_3)$ (Figure VI-4), $(\text{Tp})(\text{ArN})\text{Mo}(\text{H})(\text{PMe}_3)$ (Figure VI-5, Figure VI-6), $(\text{ArN})\text{Mo}(\text{Cl})_2(\text{PMe}_3)_3$, $(\text{ArN})_2\text{MoCl}_2 \cdot \text{DME}$, $(\text{PPh}_3)_2(\text{I})\text{ReO}_2$, $(\text{PPh}_3)_3\text{ReOCl}_3$.

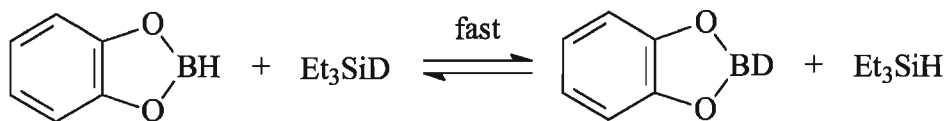
III.8.2 Boranes

Given the generality of the silane/hydrogen exchange discussed above, we reckoned that such a simple Lewis acid as borane can also catalyze this unusual reaction. For instance, triphenylborane is a relatively weak Lewis acid. Nevertheless, we were able to observe a slow formation of protosilane PhSiHD_2 and *H-D* in the solution of PhSiD_3 under hydrogen atmosphere after one month at RT (compare Figure VI-7 and Figure VI-8). This clearly indicates that the $\text{H}_2/\text{Si-H}$ exchange can be initiated in a metal-free medium by boranes. The tris(pentafluorophenyl)borane activates the exchange more effectively, and the appearance of protosilane *Si-H* and *H-D* in ^1H NMR was observed immediately after mixing the reagents (Figure VI-9, Figure VI-10, Figure VI-11). Unfortunately, it is still unclear how this exchange proceeds. The presence of the aryl groups in silanes may not play a key role in the exchange because the exchange was observed with Et_3SiD as well. We considered an opportunity that dihydrogen is first being activated by aryl boranes with the formation of $[\text{C}_6\text{F}_5\text{H}^+ - \text{BH}^-]$ intermediates¹³⁸ followed by a *H/H* exchange between *B-H* and *Si-H*. The other option is the formation of $(\text{C}_6\text{F}_5)_2\text{BH}^{153}$ in catalytic amounts in the reaction mixture to initiate the exchange. The exchange may also be a result of an intermolecular bifunctional activation (Scheme III-64).



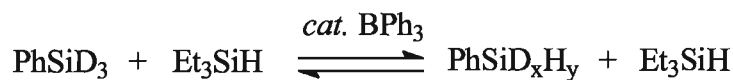
Scheme III-64. Possible activation of the H/D exchange between silane and dihydrogen.

We intended to prove the activation of molecular hydrogen and/or silane by $(\text{C}_6\text{F}_5)_2\text{BD}$. The generation of $(\text{C}_6\text{F}_5)_2\text{BD}$ by the reaction between $(\text{C}_6\text{F}_5)_3\text{B}$ and Et_3SiD unexpectedly gives a broad peak at ~ 4.0 ppm in ^1H NMR presumably due to C-H bond activation in ethyl groups of Et_3SiD since they are the only source of protons. The reaction is not clean overall and it is still under investigation. However, we found a fast H/D scrambling in the mixture of catecholborane and triethylsilane- d_1 (Scheme III-65). That could also be observed between $(\text{C}_6\text{F}_5)_2\text{BD}$ and Et_3SiH . Such hydrogen exchange between boranes (BH) and silanes (SiH) has not been previously known.



Scheme III-65. H/D exchange between catecholborane and triethylsilane- d_1 .

Piers *et al.* reported that H/D exchange between different silanes is mediated by $\text{B}(\text{C}_6\text{F}_5)_3$.⁹⁰ We hereby provide evidence that such an exchange can also be observed in the presence of significantly cheaper and more affordable triphenylborane (Figure VI-12).



Scheme III-66. H/D exchange between PhSiD_3 and Et_3SiH .

IV Conclusions and Future Work

In the course of our studies of hydrosilylation and hydroboration catalyses, we developed a synthetic approach to the novel molybdenum (IV) imido complexes, $(\text{Cp})(\text{ArN})\text{Mo}(\text{H})(\text{PMe}_3)$ and $(\text{Tp})(\text{ArN})\text{Mo}(\text{H})(\text{PMe}_3)$, investigated their structural features and carried out detailed mechanistic studies of stoichiometric reactions of these complexes with various substrates. Some further work will be focused on screening of a broader variety of substrates in the hydrosilylation catalysis.

Our initial kinetic and DFT studies indicated that, unlike its isolobal precursor $(\text{ArN})\text{Mo}(\text{H})(\text{Cl})(\text{PMe}_3)_3$ ^{5a}, the complex $(\text{Cp})(\text{ArN})\text{Mo}(\text{H})(\text{PMe}_3)$ catalyzes the hydrosilylation via an unexpected associative mechanism.^{5b} The initial step of the hydrosilylation catalysis involves the insertion of benzaldehyde into the Mo—H bond to give the alkoxy derivative $(\text{Cp})(\text{ArN})\text{Mo}(\text{OCH}_2\text{Ph})(\text{PMe}_3)$. The latter was characterized by X-ray diffraction analysis. The last step in the proposed mechanism is the reaction of the alkoxy complex with phenylsilane to give the starting hydride complex and the silyl ether. We also showed that, in spite of the d^2 electronic configuration of Mo in complex $(\text{Cp})(\text{ArN})\text{Mo}(\text{H})(\text{PMe}_3)$, its reaction with PhSiH_3 proceeds via an unexpected σ -bond metathesis mechanism that avoids the formation of an unfavourable Mo(VI) species. We, however, managed to observe the first hydrido silyl Mo(VI) derivatives when the reaction of $(\text{Cp})(\text{ArN})\text{Mo}(\text{H})(\text{PMe}_3)$ with PhSiH_3 was carried out in the presence of BPh_3 . A later experiment employing stoichiometric amounts of $(\text{Cp})(\text{ArN})\text{Mo}(\text{H})(\text{PMe}_3)$, benzaldehyde and D_3 -labeled phenylsilane (1:1:1 ratio) showed that the hydrosilylation actually does not involve the hydride transfer molybdenum to the carbonyl.

Analogous 1:1:1 reaction between $(\text{Tp})(\text{ArN})\text{Mo}(\text{H})(\text{PMe}_3)$, PhSiD_3 and carbonyl substrate established that the hydrosilylation is not accompanied by deuterium incorporation into the hydride position of the catalyst. Likewise, the hydrosilylation of carbonyl substrates by deuterated silane in the presence of catalytic amounts of $(\text{Tp})(\text{ArN})\text{Mo}(\text{H})(\text{PMe}_3)$ (5 mol%) does not result in deuterium incorporation into the hydride position. Thus, the conventional hydride mechanism based on carbonyl insertion

into the M-H bond can be reliably ruled out. As $(\text{Tp})(\text{ArN})\text{Mo}(\text{H})(\text{PMe}_3)$ is nonreactive to both the silane and ketone, the only mechanistic alternative we are left with is that the metal center activates the carbonyl as a Lewis acid.

The nonhydride mechanism was also established for the catalyzes by $(\text{ArN})\text{Mo}(\text{H})(\text{Cl})(\text{PMe}_3)$, $(\text{Ph}_3\text{P})_2(\text{I})(\text{O})\text{Re}(\text{H})(\text{OSiMe}_2\text{Ph})$ and $(\text{PPh}_3\text{CuH})_6$. This work clearly demonstrated that the generally accepted hydride mechanism does not work as the major catalysis pathway in these systems. Understanding the mechanism of hydrosilylation catalysis is important for the rational design of new catalysts. Further work must be aimed at the detailed investigation of the nonhydride mechanism to reveal the features of how substrates are activated by the metal centre. For example, replacement of the hydrogen ligand with fluorine may provide related complexes, $(\text{Tp})(\text{ArN})\text{Mo}(\text{F})(\text{PMe}_3)$ and $(\text{Cp})(\text{ArN})\text{Mo}(\text{F})(\text{PMe}_3)$, where the fluorine atom is small enough to offer space for electrophilic activation of substrates but should be unreactive toward carbonyls, thus eliminating the possibility of side reactions such as the formation of alkoxide. The fluorine atom is a strong electron-withdrawing element, and therefore we may anticipate a significant increase in the electrophilic character of Mo. On the other hand, the possible donation of the lone pair of electrons from fluorine to metal also should be considered.

The other major objective of the present Thesis was to investigate the catalytic activity of $(\text{Tp})(\text{ArN})\text{Mo}(\text{H})(\text{PMe}_3)$ in hydroboration reactions. This complex effectively catalyzes hydroboration at room temperature of a wide variety of aldehydes and ketones and with the catalyst load of $< 1\text{mol}\%$. For the first time, we reported the catalytic hydroboration of nitriles with catecholborane. Hydroboration of nitriles produces N,N-bis(borylated) amines, a very rare class of organic compounds.¹⁵⁴ We intend to prepare, isolate and characterize these compounds, and study their reactivity and properties.

In terms of chemoselectivity of hydroboration, we demonstrated that aldehydes and ketones may be reduced in the presence of nitrile groups, keeping the latter unreacted. The further work will be focused on the investigation of hydroboration of a variety of other functional groups such as alkenes, alkynes, imines, imides, esters and studying the selectivity of these reaction.

The hydroboration catalysed by early transition metals is extremely rare. Little is known about the mechanism of the catalysis. We found that the mechanism of hydroboration of carbonyls and nitriles is apparently different. We propose that the hydroboration of carbonyls apparently proceeds via the Lewis-acid activation, while nitriles insert into the MoH bond. We intend to search for the possible intermediates in hydroboration reactions as well as to study their kinetics and obtain the activation parameters.

The silyl complex $(\text{ArN})\text{Mo}(\text{SiH}_2\text{Ph})(\text{Cl})(\text{PMe}_3)_2$, an unusual example of an unsaturated molybdenum(IV) complex (16 electrons in the valence electron shell of Mo), was prepared and fully characterized by NMR. We briefly examined its reactivity. This complex is expected to be highly reactive toward organic substrates. Its reactivity towards alkenes, alkynes, carbonyls, nitriles, etc. should be examined.

Also, for the first time, we reported an unusual activation of dihydrogen by a wide range of metal complexes and boranes, which results in the exchange between H_2 and silane Si-H bonds. Our on-going investigations (stoichiometric reactions, DFT studies) are aimed at understanding the mechanistic features of this exchange. It is still unclear to us if the hydrogen exchange is a result of an intermolecular bifunctional catalysis, and if $\text{B}(\text{C}_6\text{F}_5)_3$ itself can mediate the hydrogen exchange between CatBH and H_2 . In order to verify the Lewis acid activation of H_2 by borane, the deuterated catecholborane CatBD, or other derivatives, such as $(\text{C}_6\text{F}_5)_2\text{BD}$, should be prepared and their reaction with hydrogen should be studied.

V Experimental

General methods and instrumentation

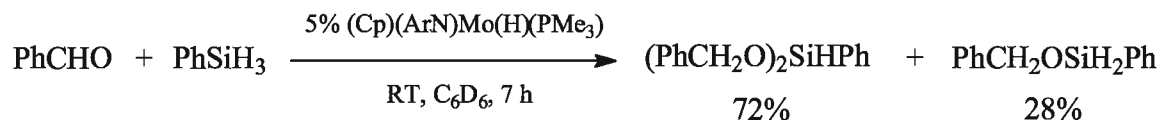
All manipulations were carried out using conventional inert atmosphere glove-box (MBraun) and Schlenk techniques. Dry ether, THF, benzene, toluene and hexanes were obtained, using Grubbs-type purification columns from Innovative Technology. NMR spectra were obtained with a Bruker AV-300 and Bruker AV-600 instruments (^1H : 300 and 600 MHz; ^2H : 92.1 MHz; ^{13}C : 75.5 and 151 MHz; ^{29}Si : 59.6 and 119.2 MHz; ^{31}P : 121.5 and 243 MHz, ^{11}B : 96.3 and 192.6 MHz). IR spectra were measured on a Perkin-Elmer 1600 FT-IR spectrometer. Elemental analyses were performed in "ANALEST" laboratories (University of Toronto). $(\text{ArN})\text{Mo}(\text{H})(\text{Cl})(\text{PMe}_3)_3$ ($\text{Ar} = 2,6\text{-(iPr)}_2\text{C}_6\text{H}_3$) was prepared by literature procedure.^{5a} PhSiH_3 was prepared from PhSiCl_3 by reaction with LiAlH_4 . PhSiD_3 , PhMeSiD_2 , PhMe_2SiD and Et_3SiD were prepared from PhSiCl_3 , PhMeSiCl_2 , PhMe_2SiCl and Et_3SiCl , respectively, by reaction with LiAlD_4 . Organic substrates (benzaldehyde, *o*-bromobenzaldehyde, acetone, acetophenone, *p*-bromobenzaldehyde, *p*-nitroacetophenone, *p*-methoxyacetophenone, 2,4-dimethyl-3-pentanone, 2-methylcyclohexanone, 2,6-dimethylcyclohexanone, cyclohexanone, acetone, butanone, benzophenone, (+)-camphor, benzonitrile, acetonitrile, isobutyronitrile, pivalonitrile, malonitrile, 1-hexynenitrile, acrylonitrile, 3-hexyne, triphenylphosphine, trimethylphosphine, triphenylborane, tris(pentafluorophenyl)borane, phenylacetylene, phenyldimethylsilane, phenylmethylsilane, triethylsilane, poly(methylhydrosiloxane), catecholborane, pinacolborane) were purchased from Aldrich and used without further purification. All catalytic, kinetic and NMR reactions were done under nitrogen atmosphere using "Young" type NMR tubes (from NewEra) equipped with Teflon valves. The structures and the yields of all hydrosilylated products were determined by NMR analysis using tetramethylsilane as an internal standard.

V. 1. Hydrosilylation catalyzed by (Cp)(ArN)Mo(H)(PMe₃)

Synthesis of (Cp)(ArN)Mo(H)(PMe₃)

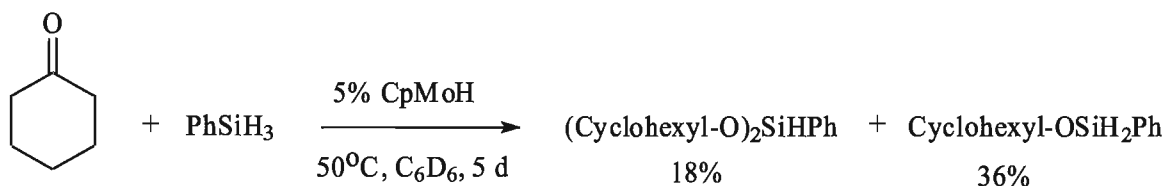
The THF solutions of (ArN)Mo(Cl)(H)(PMe₃)₃ (0.30 g, 0.56 mmol) and CpNa (0.12 g, 1.4 mmol) were mixed at RT, and the reaction mixture was stirred overnight. The solvent was removed under vacuum, and the product was extracted with hexanes giving 0.22 g of (Cp)(ArN)Mo(H)(PMe₃) as a dark-green solid. Yield: 95%. ¹H-NMR (300 MHz; C₆D₆; 298K; δ, ppm): -5.81 (d, ²J_{H-P} = 33.9 Hz, 1H, *Mo-H*), 1.06 (d, ²J_{H-P} = 9.0 Hz, 9H, *PMe*₃), 1.30 (d, ³J_{H-H} = 6.9 Hz, 6H, *iPr*), 1.37 (d, ³J_{H-H} = 6.9 Hz, 6H, *iPr*), 4.54 (sept, ³J_{H-H} = 6.9 Hz, 2H, *iPr*), 4.80 (s, 5H, *Cp*), 7.10 (m, 3H, *ArN*). ¹³C-NMR (75.5 MHz; C₆D₆; 298 K; δ, ppm): 23.7 (CH₃, *iPr*), 23.7 (d, ²J_{C-P} = 27.5 Hz, *PMe*₃), 24.0 (CH₃, *iPr*), 28.3 (CH, *iPr*), 87.0 (*Cp*), 123.0 (*Ar*), 124.5 (*Ar*), 144.2 (*Ar*). ³¹P-NMR (121.5 MHz; C₆D₆; 298 K; δ, ppm): 20.5 (s, 1P, *PMe*₃). IR (nujol, cm⁻¹): 1778 (Mo-H).

Hydrosilylation of benzaldehyde with phenylsilane



(Cp)(ArN)Mo(H)(PMe₃) (5.0 mg, 5 mol%) was added to a solution of benzaldehyde (26.0 mg, 0.242 mmol) and phenylsilane (26.2 mg, 0.242 mmol) in C₆D₆ (0.60 ml). The reaction was complete in approximately 7 hours giving (PhCH₂O)₂SiHPh (72%) and PhCH₂OSiH₂Ph (28%) as the final products.

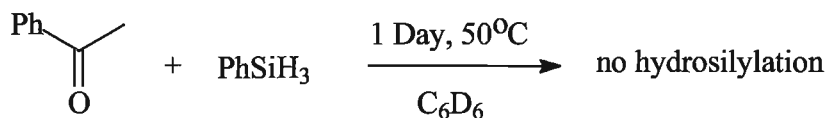
Hydrosilylation of cyclohexanone



(Cp)(ArN)Mo(H)(PMe₃) (5.0 mg, 5 mol%) was added to a solution of cyclohexanone (35.0 mg, 0.356 mmol) and phenylsilane (38.6 mg, 0.356 mmol) in C₆D₆ (0.60 ml). The reaction mixture was being heated at 50 °C for five days. The reaction provided

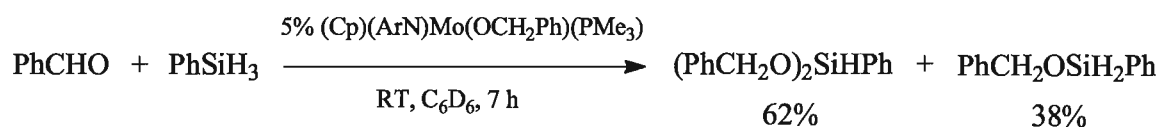
formation of (CyO)₂SiHPh (18%) and CyOSiH₂Ph (36%) as the final products.

Hydrosilylation of acetophenone



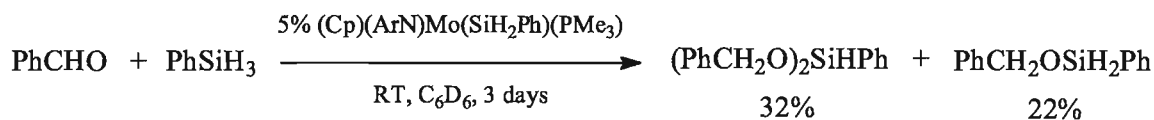
(Cp)(ArN)Mo(H)(PMe₃) (7.4 mg, 5 mol%) was added to a solution of acetophenone (42.4 mg, 0.356 mmol) and phenylsilane (38.6 mg, 0.356 mmol). The reaction mixture was heated at 50 °C for one day. Hydrosilylation of acetophenone was not observed. The catalyst reacted with the phenylsilane giving (Cp)(ArN)Mo(SiH₂Ph)(PMe₃).

Hydrosilylation of benzaldehyde with phenylsilane catalyzed by (Cp)(ArN)Mo(OCH₂Ph)(PMe₃)



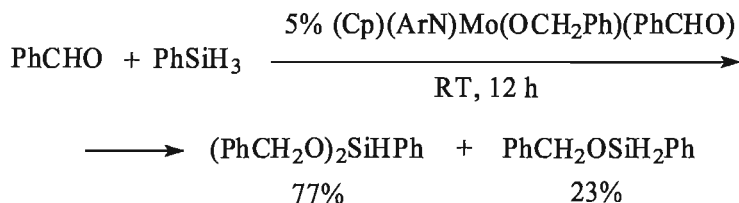
(Cp)(ArN)Mo(OCH₂Ph)(PMe₃) (6.0 mg, 5 mol%) was added to a solution of benzaldehyde (26.0 mg, 0.242 mmol) and phenylsilane (26.2 mg, 0.242 mmol) in C₆D₆ (0.60 ml). The reaction was complete in approximately 7 hours giving (PhCH₂O)₂SiHPh (62%) and PhCH₂OSiH₂Ph (38%) as the final products.

Hydrosilylation of benzaldehyde with phenylsilane catalyzed by (Cp)(ArN)Mo(SiH₂Ph)(PMe₃)



(Cp)(ArN)Mo(SiH₂Ph)(PMe₃) (6.0 mg, 5 mol%) was added to a solution of benzaldehyde (26.0 mg, 0.242 mmol) and phenylsilane (26.2 mg, 0.242 mmol) in C₆D₆ (0.60 ml). The reaction provided formation of (PhCH₂O)₂SiHPh (32%) and PhCH₂OSiH₂Ph (22%) after three days at RT. The overall yield is 54%.

Hydrosilylation of benzaldehyde with phenylsilane catalyzed by (Cp)(ArN)Mo(OCH₂Ph)(PhCHO)



(Cp)(ArN)Mo(OCH₂Ph)(PhCHO) (5.0 mg, 5 mol%) was added to a solution of benzaldehyde (26.0 mg, 0.242 mmol) and phenylsilane (26.2 mg, 0.242 mmol) in C₆D₆ (0.60 ml). Reaction was complete in approximately 12 hours giving (PhCH₂O)₂SiHPh (77%) and PhCH₂OSiH₂Ph (23%) as the final products.

The diagram below (Figure V-1) shows the change of benzaldehyde concentration in its reaction with phenylsilane in the presence of (Cp)(ArN)Mo(H)(PMe₃), (Cp)(ArN)Mo(OCH₂Ph)(PMe₃), (Cp)(ArN)Mo(OCH₂Ph)(PhCHO), and (Cp)(ArN)Mo(SiH₂Ph)(PMe₃):

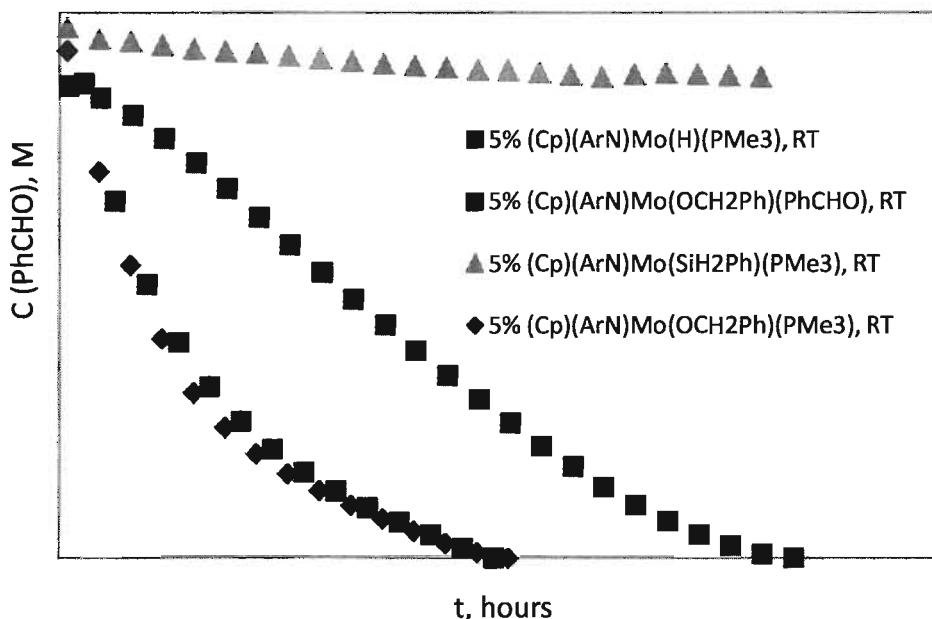
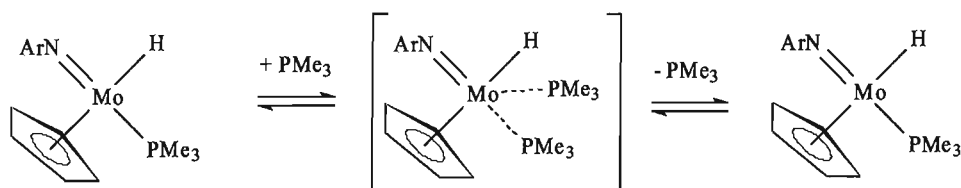


Figure V-1. $C(\text{PhCHO})$ /time plot for hydrosilylation of benzaldehyde with phenylsilane in the presence of different catalytic species.

Activation parameters for phosphine exchange: (Cp)(ArN)Mo(H)(PMe₃) + PMe₃



Trimethylphosphine (1.7 mg, 0.022 mmol) was added to a solution of (Cp)(ArN)Mo(H)(PMe₃) (5.0 g, 0.012 mmol). Selective ge-1D EXSY NMR experiments were performed to determine the exchange rate constants at four temperatures: $k(12.0\text{ }^{\circ}\text{C}) = (2.89 \pm 0.04) \cdot 10^1\text{ s}^{-1}$, $k(22.0\text{ }^{\circ}\text{C}) = (4.29 \pm 0.07) \cdot 10^1\text{ s}^{-1}$, $k(32.0\text{ }^{\circ}\text{C}) = (6.22 \pm 0.12) \cdot 10^1\text{ s}^{-1}$, $k(42.0\text{ }^{\circ}\text{C}) = (8.56 \pm 0.15) \cdot 10^1\text{ s}^{-1}$

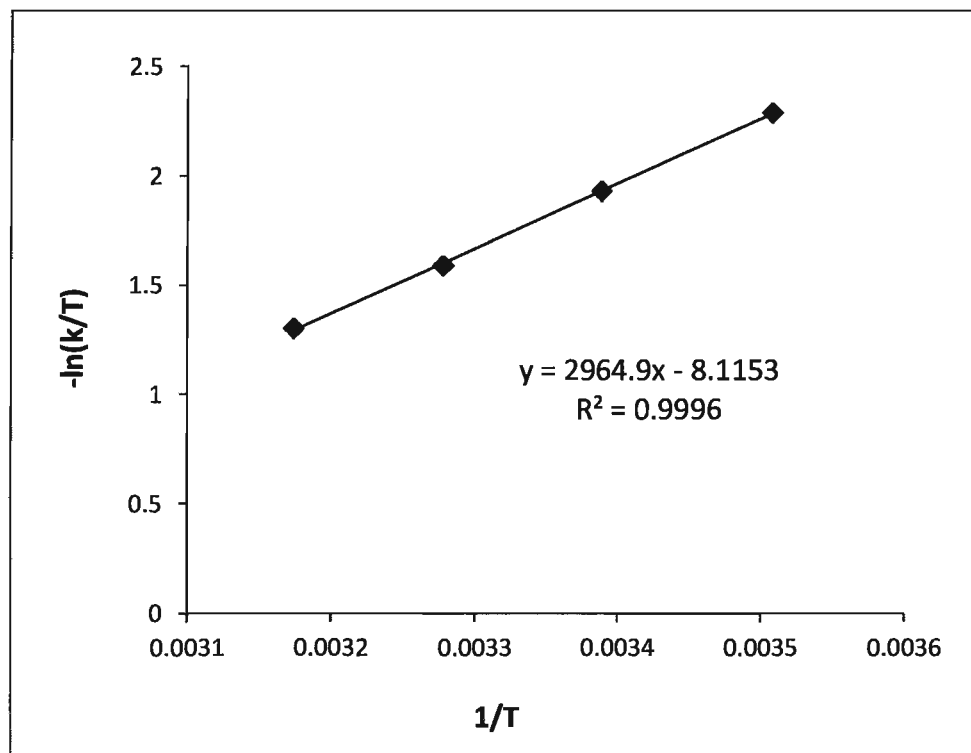
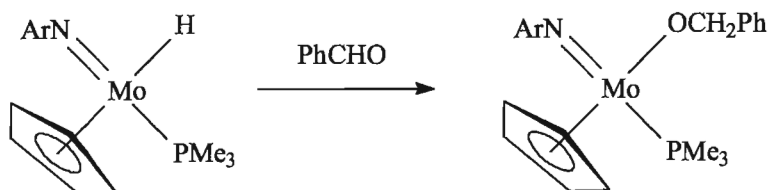


Figure V-2. Eyring plot for phosphine exchange between (Cp)(ArN)Mo(H)(PMe₃) and free PMe₃.

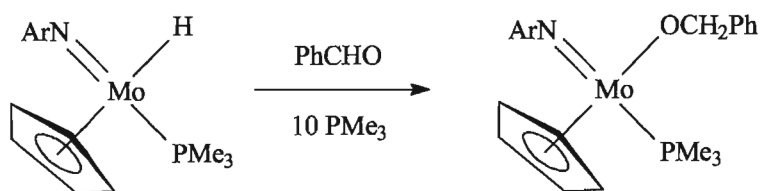
Activation parameters have been extracted from the Eyring plot (Figure V-2): $\Delta H^{\ddagger} = (2.47 \pm 0.04) \cdot 10^1\text{ kJ/mol}$, $\Delta S^{\ddagger} = -(1.30 \pm 0.01) \cdot 10^2\text{ J/(K}\cdot\text{mol)}$

Synthesis of (ArN)Mo(Cp)(OCH₂Ph)(PMe₃)



Benzaldehyde (53.0 mg, 0.501 mmol) was added to a solution of (Cp)(ArN)Mo(H)(PMe₃) (207.0 mg, 0.501 mmol) in hexane. The reaction mixture was stirred at RT for several days until the reaction was complete. The product, (Cp)(ArN)Mo(OCH₂Ph)(PMe₃), was filtered off, washed with hexane (2 x 10 ml) and dried in vacuum. Yield: 135 mg, 52%. ¹H-NMR (300 MHz; C₆D₆; 298K; δ, ppm): 1.01 (d, ²J_{H-P} = 9.3 Hz, 9H, PMe₃), 1.12 (d, ³J_{H-H} = 6.8 Hz, 6H, *iPr*), 1.26 (d, ³J_{H-H} = 6.8 Hz, 6H, *iPr*), 4.08 (sept, ³J_{H-H} = 6.8 Hz, 2H, *iPr*), 5.06 (s, 5H, Cp), 5.22 (dd, ²J_{H-H} = 180.3 Hz, ³J_{H-P} = 14.3 Hz, 2H, OCH₂Ph), 7.02-7.20 (m, 4H, Ar), 7.30-7.39 (m, 2H, Ar), 7.46-7.53 (m, 2H, Ar). ³¹P-NMR (121.5 MHz; C₆D₆; 298 K; δ, ppm): 16.1 (s, 1P, PMe₃). ¹³C-NMR (75.5 MHz; C₆D₆; 298 K; δ, ppm): 17.1 (d, ²J_{C-P} = 25.2 Hz, PMe₃), 24.1 (Me, *iPr*), 24.2 (Me, *iPr*), 28.3 (CH, *iPr*), 86.0 (d, ³J_{C-P} = 5.3 Hz, OCH₂Ph), 94.7 (Cp), 123.4 (CH, Ar), 125.2 (CH, Ar), 126.1 (CH, Ar), 126.4 (CH, Ar), 128.5 (CH, Ar, the position of this carbon was determined by HSQC NMR), 145.1 (*ipso*-C, Ar), 148.7 (*ipso*-C, Ar), 153.9 (*ipso*-C, Ar).

Kinetic study of the formation of (Cp)(ArN)Mo(OCH₂Ph)(PMe₃)



Benzaldehyde (2.7 mg, 0.026 mmol) was added to a solution of (Cp)(ArN)Mo(H)(PMe₃) (10.7 g, 0.026 mmol) in the presence of PMe₃ (19.7 mg, 0.259 mmol) in C₆D₆ (0.60 ml). The formation of the product was monitored by ¹H NMR at 26 °C (Figure V-3), 40 °C (Figure V-4), 50 °C (Figure V-5) and 60 °C (Figure V-6).

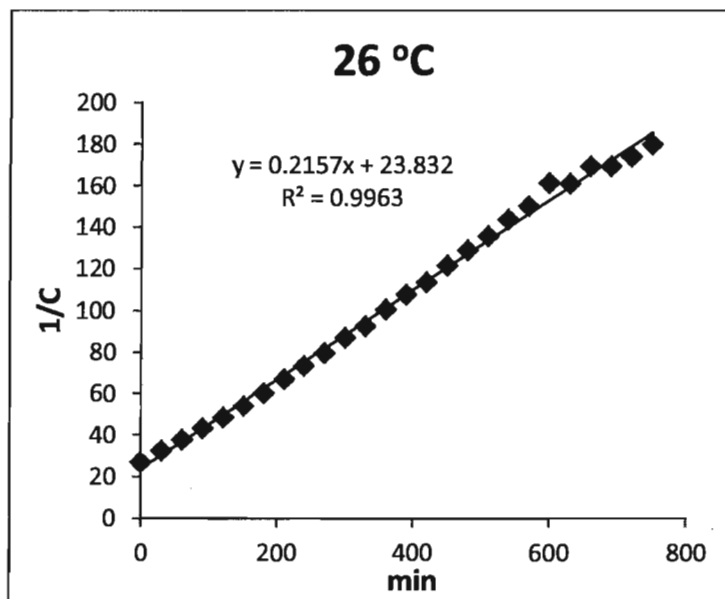


Figure V-3. (1/C)/time plot for the reaction of (Cp)(ArN)Mo(H)(PMe₃) with PhCHO (1eq.) in the presence of PMe₃ (10 eq.) at 26.0 °C

$$k(26.0\text{ °C}) = (2.157 \pm 0.027) \cdot 10^{-1} \text{ M}^{-1} \cdot \text{min}^{-1} = (3.60 \pm 0.05) \cdot 10^{-3} \text{ M}^{-1} \cdot \text{s}^{-1}$$

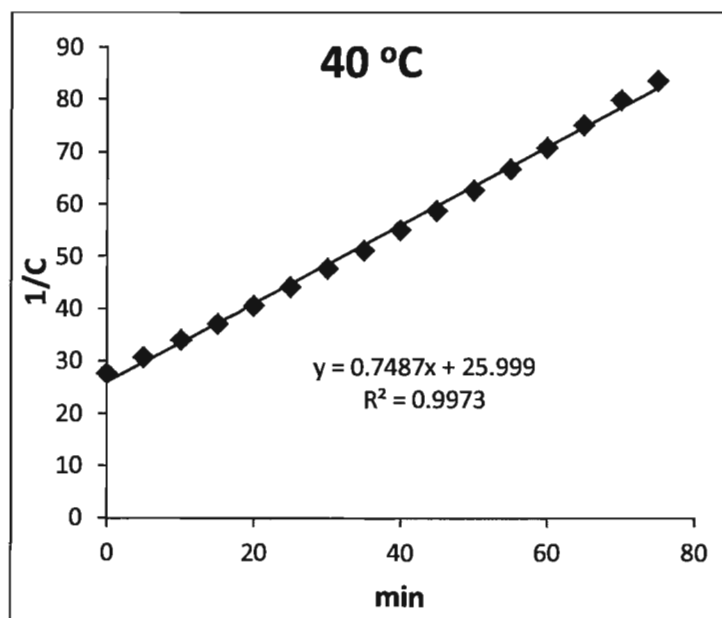


Figure V-4. (1/C)/time plot for the reaction of (Cp)(ArN)Mo(H)(PMe₃) with PhCHO (1eq.) in the presence of PMe₃ (10 eq.) at 40.0 °C

$$k(40.0\text{ °C}) = (7.487 \pm 0.104) \cdot 10^{-1} \text{ M}^{-1} \cdot \text{min}^{-1} = (1.25 \pm 0.17) \cdot 10^{-2} \text{ M}^{-1} \cdot \text{s}^{-1}$$

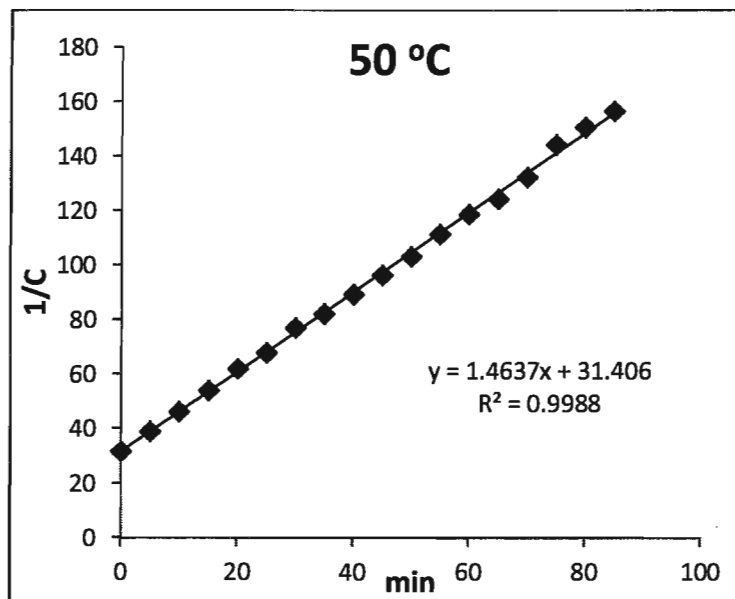


Figure V-5. (1/C)/time plot for the reaction of (Cp)(ArN)Mo(H)(PMe₃) with PhCHO (1eq.) in the presence of PMe₃ (10 eq.) at +50.0 °C

$$k(50.0\text{ }^{\circ}\text{C}) = (1.464 \pm 0.013) \text{ M}^{-1} \cdot \text{min}^{-1} = (2.44 \pm 0.17) \cdot 10^{-2} \text{ M}^{-1} \cdot \text{s}^{-1}$$

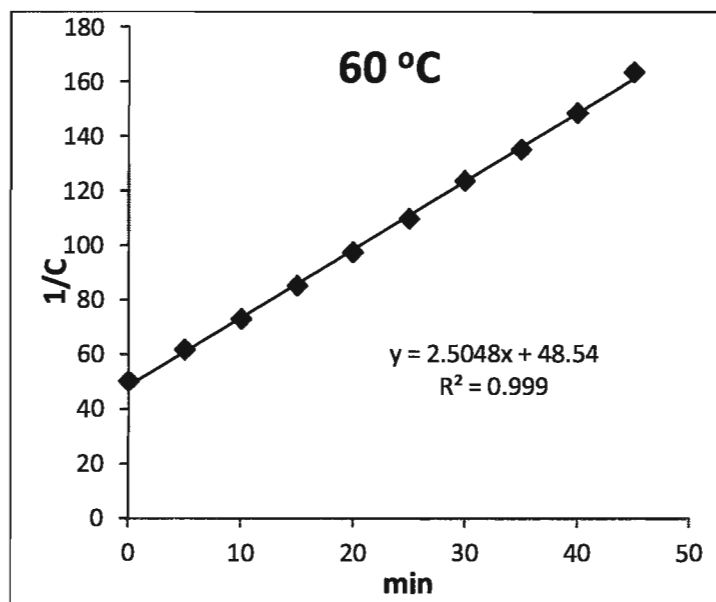


Figure V-6. (1/C)/time plot for the reaction of (Cp)(ArN)Mo(H)(PMe₃) with PhCHO (1eq.) in the presence of PMe₃ (10 eq.) at 60.0 °C

$$k(60.0\text{ }^{\circ}\text{C}) = (2.505 \pm 0.028) \text{ M}^{-1} \cdot \text{min}^{-1} = (4.17 \pm 0.05) \cdot 10^{-2} \text{ M}^{-1} \cdot \text{s}^{-1}$$

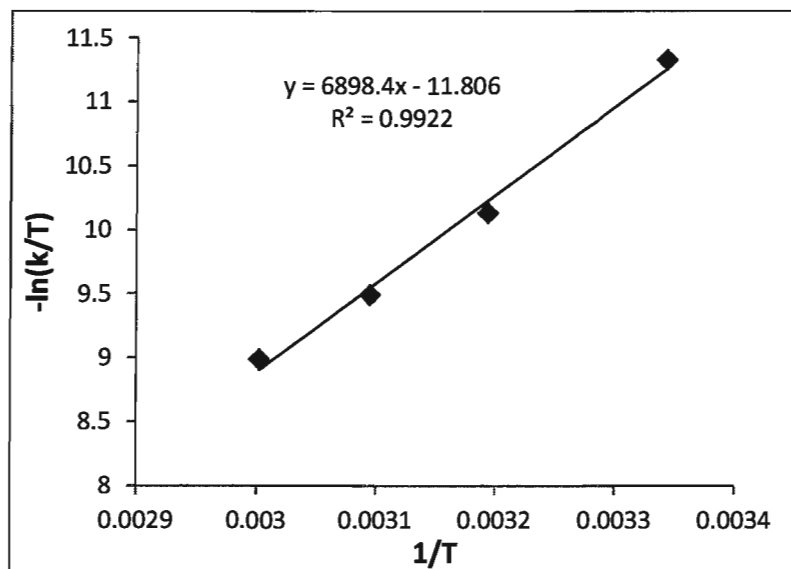


Figure V-7. Eyring plot for the reaction of $(\text{Cp})(\text{ArN})\text{Mo}(\text{H})(\text{PMe}_3)$ with PhCHO (1eq.) in the presence of PMe_3 (10 eq.)

Activation parameters have been extracted from the Eyring plot (Figure V-7): $\Delta H^\ddagger = (5.76 \pm 0.36) \cdot 10^1 \text{ kJ/mol}$, $\Delta S^\ddagger = -(9.97 \pm 1.14) \cdot 10^1 \text{ J/(K} \cdot \text{mol)}$

Kinetics of reaction between $(\text{Cp})(\text{ArN})\text{Mo}(\text{H})(\text{PMe}_3)$ and PhCHO was studied in the presence of different amount of PMe_3 (8, 9, 10, 11 and 15 eq.) (Figure V-8).

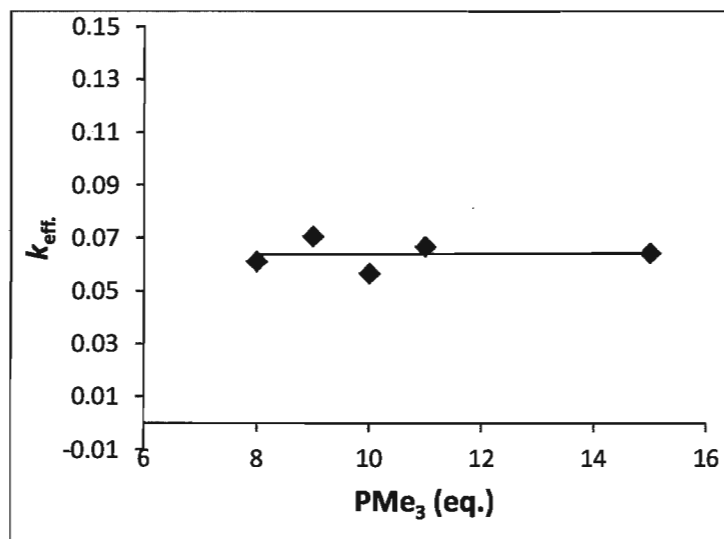
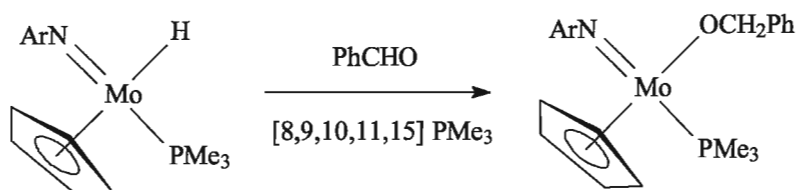


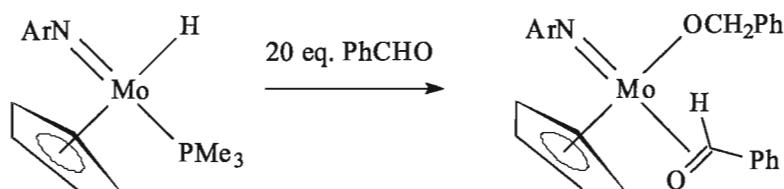
Figure V-8. $k_{\text{eff}}/\text{PMe}_3(\text{eq.})$ plot for the reaction between $(\text{Cp})(\text{ArN})\text{Mo}(\text{H})(\text{PMe}_3)$ and PhCHO .

Formation of (Cp)(ArN)Mo(OCH₂Ph)(PMe₃)



Benzaldehyde (2.7 mg, 0.026 mmol) was added to a solution of (Cp)(ArN)Mo(H)(PMe₃) (10.7 mg, 0.026 mmol) in the presence of different amounts of PMe₃ (8 eq. (15.8 mg, 0.207 mmol), 9 eq. (17.7 mg, 0.233 mmol), 10 eq. (19.7 mg, 0.259 mmol), 11 eq. (21.7 mg, 0.285 mmol), 15 eq. (29.6 mg, 0.388 mmol)) in C₆D₆ (0.60 ml). The reaction was monitored by ¹H NMR at 22.0 °C. The reaction rate constant did not depend on the PMe₃ concentration.

Formation of (Cp)(ArN)Mo(OCH₂Ph)(PhCHO)



Benzaldehyde (25.7 mg, 0.242 mmol) was added to a solution of (Cp)(ArN)Mo(H)(PMe₃) (5.3 mg, 0.010 mmol) in C₆D₆ (0.60 ml). Two isomers of (Cp)(ArN)Mo(OCH₂Ph)(PhCHO) (**A**, 71% and **B**, 29%) formed within an hour at RT.

Isomer **A**:

¹H-NMR (300 MHz; C₆D₆; 298K; δ, ppm): 0.87 (d, ³J_{H-H} = 6.85 Hz, 6H, 2CH₃, iPr), 1.09 (d, ³J_{H-H} = 6.85 Hz, 6H, 2CH₃, iPr), 3.39 (sept, ³J_{H-H} = 6.85 Hz, 2H, iPr), 5.58 (s, 1H, PhCHO), 5.65 (s, 5H, Cp), 5.84 (d, ²J_{H-H} = 13.8 Hz, CH^aH-O), 6.25 (d, ²J_{H-H} = 13.8 Hz, CHH^b-O), 6.77-6.81 (m, 3H, Ar), 6.87-7.42 (mm, 8H, 2Ph), 7.72-7.77 (m, 2H, Ph, PhCHO).

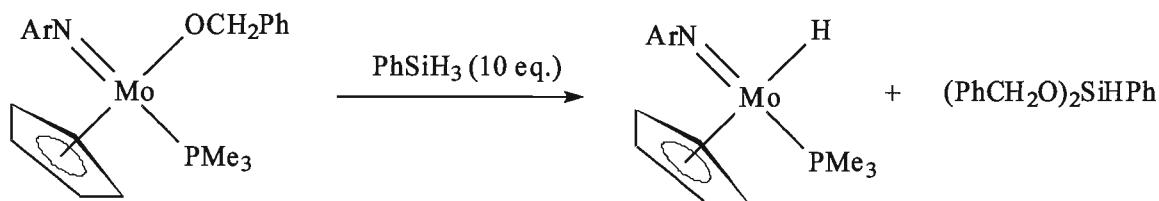
Isomer **B**:

¹H-NMR (300 MHz; C₆D₆; 298K; δ, ppm): 1.16 (d, ³J_{H-H} = 6.92 Hz, 6H, 2CH₃, iPr), 1.21 (d, ³J_{H-H} = 6.92 Hz, 6H, 2CH₃, iPr), 3.94 (sept, ³J_{H-H} = 6.85 Hz, 2H, iPr), 5.38 (s, 5H, Cp), 5.92 (d, ²J_{H-H} = 13.8 Hz, CH^aH-O), 6.08 (s, 1H, PhCHO), 6.15 (d, ²J_{H-H} = 13.8 Hz,

CHH^b-O), 6.91-6.94 (m, 3H, Ar), 6.87-7.42 (mm, 8H, 2Ph), 7.69-7.74 (m, 2H, Ph, PhCHO).

¹³C-NMR (both isomers) (75.5 MHz; C₆D₆; 298 K; δ, ppm): 24.0 (CH₃, iPr, A), 24.2 (CH₃, iPr, B), 24.6 (CH₃, iPr, B), 25.3 (CH₃, iPr, A), 27.9 (CH, iPr, A), 28.5 (CH, iPr, B), 70.5 (CH₂-O, A), 71.3 (CH₂-O, B), 88.7 (-CHO, B), 89.0 (-CHO, A), 108.0 (Cp, B), 109.9 (Cp, A), 123.3 (CH, Ar, A), 123.5 (CH, Ar, B), 125.4 (CH, PhCHO, A), 126.8, 126.9, 127.3, 127.4, 127.5, 127.6, 127.6, 127.7, 128.0, 128.2, 128.6, 128.9, 146.0 (C-Pr^I, Ar, B), 146.6, 146.7 (C-CHO, A), 147.0 (C-Pr^I, Ar, A), 148.3 (C-CHO, B), 152.7 (C-N, Ar, A) 154.0 (C-N, Ar, B).

Kinetic study of reaction between (Cp)(ArN)Mo(OCH₂Ph)(PMe₃) and PhSiH₃ (10 eq.)



Phenylsialne (11.7 mg, 0.108 mmol) was added to a solution of (Cp)(ArN)Mo(OCH₂Ph)(PMe₃) (5.6 mg, 0.011 mmol) in C₆D₆ (0.60 mL). The reaction was monitored by NMR at 16 °C (Figure V-9), 26 °C (Figure V-10), 36 °C (Figure V-11) and 46 °C (Figure V-12).

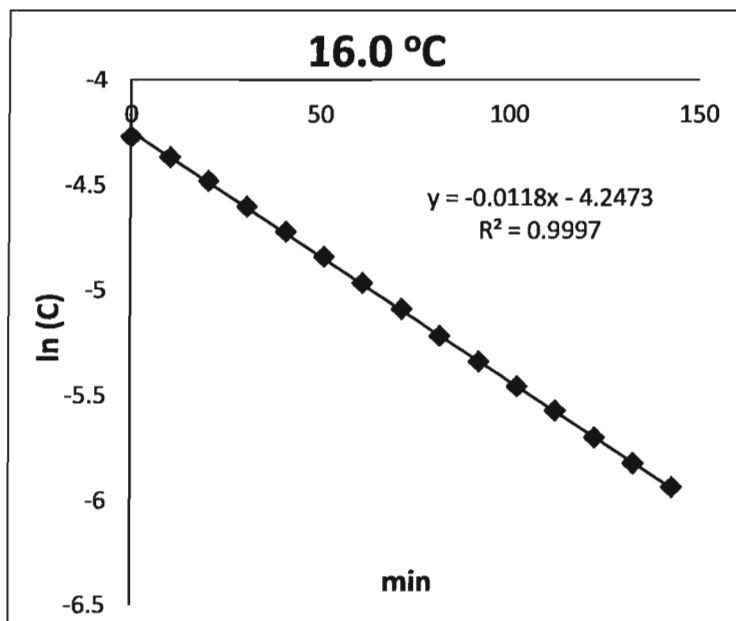


Figure V-9. ln(C)/time plot for the reaction of (Cp)(ArN)Mo(OCH₂Ph)(PMe₃) with PhSiH₃ (10 eq.) at 16.0 °C

$$k_H(16.0\text{ °C}) = (1.18 \pm 0.01) \cdot 10^{-2} \text{ min}^{-1} = (1.97 \pm 0.02) \cdot 10^{-4} \text{ s}^{-1}$$

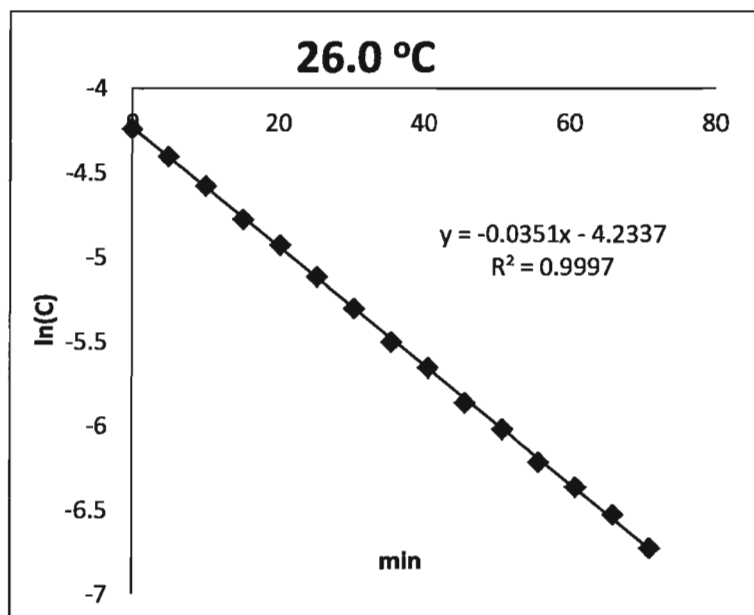


Figure V-10. ln(C)/time plot for the reaction of (Cp)(ArN)Mo(OCH₂Ph)(PMe₃) with PhSiH₃ (10 eq.) at 26.0 °C

$$k_H(26.0\text{ °C}) = (3.51 \pm 0.02) \cdot 10^{-2} \text{ min}^{-1} = (5.85 \pm 0.03) \cdot 10^{-4} \text{ s}^{-1}$$

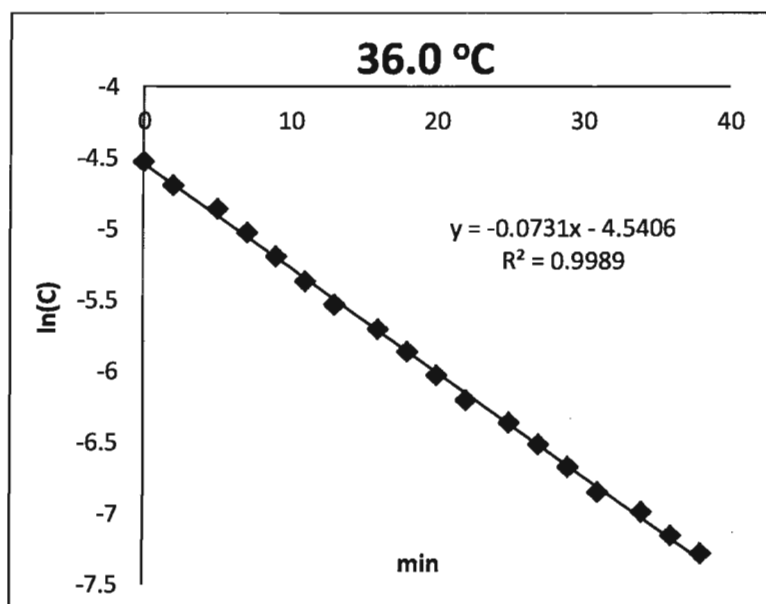


Figure V-11. ln(C)/time plot for the reaction of (Cp)(ArN)Mo(OCH₂Ph)(PMe₃) with PhSiH₃ (10 eq.) at 36.0 °C

$$k_H(36.0\text{ }^{\circ}\text{C}) = (7.31 \pm 0.06) \cdot 10^{-2} \text{ min}^{-1} = (1.22 \pm 0.01) \cdot 10^{-3} \text{ s}^{-1}$$

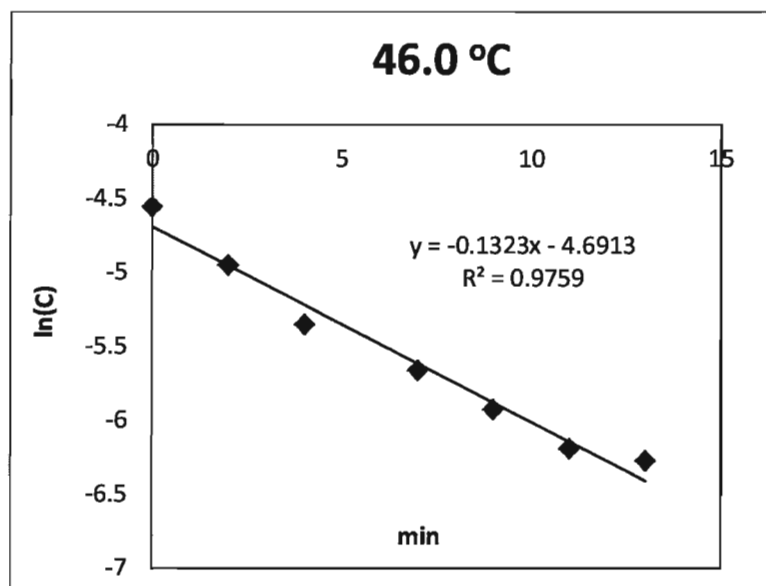


Figure V-12. ln(C)/time plot for the reaction of (Cp)(ArN)Mo(OCH₂Ph)(PMe₃) with PhSiH₃ (10 eq.) at 46.0 °C

$$k_H(46.0\text{ }^{\circ}\text{C}) = (1.32 \pm 0.09) \cdot 10^{-1} \text{ min}^{-1} = (2.21 \pm 0.16) \cdot 10^{-3} \text{ s}^{-1}$$

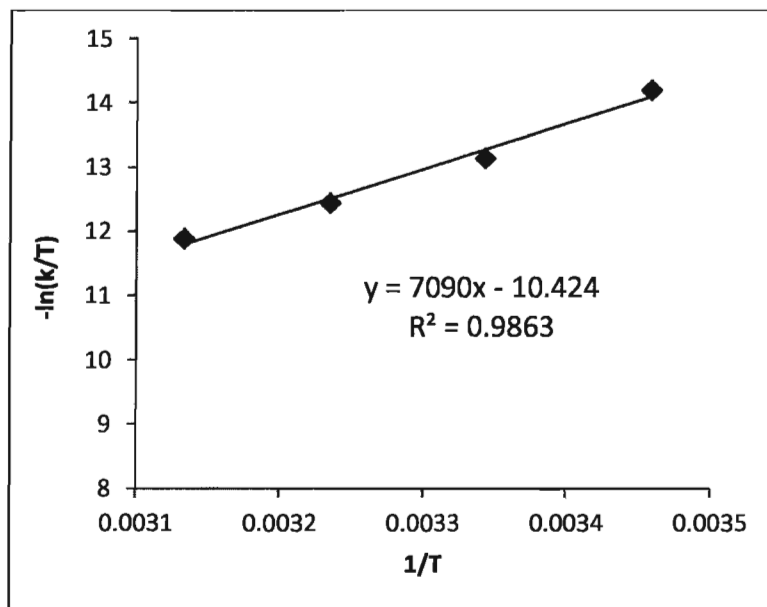
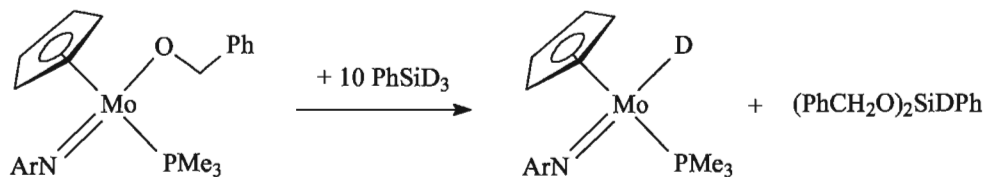


Figure V-13. Eyring plot for the reaction of (Cp)(ArN)Mo(OCH₂Ph)(PMe₃) with PhSiH₃ (10 eq.).

Activation parameters have been extracted from the Eyring plot (Figure V-13): $\Delta H^\ddagger = (5.89 \pm 0.49) \cdot 10^1$ kJ/mol, $\Delta S^\ddagger = -(1.11 \pm 1.6) \cdot 10^2$ J/(K·mol)

Kinetic study of the reaction of (Cp)(ArN)Mo(OCH₂Ph)(PMe₃) with excess PhSiD₃ under pseudo-first order conditions



PhSiD₃ (12.0 mg, 0.108 mmol) was added to a solution of (Cp)(ArN)Mo(OCH₂Ph)(PMe₃) (5.6 mg, 0.011 mmol) in C₆D₆ (0.60 mL). The reaction was monitored by ¹H NMR at 16 °C (Figure V-14), 26 °C (Figure V-15), 36 °C (Figure V-16) and 46 °C (Figure V-17).

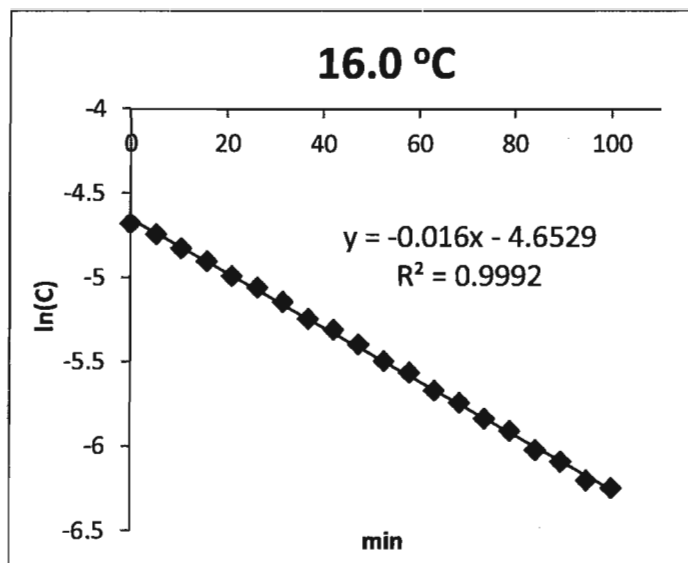


Figure V-14. $\ln(C)$ /time plot the reaction of $(Cp)(ArN)Mo(OCH_2Ph)(PMe_3)$ with $PhSiD_3$ (10 eq.) 16.0 °C.

$$k_D(16\text{ °C}) = (1.60 \pm 0.01) \cdot 10^{-2} \text{ min}^{-1} = (2.7 \pm 0.02) \cdot 10^{-4} \text{ s}^{-1}$$

$$KIE(16\text{ °C}) = \frac{k_H(16\text{ °C})}{k_D(16\text{ °C})} = \frac{0.0118}{0.0160} \cong 0.7$$

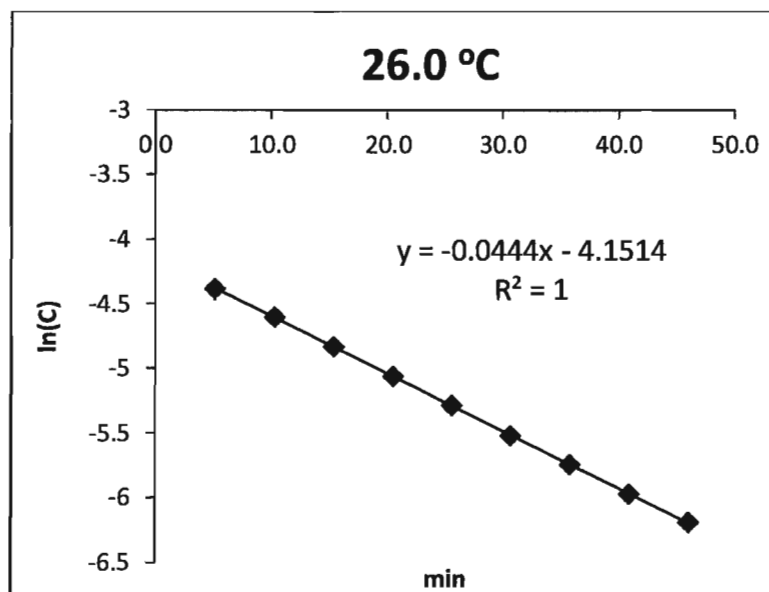


Figure V-15. $\ln(C)$ /time plot the reaction of $(Cp)(ArN)Mo(OCH_2Ph)(PMe_3)$ with $PhSiD_3$ (10 eq.) at 26.0 °C.

$$k_D(26.0\text{ }^{\circ}\text{C}) = (4.44 \pm 0.01) \cdot 10^{-2} \text{ min}^{-1} = (7.40 \pm 0.02) \cdot 10^{-4} \text{ s}^{-1}$$

$$\text{KIE}(26\text{ }^{\circ}\text{C}) = \frac{k_H(26\text{ }^{\circ}\text{C})}{k_D(26\text{ }^{\circ}\text{C})} = \frac{0.0351}{0.0444} \cong 0.8$$

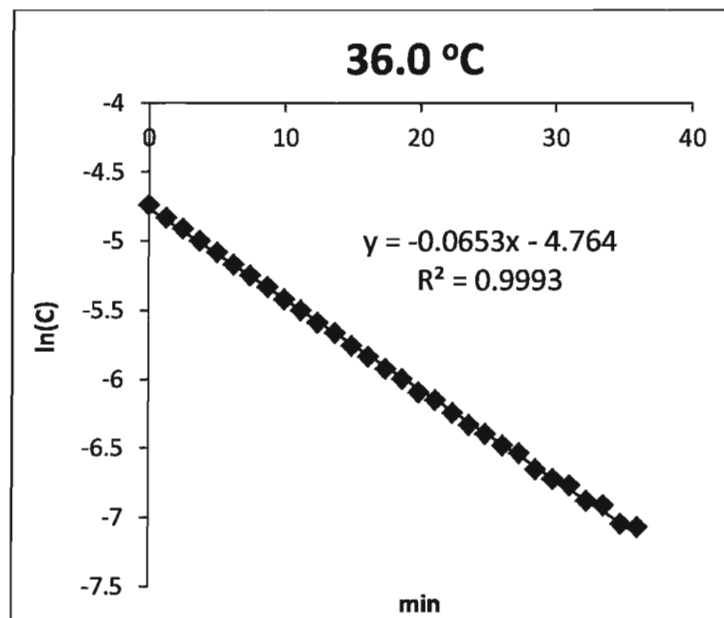


Figure V-16. ln(C)/time plot the reaction of (Cp)(ArN)Mo(OCH₂Ph)(PMe₃) with PhSiD₃ (10 eq.) at 36.0 °C.

$$k_D(36\text{ }^{\circ}\text{C}) = (6.53 \pm 0.03) \cdot 10^{-2} \text{ min}^{-1} = (1.09 \pm 0.01) \cdot 10^{-3} \text{ s}^{-1}$$

$$\text{KIE}(36\text{ }^{\circ}\text{C}) = \frac{k_H(36\text{ }^{\circ}\text{C})}{k_D(36\text{ }^{\circ}\text{C})} = \frac{0.0731}{0.0653} \cong 1.1$$

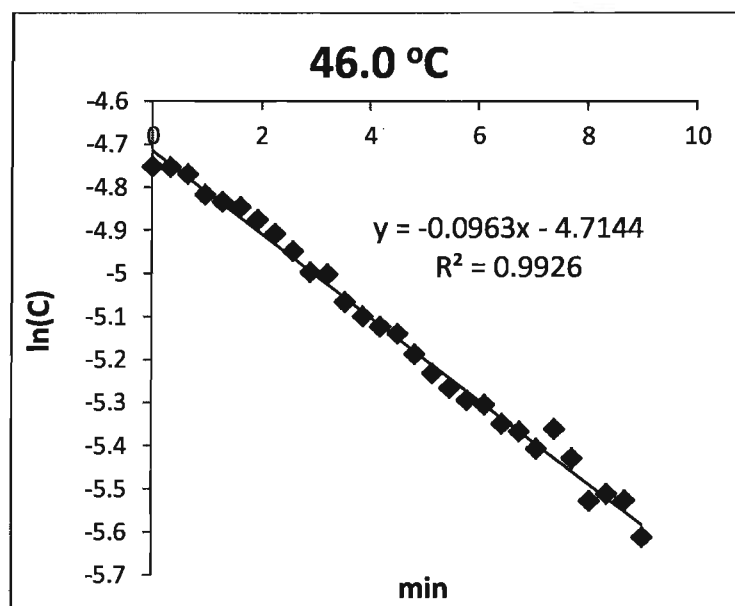


Figure V-17. ln(C)/time plot the reaction of (Cp)(ArN)Mo(OCH₂Ph)(PMe₃) with PhSiD₃ (10 eq.) at 46.0 °C.

$$k_D(46.0\text{ }^\circ\text{C}) = (9.63 \pm 0.16) \cdot 10^{-2} \text{ min}^{-1} = (1.60 \pm 0.03) \cdot 10^{-3} \text{ s}^{-1}$$

$$\text{KIE}(46\text{ }^\circ\text{C}) = \frac{k_H(46\text{ }^\circ\text{C})}{k_D(46\text{ }^\circ\text{C})} = \frac{0.1323}{0.0963} \cong 1.4$$

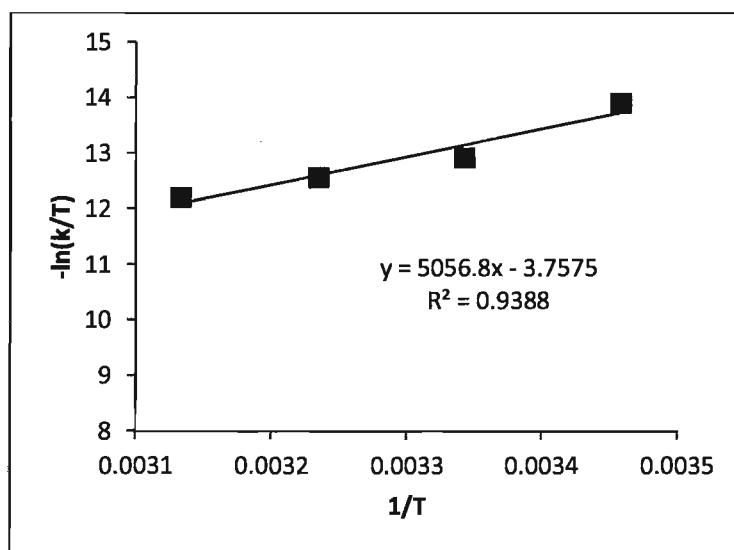
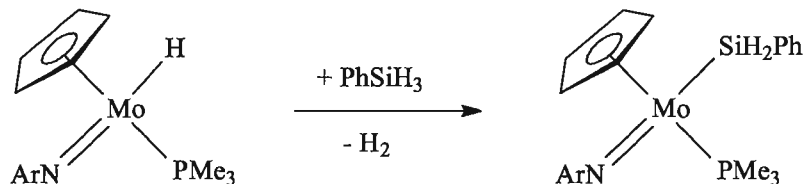


Figure V-18. Eyring plot for the reaction of (Cp)(ArN)Mo(OCH₂Ph)(PMe₃) with PhSiD₃ (10 eq.).

Activation parameters have been extracted from the Eyring plot (Figure V-21): $\Delta H^\ddagger = (4.20 \pm 0.76) \cdot 10^1$ kJ/mol, $\Delta S^\ddagger = -(1.67 \pm 0.25) \cdot 10^2$ J/(K·mol)

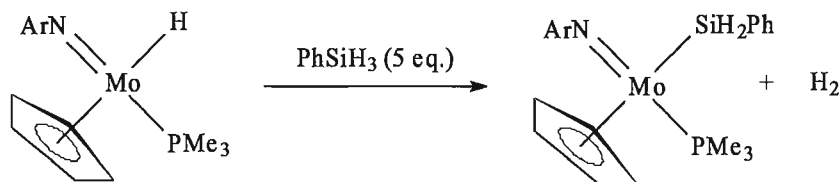
Synthesis of (Cp)(ArN)Mo(SiH₂Ph)(PMe₃)



Phenylsilane (0.140 g, 0.970 mmol) was added to a solution of (Cp)(ArN)Mo(H)(PMe₃) (0.270 g, 0.480 mmol) in Et₂O. The reaction mixture was left for one week at RT until the reaction was complete. Evaporation of all volatiles afforded (Cp)(ArN)Mo(SiH₂Ph)(PMe₃) (0.326 mg, 96% yield) as a brown-green oil.

¹H-NMR (300 MHz; C₆D₆; 298K; δ , ppm): 1.04 (d, $^2J_{H-P} = 9.0$ Hz, 9H, PMe₃), 1.16 (d, $^3J_{H-H} = 6.9$ Hz, 6H, iPr), 1.19 (d, $^3J_{H-H} = 6.9$ Hz, 6H, iPr), 4.30 (sept, $^3J_{H-H} = 6.9$ Hz, 2H, iPr), 4.70 (s, 5H, Cp), 5.18 (d, $^3J_{H-P} = 1.5$ Hz, 1H, SiH₂Ph), 5.56 (d, $^3J_{H-P} = 4.2$ Hz, 1H, SiH₂Ph), 6.89 (t, $^3J_{H-H} = 7.5$ Hz, 1H, *p*-H, ArN), 7.05 (m, 2H, *p*-H, ArN), 7.25 (m, 1H, *p*-H, SiPh), 7.34 (t, $^3J_{H-H} = 7.5$ Hz, 2H, *m*-H, SiPh), 8.12 (d, $^3J_{H-H} = 6.5$ Hz, 2H, *o*-H, SiPh). ¹³C-NMR (75.5 MHz; C₆D₆; 298 K; δ , ppm): 21.5 (d, $^2J_{C-P} = 25.7$ Hz, PMe₃), 23.8 (s, CH₃), 24.8 (s, CH₃), 28.2 (s, CH), 90.0 (s, Cp), 119.3, 123.4, 125.3, 127.8, 130.5, 136.4, 137.3, 145.0 (s, aromatic). ³¹P-NMR (121.5 MHz; C₆D₆; 298 K; δ , ppm): 18.60 (s, 1P, PMe₃). ²⁹Si-NMR (119.24 MHz; C₆D₆; 298 K; δ , ppm): -4.0 (dt, $^1J_{Si-P} = 29.8$ Hz, $^1J_{Si-H} = 156.8$ Hz, SiH₂Ph).

The reaction of (Cp)(ArN)Mo(H)(PMe₃) with PhSiH₃ (5 eq.) in the presence of different amounts of PMe₃



Phenylsilane (13.6 mg, 0.125 mmol) was added to a solution (Cp)(ArN)Mo(H)(PMe₃)

(10.5 mg, 0.025 mmol) in C₆D₆ (0.60 ml). The reaction was monitored by ¹H NMR. The experiment repeated in the presence of 10 eq. PMe₃ (19.3 mg, 0.250 mmol) and 20 eq. PMe₃ (38.6 mg, 0.508 mmol) (Figure V-19).

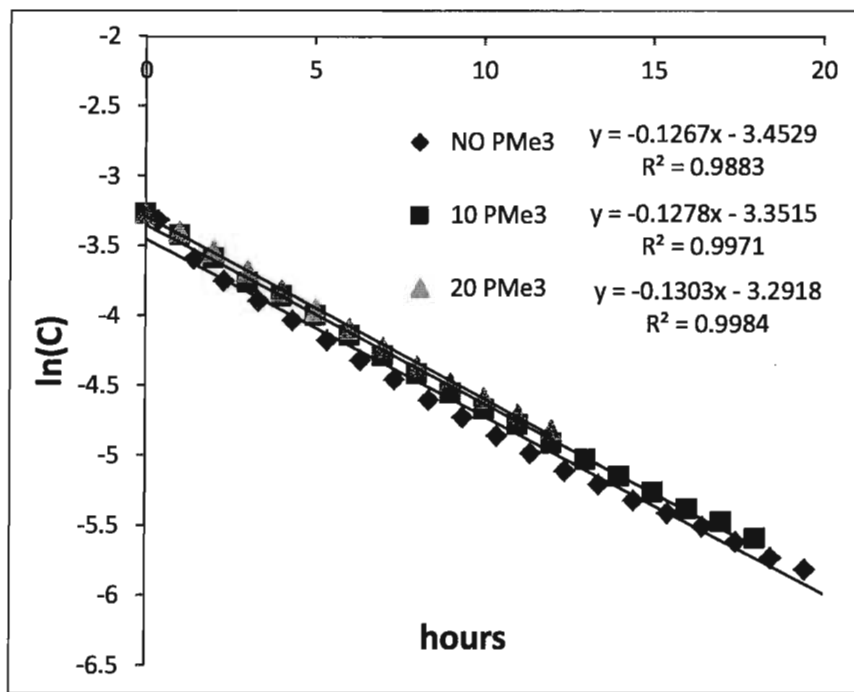
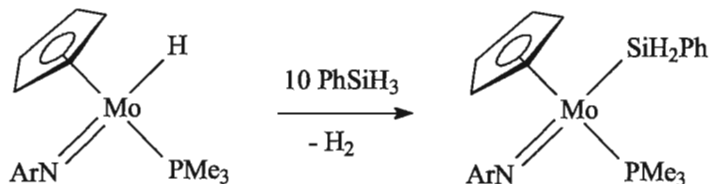


Figure V-19. Ln(C)/time plot for the reaction of (Cp)(ArN)Mo(H)(PMe₃) with PhSiH₃ (5 eq.) in the presence of 0, 10, and 20 eq. of PMe₃

$$k(\text{no PMe}_3) = (1.27 \pm 0.03) \cdot 10^{-1} \text{ h}^{-1}, k(10 \text{ PMe}_3) = (1.28 \pm 0.02) \cdot 10^{-1} \text{ h}^{-1}, k(20 \text{ PMe}_3) = (1.30 \pm 0.02) \cdot 10^{-1} \text{ h}^{-1}$$

Reaction between (Cp)(ArN)Mo(H)(PMe₃) and PhSiH₃ (5 eq.)



Phenylsilane (13.1 mg, 0.121 mmol) was added to a solution (Cp)(ArN)Mo(H)(PMe₃) (10.5 mg, 0.025 mmol) in C₆D₆ (0.60 ml). The reaction was monitored by ¹H NMR at 25.0 °C (Figure V-20), 35.0 °C (Figure V-21), 45.0 °C (Figure V-22), and 55.0 °C (Figure V-23).

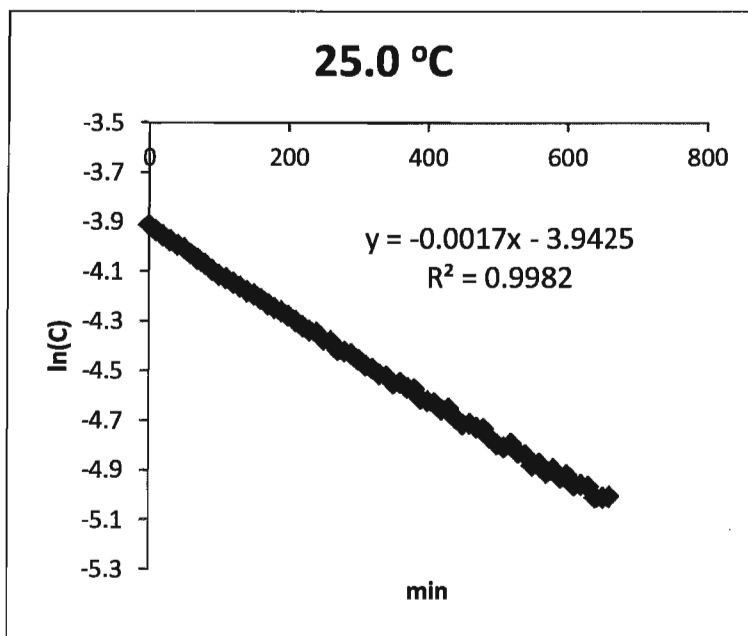


Figure V-20. Ln(C)/time plot for the reaction of (Cp)(ArN)Mo(H)(PMe₃) with PhSiH₃ (10 eq.) at 25.0 °C.

$$k_H(25.0\text{ °C}) = (1.70 \pm 0.01) \cdot 10^{-3} \text{ min}^{-1} = (2.83 \pm 0.02) \cdot 10^{-5} \text{ s}^{-1}$$

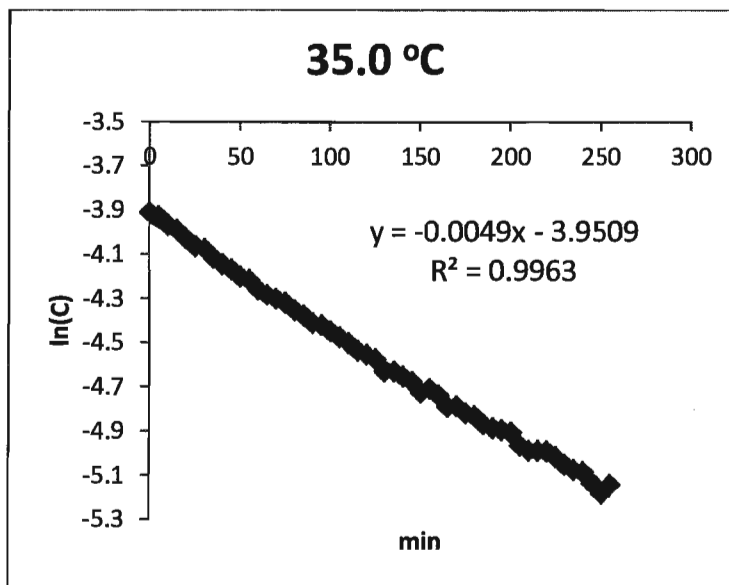


Figure V-21. Ln(C)/time plot for the reaction of (Cp)(ArN)Mo(H)(PMe₃) with PhSiH₃ (10 eq.) at 35.0 °C.

$$k_H(35.0\text{ °C}) = (4.9 \pm 0.1) \cdot 10^{-3} \text{ min}^{-1} = (8.17 \pm 0.02) \cdot 10^{-5} \text{ s}^{-1}$$

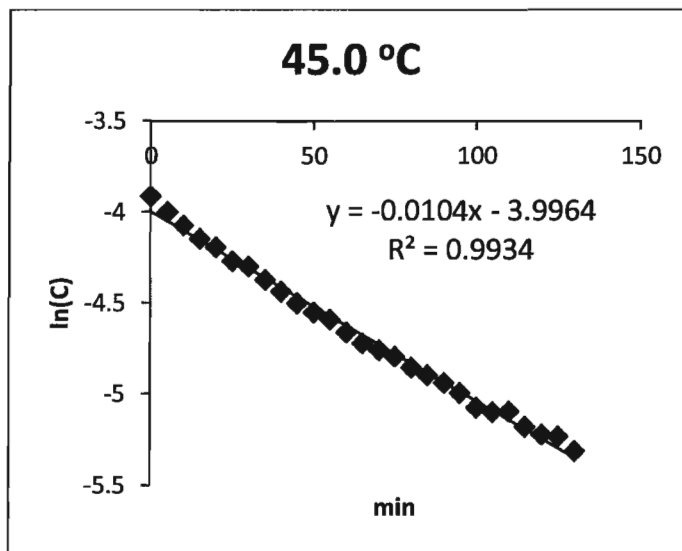


Figure V-22. Ln(C)/time plot for the reaction of (Cp)(ArN)Mo(H)(PMe₃) with PhSiH₃ (10 eq.) at 45.0 °C.

$$k_H(45.0\text{ °C}) = (1.04 \pm 0.02) \cdot 10^{-2} \text{ min}^{-1} = (1.73 \pm 0.03) \cdot 10^{-4} \text{ s}^{-1}$$

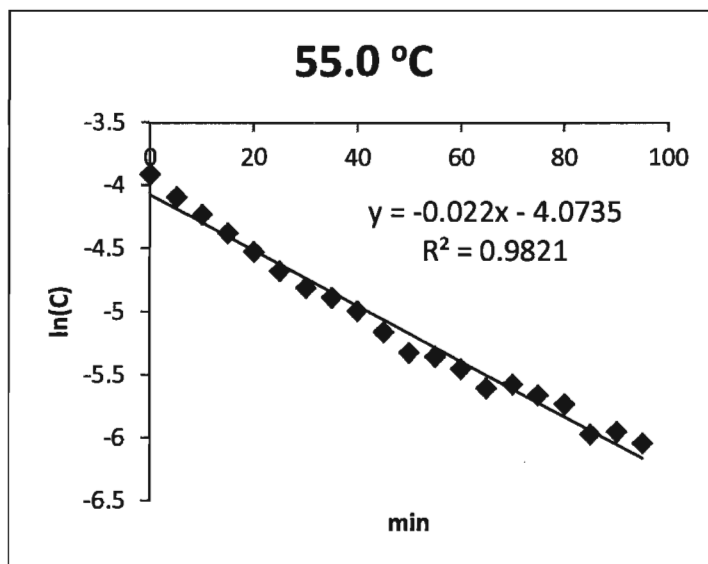


Figure V-23. Ln(C)/time plot for the reaction of (Cp)(ArN)Mo(H)(PMe₃) with PhSiH₃ (10 eq.) at 55.0 °C.

$$k_H(55.0\text{ °C}) = (2.2 \pm 0.1) \cdot 10^{-2} \text{ min}^{-1} = (3.67 \pm 0.17) \cdot 10^{-4} \text{ s}^{-1}$$

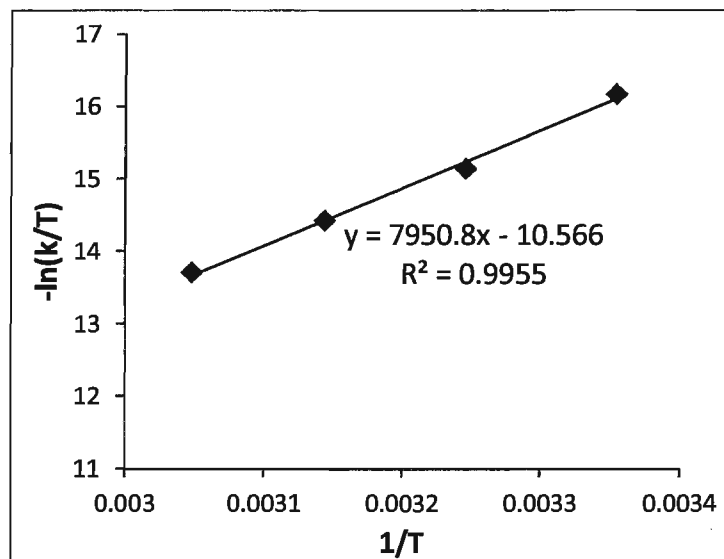
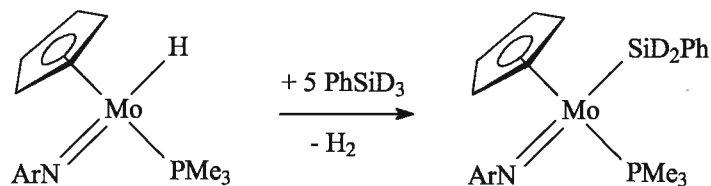


Figure V-24. Eyring plot for the reaction of (Cp)(ArN)Mo(H)(PMe₃) with PhSiH₃ (10 eq.).

Activation parameters have been extracted from the Eyring plot (Figure V-24): $\Delta H^\ddagger = (6.61 \pm 0.31) \cdot 10^1$ kJ/mol, $\Delta S^\ddagger = -(1.10 \pm 0.10) \cdot 10^2$ J/(K·mol)

Reaction between (Cp)(ArN)Mo(H)(PMe₃) and PhSiD₃ (5 eq.)



PhSiD₃ (0.0136 g, 0.121 mmol) was added to a solution (Cp)(ArN)Mo(H)(PMe₃) (10.5 mg, 0.025 mmol) in C₆D₆ (0.60 ml). The reaction was monitored by ¹H NMR at 25 °C (Figure V-25).

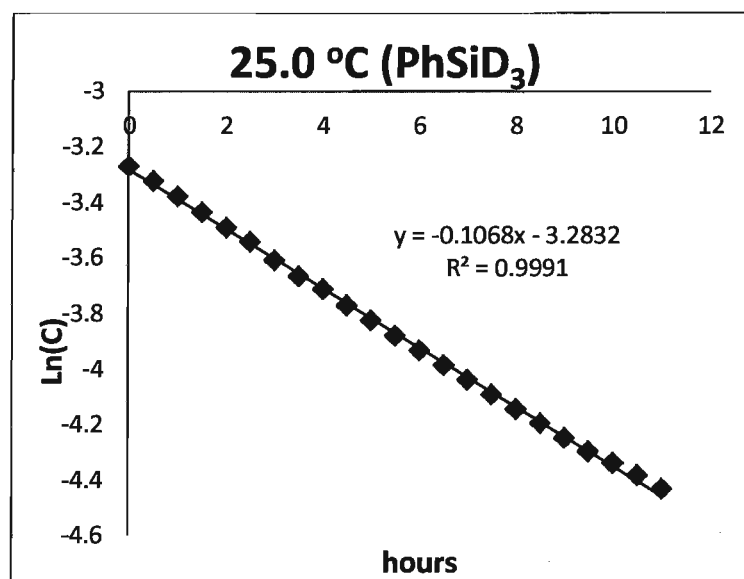


Figure V-25. Ln(C)/time plot for reaction between (Cp)(ArN)Mo(H)(PMe₃) and PhSiD₃ (5 eq) at 25.0 °C.

$$k_D(25.0\text{ }^\circ\text{C}) = (1.068 \pm 0.007) \cdot 10^{-1} \text{ h}^{-1} = (2.97 \pm 0.02) \cdot 10^{-5} \text{ s}^{-1}.$$

$$\text{KIE}(25^\circ\text{C}) = \frac{k_H(25^\circ\text{C})}{k_D(25^\circ\text{C})} = \frac{2.83 \cdot 10^{-5}}{2.97 \cdot 10^{-5}} \cong 1.0$$

The chart below illustrates the time profile (relative integral intensity vs. time) of two concurrent reactions: 1) formation of (Cp)(ArN)Mo(D)(PMe₃) from (Cp)(ArN)Mo(H)(PMe₃) and PhSiD₃, 2) formation of (Cp)(ArN)Mo(SiD₂Ph)(PMe₃) as a result of the dehydrogenative addition of PhSiD₃ to (Cp)(ArN)Mo(H)(PMe₃) (Figure V-26).

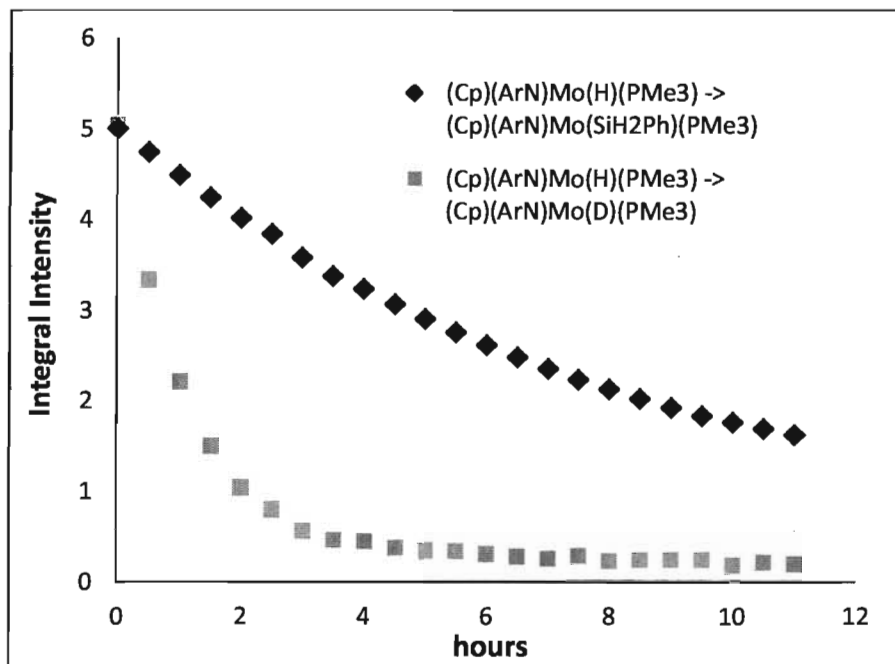


Figure V-26. Relative integral intensity vs. time plot for concurrent formation of $(\text{Cp})(\text{ArN})\text{Mo}(\text{D})(\text{PMe}_3)$ and $(\text{Cp})(\text{ArN})\text{Mo}(\text{SiH}_2\text{Ph})(\text{PMe}_3)$ from $(\text{Cp})(\text{ArN})\text{Mo}(\text{H})(\text{PMe}_3)$ and PhSiD_3 (5 eq.) at 25 °C.

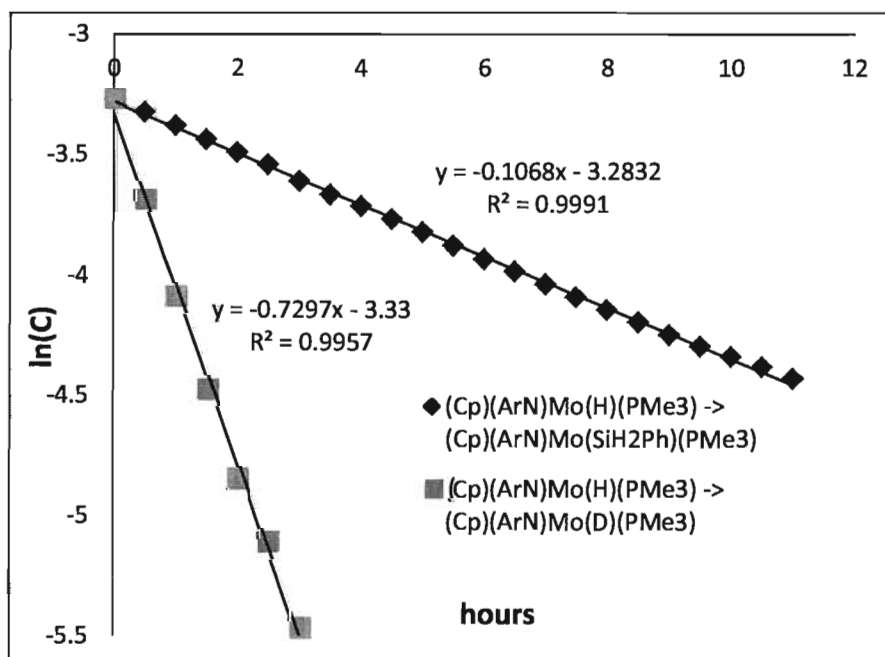
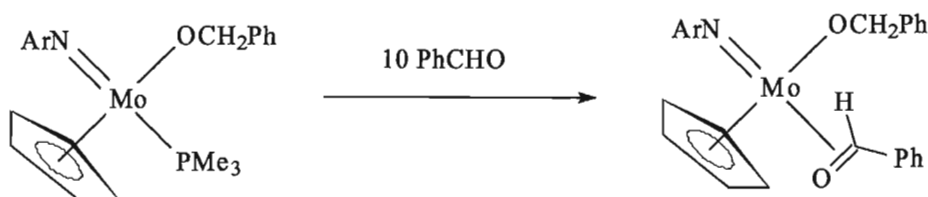


Figure V-27. $\text{Ln}(\text{C})/\text{time}$ plot for the reaction of $(\text{Cp})(\text{ArN})\text{Mo}(\text{H})(\text{PMe}_3)$ with PhSiD_3 (5 eq) at 25 °C.

Rate constant for reaction between (Cp)(ArN)Mo(H)(PMe₃) and PhSiD₃ (5 eq.) to produce (Cp)(ArN)Mo(D)(PMe₃) have been extracted from Figure V-27.

$$k_{H/D} = [(0.7297 \pm 0.0214) - (0.1068 \pm 0.0007)] \text{ hours}^{-1} = (0.6230 \pm 0.0207) \text{ hours}^{-1} = (1.73 \pm 0.06) \cdot 10^{-4} \text{ s}^{-1}$$

Reaction between (Cp)(ArN)Mo(OCH₂Ph)(PMe₃) with PhCHO (10 eq.)



Benzaldehyde (10.8 mg, 0.102 mmol) was added to a solution of (Cp)(ArN)Mo(OCH₂Ph)(PMe₃) (5.3 g, 0.010 mmol) in C₆D₆ (0.60 mL). The reaction was monitored by ¹H NMR at 26.0 °C (Figure V-28), 40.0 °C (Figure V-29), and 55.0 °C (Figure V-30).

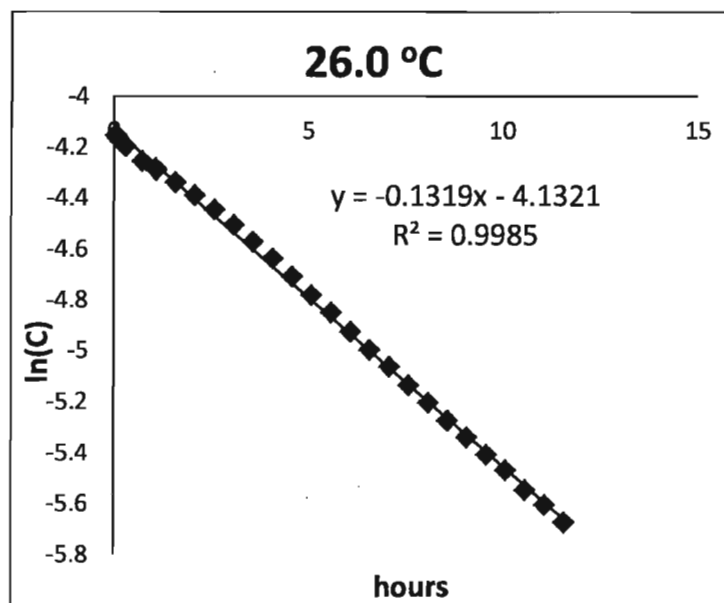


Figure V-28. Ln(C)/time plot for reaction between (Cp)(ArN)Mo(OCH₂Ph)(PMe₃) and PhCHO (10 eq.) at 26.0 °C.

$$k(26.0 \text{ } ^\circ\text{C}) = (0.132 \pm 0.001) \text{ h}^{-1} = (3.66 \pm 0.03) \cdot 10^{-5} \text{ s}^{-1}$$

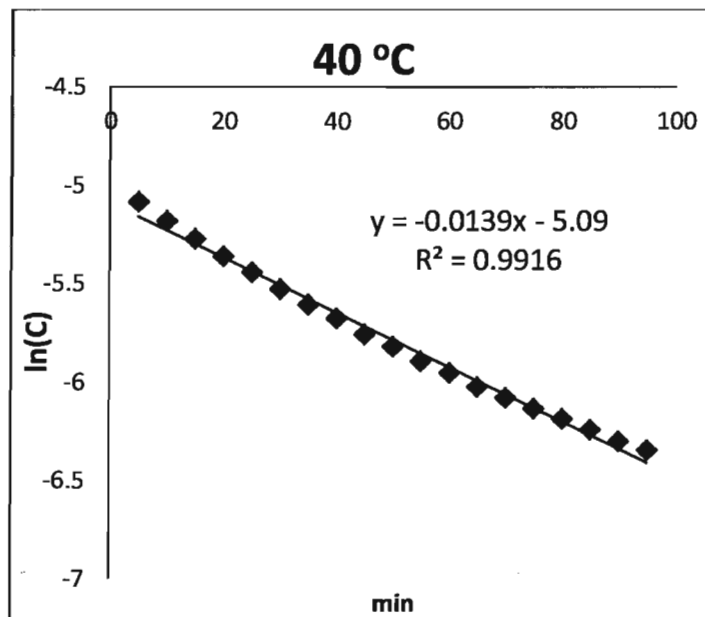


Figure V-29. Ln(C)/time plot for reaction between (Cp)(ArN)Mo(OCH₂Ph)(PMe₃) and PhCHO (10 eq.) at 40.0 °C.

$$k(40.0\text{ °C}) = (1.39 \pm 0.03) \cdot 10^{-2} \text{ min}^{-1} = (2.31 \pm 0.05) \cdot 10^{-4} \text{ s}^{-1}$$

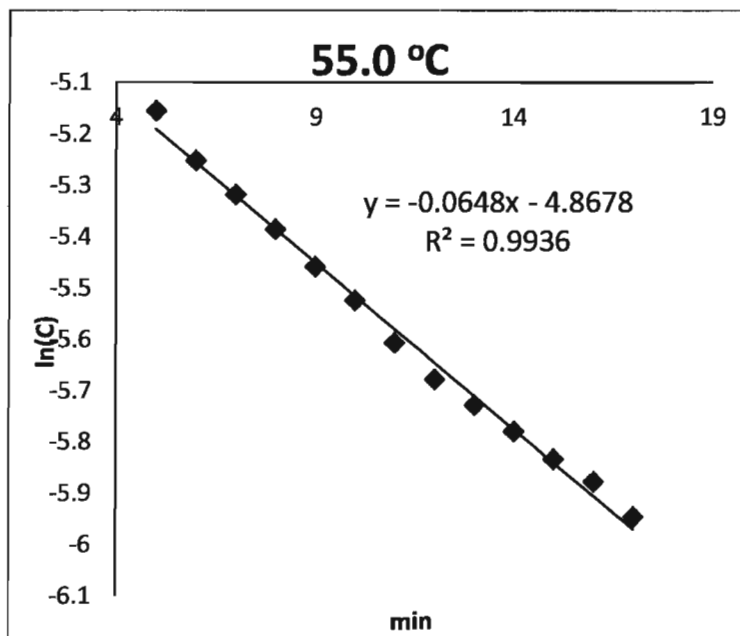


Figure V-30. Ln(C)/time plot for the reaction between (Cp)(ArN)Mo(OCH₂Ph)(PMe₃) and PhCHO (10 eq.) at 55.0 °C.

$$k(55.0\text{ °C}) = (6.48 \pm 0.16) \cdot 10^{-2} \text{ min}^{-1} = (1.08 \pm 0.03) \cdot 10^{-3} \text{ s}^{-1}$$

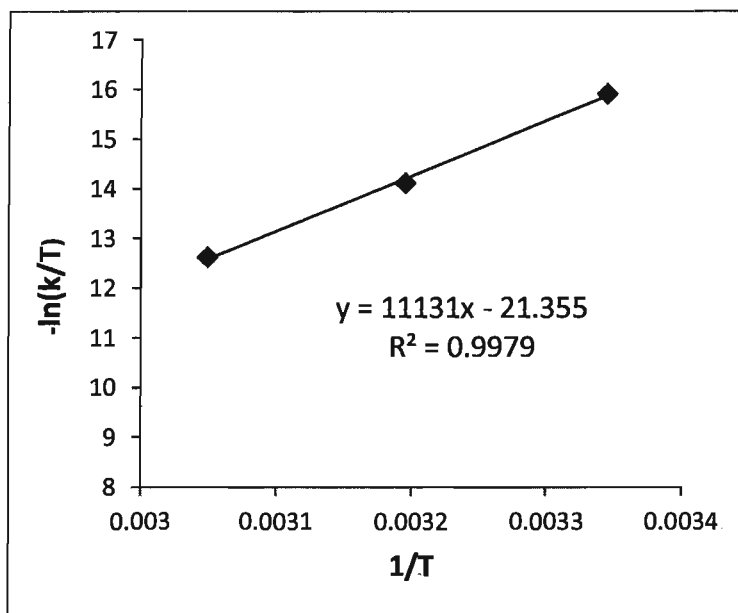


Figure V-31. Eyring plot for the reaction of (Cp)(ArN)Mo(OCH₂Ph)(PMe₃) with PhCHO (10 eq.)

Activation parameters have been extracted from the Eyring plot (Figure V-31): $\Delta H^\ddagger = (9.25 \pm 0.43) \cdot 10^1$ kJ/mol, $\Delta S^\ddagger = -(2.03 \pm 1.36) \cdot 10^1$ J/(K·mol).

Reaction between (Cp)(ArN)Mo(OCH₂Ph)(η^2 -PhCHO) and PhSiH₃ (excess)

Benzaldehyde (25.7 mg, 0.242 mmol) was added to a solution of (Cp)(ArN)Mo(H)(PMe₃) (5.3 mg, 0.010 mmol) in C₆D₆ (0.60 ml) to generate complex (Cp)(ArN)Mo(OCH₂Ph)(η^2 -PhCHO) *in situ*. The complex was formed within one hour at RT. All volatiles were evaporated, and the residue was re-dissolved in C₆D₆ (0.60 mL). Phenylsilane (13.0 mg, 0.121 mmol) was added, and the reaction was monitored by ¹H NMR (Figure V-32). The reaction provided formation of (Cp)(ArN)Mo(H)₂(SiH₂Ph), (Cp)(ArN)Mo(H)(SiH₂Ph)(H) and other unidentified products.

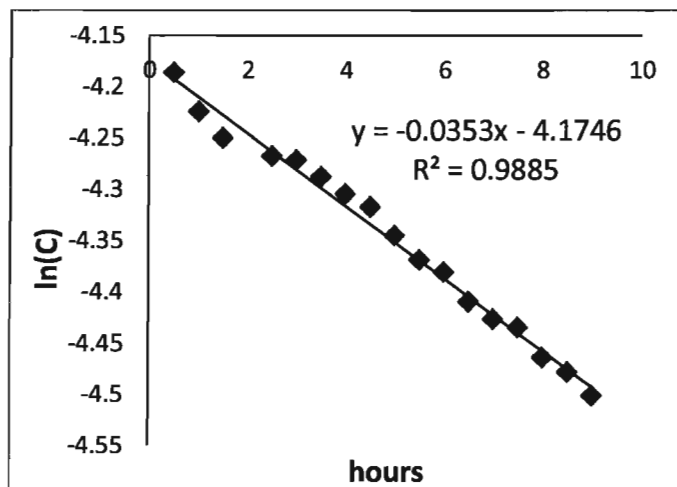


Figure V-32. Ln(C)/time plot for the reaction of (Cp)(ArN)Mo(OCH₂Ph)(PhCHO) with PhSiH₃ (12 eq.)

$$k(26.0\text{ }^{\circ}\text{C}) = (3.53 \pm 0.10) \cdot 10^{-2} \text{ h}^{-1} = (9.8 \pm 0.3) \cdot 10^{-6} \text{ s}^{-1}$$

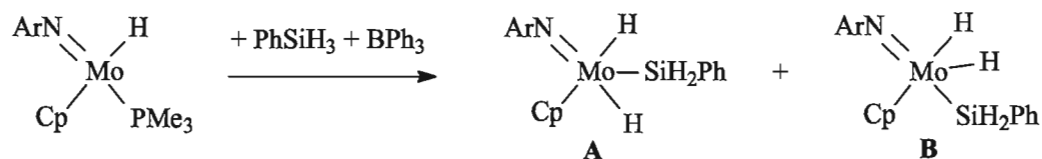
Reaction of (Cp)(ArN)Mo(SiH₂Ph)(PMe₃) with excess of PhCHO

Benzaldehyde (14.3 g, 0.135 mmol) was added to a solution of (Cp)(ArN)Mo(SiH₂Ph)(PMe₃) (5.0 mg, 0.010 mmol) in C₆D₆ (0.60 mL). No reaction was observed after one day at RT.

Reaction between (Cp)(ArN)Mo(OCH₂Ph)(PMe₃) and *o*-bromobenzaldehyde

o-Bromobenzaldehyde (16.0 mg, 0.0863 mmol) was added to a solution of (Cp)(ArN)Mo(OCH₂Ph)(PMe₃) (12.4 mg, 0.0242 mmol) in C₆D₆ (0.60 mL). The reaction mixture was heated for 20 minutes at 60 °C. Formation of free benzaldehyde was observed by ¹H NMR.

Reaction between (Cp)(ArN)Mo(H)(PMe₃), PhSiH₃ (1 eq.) and Ph₃B (1 eq.)



Phenylsilane (6.23 mg, 0.057 mmol) and Ph₃B (13.9 g, 0.057 mmol) were added to a

solution of (Cp)(ArN)Mo(H)(PMe₃) (23.8 mg, 0.057 mmol) in C₆D₆ at RT. The formation of isomers (Cp)(ArN)Mo(H)(SiH₂Ph)(H) (**A**) and (Cp)(ArN)Mo(H)₂(SiH₂Ph) (**B**) was detected by ²⁹Si INEPT+ NMR (Figure V-33).

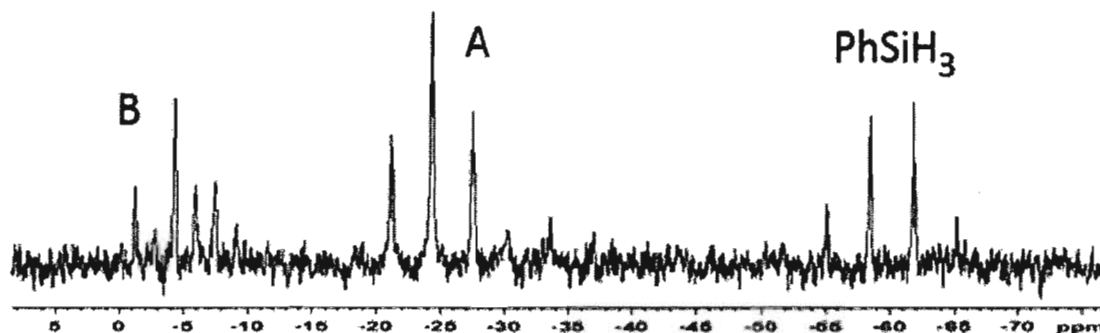


Figure V-33. ²⁹Si INEPT+ NMR spectrum of a reaction mixture containing (Cp)(ArN)Mo(H)(SiH₂Ph)(H) (**A**), (Cp)(ArN)Mo(H)₂(SiH₂Ph) (**B**) and PhSiD₃.

The detected intermediates **A** and **B** were unstable and decomposed within day.

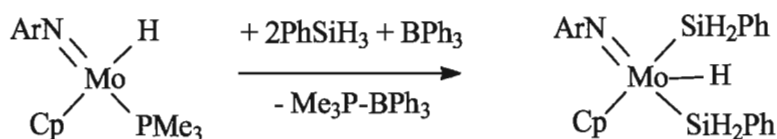
(ArN)(ArN)(Cp)Mo(H)(SiH₂Ph)(H), **A**

¹H-NMR (300 MHz; C₆D₆; 298K; δ, ppm): -1.30 (s, 2H, Mo(H)(SiH₂)(H)), 5.82 (s, 2H, SiH₂Ph). ²⁹Si-NMR INEPT+ (300 MHz; C₆D₆; 298K; δ, ppm): -24.32 (tt, ¹J_{Si-H} = 188.2 Hz, ²J_{Si-H} = 6.9 Hz, 1Si).

(ArN)(Cp)Mo(H)(H)(SiH₂Ph), **B**

¹H-NMR (300 MHz; C₆D₆; 298K; δ, ppm): -0.52 (d, ²J_{H-H} = 4.9 Hz, 1H, Mo-H^a), 0.58 (d, ²J_{H-H} = 4.9 Hz, 1H, Mo-H^b). ²⁹Si-NMR INEPT+ (300 MHz; C₆D₆; 298K; δ, ppm): -4.33 (vt, ¹J_{Si-H} = 185.6 Hz, 1Si).

Reaction between (Cp)(ArN)Mo(H)(PMe₃), PhSiH₃ (2 eq.) and Ph₃B (1 eq.)



Phenylsilane (0.400 g, 3.70 mmol) and Ph₃B (0.176 g, 0.726 mmol) were added to a

solution of (Cp)(ArN)Mo(H)(PMe₃) (0.300 g, 0.726 mmol) in Et₂O. The reaction mixture was stirred for a week at RT. All volatiles were removed under vacuum to give 0.420 g of an amorphous black crude residue containing (Cp)(ArN)Mo(H)(SiH₂Ph)₂ (~85%), (Cp)(ArN)Mo(SiH₂Ph)(PMe₃) (~10%) and Ph₂SiH₂ (~5%).

(Cp)(ArN)Mo(SiH₂Ph)₂(H)

¹H-NMR (300 MHz; C₆D₆; 298K; δ, ppm): 0.28 (m, 1H, Mo-*H*), 4.84 (s, 5H, *Cp*), 5.61 (dd, ²*J*_{H-H} = 4.5 Hz, ³*J*_{H-H} = 2.1 Hz, 2H, 2SiH^{*a*}HPh), 5.80 (dd, ²*J*_{H-H} = 4.5 Hz, ³*J*_{H-H} = 2.1 Hz, 2H, 2SiH^{*b*}HPh). ²⁹Si-NMR INEPT+ (300 MHz; C₆D₆; 298K; δ, ppm): -5.90 (t, ¹*J*_{Si-H} = 189.7 Hz, 2Si) (Figure V-34).

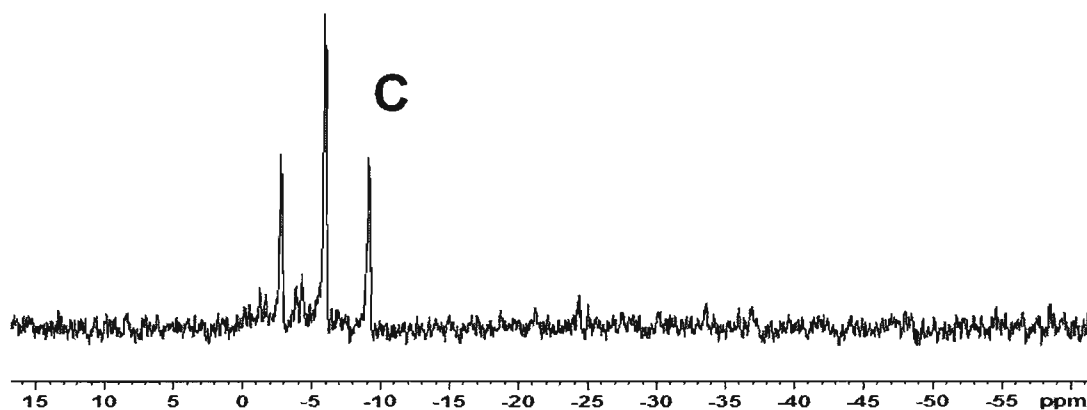


Figure V-34. ²⁹Si INEPT+ NMR spectrum of (Cp)(ArN)Mo(SiH₂Ph)₂(H), C.

Table V-1. Hydrosilylation of carbonyls with PhSiH₃ catalyzed by (Cp)(ArN)Mo(H)(PMe₃).

<i>Entry</i>	<i>Substrate</i>	<i>Conversion of org. substrate</i>	<i>Product(s)</i>	<i>Conditions</i>	<i>Yield, %</i>
1	PhC(O)H	100%	PhCH ₂ OSiH ₂ Ph, (PhCH ₂ O) ₂ SiHPh	0.5 day, RT	21, 79
2	PhC(O)Me	0%	-	5 days, 50 °C	0, 0
3	Cyclohexanone	54%	CyOSiH ₂ Ph, (CyO) ₂ SiHPh	5 days, 50 °C	36, 18
4	PhCN	10%	PhCH=NSiH ₂ Ph	3 days, 50 °C	10

Table V-2. Hydrosilylation of PhCHO with PhSiH₃.

<i>CATALYST</i>	<i>Products</i>	<i>Reactions conditions</i>	<i>Yield, according to ¹H-NMR</i>	<i>Catalyst mol, %</i>	<i>Turnover number (TON)</i>
(Cp)(ArN)Mo(H)(PMe ₃)	PhCH ₂ OSiH ₂ Ph	7 h	21%	5	20
	(PhCH ₂ O) ₂ SiHPh		79%		
(Cp)(ArN)Mo(OCH ₂ Ph)(PMe ₃)	PhCH ₂ OSiH ₂ Ph	7 h	38%	5	20
	(PhCH ₂ O) ₂ SiHPh		62%		
(Cp)(ArN)Mo(OCH ₂ Ph)(PhCHO)	PhCH ₂ OSiH ₂ Ph	12 h, RT	23%	5	20
	(PhCH ₂ O) ₂ SiHPh		77%		
(Cp)(ArN)Mo(SiH ₂ Ph)(PMe ₃)	PhCH ₂ OSiH ₂ Ph	3 d, RT	22%	5	11
	(PhCH ₂ O) ₂ SiHPh		32%		

Table V-3. Hydrosilylation of PhCHO with PhSiH₃ (and PhSiD₃) catalyzed by (Cp)(ArN)Mo(H)(PMe₃): reaction rate constants of individual steps and activation parameters

REACTION	Rate constant, <i>k</i>	ΔH^\ddagger , kJ/mol	ΔS^\ddagger , J/(K·mol)
(Cp)(ArN)Mo(H)(PMe ₃) + PMe ₃ , phosphine exchange	(2.89 ± 0.04)·10 ¹ s ⁻¹ (12.0 °C) (4.29 ± 0.07)·10 ¹ s ⁻¹ (22.0 °C) (6.22 ± 0.12)·10 ¹ s ⁻¹ (32.0 °C) (8.56 ± 0.15)·10 ¹ s ⁻¹ (42.0 °C)	(2.47±0.04)·10 ¹	-(1.30 ± 0.01)·10 ²
(Cp)(ArN)Mo(H)(PMe ₃) + PhCHO (1 eq) + PMe ₃ (10 eq) => (Cp)(ArN)Mo(OCH ₂ Ph)(PMe ₃)	(3.6 ± 0.1)·10 ⁻³ M ⁻¹ ·s ⁻¹ (26.0 °C) (1.25 ± 0.17)·10 ⁻² M ⁻¹ ·s ⁻¹ (40.0 °C) (2.44 ± 0.17)·10 ⁻² M ⁻¹ ·s ⁻¹ (50.0 °C) (4.17 ± 0.05)·10 ⁻² M ⁻¹ ·s ⁻¹ (60.0 °C)	(5.76 ± 0.36)·10 ¹	-(9.97 ± 1.14)·10 ¹
(Cp)(ArN)Mo(OCH ₂ Ph)(PMe ₃) + PhSiH ₃ (10 eq) => (Cp)(ArN)Mo(H)(PMe ₃) + (PhCH ₂ O) ₂ SiHPh	(1.97 ± 0.02)·10 ⁻⁴ s ⁻¹ (16.0 °C) (5.85 ± 0.03)·10 ⁻⁴ s ⁻¹ (26.0 °C) (1.22 ± 0.01)·10 ⁻³ s ⁻¹ (36.0 °C) (2.21 ± 0.16)·10 ⁻³ s ⁻¹ (46.0 °C)	(5.89 ± 0.49)·10 ¹	-(1.11 ± 0.16)·10 ²
(Cp)(ArN)Mo(OCH ₂ Ph)(PMe ₃) + PhSiD ₃ (10 eq) => (Cp)(ArN)Mo(D)(PMe ₃) + (PhCH ₂ O) ₂ SiDPh	(2.7 ± 0.02)·10 ⁻⁴ s ⁻¹ (16.0 °C) (7.40 ± 0.02)·10 ⁻⁴ s ⁻¹ (26.0 °C) (1.09 ± 0.01)·10 ⁻³ s ⁻¹ (36.0 °C) (1.60 ± 0.03)·10 ⁻³ s ⁻¹ (46.0 °C)	(4.20 ± 0.76)·10 ¹	-(1.67 ± 0.25)·10 ²
(Cp)(ArN)Mo(H)(PMe ₃) + PhSiH ₃ (10 eq) => (Cp)(ArN)Mo(SiH ₂ Ph)(PMe ₃) + H ₂	(1.57 ± 0.01)·10 ⁻⁴ M ⁻¹ ·s ⁻¹ (25.0 °C) (4.54 ± 0.01)·10 ⁻⁴ M ⁻¹ ·s ⁻¹ (35.0 °C) (9.61 ± 0.17)·10 ⁻⁴ M ⁻¹ ·s ⁻¹ (45.0 °C) (2.04 ± 0.09)·10 ⁻³ M ⁻¹ ·s ⁻¹ (55.0 °C)	(6.61 ± 0.31)·10 ¹	-(9.58 ± 1.00)·10 ¹
(Cp)(ArN)Mo(H)(PMe ₃) + PhSiD ₃ (5 eq) => (Cp)(ArN)Mo(SiD ₂ Ph)(PMe ₃) + HD	(1.65 ± 0.01)·10 ⁻⁴ M ⁻¹ ·s ⁻¹ (26.0 °C)	-	-
(Cp)(ArN)Mo(OCH ₂ Ph)(PMe ₃) + PhCHO (10 eq) => (Cp)(ArN)Mo(OCH ₂ Ph)(PhCHO)	(2.15 ± 0.02)·10 ⁻⁴ M ⁻¹ ·s ⁻¹ (26.0 °C) (1.36 ± 0.03)·10 ⁻³ M ⁻¹ ·s ⁻¹ (40.0 °C) (6.35 ± 0.02)·10 ⁻³ M ⁻¹ ·s ⁻¹ (55.0 °C)	(9.25 ± 0.43)·10 ¹	-(5.6 ± 13.6)
(Cp)(ArN)Mo(OCH ₂ Ph)(PhCHO) + PhSiH ₃ => N/A	(1.08 ± 0.03)·10 ⁻⁴ M ⁻¹ ·s ⁻¹ (26.0 °C)	-	-

Computational studies

Density Functional Theory (DFT) calculations have been performed using the *Gaussian 03* program.¹⁵⁵ In all calculations, the spin-restricted method was employed. Wave function stability calculations were performed to confirm that the calculated wave functions corresponded to the electronic ground state. The structures of all species were optimized using the B3LYP exchange-correlation (XC) functional^{156, 157} with the all-electron, mixed basis set (DZVP¹⁵⁸ on Mo and TZVP¹⁵⁹ on all other atoms). Tight SCF convergence criteria (10^{-8} a.u.) were used for all calculations. Harmonic frequency calculations with the analytic evaluation of force gradients (OPT=CalcAll) were used to determine the nature of the stationary points. Intrinsic reaction coordinate (IRC)¹⁶⁰ calculations were used to confirm the reaction pathways through transition states (TSs) for all reactions. Free energies of species were evaluated at 298K and 1 atm.

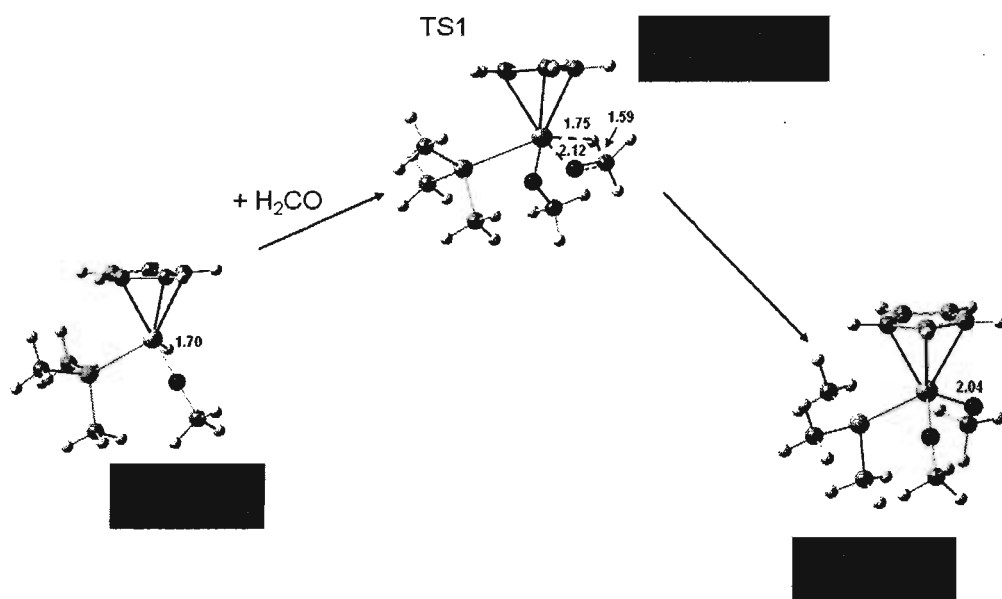


Figure V-35. Computed reaction pathways for the formation of $(\text{Cp})(\text{MeN})\text{Mo}(\text{OCH}_3)(\text{PMe}_3)$

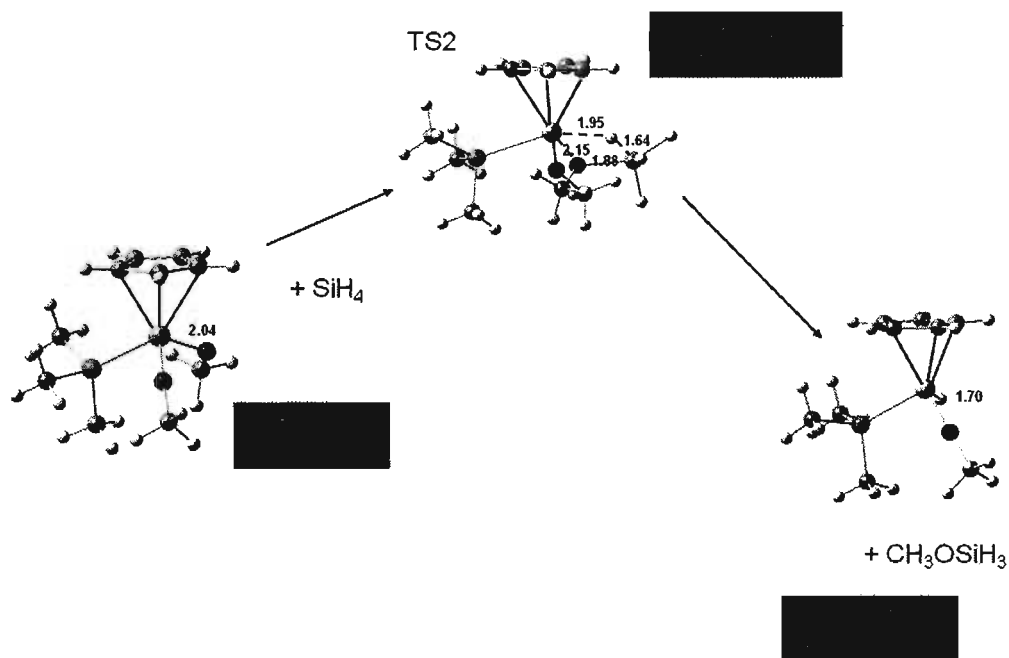


Figure V-36. Computed reaction pathways for the addition of SiH_4 to $(\text{Cp})(\text{MeN})\text{Mo}(\text{OCH}_3)(\text{PMe}_3)$.

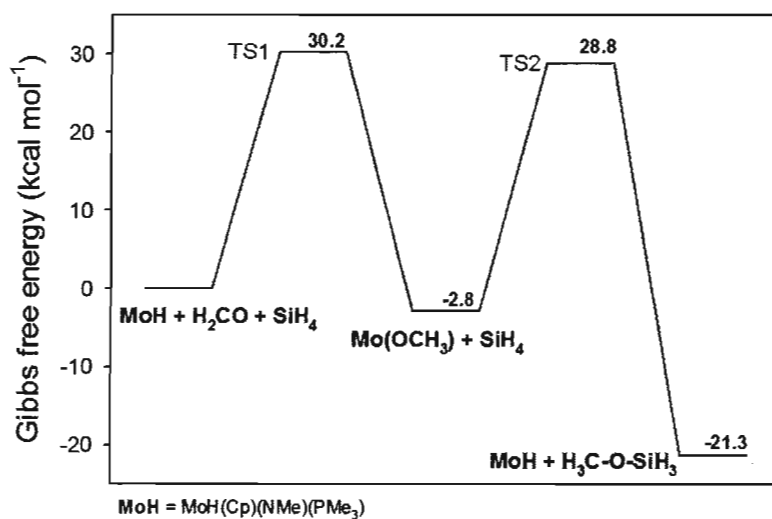


Figure V-37. Energy profile for the addition of SiH₄ to CH₂=O mediated by (Cp)(MeN)Mo(H)(PMe₃) (at 298 K).

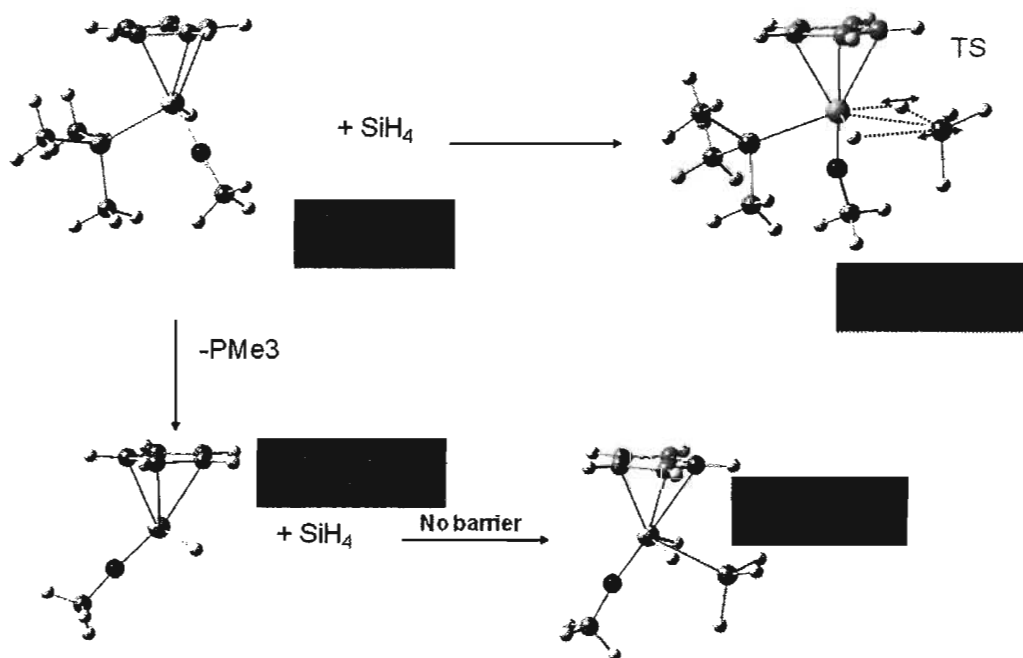


Figure V-38. Computed reaction pathways for the formation of (Cp)(MeN)Mo(H)₂(SiH₃) (at 298 K).

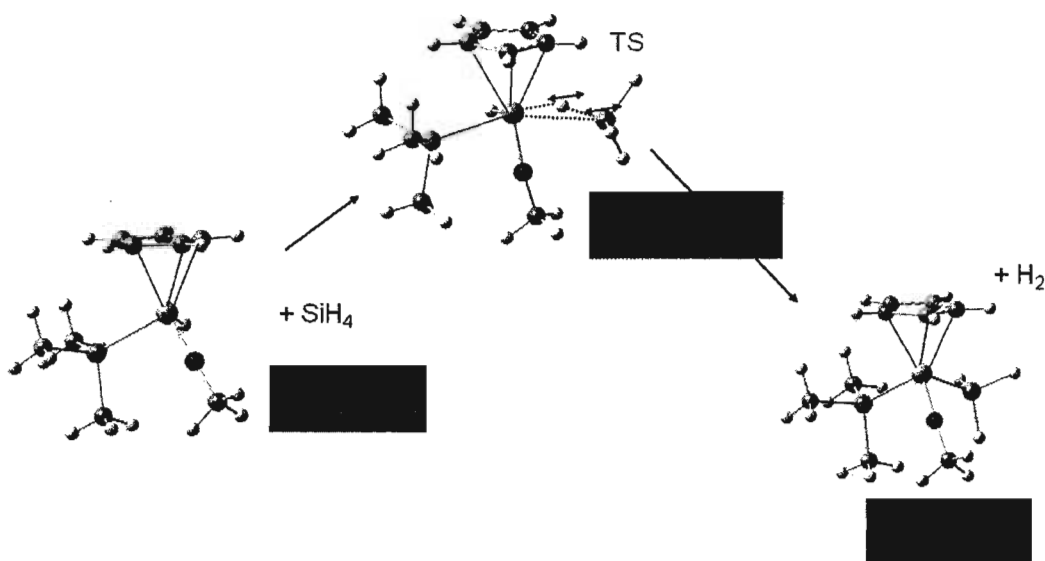


Figure V-39. Computed reaction pathway for the formation of $(\text{Cp})(\text{MeN})\text{Mo}(\text{SiH}_3)(\text{PMe}_3)$ (at 298 K).

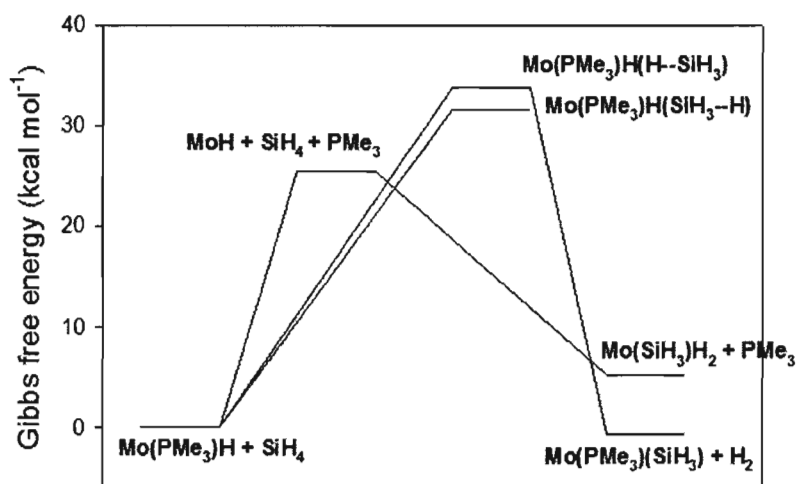


Figure V-40. Energy profile for the reactions of SiH_4 with $\text{Cp}(\text{MeN})\text{Mo}(\text{PMe}_3)(\text{H})$ (at 298 K)

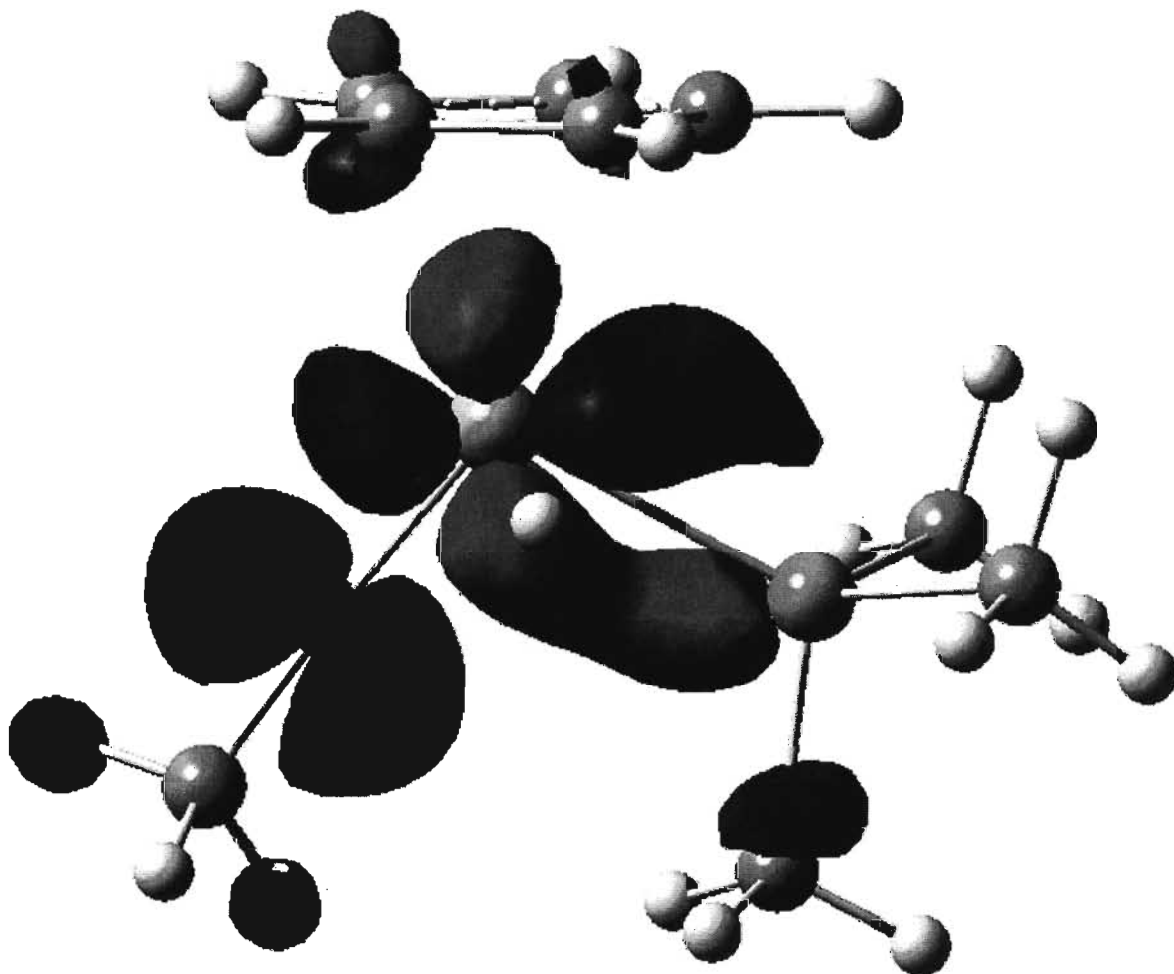


Figure V-41. The lowest unoccupied molecular orbital (LUMO) of $(\text{Cp})(\text{MeN})\text{Mo}(\text{H})(\text{PMe}_3)$.

Crystallographic study

A crystal of $(\text{Cp})(\text{ArN})\text{Mo}(\text{OCH}_2\text{Ph})(\text{PMe}_3)$ was coated with polyperfluoro oil and mounted on the Bruker Smart three-circle diffractometer with CCD area detector at 123 K.^k The crystallographic data and the characteristics of structure solution and refinement are given in Table VI-1. The structure factor amplitudes for all independent reflections were obtained after the Lorentz and polarization corrections. The Bruker SAINT program^l was used for data reduction. An absorption correction based on measurements of equivalent reflections was applied (SADABS).^m The structures were solved by direct methodsⁿ and refined by full-matrix least squares procedures, using $\omega(|F_o|^2 - |F_c|^2|)^2$ as the refined function. All non-hydrogen atoms were found from the difference electron density map and refined with anisotropic thermal parameters, whereas all hydrogen atoms were refined using the “riding” model.

^k SMART Version 5.625. Bruker AXS Inc., Madison, Wisconsin, USA, 2001.

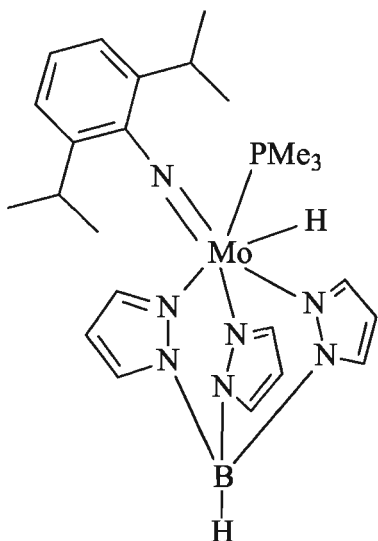
^l SAINT, Version 6.02A, Bruker AXS Inc., Madison, Wisconsin, USA, 2001.

^m SMART and SADABS Software Reference Manuals. Bruker AXS Inc. Madison, Wisconsin, USA, 1998.

ⁿ SHELXTL-Plus, Release 5.10, Bruker AXS Inc., Madison, Wisconsin, USA, 1997.

V. 2. Hydrosilylation catalyzed by (Tp)(ArN)Mo(H)(PMe₃)

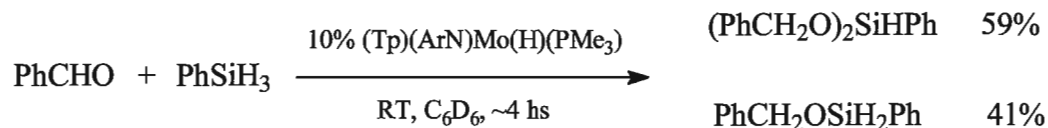
Synthesis of (Tp)(ArN)Mo(H)(PMe₃)



(ArN)Mo(H)(Cl)(PMe₃)₃ (2.2 g, 4.11 mmol) and KTp (1.6 g, 6.16 mmol) were dissolved in THF at RT, and the solution was heated for 2 days at 50 °C. The solvent was evaporated, and the residue was recrystallized from hexane giving (Tp)(ArN)Mo(H)(PMe₃) (1.7 g, 74%) as a dark-brown solid. ¹H-NMR (300 MHz; C₆D₆; 298K; δ, ppm): 1.04 (m, 6H, 2CH₃, *i*Pr), 1.34 (d, ²*J*_{H-H} = 6.6 Hz, 6H, 2CH₃, *i*Pr), 1.36 (d, ²*J*_{H-P} = 7.4 Hz, 9H, PMe₃), 3.67 (d, ²*J*_{H-P} = 21.4 Hz, Mo-H), 4.35 (m, 2H, *i*Pr), 5.68 (t, *J* = 2.1 Hz, 1H^a, Pz), 5.90 (t, *J* = 2.1 Hz, 1H^b, Pz), 6.09 (t, *J* = 2.1 Hz, 1H^c, Pz), 7.24 (d, ²*J*_{H-H} = 2.1 Hz, 1H^a, Pz), 7.45 (d, ²*J*_{H-H} = 2.1 Hz, 1H^a, Pz), 7.52 (d, ²*J*_{H-H} = 2.1 Hz, 1H^b, Pz), 7.56 (d, ²*J*_{H-H} = 2.1 Hz, 1H^c, Pz), 7.76 (d, ²*J*_{H-H} = 2.1 Hz, 1H^c, Pz), 7.88 (d, ²*J*_{H-H} = 2.1 Hz, 1H^b, Pz). ¹³C-NMR (150.92 MHz; C₆D₆; 298 K; δ, ppm): 22.2 (d, ²*J*_{P-H} = 22.0 Hz, PMe₃), 23.2 (bs, CH₃, *i*Pr), 27.3 (bs, CH, *i*Pr), 104.0 (Pz^a), 105.0 (Pz^c), 105.5 (Pz^b), 123.2 (*m*-C, 2CH, Ar), 123.8 (*p*-C, CH, Ar), 133.6 (Pz^a), 134.8 (Pz^b), 134.9 (Pz^c), 141.9 (Pz^b), 142.5 (Pz^a), 143.7 (Pz^c), 152.7 (*ipso*-C, C-N, Ar). ³¹P-NMR (121.5 MHz; C₆D₆; 298 K; δ, ppm): 15.6 (s, 1P, PMe₃). ¹¹B-NMR (96.3 MHz; C₆D₆; 298 K; δ, ppm): -4.1 (bs). Elem. Anal. (%): calc. for C₂₄H₃₇BMoN₇P (561.33): C 51.35, H 6.64, N 17.47; found (±0.3%) C 51.09, H 6.92, N 16.28. IR (nujol, cm⁻¹): 1683.56 (Mo-H), 2472.31 (B-H).

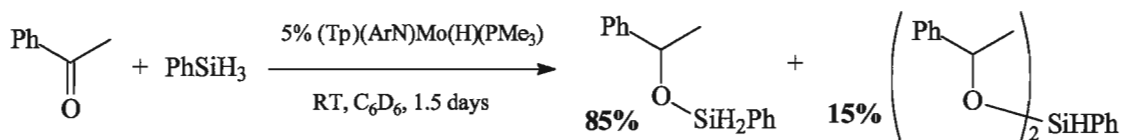
Hydrosilylation catalyzed by (Tp)(ArN)Mo(H)(PMe₃)

Hydrosilylation of benzaldehyde with PhSiH₃



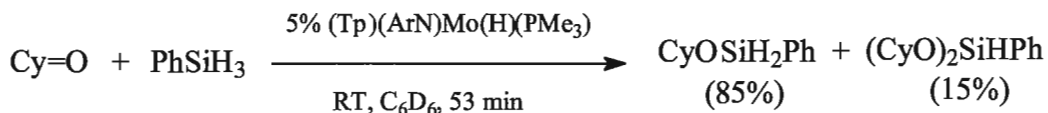
Benzaldehyde (19.0 mg, 0.177 mmol) and phenylsilane (19.3 mg, 0.177 mmol) were added to a solution of (Tp)(ArN)Mo(H)(PMe₃) (10.0 mg, 10 mol% in 0.60 ml C₆D₆) at RT. The reaction was complete in 4 hours giving (PhCH₂O)₂SiHPh (59%) and PhCH₂OSiH₂Ph (41%) as the final products.

Hydrosilylation of acetophenone with PhSiH₃



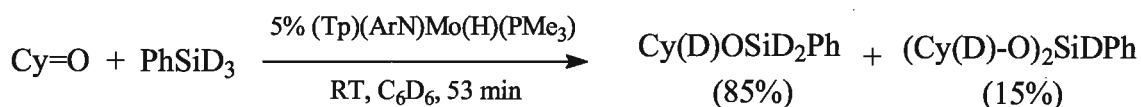
Acetophenone (42.8 mg, 0.3563 mmol) and phenylsilane (38.6 mg, 0.356 mmol) were added to a solution of (Tp)(ArN)Mo(H)(PMe₃) (10.0 mg, 5 mol%) in C₆D₆ (0.60 ml). The reaction was complete in 1.5 days at RT giving PhCH(OSiH₂Ph)CH₃ (85%) and (PhCH(CH₃)O)₂SiHPh (15%) as the final products.

Hydrosilylation of cyclohexanone with PhSiH₃



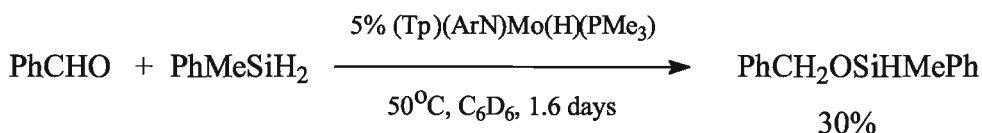
Cyclohexanone (35.0 mg, 0.356 mmol) and phenylsilane (38.6 mg, 0.356 mmol) were added to a solution of (Tp)(ArN)Mo(H)(PMe₃) (10.0 mg, 5 mol%) in C₆D₆ (0.60 ml). The reaction was complete in ~50 min at RT giving (CyO)₂SiHPh (15%) and CyOSiH₂Ph (85%) as the final products.

Hydrosilylation of cyclohexanone with PhSiD₃



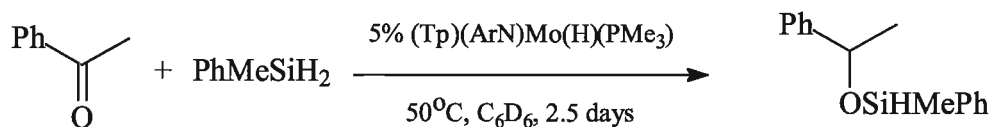
Cyclohexanone (17.5 mg, 0.174 mmol) and PhSiD₃ (19.3 mg, 0.174 mmol) were added to a solution of (Tp)(ArN)Mo(H)(PMe₃) (5.0 mg, 5 mol%) in C₆D₆ (0.60 ml). The reaction was complete in ~50 min at RT giving (CyO)₂SiDPh (15%) and CyOSiH₂Ph (85%) as the final products. Substitution of the molybdenum hydride Mo-H by deuterium was not observed.

Hydrosilylation of benzaldehyde with PhMeSiH₂



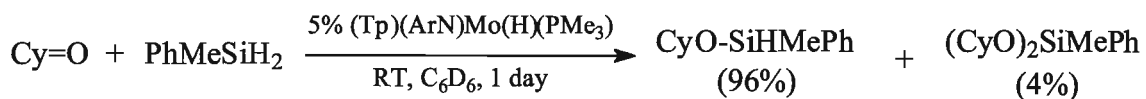
Benzaldehyde (37.8 mg, 0.356 mmol) and methylphenylsilane (43.6 mg, 0.356 mmol) were added to a solution of (Tp)(ArN)Mo(H)(PMe₃) (10.0 mg, 5 mol%) in C₆D₆ (0.60 ml). The reaction mixture was heated at 50 °C for 1.6 days giving PhCH₂OSiHMePh (30%) as the only product. The catalysis was terminated.

Hydrosilylation of acetophenone with PhMeSiH₂



Acetophenone (42.8 mg, 0.356 mmol) and methylphenylsilane (38.6 mg, 0.356 mmol) were added to a solution of (Tp)(ArN)Mo(H)(PMe₃) (10.0 mg, 5 mol%) in C₆D₆ (0.60 ml). The reaction was complete in 2.5 days at 50 °C giving PhCH(OSiHCH₃Ph)CH₃ (100%) as the only product.

Hydrosilylation of cyclohexanone with PhMeSiH₂



Cyclohexanone (35.0 mg, 0.356 mmol) and methylphenylsilane (38.6 mg, 0.356 mmol) were added to a solution of (Tp)(ArN)Mo(H)(PMe₃) (10.0 mg, 5 mol%) in C₆D₆ (0.60 ml). The reaction was complete in 1 day at RT giving (CyO)₂SiMePh (4%) and CyOSiHMePh (96%).

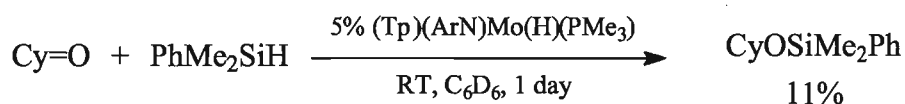
Hydrosilylation of benzaldehyde with PhMe₂SiH

Benzaldehyde (37.8 mg, 0.356 mmol) and dimethylphenylsilane (48.6 mg, 0.356 mmol) were added to a solution of (Tp)(ArN)Mo(H)(PMe₃) (10.0 mg, 5 mol%) in C₆D₆ (0.60 ml). The reaction mixture was heated for 1 day at 50 °C. Hydrosilylation was not observed.

Hydrosilylation of acetophenone with PhMe₂SiH

Acetophenone (42.8 mg, 0.356 mmol) and dimethylphenylsilane (48.6 mg, 0.356 mmol) were added to a solution of (Tp)(ArN)Mo(H)(PMe₃) (10.0 mg, 5 mol%) in C₆D₆ (0.60 ml). The reaction mixture was heated for 1 day at 50 °C. Hydrosilylation was not observed.

Hydrosilylation of cyclohexanone with PhMe₂SiH



Cyclohexanone (35.0 mg, 0.356 mmol) and dimethylphenylsilane (48.6 mg, 0.356 mmol) were added to a solution of (Tp)(ArN)Mo(H)(PMe₃) (10.0 mg, 5 mol%) in C₆D₆ (0.60 ml). The reaction was heated at 50 °C for 1.5 days. CyO-SiMe₂Ph was formed in 11% yield as the only product. The catalysis was terminated.

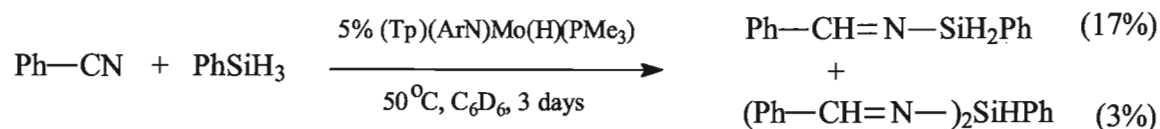
Hydrosilylation of benzaldehyde with (EtO)₃SiH

Benzaldehyde (37.8 mg, 0.356 mmol) and triethoxysilane (58.5 mg, 0.356 mmol) were added to a solution of (Tp)(ArN)Mo(H)(PMe₃) (10.0 mg, 5 mol%) in C₆D₆ (0.60 ml). The reaction mixture was heated for 1 day at 50 °C. Hydrosilylation was not observed.

Hydrosilylation of acetophenone with (EtO)₃SiH

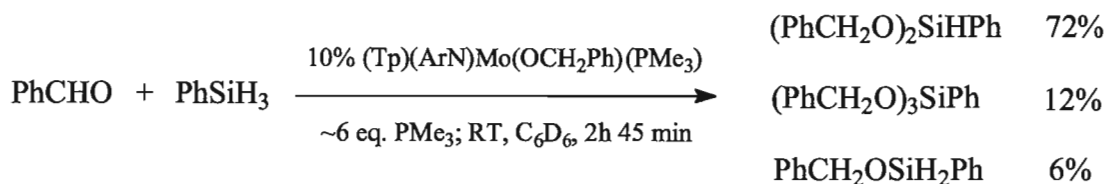
Acetophenone (42.8 mg, 0.356 mmol) and triethoxysilane (58.5 mg, 0.356 mmol) were added to a solution of (Tp)(ArN)Mo(H)(PMe₃) (10.0 mg, 5 mol%) in C₆D₆ (0.60 ml). The reaction mixture was heated for 1 day at 50 °C. Hydrosilylation was not observed.

Hydrosilylation of benzonitrile with phenylsilane



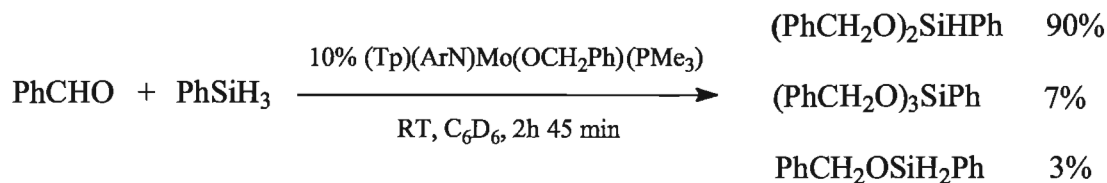
Phenylsilane (61.7 mg, 0.570 mmol) and benzonitrile (29.4 mg, 0.285 mmol) were added to a solution of (Tp)(ArN)Mo(H)(PMe₃) (8.0 mg, 5 mol%) in C₆D₆ (0.60 ml). The reaction mixture was heated for 3 days at 50 °C affording Ph-CH=N-SiH₂Ph (17%) and (Ph-CH=N-)₂SiHPh (3%) in 20% overall yield. The catalysis was terminated at this step. For Ph-CH=N-SiH₂Ph: ¹H-NMR (300 MHz; C₆D₆; 298K; δ, ppm): 5.43 (s, 2H, Si-H), 8.91 (s, 1H, -CH=N-). For (Ph-CH=N-)₂SiHPh: ¹H-NMR (300 MHz; C₆D₆; 298K; δ, ppm): 6.04 (s, 1H, Si-H), 9.21 (s, 2H, -CH=N-).

Hydrosilylation of benzaldehyde with phenylsilane catalyzed by (Tp)(ArN)Mo(OCH₂Ph)(PMe₃) in the presence of PMe₃.



Benzaldehyde (19.0 mg, 0.177 mmol) and phenylsilane (19.3 mg, 0.177 mmol) were added to a solution of (Tp)(ArN)Mo(OCH₂Ph)(PMe₃) (11.9 mg, 10 mol%) in the presence of PMe₃ (8.1 mg, 0.106 mmol) in C₆D₆ (0.60 ml) at RT. The reaction was complete in 2 hours and 45 min giving (PhCH₂O)₂SiHPh (82%), (PhCH₂O)₃SiPh (12%), PhCH₂OSiH₂Ph (6%).

Hydrosilylation of benzaldehyde with phenylsilane catalyzed by (Tp)(ArN)Mo(OCH₂Ph)(PMe₃).



Benzaldehyde (19.0 mg, 0.177 mmol) and phenylsilane (19.3 mg, 0.177 mmol) were added to a solution of (Tp)(ArN)Mo(OCH₂Ph)(PMe₃) (11.9 mg, 10 mol%) in C₆D₆ (0.60 ml) at RT. The reaction was complete in 2 hours and 45 min giving (PhCH₂O)₂SiHPh (90%), (PhCH₂O)₃SiPh (7%), PhCH₂OSiH₂Ph (3%) as the final products.

Stoichiometric reactions with (Tp)(ArN)Mo(H)(PMe₃)

Phosphine exchange between (Tp)(ArN)Mo(H)(PMe₃) and PMe₃

Trimethylphosphine (1.8 mg, 0.023 mmol) was added to a solution of (Tp)(ArN)Mo(H)(PMe₃) (13 mg, 0.023 mmol). The reaction mixture was studied by ³¹P-³¹P EXSY NMR (d8 = 0.300 s, T = 22 °C). Exchange between the free and the bound phosphines was not observed.

Phosphine exchange between (Tp)(ArN)Mo(OCH₂Ph)(PMe₃) and PMe₃

Trimethylphosphine (6.8 mg, 0.089 mmol) was added to a solution of (Tp)(ArN)Mo(H)(PMe₃) (11.8 mg, 0.018 mmol). The reaction mixture was studied by ³¹P-³¹P EXSY NMR (d8 = 0.300 s, T = 22 °C). Exchange between the free and the bound phosphines was not observed.

(Tp)(ArN)Mo(H)(PMe₃): exchange of pyrazolyl ligands

Exchange between three Pz groups in (Tp)(ArN)Mo(H)(PMe₃) was observed by ¹H-¹H EXSY experiment at 22.0 °C (d8 = 0.300 s) (Figure V-42). At -50.0 °C (d8 = 0.300 s) the exchange was not observed (Figure V-43).

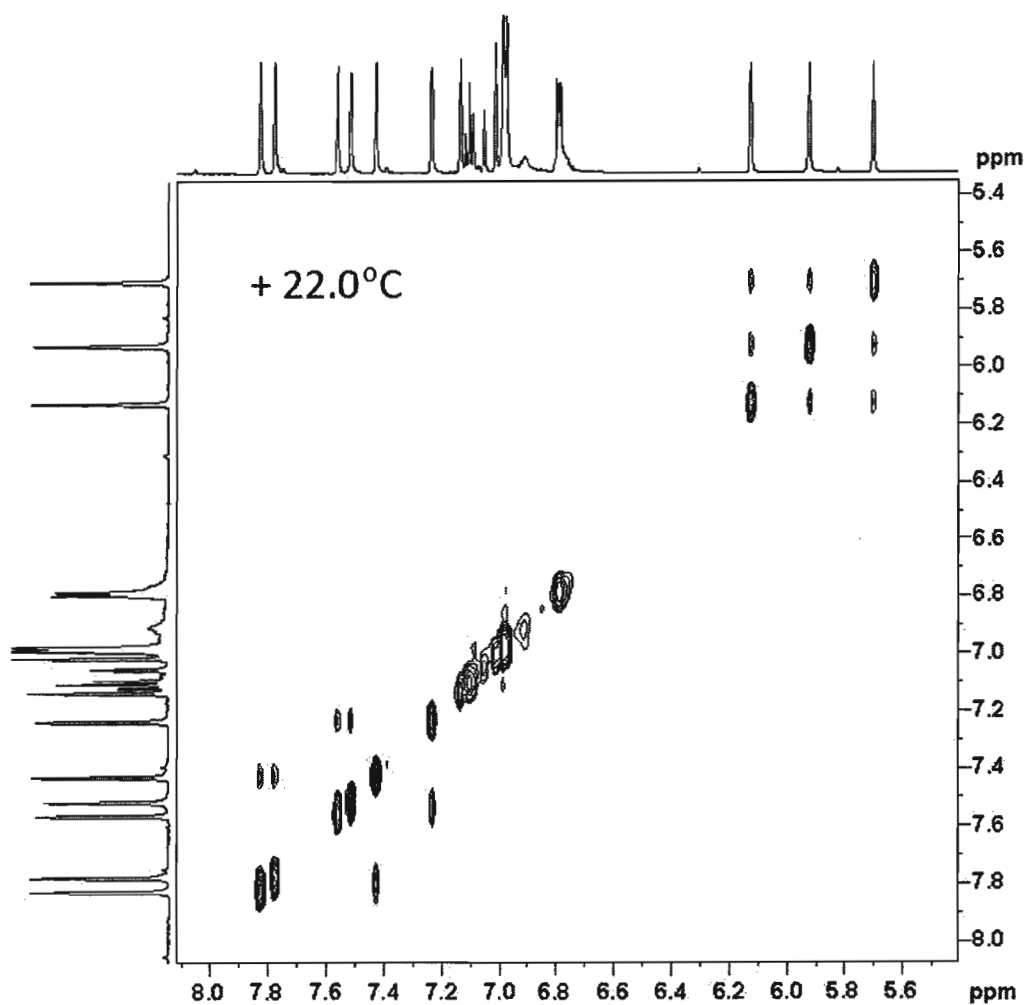


Figure V-42. ^1H - ^1H EXSY NMR spectrum of $(\text{Tp})(\text{ArN})\text{Mo}(\text{H})(\text{PMe}_3)$ at $22.0\text{ }^\circ\text{C}$ ($d_8 = 0.300\text{ s}$).

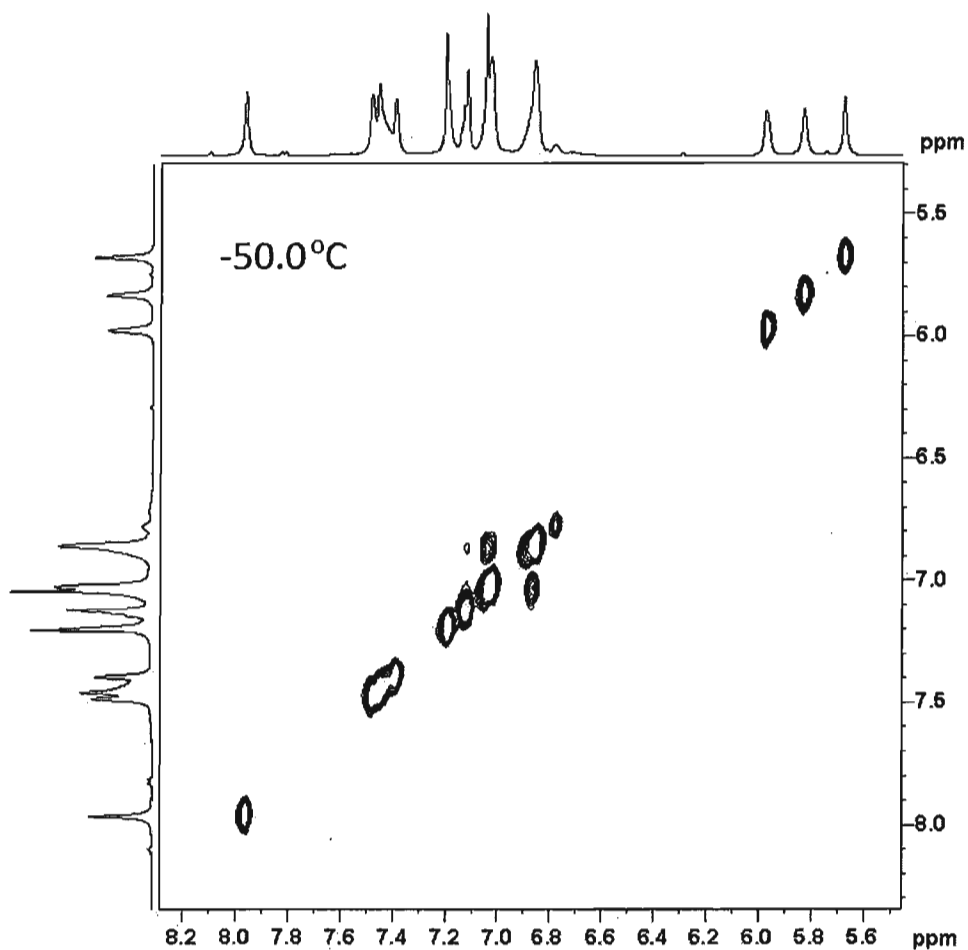


Figure V-43. ^1H - ^1H EXSY NMR spectrum of $(\text{Tp})(\text{ArN})\text{Mo}(\text{H})(\text{PMe}_3)$ at $-50.0\text{ }^\circ\text{C}$ ($d_8 = 0.300\text{ s}$).

$(\text{Tp})(\text{ArN})\text{Mo}(\text{H})(\text{PMe}_3)$: kinetic studies of Pz ligand dissociation

SELNOGP ge-1D EXSY NMR (Bruker 600 MHz machine) experiments were used to determine the exchange rate constants at $17.0\text{ }^\circ\text{C}$ (Figure V-44), $22.0\text{ }^\circ\text{C}$ (Figure V-45), $27.0\text{ }^\circ\text{C}$ (Figure V-46) and $32.0\text{ }^\circ\text{C}$ (Figure V-47).

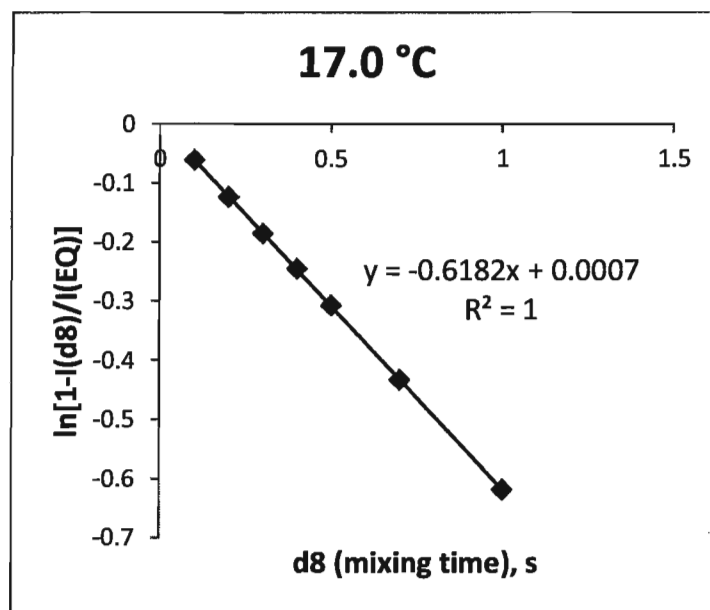


Figure V-44. $\ln[1-I(d8)/I(EQ)]/d8$ plot for Pz-ring dissociation in $(Tp)(ArN)Mo(H)(PMe_3)$ at 17.0 °C.

$$k(17.0\text{ °C}) = 0.618\text{ s}^{-1}$$

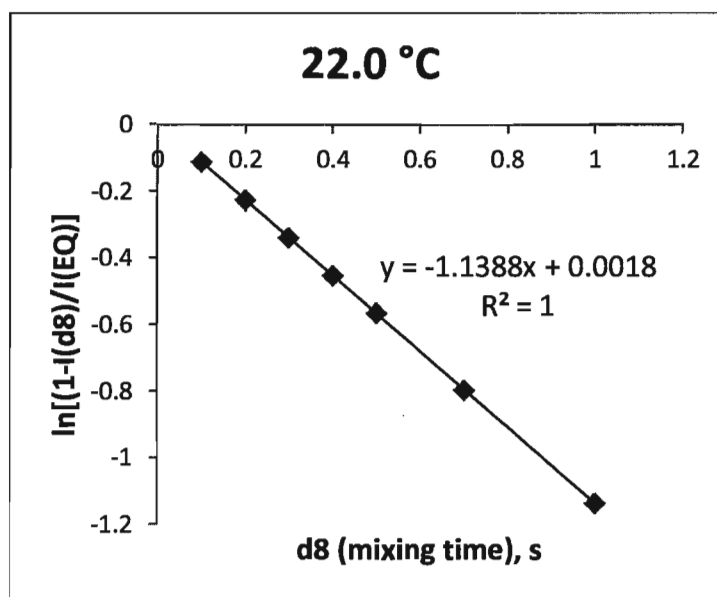


Figure V-45. $\ln[1-I(d8)/I(EQ)]/d8$ plot for Pz-ring dissociation in $(Tp)(ArN)Mo(H)(PMe_3)$ at 22.0 °C.

$$k(22.0\text{ °C}) = 1.138\text{ s}^{-1}$$

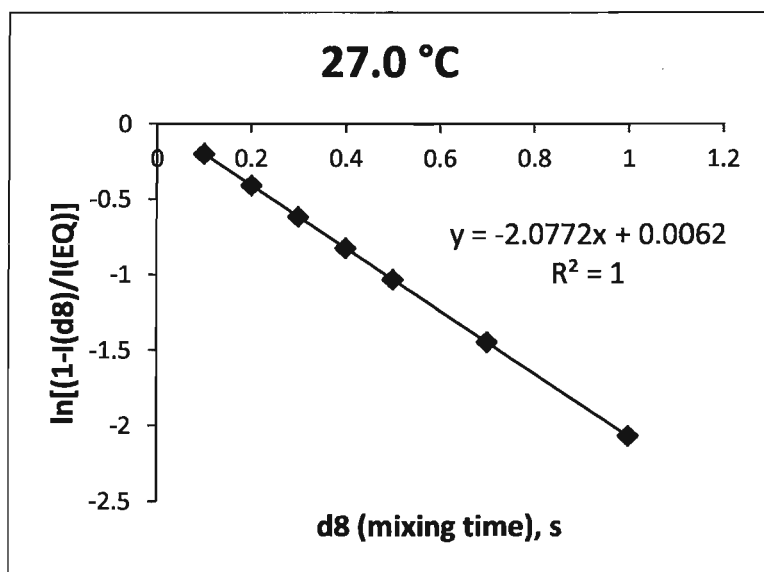


Figure V-46. $\ln[1-I(d8)/I(EQ)]/d8$ plot for Pz-ring dissociation in $(Tp)(ArN)Mo(H)(PMe_3)$ at 27.0 °C.

$$k(27.0\text{ °C}) = 2.077\text{ s}^{-1}$$

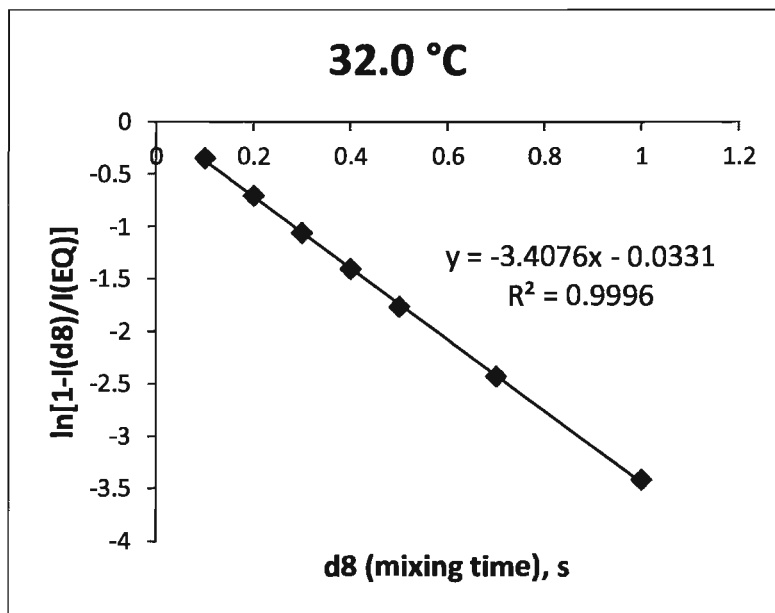


Figure V-47. $\ln[1-I(d8)/I(EQ)]/d8$ plot for Pz-ring dissociation in $(Tp)(ArN)Mo(H)(PMe_3)$ at 32.0 °C.

$$k(32.0\text{ °C}) = 3.407\text{ s}^{-1}$$

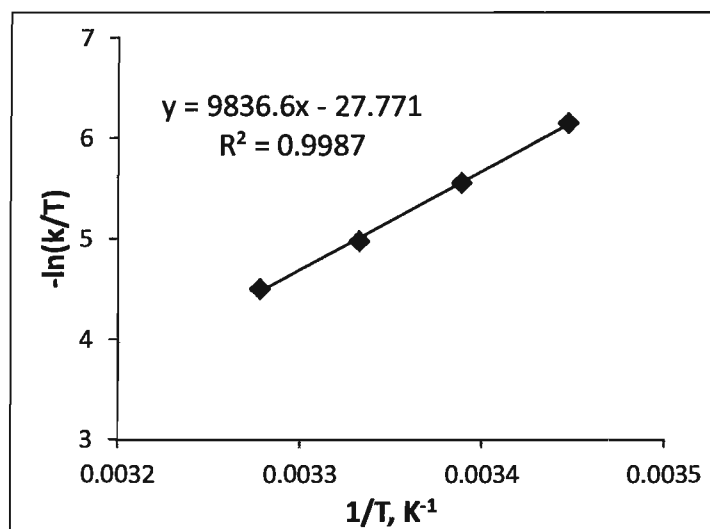


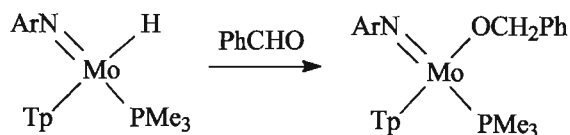
Figure V-48. Eyring plot for pyrazolyl ligand dissociation in (Tp)(ArN)Mo(H)(PMe₃).

Activation parameters were extracted from the Eyring plot (Figure V-48): $\Delta H^\ddagger = (8.18 \pm 0.21) \cdot 10^1$ kJ/mol, $\Delta S^\ddagger = (3.24 \pm 0.70) \cdot 10^1$ J/(K·mol)

(Tp)(ArN)Mo(OCH₂Ph)(PMe₃): dissociation of Pz ligands

A solution of (Tp)(ArN)Mo(OCH₂Ph)(PMe₃) (12.1 mg, 0.018 mmol) in C₆D₆ (0.60 ml) was studied by SELNOGP ge-1D EXSY NMR at 17.0, 22.0, 27.0 and 32.0 °C. Dissociation of the Pz ligands was not observed.

Synthesis of (Tp)(ArN)Mo(OCH₂Ph)(PMe₃)



Benzaldehyde (56.7 mg, 0.535 mmol) was added to a solution of (Tp)(ArN)Mo(H)(PMe₃) (300.0 mg, 0.535 mmol) in Et₂O at RT. The reaction mixture was left for one week until the reaction was complete. All volatiles were evaporated in vacuum. The product, (Tp)(ArN)Mo(OCH₂Ph)(PMe₃), was a green oil, and could not be individually isolated or purified because of its instability. ¹H-NMR (300 MHz; C₆D₆; 298K; δ, ppm): 0.91 (m, 6H, 2CH₃, iPr), 1.19 (d, ³J_{H-H} = 6.8 Hz, 6H, 2CH₃, iPr), 1.21 (d,

$^2J_{P-H} = 7.1$ Hz, 9H, PMe_3), 3.86 (m, 2H, 2CH, iPr), 4.94 (dd, $^2J_{H-H} = 244.5$ Hz, $^3J_{H-P} = 14.0$ Hz, 2H, OCH_2Ph), 5.76 (m, 3H, Pz), 5.96 (m, 3H, Pz), 5.98 (m, 3H, Pz), 6.96-7.02 (m, 2H), 7.10-7.20 (m, 2H), 7.21-7.25 (m, 1H), 7.30-7.38 (m, 2H), 7.39-7.43 (m, 1H), 7.47-7.58 (m, 4H), 7.63-7.68 (m, 2H). ^{31}P -NMR (121.5 MHz; C_6D_6 ; 298 K; δ , ppm): 9.9 (s, 1P, PMe_3). ^{13}C -NMR (75.5 MHz; C_6D_6 ; 298 K; δ , ppm): 16.4 (d, $^2J_{C-P} = 21.9$ Hz, PMe_3), 23.9 (Me, iPr), 24.2 (Me, iPr), 28.1 (CH, iPr), 79.2 (d, $^3J_{C-P} = 5.5$ Hz, OCH_2Ph), 105.1 (Pz), 105.6 (Pz), 106.4 (Pz), 124.3, 124.4, 125.9, 127.2, 128.3, 133.5, 136.0, 136.3, 142.2, 143.4, 145.9, 146.5, 150.0, 155.2.

Reaction between $(\text{Tp})(\text{ArN})\text{Mo}(\text{H})(\text{PMe}_3)$ and benzaldehyde

Benzaldehyde (1.9 mg, 0.0178 mmol) was added to a solution of $(\text{Tp})(\text{ArN})\text{Mo}(\text{H})(\text{PMe}_3)$ (10.0 mg, 0.0178 mmol) in C_6D_6 (0.60 ml). The reaction was monitored by ^1H NMR (Figure V-49). The experiment has been repeated in the presence of 5 eq. PMe_3 (6.8 mg, 0.089 mmol) (Figure V-50), 10 eq. PMe_3 (13.6 mg, 0.178 mmol) (Figure V-51), and 20 eq. PMe_3 (27.2 mg, 0.356 mmol) (Figure V-52).

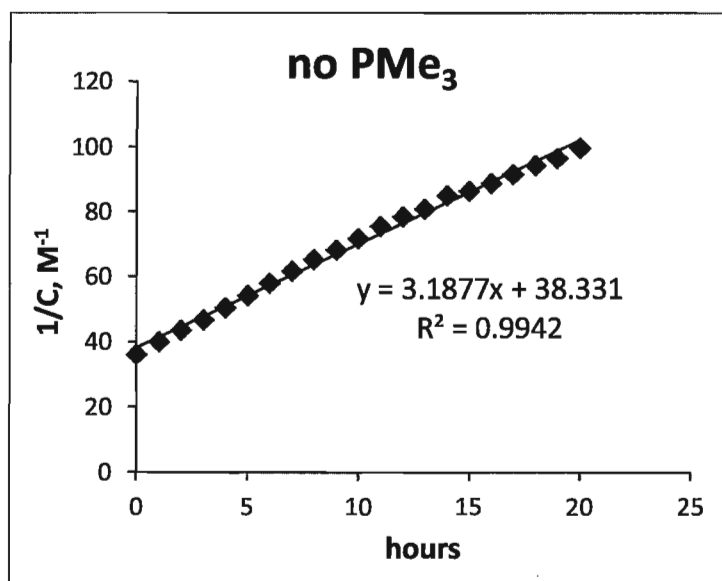


Figure V-49. $(1/C)/\text{time}$ plot for the reaction of $(\text{Tp})(\text{ArN})\text{Mo}(\text{H})(\text{PMe}_3)$ with PhCHO (1eq.).

$$k(\text{no } \text{PMe}_3) = (3.19 \pm 0.04) \text{ M}^{-1} \cdot \text{h}^{-1} = (8.85 \pm 0.10) \cdot 10^{-4} \text{ M}^{-1} \cdot \text{s}^{-1}$$

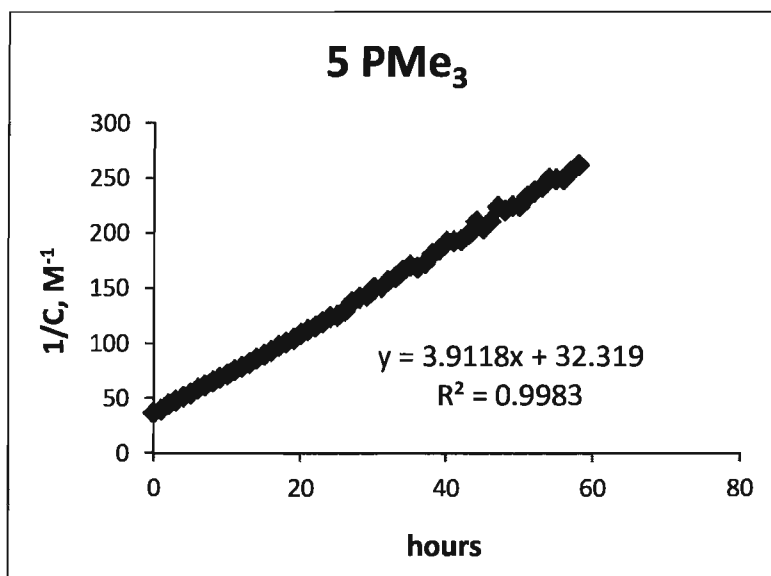


Figure V-50. $(1/C)/\text{time}$ plot for the reaction of $(\text{Tp})(\text{ArN})\text{Mo}(\text{H})(\text{PMe}_3)$ with PhCHO (1eq.) in the presence of 5 eq. of PMe_3 .

$$k(5 \text{ PMe}_3) = (3.91 \pm 0.02) \text{ M}^{-1} \cdot \text{h}^{-1} = (1.09 \pm 0.01) \cdot 10^{-3} \text{ M}^{-1} \cdot \text{s}^{-1}$$

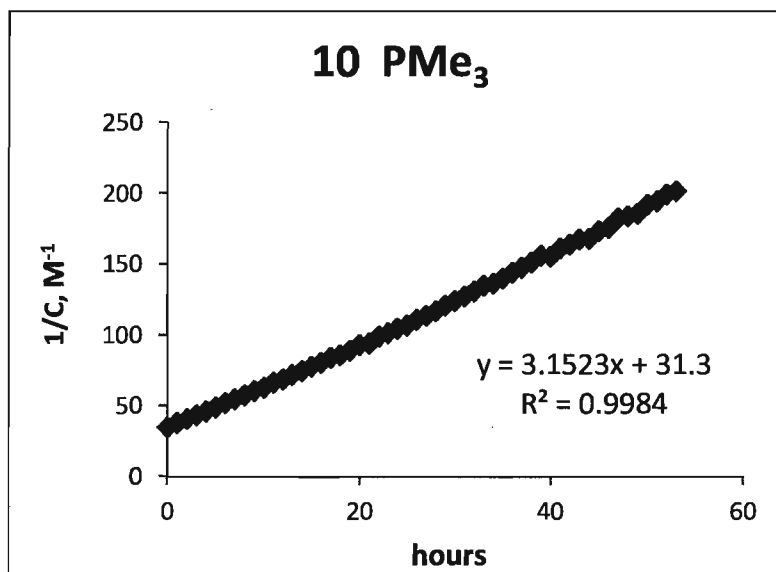


Figure V-51. $(1/C)/\text{time}$ plot for the reaction of $(\text{Tp})(\text{ArN})\text{Mo}(\text{H})(\text{PMe}_3)$ with PhCHO (1eq.) in the presence of 10 eq. of PMe_3 .

$$k(10 \text{ PMe}_3) = (3.15 \pm 0.02) \text{ M}^{-1} \cdot \text{h}^{-1} = (8.75 \pm 0.10) \cdot 10^{-4} \text{ M}^{-1} \cdot \text{s}^{-1}$$

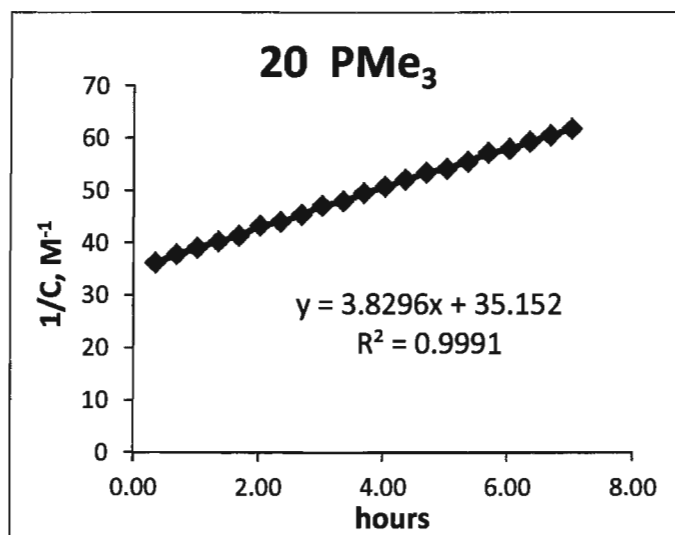


Figure V-52. $(1/C)/\text{time}$ plot for the reaction of $(\text{Tp})(\text{ArN})\text{Mo}(\text{H})(\text{PMe}_3)$ with PhCHO (1eq.) in the presence of 20 eq. of PMe_3 .

$$k(20 \text{ PMe}_3) = (3.83 \pm 0.03) \text{ M}^{-1} \cdot \text{h}^{-1} = (1.06 \pm 0.01) \cdot 10^{-3} \text{ M}^{-1} \cdot \text{s}^{-1}$$

The rate constants for reaction between $(\text{Tp})(\text{ArN})\text{Mo}(\text{H})(\text{PMe}_3)$ and PhCHO (1:1) have been determined at 36.0°C (Figure V-53), 46.0°C (Figure V-54) and 55.6°C (Figure V-55).

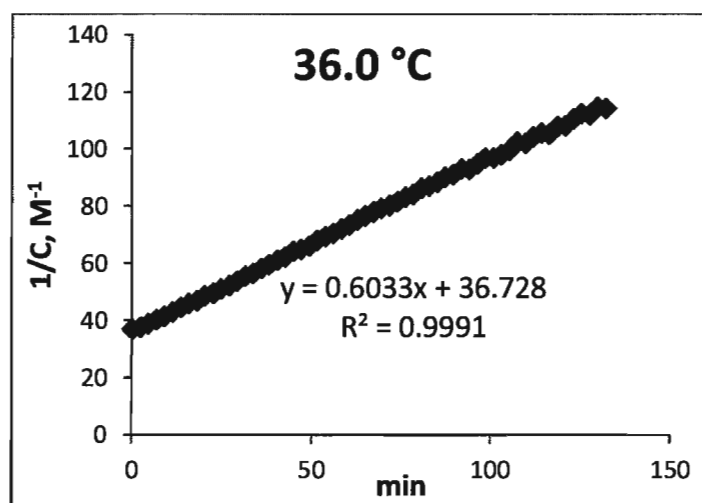


Figure V-53. $(1/C)/\text{time}$ plot for the reaction of $(\text{Tp})(\text{ArN})\text{Mo}(\text{H})(\text{PMe}_3)$ with PhCHO (1eq.) in the presence of 10 eq. of PMe_3 at 36.0°C .

$$k(36.0^\circ\text{C}) = (6.03 \pm 0.02) \cdot 10^{-1} \text{ M}^{-1} \cdot \text{min}^{-1} = (1.005 \pm 0.003) \cdot 10^{-2} \text{ M}^{-1} \cdot \text{s}^{-1}$$

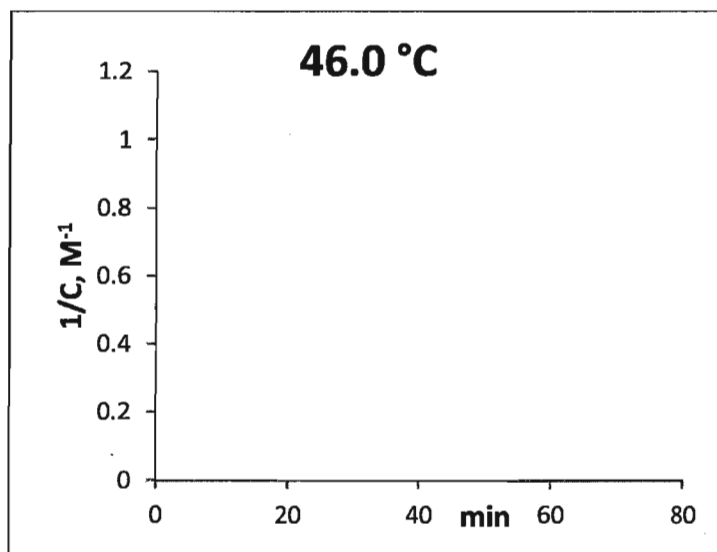


Figure V-54. (1/C)/time plot for the reaction of (Tp)(ArN)Mo(H)(PMe₃) with PhCHO (1eq.) in the presence of 10 eq. of PMe₃ at 46.0 °C.

$$k(46.0\text{ }^{\circ}\text{C}) = (8.99 \pm 0.17) \cdot 10^{-1} \text{ M}^{-1} \cdot \text{min}^{-1} = (1.50 \pm 0.03) \cdot 10^{-2} \text{ M}^{-1} \cdot \text{s}^{-1}$$

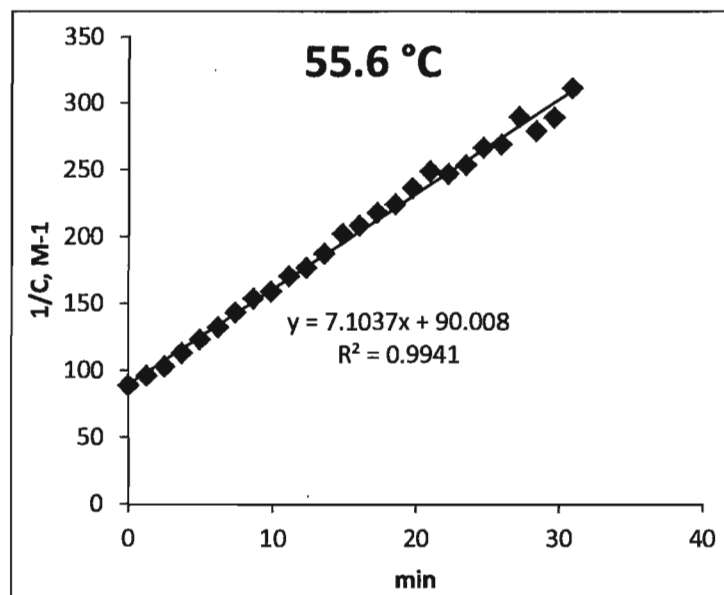


Figure V-55. (1/C)/time plot for the reaction of (Tp)(ArN)Mo(H)(PMe₃) with PhCHO (1eq.) in the presence of 10 eq. of PMe₃ at 55.6 °C.

$$k(55.6\text{ }^{\circ}\text{C}) = (7.103 \pm 0.112) \text{ M}^{-1} \cdot \text{min}^{-1} = (1.18 \pm 0.02) \cdot 10^{-1} \text{ M}^{-1} \cdot \text{s}^{-1}$$

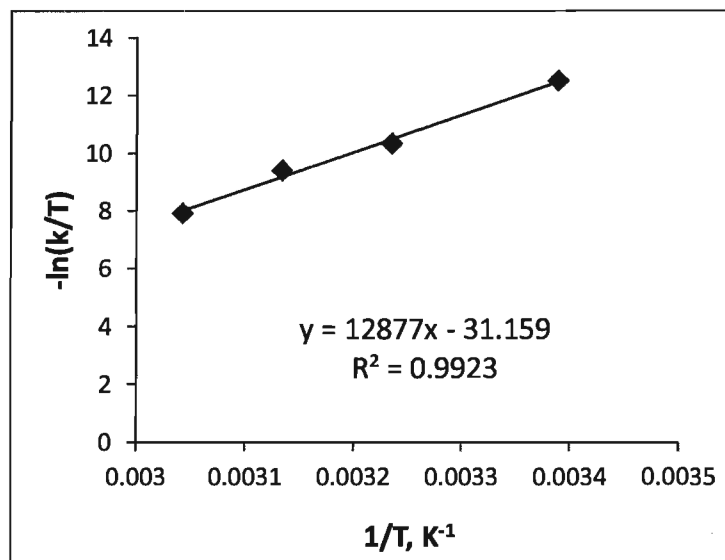


Figure V-56. Eyring plot for the reaction of (Tp)(ArN)Mo(H)(PMe₃) with PhCHO (1eq.) in the presence of 10 eq. of PMe₃.

Activation parameters were extracted from the Eyring plot (Figure V-56): $\Delta H^\ddagger = (1.03 \pm 0.07) \cdot 10^2$ kJ/mol, $\Delta S^\ddagger = (4.53 \pm 5.35) \cdot 10^1$ J/(K·mol)

Synthesis of (Tp)(ArN)Mo(OCH₂Ph)(η^2 -PhCHO)

Solution of (Tp)(ArN)Mo(H)(PMe₃) (300.0 mg, 0.534 mmol) and benzaldehyde (113.42 mg, 1.069 mmol) in Et₂O was stirred for one week at RT. The pale-yellow precipitate, (Tp)(ArN)Mo(OCH₂Ph)(η^2 -PhCHO), was filtered and washed with Et₂O. Yield: 187 mg, 50%. ¹H-NMR (300 MHz; C₆D₆; 298K; δ , ppm): 0.13-1.84 (bm, 12H, CH₃, iPr), 5.38 (s, CHO, PhCHO), 5.56 (m, 1H, Pz^a), 5.84 (m, 1H, Pz^b), 5.93 (m, 1H, Pz^c), 6.52 (d, ²J_{H-H} = 15.4 Hz, CH^aH^bPh), 6.63 (d, ²J_{H-H} = 15.4Hz, CH^aH^b), 6.70-6.97 (bm, 1H), 6.80-6.85 (m, 2H), 7.00-7.05 (3H), 7.12 (m, 1H), 7.16 (pt, 3H), 7.30 (1H), 7.37-7.41 (m, 3H), 7.43-7.64 (2H), 7.62 (1H), 8.14 (m, 2H). ¹³C-NMR (75.5 MHz; C₆D₆; 298 K; δ , ppm): 24.3 (iPr), 27.9 (iPr), 69.8 (-OCH₂Ph), 105.2 (Mo-PhCHO), 105.5 (Pz^a), 105.6 (Pz^c), 106.3 (Pz^b), 123.7 (bs), 126.1, 126.8, 127.3, 127.9, 127.9, 128.3, 134.5, 134.7, 136.0, 140.1, 142.8, 143.8, 145.1, 147.3, 150.9. ¹¹B-NMR (96.3 MHz; C₆D₆; 298 K; δ , ppm): -4.3 (bs). IR (nujol, cm⁻¹): 1597 (C-H, -CH=O), 2520 (B-H).

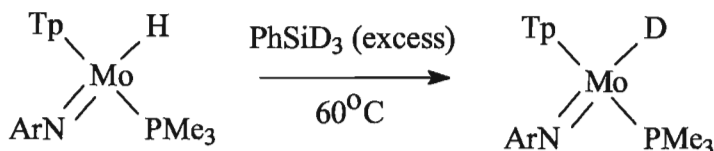
Reaction of (Tp)(ArN)Mo(H)(PMe₃) with PhSiH₃

Phenylsilane (5.4 mg, 0.050 mmol) was added to a solution of (Tp)(ArN)Mo(H)(PMe₃) (28.0 mg, 0.050 mmol) in C₆D₆ (0.60 ml). No reaction was observed.

Reaction of (Tp)(ArN)Mo(H)(PMe₃) with PhSiH₃ and BPh₃

Phenylsilane (19.3 mg, 0.178 mmol) and triphenylborane (10.8 mg, 0.045 mmol) were added to a solution of (Tp)(ArN)Mo(H)(PMe₃) (25.0 mg, 0.045 mmol) in C₆D₆ (0.60 ml). The reaction mixture was left for one day at RT, and then heated for one day at 50 °C. No reaction was observed.

Reaction of (Tp)(ArN)Mo(H)(PMe₃) with PhSiD₃



PhSiD₃ (9.9 mg, 0.089 mol) was added to a solution of (Tp)(ArN)Mo(H)(PMe₃) (10.0 mg, 0.018 mmol) in C₆D₆ (0.60 ml). The reaction was monitored at 60.0 °C by ¹H NMR (Figure V-57).

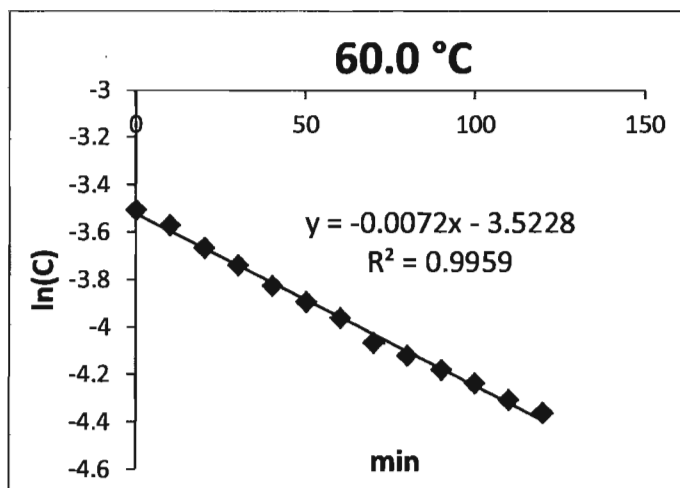


Figure V-57. ln(C)/time plot for the reaction of (Tp)(ArN)Mo(H)(PMe₃) with PhSiD₃ (5 eq.) at 60.0 °C.

$$k_{\text{H/D}}(60.0\text{ }^\circ\text{C}) = (7.22 \pm 0.14) \cdot 10^{-3} \text{ min}^{-1} = (1.20 \pm 0.23) \cdot 10^{-4} \text{ s}^{-1}$$

Reaction of (Tp)(ArN)Mo(H)(PMe₃) with PhSiD₃

Et₃SiD (14.0 μ l, 0.100 mol) was added to a solution of (Tp)(ArN)Mo(H)(PMe₃) (11.3 mg, 0.020 mmol) in C₆D₆ (0.60 ml). The reaction was heated at 50.0 $^{\circ}$ C during two days. H/D exchange was not observed.

Reaction of (Tp)(ArN)Mo(OCH₂Ph)(PMe₃) with PhSiH₃

Phenylsilane (13.5 mg, 0.125 mmol) was added to a solution of (Tp)(ArN)Mo(OCH₂Ph)(PMe₃) (8.3 mg, 0.013 mmol) in C₆D₆ (0.60 ml). The reaction was monitored by ¹H NMR at 17.0 $^{\circ}$ C (Figure V-58), 22.0 $^{\circ}$ C (Figure V-59), 27.0 $^{\circ}$ C (Figure V-60) and 32.0 $^{\circ}$ C (Figure V-61).

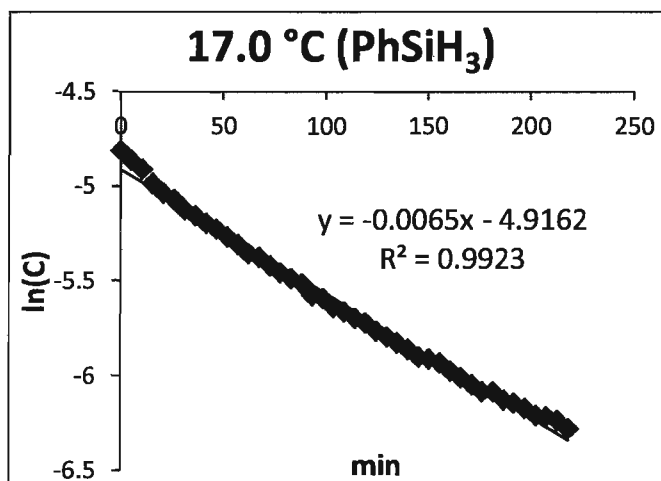


Figure V-58. ln(C)/time plot for the reaction between (Tp)(ArN)Mo(OCH₂Ph)(PMe₃) and PhSiH₃ (10 eq.) at 17.0 $^{\circ}$ C.

$$k(17.0\text{ }^{\circ}\text{C}) = (6.78 \pm 0.09) \cdot 10^{-3} \text{ min}^{-1} = (1.13 \pm 0.02) \cdot 10^{-4} \text{ s}^{-1}$$

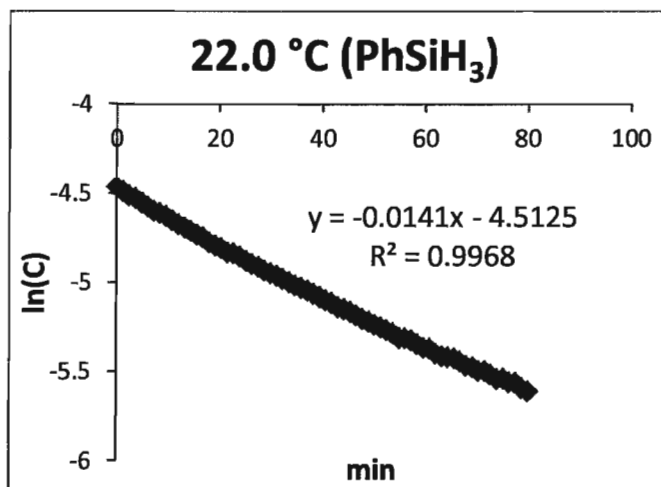


Figure V-59. ln(C)/time plot for the reaction between (Tp)(ArN)Mo(OCH₂Ph)(PMe₃) and PhSiH₃ (10 eq.) at 22.0 °C.

$$k(22.0\text{ °C}) = (1.41 \pm 0.01) \cdot 10^{-2} \text{ min}^{-1} = (2.35 \pm 0.02) \cdot 10^{-4} \text{ s}^{-1}$$

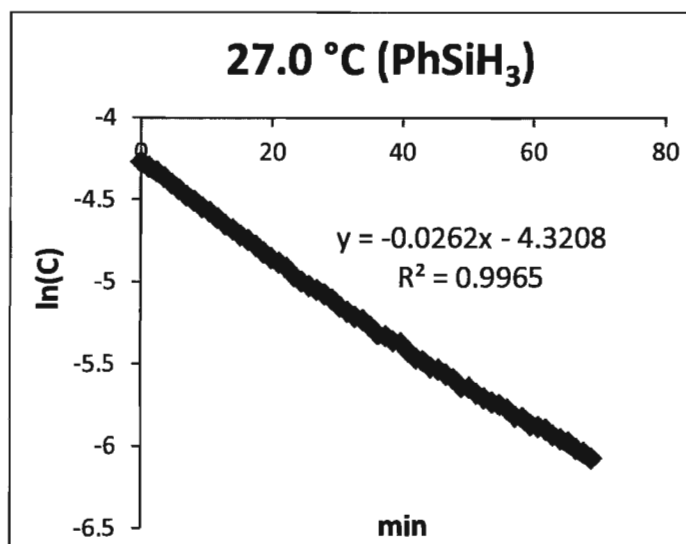


Figure V-60. ln(C)/time plot for the reaction between (Tp)(ArN)Mo(OCH₂Ph)(PMe₃) and PhSiH₃ (10 eq.) at 27.0 °C.

$$k(27.0\text{ °C}) = (2.62 \pm 0.02) \cdot 10^{-2} \text{ min}^{-1} = (4.37 \pm 0.04) \cdot 10^{-4} \text{ s}^{-1}$$

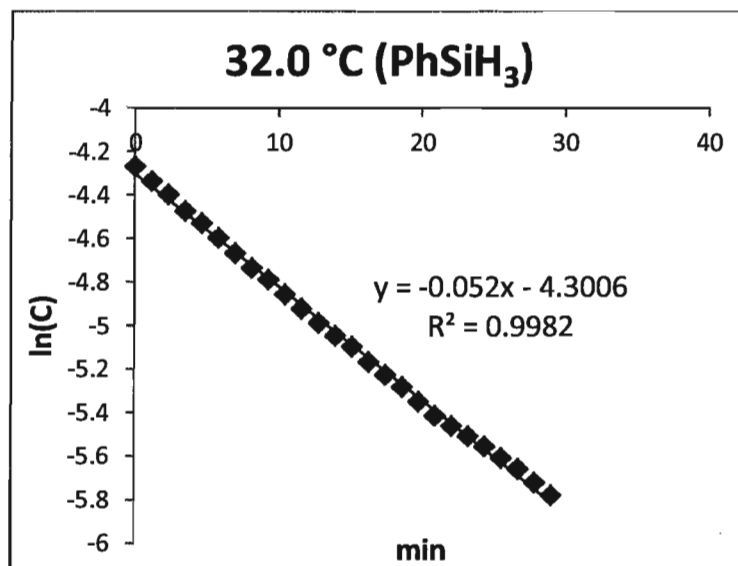


Figure V-61. ln(C)/time plot for the reaction between (Tp)(ArN)Mo(OCH₂Ph)(PMe₃) and PhSiH₃ (10 eq.) at 32.0 °C.

$$k(32.0\text{ }^{\circ}\text{C}) = (5.20 \pm 0.05) \cdot 10^{-2} \text{ min}^{-1} = (8.67 \pm 0.01) \cdot 10^{-4} \text{ s}^{-1}$$

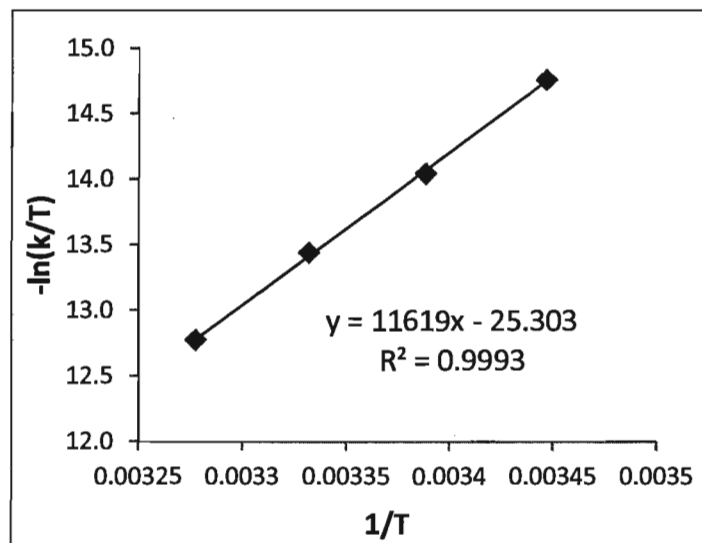


Figure V-62. Eyring plot for the reaction of (Tp)(ArN)Mo(OCH₂Ph)(PMe₃) with PhSiH₃ (10 eq.).

Activation parameters were extracted from the Eyring plot (Figure V-62): $\Delta H^{\ddagger} = (96.6 \pm 1.8) \text{ kJ/mol}$, $\Delta S^{\ddagger} = (12.5 \pm 6.2) \text{ J/(K}\cdot\text{mol)}$

Reaction of (Tp)(ArN)Mo(OCH₂Ph)(PMe₃) with PhSiD₃

PhSiD₃ (13.9 mg, 0.125 mmol) was added to a solution of (Tp)(ArN)Mo(OCH₂Ph)(PMe₃) (8.3 mg, 0.013 mmol) in C₆D₆ (0.60 ml). The reaction was monitored by ¹H NMR at 17.0 °C (Figure V-63), 22.0 °C (Figure V-64), 27.0 °C (Figure V-65) and 32.0 °C (Figure V-66).

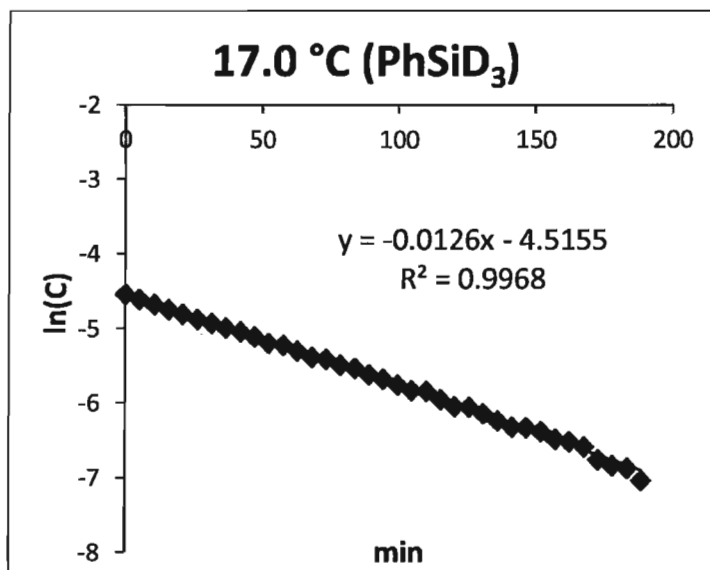


Figure V-63. ln(C)/time plot for reaction between (Tp)(ArN)Mo(OCH₂Ph)(PMe₃) and PhSiD₃ (10 eq.) at 17.0 °C.

$$k(17.0\text{ }^{\circ}\text{C}) = (1.26 \pm 0.01) \cdot 10^{-2} \text{ min}^{-1} = (2.10 \pm 0.02) \cdot 10^{-4} \text{ s}^{-1}$$

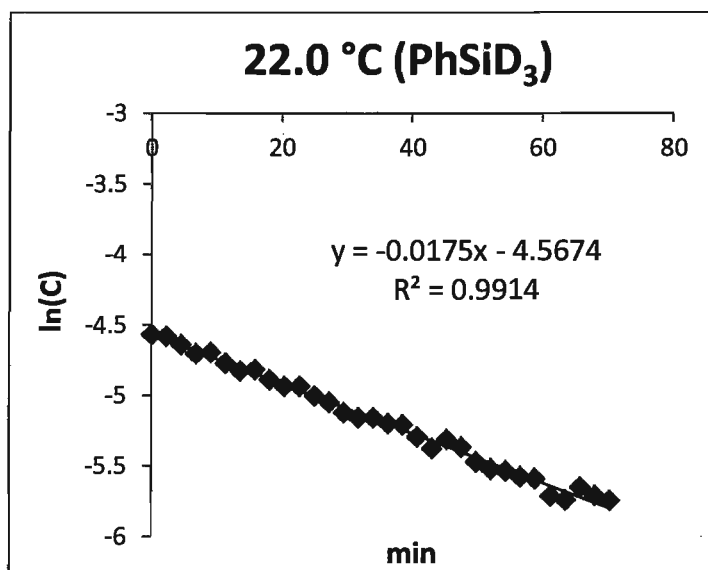


Figure V-64. ln(C)/time plot for reaction between (Tp)(ArN)Mo(OCH₂Ph)(PMe₃) and PhSiD₃ (10 eq.) at 22.0 °C.

$$k(22.0\text{ °C}) = (1.75 \pm 0.01) \cdot 10^{-2} \text{ min}^{-1} = (2.92 \pm 0.02) \cdot 10^{-4} \text{ s}^{-1}$$

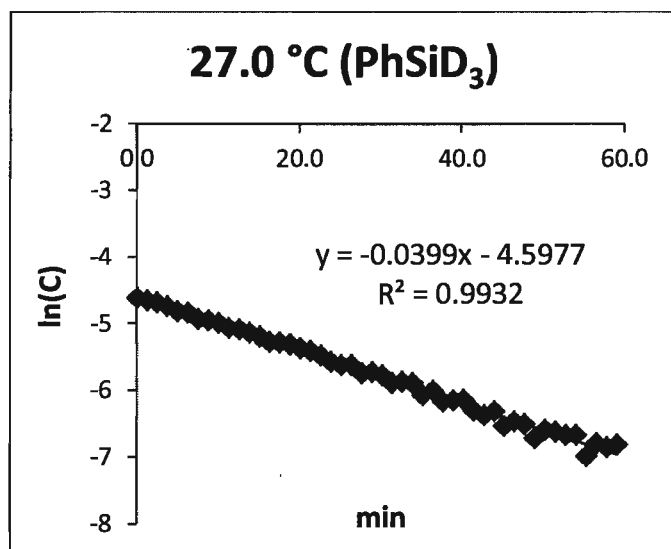


Figure V-65. ln(C)/time plot for reaction between (Tp)(ArN)Mo(OCH₂Ph)(PMe₃) and PhSiD₃ (10 eq.) at 27.0 °C.

$$k(27.0\text{ °C}) = (3.99 \pm 0.02) \cdot 10^{-2} \text{ min}^{-1} = (6.60 \pm 0.04) \cdot 10^{-4} \text{ s}^{-1}$$

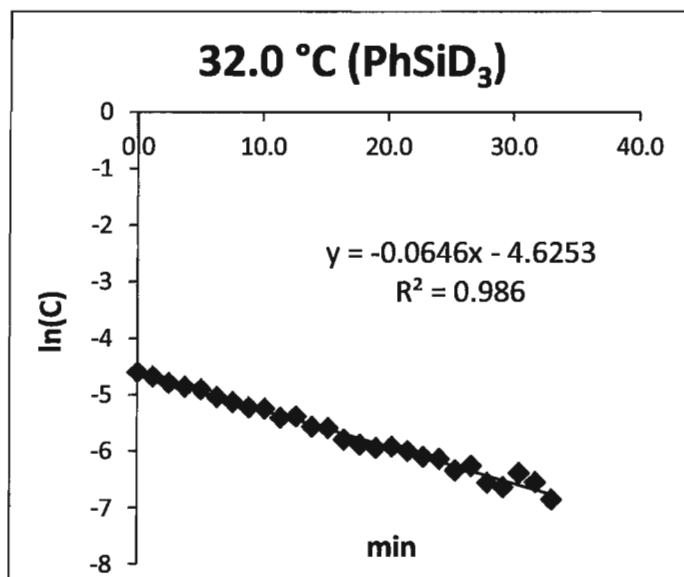


Figure V-66. ln(C)/time plot for reaction between (Tp)(ArN)Mo(OCH₂Ph)(PMe₃) and PhSiD₃ (10 eq.) at 32.0 °C.

$$k(32.0\text{ °C}) = (6.46 \pm 0.05) \cdot 10^{-2} \text{ min}^{-1} = (1.08 \pm 0.01) \cdot 10^{-3} \text{ s}^{-1}$$

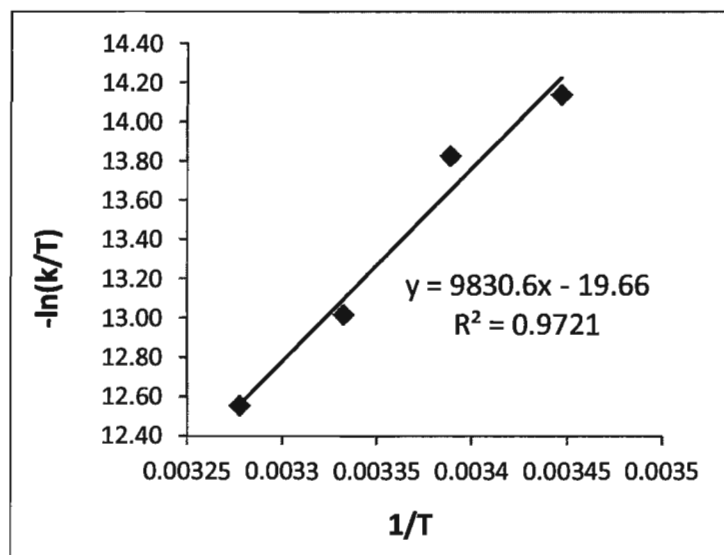


Figure V-67. Eyring plot for the reaction of (Tp)(ArN)Mo(OCH₂Ph)(PMe₃) with PhSiD₃ (10 eq.).

Activation parameters for reaction between (Tp)(ArN)Mo(OCH₂Ph)(PMe₃) and PhSiD₃ (10 eq.) were extracted from the Eyring plot (Figure V-67): $\Delta H^\ddagger = (8.17 \pm 0.98) \cdot 10^1$ kJ/mol, $\Delta S^\ddagger = -(3.44 \pm 3.29) \cdot 10^1$ J/(K·mol).

Reaction of (Tp)(ArN)Mo(H)(PMe₃) with PhSiD₃ and cyclohexane

Experiment 1. Cyclohexanone (1.9 mg, 0.018 mmol) and PhSiD₃ (2.0 mg, 0.018 mmol) were added to a solution of (Tp)(ArN)Mo(H)(PMe₃) (10.0 mg, 0.018 mmol) in C₆D₆ (0.60 ml). The reaction was monitored by ¹H NMR (Figure V-68, green). Substitution of the hydride by deuterium was not observed.

Experiment 2. Cyclohexanone (3.4 mg, 0.036 mmol) and PhSiD₃ (2.0 mg, 0.018 mmol) were added to a solution of (Tp)(ArN)Mo(H)(PMe₃) (10.0 mg, 0.018 mmol) in C₆D₆ (0.60 ml). The reaction was monitored by ¹H NMR (Figure V-68, red).

Experiment 3. Cyclohexanone (1.9 mg, 0.018 mmol) and PhSiD₃ (4.0 mg, 0.018 mmol) were added to a solution of (Tp)(ArN)Mo(H)(PMe₃) (10.0 mg, 0.018 mmol) in C₆D₆ (0.60 ml). The reaction was monitored by ¹H NMR (Figure V-68, blue).

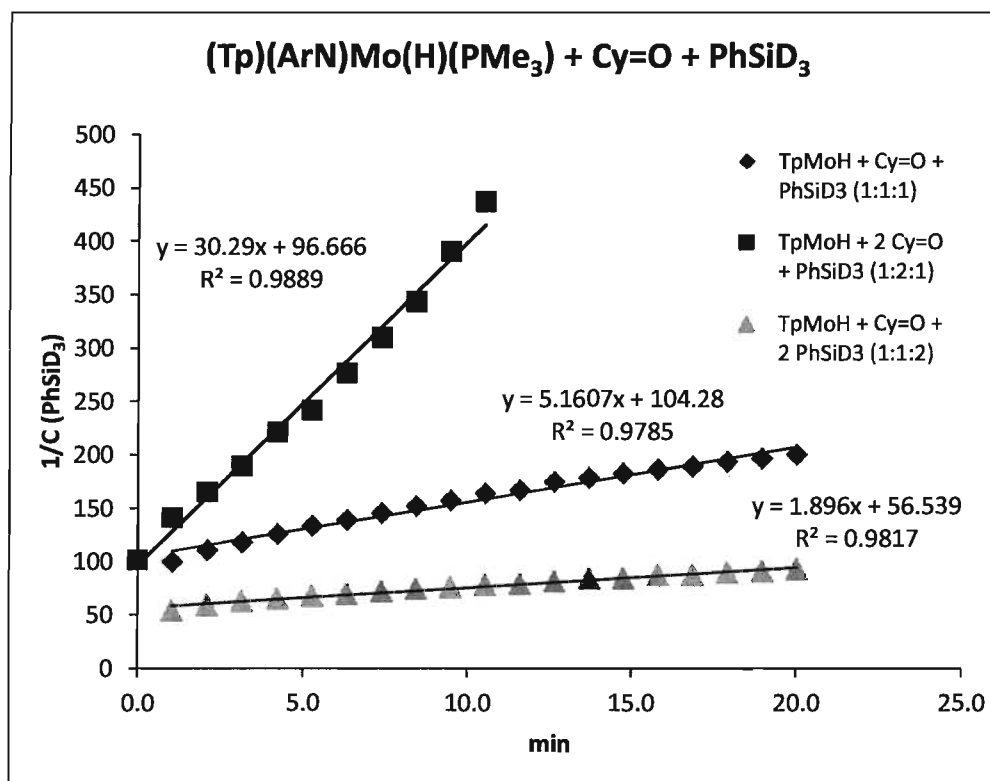


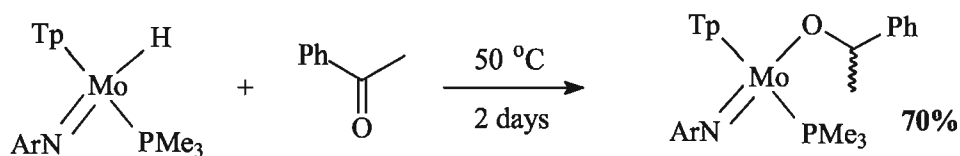
Figure V-68. (1/C)/time plot for the reactions

(Tp)(ArN)Mo(H)(PMe₃)+cyclohexanol+PhSiD₃ (1:1:1) (green),
 (Tp)(ArN)Mo(H)(PMe₃)+2cyclohexanol+PhSiD₃ (1:2:1) (red), and
 (Tp)(ArN)Mo(H)(PMe₃)+cyclohexanol+2PhSiD₃ (1:1:2) (blue).

Reaction of (Tp)(ArN)Mo(H)(PMe₃) with PhSiD₃ and PhCHO

Benzaldehyde (1.9 mg, 0.018 mmol) and PhSiD₃ (2.0 mg, 0.018 mmol) were added to a solution of (Tp)(ArN)Mo(H)(PMe₃) (10.0 mg, 0.018 mmol) in C₆D₆ (0.60 ml). The reaction provided formation of PhCHDOSiD₂Ph and (PhCHDO)₂SiDPh. The catalyst (Tp)(ArN)Mo(H)(PMe₃) did not form derivatives and remained unchanged during the reaction.

Reaction of (Tp)(ArN)Mo(H)(PMe₃) with acetophenone

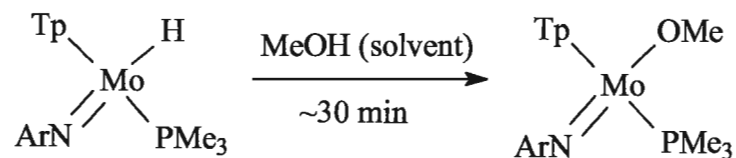


Acetophenone (10.2 mg, 0.083 mmol) was added to a solution of (Tp)(ArN)Mo(H)(PMe₃) (10.0 mg, 0.018 mmol) in C₆D₆ (0.60 ml). The reaction mixture was heated at 50 °C for two days. The reaction afforded formation of two diastereomers of (Tp)(ArN)Mo(OCH(Me)Ph)(PMe₃) with 1.38 (A) : 1 (B) ratio and 70% total yield. ¹H-NMR (300 MHz; C₆D₆; 298K; δ, ppm): 0.93-1.02 (m, 12H, 4CH₃, iPr, A), 1.18 (d, *J* = 7.35, 9H, PMe₃, A), 1.20 (d, *J* = 6.2 Hz, 6H, 2CH₃, iPr, B), 1.23 (d, *J* = 7.35, 9H, PMe₃, B), 1.49 (d, *J* = 6.2 Hz, 6H, 2CH₃, iPr, B), 3.67 (sept, *J* = 6.85 Hz, 2H, iPr, B), 3.78 (bm, 2H, iPr, A), 4.60 (q, *J* = 6.1 Hz, 1H, -OCHMePh, A), 5.34 (q, *J* = 6.2 Hz, 1H, -OCHMePh, B), 5.58 (m, 1H, Pz, A), 5.81 (m, 1H, Pz, B), 5.92 (m, 1H, Pz, A), 5.95 (m, 1H, Pz, B), 6.03 (m, 1H, Pz, A), 6.04 (m, 1H, Pz, B), 6.92 (m, 1H, Pz), 6.95 (m, 1H, Pz), 6.99-7.40 (mm, 20H, Pz+Ar+Ph, A+B), 7.45 (m, 1H, Pz, A), 7.47 (m, 1H, Pz, B), 7.59 (m, 1H, Pz), 7.61 (m, 1H, Pz), 7.64 (m, 1H, Pz), 7.66 (m, 1H, Pz). ³¹P-NMR (121.5 MHz; C₆D₆; 298 K; δ, ppm): 9.2 (s, PMe₃, B), 9.3 (s, PMe₃, A).

Reaction of (Tp)(ArN)Mo(H)(PMe₃) with acetone

Acetone (1.0 mg, 0.018 mmol) was added to a solution of (Tp)(ArN)Mo(H)(PMe₃) (10.0 mg, 0.018 mmol) in C₆D₆ (0.60 ml). No reaction was observed during one day at RT. An additional amount of acetone (5.2 mg, 0.065 mmol) was added, and the reaction mixture was heated at 50 °C during two days. The acetone condensation and formation of unknown products were observed in ¹H NMR:

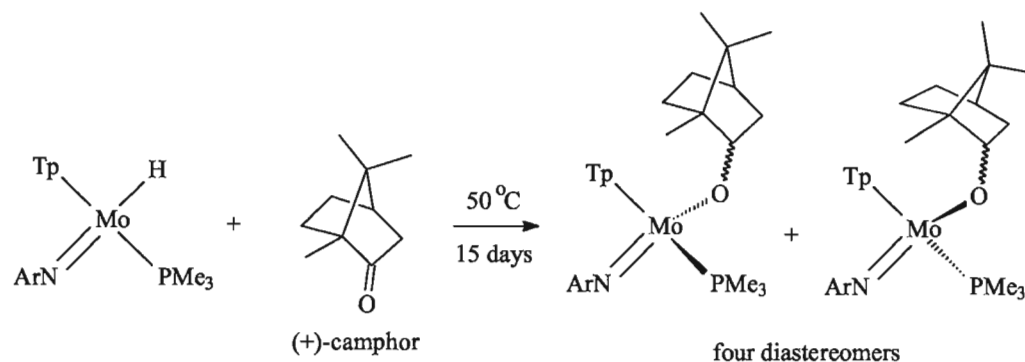
Formation of (Tp)(ArN)Mo(OCH₃)(PMe₃)



(Tp)(ArN)Mo(H)(PMe₃) (10.0 mg, 0.018 mmol) was dissolved in MeOH (0.60 ml). The color of the solution gradually changed from dark brown to green within 30 min. The solvent was evaporated, and the residue was re-dissolved in C₆D₆ (0.60 ml). Reaction provided formation of (Tp)(ArN)Mo(OCH₃)(PMe₃) as the only product. ¹H-NMR (300 MHz; CDCl₃; 298K; δ, ppm): 0.83-0.99 (bm, 6H, 2CH₃, iPr), 1.20 (d, *J* = 7.28 Hz, 9H,

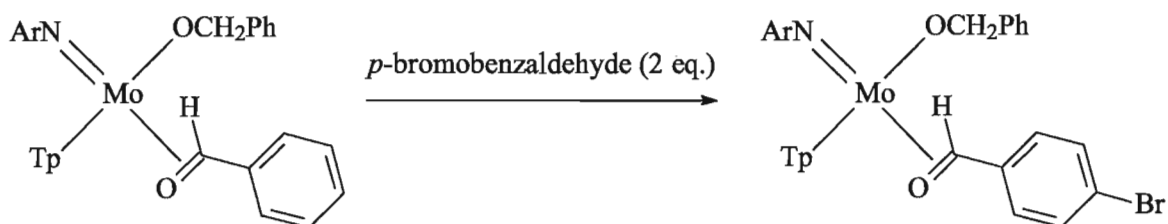
PMe₃), 1.25-1.31 (bm, 6H, 2CH₃, iPr), 3.83 (bm, 2H, iPr), 4.09 (s, 3H, OCH₃), 5.89 (m, 1H, Pz), 5.94 (m, 1H, Pz), 5.97 (m, 1H, Pz), 6.99-7.04 (m, 2H, Ar), 7.14-7.20 (m, 1H, Ar), 7.26 (m, 1H, Pz), 7.41 (m, 1H, Pz), 7.50 (m, 1H, Pz), 7.53 (m, 1H, Pz), 7.61 (m, 1H, Pz), 7.85 (m, 1H, Pz). ³¹P-NMR (121.5 MHz; C₆D₆; 298 K; δ, ppm): 9.3 (1P, PMe₃)

Reaction of (Tp)(ArN)Mo(H)(PMe₃) with (+)-camphor



(+)-Camphor (5.8 mg, 0.038 mmol) was added to a solution of (Tp)(ArN)Mo(H)(PMe₃) (42.8 mg, 0.076 mmol) in C₆D₆ (0.60 ml). The reaction mixture was heated at 50 °C for 15 days. The reaction afforded a mixture of four diastereomers in 100% NMR yield. ³¹P-NMR (121.5 MHz; C₆D₆; 298 K; δ, ppm): 7.8 (s, PMe₃, isomer-I, 27%), 8.3 (s, PMe₃, isomer-II, 16%), 8.5 (s, PMe₃, isomer-III, 5%), 9.0 (s, PMe₃, isomer-IV, 52%).

Reaction of (Tp)(ArN)Mo(OCH₂Ph)(PhCHO) with *p*-bromobenzaldehyde



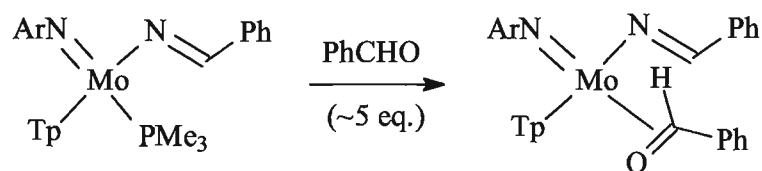
p-Bromobenzaldehyde (2.6 mg, 0.0143 mmol) was added to a solution of (Tp)(ArN)Mo(OCH₂Ph)(PhCHO) (5.0 mg, 0.0072 mmol) in C₆D₆ (0.60 ml). The reaction mixture was heated at 60 °C for one hour. The coordinated benzaldehyde was replaced by *p*-bromobenzaldehyde. No further reaction was observed. ¹H-NMR (300 MHz; CDCl₃; 298K; δ, ppm): 0.14-1.88 (bm, 12H, 4CH₃, i-Pr, Ar), 5.19 (s, 1H, Mo-ArCHO), 5.58 (m,

1H, Pz), 5.84 (m, 1H, Pz), 5.93 (m, 1H, Pz), 6.45 (d, $J = 15.9$ Hz, $-\text{OCH}^a\text{H}^b\text{Ph}$), 6.56 (d, $J = 15.9$ Hz, $-\text{OCH}^a\text{H}^b\text{Ph}$), 6.76-6.87 (m, 3H, Ar), 6.93-7.00 (m, 3H, Ph), 7.02 (m, 1H), 7.05 (m, 1H), 7.12 (m, 1H, Pz), 7.33-7.38 (m, 2H, aromatic C-H, $p\text{-BrC}_6\text{H}_4\text{CHO}$), 7.49-7.54 (m, 2H, aromatic C-H, $p\text{-BrC}_6\text{H}_4\text{CHO}$), 7.60 (m, 1H, Pz), 7.30 (m, 1H, Pz), 7.98 (m, 1H, Pz), 8.10 (m, 1H, Pz).

Synthesis of (Tp)(ArN)Mo(-N=CHPh)(PMe₃)

The solution of (Tp)(ArN)Mo(H)(PMe₃) (304 mg, 0.542 mmol) and benzonitrile (55.8 mg, 0.542 mmol) in C₆D₆ (0.60 ml) was heated at 50 °C for 4 days. Then, the solvent was evaporated in vacuum. The reaction provided formation of (Tp)(ArN)Mo(-N=CHPh)(PMe₃). Yield: 349 mg (97%). ¹H-NMR (300 MHz; C₆D₆; 298K; δ , ppm): 0.96 (d, $^3J_{\text{H-H}} = 6.8$ Hz, 6H, 2CH₃, iPr), 1.07 (d, $^2J_{\text{P-H}} = 7.7$ Hz, 9H, PMe₃), 1.31 (bd, $^3J_{\text{H-H}} = 6.7$ Hz, 6H, 2CH₃, iPr), 3.92 (bsept, $^3J_{\text{H-H}} = 6.8$ Hz, 2H, iPr), 5.78 (m, 1H, Pz), 5.87 (m, 1H, Pz), 6.01 (m, 1H, Pz), 6.90 (bm, 1H, Ar), 7.07 (m, 3H, Ar), 7.19-7.53 (bm, 5H), 7.30 (m, 1H, Pz), 7.46 (m, 1H, Pz), 7.49 (m, 1H, Pz), 7.54 (m, 1H, Pz), 7.57 (m, 1H, Pz), 7.68 (m, 1H, Pz), 8.07 (d, $^4J_{\text{H-P}} = 2.2$ Hz, CH=N). ³¹P-NMR (121.5 MHz; C₆D₆; 298 K; δ , ppm): -0.1 (1P, PMe₃). ¹³C-NMR (75.5 MHz; C₆D₆; 298 K; δ , ppm): 16.4 (d, $^3J_{\text{C-P}} = 23.7$ Hz, PMe₃), 24.7, 25.6, 27.5, 104.6, 105.7, 106.7, 123.7, 125.0, 125.4, 125.6, 128.2, 133.8, 135.4, 135.9, 141.3, 143.0, 143.5, 144.3, 145.8, 148.4, 154.3. IR (nujol, cm⁻¹): 1592 ($-\text{N}=\text{C}-\text{H}$), 2476 (B-H). Elem. Anal. (%): calc. for C₃₁H₄₂BMoN₈P (664.45): C 56.04, H 6.37, N 16.86; found ($\pm 0.3\%$) C 54.96, H 6.54, N 15.64

Reaction of (Tp)(ArN)Mo(-N=CHPh)(PMe₃) with PhCHO



The excess of benzaldehyde was added to the solution containing (Tp)(ArN)Mo(-N=CHPh)(PMe₃). The product was not isolated. ¹H-NMR (300 MHz; C₆D₆; 298K; δ , ppm): 5.37 (s, 1H, CHO, PhCHO), 5.57 (m, 1H, Pz), 5.85 (m, 1H, Pz), 5.94 (m, 1H, Pz),

6.60-6.67 (m, 3H), 6.75-6.87 (m, 5H), 7.13 (m, 2H), 7.31 (m, 1H), 7.37 (m, 2H), 7.63 (m, 1H), 8.15 (m, 2H).

Reaction of (Tp)(ArN)Mo(-N=CHPh)(PMe₃) with PhSiH₃

Phenylsilane (4.2 mg, 0.039 mmol) was added to a solution of (Tp)(ArN)Mo(-N=CHPh)(PMe₃) (26.0 mg, 0.0390 mmol), and the reaction mixture was left to two days at RT, and then, heated for one day at 50 °C. No reaction was observed. BPh₃ (9.4 mg, 0.039 mmol) was added to the reaction mixture, and the sample was heated for two hours at 50 °C, and then, overnight at RT. No reaction was observed.

Preparation of (Tp)(ArN)Mo(-CHMeCN)(PMe₃)

Acrylonitrile (1.8 μ l, 0.027 mmol) was added to a solution of (Tp)(ArN)Mo(H)(PMe₃) (15.0 mg, 0.0367 mmol) in C₆D₆ (0.60 ml). The reaction provided clean formation of (Tp)(ArN)Mo(-CHMeCN)(PMe₃) within one hour at RT. ¹H-NMR (300 MHz; C₆D₆; 298K; δ , ppm): 0.96 (d, ³J_{H-H} = 6.8 Hz, 6H, 2CH₃, *i*-Pr), 1.07 (d, ³J_{H-H} = 6.8 Hz, 6H, 2CH₃, *i*-Pr), 1.29 (d, ²J_{H-P} = 7.7 Hz, 9H, PMe₃), 1.84 (d, ³J_{H-H} = 7.2 Hz, 3H, -CHMeCN), 2.62 (qd, ³J_{H-H} = 7.2 Hz, ³J_{H-P} = 2.4 Hz, 1H, Mo-CHMeCN), 3.64 (sept, ³J_{H-H} = 6.8 Hz, 2H, *i*Pr), 5.68 (t, ³J_{H-H} = 2.1 Hz, 1H, Pz), 5.95 (t, ³J_{H-H} = 2.1 Hz, 1H, Pz), 5.98 (t, ³J_{H-H} = 2.1 Hz, 1H, Pz), 6.91 (d, ³J_{H-H} = 7.7 Hz, 2H, *m*-H, Ar), 7.10 (t, ³J_{H-H} = 7.7 Hz, 1H, *p*-H, Ar), 7.16 (d, ³J_{H-H} = 2.1 Hz, 1H, Pz), 7.42 (d, ³J_{H-H} = 2.1 Hz, 1H, Pz), 7.46 (d, ³J_{H-H} = 2.1 Hz, 1H, Pz), 7.51 (d, ³J_{H-H} = 2.1 Hz, 1H, Pz), 7.69 (d, ³J_{H-H} = 2.1 Hz, 1H, Pz), 8.18 (d, ³J_{H-H} = 2.1 Hz, 1H, Pz). ³¹P-NMR (121.5 MHz; C₆D₆; 298 K; δ , ppm): 5.5 (1P, PMe₃). ¹³C-NMR (150.9 MHz; C₆D₆; 298 K; δ , ppm): 10.9 (d, ²J_{C-P} = 2.9 Hz, Mo-CH), 18.2 (d, ¹J_{C-P} = 22.5 Hz, PMe₃), 24.1 (Mo-CHMeCN), 24.5 (CH₃, *i*-Pr), 25.2 (CH₃, *i*-Pr), 27.0 (CH, *i*-Pr), 104.5 (Pz), 105.8 (Pz), 106.3 (Pz), 123.7 (CH, *m*-C, Ar), 125.7 (CH, *p*-C, Ar), 134.2 (Pz), 135.6 (Pz), 135.8 (Pz), 139.5 (CN), 141.5 (Pz), 142.1 (Pz), 143.6 (Pz), 145.6 (*ipso*-C, C-C, Ar), 152.1 (*ipso*-C, C-N, Ar).

Table V-4. Hydrosilylation of various organic substrates catalyzed by (Tp)(ArN)Mo(H)(PMe₃) (5 mol%).

<i>Substrate</i>	<i>Silane</i>	<i>Product</i>	<i>Reaction conditions</i>	<i>Conversion of organic substrate</i>	<i>Yield, according to ¹H-NMR</i>	<i>Turnover number (TON)</i>
PhCHO	PhSiH ₃	PhCH ₂ OSiH ₂ Ph (PhCH ₂ O) ₂ SiHPh	0.5 day, RT	100%	38% 62%	20
PhCOCH ₃	PhSiH ₃	PhSiH ₂ OCH(Me)Ph PhSiH(OCH(Me)Ph) ₂	1.5 days, RT	100%	85% 15%	20
Cyclohexanone	PhSiH ₃	CyOSiH ₂ Ph (CyO) ₂ SiHPh	53 min, RT	100%	85% 15%	20
PhCHO	PhMeSiH ₂	PhCH ₂ OSiHMePh	1.5 days, 50 °C	30%	30%	6
PhCOCH ₃	PhMeSiH ₂	PhMeSiHOCH(Me)Ph	2.5 days, 50 °C	100%	100%	20
Cyclohexanone	PhMeSiH ₂	CyOSiHMePh (CyO) ₂ SiMePh	1 day, RT	100%	96% 4%	20
PhCHO	PhMe ₂ SiH		2 days, 50 °C	0%	0%	0
PhCOCH ₃	PhMe ₂ SiH		2 days, 50 °C	0%	0%	0
Cyclohexanone	PhMe ₂ SiH	CyOSiMe ₂ Ph	1.5 days, 50 °C	11%	11%	2
PhCHO	(EtO) ₃ SiH		2 days, 50 °C	0%	0%	0
PhCOCH ₃	(EtO) ₃ SiH		2 days, 50 °C	0%	0%	0
PhCHO	Et ₃ SiH		1 day, 60 °C	0%	0%	0
PhCN	PhSiH ₃	PhCH=NSiH ₂ Ph (PhCH=N) ₂ SiHPh	3 days, 50 °C	20%	86% 14%	5

Table V-5. Hydrosilylation of PhCHO with PhSiH₃ (and PhSiD₃) catalyzed by (Tp)(ArN)Mo(H)(PMe₃): reaction rate constants of individual steps and activation parameters.

REACTION	Rate constant, <i>k</i>	ΔH^\ddagger , kJ/mol	ΔS^\ddagger , J/(K·mol)
(Tp)(ArN)Mo(H)(PMe ₃), Pz-ring dissociation	$k(290.1 \text{ K}) = 0.618 \text{ s}^{-1}$ $k(295.1 \text{ K}) = 1.138 \text{ s}^{-1}$ $k(300.1 \text{ K}) = 2.077 \text{ s}^{-1}$ $k(305.1 \text{ K}) = 3.407 \text{ s}^{-1}$	81.8 ± 2.1	32.4 ± 7.0
(Tp)(ArN)Mo(H)(PMe ₃) + PhCHO (1 eq) + PMe ₃ (10 eq) → (Tp)(ArN)Mo(OCH ₂ Ph)(PMe ₃)	$k(309.1 \text{ K}) = (1.005 \pm 0.003) \cdot 10^{-2} \text{ M}^{-1} \cdot \text{s}^{-1}$ $k(319.1 \text{ K}) = (1.50 \pm 0.03) \cdot 10^{-2} \text{ M}^{-1} \cdot \text{s}^{-1}$ $k(328.7 \text{ K}) = (1.18 \pm 0.02) \cdot 10^{-1} \text{ M}^{-1} \cdot \text{s}^{-1}$	102.5 ± 6.6	45.3 ± 53.45
(Tp)(ArN)Mo(OCH ₂ Ph)(PMe ₃) + PhSiH ₃ (10 eq) → (Cp)(ArN)Mo(H)(PMe ₃) + (PhCH ₂ O) ₂ SiHPh	$k(290.1 \text{ K}) = (1.13 \pm 0.02) \cdot 10^{-4} \text{ s}^{-1}$ $k(295.1 \text{ K}) = (2.35 \pm 0.02) \cdot 10^{-4} \text{ s}^{-1}$ $k(300.1 \text{ K}) = (4.37 \pm 0.04) \cdot 10^{-4} \text{ s}^{-1}$ $k(305.1 \text{ K}) = (8.67 \pm 0.01) \cdot 10^{-4} \text{ s}^{-1}$	96.6 ± 1.8	12.5 ± 6.2
(Tp)(ArN)Mo(H)(PMe ₃) + PhSiD ₃ (5 eq.) → (Tp)(ArN)Mo(D)(PMe ₃)	$k(333.1 \text{ K}) = (1.20 \pm 0.23) \cdot 10^{-4} \text{ s}^{-1}$	-	-

V. 3. Hydrosilylation catalyzed by (PPh₃)CuH

Preparation of (PPh₃)CuH

A crude mixture of triphenylphosphine (1.06 g, 4.04 mmol), copper(I) chloride (0.2 g, 2.02 mmol) and *t*-BuOK (0.23 g, 2.02 mmol) was suspended in toluene, and PhMe₂SiH (0.31 ml, 2.02 mmol) was added to the resulting solution. All the solids dissolved, and the reaction mixture turned dark red within one hour. Acetonitrile (~200%) was added, and the resulting solution was placed in freezer (-40 °C) for two days. The crystallized product was filtered, washed with acetonitrile and dried under vacuum. Crude yield: 0.31 g (47%). Additional purification from inorganic salts (*e.g.* KCl) was not performed. The isolated compound was NMR-pure CuH(PPh₃). ¹H-NMR (300 MHz; C₆D₆; 298K; δ, ppm): 3.51 (bs, 1H, Cu-H), 6.65-6.82 (m, 6H, *m*-H, Ph), 6.95 (t, *J* = 7.14 Hz, 3H, *p*-H, Ph), 7.60-7.74 (m, 6H, *o*-H, Ph). ³¹P-NMR (121.5 MHz; C₆D₆; 298 K; δ, ppm): -5.9 (bs, 1P, PPh₃).

Stoichiometric reaction between (PPh₃)CuH, PhCHO and PhMe₂SiD

(PPh₃)CuH (14.5 mg, 0.044 mmol) was added to a solution of PhCHO (4.7 mg, 0.044 mmol) and PhMe₂SiD (6.1 mg, 0.044 mmol). The reaction resulted in formation of PhCHDOSiMe₂Ph as the only product. (PPh₃)CuH remained unchanged during the reaction. The hydride retention on Cu was demonstrated by the relative integral intensities in the ¹H NMR spectrum (Figure III-4, page 90; Figure III-5, page 91), and 100%-absence of Cu-D in 2D NMR spectrum (Figure III-6, page 92). By the end of conversion, PhCHO (47.0 mg, 0.440 mmol) and PhMe₂SiD (61.0 mg, 0.440 mmol) were added to the same NMR tube to perform the reaction catalytically. The signal of Cu-H was observable by ¹H NMR during the catalysis (Figure III-7, page 93).

Stoichiometric reaction between (PPh₃)CuH, acetophenone and PhMe₂SiD

(PPh₃)CuH (0.6 mg, 0.020 mmol) was added to a solution of PhCOCH₃ (3.7 mg, 0.031 mmol) and PhMe₂SiD (4.2 mg, 0.031 mmol). Hydrosilylation was not observed.

Stoichiometric reaction between (PPh₃)CuH, cyclohexanone and PhMe₂SiD

(PPh₃)CuH (10.0 mg, 0.031 mmol) was added to a solution of cyclohexanol (3.0 mg, 0.031 mmol) and PhMe₂SiD (4.2 mg, 0.031 mmol). The reaction was left overnight. Next day, only 11% of the product Cy(D)OSiMe₂Ph was formed.

Hydrosilylation of PhCN by PhMe₂SiH in the presence of 10% (PPh₃)CuH

(PPh₃)CuH (5.0 mg, 0.015 mmol) was added to a solution of benzonitrile (15.9 mg, 0.154 mmol) and PhMe₂SiH (21.0 mg, 0.154 mmol) in C₆H₆ (0.6 ml). The reaction mixture was kept at RT for several days, and then was heated at 50 °C overnight. Hydrosilylation of benzonitrile was not observed.

Stoichiometric reaction between (PPh₃)CuH and PhCHO

Benzaldehyde (3.2 mg, 0.031 mmol) was added to a solution of (PPh₃)CuH (10.0 mg, 0.031 mmol) in C₆H₆ (0.6 ml). Next day, the reaction provided formation of (PPh₃)CuOCH₂Ph (65% NMR yield) and a relatively large amounts of a black precipitate (metallic copper). ¹H-NMR (300 MHz; C₆D₆; 298K; δ, ppm): 5.23 (s, 2H, -OCH₂Ph), 6.91-7.10 (m, 12H, *m*- and *p*-H, OPh, PPh₃), 7.38-7.57 (m, 8H, *o*-H, OPh, PPh₃). ³¹P-NMR (121.5 MHz; C₆D₆; 298 K; δ, ppm): -1.0 (bs, 1P, PPh₃). ¹³C-NMR (75.5 MHz; C₆D₆; 298 K; δ, ppm): 71.3 (bs, -OCH₂Ph), 134.0 (*o*-C, -OCH₂Ph), 128.5 (*m*-C, -OCH₂Ph), 128.6 (*p*-C, -OCH₂Ph), 148.2 (bs, *ipso*-C, -OCH₂Ph)

Reaction between (PPh₃)CuOCH₂Ph and PhMe₂SiH

PhMe₂SiH (0.020 mmol) was added to a solution of (PPh₃)CuOCH₂Ph (0.020 mmol) in C₆H₆ (0.6 ml). Formation of PhCH₂OSiMe₂Ph was observed immediately by ¹H NMR. Several forms of copper hydride were present in the resulting mixture. ¹H-NMR (300 MHz; C₆D₆; 298K; δ, ppm): 2.55 (CuH), 3.14 (CuH), 3.63 (CuH), 4.69 (s, 2H, PhCH₂OSiMe₂Ph).

V. 4. Hydrosilylation catalyzed by oxo-Re(V) complexes

Reaction of $(PPh_3)_2(O)(I)Re(H)SiMe_2Ph$ with PhCHO and PhMe₂SiD

Benzaldehyde (2.3 μ l, 0.023 mmol) and PhMe₂SiD (2.8 μ l, 0.023 mmol) were added to a solution of $(I)(O)Re(H)(OSiMe_2Ph)(PPh_3)_2$ prepared *in situ* from PhMe₂SiD (3.1 mg, 0.023 mmol) and $(PPh_3)_2Re(O)_2(I)$ (20.0 mg, 0.023 mmol) in CDCl₃ (Figure III-8, page 98). The reaction was monitored by ¹H NMR (Figure III-9, page 99 and Figure III-10, page 100), and was complete in approximately 40 min. By the end of reaction, the integral intensity of Re-H peak was decreased by 19%.

Preparation of $(PCy_3)_2ReOCl_3$ ¹⁶¹

Tricyclohexylphosphine (305.0 mg, 1.09 mmol) was added to a solution of $(PPh_3)_2ReOCl_3$ (200.0 mg, 0.240 mmol) in benzene. The reaction mixture was stirred for several hours at RT. The solvent was evaporated, and the crude residue was washed with diethyl ether to remove the excess of PPh₃. The residue was dried under vacuum to give 205.0 mg of $(PCy_3)_2ReOCl_3$. Yield: 98%. ¹H-NMR (300 MHz; C₆D₆; 298K; δ , ppm): 1.07-1.35 (m, 20H, Cy), 1.47-1.85 (m, 30H, Cy), 2.25-2.42 (m, 10H, Cy), 2.91-3.10 (m, 6H, Cy). ³¹P-NMR (121.5 MHz; C₆D₆; 298 K; δ , ppm): -28.0 (s, PCy₃).

Preparation of $(PCy_3)_2Re(H)OCl_2$ ^{10b}

Triethylsilane (2.0 μ l, 0.012 mmol) was added to a solution of $ReOCl_3(PCy_3)_2$ (10.8 mg, 0.012 mmol) in C₆D₆ (0.60 ml). The reaction mixture was heated at 100 °C for several days until the reaction is complete. NMR yield: ~100%. ¹H-NMR (300 MHz; C₆D₆; 298K; δ , ppm): 1.08-2.62 (m, 66H, PCy₃), 7.38 (t, ²J_{H-P} = 15.4 Hz, 1H, Re-H). ³¹P-NMR (121.5 MHz; C₆D₆; 298 K; δ , ppm): 8.8 (s, PCy₃).

Reaction of $(PCy_3)_2Re(H)OCl_2$ with propanal and Et₃SiD

Triethylsilane-*d*₁ (2.0 μ l, 0.012 mmol) and propanal (0.9 μ l, 0.012 mmol) were added to a solution of $(PCy_3)_2Re(H)OCl_2$ (10.0 mg, 0.012 mmol) in C₆D₆ (0.60 ml). The reaction was monitored by ¹H NMR during one week at RT. Formation of

(PCy₃)₂Re(OCH₂CH₂CH₃)OCl₂ and Et₃SiOCH₂CH₂CH₃ was observed. ¹H-NMR (300 MHz; C₆D₆; 298K; δ, ppm): 3.49 (t, ³J_{H-H} = 6.59 Hz, Et₃SiOCH₂CH₂CH₃), 3.69 (t, ³J_{H-H} = 6.59 Hz, ReOCH₂CH₂CH₃). ³¹P-NMR (121.5 MHz; C₆D₆; 298 K; δ, ppm): -17.2 (s, PCy₃, (PCy₃)₂Re(OCH₂CH₂CH₃)OCl₂).

Reaction of (PCy₃)₂Re(H)OCl₂ with butanone and Et₃SiD

Triethylsilane-*d*₁ (2.0 μl, 0.012 mmol) and butanone (1.1 μl, 0.012 mmol) were added to a solution of (PCy₃)₂Re(H)OCl₂ (10.0 mg, 0.012 mmol) in C₆D₆ (0.60 ml). The reaction was monitored by ¹H NMR during several days at RT, followed by heating overnight at 70 °C. Butanone did not react with the other substrates. A slow exchange between Re-*H* and Si-*D* was observed.

Preparation of (PPh₃)₂Re(D)OCl₂ ^{10b}

Triethylsilane-*d*₁ (2.8 μl, 0.017 mmol) was added to a solution of ReOCl₃(PPh₃)₂ (14.5 mg, 0.017 mmol) in C₆D₆ (0.60 ml), and the reaction mixture was heated at 50 °C for 3 hours. The reaction provided formation of (PPh₃)₂Re(D)OCl₂. NMR yield: ~100%. ¹H-NMR (300 MHz; C₆D₆; 298K; δ, ppm): 6.89-7.07 (m, 12H, PPh₃), 8.00-8.10 (m, 18H, PPh₃). ³¹P-NMR (121.5 MHz; C₆D₆; 298 K; δ, ppm): 7.3 (s, PPh₃).

Reaction of (PPh₃)₂Re(D)OCl₂ with PhCHO and Et₃SiH

Triethylsilane (2.8 μl, 0.017 mmol) and benzaldehyde (1.8 μl, 0.017 mmol) were added to a solution of (PPh₃)₂Re(D)OCl₂ (13.6 mg, 0.017 mmol) in C₆D₆ (0.60 ml). The reaction was monitored by ¹H NMR. Formation of benzyloxy complex (PCy₃)₂Re(OCHDPh)OCl₂ and Et₃SiOCHDPh was observed. ¹H-NMR (300 MHz; C₆D₆; 298K; δ, ppm): 3.56 (bs, ReOCHDPh), 4.63 (s, Et₃SiOCHDPh). ³¹P-NMR (121.5 MHz; C₆D₆; 298 K; δ, ppm): -10.2 (s, PPh₃, (PCy₃)₂Re(OCHDPh)OCl₂).

H/D exchange between Et₃SiH and (PCy₃)₂Re(D)OCl₂

Triethylsilane (2.8 μl, 0.017 mmol) was added to a solution of ReOCl₂(D)(PCy₃)₂ (0.017 mmol) in C₆D₆ (0.60 ml). The reaction mixture was heated at 70 °C overnight. Formation

of Re-*H* was observed by ^1H NMR. ^1H -NMR (300 MHz; C_6D_6 ; 298K; δ , ppm): 1.08-2.62 (m, 66H, PCy_3), 7.38 (t, $^2J_{\text{H-P}} = 15.4$ Hz, 1H, Re-*H*).

V. 5. Hydrosilylation catalyzed by Zn(II) complexes

Hydrosilylation of benzaldehyde with PMHS catalyzed by Zn(II)

Solution of zinc 2-ethylhexanoate (51.7 mg, 0.147 mmol) in *tert*-butyl methyl ether (0.7 ml) was added to NaBD_4 (6.2 mg, 0.147 mmol), and the mixture was left overnight at RT. The suspension was transferred into a separate NMR tube. PMHS (8.8 mg, 0.147 mmol) and benzaldehyde (15.6 mg, 0.147 mmol) were added, and the reaction mixture was heated at 70 °C overnight. ^1H -NMR (300 MHz; C_6D_6 ; 298K; δ , ppm): 4.90-4.97 (m, PhCHDO-PMHS).

V. 6. Hydrosilylation catalyzed by $(\text{ArN})\text{Mo}(\text{H})(\text{Cl})(\text{PMe}_3)_3$

Stoichiometric reaction between $(\text{ArN})\text{Mo}(\text{H})(\text{Cl})(\text{PMe}_3)_3$, PhCHO and PhSiD_3

$(\text{ArN})\text{Mo}(\text{H})(\text{Cl})(\text{PMe}_3)_3$ (10.0 mg, 0.019 mmol) was added to a solution of benzaldehyde (2.0 mg, 0.019 mmol) and PhSiD_3 (2.1 mg, 0.019 mmol). A quick formation of $(\text{ArN})\text{Mo}(\text{H})(\eta^2\text{-PhCHO})(\text{Cl})(\text{PMe}_3)_2$ was observed by ^1H NMR. The adduct was slowly re-arranging into the benzyloxy complex $(\text{ArN})\text{Mo}(\text{OCH}_2\text{Ph})(\text{Cl})(\text{PMe}_3)_3$, and the latter reacted with PhSiD_3 producing the silyl ether $\text{PhCH}_2\text{OSiD}_2\text{Ph}$ and $(\text{ArN})\text{Mo}(\text{D})(\text{Cl})(\text{PMe}_3)_3$.

Stoichiometric reaction between $(\text{ArN})\text{Mo}(\text{H})(\text{Cl})(\text{PMe}_3)_3$, cyclohexanone and PhSiD_3

$(\text{ArN})\text{Mo}(\text{H})(\text{Cl})(\text{PMe}_3)_3$ (10.0 mg, 0.019 mmol) was added to a solution of cyclohexanone (1.8 mg, 0.019 mmol) and PhSiD_3 (2.1 mg, 0.019 mmol). The reaction was 50% complete in 7 min at RT and yielded $\text{Cy}(\text{H})\text{OSiD}_2\text{Ph}$ (19%), $\text{Cy}(\text{D})\text{OSiD}_2\text{Ph}$ (32%). The initial catalyst was present as $(\text{ArN})\text{Mo}(\text{H})(\text{Cl})(\text{PMe}_3)_3$ (63%), and $(\text{ArN})\text{Mo}(\text{D})(\text{Cl})(\text{PMe}_3)_3$ (37%). The reaction was complete in approximately one hour at RT and finally yielded CyOSiD_2Ph (77%), $(\text{CyO})_2\text{SiDPh}$ (23%). The initial catalyst was present as $(\text{ArN})\text{Mo}(\text{H})(\text{Cl})(\text{PMe}_3)_3$ (44%), and $(\text{ArN})\text{Mo}(\text{D})(\text{Cl})(\text{PMe}_3)_3$ (66%).

Stoichiometric reaction between (ArN)Mo(H)(Cl)(PMe₃), PhCOCH₃ and PhSiD₃

(ArN)Mo(H)(Cl)(PMe₃)₃ (10.0 mg, 0.019 mmol) was added to a solution of acetophenone (2.2 mg, 0.019 mmol) and PhSiD₃ (2.1 mg, 0.019 mmol). When the reaction was complete, the reaction mixture consisted of PhCH(-OSiD₂Ph)CH₃, (ArN)Mo(H)(Cl)(PMe₃) (85%) and (ArN)Mo(D)(Cl)(PMe₃) (25%).

Synthesis of (ArN)Mo(OCy)(Cl)(PMe₃)₃

Cyclohexanone (64.0 mg, 0.650 mmol) was added to a toluene solution of (ArN)Mo(H)(Cl)(PMe₃)₃ (350.0 mg, 0.650 mmol). The reaction mixture was left for one day at RT. The product was crystallized at -80 °C, filtered off and dried in vacuum, affording 120 mg (51%) of (ArN)Mo(O-Cy)(Cl)(PMe₃)₃ as light-green crystalline solid.

¹H-NMR (300 MHz; C₆D₆; 298K; δ, ppm): 0.72-1.53 (mm, 8H, Cy; 12H, 4CH₃, iPr), 1.25 (d, ²J_{H-P} = 7.3 Hz, 9H, PMe₃), 1.29 (vt, ²J_{H-P} = 2.9 Hz, 18H, 2PMe₃), 1.53-1.64 (m, 1H, Cy), 1.67-1.80 (m, 2H, Cy), 1.92-2.04 (m, 2H, Cy), 3.1-4.3 (bm, 1H, CH, iPr), 4.07 (m, 1H, CH-O), 4.3-5.4 (bm, 1H, CH, iPr), 6.85-7.08 (m, 3H, Ar). ³¹P-NMR (121.5 MHz; C₆D₆; 298 K; δ, ppm): -12.2 (d, ²J_{P-P} = 14.8 Hz, 2P, PMe₃), 7.0 (t, ²J_{P-P} = 14.8 Hz, 1P, PMe₃). ¹³C-NMR (75.5 MHz; C₆D₆; 298 K; δ, ppm): 17.3 (vt, ¹J_{C-P} = 9.4 Hz, 2PMe₃), 22.7 (d, ¹J_{C-P} = 20.7 Hz, PMe₃), 26.3 (Cy), 27.2 (Cy), 39.8 (Cy), 76.1 (C-O, Cy), 124.3 (C-H, Ar), 128.7 (C-H, Ar), 151.4 (C-N, Ar). Signals of ^{Ar}C-CH(CH₃)₂ were not observed due to fluxionality. X-Ray: Single crystals for X-Ray analysis have been formed in NMR tube contained the solution of (ArN)Mo(O-Cy)(Cl)(PMe₃)₃ in C₆D₆ (0.60 ml).

(ArN)Mo(OCy)(Cl)(PMe₃)₃ + PMe₃: PHOSPHINE EXCHANGE

Trimethylphosphine (1.5 mg, 0.020 mmol) was added to a solution of (ArN)Mo(O-Cy)(Cl)(PMe₃)₃ (26.0 mg, 0.041 mmol) in C₆D₆ (0.60 ml). Below is a picture of ³¹P-³¹P EXSY NMR spectrum of the sample containing (ArN)Mo(OCy)(Cl)(PMe₃)₃ demonstrating the exchange between *cis*-, *trans*- and free PMe₃ (Figure V-69).

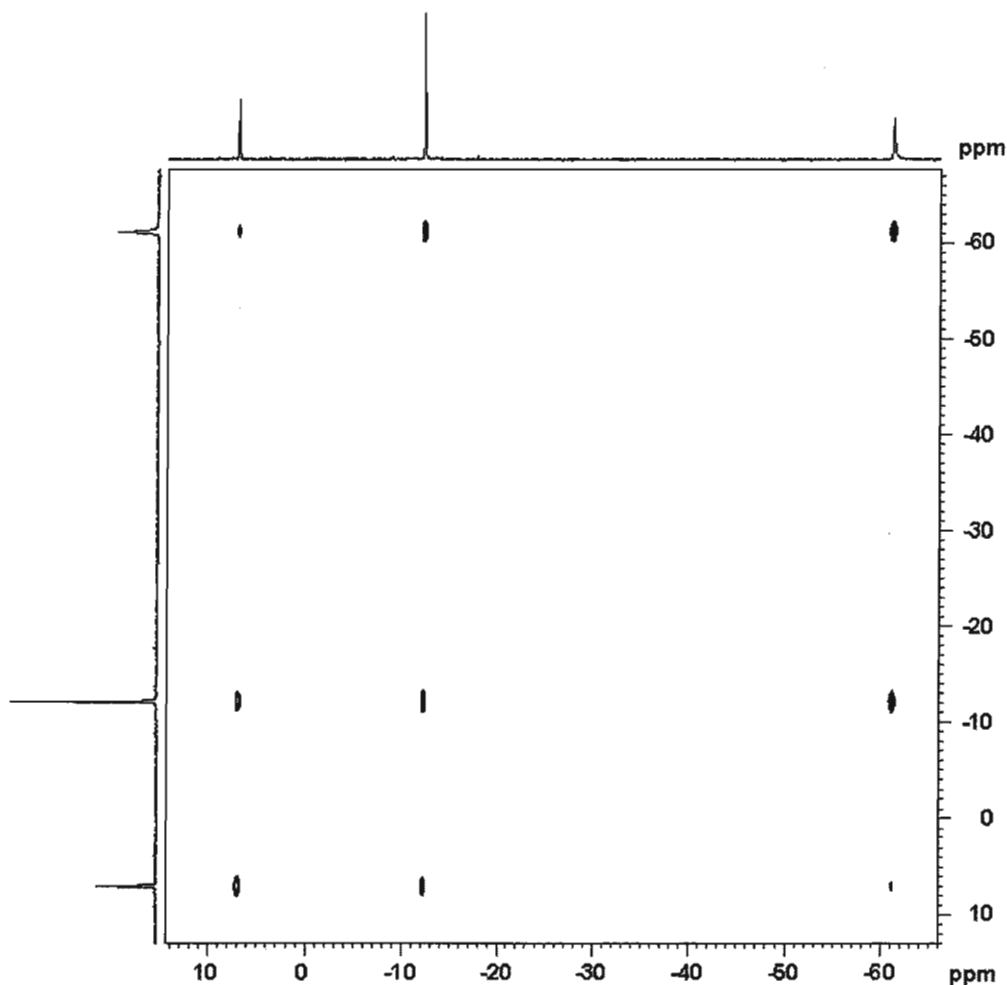


Figure V-69. ^{31}P - ^{31}P EXSY NMR spectrum of $(\text{ArN})\text{Mo}(\text{OCy})(\text{Cl})(\text{PMe}_3)_3$ in the presence of PMe_3 in C_6D_6 with the mixing time of 0.500 s showing fast exchange between all bound and free phosphines (Bruker 600 MHz NMR machine).

$(\text{ArN})\text{Mo}(\text{OCy})(\text{Cl})(\text{PMe}_3)_3$: PHOSPHINE DISSOCIATION

An NMR sample containing $(\text{ArN})\text{Mo}(\text{OCy})(\text{Cl})(\text{PMe}_3)_3$ (10.0 mg, 0.016 mmol) was studied by Selective ge-1D EXSY NMR. The bound phosphines were irradiated at 1.356 ppm (*trans*- PMe_3 , Figure 3), and at 1.402 ppm (*cis*- PMe_3 , Figure 4). The experiment explicitly demonstrated that the bound phosphines are in fast exchange. The peak at 0.908 ppm corresponds to the free PMe_3 formed as a result of dissociation.

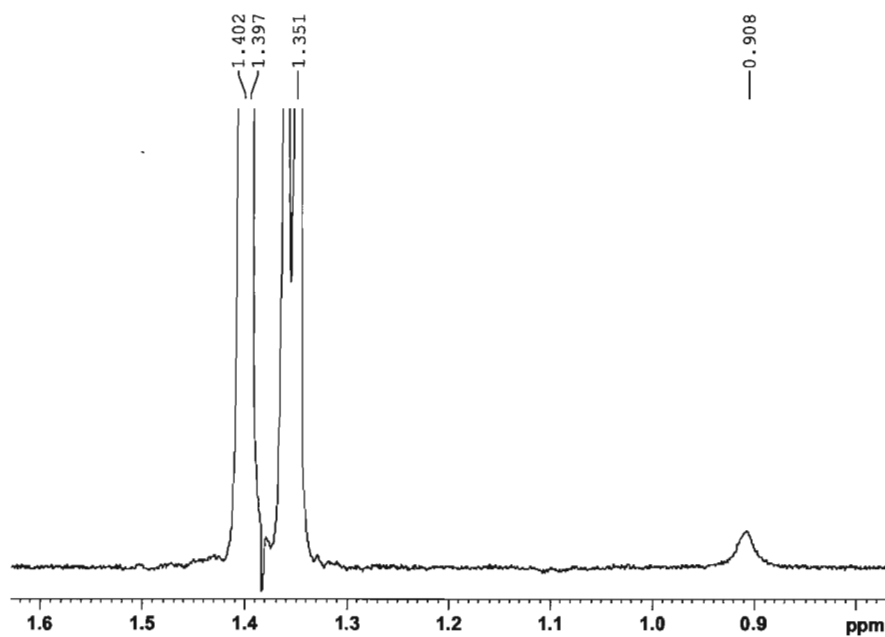


Figure V-70. Selective ge-1D EXSY experiment of the sample containing $(\text{ArN})\text{Mo}(\text{OCy})(\text{Cl})(\text{PMe}_3)_3$: irradiation of the area of *trans*- PMe_3 groups at 1.356 ppm with the mixing time of 1.000 s (Bruker 600 MHz NMR machine).

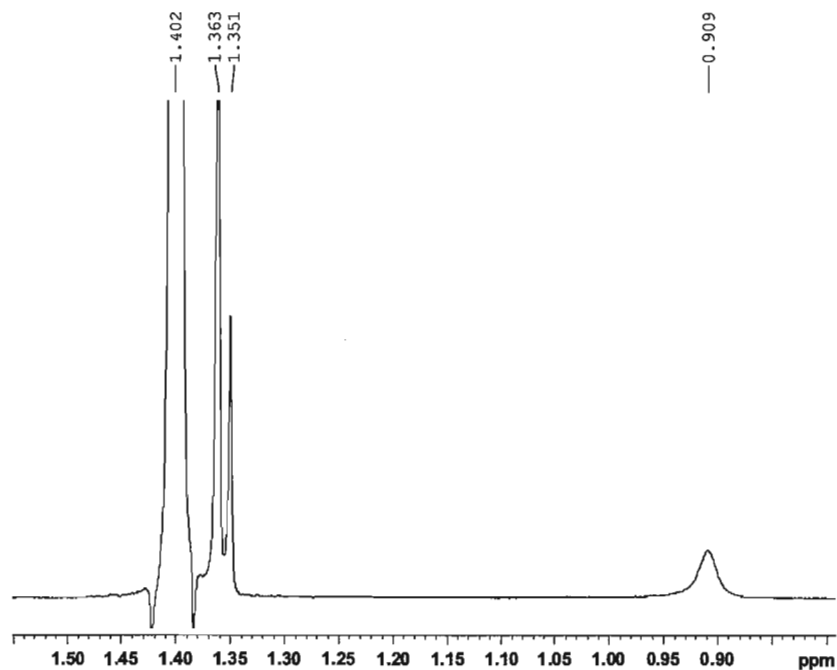
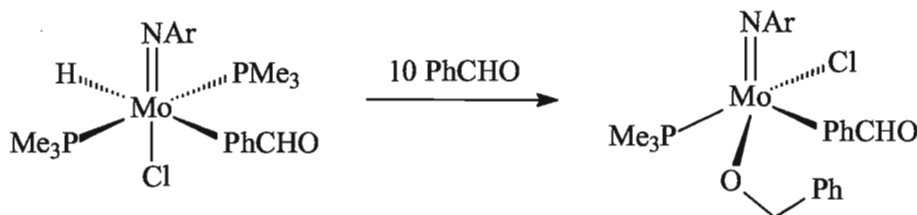


Figure V-71. Selective ge-1D EXSY experiment of the sample containing $(\text{ArN})\text{Mo}(\text{OCy})(\text{Cl})(\text{PMe}_3)_3$: irradiation of the area of *cis*- PMe_3 groups at 1.402 ppm with the mixing time of 1.000 s (Bruker 600 MHz NMR machine).

Kinetic investigation of the reaction $(\text{ArN})\text{Mo}(\text{H})(\text{PhCHO})(\text{Cl})(\text{PMe}_3)_2$ with PhCHO (10 eq.)



Benzaldehyde (31.7 mg, 0.300 mmol) was added to a solution of $(\text{ArN})\text{Mo}(\text{H})(\text{Cl})(\text{PMe}_3)_3$ (16.0 mg, 0.030 mmol), and $(\text{ArN})\text{Mo}(\text{H})(\text{PhCHO})(\text{Cl})(\text{PMe}_3)_3$ immediately formed. The further formation of $(\text{ArN})\text{Mo}(\text{OCH}_2\text{Ph})(\text{PhCHO})(\text{Cl})(\text{PMe}_3)_3$ was monitored by ^1H NMR at 10.0 (Figure V-72), 18.0 (Figure V-73), 23.4 (Figure V-74) and 34.0 $^\circ\text{C}$ (Figure V-75).

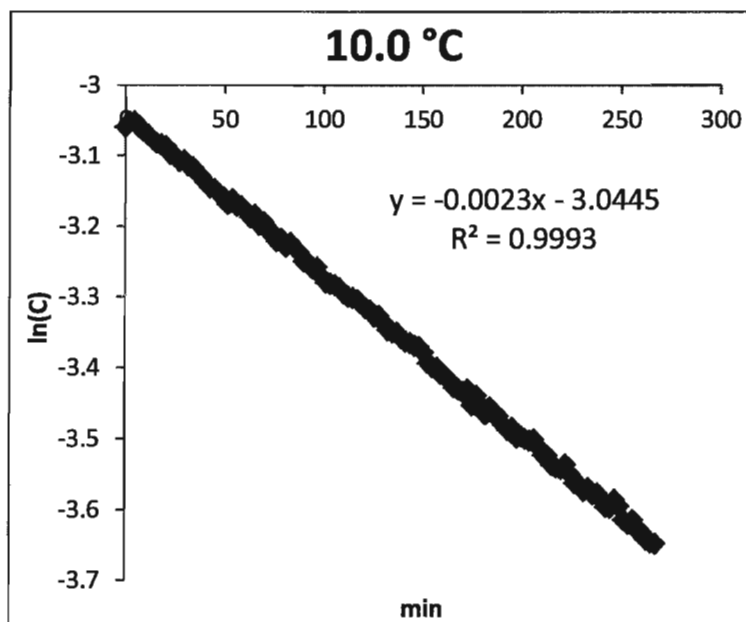


Figure V-72. $\text{Ln}(\text{C})$ vs. time plot for the reaction of $(\text{ArN})\text{Mo}(\text{H})(\text{PhCHO})(\text{Cl})(\text{PMe}_3)_2$ with PhCHO (10 eq.) at 10.0 $^\circ\text{C}$.

$$k(10.0\text{ }^\circ\text{C}) = (2.26 \pm 0.01) \cdot 10^{-3} \text{ min}^{-1} = (3.77 \pm 0.02) \cdot 10^{-5} \text{ s}^{-1}$$

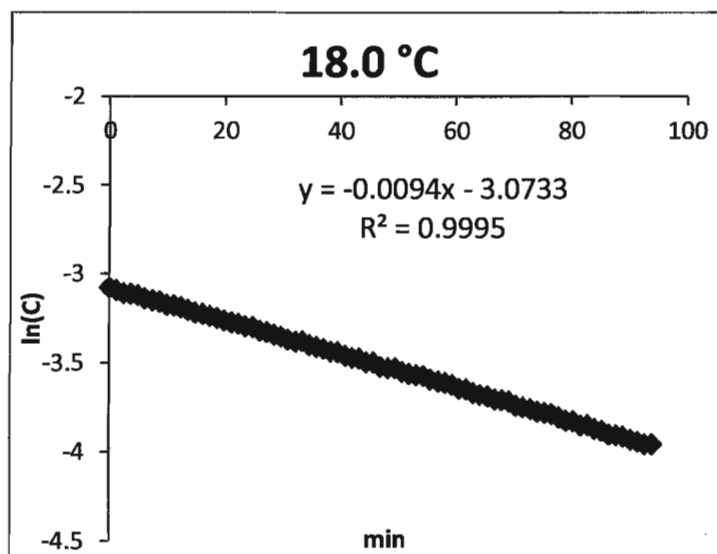


Figure V-73. Ln(C) vs. time plot for the reaction of (ArN)Mo(H)(PhCHO)(Cl)(PMe₃)₂ with PhCHO (10 eq.) at 18.0 °C.

$$k(18.0\text{ }^{\circ}\text{C}) = (9.40 \pm 0.02) \cdot 10^{-3} \text{ min}^{-1} = (1.57 \pm 0.03) \cdot 10^{-4} \text{ s}^{-1}$$

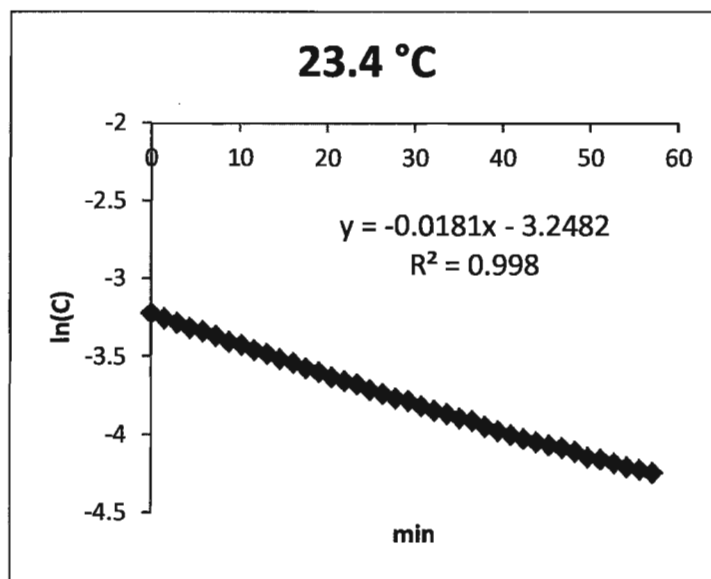


Figure V-74. Ln(C) vs. time plot for the reaction of (ArN)Mo(H)(PhCHO)(Cl)(PMe₃)₂ with PhCHO (10 eq.) at 23.4 °C.

$$k(23.4\text{ }^{\circ}\text{C}) = (1.81 \pm 0.01) \cdot 10^{-2} \text{ min}^{-1} = (3.02 \pm 0.02) \cdot 10^{-4} \text{ s}^{-1}$$

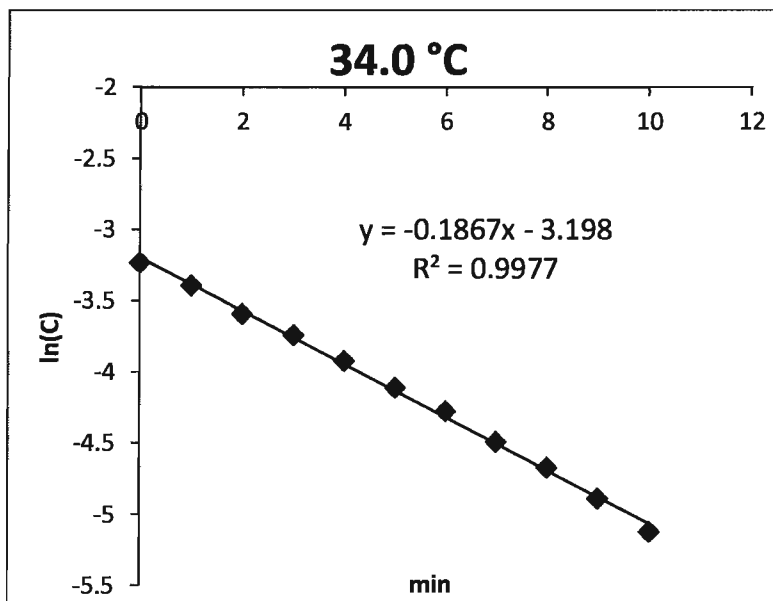


Figure V-75. Ln(C) vs. time plot for the reaction of (ArN)Mo(H)(PhCHO)(Cl)(PMe₃)₂ with PhCHO (10 eq.) at 34.0 °C.

$$k(34.0\text{ °C}) = (1.87 \pm 0.03) \cdot 10^{-1} \text{ min}^{-1} = (3.12 \pm 0.05) \cdot 10^{-3} \text{ s}^{-1}$$

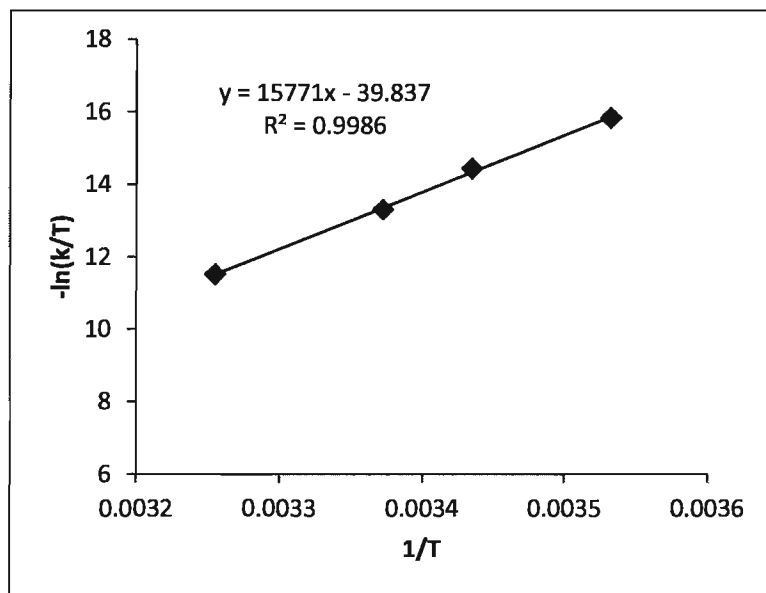


Figure V-76. Eyring plot for the reaction of (ArN)Mo(H)(PhCHO)(Cl)(PMe₃)₂ with PhCHO (10 eq.).

Activation parameters were extracted from the Eyring plot (Figure V-76): $\Delta H^\ddagger = (1.31 \pm 0.11) \cdot 10^2$ kJ/mol, $\Delta S^\ddagger = (1.33 \pm 0.38) \cdot 10^2$ J/(K·mol).

Reaction (ArN)Mo(H)(PhCHO)(Cl)(PMe₃)₂ with PhCHO

Benzaldehyde (15.9 mg, 0.150 mmol, 5 eq.; 31.7 mg, 0.300 mmol, 10 eq.; 47.7 mg, 0.45 mmol, 15 eq.) was added to a solution of (ArN)Mo(H)(Cl)(PMe₃)₃ (16.0 mg, 0.030 mmol), and (ArN)Mo(H)(PhCHO)(Cl)(PMe₃)₃ immediately formed. Disappearance of the starting material was monitored by ¹H NMR. Two products were formed, (ArN)Mo(OCH₂Ph)(PhCHO)(Cl)(PMe₃) (major) and (ArN)Mo(OCH₂Ph)(Cl)(PMe₃)₃ (minor).

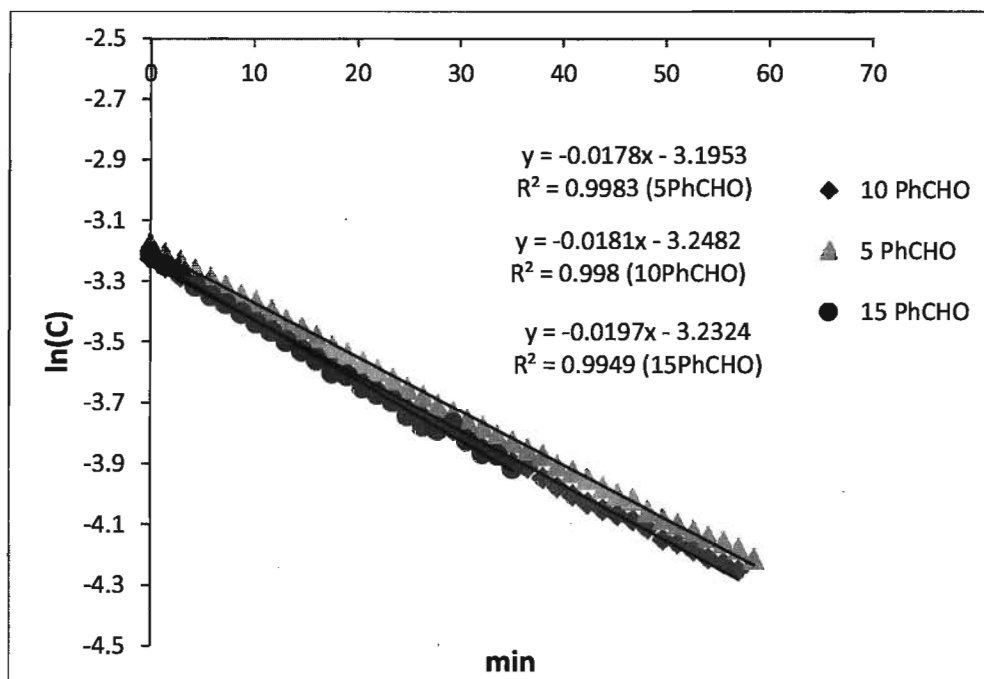


Figure V-77. $\ln(C)$ vs. time plot for the reaction (ArN)Mo(H)(PhCHO)(Cl)(PMe₃)₂ with PhCHO (5, 10, 15, and 20 eq.)

(ArN)Mo(H)(PhCHO)(Cl)(PMe₃)₂: Intermolecular exchange of benzaldehyde

Irradiation of the C-H proton of the carbonyl group of the coordinated benzaldehyde in (ArN)Mo(H)(PhCHO)(Cl)(PMe₃)₂ showed that it is in fast exchange with the free benzaldehyde (9.630 ppm) and with the coordinated aldehyde of the minor isomer (5.417 ppm) (Figure V-78).

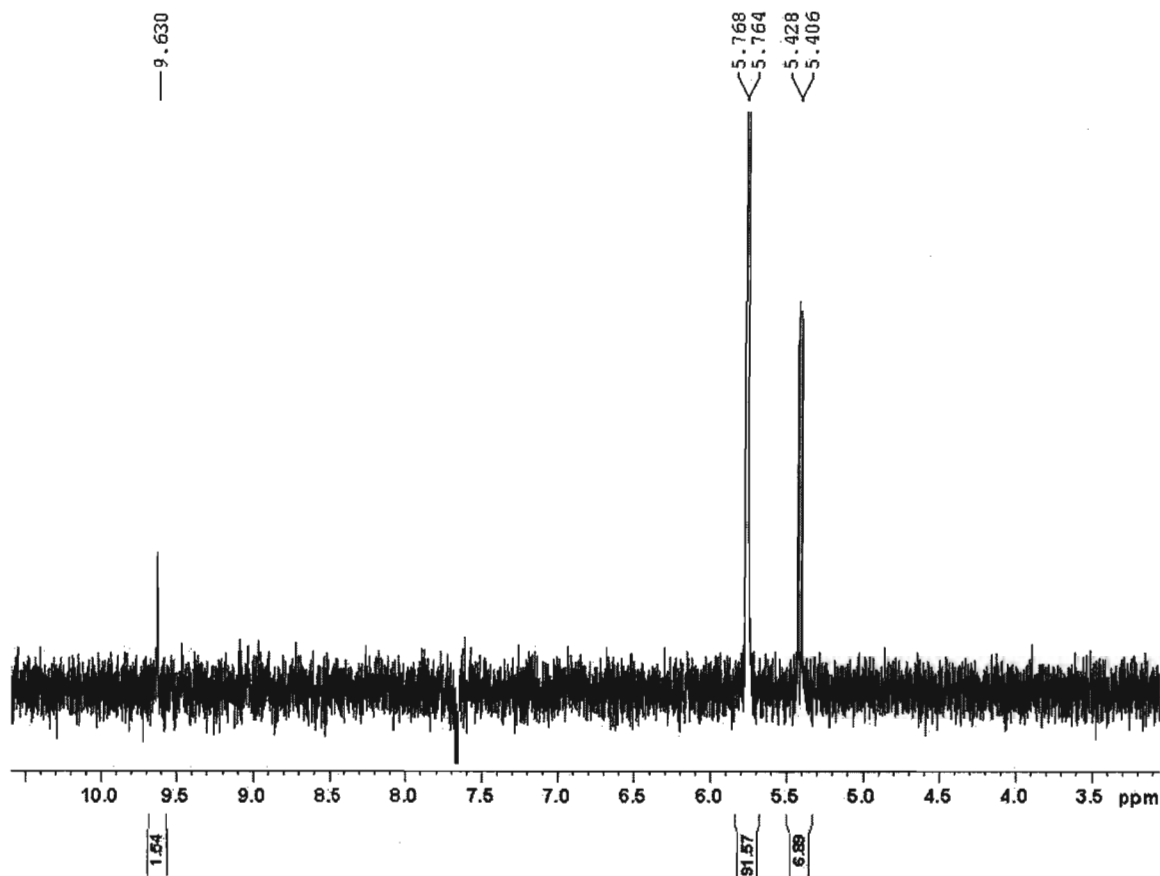


Figure V-78. Selective ge-1D EXSY NMR experiment of the sample containing (ArN)Mo(H)(PhCHO)(Cl)(PMe₃)₂: irradiation of the C-H proton of coordinated aldehyde at the frequency of 5.763 ppm with mixing time of 0.300 s (600 MHz machine).

The $-CHO$ protons of the free benzaldehyde (9.630 ppm) and the minor isomer of (ArN)Mo(H)(PhCHO)(Cl)(PMe₃)₂ (5.417 ppm) were also irradiated to demonstrate their exchange (Figure V-79, Figure V-80).

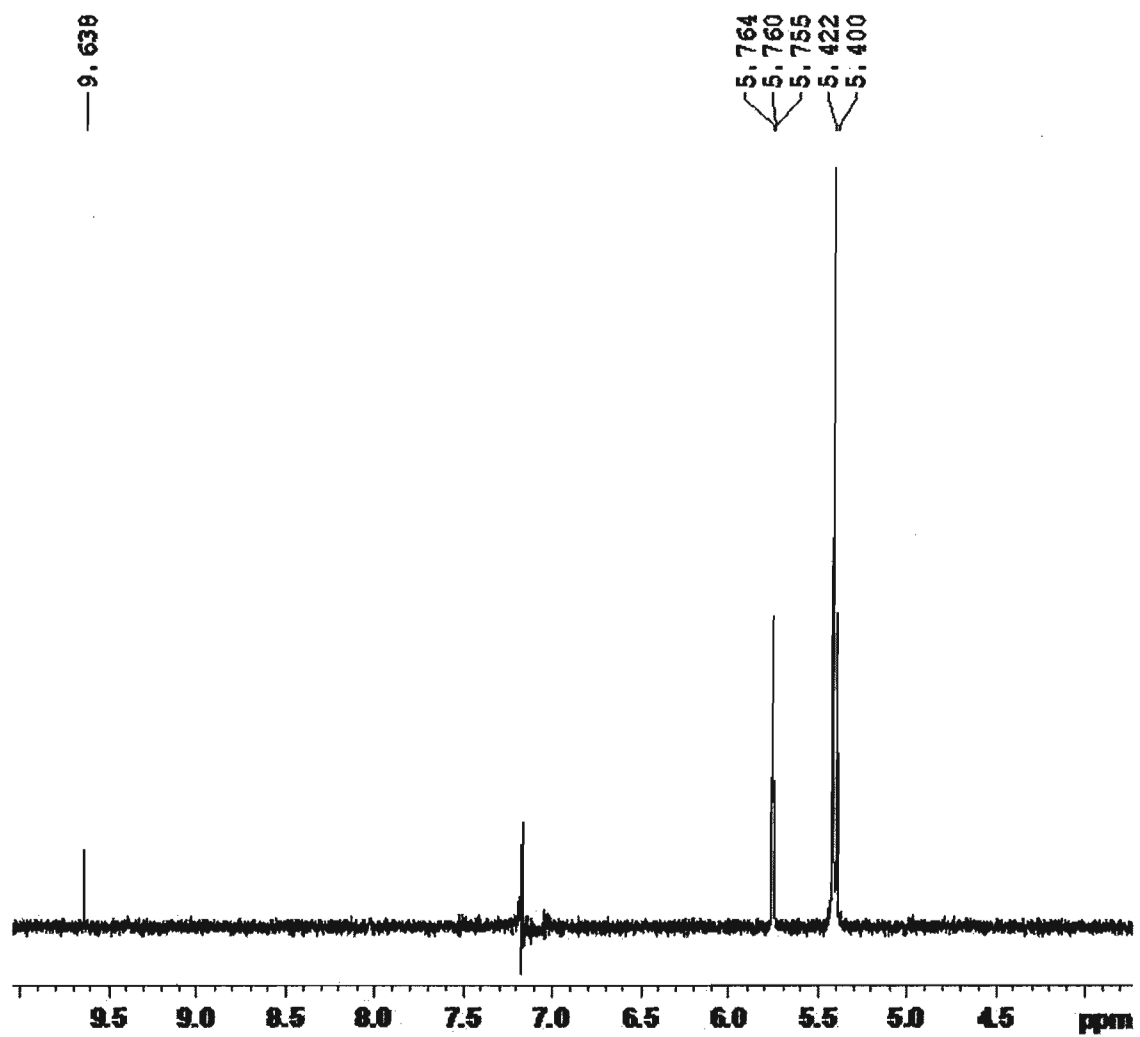


Figure V-79. Selective ge-1D EXSY NMR experiment of the sample containing $(\text{ArN})\text{Mo}(\text{H})(\text{PhCHO})(\text{Cl})(\text{PMe}_3)_2$: irradiation of the C-H proton of coordinated aldehyde of its minor isomer at the frequency of 5.417 ppm with mixing time of 0.300 s (600 MHz machine).

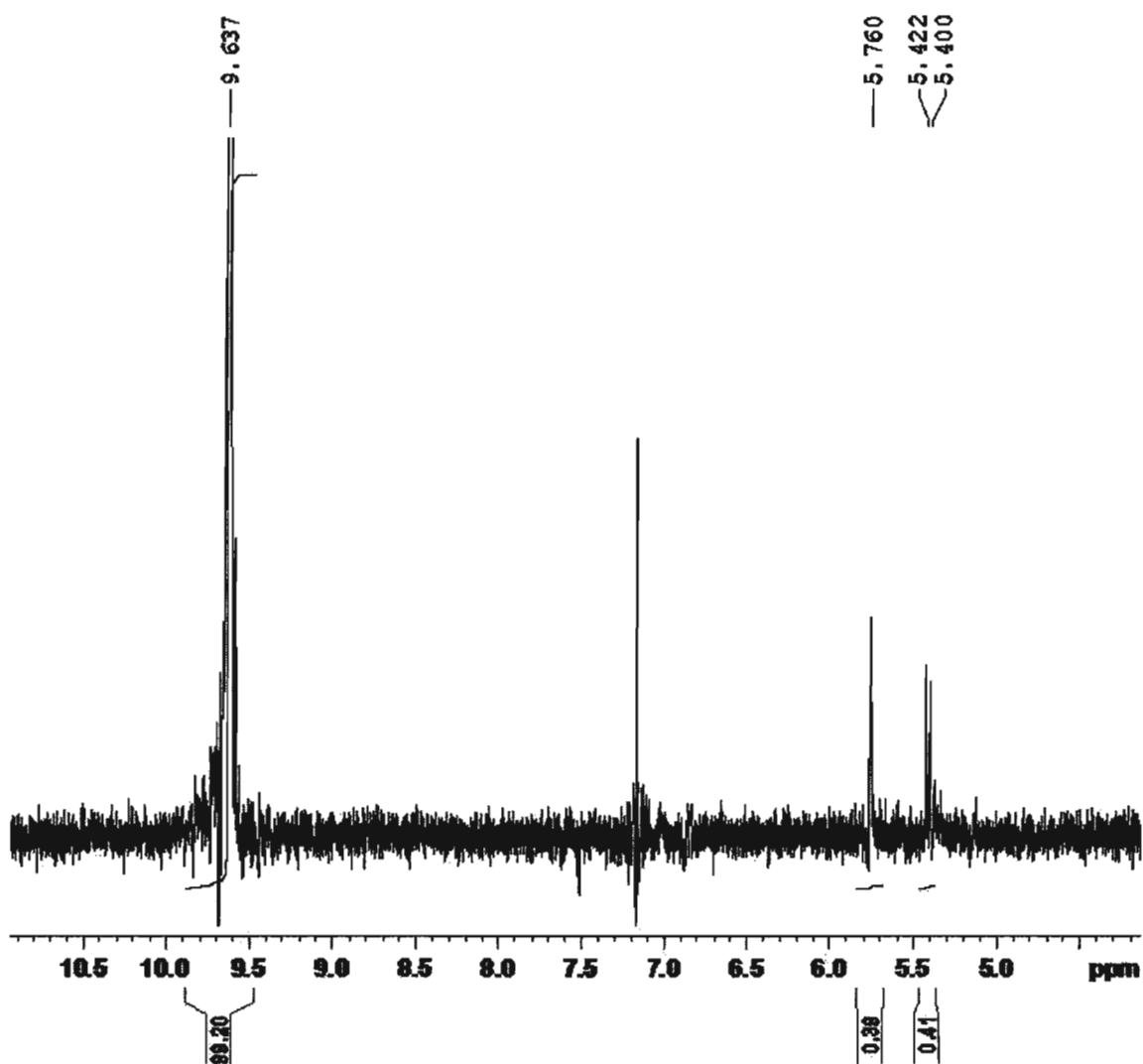


Figure V-80. Selective ge-1D EXSY NMR experiment of the sample containing $(\text{ArN})\text{Mo}(\text{H})(\text{PhCHO})(\text{Cl})(\text{PMe}_3)_2$: irradiation of the C-H proton of free benzaldehyde at the frequency of 9.638 ppm with the mixing time of 0.300 s (600 MHz machine).

(ArN)Mo(H)(PhCHO)(Cl)(PMe₃)₂: intramolecular phosphines exchange

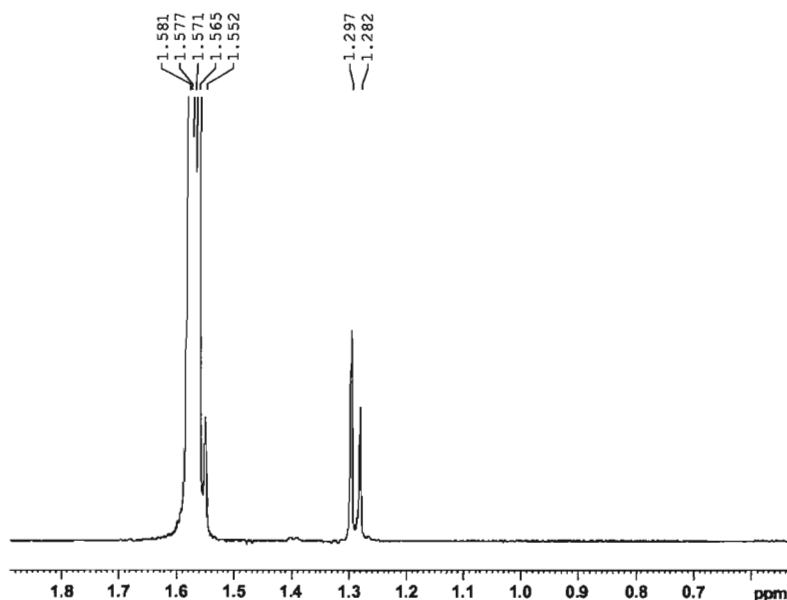


Figure V-81. Selective ge-1D EXSY NMR experiment of the sample containing (ArN)Mo(H)(PhCHO)(Cl)(PMe₃)₂: irradiation of the PMe₃ protons at the frequency of 1.572 ppm with the mixing time of 1.000 s (600 MHz machine).

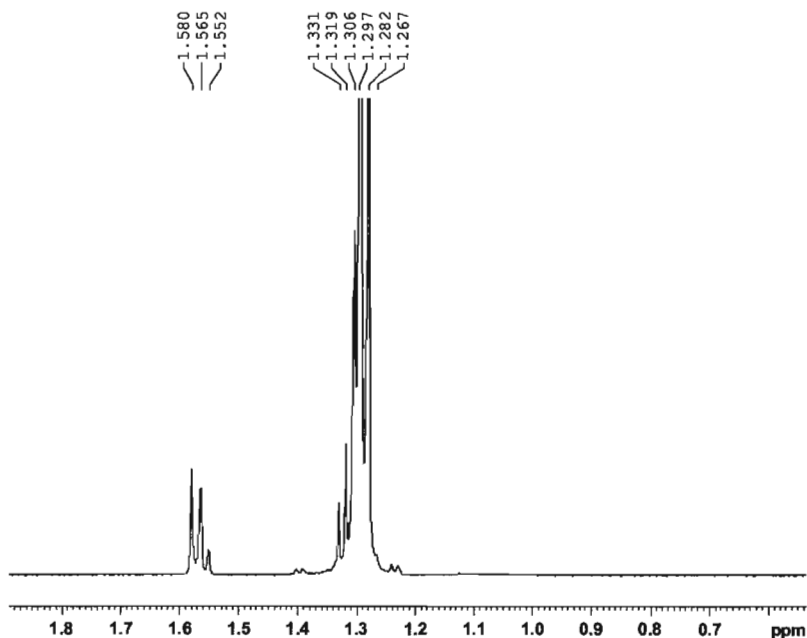
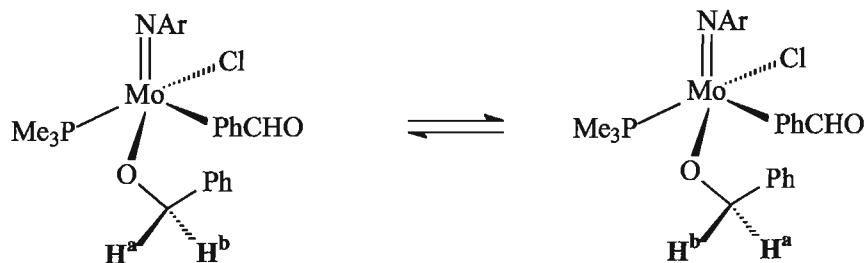


Figure V-82. Selective ge-1D EXSY NMR experiment of the sample containing (ArN)Mo(H)(PhCHO)(Cl)(PMe₃)₂: irradiation of the PMe₃ protons at the frequency of 1.290 ppm with the mixing time of 1.000 s (600 MHz machine).

(ArN)Mo(OCH₂Ph)(PhCHO)(Cl)(PMe₃): kinetic investigation of the exchange of two enantiomers



Selective ge-1D EXSY NMR experiments demonstrated that two enantiomeric protons of the benzyloxy group in (ArN)Mo(OCH₂Ph)(PhCHO)(Cl)(PMe₃) are in fast exchange at RT. The kinetics of this exchange was studied at 18.1 °C (Figure V-83), 22.0 °C (Figure V-84), 26.0 °C (Figure V-85), and 30.0 °C (Figure V-86). $R = \frac{B, \%}{50\%}$ B – The saturation (%) of the non-irradiated signal at a certain mixing time (d8, s).

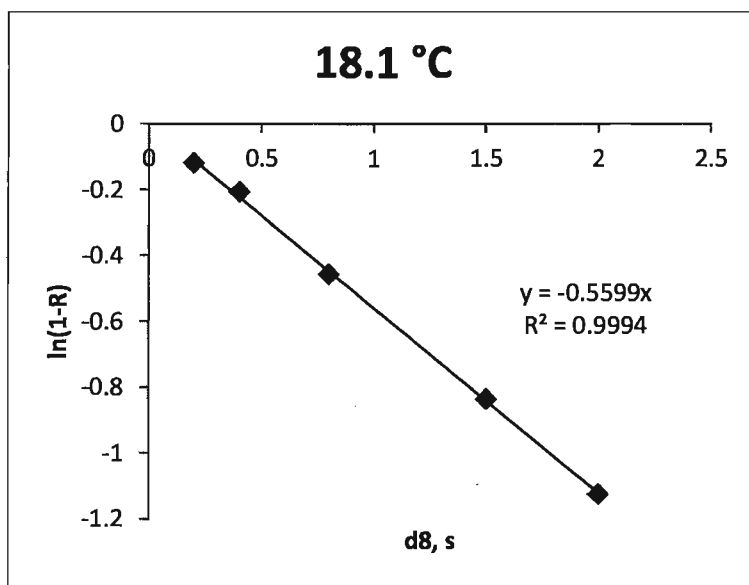


Figure V-83. Ln(1-R) vs. mixing time (d8, s) plot for the exchange of two enantiomers of (ArN)Mo(OCH₂Ph)(PhCHO)(Cl)(PMe₃) at 18.1 °C.

$$k(18.1\text{ }^{\circ}\text{C}) = (5.60 \pm 0.08) \cdot 10^{-1} \text{ s}^{-1}$$

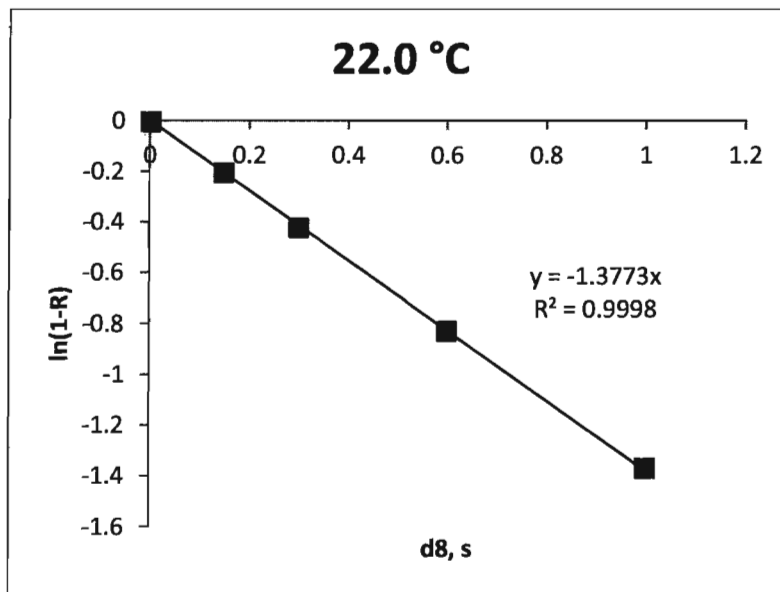


Figure V-84. Ln(1-R) vs. mixing time (d8) plot for the exchange of two enantiomers of (ArN)Mo(OCH₂Ph)(PhCHO)(Cl)(PMe₃) at 22.0 °C.

$$k(22.0\text{ °C}) = (1.378 \pm 0.007)\text{ s}^{-1}$$

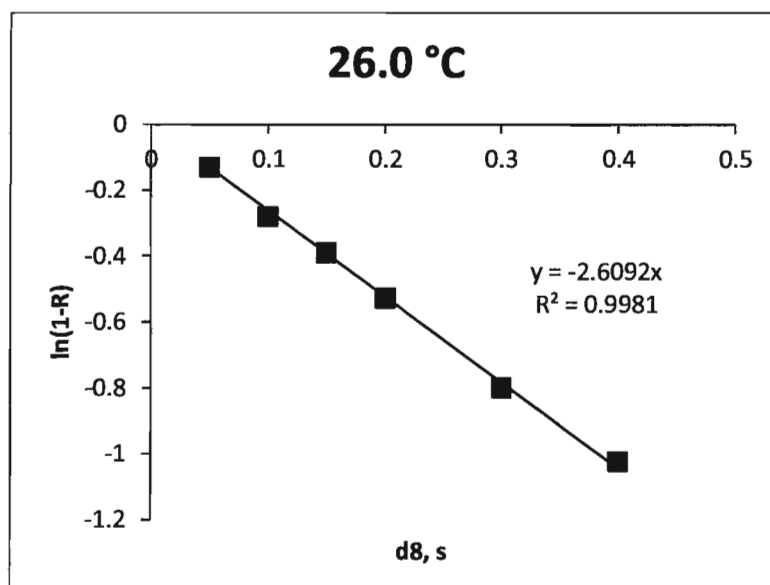


Figure V-85. Ln(1-R) vs. mixing time (d8) plot for the exchange of two enantiomers of (ArN)Mo(OCH₂Ph)(PhCHO)(Cl)(PMe₃) at 26.0 °C.

$$k(26.0\text{ °C}) = (2.61 \pm 0.05)\text{ s}^{-1}$$

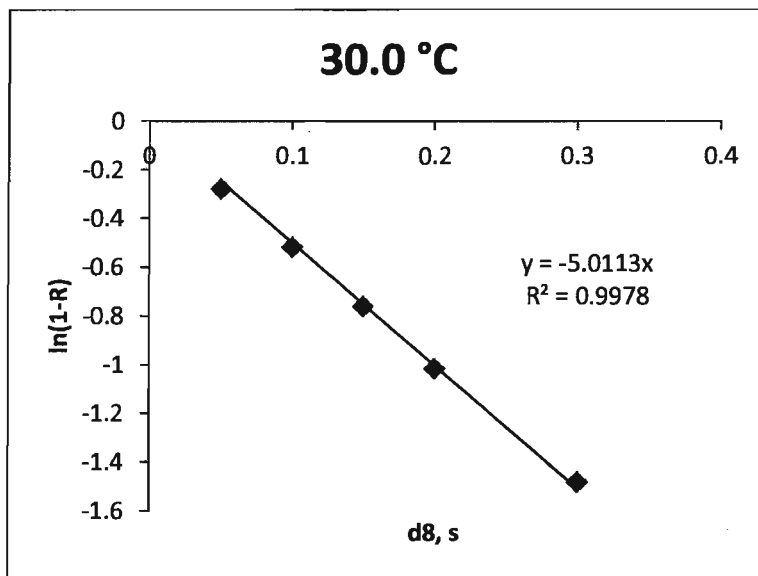


Figure V-86. Ln(1-R) vs. mixing time (d8) plot for the exchange of two enantiomers of (ArN)Mo(OCH₂Ph)(PhCHO)(Cl)(PMe₃) at 30.0 °C.

$$k(30.0\text{ °C}) = (5.01 \pm 0.04)\text{ s}^{-1}$$

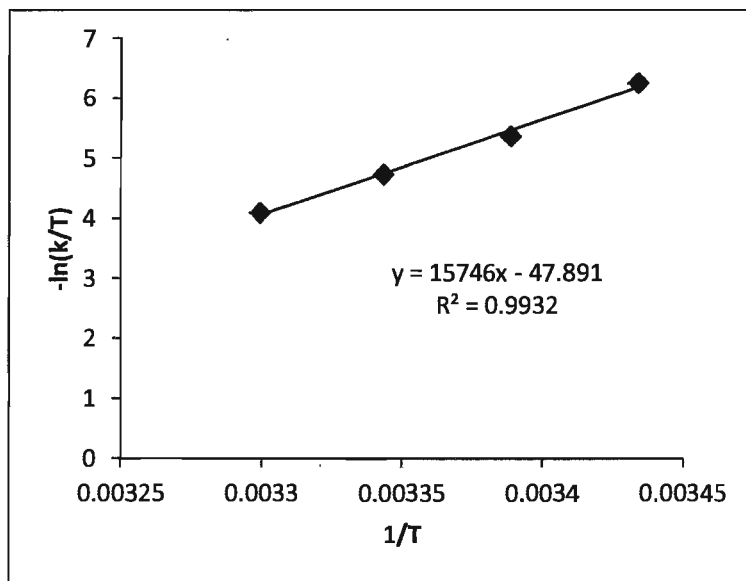


Figure V-87. Eyring plot for the exchange of two enantiomers of (ArN)Mo(OCH₂Ph)(PhCHO)(Cl)(PMe₃).

Activation parameters were extracted from the Eyring plot (Figure V-87): $\Delta H^\ddagger = (1.31 \pm 0.08) \cdot 10^2$ kJ/mol, $\Delta S^\ddagger = (2.00 \pm 0.27) \cdot 10^2$ J/(K·mol).

(ArN)Mo(OCH₂Ph)(PhCHO)(Cl)(PMe₃): no exchange of phosphines

Irradiation of the free phosphine peak at 0.913 ppm showed no exchange with the bound PMe₃ in the timescale of EXSY NMR experiment (Figure V-88).

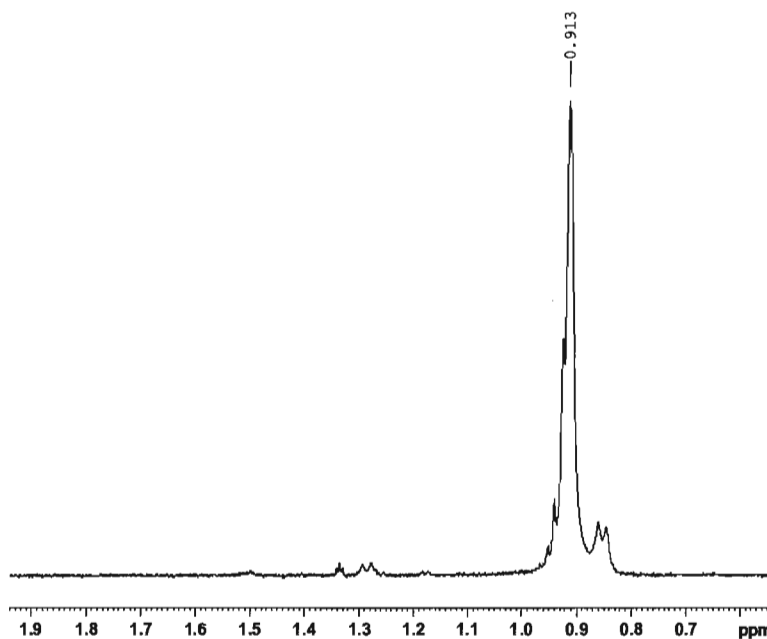


Figure V-88. Selective ge-1D EXSY NMR experiment of the sample containing (ArN)Mo(OCH₂Ph)(PhCHO)(Cl)(PMe₃): irradiation of the PMe₃ protons at the frequency of 0.913 ppm with the mixing time of 1.000 s (600 MHz machine).

(ArN)Mo(OCH₂Ph)(PhCHO)(Cl)(PMe₃): exchange of aldehydes

Irradiation of the free benzaldehyde peak at 9.768 ppm with the Selective ge-1D EXSY NMR experiment in a solution with (ArN)Mo(OCH₂Ph)(PhCHO)(Cl)(PMe₃) showed fast exchange between the coordinated and the external benzaldehyde (Figure V-89). The experiment for the same sample has been repeated with the irradiation of the coordinated benzaldehyde at 5.505 ppm (Figure V-90).

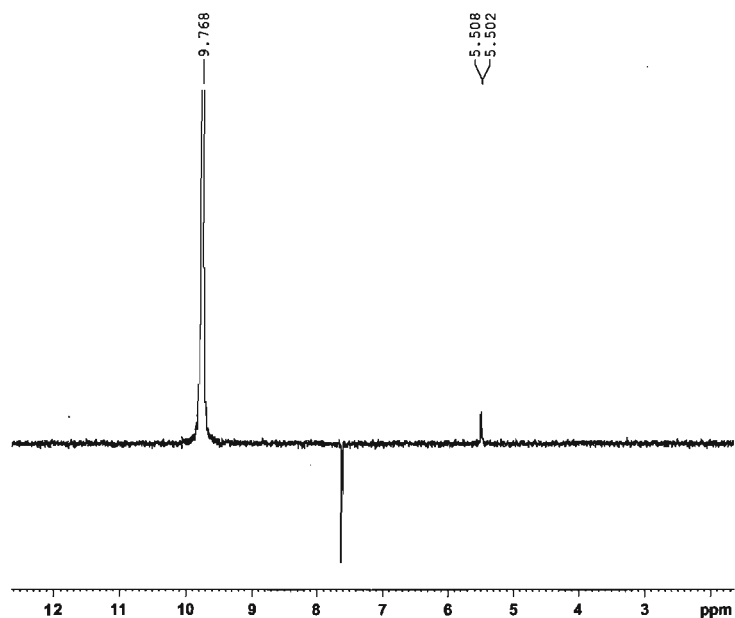


Figure V-89. Selective ge-1D EXSY NMR experiment of the sample containing $(\text{ArN})\text{Mo}(\text{OCH}_2\text{Ph})(\text{PhCHO})(\text{Cl})(\text{PMe}_3)$: irradiation of free PhCHO protons at the frequency of 9.766 ppm with the mixing time of 1.000 s (600 MHz machine).

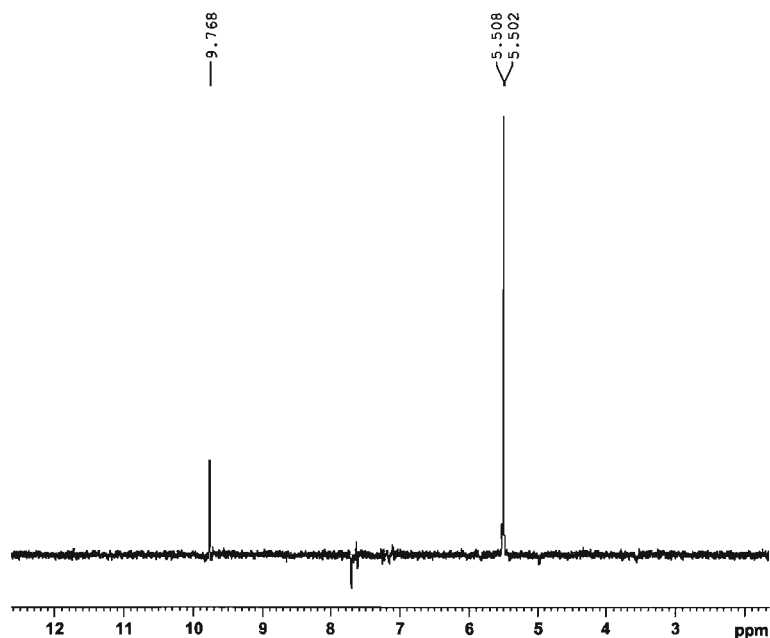


Figure V-90. Selective ge-1D EXSY NMR experiment of the sample containing $(\text{ArN})\text{Mo}(\text{OCH}_2\text{Ph})(\text{PhCHO})(\text{Cl})(\text{PMe}_3)$: irradiation of free PhCHO protons at the frequency of 5.505 ppm with the mixing time of 1.000 s (600 MHz machine).

Reaction of (ArN)Mo(OCH₂Ph)(Cl)(PMe₃)₃ with PhSiH₃ (5 eq)

Phenylsilane (15.1 mg, 0.140 mmol) was added to a solution of (ArN)Mo(OCH₂Ph)(Cl)(PMe₃)₃ (18.0 mg, 0.028 mmol) in the presence of PMe₃ (64.0 mg, 0.840 mmol). The reaction was monitored by ¹H NMR at 10.0 °C. The reaction provided formation of (ArN)Mo(H)(Cl)(PMe₃)₃ as the end-product and (ArN)Mo(Cl)₂(PMe₃)₃ (~18%) as a result of partial redistribution/decomposition. Kinetic data were linearized in Ln(C)-time coordinates (Figure V-91).

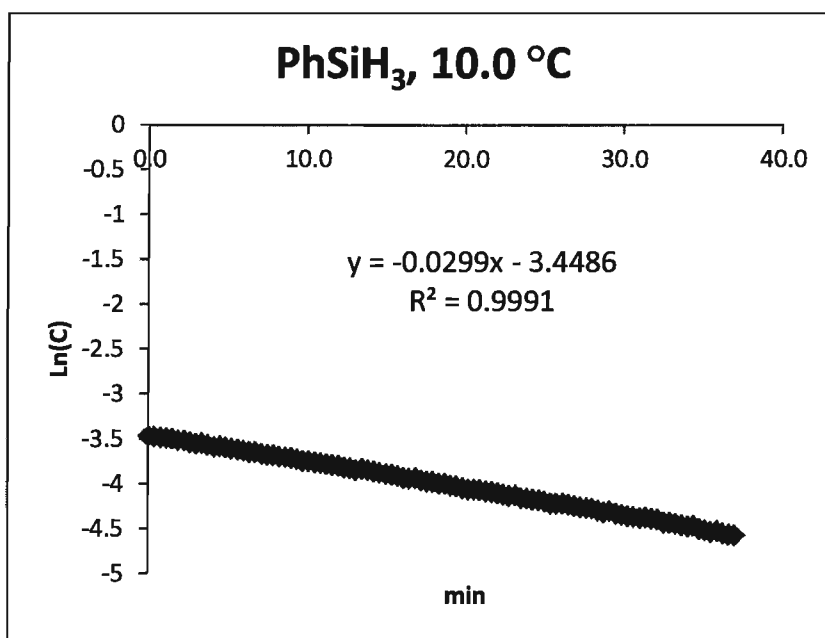


Figure V-91. Ln(C) vs. time plot for the reaction of (ArN)Mo(OCH₂Ph)(Cl)(PMe₃)₃ with PhSiH₃ (5 eq.) in the presence of PMe₃ (30 eq.) at 10.0 °C.

$$k_H(10.0\text{ °C}) = (2.99 \pm 0.01) \cdot 10^{-2} \text{ min}^{-1} = (4.98 \pm 0.02) \cdot 10^{-4} \text{ s}^{-1}$$

Reaction of (ArN)Mo(OCH₂Ph)(Cl)(PMe₃)₃ with PhSiD₃ (5 eq)

Phenylsilane-*d*₃ (15.6 mg, 0.140 mmol) was added to a solution of (ArN)Mo(OCH₂Ph)(Cl)(PMe₃)₃ (18.0 mg, 0.028 mmol) in the presence of PMe₃ (64.0 mg, 0.840 mmol). The reaction was monitored by ¹H NMR at 10 °C. The reaction provided formation of (ArN)Mo(D)(Cl)(PMe₃)₃ as the end-product and (ArN)Mo(Cl)₂(PMe₃)₃ (~18%) as a result of partial redistribution/decomposition. Kinetic data were linearized in Ln(C)-time plot (Figure V-92).

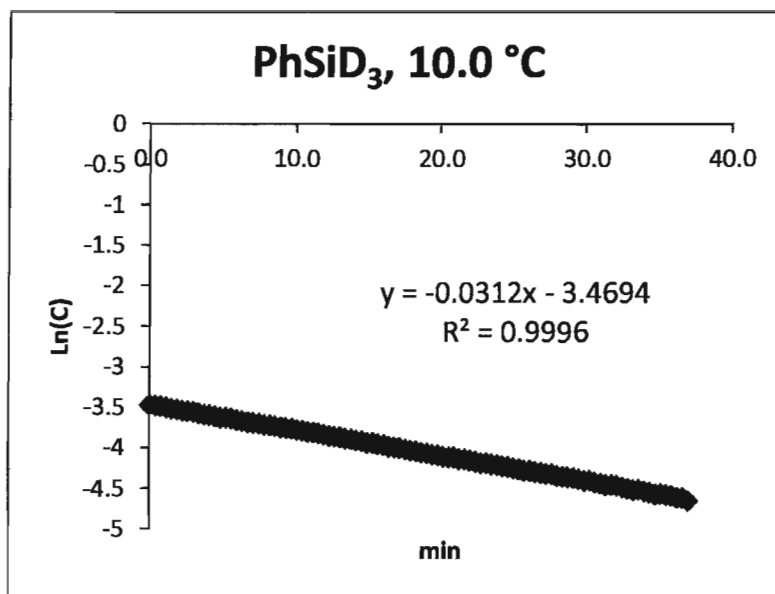


Figure V-92. Ln(C) vs. time plot for the reaction of (ArN)Mo(OCH₂Ph)(Cl)(PMe₃)₃ with PhSiD₃ (5 eq.) in the presence of PMe₃ (30 eq.) at 10.0 °C.

$$k_D(10.0\text{ °C}) = (3.12 \pm 0.01) \cdot 10^{-2} \text{ min}^{-1} = (5.20 \pm 0.02) \cdot 10^{-4} \text{ s}^{-1},$$

$$\text{KIE} = \frac{k_H}{k_D} = \frac{2.99}{3.12} \cong 0.96$$

Reversible formation of (ArN)Mo(OCH₂Ph)(η^2 -PhCHO)(Cl)(PMe₃) from (ArN)Mo(OCH₂Ph)(Cl)(PMe₃)

Benzaldehyde (28.6 μ l, 0.280 mmol) was added to a solution of (ArN)Mo(OCH₂Ph)(Cl)(PMe₃) (18.0 mg, 0.0280 mmol) in C₆D₆ (0.60 ml). NMR analysis showed fast formation of (ArN)Mo(OCH₂Ph)(η^2 -PhCHO)(Cl)(PMe₃). The excess of benzaldehyde was evaporated, and the residue was re-dissolved in C₆D₆. Addition of PMe₃ (28.9 μ l, 0.280 mmol) fully regenerated the starting material.

Reaction of (ArN)Mo(OCH₂Ph)(Cl)(PMe₃)₃ with pivalaldehyde (*t*-BuCHO)

Pivalaldehyde (10.0 μ l, 0.092 mmol) was added to a solution of (ArN)Mo(OCH₂Ph)(Cl)(PMe₃)₃ (45.6 mg, 0.071 mmol) in C₆D₆ (0.60 ml). Next day, 50% of the benzyloxy complex reacted, and free benzaldehyde peak was observed at 9.64 ppm in ¹H NMR spectrum.

Attempts to prepare (ArN)Mo(OCy)(Cy=O)(Cl)(PMe₃)

Cyclohexanone (2.5 μ l, 0.022 mmol) was added to a solution of (ArN)Mo(OCy)(Cl)(PMe₃)₃ (14.0 mg, 0.022 mmol) in C₆D₆ (0.60 ml). Triphenylborane (5.3 mg, 0.022 mmol) was added, and colour of the solution quickly changed from green to brown. After 10 min, the reaction mixture consisted of (ArN)Mo(OCy)(Cl)(PMe₃)₃ (~50%) and (ArN)Mo(Cl)₂(PMe₃)₃ (~50%) and Ph₃P*BPh₃. The starting material finally decomposed giving a mixture of unidentified products and (ArN)Mo(Cl)₂(PMe₃)₃.

Reactivity of (ArN)Mo(H)(Cl)(PMe₃)₃ with PhSiD₃

Phenylsilane-*d*₃ (10.0 μ l, 0.0788 mmol) was added to a solution of (ArN)Mo(H)(Cl)(PMe₃)₃ (10.0 mg, 0.0187 mmol) in C₆D₆ (0.60 ml). The reaction mixture was monitored by ¹H NMR at RT. Formation of (ArN)Mo(D)(Cl)(PMe₃)₃ was observed: ~9% (10 min), ~55% (6 hours), and ~100% (26 hours).

Hydrosilylation of benzaldehyde with PMHS catalyzed by (ArN)Mo(H)(Cl)(PMe₃)₃

Benzaldehyde (39.6 mg, 0.371 mmol) and PMHS (23.0 μ l, 0.371 mmol) were added to a solution of (ArN)Mo(H)(Cl)(PMe₃)₃ (10.0 mg, 0.0190 mmol, 5 mol%) in C₆D₆ (0.60 ml). The reaction mixture was heated for two days at 50 °C. with the ~50% conversion of the benzaldehyde.

Hydrosilylation of acetophenone with PMHS catalyzed by (ArN)Mo(H)(Cl)(PMe₃)₃

Acetophenone (44.8 mg, 0.371 mmol) and PMHS (23.0 μ l, 0.371 mmol) were added to a solution of (ArN)Mo(H)(Cl)(PMe₃)₃ (10.0 mg, 0.0190 mmol, 5 mol%) in C₆D₆ (0.60 ml). The reaction mixture was heated for two days at 50 °C with 100% conversion of the acetophenone.

Hydrosilylation of cyclohexanone with PMHS catalyzed by (ArN)Mo(H)(Cl)(PMe₃)₃

Cyclohexanone (36.6 mg, 0.371 mmol) and PMHS (23.0 μ l, 0.371 mmol) were added to a solution of (ArN)Mo(H)(Cl)(PMe₃)₃ (10.0 mg, 0.0190 mmol, 5 mol%) in C₆D₆ (0.60 ml). The reaction was complete in three hours at RT.

Hydrosilylation of cyclohexanone with PhSiH₃ catalyzed by (ArN)Mo(H)(Cl)(PMe₃)₃

Cyclohexanone (11.0 mg, 0.112 mmol) and PhSiH₃ (12.1, 0.112 mmol) were added to a solution of (ArN)Mo(H)(Cl)(PMe₃)₃ (3.0 mg, 0.0060 mmol, 5 mol%) in C₆D₆ (0.60 ml). The reaction was complete in 35 min at RT.

Hydrosilylation of cyclohexanone with PhSiH₃ catalyzed by (ArN)Mo(O-Cy)(Cl)(PMe₃)₃

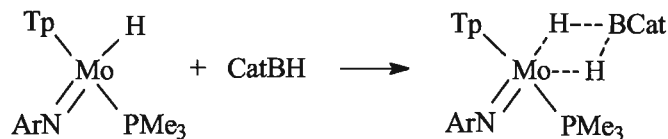
Cyclohexanone (11.0 mg, 0.112 mmol) and PhSiH₃ (12.1, 0.112 mmol) were added to a solution of (ArN)Mo(O-Cy)(Cl)(PMe₃)₃ (3.5 mg, 0.006 mmol, 5 mol%) in C₆D₆ (0.60 ml). The reaction was complete in 3 hours at RT.

Table V-6. Hydrosilylation of organic substrates using (ArN)Mo(H)(Cl)(PMe₃)₃ as a catalyst

Substrate	Silane	Product	Reaction conditions	Conversion of organic substrate	Yield, according to ¹ H-NMR	Catalyst mol, %	Turnover number (TON)
Cyclohexanone	PhSiH ₃	CyOSiH ₂ Ph, (CyO) ₂ SiHPh	35 min, RT	100%	79% 21%	5	20
Cyclohexanone	PhSiH ₃	CyOSiH ₂ Ph (CyO) ₂ SiHPh	3 h, RT	100%	60% 40%	5	20
PhCHO	PMHS	(PhCH ₂ O) _x (PMHS)	2 days, 50 °C	~50%	~50%	6	~8
PhCOCH ₃	PMHS	(Ph(Me)CHO) _x (PMHS)	2 days, 50 °C	100 %	100%	6	17
Cyclohexanone	PMHS	(CyO) _x (PMHS)	3 hours, RT	100 %	100%	6	17

V. 7. Hydroboration catalyzed by (Tp)(ArN)Mo(H)(PMe₃)

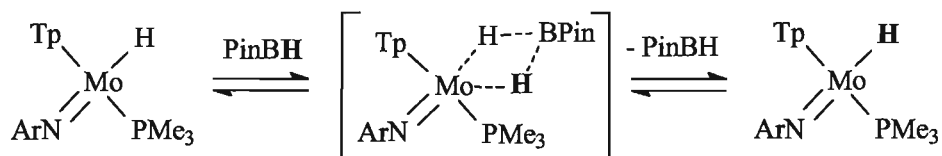
Reaction between (Tp)(ArN)Mo(H)(PMe₃) and catecholborane



Catecholborane (4.3 mg, 0.036 mmol) was added to a solution of (Tp)(ArN)Mo(H)(PMe₃) (20.0 mg, 0.036 mmol) in toluene-*d*₈ (0.60 ml). ¹H NMR spectrum of the resulting mixture showed a broad singlet at 4.06 ppm (bs, 2H, Mo(H)₂B) resulted from the coalescence of the Mo-H doublet (3.66 ppm) with the H-B quartet of catecholborane. All other signals of (Tp)(ArN)Mo(H)(PMe₃) were observed unchanged in ¹H NMR spectrum. ¹¹B NMR spectrum of catecholborane, in the presence of (Tp)(ArN)Mo(H)(PMe₃), showed the singlet at 28.7 ppm (bs, 1B).

Several ¹H NMR experiments have been done in attempts to split the broadened singlet 4.06 (bs, 2H, Mo-H, B-H) into two parts by slowing down the exchange at lower temperatures (-24.6, -44.5, -47.3, -52.0 and -70 °C). The broadness of the signal did not change. The exchange was too fast and did not allow us to reach the coalescence temperature. At the elevated temperatures (22.0, 31.2, 48.6 °C) the broad peak did not become less broadened either. That also proved B-H interactions, and influence of the quadruple nature of the boron atom.

The reaction of (Tp)(ArN)Mo(H)(PMe₃) with pinacolborane



Pinacolborane, (Tp)(ArN)Mo(H)(PMe₃) and their mixture were analyzed by ¹H and ¹¹B NMR. The characteristic NMR signals of each reagent were not affected by the presence

of the other reagent (Table V-7). No peak shifting, broadening or coalescence were observed.

Table V-7. Characteristic signals in the ^1H and ^{11}B NMR spectra for pinacolborane, $(\text{Tp})(\text{ArN})\text{Mo}(\text{H})(\text{PMe}_3)$ and their mixture.

^1H NMR, C_6D_6 (solvent)	B-H	CH_3	Mo-H
PinBH	4.28 ppm (q, $^1J_{\text{B-H}} = 129.8$ Hz)	0.99 ppm (s, 12H, 4 CH_3)	-
$(\text{Tp})(\text{ArN})\text{Mo}(\text{H})(\text{PMe}_3)$	-	-	3.67 ppm (d, $^2J_{\text{H-P}} = 21.4$ Hz)
PinBH + $(\text{Tp})(\text{ArN})\text{Mo}(\text{H})(\text{PMe}_3)$	4.28 ppm (q, $^1J_{\text{B-H}} = 129.8$ Hz)	0.99 ppm (s, 12H, 4 CH_3)	3.67 ppm (d, $^2J_{\text{H-P}} = 21.4$ Hz)

^{11}B NMR	B-H, PinBH
PinBH	28.6 ppm (d, $^1J_{\text{B-H}} = 174.1$ Hz)
PinBH + $(\text{Tp})(\text{ArN})\text{Mo}(\text{H})(\text{PMe}_3)$	28.6 ppm (d, $^1J_{\text{B-H}} = 174.1$ Hz)

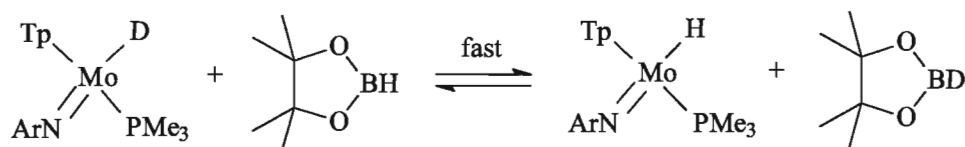
The exchange between Mo-H and B-H was not observed by the Selective ge-1D EXSY NMR experiment at 22 °C (d8 = 0.300 s, O1P = 3.776 ppm (Mo-H)), 50 °C (d8 = 0.300 ppm, O1P = 3.745 ppm (Mo-H)), and 70 °C (d8 = 0.300 s, O1P = 3.700 ppm (Mo-H)).

Preparation of $(\text{Tp})(\text{ArN})\text{Mo}(\text{D})(\text{PhCHO})$

$(\text{Tp})(\text{ArN})\text{Mo}(\text{H})(\text{PMe}_3)$ (10.0 mg, 0.018 mmol) was dissolved in isopropanol- d_8 (0.60 ml). All Mo-H hydrides were replaced by deuterium within 3 hours at 40 °C. The solvent was evaporated. The crude residue was dried under vacuum, then re-dissolved in C_6D_6 (0.60 ml). ^1H -NMR (300 MHz; C_6D_6 ; 298K; δ , ppm): 1.04 (m, 6H, 2 CH_3 , *iPr*), 1.34 (d, $^2J_{\text{H-H}} = 6.6$ Hz, 6H, 2 CH_3 , *iPr*), 1.36 (d, $^2J_{\text{H-P}} = 7.4$ Hz, 9H, PMe_3), 4.35 (m, 2H, *iPr*), 5.68 (dd, $^2J_{\text{H-H}} = 2.1$ Hz, 1H^a, *Pz*), 5.90 (dd, $^2J_{\text{H-H}} = 2.1$ Hz, 1H^b, *Pz*), 6.09 (dd, $^2J_{\text{H-H}} = 2.1$ Hz,

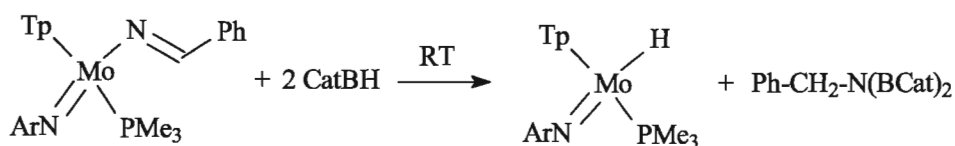
1H^c , Pz), 7.24 (d, $^2J_{\text{H-H}} = 2.1$ Hz, 1H^a , Pz), 7.45 (d, $^2J_{\text{H-H}} = 2.1$ Hz, 1H^a , Pz), 7.52 (d, $^2J_{\text{H-H}} = 2.1$ Hz, 1H^b , Pz), 7.56 (d, $^2J_{\text{H-H}} = 2.1$ Hz, 1H^c , Pz), 7.76 (d, $^2J_{\text{H-H}} = 2.1$ Hz, 1H^c , Pz), 7.88 (d, $^2J_{\text{H-H}} = 2.1$ Hz, 1H^b , Pz). ^{13}C -NMR (150.92 MHz; C_6D_6 ; 298 K; δ , ppm): 22.2 (d, $^2J_{\text{P-H}} = 22.0$ Hz, PMe_3), 23.2 (bs, CH_3 , iPr), 27.3 (bs, CH, iPr), 104.0 (Pz^a), 105.0 (Pz^c), 105.5 (Pz^b), 123.2 (*m*-C, 2CH, Ar), 123.8 (*p*-C, CH, Ar), 133.6 (Pz^a), 134.8 (Pz^b), 134.9 (Pz^c), 141.9 (Pz^b), 142.5 (Pz^a), 143.7 (Pz^c), 152.7 (*ipso*-C, C-N, Ar). ^{31}P -NMR (121.5 MHz; C_6D_6 ; 298 K; δ , ppm): 15.6 (s, 1P, PMe_3). ^{11}B -NMR (96.3 MHz; C_6D_6 ; 298 K; δ , ppm): -4.1 (bs). ^{31}P -NMR (121.5 MHz; C_6D_6 ; 298 K; δ , ppm): 15.6 (s, 1P, PMe_3).

The reaction of $(\text{Tp})(\text{ArN})\text{Mo}(\text{D})(\text{PMe}_3)$ with pinacolborane



Pinacolborane (2.3 mg, 0.018 mmol) was added to a solution of $(\text{Tp})(\text{ArN})\text{Mo}(\text{D})(\text{PMe}_3)$ (10.0 mg, 0.018 mmol). Deuterium scrambling occurred within 5 min. ^{11}B -NMR (96.3 MHz; C_6D_6 ; 298 K; δ , ppm): 28.6 (d, $^1J_{\text{B-H}} = 174.1$ Hz, PinBH, ~50%), 28.6 (bs, PinBD, ~50%).

Reaction of $(\text{Tp})(\text{ArN})\text{Mo}(-\text{N}=\text{CHPh})(\text{PMe}_3)$ with catecholborane

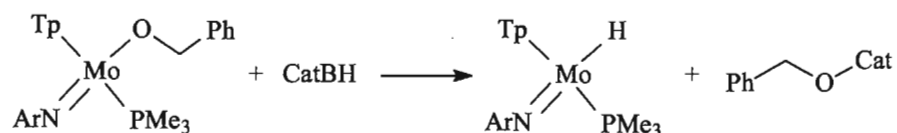


Catecholborane (5.8 mg, 0.0486 mmol) was added to a solution of $(\text{Tp})(\text{ArN})\text{Mo}(-\text{N}=\text{CHPh})(\text{PMe}_3)$ (16.2 mg, 0.0243 mmol). The reaction provided formation of $\text{Ph-CH}_2\text{-N(BCat)}_2$ and $(\text{Tp})(\text{ArN})\text{Mo}(\text{H})(\text{PMe}_3)$ in less than 10 min. ^1H -NMR (300 MHz; CDCl_3 ; 298K; δ , ppm): 4.73 (s, 2H, $\text{CH}_2\text{-N}$), 6.99-7.06 (m, 4H, Ar, BCat), 7.18-7.24 (m, 4H, Ar, BCat), 7.24-7.34 (m, 3H, Ph), 7.44-7.49 (m, 2H, Ph). ^{11}B -NMR (96.3 MHz; C_6D_6 ; 298 K; δ , ppm): 27.58 (bs).

Reaction of (Tp)(ArN)Mo(-N=CHPh)(PMe₃) with pinacolborane

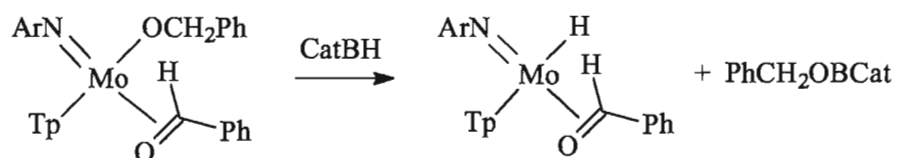
Pinacolborane (2.9 mg, 0.023 mmol) was added to a solution of (Tp)(ArN)Mo(-N=CHPh)(PMe₃) (15.0 mg, 0.023 mmol) in C₆D₆ (0.60 ml). The sample was left for one month at RT, and then heated at 50 °C for several days. Reaction was not observed.

Reaction of (Tp)(ArN)Mo(OCH₂Ph)(PMe₃) with catecholborane



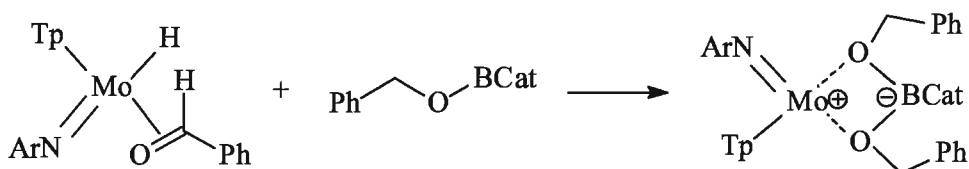
Catecholborane (1.8 mg, 0.015 mmol) was added to a solution of (Tp)(ArN)Mo(-N=CHPh)(PMe₃) (10.0 mg, 0.015 mmol). The reaction provided formation of PhCH₂OCat and (Tp)(ArN)Mo(H)(PMe₃) in less than 10 min. ¹H-NMR (300 MHz; CDCl₃; 298K; δ, ppm): 4.85 (s, 2H, -CH₂OCat)

Reaction of (Tp)(ArN)Mo(OCH₂Ph)(PhCHO) with CatBH



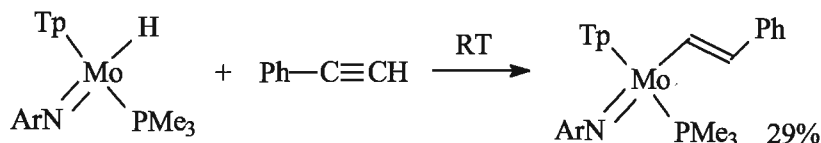
Catecholborane (1.7 mg, 0.014 mmol) was added to a solution of (Tp)(ArN)Mo(OCH₂Ph)(PhCHO) (10.0 mg, 0.014 mmol) in C₆D₆ (0.60 ml). The reaction provided immediate formation of (Tp)(ArN)Mo(H)(PhCHO) and PhCH₂OCat. ¹H-NMR (300 MHz; CDCl₃; 298K; δ, ppm): 0.54 (bd, *J* = 6.7 Hz, 3H, CH₃, iPr), 0.64 (bd, *J* = 6.7 Hz, 3H, CH₃, iPr), 1.52 (m, 6H, 2CH₃, iPr), 3.22 (m, 1H, iPr), 4.51 (s, 1H, Mo-PhCHO), 5.60 (m, 1H, Pz), 5.66 (m, 1H, Pz), 6.02 (m, 1H, Pz), 6.98-7.23 (5H, m, Ph), 7.39 (m, 1H, Pz), 7.44 (m, 1H, Pz), 7.47 (m, 1H, Pz), 7.70 (m, 1H, Pz), 8.10 (m, 1H, Pz), 8.42 (m, 1H, Pz), 8.89 (s, 1H, Pz).

Reaction of (Tp)(ArN)Mo(H)(PhCHO) with PhCH₂OBCat



(Tp)(ArN)Mo(H)(PhCHO) (8.5 mg, 0.014 mmol), prepared *in situ* by the reaction between (Tp)(ArN)Mo(OCH₂Ph)(PhCHO) and CatBH, further reacts with PhCH₂OBCat (3.2 mg, 0.014 mmol) within one hour at RT giving (Tp)(ArN)Mo(OCH₂Ph)₂(BCat). ¹H-NMR (600 MHz; CDCl₃; 298K; δ, ppm): 1.13 (bd, *J* = 6.77 Hz, 12H, 4CH₃, iPr), 3.75 (m, 2H, 2CH, iPr), 4.69 (d, *J* = 13.0 Hz, 2H, CH₂-O), 4.89 (d, *J* = 13.0 Hz, 2H, CH₂-O), 5.67 (m, 2H, 2Pz), 5.83 (m, 1H, Pz), 6.33 (m, 2H, Pz), 6.80-6.87 (m, 2H, BCat), 6.80-6.96 (m, 10H, 2Ph), 7.08-7.12 (d, *J* = 7.7 Hz, 2 *m*-H, Ar), 7.13-7.20 (m, 2H, BCat), 7.22 (m, 1H, Pz), 7.26-7.31 (t, *J* = 7.7, 1 *p*-H, Ar), 7.41 (m, 2H, Pz), 9.19 (m, 1H, Pz). ¹³C-NMR (75.5 MHz; C₆D₆; 298 K; δ, ppm): 25.0 (CH₃, iPr), 28.1 (CH, iPr), 72.2 (OCH₂), 105.7 (Pz), 107.0 (2Pz), 110.2 (2C, BCat), 119.7 (1C, BCat), 120.3 (1C, BCat), 124.1 (*m*-C, 2C, Ar) 126.3 (*p*-C, 1C, Ar), 127.9 (4C, *m*-C, 2Ph), 129.3 (4C, *o*-C, 2Ph), 133.7 (1C, Pz), 137.1 (2Pz), 138.8 (2C, *ipso*-C, 2Ph), 145.6 (Pz), 145.8 (2Pz), 147.8 (1C, C-N, Ar), 152.56 (2C, BCat), 153.2 (2C, *p*-C, 2Ph), 155.7 (*o*-C, 2C, Ar). ¹¹B-NMR (96.3 MHz; C₆D₆; 298 K; δ, ppm): 16.7 (s).

Reaction of (Tp)(ArN)Mo(H)(PMe₃) with PhC≡CH



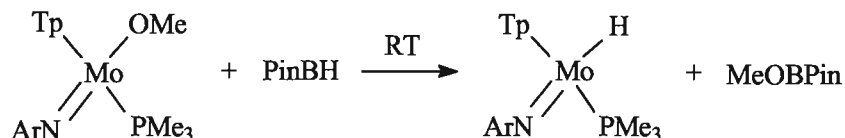
(Tp)(ArN)Mo(H)(PMe₃) (19.0 mg, 0.034 mmol) and phenylacetylene (3.5 mg, 3.7 μl, 0.034 mmol) were mixed in C₆D₆ (0.60 ml). The reaction provided formation of (Tp)(ArN)Mo(-CH=CH-Ph)(PMe₃) with 29% yield in 3.5 d at RT. Formation of other by-products and partial polymerization of the phenylsilane were observed. ¹H-NMR (300 MHz; CDCl₃; 298K; δ, ppm): 0.97 (d, *J* = 6.82 Hz, 6H, 2CH₃, iPr), 1.15 (d, *J* = 7.68 Hz, 9H, PMe₃), 1.24 (d, *J* = 6.82 Hz, 6H, 2CH₃, iPr), 3.86 (sept, *J* = 6.82 Hz, 2H, CH, iPr),

5.74 (m, 1H, Pz), 5.93 (m, 1H, Pz), 6.04 (m, 1H, Pz), 6.19 (1H, =CH-Ph, position determined by ^1H - ^1H COSY experiment), 10.59 (dd, $^3J_{\text{H-H}} = 17.06$ Hz, $^3J_{\text{H-P}} = 4.40$ Hz, 1H, Mo-CH=). ^{31}P -NMR (121.5 MHz; C_6D_6 ; 298 K; δ , ppm): 7.41 (1P, PMe_3)

Preparation of $(\text{Tp})(\text{ArN})\text{Mo}(\text{OCH}_3)(\text{PMe}_3)$

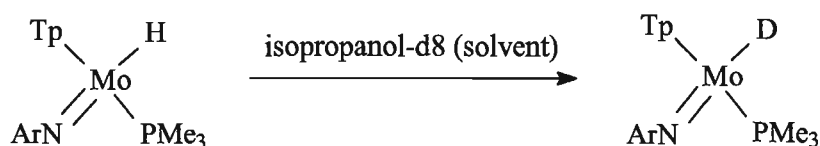
$(\text{Tp})(\text{ArN})\text{Mo}(\text{H})(\text{PMe}_3)$ (10.0 mg, 0.0180 mmol) was dissolved in methanol (0.60 ml). The color of the solution gradually changed from dark brown to green within 30 min at RT. The solvent was evaporated. The residue was dried under vacuum and re-dissolved in C_6D_6 (0.60 ml). Reaction provided formation of $(\text{Tp})(\text{ArN})\text{Mo}(\text{OCH}_3)(\text{PMe}_3)$. NMR yield: 100%. ^1H -NMR (300 MHz; CDCl_3 ; 298K; δ , ppm): 0.83-0.99 (bm, 6H, 2CH_3 , iPr), 1.20 (d, $J = 7.28$ Hz, 9H, PMe_3), 1.25-1.31 (bm, 6H, 2CH_3 , iPr), 3.83 (bm, 2H, iPr), 4.09 (s, 3H, OCH_3), 5.89 (m, 1H, Pz), 5.94 (m, 1H, Pz), 5.97 (m, 1H, Pz), 6.99-7.04 (m, 2H, Ar), 7.14-7.20 (m, 1H, Ar), 7.26 (m, 1H, Pz), 7.41 (m, 1H, Pz), 7.50 (m, 1H, Pz), 7.53 (m, 1H, Pz), 7.61 (m, 1H, Pz), 7.85 (m, 1H, Pz). ^{31}P -NMR (121.5 MHz; C_6D_6 ; 298 K; δ , ppm): 9.29 (1P, PMe_3)

Reaction of $(\text{Tp})(\text{ArN})\text{Mo}(\text{OCH}_3)(\text{PMe}_3)$ with PinBH



Pinacolborane (2.3 mg, 0.018 mmol) was added to a solution of $(\text{Tp})(\text{ArN})\text{Mo}(\text{OCH}_3)(\text{PMe}_3)$ (11.0 mg, 0.0180 mmol) in C_6D_6 (0.60 ml). The reaction provided immediate formation of $(\text{Tp})(\text{ArN})\text{Mo}(\text{H})(\text{PMe}_3)$ and PinBOMe. ^1H -NMR (300 MHz; CDCl_3 ; 298K; δ , ppm): 1.04 (s, 12H, 4CH_3 , PinBOMe), 3.51 (s, 3H, OCH_3 , PinBOMe). ^{11}B -NMR (96.3 MHz; C_6D_6 ; 298 K; δ , ppm): 22.9 (bs, PinBOMe).

Preparation of $(\text{Tp})(\text{ArN})\text{Mo}(\text{D})(\text{PMe}_3)$



(Tp)(ArN)Mo(H)(PMe₃) (10.0 mg, 0.018 mmol) was dissolved in isopropanol-*d*₈. The reaction was monitored by ¹H NMR until the signal of Mo-H disappeared. Then, the solvent was evaporated, and the sample was re-dissolved in C₆D₆ (0.60 ml). ¹H-NMR (300 MHz; C₆D₆; 298K; δ, ppm): 1.04 (m, 6H, 2CH₃, *iPr*), 1.34 (d, ²J_{H-H} = 6.6 Hz, 6H, 2CH₃, *iPr*), 1.36 (d, ²J_{H-P} = 7.4 Hz, 9H, PMe₃), 4.35 (m, 2H, *iPr*), 5.68 (m, 1H^a, Pz), 5.90 (m, 1H^b, Pz), 6.09 (m, 1H^c, Pz), 7.24 (m, 1H^a, Pz), 7.45 (m, 1H^a, Pz), 7.52 (m, 1H^b, Pz), 7.56 (m, 1H^c, Pz), 7.76 (m, 1H^c, Pz), 7.88 (m, 1H^b, Pz). ³¹P-NMR (121.5 MHz; C₆D₆; 298 K; δ, ppm): 15.62 (s, 1P, PMe₃). ¹¹B-NMR (96.3 MHz; C₆D₆; 298 K; δ, ppm): -4.1 (bs)

Reaction of (Tp)(ArN)Mo(H)(PMe₃) with *p*-nitroacetophenone

p-Nitroacetophenone (2.9 mg, 0.018 mmol) was added to a solution of (Tp)(ArN)Mo(H)(PMe₃) (10.0 mg, 0.018 mmol) in C₆D₆ (0.60 ml). The color changed immediately from brown to black, following by formation of a large amount of black precipitate.

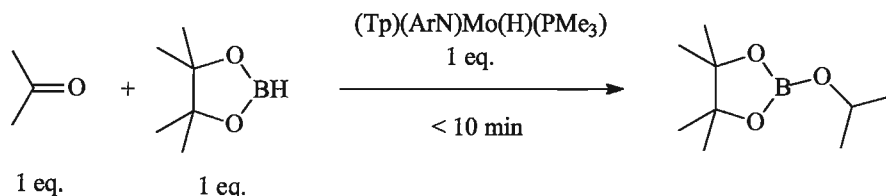
Studying the effect of ketones and nitriles coordination to catecholborane

Several experiments were made to reveal the effect of ketones and nitriles coordination to catecholborane. The table below represents the chemical shifts of B-H signal for catecholborane and its mixture with various carbonyls and benzonitrile (Table V-8).

Table V-8. Chemical shifts of the B-H signal (¹H NMR) for catecholborane and its mixture with various carbonyls and benzonitrile.

¹ H NMR, C ₆ D ₆ (solvent)	B-H
CatBH	4.57 ppm (q, ¹ J _{H-B} = 142.5 Hz)
CatBH + PhCOCH ₃	4.57 ppm (q, ¹ J _{H-B} = 142.5 Hz)
CatBH + cyclohexanone	4.57 ppm (q, ¹ J _{H-B} = 142.5 Hz)
CatBH + 2-methylcyclohexanone	4.57 ppm (q, ¹ J _{H-B} = 142.5 Hz)
CatBH + PhCN	4.57 ppm (q, ¹ J _{H-B} = 142.5 Hz)

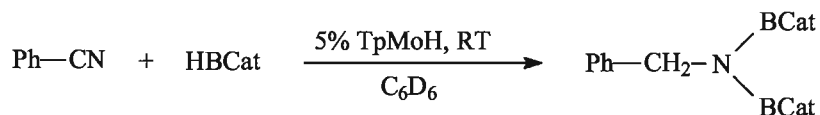
Stoichiometric reaction between (Tp)(ArN)Mo(H)(PMe₃), acetone and pinacolborane



Acetone (1.0 mg, 0.018 mmol), pinacolborane (2.3 mmol, 0.018 mmol) and (Tp)(ArN)Mo(H)(PMe₃) (10 mg, 0.018 mmol) were dissolved in C₆D₆ (0.60 ml). The reaction proceeded within 10 min at RT.

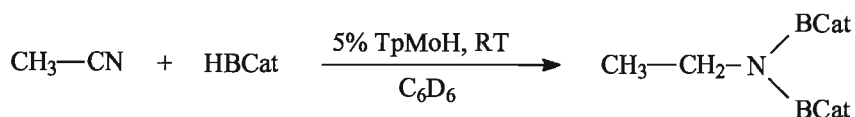
HYDROBORATION CATALYSED BY (Tp)(ArN)Mo(H)(PMe₃)

Hydroboration of PhCN with catecholborane



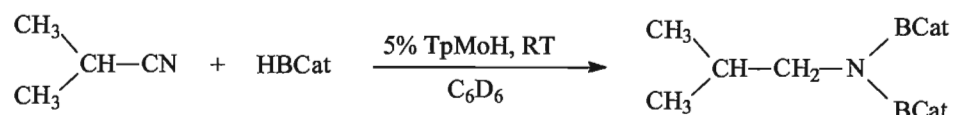
Catecholborane (31.4 mg, 0.262 mmol) was added to a solution of benzonitrile (13.5 mg, 0.131 mmol) in C₆D₆ (0.60 ml) in the presence of (Tp)(ArN)Mo(H)(PMe₃) (3.7 mg, 5 mol%) at RT. The reaction provided formation of PhCH₂N(BCat)₂ in 0.5 d at RT. The product precipitated in benzene. NMR yield: ~100%. ¹H-NMR (300 MHz; CDCl₃; 298K; δ, ppm): 4.73 (s, 2H, CH₂-N), 6.99-7.06 (m, 4H, Ar, BCat), 7.18-7.24 (m, 4H, Ar, BCat), 7.24-7.34 (m, 3H, Ph), 7.44-7.49 (m, 2H, Ph). ¹³C-NMR (75.5 MHz; CDCl₃; 298 K; δ, ppm): 48.0 (CH₂N), 112.5 (CH, Ar, BCat), 122.6 (CH, Ar, BCat), 127.5 (CH, Ph), 127.9 (CH, Ph), 128.7 (CH, Ph), 140.3 (*ipso*-C^a), 148.5 (*ipso*-C^b). ¹¹B-NMR (96.3 MHz; C₆D₆; 298 K; δ, ppm): 27.6 (bs).

Hydroboration of CH₃CN with catecholborane



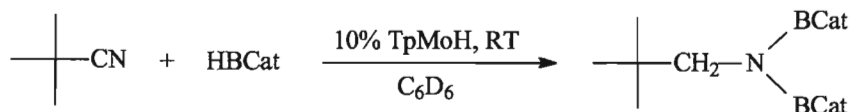
Catecholborane (16.9 mg, 0.140 mmol) was added to a solution of acetonitrile (2.9 mg, 0.070 mmol) in the presence of (Tp)(ArN)Mo(H)(PMe₃) (2.0 mg, 5 mol%) at RT. The reaction provided formation of CH₃CH₂N(BCat)₂ in 57% yield in 3 d at RT. in C₆D₆ (0.60 ml) NMR yield (final) is ~100%. ¹H-NMR (300 MHz; C₆D₆; 298K; δ, ppm): 1.10 (t, ³J_{H-H} = 7.14 Hz, 3H, CH₃), 3.36 (q, ³J_{H-H} = 7.14 Hz, 2H, CH₂-N), 6.73-6.79 (4H, Ar, BCat), 7.01-7.06 (4H, Ar, BCat). ¹¹B-NMR (96.3 MHz; C₆D₆; 298 K; δ, ppm): 27.8 (bs).

Hydroboration of (CH₃)₂CH-CN with catecholborane



Catecholborane (16.9 mg, 0.140 mmol) was added to a solution of isobutyronitrile (4.83 mg, 0.070 mmol) in the presence of (Tp)(ArN)Mo(H)(PMe₃) (2.0 mg, 5 mol%) in C₆D₆ (0.60 ml) at RT. The reaction provided formation of (CH₃)₂CHCH₂N(BCat)₂ in 82% yield in 3 d at RT. Then, the reaction mixture was heated up to 60 °C to complete the reaction. NMR yield (final) is ~100%. ¹H-NMR (300 MHz; C₆D₆; 298K; δ, ppm): 0.83 (d, ³J_{H-H} = 6.5 Hz, 6H, 2CH₃), 1.90 (m, 1H, CH), 3.24 (d, ³J_{H-H} = 7.3 Hz, 2H, CH₂-N), 6.71-6.79 (m, 4H, Ar, BCat), 7.00-7.08 (m, 4H, Ar, BCat). ¹³C-NMR (75.5 MHz; C₆D₆; 298 K; δ, ppm): 20.4, 30.7, 52.3, 112.7, 122.9, 149.3. ¹¹B-NMR (96.3 MHz; C₆D₆; 298 K; δ, ppm): 27.8 (bs).

Hydroboration of (CH₃)₃C-CN with catecholborane



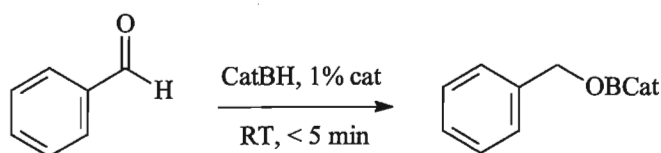
Catecholborane (16.9 mg, 0.140 mmol) was added to a solution of pivalonitrile (5.8 mg, 0.070 mmol) in the presence of (Tp)(ArN)Mo(H)(PMe₃) (3.5 mg, 9 mol%) in C₆D₆ (0.60 ml) at RT. The reaction provided formation of (CH₃)₃C-CH₂N(BCat)₂ in 86% yield in 3 d at RT. Then, the reaction mixture was heated at 60 °C to complete the reaction. NMR yield (final) is ~100%. ¹H-NMR (300 MHz; C₆D₆; 298K; δ, ppm): 0.86 (s, 9H, *t*-Bu), 3.31 (s, 2H, CH₂), 6.70-6.78 (m, 4H, Ar, HBCat), 7.01-7.08 (m, 4H, Ar, BCat). ¹³C-NMR

(75.5 MHz; C₆D₆; 298 K; δ , ppm): 27.8, 33.5, 55.7, 112.6, 123.0, 149.2. ¹¹B-NMR (96.3 MHz; C₆D₆; 298 K; δ , ppm): 27.5 (bs).

Competitive hydroboration of CH₃CN, (CH₃)₂CH-CN and (CH₃)₃C-CN with catecholborane

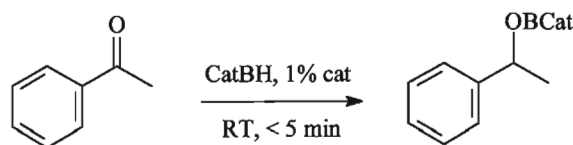
Catecholborane (16.9 mg, 0.140 mmol) was added to a solution of acetonitrile (2.9 mg, 0.070 mmol), isobutyronitrile (4.8 mg, 0.07 mmol) and pivalonitrile (5.8 mg, 0.070 mmol) in the presence of (Tp)(ArN)Mo(H)(PMe₃) (3.9 mg, 10 mol%) in C₆D₆ (0.60 ml) at RT. When catecholborane was consumed (~4 d), the reaction mixture contained CH₃CH₂N(BCat)₂ (36%), (CH₃)₂CHCH₂N(BCat)₂ (35%) and (CH₃)₃C-CH₂N(BCat)₂ (29%).

Hydroboration of benzaldehyde with catecholborane



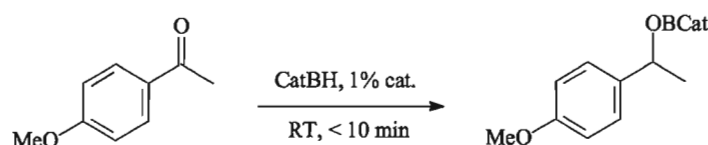
Catecholborane (21.4 mg, 0.178 mmol) was added to a solution of benzaldehyde (18.9 mg, 0.178 mmol) in the presence of (Tp)(ArN)Mo(H)(PMe₃) (1.0 mg, 1 mol%) in C₆D₆ (0.60 ml) at RT. The reaction resulted in formation of PhCH₂OBCat in less than 5 min. ¹H-NMR (300 MHz; C₆D₆; 298K; δ , ppm): 4.85 (s, CH₂, 2H), 6.70-6.80 (m, 2H, Ar, BCat), 6.86-6.96 (m, 2H, Ar, BCat), 7.02-7.27 (m, 5H, Ph). ¹³C-NMR (75.5 MHz; C₆D₆; 298 K; δ , ppm): 68.3, 112.6, 122.9, 127.7, 129.1, 138.7, 148.9. ¹¹B-NMR (96.3 MHz; C₆D₆; 298 K; δ , ppm): 23.6 (bs)

Hydroboration of acetophenone with catecholborane



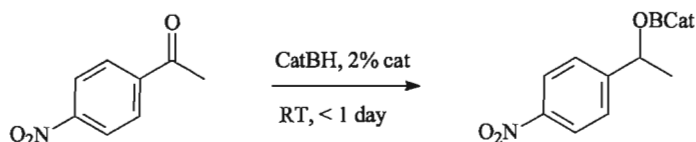
Catecholborane (21.4 mg, 0.178 mmol) was added to a solution of acetophenone (21.4 mg, 0.178 mmol) in the presence of (Tp)(ArN)Mo(H)(PMe₃) (1.0 mg, 1 mol%) in C₆D₆ (0.60 ml) at RT. The reaction resulted in formation of PhCH(OBCat)CH₃ in less than 5 minutes. NMR yield: 100%. ¹H-NMR (300 MHz; C₆D₆; 298K; δ, ppm): 1.38 (d, *J* = 6.59 Hz, 3H, CH₃), 5.38 (q, *J* = 6.59 Hz, 1H, CH-O), 6.68-6.75 (m, 2H, Ar, BCat), 6.85-6.92 (m, 2H, Ar, BCat), 7.01-7.15 (m, 3H, Ph), 7.26-7.31 (m, 2H, Ph). ¹³C-NMR (75.5 MHz; C₆D₆; 298 K; δ, ppm): 25.5, 75.0, 112.6, 122.8, 126.0, 128.2, 129.1, 144.2, 148.9. ¹¹B-NMR (96.3 MHz; C₆D₆; 298 K; δ, ppm): 23.4 (bs).

Hydroboration of *p*-methoxyacetophenone with catecholborane



Catecholborane (8.6 mg, 0.071 mmol) was added to a solution of *p*-methoxyacetophenone (13.0 mg, 0.071 mmol) in the presence of (Tp)(ArN)Mo(H)(PMe₃) (0.4 mg, 1 mol%) in C₆D₆ (0.60 ml) at RT. The reaction resulted in formation of *p*-MeOC₆H₄CH(OBCat)Ph in less than 10 min. ¹H-NMR (300 MHz; C₆D₆; 298K; δ, ppm): 1.43 (d, *J* = 6.3 Hz, 3H, CH₃), 3.28 (s, 3H, OCH₃), 5.40 (q, *J* = 6.3 Hz, 1H, CH-O), 6.67-6.82 (m, 4H, Ar, BCat and Ph), 6.84-6.95 (m, 2H, Ar, BCat), 7.20-7.28 (m, 2H, Ar). ¹³C-NMR (75.5 MHz; C₆D₆; 298 K; δ, ppm): 25.4, 55.1, 74.8, 112.5, 114.6, 122.8, 127.4, 136.3, 148.9, 160.1. ¹¹B-NMR (96.3 MHz; C₆D₆; 298 K; δ, ppm): 23.4 (bs).

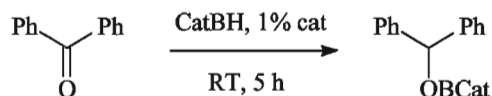
Hydroboration of *p*-nitroacetophenone with catecholborane



Catecholborane (11.3 mg, 0.0940 mmol) was added to a solution of *p*-nitroacetophenone (15.5 mg, 0.094 mmol) in the presence of (Tp)(ArN)Mo(H)(PMe₃) (0.4 mg, 1 mol%) in C₆D₆ (0.60 ml) at RT. The reaction provided formation of *p*-NO₂-C₆H₄-CH(OBCat)CH₃ and lots of black precipitate resulted from catalyst decomposition. NMR yield: ~45%. ¹H-

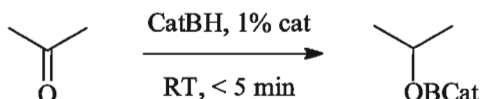
NMR (300 MHz; C₆D₆; 298K; δ , ppm): 1.17 (d, J = 6.60 Hz, 3H, CH₃), 5.12 (q, J = 6.60 Hz, 1H, CH-O), 6.69-6.79 (m, 2H, BCat), 6.84-6.94 (m, 4H, BCat and Ar), 7.74-7.82 (m, 2H, BCat). ¹¹B-NMR (96.3 MHz; C₆D₆; 298 K; δ , ppm): 23.6 (bs).

Hydroboration of benzophenone with catecholborane



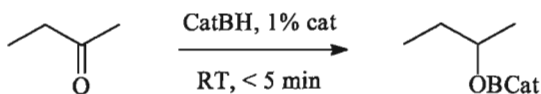
Catecholborane (8.6 mg, 0.071 mmol) was added to a solution of benzophenone (13.0 mg, 0.071 mmol) in the presence of (Tp)(ArN)Mo(H)(PMe₃) (0.4 mg, 1 mol%) in C₆D₆ (0.60 ml) at RT. The reaction resulted in formation of PhCH(OBCat)Ph in 5 hs. ¹H-NMR (300 MHz; C₆D₆; 298K; δ , ppm): 6.44 (s, CH, 1H), 6.67-6.72 (m, 2H, Ar, BCat), 6.83-6.90 (m, 2H, Ar, BCat), 6.96-7.12 (m-, p-H, 6H, Ar), 7.34-7.40 (m, o-H, 4H, Ar). ¹³C-NMR (75.5 MHz; C₆D₆; 298 K; δ , ppm): 80.2 (C-H), 112.6 (CH, Ar, BCat), 122.8 (CH, Ar, BCat), 127.3 (CH, Ar, Ph), 128.3 (CH, Ph, determined by HSQC), 129.1 (CH, Ph), 142.8 (*ipso*-C), 148.8 (*ipso*-C). ¹¹B-NMR (96.3 MHz; C₆D₆; 298 K; δ , ppm): 23.7 (bs).

Hydroboration of acetone with catecholborane



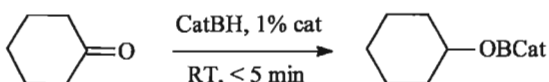
Catecholborane (11.3 mg, 0.094 mmol) was added to a solution of acetone (5.5 mg, 0.094 mmol) in the presence of (Tp)(ArN)Mo(H)(PMe₃) (1.0 mg, 1 mol%) in C₆D₆ (0.60 ml) at RT. The reaction resulted in formation CH₃CH(OBCat)CH₃ in less than 5 min. ¹H-NMR (300 MHz; C₆D₆; 298K; δ , ppm): 1.06 (d, J = 6.3 Hz, 6H, 2CH₃), 4.43 (sept, J = 6.3 Hz, 1H, CH-O), 6.71-6.78 (m, 2H, BCat), 6.90-6.97 (m, 2H, BCat). ¹³C-NMR (75.5 MHz; C₆D₆; 298 K; δ , ppm): 24.4, 69.7, 112.5, 122.8, 149.0. ¹¹B-NMR (96.3 MHz; C₆D₆; 298 K; δ , ppm): 23.2 (bs).

Hydroboration of butanone with catecholborane



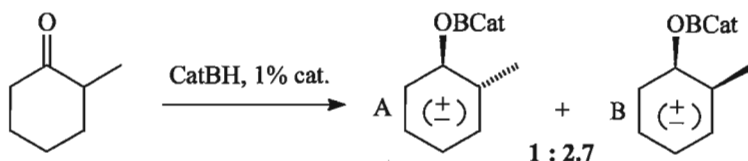
Catecholborane (11.3 mg, 0.094 mmol) was added to a solution of butanone (6.8 mg, 0.094 mmol) in the presence of (Tp)(ArN)Mo(H)(PMe₃) (1.0 mg, 1 mol%) in C₆D₆ (0.60 ml) at RT. The reaction resulted in formation CH₃CH₂CH(OBCat)CH₃ in less than 5 min. ¹H-NMR (300 MHz; C₆D₆; 298K; δ, ppm): 0.76 (t, *J* = 7.5 Hz, 3H, CH₃), 1.08 (d, *J* = 6.3, 3H, CH₃), 1.23-1.54 (m, 2H, CH₂), 4.27 (hept, *J* = 6.2 Hz, 1H, CH-O), 6.71-6.78 (m, 2H, BCat), 6.90-6.97 (m, 2H, BCat). ¹³C-NMR (75.5 MHz; C₆D₆; 298 K; δ, ppm): 10.2, 22.1, 31.4, 74.6, 112.5, 122.8, 149.0. ¹¹B-NMR (96.3 MHz; C₆D₆; 298 K; δ, ppm): 23.4 (bs).

Hydroboration of cyclohexanone with catecholborane



Catecholborane (21.4 mg, 0.178 mmol) was added to a solution of cyclohexanone (17.5 mg, 0.178 mmol) in the presence of (Tp)(ArN)Mo(H)(PMe₃) (1.0 mg, 1 mol%) in C₆D₆ (0.60 ml) at RT. The reaction resulted in formation CyOBCat in less than 5 min. ¹H-NMR (300 MHz; C₆D₆; 298K; δ, ppm): 0.95-1.16 (m, 3H), 1.18-1.31 (m, 1H), 1.34-1.48 (m, 2H), 1.49-1.62 (m, 2H), 1.71-1.82 (m, 2H), 4.21 (m, 1H, CH-O), 6.72-6.79 (m, 2H, Ar, BCat), 6.91-6.98 (m, 2H, Ar, BCat). ¹³C-NMR (75.5 MHz; C₆D₆; 298 K; δ, ppm): 24.2, 25.9, 34.5, 74.9, 112.5, 122.8, 149.0. ¹¹B-NMR (96.3 MHz; C₆D₆; 298 K; δ, ppm): 23.4.

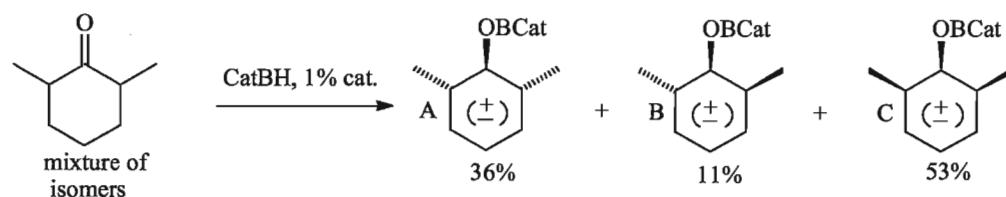
Hydroboration of 2-methylcyclohexanone with catecholborane



Catecholborane (11.3 mg, 0.094 mmol) was added to a solution of 2-methylcyclohexanone (11.8 mg, 0.094 mmol) in the presence of (Tp)(ArN)Mo(H)(PMe₃)

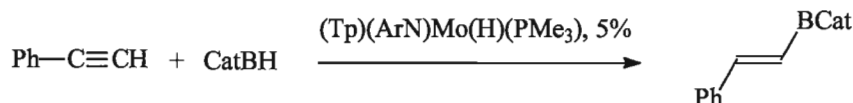
(0.5 mg, 1 mol%) in C₆D₆ (0.60 ml) at RT. The reaction resulted in formation of two isomers A (27%) and B (73%) in less than 10 min. ¹H-NMR (300 MHz; C₆D₆; 298K; δ, ppm): 0.88 (d, *J* = 6.6 Hz, 3H, CH₃, A), 0.92 (d, *J* = 6.1 Hz, 3H, CH₃, B), 0.75-1.15 (m, 2H, A and B), 1.19-1.69 (m, 6H, A and B), 1.73-1.86 (m, 1H, A), 1.88-1.98 (m, 1H, B), 3.85 (m, 1H, CH-O, B), 4.40 (m, 1H, CH-O, A), 6.71-6.79 (m, 2H, Ar, BCat), 6.90-6.98 (m, 2H, Ar, BCat). ¹³C-NMR (75.5 MHz; C₆D₆; 298 K; δ, ppm): 17.9, 19.0, 21.0, 25.4, 25.9, 29.2, 32.6, 33.8, 34.7, 36.3, 39.5, 76.5, 81.3, 112.5, 122.8, 149.1. ¹¹B-NMR (96.3 MHz; C₆D₆; 298 K; δ, ppm): 23.5.

Hydroboration of 2,6-dimethylcyclohexanone with catecholborane



Catecholborane (11.3 mg, 0.094 mmol) was added to a solution of 2,6-dimethylcyclohexanone (11.8 mg, 0.094 mmol) in the presence of (Tp)(ArN)Mo(H)(PMe₃) (0.5 mg, 1 mol%) at RT. The reaction resulted in formation of three isomers A (36%), B (11%) and C (53%) in less than 10 min. ¹H-NMR (300 MHz; C₆D₆; 298K; δ, ppm): 0.76-1.95 (m, 14H, Cy*), 3.58 (t, ³*J*_{trans-H-H} = 9.6 Hz, 1H, CH-O, A), 4.09 (dd, ³*J*_{trans-H-H} = 7.8 Hz, ³*J*_{cis-H-H} = 3.8 Hz, 1H, CH-O, B), 4.27 (m, 1H, CH-O, C), 6.70-6.79 (m, 2H, Ar, BCat), 6.89-6.99 (m, 2H, Ar, BCat). ¹³C-NMR (75.5 MHz; C₆D₆; 298 K; δ, ppm): 15.4, 19.1, 19.2, 25.9, 26.5, 28.2, 34.3, 37.5, 39.3, 45.6, 80.7, 87.3, 112.6, 122.8. ¹¹B-NMR (96.3 MHz; C₆D₆; 298 K; δ, ppm): 23.7 (bs).

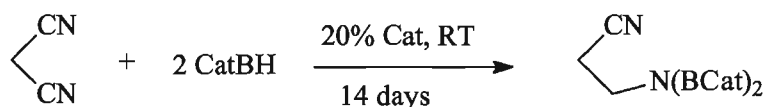
Hydroboration of Ph-C≡CH with catecholborane



Catecholborane (11.6 mg, 0.094 mmol) and phenylsilane (9.6 mg, 0.094 mmol) were added to a solution of (Tp)(ArN)Mo(H)(PMe₃) (2.6 mg, 5 mol%) in C₆D₆ (0.60 ml). The

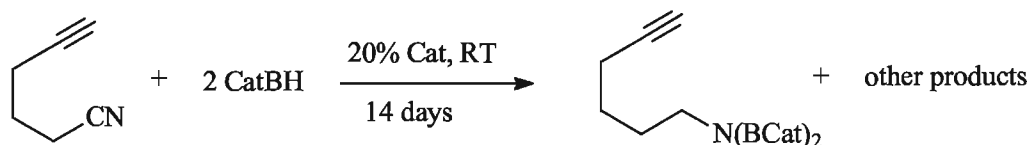
reaction provided formation of *trans*-Ph-CH=CH-BCat in one day at RT. The presence of catalyst also caused a partial polymerization of phenylacetylene as a side reaction. ¹H-NMR (300 MHz; C₆D₆; 298K; δ, ppm): 6.43 (d, *J* = 18.5 Hz, 1H, -CH=), 6.80-6.88 (m, 2H, Ar, BCat), 7.02-7.12 (m, 3H, Ph; 2H, BCat), 7.24-7.30 (m, 2H, Ph). ¹³C-NMR (75.5 MHz; C₆D₆; 298 K; δ, ppm): 113.0, 123.3, 129.3, 130.0, 132.7, 137.7, 149.3, 152.7. ¹¹B-NMR (96.3 MHz; C₆D₆; 298 K; δ, ppm): 31.4 (bs)

Hydroboration of malononitrile with catecholborane



Malononitrile (3.1 mg, 0.047 mmol) and catecholborane (11.3 mg, 0.047 mmol) were added to a solution of (Tp)(ArN)Mo(H)(PMe₃) (5 mg, 20 mol%) in C₆D₆ (0.60 ml). The reaction mixture was left for 14 days at RT. The reaction provided formation of (CatB)₂NCH₂CH₂CN in 20% yield. ¹H-NMR (300 MHz; C₆D₆; 298K; δ, ppm): 1.77 (t, *J* = 7.15 Hz, 2H, CH₂-N), 3.17 (t, *J* = 7.12 Hz, 2H, CH₂-CN).

Hydroboration of 1-hexynenitrile with catecholborane

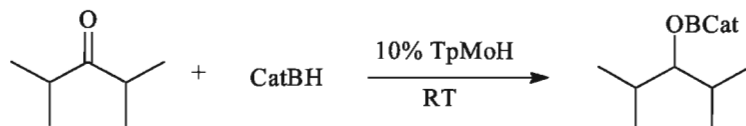


1-Hexynenitrile (4.4 mg, 0.047 mmol) and catecholborane (11.3 mg, 0.047 mmol) were added to a solution of (Tp)(ArN)Mo(H)(PMe₃) (5.0 mg, 20 mol%) in C₆D₆ (0.60 ml). The reaction provided formation of HC≡C-(CH₂)₄-N(BCat)₂ in one day at RT in 37% NMR yield. Then, hydroboration of the C≡C bond was also observed. ¹H-NMR (300 MHz; C₆D₆; 298K; δ, ppm): 1.90 (td, ³*J*_{H-H} = 7.12 Hz, ⁴*J*_{H-H} = 2.73 Hz, 2H, -CH₂-C≡), 3.29 (t, ³*J*_{H-H} = 7.45 Hz, 2H, -CH₂-N(BCat)₂), 5.90 (d, ³*J*_{H-H} = 17.79 Hz, 1H, -CH=), 7.07 (1H, -CH=, position determined by ¹H-¹H COSY NMR). ¹¹B-NMR (96.3 MHz; C₆D₆; 298 K; δ, ppm): 15.5 (bm), 26.9 (bm).

Hydroboration of acrylonitrile

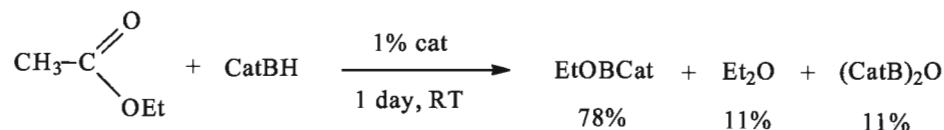
Acrylonitrile (2.3 μ l, 0.036 mmol) and CatBH (3.8 μ l, 0.036 mmol) were mixed in the presence of (Tp)(ArN)Mo(H)(PMe₃) (2.0 mg, 10 mol%) in C₆D₆ (0.60 ml). Hydroboration was not observed.

Hydroboration of 2,4-dimethyl-3-pentanone with catecholborane



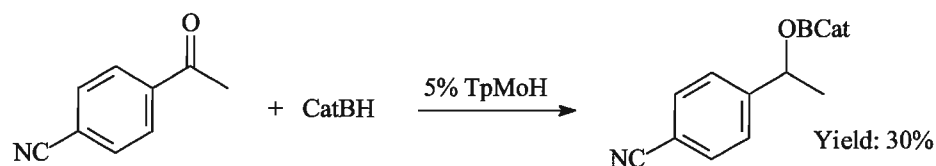
2,4-Dimethyl-3-pentanone (13.3 μ l, 0.094 mmol) and catecholborane (10 μ l, 0.094 mmol) were mixed in the presence of (Tp)(ArN)Mo(H)(PMe₃) (5.3 mg, 10 mol%) in C₆D₆ (0.60 ml). The reaction provided formation of (i-Pr)₂CHOBCat in one day at RT. NMR yield: 76%. ¹H-NMR (300 MHz; C₆D₆; 298K; δ , ppm): 0.78 (d, J = 7.14 Hz, 6H, 2CH₃), 0.88 (d, J = 7.14 Hz, 6H, 2CH₃), 1.74 (hept, J = 6.59 Hz, 2H, -CH(CH₃)₂), 3.89 (t, J = 5.77 Hz, 1H, CH-O), 6.81-6.89 (m, 2H, BCat), 7.01-7.10 (m, 2H, BCat). ¹¹B-NMR (96.3 MHz; C₆D₆; 298 K; δ , ppm): 22.7 (bs)

Hydroboration of ethyl acetate with catecholborane



Ethyl acetate (8.3 mg, 0.094 mmol) and catecholborane (11.3 mg, 0.094 mmol) were added to a solution of (Tp)(ArN)Mo(H)(PMe₃) (2.5 mg, 5 mol%) in C₆D₆ (0.60 ml). The reaction provided formation of CH₃CH₂OBCat (78%), (CH₃CH₂)₂O (11%) and (CatB)₂O (11%) in one day at RT. ¹H-NMR (300 MHz; C₆D₆; 298K; δ , ppm): 0.99 (t, J = 6.88 Hz, 3H, CH₃, EtOBCat), 1.11 (t, J = 7.14, 6H, 2CH₃, Et₂O), 3.26 (q, J = 7.14 Hz, 4H, 2CH₂, Et₂O), 3.81 (q, J = 6.88 Hz, 2H, CH₂, EtOBCat), 6.70-6.78 (m, 2H, Ar, EtOBCat and (CatB)₂O), 6.87-6.96 (m, 2H, Ar, EtOBCat and (CatB)₂O). ¹¹B-NMR (96.3 MHz; C₆D₆; 298 K; δ , ppm): 23.4 (bs, C₂H₅OBCat), 28.8 (bs, (CatB)₂O).

Hydroboration of 4-acetylbenzonitrile



4-Acetylbenzonitrile (17.4 μ l, 0.121 mmol) and catecholborane (12.8 μ l, 0.121 mmol) were mixed in the presence of (Tp)(ArN)Mo(H)(PMe₃) (2.5 mg, 5 mol%) in C₆D₆ (0.60 ml). The colour of the reaction mixture immediately turned dark-brown. The reaction provided formation of *p*-CN-C₆H₄CH(OBCat)CH₃ as the only product in 30% yield. Hydroboration of the nitrile group was not observed. The catalyst decomposed during the reaction. ¹H-NMR (300 MHz; C₆D₆; 298K; δ , ppm): 1.15 (d, ³J_{H-H} = 6.50 Hz, 3H, CH₃), 5.09 (q, ³J_{H-H} = 6.50, 1H, CH-CH₃). ¹¹B-NMR (96.3 MHz; C₆D₆; 298 K; δ , ppm): 23.4 (bs).

Competitive hydroboration of benzaldehyde and benzonitrile

Benzaldehyde (9.1 μ l, 0.0982 mmol), benzonitrile (8.7 μ l, 0.0982 mmol) and catecholborane (9.5 μ l, 0.0892 mmol) were mixed in the presence of (Tp)(ArN)Mo(H)(PMe₃) (0.5 mg, 1 mol%) in C₆D₆ (0.60 ml). The reaction provided formation of PhCH₂OBCat in less than 5 min. Conversion of the benzonitrile was not observed.

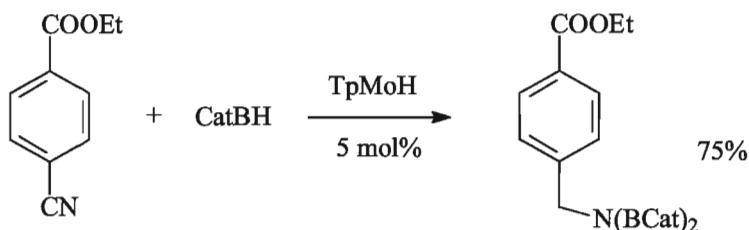
Competitive hydroboration of acetophenone and isobutyronitrile

Acetophenone (10.4 μ l, 0.0892 mmol), isobutyronitrile (8.0 μ l, 0.0892 mmol) and catecholborane (9.5 μ l, 0.0892 mmol) were mixed in the presence of (Tp)(ArN)Mo(H)(PMe₃) (2.5 mg, 5 mol%) in C₆D₆ (0.60 ml). The colour of the reaction mixture quickly changed from brown to purple, and then gradually to green-brown. The reaction provided formation of PhCH(OBCat)CH₃ as the only product within one hour at RT. Hydroboration of isobutyronitrile was not observed. ¹³P NMR spectrum of the reaction mixture showed the presence of a single peak at -1.73 ppm previously observed during the individual hydroboration of isobutyronitrile.

Hydroboration of 3-hexyne

3-Hexyne (15.0 μ l, 0.132 mmol) and catecholborane (14.1 μ l, 0.132 mmol) were mixed in the presence of (Tp)(ArN)Mo(H)(PMe₃) (3.7 mg, 5 mol%) in C₆D₆ (0.60 ml). No reaction was observed during one day at RT.

Hydroboration of ethyl 4-cyanobenzoate



Ethyl 4-cyanobenzoate (15.6 mg, 0.0892 mmol) and catecholborane (19.0 μ l, 0.178 mmol) were mixed in the presence of (Tp)(ArN)Mo(H)(PMe₃) (2.5 mg, 5 mol%) in C₆D₆ (0.60 ml). The reaction provided formation of EtOOC-C₆H₄-CH₂N(BCat)₂ in 1.5 days as the major product. NMR yield/selectivity: 75%. ¹H-NMR (300 MHz; C₆D₆; 298K; δ , ppm): 0.99 (t, ³J_{H-H} = 7.10 Hz, 3H, CH₃), 4.10 (q, ³J_{H-H} = 7.10 Hz, 2H, OCH₂), 4.46 (s, CH₂N), 6.68-6.67 (m, 2H, BCat), 6.95-7.03 (m, 2H, BCat), 7.28 (d, ³J_{H-H} = 8.10, 2H, Ar), 8.06 (d, ³J_{H-H} = 8.10, 2H, Ar). ¹³C-NMR (150.9 MHz; C₆D₆; 298 K; δ , ppm): 13.8 (CH₃), 47.5 (CH₂N), 60.5 (OCH₂), 112.2 (CH, BCat), 127.0 (CH, BCat), 129.9 (CH, Ar), 144.9 (*ipso*-C, C(Ar)-CH₂N), 148.3 (*ipso*-C, BCat), 165.7 (*ipso*-C, C(Ar)-COOEt). ¹¹B-NMR (96.3 MHz; C₆D₆; 298 K; δ , ppm): 28.0 (bs, B-N).

Hydroboration of N-benzylidenaniline¹⁵⁴

N-benzylidenaniline (16.2 mg, 0.0892 mmol) and catecholborane (9.5 μ l, 0.0892 mmol) were mixed in C₆D₆ (0.60 ml). The reaction provided fast formation of PhCH₂N(BCat)Ph.

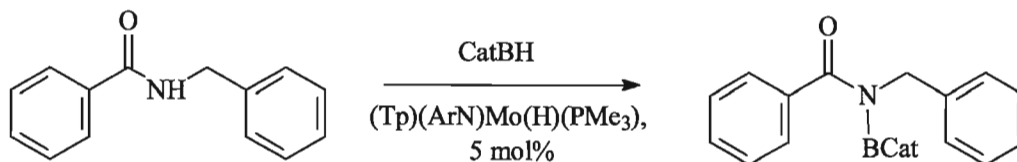
Competitive hydroboration of acetophenone and benzonitrile mediated by (Tp)(ArN)Mo(-N=CHPh)(PMe₃)

Acetophenone (10.4 μ l, 0.0892 mmol), benzonitrile (8.7 μ l, 0.0892 mmol) and catecholborane (9.5 μ l, 0.0892 mmol) were mixed in the presence of (Tp)(ArN)Mo(-N=CHPh)(PMe₃) (3.0 mg, 5 mol%) in C₆D₆ (0.60 ml). Hydroboration of acetophenone was complete within one hour at RT. ³¹P NMR spectrum showed the presence of an unknown catalyst derivative. The colour of the solution was orange-brown. ¹H-NMR (300 MHz; C₆D₆; 298K; δ , ppm): 0.85 (bm, 6H, 2CH₃, *i*-Pr), 0.99 (bd, ³J_{H-H} = 6.70 Hz, 2CH₃, *i*-Pr), 1.23 (d, ²J_{H-P} = 8.23 Hz, PMe₃), 5.93 (t, ³J_{H-H} = 2.20 Hz, 1H, Pz), 5.99 (t, ³J_{H-H} = 2.20 Hz, 1H, Pz), 6.02 (t, ³J_{H-H} = 2.20 Hz, 1H, Pz). ³¹P-NMR (121.5 MHz; C₆D₆; 298 K; δ , ppm): -1.92 (s).

Hydroboration of acetophenone mediated by (Tp)(ArN)Mo(-N=CHPh)(PMe₃)

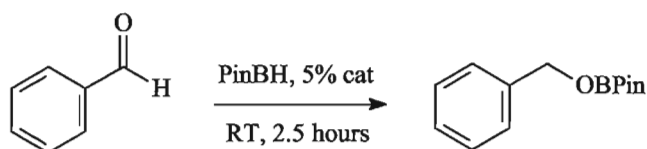
Acetophenone (10.4 μ l, 0.0892 mmol) and catecholborane (9.5 μ l, 0.0892 mmol) were mixed in the presence of (Tp)(ArN)Mo(-N=CHPh)(PMe₃) (3.0 mg, 5 mol%) in C₆D₆ (0.60 ml). The reaction provided fast (<10 min) formation of PhCH(OBCat)CH₃. The solution was bright purple. NMR analysis showed the presence of an unknown catalyst derivative. ¹H-NMR (300 MHz; C₆D₆; 298K; δ , ppm): 0.84 (bd, ³J_{H-H} = 6.59 Hz, 2CH₃, *i*-Pr), 0.89 (bd, ³J_{H-H} = 6.59 Hz, 2CH₃, *i*-Pr), 1.17 (d, ²J_{H-P} = 8.78 Hz, PMe₃), 3.31 (sept, ³J_{H-H} = 6.59 Hz, 2H, CH, *i*-Pr), 5.77 (t, ³J_{H-H} = 2.20 Hz, 1H, Pz), 5.93 (t, ³J_{H-H} = 2.20 Hz, 1H, Pz), 6.05 (t, ³J_{H-H} = 2.20 Hz, 1H, Pz). ³¹P-NMR (121.5 MHz; C₆D₆; 298 K; δ , ppm): -1.35 (s).

Hydroboration of N-benzylbenzamide



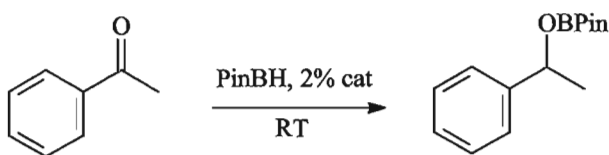
N-benzylbenzamide (18.8 mg, 0.0892 mmol) and catecholborane (9.5 μ l, 0.0892 mmol) were mixed in the presence of (Tp)(ArN)Mo(H)(PMe₃) (3.0 mg, 5 mol%) in C₆D₆ (0.60 ml). Formation of gas (H₂) was observed. The reaction provided fast formation of N-benzyl-N-catecholborylbenzamide precipitated as a pale-yellow solid. The product was filtered, washed with benzene, and dissolved in CDCl₃. ¹H-NMR (300 MHz; CDCl₃; 298K; δ , ppm): 4.95 (s, 2H, CH₂N), 6.96-7.66 (m, 14H, Ar).

Hydroboration of benzaldehyde with pinacolborane



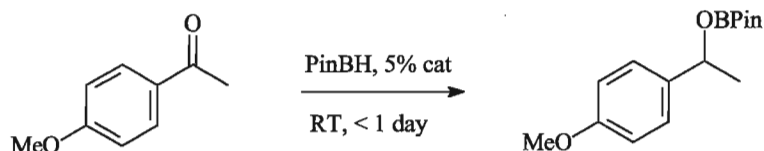
Pinacolborane (8.8 mg, 0.069 mmol) and benzaldehyde (10.9 mg, 0.069 mmol) were added to a solution of (Tp)(ArN)Mo(H)(PMe₃) (3.0 mg, 5 mol%) in C₆D₆ (0.60 ml) at RT. The reaction provided formation of PhCH₂OBPin in 2.5 hours. ¹H-NMR (300 MHz; C₆D₆; 298K; δ , ppm): 1.04 (s, 12H, 4CH₃), 4.96 (s, 2H, CH₂), 6.98-7.17 (m, 3H, Ph), 7.28-7.34 (m, 2H, Ph). ¹³C-NMR (75.5 MHz; C₆D₆; 298 K; δ , ppm): 25.0, 67.3, 83.1, 127.4, 127.9, 128.9, 140.4. ¹¹B-NMR (96.3 MHz; C₆D₆; 298 K; δ , ppm): 23.0 (bs).

Hydroboration of acetophenone with pinacolborane



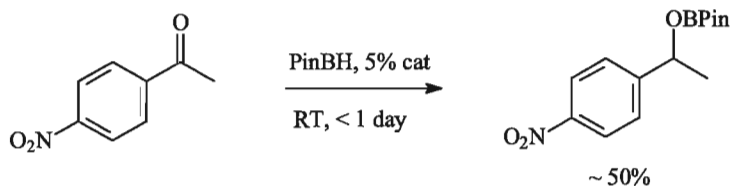
Pinacolborane (8.8 mg, 0.069 mmol) and acetophenone (8.3 mg, 0.069 mmol) were added to a solution of (Tp)(ArN)Mo(H)(PMe₃) (1.0 mg, 2 mol%) in C₆D₆ (0.60 ml) at RT. The reaction resulted in formation PhCH(OBPin)CH₃ in 0.5 days. ¹H-NMR (300 MHz; C₆D₆; 298K; δ , ppm): 1.00 (s, 6H, Pin), 1.03 (s, 6H, Pin), 1.46 (d, *J* = 6.39 Hz, 3H, CH₃), 5.42 (q, *J* = 6.39 Hz, 1H, CH-O), 6.98-7.19 (m, 3H, Ph), 7.34-7.40 (m, 2H, Ph). ¹³C-NMR (75.5 MHz; C₆D₆; 298 K; δ , ppm): 24.9, 25.0, 26.1, 73.3, 82.9, 126.1, 127.7, 128.9, 145.8. ¹¹B-NMR (96.3 MHz; C₆D₆; 298 K; δ , ppm): 22.7 (bs)

Hydroboration of 4-methoxyacetophenone with pinacolborane



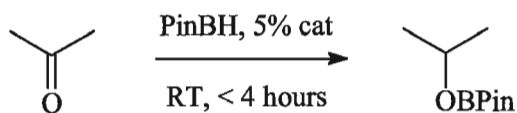
Pinacolborane (13.2 mg, 0.103 mmol) and 4-methoxyacetophenone (15.5 mg, 0.103 mmol) were added to a solution of (Tp)(ArN)Mo(H)(PMe₃) (3.0 mg, 5 mol%) in C₆D₆ (0.60 ml) at RT. The reaction provided formation of MeOC₆H₄CH(OBPin)CH₃ in less than 1 day. ¹H-NMR (300 MHz; C₆D₆; 298K; δ, ppm): 1.02 (s, 6H, 2CH₃), 1.04 (s, 6H, 2CH₃), 1.50 (d, *J* = 6.58 Hz, 3H, CH₃), 3.29 (s, 3H, OCH₃), 5.42 (q, *J* = 6.58 Hz, 1H, CH-O), 6.73-6.79 (m, 2H, Ar), 7.28-7.34 (m, 2H, Ar). ¹³C-NMR (75.5 MHz; C₆D₆; 298 K; δ, ppm): 25.0, 25.1, 26.1, 55.1, 73.0, 82.8, 114.4, 127.3, 137.9, 159.8. ¹¹B-NMR (96.3 MHz; C₆D₆; 298 K; δ, ppm): 22.7 (bs).

Hydroboration of 4-nitroacetophenone with pinacolborane



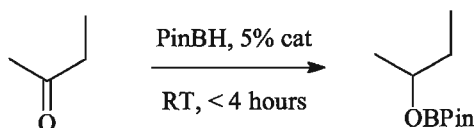
Pinacolborane (13.2 mg, 0.103 mmol) and 4-nitroacetophenone (17.0 mg, 0.103 mmol) were added to a solution of (Tp)(ArN)Mo(H)(PMe₃) (3.0 mg, 5 mol%) in C₆D₆ (0.60 ml) at RT. The reaction provided formation of MeOC₆H₄CH(OBPin)CH₃ in 0.5 day, and then stopped due to the catalyst decomposition. NMR yield: ~50%. ¹H-NMR (300 MHz; C₆D₆; 298K; δ, ppm): 1.01 (s, 6H, 2CH₃), 1.03 (s, 6H, 2CH₃), 1.25 (d, *J* = 6.59 Hz, 3H, CH₃), 5.19 (q, *J* = 6.59 Hz, 1H, CH-O), 6.97-7.02 (m, 2H, Ar), 7.77-7.83 (m, 2H, Ar). ¹¹B-NMR (96.3 MHz; C₆D₆; 298 K; δ, ppm): 22.0 (bs).

Hydroboration of acetone with pinacolborane



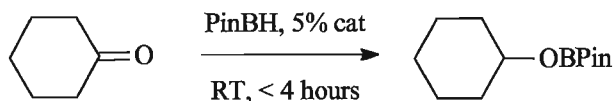
Pinacolborane (13.2 mg, 0.103 mmol) and acetone (6.0 mg, 0.103 mmol) were added to a solution of (Tp)(ArN)Mo(H)(PMe₃) (3.0 mg, 5 mol%) in C₆D₆ (0.60 ml) at RT. The reaction resulted in formation CH₃C(OBPin)CH₃ in less than one hour. ¹H-NMR (300 MHz; C₆D₆; 298K; δ, ppm): 1.06 (s, 12H, 4CH₃, Pin), 1.17 (d, *J* = 6.26 Hz, 6H, 2CH₃), 4.47 (sept, *J* = 6.26 Hz, 1H, CH). ¹³C-NMR (75.5 MHz; C₆D₆; 298 K; δ, ppm): 24.9, 25.0, 67.7, 82.5. ¹¹B-NMR (96.3 MHz; C₆D₆; 298 K; δ, ppm): 22.5 (bs)

Hydroboration of butanone with pinacolborane



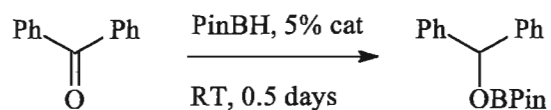
Pinacolborane (13.2 mg, 0.103 mmol) and butanone (7.4 mg, 0.103 mmol) were added to a solution of (Tp)(ArN)Mo(H)(PMe₃) (3.0 mg, 5 mol%) in C₆D₆ (0.60 ml) at RT. The reaction provided formation of CH₃CH₂C(OBPin)CH₃ in less than one hour. ¹H-NMR (300 MHz; C₆D₆; 298K; δ, ppm): 0.88 (t, *J* = 7.3 Hz, 3H, CH₃), 1.07 (s, 12H, 4CH₃, Pin), 1.17 (d, *J* = 6.03 Hz, 3H, CH₃), 1.30-1.62 (m, 2H, CH₂), 4.26 (m, 1H, CH-O). ¹³C-NMR (75.5 MHz; C₆D₆; 298 K; δ, ppm): 10.4, 22.7, 25.0, 31.8, 72.6, 82.5. ¹¹B-NMR (96.3 MHz; C₆D₆; 298 K; δ, ppm): 22.5 (bs).

Hydroboration of cyclohexanone with pinacolborane



Pinacolborane (13.2 mg, 0.103 mmol) and cyclohexanone (10.1 mg, 0.103 mmol) were added to a solution of (Tp)(ArN)Mo(H)(PMe₃) (3.0 mg, 5 mol%) in C₆D₆ (0.60 ml) at RT. The reaction provided formation of CyOBPin in less than one hour. ¹H-NMR (300 MHz; C₆D₆; 298K; δ, ppm): 1.02-1.21 (m, 2H), 1.08 (s, 12H, 4CH₃, Pz), 1.23-1.37 (m, 2H), 1.42-1.56 (m, 2H), 1.56-1.67 (m, 2H), 1.85-1.95 (m, 2H), 4.23 (m, 1H, CH-O). ¹³C-NMR (75.5 MHz; C₆D₆; 298 K; δ, ppm): 24.5, 25.1, 26.1, 35.1, 73.1, 82.5. ¹¹B-NMR (96.3 MHz; C₆D₆; 298 K; δ, ppm): 22.5 (bs).

Hydroboration of benzophenone with pinacolborane



Pinacolborane (13.2 mg, 0.103 mmol) and benzophenone (10.9 mg, 0.103 mmol) were added to a solution of (Tp)(ArN)Mo(H)(PMe₃) (3.0 mg, 5 mol%) in C₆D₆ (0.60 ml) at RT. The reaction resulted in formation (C₆H₅)₂CHOBPin in one hour. ¹H-NMR (300 MHz; C₆D₆; 298K; δ, ppm): 0.98 (s, 12H, 4CH₃), 6.44 (s, 1H, CH-O), 6.96-7.05 (m, 2H, Ar), 7.05-7.14 (m, 4H, Ar), 7.41-7.49 (m, 4H, Ar). ¹³C-NMR (75.5 MHz; C₆D₆; 298 K; δ, ppm): 24.9, 78.9, 83.2, 127.3, 127.9, 128.9, 144.3. ¹¹B-NMR (96.3 MHz; C₆D₆; 298 K; δ, ppm): 23.0 (bs).

V. 8. Silyl Imido Molybdenum(IV) Complexes

Synthesis of (ArN)Mo(SiH₂Ph)(Cl)(PMe₃)₃

Phenylsilane (50.0 μ l, 0.527 mmol) was added to a solution of (ArN)Mo(OCy)(Cl)(PMe₃) (20.0 mg, 0.032 mmol) in toluene. The quick release of hydrogen has been observed. The solution was stored at -30 °C. The product (ArN)Mo(SiH₂Ph)(Cl)(PMe₃)₃ crystallized as tetragonal crystals. ¹H NMR (300 MHz, C₆D₆; 297 K, δ , ppm): 1.16 (bd, J = 4.6 Hz, 9H, 1PMe₃), 1.22 (d, J = 6.7 Hz, 12H, 4CH₃, 2Prⁱ), 1.25 (vt, J = 3.2 Hz, 18H, 2PMe₃), 4.00 (sept, J = 6.7 Hz, 2H, 2Prⁱ), 5.78 (t+sat, ³ $J_{\text{H-P}}$ = 3.4 Hz, ¹ $J_{\text{H-Si}}$ = 153.8 Hz, 2H, SiH₂Ph), 6.86-6.93 (m, 2H, *m*-H, Ar), 6.95-7.02 (m, 1H, *p*-H, Ar), 7.21-7.26 (m, 1H, *p*-H, Ph), 7.28-7.33 (m, 2H, *m*-H, Ph), 8.31-8.49 (m, 2H, *o*-H, Ph). ³¹P NMR (121.5 MHz; C₆D₆; 297 K, δ , ppm): -4.7 (bs, PMe₃). ¹³C-NMR (75.5 MHz; C₆D₆; 298 K; δ , ppm): 19.4 (bs, 2PMe₃), 19.9 (bs, 1PMe₃), 25.3 (s, 4CH₃, 2Prⁱ), 27.6 (bs, 2C-H, 2Prⁱ), 124.4 (2 *m*-C-H, Ar), 126.3 (*p*-C-H, Ar), 127.6 (2*m*-C-H, Ph), 127.8 (*p*-C-H, Ph), 137.9 (2 *o*-C-H, Ph), 145.6 (*ipso*-C-C, Ar), 152.1 (*ipso*-C-N, Ar). A signal for the *ipso*-C-Si carbon atom was not detected. Elem. Anal. (%): calc. for C₂₇H₅₁ClMoNP₃Si (642.100): C 50.50, H 8.01, N 2.18; found (\pm 0.3%) C 49.95, H 7.52, N 2.35.

Preparation of (ArN)Mo(SiH₂Ph)(Cl)(PMe₃)₂^o

BPh₃ (9.4 mg, 0.040 mmol) was added to a solution of (ArN)Mo(H)(Cl)(PMe₃)₃ (21.0 mg, 0.04 mmol) and PhSiH₃ (4.8 μ l, 0.04 mmol) in C₆D₆ (0.60 ml) in a separate vial under the glovebox. Immediate formation of precipitate of Me₃B*PMe₃ was observed. The solution was filtered and transferred into an NMR tube. NMR analysis showed quantitative formation of (ArN)Mo(SiH₂Ph)(Cl)(PMe₃)₂. ¹H NMR (300 MHz, C₆D₆; 297 K, δ , ppm): 1.21-1.25 (m, 30H, 4CH₃ of NAr and 2PMe₃), 3.77 (sept, ³ $J_{\text{H-H}}$ = 6.9 Hz, 2H,

^o NMR-scale *in situ* preparation of (ArN)Mo(SiH₂Ph)(Cl)(PMe₃)₂ was originally developed by Eric Peterson (undergraduate student in Nikonov's group).

2CH, NAr), 5.93 (t+sat, $^3J_{\text{H-P}} = 3.3$ Hz, $^1J_{\text{H-Si}} = 158.2$ Hz, 2H, SiH₂Ph), 6.87-7.31 (m, 6H, *m*-H and *p*-H of SiH₂Ph and NAr), 7.88 (d, $^3J_{\text{H-H}} = 7.5$ Hz, 2H, *o*-H, SiH₂Ph). ^{31}P NMR (121.5 MHz; C₆D₆; 297 K, δ , ppm): 0.3 (s, PMe₃). ^1H - ^{13}C HSQC NMR (f1: 300 MHz; f2: 75.5 MHz; $J = 145.0$ Hz; C₆D₆; 297 K, δ , ppm): 15.8 (PMe₃), 23.7 (CH₃, NAr), 29.2 (CH, NAr), 123.0 (*m*-C and *p*-C of NAr and SiH₂Ph), 125.9, 126.5, 127.5, 136.5 (*o*-C, SiH₂Ph). ^1H - ^{29}Si HSQC NMR (f1: 300 MHz; f2: 59.6 MHz; $J = 200.0$ Hz; C₆D₆; 297 K, δ , ppm): 6.3 (SiH₂Ph).

Reaction between (ArN)Mo(H)(Cl)(PMe₃)₃ (1 eq), PhSiH₃ (1 eq) and B(C₆F₅)₃ (2 eq)

Proposed product: [(ArN)Mo(Cl)(SiH₂Ph)(PMe₃)₂]⁺[HB(C₆F₅)₃]⁻. ^1H NMR (300 MHz, C₆D₆; 297 K, δ , ppm)^p: 1.02 (d, $J = 6.2$ Hz, 9H, 1PMe₃), 1.27 (d, $J = 6.6$ Hz, 6H, 2CH₃, *i*Pr), 1.29 (d, $J = 6.6$ Hz, 6H, 2CH₃, *i*Pr), 1.39 (d, $J = 6.2$ Hz, 9H, 1PMe₃), 3.87 (sept, $J = 6.7$ Hz, 2H, *i*Pr), 6.87-6.94 (m, 2H, Ar), 6.97-7.03 (m, 1H, Ar), 7.23-7.31 (m, 3H, Ph), 7.72 (d, $^3J_{\text{H-31P}} = 2.0$ Hz, $^1J_{\text{H-29Si}} = 188.7$ Hz, 1H, Si-H), 7.93-7.99 (m, 2H, *o*-H, Ph). ^{31}P NMR (121.5 MHz; C₆D₆; 297 K, δ , ppm): -1.49 (d, $J = 176.7$ Hz, 1P, PMe₃), 0.34 (d, $J = 176.7$ Hz, 1P, PMe₃). ^1H - ^{29}Si HSQC NMR (f1: 600.2 MHz; f2: 119.2 MHz; $J = 200.0$ Hz; C₆D₆; 297 K, δ , ppm): 97.8 (SiHPh). ^{19}F NMR (282.4 MHz, C₆D₆; 297 K, δ , ppm): no signals observed. ^1H - ^{13}C HSQC NMR (f1: 600.2 MHz; f2: 150.9 MHz; C₆D₆; 297 K, δ , ppm): 15.7 (PMe₃), 16.1 (PMe₃), 23.8 (2CH₃, *i*Pr), 24.1 (2CH₃, *i*Pr), 29.3 (CH, *i*Pr), 123.3 (2CH, *m*-C, Ar), 126.5 (*p*-CH, Ar), 127.8 (CH, Ph), 135.4 (CH, *o*-CH, Ph)

Synthesis of (ArN)Mo(-N=C(SiH₂Ph)Ph)(Cl)(PMe₃)₂^q

^1H NMR (300 MHz, C₆D₆; 297 K, δ , ppm): 0.89 (vt, $^2J_{\text{H-P}} = 3.30$ Hz, 2PMe₃), 1.33 (bd, $^2J_{\text{H-H}} = 6.90$ Hz, 12H, 4CH₃, *i*-Pr), 4.58 (sept, $^2J_{\text{H-H}} = 6.90$ Hz, 2H, *i*-Pr), 6.07 (s, 2H,

^p H-B signal was not observed in ^1H NMR in the range from -40 to +40 ppm.

^q The structure of (ArN)Mo(-N=C(SiH₂Ph)Ph)(Cl)(PMe₃)₂ is proposed. The alternative suggested structure is (ArN)Mo(-C(Ph)=N-SiH₂Ph)(Cl)(PMe₃)₂

$^{28}\text{SiH}_2\text{Ph}$; d, $^1J_{\text{Si-H}} = 206.9$ Hz, $^{29}\text{SiH}_2\text{Ph}$), 6.99-7.06 (m, 3H, Ar), 7.07-7.38 (m, 6H, Ph), 7.72-7.78 (m, 2H, *o*-H, SiH_2Ph). ^{31}P NMR (121.5 MHz; C_6D_6 ; 297 K, δ , ppm): -9.5 (s, 2PMe_3). ^1H - ^{13}C HSQC NMR (f1: 300 MHz; f2: 75.5 MHz; $J = 145.0$ Hz; C_6D_6 ; 297 K, δ , ppm): -39.5 (SiH_2Ph). ^{13}C -NMR (75.5 MHz; C_6D_6 ; 298 K; δ , ppm): 14.4 (vt, $^1J_{\text{C-P}} = 10.7$ Hz, 2PMe_3), 24.1 (s, CH_3 , *i*-Pr), 27.4 (bs, CH, *i*-Pr), 55.4 ($-\text{N}=\text{C}(\text{Ph})(\text{SiH}_2\text{Ph})$, the signal was found by HMBC correlation), 123.1 (CH, Ar), 125.9 (CH, Ar), 128.3 (*o*-C, C-Ph), 128.4 (CH, Ph), 128.5 (CH, Ph), 128.6 (CH, Ph), 129.3 (CH, Ph), 129.8 (CH, Ph), 135.6 (*ipso*-C), 135.9 (*o*-C, SiH_2Ph), 139.8 (*ipso*-C), 151.9 (*ipso*-C, C-N, Ar).

Reaction of $(\text{ArN})\text{Mo}(-\text{N}=\text{C}(\text{SiH}_2\text{Ph})\text{Ph})(\text{Cl})(\text{PMe}_3)_2$ with CatBH

Catecholborane was added to a solution of $(\text{ArN})\text{Mo}(-\text{N}=\text{C}(\text{SiH}_2\text{Ph})\text{Ph})(\text{Cl})(\text{PMe}_3)_2$ in C_6D_6 (0.60 ml).

Reaction of $(\text{ArN})\text{Mo}(\text{SiH}_2\text{Ph})(\text{Cl})(\text{PMe}_3)_2$ with cyclohexanone

Cyclohexanone (2.9 μl , 0.028 mmol) was added to a solution of $(\text{ArN})\text{Mo}(\text{SiH}_2\text{Ph})(\text{Cl})(\text{PMe}_3)_2$ (0.028 mmol) in C_6D_6 (0.6 μl). Next day, additional amount of cyclohexanone (1.5 μl , 0.014 mmol) were added to complete the reaction.

V. 9. H₂/Si-H exchange mediated by metal complexes and boranes

Table V-9. Rate constants for H/H exchange between H₂ and PhSiH₃ in the presence of
(ArN)Mo(SiH₂Ph)(Cl)(PMe₃)₂

T, K	1/T, K ⁻¹	k, s ⁻¹	-ln(k/T)
283.1	0.003532	0.0148	-5.22783E-05
295.1	0.003389	0.0706	-0.000239241
304.1	0.003288	0.1135	-0.000373232
314.1	0.003184	0.1573	-0.000500796

$$\Delta H^\ddagger, \text{ J/mol}$$

$$10.7 \pm 0.1$$

$$\Delta S^\ddagger, \text{ J/(K}\cdot\text{mol)}$$

$$-197.8 \pm 0.0$$

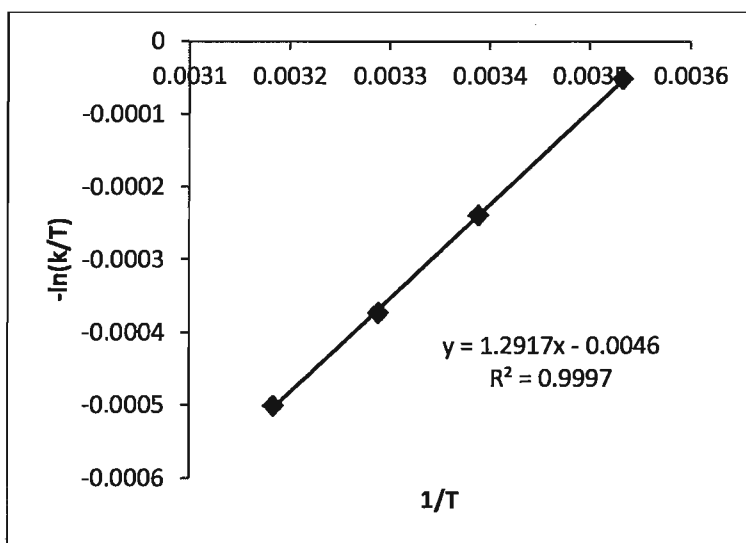


Figure V-93. Eyring plot for H/H exchange between H₂ and PhSiH₃ in the presence of
(ArN)Mo(SiH₂Ph)(Cl)(PMe₃)₂

Metal-mediated H₂/Si-H exchange: general procedure

Hydrogen atmosphere was applied to a solution of a metal complex and PhSiD₃ in C₆D₆. Formation of H-D and PhSiH_xD_y was observed by ¹H NMR. ¹H-NMR (300 MHz; C₆D₆; 298K; δ , ppm): 4.32 (s, PhSiH_xD_y), 4.54 (t, ¹J_{H-D} = 42.6 Hz, H-D). The following complexes observed to mediate the H₂/Si-H exchange: ZnCl₂ (Figure VI-1), (PPh₃)CuH (Figure VI-2), (ArN)Mo(H)(Cl)(PMe)₃ (Figure VI-3), (Cp)(ArN)Mo(H)(PMe₃) (Figure

VI-4), (Tp)(ArN)Mo(H)(PMe₃) (Figure VI-5, Figure VI-6), (ArN)Mo(Cl)₂(PMe₃)₃, (ArN)Mo(SiH₂Ph)(Cl)(PMe₃)₂, (ArN)Mo(SiH₂Ph)(Cl)(PMe₃)₃, (ArN)Mo(-C(Ph)=N-SiH₂Ph)(Cl)(PMe₃)₂.

H/D exchange between PhSiD₃ and H₂ (control experiment)

A hydrogen atmosphere was applied to the solution of PhSiD₃ (5 μl, 0.0040 mmol) in C₆D₆ (0.60 ml). Formation of either PhSiH_xD_y or H-D was not observed during one month at RT.

H/D exchange between PhSiD₃ and H₂ mediated by BPh₃

A hydrogen atmosphere was applied to the solution of PhSiD₃ (5 μl, 0.0040 mmol) and BPh₃ (1.0 mg, 0.0040 mmol) in C₆D₆ (0.60 ml). Formation of PhSiH_xD_y and H-D was observed by ¹H NMR after one month at RT. ¹H-NMR (300 MHz; C₆D₆; 298K; δ, ppm): 4.32 (s, PhSiH_xD_y), 4.54 (t, ¹J_{H-D} = 42.5 Hz, H-D).

H/D exchange between PhSiD₃ and H₂ mediated by B(C₆F₅)₃

A hydrogen atmosphere was applied to the solution of PhSiD₃ (4.4 mg, 0.040 mmol) and B(C₆F₅)₃ (5.0 mg, 0.010 mmol) in C₆D₆ (0.60 ml). Appearance of PhSiH_xD_y and H-D was observed in ¹H NMR after 10 min at RT. The reaction was left overnight. Next day, a large broad peak of PhSiH₃ was observed. The exchange was slow. ¹H-NMR (300 MHz; C₆D₆; 298K; δ, ppm): 4.32 (s, PhSiH_xD_y), 4.54 (t, ¹J_{H-D} = 42.5 Hz, H-D).

H/D exchange between PhMeSiD₂ and H₂ mediated by B(C₆F₅)₃

A hydrogen atmosphere was applied to the solution of PhMeSiD₂ (4.8 mg, 0.039 mmol) and B(C₆F₅)₃ (2.0 mg, 0.0039 mmol) in C₆D₆ (0.60 ml). Formation of PhMeSiH_xD_y and H-D was observed. ¹H-NMR (300 MHz; C₆D₆; 298K; δ, ppm): 4.32 (s, PhSiH_xD_y), 4.54 (t, ¹J_{H-D} = 42.3 Hz, H-D).

H/D exchange between PhMe₂SiD and H₂ mediated by B(C₆F₅)₃

A hydrogen atmosphere was applied to the solution of PhMe₂SiD (5.4 mg, 0.039 mmol) and B(C₆F₅)₃ (2.0 mg, 0.0039 mmol) in C₆D₆ (0.60 ml). Formation of PhMe₂SiH and H-D was observed. ¹H-NMR (300 MHz; C₆D₆; 298K; δ, ppm): 4.32 (s, PhSiH_xD_y), 4.54 (t, ¹J_{H-D} = 42.3 Hz, H-D).

H/D exchange between Et₃SiD and H₂ mediated by B(C₆F₅)₃

A hydrogen atmosphere was applied to the solution of Et₃SiD (4.6 mg, 0.039 mmol) and B(C₆F₅)₃ (2.0 mg, 0.0039 mmol) in C₆D₆ (0.60 ml). Formation of Et₃SiH and H-D was observed. ¹H-NMR (300 MHz; C₆D₆; 298K; δ, ppm): 4.32 (s, PhSiH_xD_y), 4.54 (t, ¹J_{H-D} = 42.3 Hz, H-D).

H/D exchange between PhSiD₃ and Et₃SiH in the presence of BPh₃

Triethylsilane (10 μl, 0.079 mmol) and PhSiD₃ (10 μl, 0.079 mmol) were mixed in the presence of BPh₃ (1.9 mg, 0.0079 mmol) in C₆D₆ (0.60 ml). The H/D exchange was not immediately observed. The reaction mixture was left for one month at RT. Formation of PhSiH_xD_y was observed by ¹H NMR. ¹H-NMR (300 MHz; C₆D₆; 298K; δ, ppm): 4.32 (s, PhSiH_xD_y).

Preparation of HB(C₆F₅)₂¹⁶²

Triethylsilane (2.9 μl, 0.018 mmol) was added to a solution of B(C₆F₅)₃ (10.0 mg, 0.018 mmol) in C₆D₆ (0.60 ml), and the reaction mixture was heated at 40 °C for several days until the reaction is complete.

H/D exchange between CatBH and Et₃SiD

Catecholborane (5 μl) and Et₃SiD (5 μl) were mixed in C₆D₆ (0.60 ml). Formation of Et₃SiH was observed in ¹H NMR and a broad singlet of CatBD in ¹¹B NMR spectrum. ¹H-NMR (300 MHz; C₆D₆; 298K; δ, ppm): 4.00 (s, 1H, Et₃SiH). ¹¹B-NMR (96.3 MHz; C₆D₆; 298 K; δ, ppm): 28.0 (bs, 1B, CatBD).

H/D exchange between PhSiH₃ and H₂ in the presence of PMe₃

Trimethylphosphine (7 μ l) was added to a solution of PhSiD_3 (5 μ l) in C_6D_6 (0.60 ml). The hydrogen atmosphere was applied, and the reaction mixture was left for one week at RT. No detectable amount of protosilane PhSiD_xH_y or HD was observed in ^1H NMR spectrum, indicating on the absence of H/D scrambling.

Reaction between acetophenone and PhSiD_3 in the presence of BPh_3

Acetophenone (6.0 mg, 0.050 mmol), phenylsilane (5.4 mg, 0.050 mmol) and triphenylborane (1.2 mg, 0.0050 mmol) were mixed in C_6D_6 (0.60 ml). Hydrosilylation of acetophenone was not observed.

Reaction between styrene and PhSiD_3 in the presence of BPh_3

Styrene (5.0 mg, 0.048 mmol), phenylsilane (5.2 mg, 0.048 mmol) and triphenylborane (11.6 mg, 0.048 mmol) were mixed in C_6D_6 (0.60 ml). Hydrosilylation of styrene was not observed.

Reaction between 1-hexane and CatBH in the presence of $\text{B}(\text{C}_6\text{F}_5)_3$

Hydroboration of 1-hexane was not observed.

H/D exchange between Et_3SiD and CatBH

Catecholborane (3.0 ml) and Et_3SiD (3.0 ml) were mixed in C_6D_6 (0.60 ml). Formation of Et_3SiH and CatBD was observed by NMR. ^1H -NMR (300 MHz; C_6D_6 ; 298K; δ , ppm): 4.00 (s, Et_3SiH).

VI Appendix

Table VI-1. Crystal structure determination parameters for

(Cp)(ArN)Mo(OCH₂Ph)(PMe₃).

Identification code	p-1
Empirical formula	C ₂₇ H ₃₈ MoNOP
Formula weight	519.49
Colour, habit	black plate
Crystal size, mm	0.38 x 0.32 x 0.04
Crystal system, space group	Triclinic, P-1
Unit cell dimensions:	a, Å 9.9782(7) α, ° 108.5940(10)
	b, Å 10.3691(7) β, ° 96.9990(10)
	c, Å 14.1074(10) γ, ° 105.3790(10)
Volume, Å ³	1299.42(16)
Z	2
Calculated density, g/cm ³	1.328
Absorption coefficient, mm ⁻¹	0.584
F(000)	544
Bruker SMART-APEX-2	Bruker SMART-APEX-2
Temperature, K	123(2)
Radiation, (λ, Å)	graphite monochromatized MoKα (0.71073)
Scan mode	omega
Step per scan, °	0.3
Theta range for data collection, °	1.56 to 30.00
Limiting indices	-14 ≤ h ≤ 12, -11 ≤ k ≤ 14, -19 ≤ l ≤ 19
Reflections collected / unique	16642 / 7517 [R(int) = 0.0238]
Completeness to theta = 30.00 °	99.2 %
Reflections with I > 2σ(I)	6610
Min. and Max. transmission	0.8085 and 0.9770
Solution method	Direct methods (SHELXS-97, G. M. Sheldrick, Acta Cryst., A46, 1990, 467-473)
Refinement method	Full-matrix least-squares on F ² (SHELXL-97, Program for the Refinement of Crystal Structures. University of Gottingen, 1997)
Hydrogen treatment	All H atoms were found from diff. Fourier synthesis and refined isotopically
Data / restraints / parameters	7517 / 0 / 229
Goodness-of-fit on F ²	1.074
Final R indices [I > 2σ(I)]	R1 = 0.0289 wR2 = 0.0713
R indices (all data)	R1 = 0.0358 wR2 = 0.0740
Largest diff. peak and hole, e/ Å ³	1.016 and -0.383

Table VI-2. Crystal structure determination parameters for (Tp)(ArN)Mo(H)(PMe₃).

Identification code	p21c
Empirical formula	C ₃₀ H ₅₄ BMoN ₇ P
Formula weight	650.52
Habit, colour	block, black
Crystal size, mm	0.45 x 0.40 x 0.36
Crystal system, space group	Monoclinic, P2(1)/c
Unit cell dimensions:	a, Å 11.4352(4) α, ° 90.00 b, Å 13.2000(4) β, ° 103.8340(10) c, Å 20.9102(7) γ, ° 90.00
Volume, Å ³	3064.73(18)
Z	4
Calculated density, g/cm ³	1.410
Absorption coefficient, mm ⁻¹	0.513
F(000)	1380
Diffractometer	Bruker SMART-APEX-2
Temperature, K	143(2)
Radiation, (λ, Å)	graphite monochromatized MoK α (0.71073)
Scan mode	omega
Theta range for data collection, °	1.83 to 30.00
Limiting indices	-16 ≤ h ≤ 16, -18 ≤ k ≤ 18, -29 ≤ l ≤ 29
Reflections collected / unique	35446 / 8933 [R(int) = 0.0208]
Completeness to theta = 30.00 °	100.0%
Reflections with I>2σ(I)	7274
Absorption correction	Semi-empirical from equivalents
Min. and Max. transmission	0.8019 and 0.8368
Solution method	Direct methods (SHELXS-97, G. M. Sheldrick, Acta Cryst., A46, 1990, 467-473)
Refinement method	Full-matrix least-squares on F ² (SHELXL-97, Program for the Refinement of Crystal Structures. University of Gottingen, 1997)
Hydrogen treatment	All H atoms were found from diff. Fourier synthesis and refined isotopically.
Data / restraints / parameters	8933 / 0 / 229
Goodness-of-fit on F ²	1.090
Final R indices [I>2σ(I)]	R1 = 0.0431, wR2 = 0.1170
R indices (all data)	R1 = 0.0541, wR2 = 0.1235
Largest diff. peak and hole, e/ Å ³	1.207 and -0.800

Table VI-3. Crystal structure determination parameters for (ArN)(CyO)Mo(Cl)(PMe₃)₃

Identification code	p21c
Empirical formula	C ₂₇ H ₅₅ ClMoNOP ₃
Formula weight	634.02
Crystal size, mm	0.30 x 0.28 x 0.04
Unit cell dimensions:	a, Å 12.6249(11) α, ° 90
	b, Å 19.6456(17) β, ° 102.5750(10)
	c, Å 13.7219(12) γ, ° 90
Volume, Å ³	3321.7(5)
Z	4
Calculated density, g/cm ³	1.268
Absorption coefficient, mm ⁻¹	0.639
F(000)	1344
Temperature, K	153(2)
Radiation, (λ, Å)	graphite monochromatized MoK α (0.71073)
Scan mode	omega
Step per scan, deg	0.3
Theta range, deg	1.65 to 30.00
Limiting indices	-17 ≤ h ≤ 17, -27 ≤ k ≤ 27, -19 ≤ l ≤ 19
Reflections collected / unique	38454 / 9652 [R(int) = 0.0355]
Completeness to theta = 30.00 °	99.7%
Reflections with I > 2σ(I)	8215
Min. and Max. transmission	0.8315 and 0.9749
Solution method	Direct methods (SHELXS-97, G. M. Shendrick, Acta Cryst., A46, 1990, 467-473)
Refinement method	Full-matrix least-squares on F ² SHELXL-97, Program for the Refinement of Crystal Structures. University of Gottingen, 1997
Hydrogen treatment	All H atoms were found from diff. Fourier synthesis and refined isotopically
Data / restraints / parameters	9652 / 0 / 307
Goodness-of-fit on F ²	1.149
Final R indices [I > 2σ(I)]	R1 = 0.0444, wR2 = 0.1258
R indices (all data)	R1 = 0.0537, wR2 = 0.1289
Largest diff. peak and hole, e/ Å ³	2.881 and -0.447

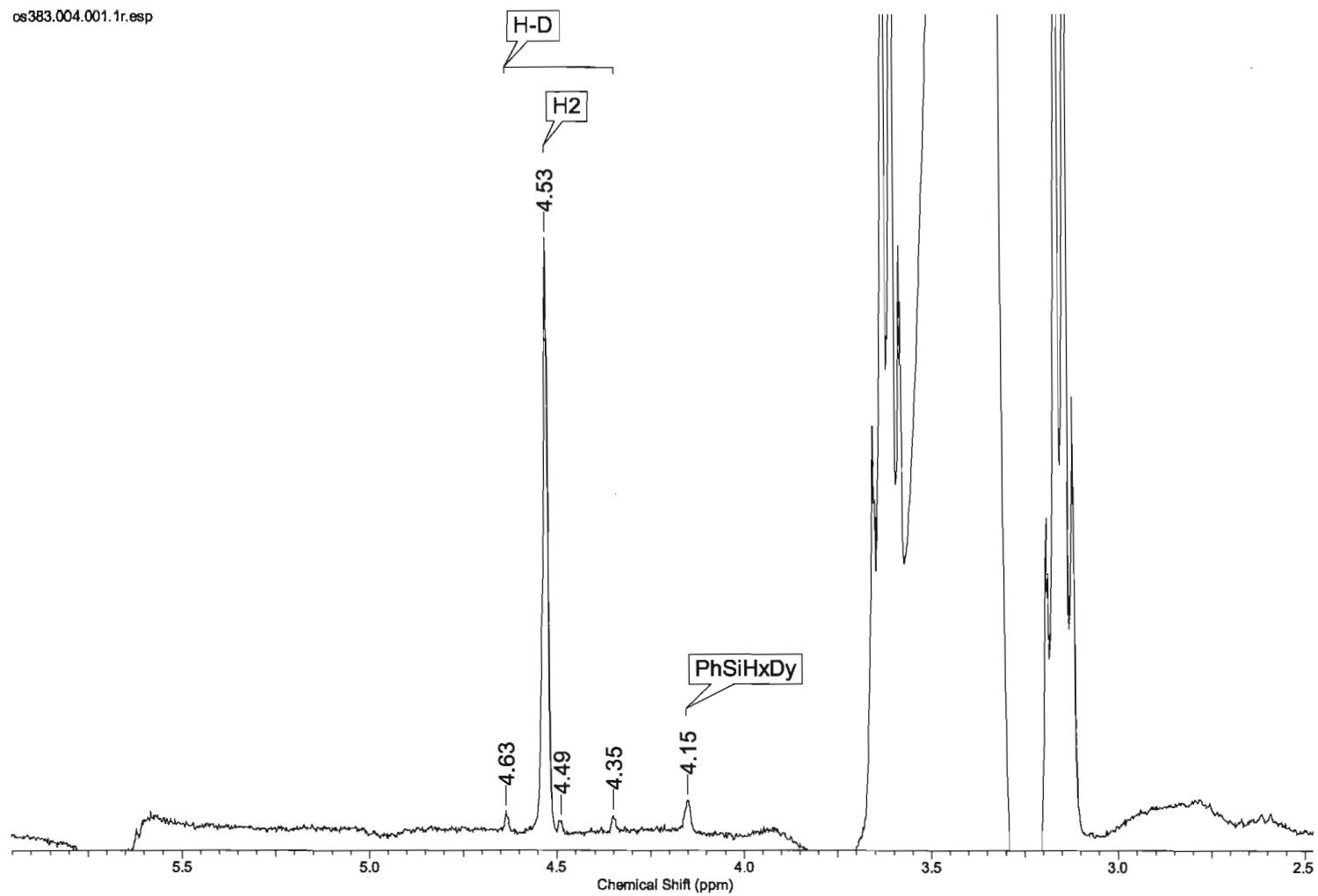


Figure VI-1. ^1H NMR spectrum of PhSiD_3 and ZnCl_2 in Et_2O under H_2 atmosphere.

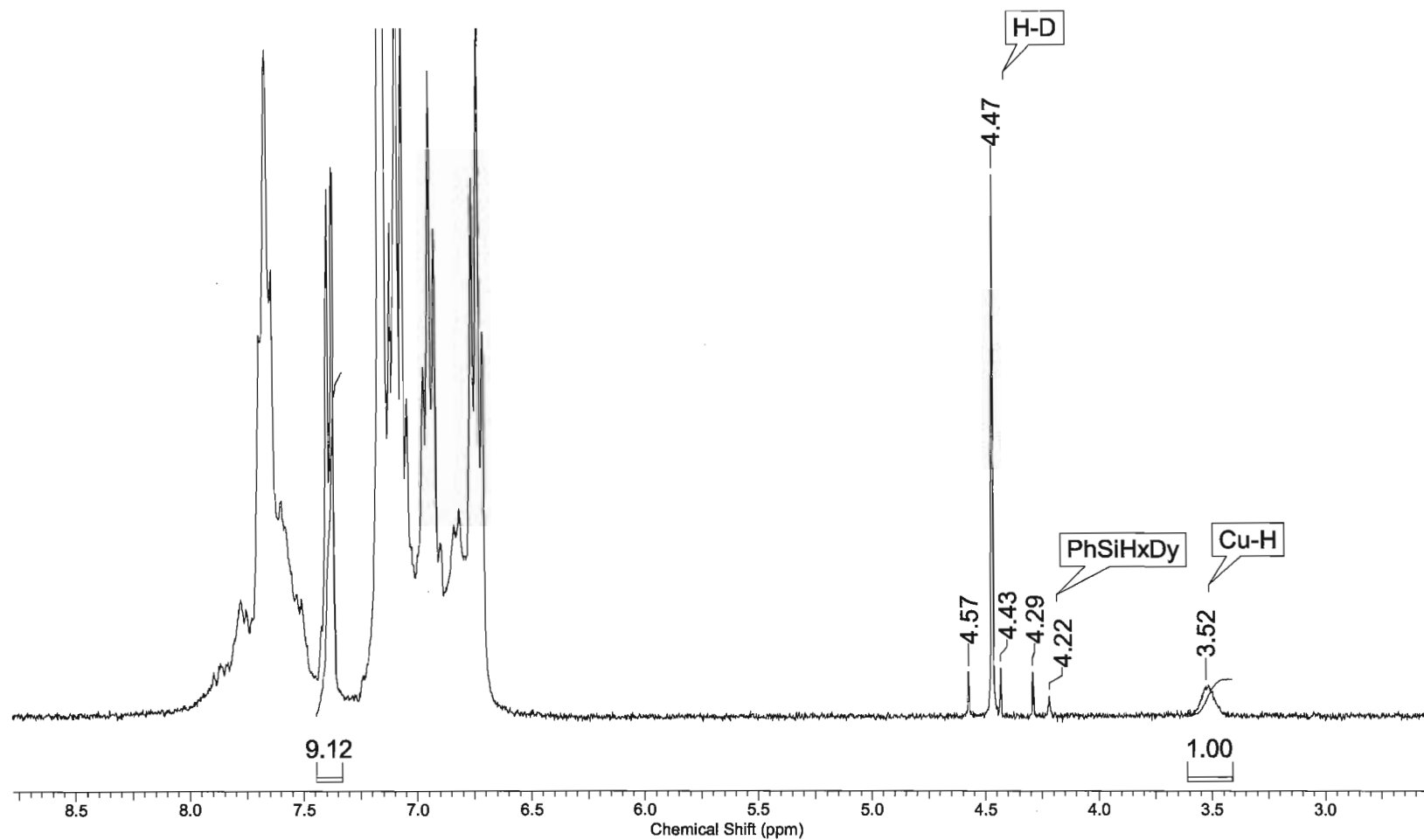


Figure VI-2. ^1H NMR spectrum of PhSiD_3 and $\text{CuH(PPh}_3\text{)}$ in C_6D_6 under H_2 atmosphere.

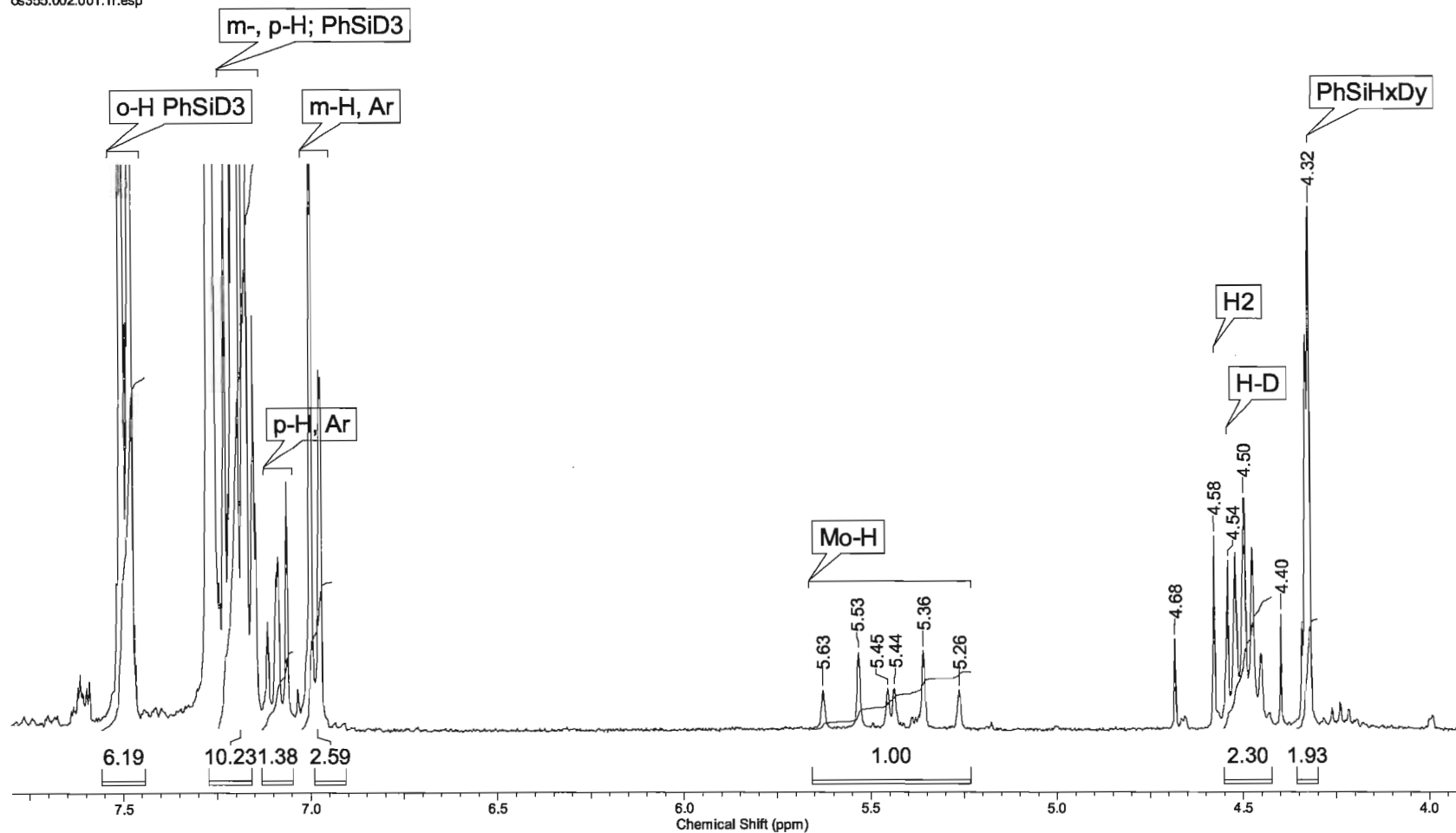


Figure VI-3. ^1H NMR spectrum of $(\text{ArN})\text{Mo}(\text{H})(\text{Cl})(\text{PMe}_3)_3$ and PhSiD_3 under H_2 atmosphere.

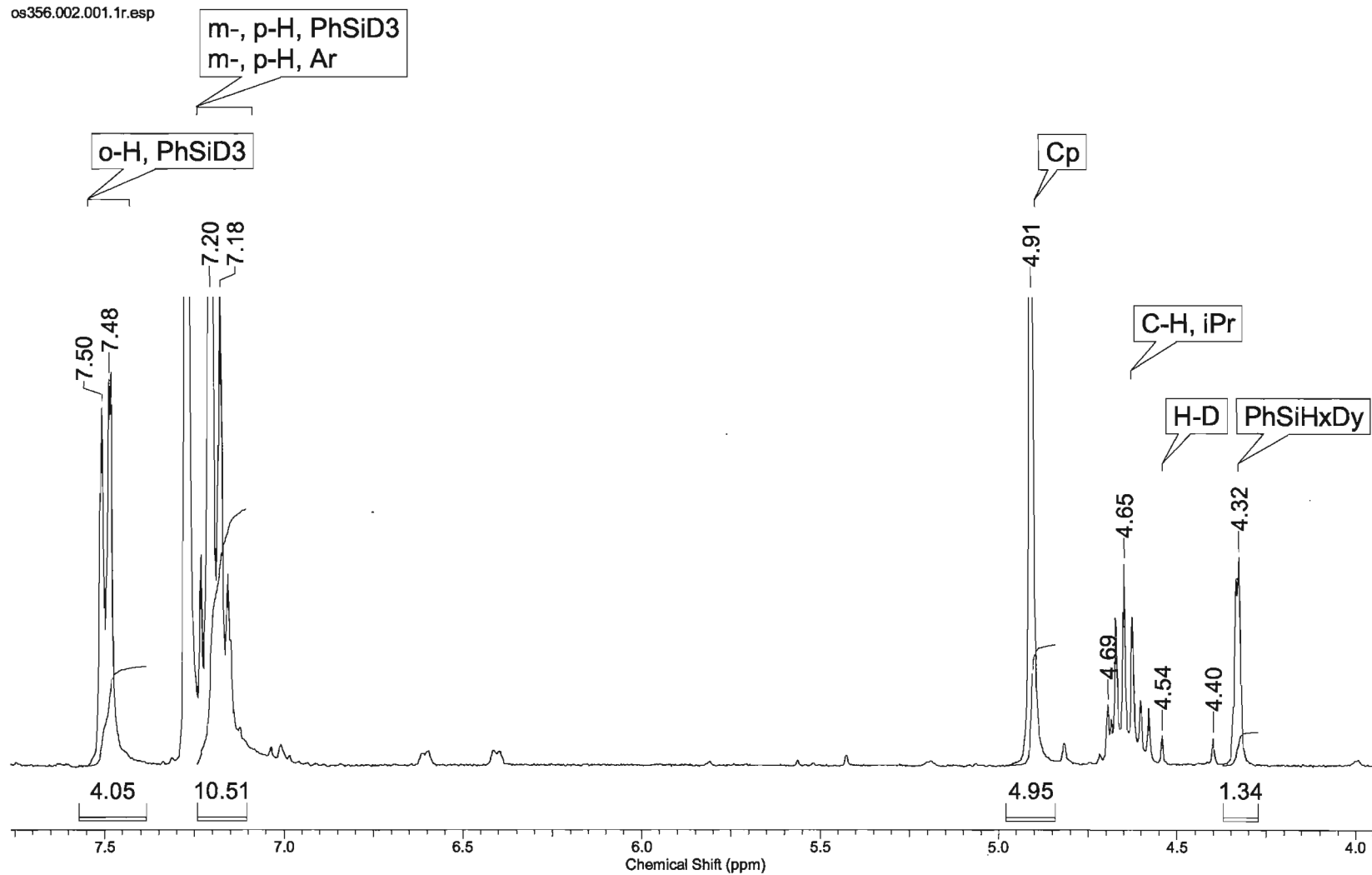


Figure VI-4. ^1H NMR spectrum of $(\text{Cp})(\text{ArN})\text{Mo}(\text{H})(\text{PMe}_3)$ and PhSiD_3 under H_2 atmosphere.

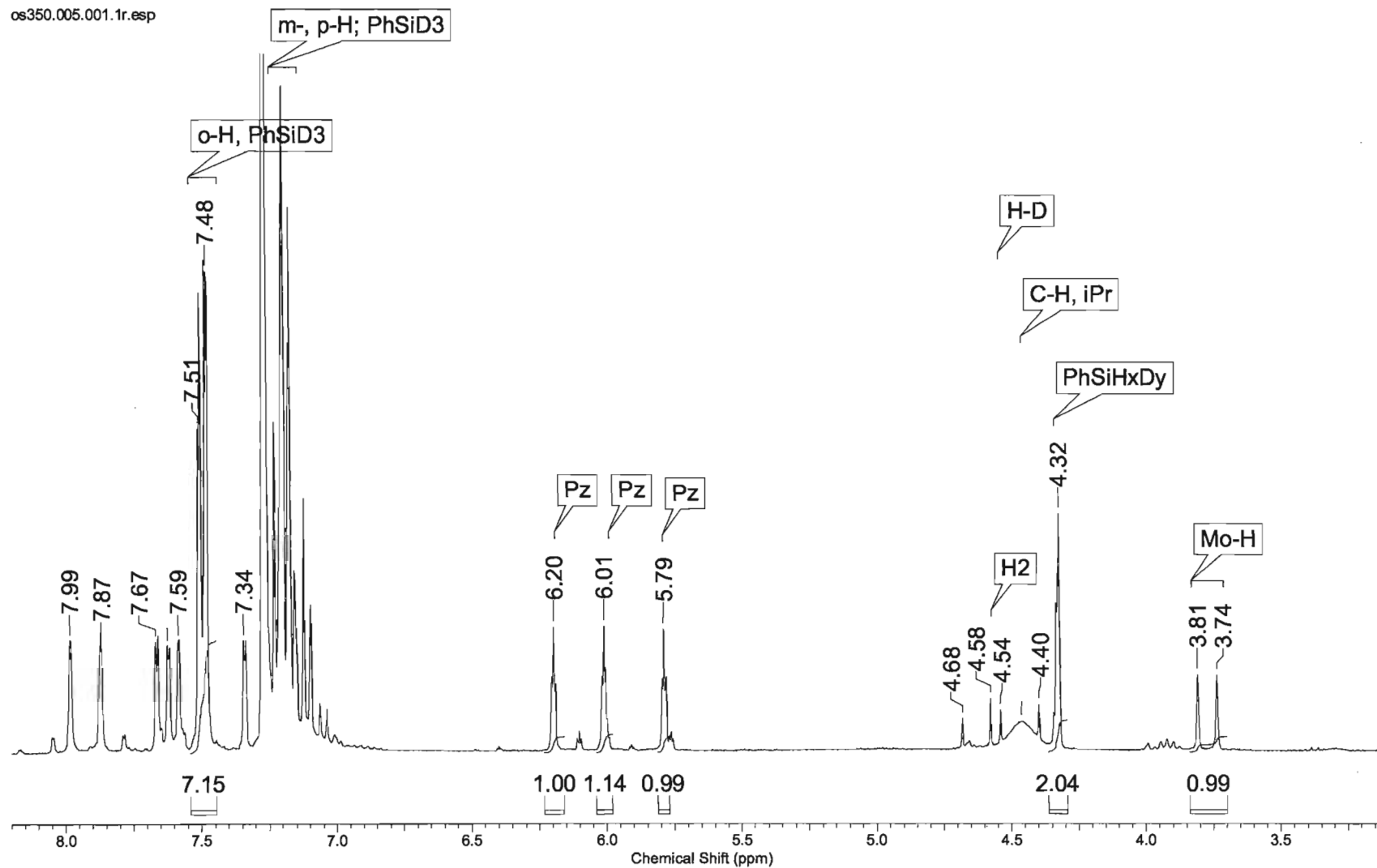


Figure VI-5. ^1H NMR spectrum of $(\text{Tp})(\text{ArN})\text{Mo}(\text{H})(\text{PMe}_3)$ and PhSiD_3 under H_2 atmosphere (30 min, RT).

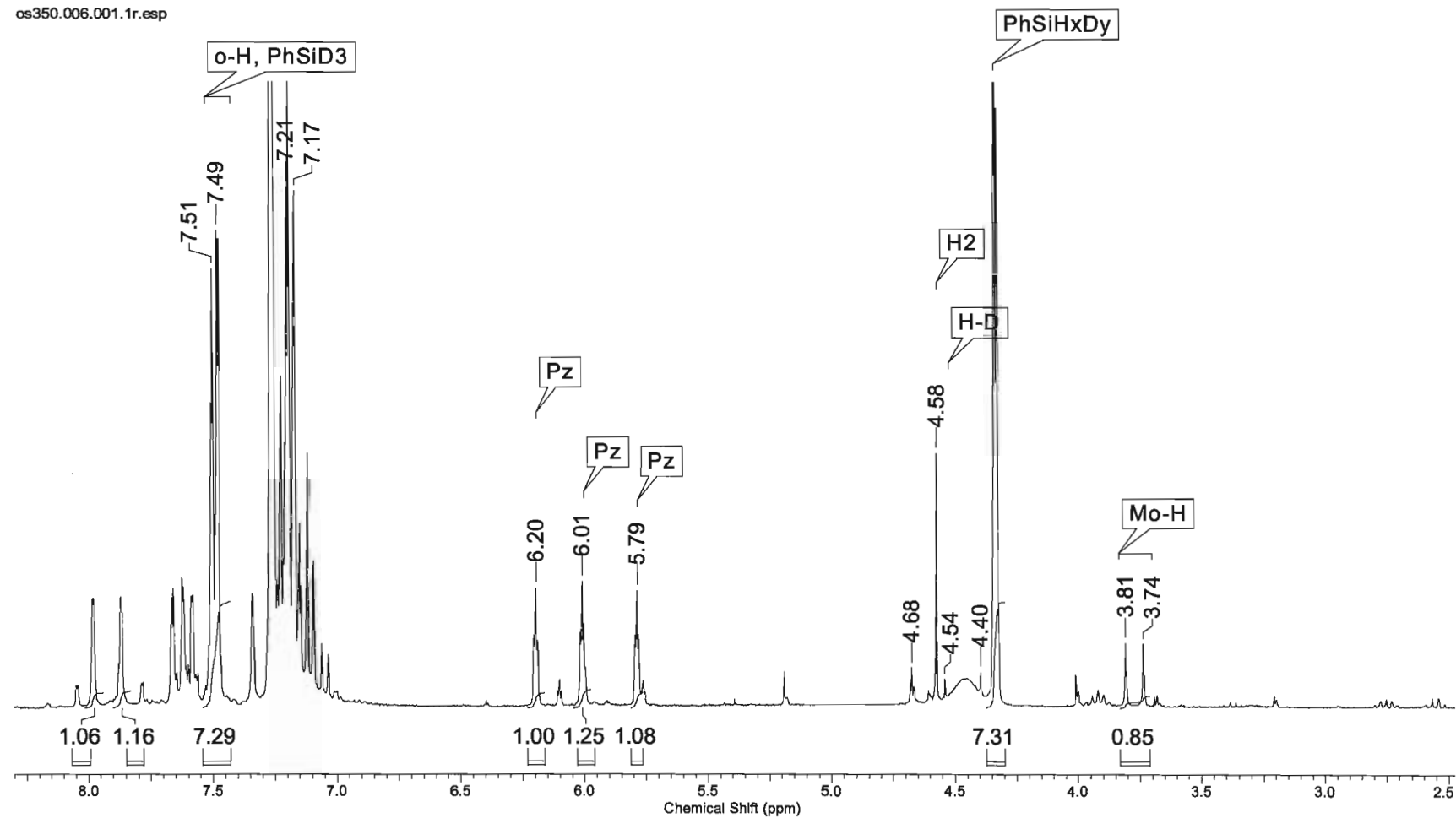


Figure VI-6. ^1H NMR spectrum of $(\text{Tp})(\text{ArN})\text{Mo}(\text{H})(\text{PMe}_3)$ and PhSiD_3 under H_2 atmosphere (3 days, RT).

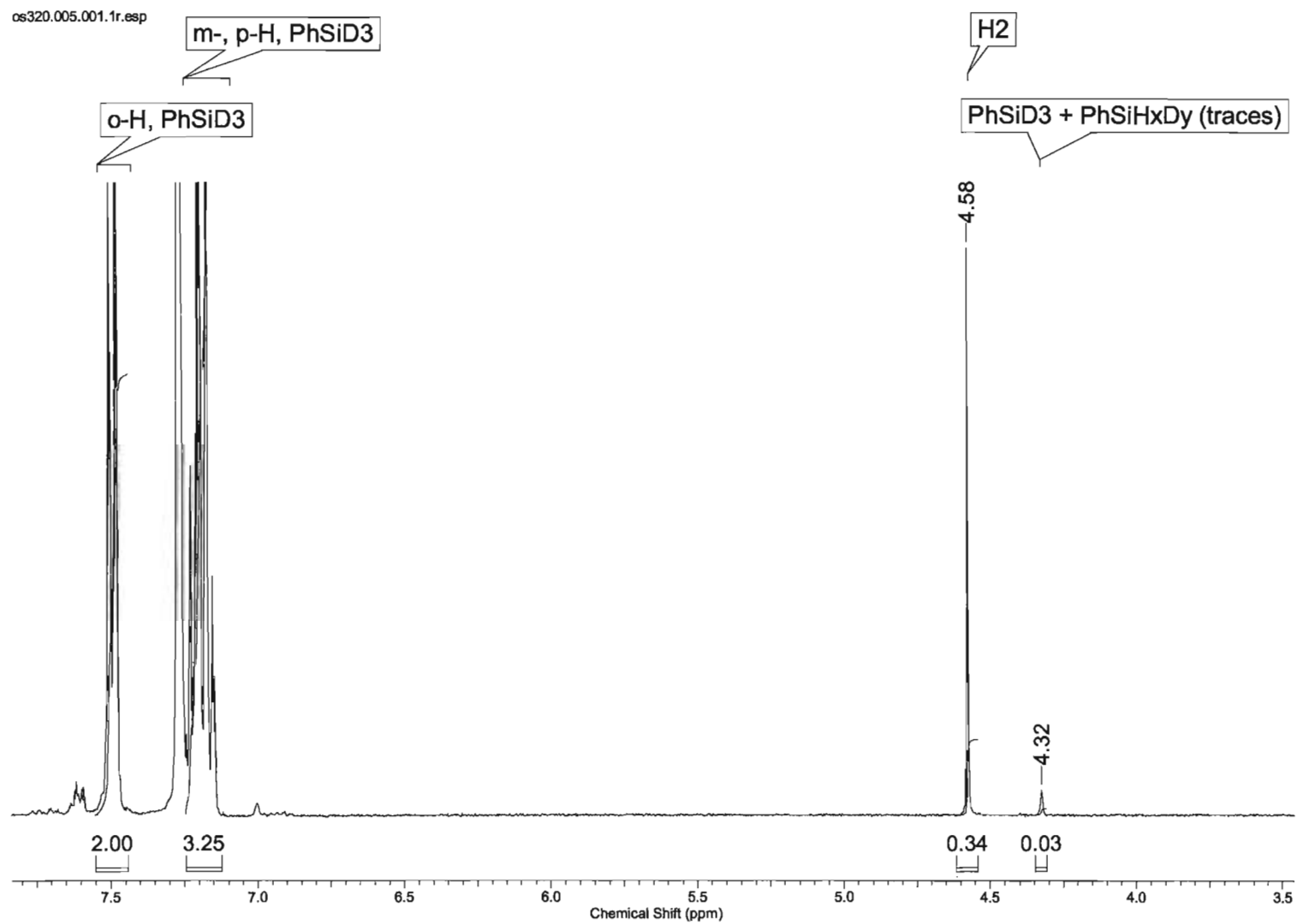


Figure VI-7. ^1H NMR spectrum of PhSiD_3 in C_6D_6 under the hydrogen atmosphere (control experiment)

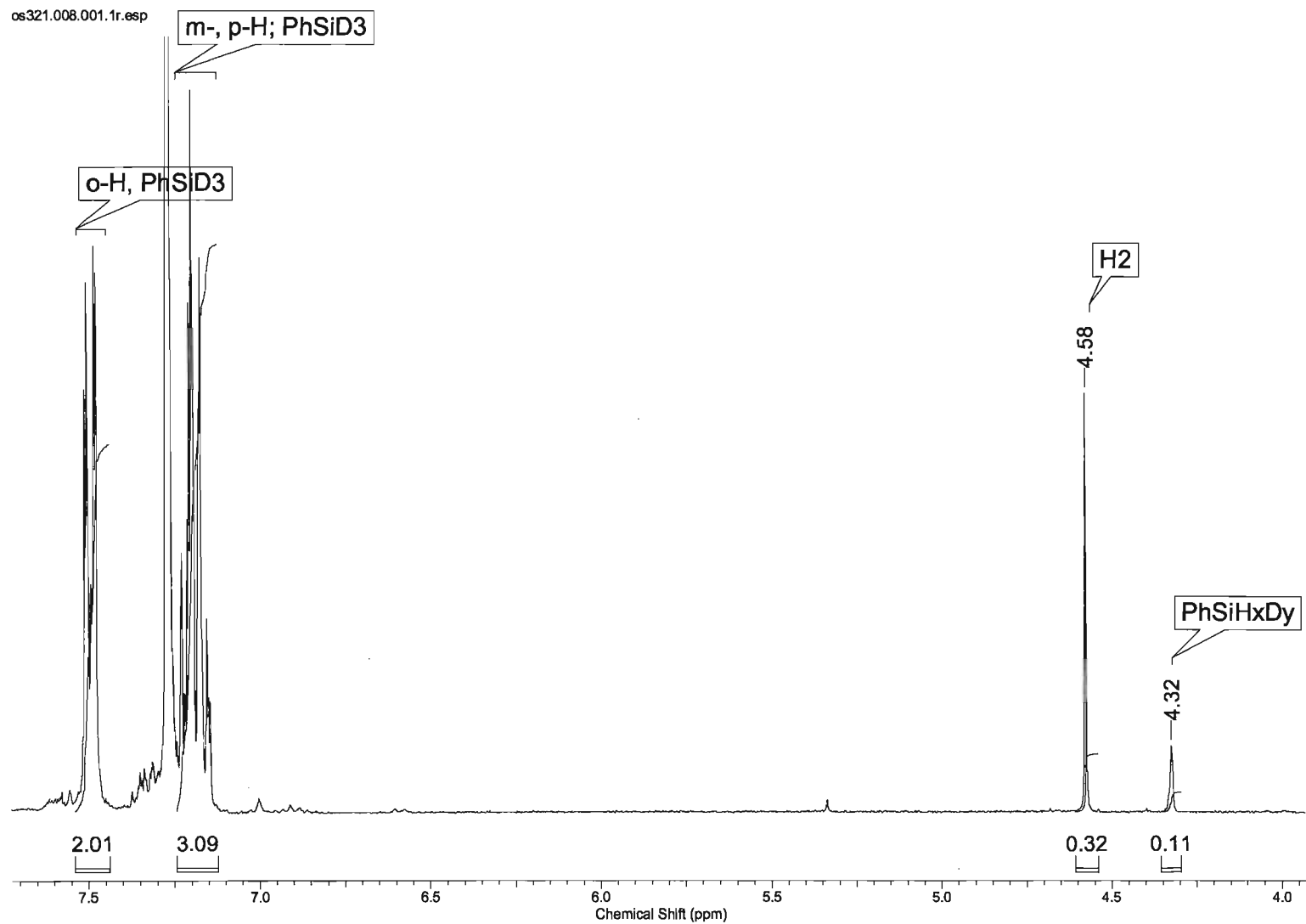


Figure VI-8. ^1H NMR spectrum of PhSiD₃ and BPh₃ in C₆D₆ under the hydrogen atmosphere

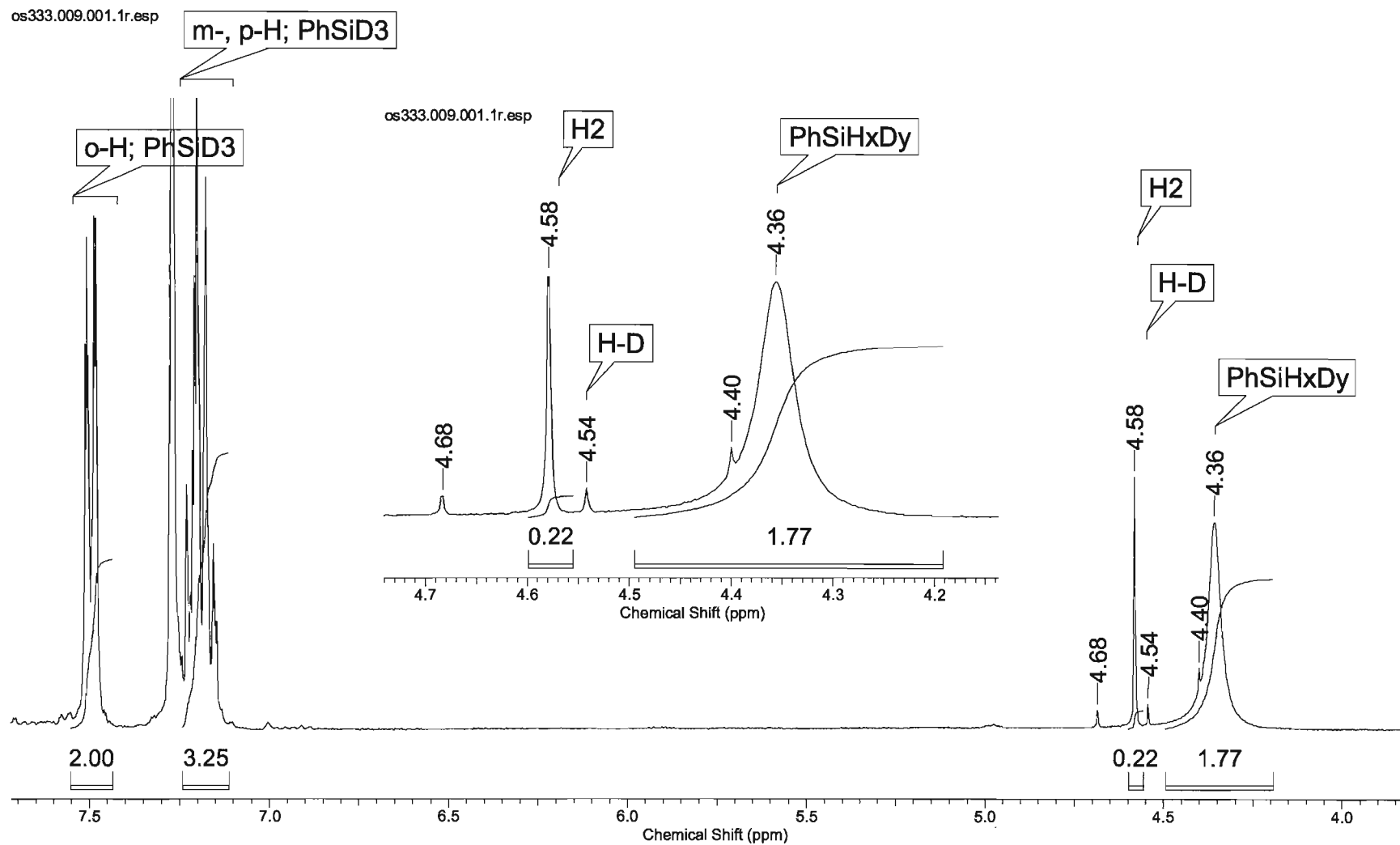


Figure VI-9. ^1H NMR spectrum of PhSiD_3 and $\text{B}(\text{C}_6\text{F}_5)_3$ in C_6D_6 under the hydrogen atmosphere

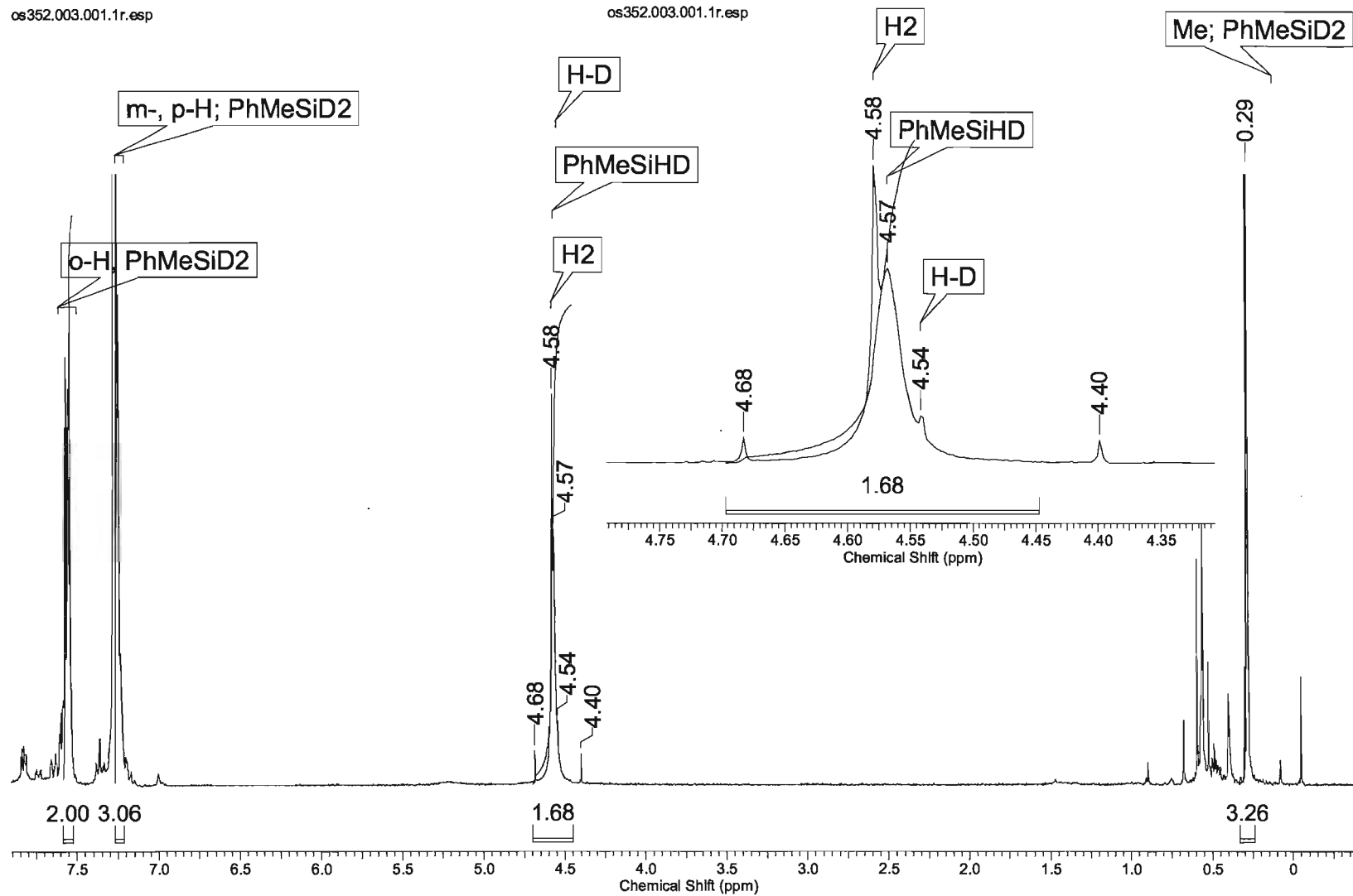


Figure VI-10. ^1H NMR spectrum of PhMeSiD_2 and $\text{B}(\text{C}_6\text{F}_5)_3$ in C_6D_6 under the hydrogen atmosphere

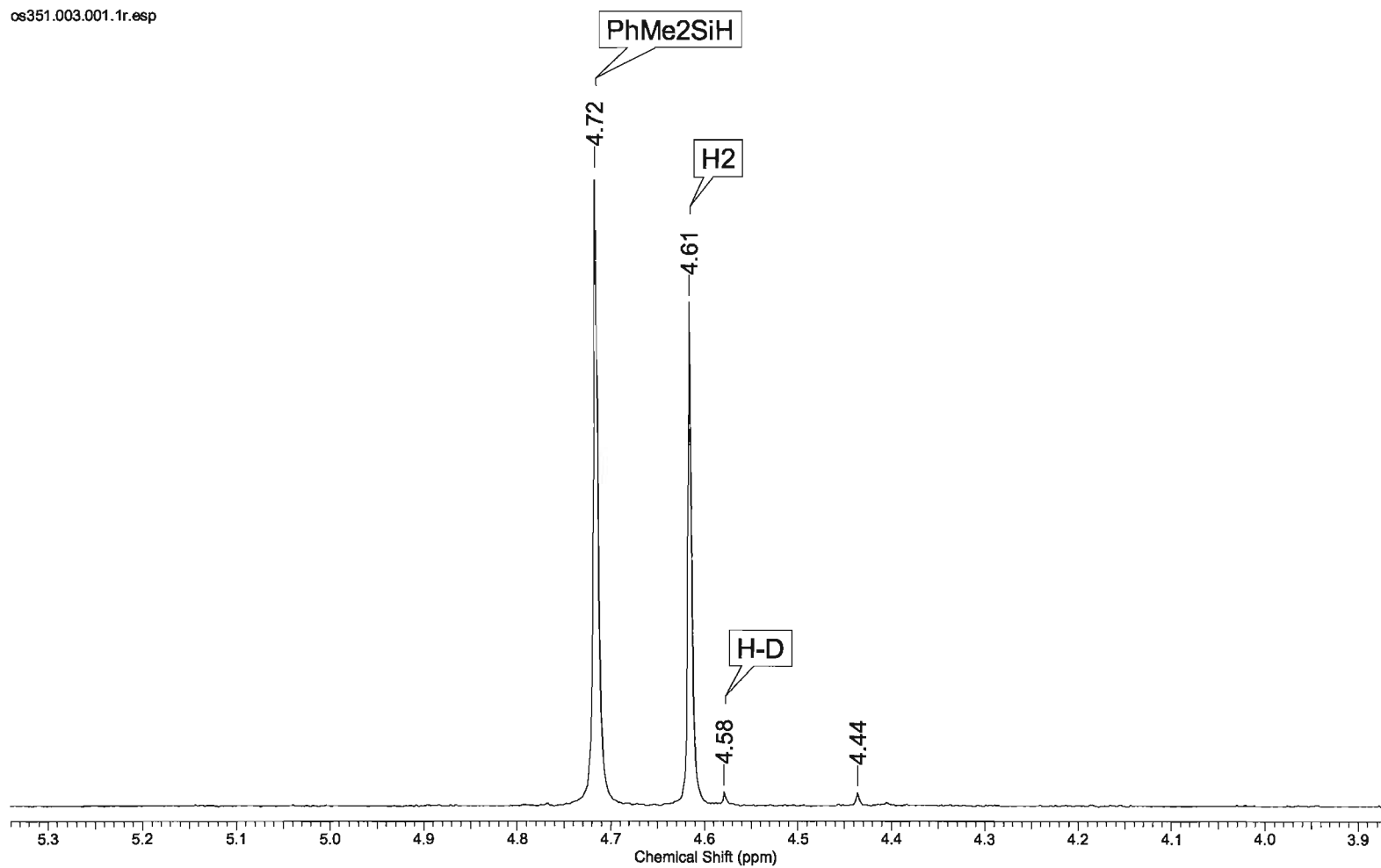


Figure VI-11. ^1H NMR spectrum of PhMe₂SiD and B(C₆F₅)₃ in C₆D₆ under the hydrogen atmosphere

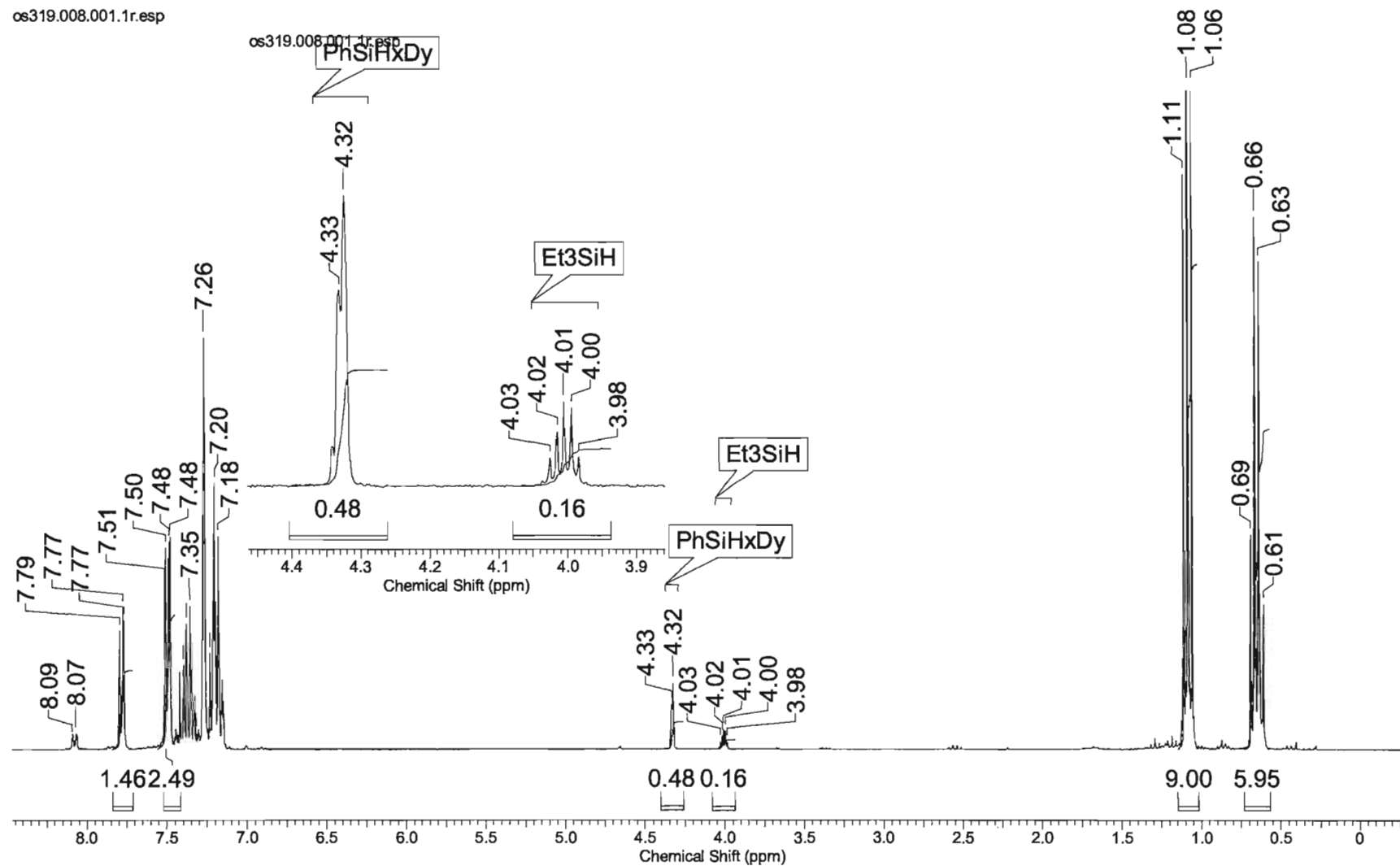


Figure VI-12. ¹H NMR spectrum of PhSiD₃, Et₃SiH and BPh₃ in C₆D₆ (after 1 month at RT).

VII References

1. (a) Roy, A. K., A Review of recent progress in catalysed homogeneous hydrosilation (hydrosilylation). *Adv. Organomet. Chem.* **2008**, *55*, 1-59; (b) Gibson, S. E.; Rudd, M., The role of secondary interactions in the asymmetric palladium-catalysed hydrosilylation of olefins with monophosphane ligands. *Adv. Synth. Catal.* **2007**, *349*, 781-795; (c) Marciniak, B., Silicometallics and catalysis. *Appl Organomet Chem* **2000**, *14* (10), 527-538; (d) Marciniak, B., *Comprehensive handbook on hydrosilylation*. Pergamon: Oxford, 1992.
2. (a) Berk, S. C.; Kreutzer, K. A.; Buchwald, S. L., A Catalytic Method for the Reduction of Esters to Alcohols. *Journal of the American Chemical Society* **1991**, *113* (13), 5093-5095; (b) Berk, S. C.; Buchwald, S. L., An Air-Stable Catalyst System for the Conversion of Esters to Alcohols. *J Org Chem* **1992**, *57* (14), 3751-3753; (c) Broene, R. D.; Buchwald, S. L., Asymmetric hydrogenation of unfunctionalized trisubstituted olefins with a chiral titanocene catalyst. *Journal of the American Chemical Society* **1993**, *115* (26), 12569-12570; (d) Carter, M. B.; Schiott, B.; Gutierrez, A.; Buchwald, S. L., Enantioselective Hydrosilylation of Ketones with a Chiral Titanocene Catalyst. *Journal of the American Chemical Society* **1994**, *116* (26), 11667-11670; (e) Halterman, R. L.; Ramsey, T. M.; Chen, Z. L., Catalytic Asymmetric Hydrosilation of Aryl Alkyl Ketones with C-2-Symmetrical Chiral Metallocene Complexes. *J Org Chem* **1994**, *59* (9), 2642-2644; (f) Xin, S. X.; Harrod, J. F., Enantioselective Hydrosilation of Ketones in the Presence of an S,S-[1,2-Bis(Tetrahydroindenyl)Ethane]Titanium Catalyst. *Can J Chem* **1995**, *73* (7), 999-1002; (g) Yun, J.; Buchwald, S. L., Titanocene-catalyzed asymmetric ketone hydrosilylation: The effect of catalyst activation protocol and additives on the reaction rate and enantioselectivity. *Journal of the American Chemical Society* **1999**, *121* (24), 5640-5644.
3. Yun, S. S.; Yang, Y. S.; Lee, S., Hydrosilation of ketones catalyzed by dimethylzirconocene. *B Kor Chem Soc* **1997**, *18* (10), 1058-1060.

4. (a) Royo, B.; Romao, C. C., Reduction of carbonyl groups by high-valent rhenium oxides. *J Mol Catal a-Chem* **2005**, *236* (1-2), 107-112; (b) Reis, P. M.; Romao, C. C.; Royo, B., Dioxomolybdenum(VI) complexes as catalysts for the hydrosilylation of aldehydes and ketones. *Dalton T* **2006**, (15), 1842-1846; (c) Ziegler, J. E.; Du, G. D.; Fanwick, P. E.; Abu-Omar, M. M., An Efficient Method for the Preparation of Oxo Molybdenum Salalen Complexes and Their Unusual Use as Hydrosilylation Catalysts. *Inorganic Chemistry* **2009**, *48* (23), 11290-11296.
5. (a) Peterson, E.; Khalimon, A. Y.; Sirnionescu, R.; Kuzmina, L. G.; Howard, J. A. K.; Nikonov, G. I., Diversity of Catalysis by an Imido-Hydrido Complex of Molybdenum. Mechanism of Carbonyl Hydrosilylation and Silane Alcoholysis. *Journal of the American Chemical Society* **2009**, *131* (3), 908-909; (b) Shirobokov, O. G.; Gorelsky, S. I.; Simionescu, R.; Kuzmina, L. G.; Nikonov, G. I., The unexpected mechanism of carbonyl hydrosilylation catalyzed by (Cp)(ArN=)Mo(H)(PMe₃). *Chem Commun* **2010**, *46* (41), 7831-7833.
6. Du, G.; Abu-Omar, M. M., Oxo and imido complexes of rhenium and molybdenum in catalytic reductions. *Curr Org Chem* **2008**, *12* (14), 1185-1198.
7. (a) Fontaine, F. G.; Nguyen, R. V.; Zargarian, D., Hydrosilylation of alkenes and ketones catalyzed by nickel(II) indenyl complexes. *Can J Chem* **2003**, *81* (11), 1299-1306; (b) Chakraborty, S.; Krause, J. A.; Guan, H., Hydrosilylation of Aldehydes and Ketones Catalyzed by Nickel PCP-Pincer Hydride Complexes. *Organometallics* **2009**, *28* (2), 582-586; (c) Tran, B. L.; Pink, M.; Mindiola, D. J., Catalytic Hydrosilylation of the Carbonyl Functionality via a Transient Nickel Hydride Complex. *Organometallics* **2009**, *28* (7), 2234-2243.
8. (a) Langlotz, B. K.; Wadepohl, H.; Gade, L. H., Chiral bis(pyridylimino)isoindoles: A highly modular class of pincer ligands for enantioselective catalysis. *Angewandte Chemie-International Edition* **2008**, *47* (25), 4670-4674; (b) Shaikh, N. S.; Enthaler, S.; Junge, K.; Beller, M., Iron-catalyzed enantioselective hydrosilylation of ketones. *Angewandte Chemie-International Edition* **2008**, *47* (13), 2497-2501; (c) Nishiyama, H.; Furuta, A., An iron-catalysed hydrosilylation of ketones. *Chem Commun* **2007**, (7), 760-762; (d) Addis, D.; Shaikh, N.; Zhou, S. L.; Das, S.;

Junge, K.; Beller, M., Chemo- and Stereoselective Iron-Catalyzed Hydrosilylation of Ketones. *Chem-Asian J* **2010**, *5* (7), 1687-1691; (e) Bart, S. C.; Lobkovsky, E.; Chirik, P. J., Preparation and molecular and electronic structures of iron(0) dinitrogen and silane complexes and their application to catalytic hydrogenation and hydrosilation. *Journal of the American Chemical Society* **2004**, *126* (42), 13794-13807; (f) Gutsulyak, D. V.; Kuzmina, L. G.; Howard, J. A. K.; Vyboishchikov, S. F.; Nikonov, G. I., Cp(*i*-Pr₂MeP)FeH₂SiR₃: Nonclassical iron silyl dihydride. *Journal of the American Chemical Society* **2008**, *130* (12), 3732-3733; (g) Shaikh, N. S.; Junge, K.; Beller, M., A Convenient and General Iron-Catalyzed Hydrosilylation of Aldehydes. *Org Lett* **2007**, *9* (26), 5429-5432; (h) Tondreau, A. M.; Lobkovsky, E.; Chirik, P. J., Bis(imino)pyridine iron complexes for aldehyde and ketone hydrosilylation. *Org Lett* **2008**, *10* (13), 2789-2792; (i) Kandepi, V. V. K. M.; Cardoso, J. M. S.; Peris, E.; Royo, B., Iron(II) Complexes Bearing Chelating Cyclopentadienyl-N-Heterocyclic Carbene Ligands as Catalysts for Hydrosilylation and Hydrogen Transfer Reactions. *Organometallics* **2010**, *29* (12), 2777-2782.

9. (a) Diez-Gonzalez, S.; Nolan, S. P., Copper, silver, and gold complexes in hydrosilylation reactions. *Accounts Chem Res* **2008**, *41* (2), 349-358; (b) Deutsch, C.; Krause, N.; Lipshutz, B. H., CuH-catalyzed reactions. *Chem Rev* **2008**, *108* (8), 2916-2927.

10. (a) Nolin, K. A.; Krumper, J. R.; Pluth, M. D.; Bergman, R. G.; Toste, F. D., Analysis of an unprecedented mechanism for the catalytic hydrosilylation of carbonyl compounds. *Journal of the American Chemical Society* **2007**, *129* (47), 14684-14696; (b) Du, G. D.; Fanwick, P. E.; Abu-Omar, M. M., Mechanistic insight into hydrosilylation reactions catalyzed by high valent Re equivalent to X (X = O, NAr, or N) complexes: The silane (SiH) does not add across the metal-ligand multiple bond. *Journal of the American Chemical Society* **2007**, *129* (16), 5180-5187.

11. Crabtree, R. H., *The Organometallic Chemistry of the Transition Metals*. 3rd edition ed.; Wiley-Interscience: 2001.

12. Vogels, C. M.; Decken, A.; Westcott, S. A., Catalyzed hydroboration of nitrostyrenes and 4-vinylaniline: a mild and selective route to aniline derivatives containing boronate esters. *Tetrahedron Lett* **2006**, 47 (14), 2419-2422.
13. Sommer, L. H.; Pietrusza, E. W.; Whitmore, F. C., Peroxide-Catalyzed Addition of Trichlorosilane to 1-Octene. *Journal of the American Chemical Society* **1947**, 69 (1), 188-188.
14. (a) Calas, R.; Duffaut, N.; Valade, J., Action Du Trichlorosilane Et Du Triphenylsilane Sur Les Cetonnes Aliphatiques Et Alicycliques. *B Soc Chim Fr* **1958**, (6), 751-751; (b) Calas, R.; Duffaut, N., Addition Du Trichlorosilane Et Du Triphenylsilane Aux Cetonnes Aliphatiques Saturees. *Cr Hebd Acad Sci* **1957**, 245 (9), 906-907.
15. Gilman, H.; Wittenberg, D., Addition of Triphenylsilane, Diphenylsilane, and Phenylsilane to Benzophenone. *J Org Chem* **1958**, 23 (3), 501-502.
16. (a) Calas, R.; Duffaut, N.; Menard, M. F., Action Du Trichlorosilane Sur Les Aldehydes Aliphatiques Satures. *B Soc Chim Fr* **1959**, (4), 562-562; (b) Calas, R.; Duffaut, N.; Bardot, C., Sur La Reactivite De Quelques Cetonnes Avec Des Hydrogenosilanes. *Cr Hebd Acad Sci* **1959**, 249 (17), 1682-1684; (c) Calas, R.; Duffaut, N.; Bardot, C., Reactivite De Quelques Cetonnes Vis-a-Vis De Divers Hydrogenosilanes. *B Soc Chim Fr* **1959**, (10), 1440-1440.
17. Calas, R., Sur Quelques Aspects de la Reactivite des Hydrogenosilanes en Chimie. *Pure Appl Chem* **1996**, 13 (1-2), 61-79.
18. Calas, R.; Frainnet, E.; Bonastre, J., Sur Une Nouvelle Methode Daddition Du Triethylsilane Aux Cetonnes. *Cr Hebd Acad Sci* **1960**, 251 (25), 2987-2989.
19. Ojima, I.; Nihonyan.M; Nagai, Y., Rhodium Complex Catalyzed Hydrosilylation of Carbonyl-Compounds. *J Chem Soc Chem Comm* **1972**, (16), 938-&.
20. de Charentenay, F.; Osborn, J. A.; Wilkinson, G., Interaction of Silanes with Tris(Triphenylphosphine)Chlororhodium(1) and Other Rhodium Complexes - Hydrosilation of 1-Hexene by Use of Trichlorosilane. *J Chem Soc A* **1968**, (4), 787-790.
21. Haszeldine, R. V.; Parish, R. V.; Parry, D. J., Organosilicon Chemistry .V. Rhodium(3)-Silyl Complexes and Hydrosilation of 1-Hexene. *J Chem Soc A* **1969**, (4), 683-690.

22. (a) Ojima, I.; Nihonyanagi, M.; Kogure, T.; Nagai, Y., Reduction of Carbonyl-Compounds with Various Hydrosilane-Rhodium(I) Complex Combinations. *B Chem Soc Jpn* **1972**, *45* (11), 3506-3511; (b) Ojima, I.; Nihonyanagi, M.; Nagai, Y., Stereoselective Reduction of Ketones with Hydrosilane-Rhodium(I) Complex Combinations. *B Chem Soc Jpn* **1972**, *45* (12), 3722-3727; (c) Ojima, I.; Nagai, Y.; Kogure, T., Selective Reduction of Alpha,Beta-Unsaturated Terpene Carbonyl-Compounds Using Hydrosilane-Rhodium(I) Complex Combinations. *Tetrahedron Lett* **1972**, (49), 5035-5038.
23. (a) Ojima, I.; Nihonyanagi, M.; Kogure, T.; Kumagai, M.; Horiuchi, S.; Nakatsugawa, K.; Nagai, Y., Reduction of Carbonyl-Compounds Via Hydrosilylation .1. Hydrosilylation of Carbonyl-Compounds Catalyzed by Tris(Triphenylphosphine)Chlororhodium. *J Organomet Chem* **1975**, *94* (3), 449-461; (b) Ojima, I.; Kogure, T.; Kumagai, M.; Horiuchi, S.; Sato, T., Reduction of Carbonyl-Compounds Via Hydrosilylation .2. Asymmetric Reduction of Ketones Via Hydrosilylation Catalyzed by a Rhodium(I) Complex with Chiral Phosphine Ligands. *J Organomet Chem* **1976**, *122* (1), 83-97; (c) Ojima, I.; Kogure, T.; Kumagai, M., Reduction of Carbonyl-Compounds Via Hydrosilylation .3. Asymmetric Reduction of Keto Esters Via Hydrosilylation Catalyzed by a Rhodium Complex with Chiral Phosphine Ligands. *J Org Chem* **1977**, *42* (10), 1671-1679; (d) Ojima, I.; Kogure, T., Reduction of Carbonyl-Compounds Via Hydrosilylation .4. Highly Regioselective Reductions of Alpha,Beta-Unsaturated Carbonyl-Compounds. *Organometallics* **1982**, *1* (10), 1390-1399; (e) Ojima, I.; Nagai, Y., Asymmetric Reduction of Ketones Via Hydrosilylation Catalyzed by a Rhodium (I) Complex with Chiral Phosphine Ligands .2. Mechanism of Induction of Asymmetry. *Chem Lett* **1974**, (3), 223-228.
24. Peyronel, J. F.; Kagan, H. B., Spin Trapping Experiments on an Asymmetric Hydrosilylation Catalytic System, Mechanistic Implications. *Nouv J Chim* **1978**, *2* (3), 211-213.
25. Ojima, I.; Kogure, T.; Nagai, Y., Selective Asymmetric Reduction of Alpha, Beta-Unsaturated Ketones Via Hydrosilylation Catalyzed by Rhodium(I) Complexes with Chiral Phosphine Ligands. *Chem Lett* **1975**, (9), 985-988.

26. Zheng, G. Z.; Chan, T. H., Regiocontrolled Hydrosilation of Alpha,Beta-Unsaturated Carbonyl-Compounds Catalyzed by Hydridotetrakis(Triphenylphosphine)Rhodium(I). *Organometallics* **1995**, *14* (1), 70-79.
27. Kolb, I.; Hetflejs, J., Catalysis by Metal-Complexes .62. Kinetics of Hydrosilylation of *Tert*-Butylphenylketone by Diphenylsilane Catalyzed by [Rh(1,5-COD)(-)-DIOP]ClO₄. *Collect Czech Chem C* **1980**, *45* (8), 2224-2239.
28. Fernandez, M. J.; Maitlis, P. M., Bis(Triethylsilyl)Dihydro(Pentamethylcyclopentadienyl)Rhodium - an Organo-Rhodium(V) Complex. *J Chem Soc Chem Comm* **1982**, (5), 310-311.
29. Fernandez, M. J.; Bailey, P. M.; Bentz, P. O.; Ricci, J. S.; Koetzle, T. F.; Maitlis, P. M., Synthesis, X-Ray, and Low-Temperature Neutron-Diffraction Study of a Rhodium(V) Complex - Dihydridobis(Triethylsilyl)-Pentamethylcyclopentadienylrhodium. *Journal of the American Chemical Society* **1984**, *106* (19), 5458-5463.
30. Millan, A.; Fernandez, M. J.; Bentz, P.; Maitlis, P. M., Rhodium-Catalyzed Hydrosilylation - the Direct Production of Alkenyl(Triethyl)Silanes from Alk-1-Enes and Triethylsilane. *J Mol Catal* **1984**, *26* (1), 89-104.
31. Goikhman, R.; Milstein, D., Reactivity of rhodium-triflate complexes with diphenylsilane: Evidence for silylene intermediacy in stoichiometric and catalytic reactions. *Chem-Eur J* **2005**, *11* (10), 2983-2988.
32. Feldman, J. D.; Peters, J. C.; Tilley, T. D., Activations of silanes with [PhB(CH₂PPh₂)₃]Ir(H)(η^3 -C₈H₁₃). Formation of iridium silylene complexes via the extrusion of silylenes from secondary silanes R₂SiH₂. *Organometallics* **2002**, *21* (20), 4065-4075.
33. (a) Gade, L. H.; Cesar, V.; Bellemin-Laponnaz, S., A modular assembly of chiral oxazolinylcarbene-rhodium complexes: Efficient phosphane-free catalysts for the asymmetric hydrosilylation of dialkyl ketones. *Angewandte Chemie-International Edition* **2004**, *43* (8), 1014-1017; (b) Cesar, V.; Bellemin-Laponnaz, S.; Wadepohl, H.; Gade, L. H., Designing the "search pathway" in the development of a new class of highly efficient stereoselective hydrosilylation catalysts. *Chem-Eur J* **2005**, *11* (9), 2862-2873.

34. (a) Schneider, N.; Finger, M.; Haferkemper, C.; Bellemin-Laponnaz, S.; Hofmann, P.; Gade, L. H., Multiple Reaction Pathways in Rhodium-Catalyzed Hydrosilylations of Ketones. *Chem-Eur J* **2009**, *15* (43), 11515-11529; (b) Schneider, N.; Finger, M.; Haferkemper, C.; Bellemin-Laponnaz, S.; Hofmann, P.; Gade, L. H., Metal Silylenes Generated by Double Silicon-Hydrogen Activation: Key Intermediates in the Rhodium-Catalyzed Hydrosilylation of Ketones. *Angewandte Chemie-International Edition* **2009**, *48* (9), 1609-1613.
35. Sato, F.; Jinbo, T.; Sato, M., Cp₂TiCl₂-Catalyzed Grignard Reactions .2. Reactions with Ketones and Aldehydes. *Tetrahedron Lett* **1980**, *21* (22), 2171-2174.
36. Nakano, T.; Nagai, Y., Bis(η^5 -Cyclopentadienyl)diphenyltitanium-catalyzed Hydrosilylation of Ketones. *Chem Lett* **1988**, (3), 481-484.
37. Harrod, J. F.; Yun, S. S., Silyltitanocene Complexes as Catalysts for the Hydrogenation, Isomerization, and Hydrosilation of Olefins. *Organometallics* **1987**, *6* (7), 1381-1387.
38. (a) Samuel, E.; Harrod, J. F., Synthesis and Characterization of a Novel Bis(Cyclopentadienyl)Titanium Hydride Complex. *Journal of the American Chemical Society* **1984**, *106* (6), 1859-1860; (b) Aitken, C.; Harrod, J. F.; Samuel, E., Polymerization of Primary Silanes to Linear Polysilanes Catalyzed by Titanocene Derivatives. *J Organomet Chem* **1985**, *279* (1-2), C11-C13; (c) Aitken, C. T.; Harrod, J. F.; Samuel, E., Identification of Some Intermediates in the Titanocene-Catalyzed Dehydrogenative Coupling of Primary Organosilanes. *Journal of the American Chemical Society* **1986**, *108* (14), 4059-4066.
39. (a) Woo, H. G.; Tilley, T. D., Dehydrogenative Polymerization of Silanes to Polysilanes by Zirconocene and Hafnocene Catalysts - a New Polymerization Mechanism. *Journal of the American Chemical Society* **1989**, *111* (20), 8043-8044; (b) Woo, H. G.; Tilley, T. D., σ -Bond Metathesis Reactions of Si-H and M-Si Bonds - New Routes to d⁰ Metal Silyl Complexes. *Journal of the American Chemical Society* **1989**, *111* (10), 3757-3758.
40. (a) Wild, F. R. W. P.; Zsolnai, L.; Huttner, G.; Brintzinger, H. H., Ansa-Metallocene Derivatives .4. Synthesis and Molecular-Structures of Chiral Ansa-

- Titanocene Derivatives with Bridged Tetrahydroindenyl Ligands. *J Organomet Chem* **1982**, 232 (3), 233-247; (b) Collins, S.; Kuntz, B. A.; Taylor, N. J.; Ward, D. G., X-Ray Structures of Ethylenebis(Tetrahydroindenyl)-Titanium and Ethylenebis(Tetrahydroindenyl)-Zirconium Dichlorides - a Revision. *J Organomet Chem* **1988**, 342 (1), 21-29; (c) Collins, S.; Kuntz, B. A.; Hong, Y., Additions of Chiral Allyltitanocenes to Aldehydes - Diastereoselective Synthesis of Homoallylic Alcohols with a Recyclable Chiral Transition-Metal Reagent. *J Org Chem* **1989**, 54 (17), 4154-4158.
41. Mimoun, H., Selective reduction of carbonyl compounds by polymethylhydrosiloxane in the presence of metal hydride catalysts. *J Org Chem* **1999**, 64 (7), 2582-2589.
42. Müller, B.; Ruf, M.; Vahrenkamp, H., On the Nature of Zinc Chloride-Aldehyde Interactions. *Angew Chem Int Edit* **1994**, 33 (20), 2089-2090.
43. Masthoff, R.; Kohler, H.; Bohland, H.; Schmeil, F., Phenoxide Der Nebengruppenelemente. *Z Chem* **1965**, 5 (4), 122-&.
44. (a) Duthaler, R. O.; Hafner, A., Chiral Titanium Complexes for Enantioselective Addition of Nucleophiles to Carbonyl Groups. *Chem Rev* **1992**, 92 (5), 807-832; (b) Otera, J., Transesterification. *Chem Rev* **1993**, 93 (4), 1449-1470; (c) Siling, M. I.; Laricheva, T. N., Titanium compounds as catalysts for esterification and transesterification reactions. *Usp Khim* **1996**, 65 (3), 296-304.
45. Ranu, B. C., Zinc Borohydride - a Reducing Agent with High-Potential. *Synlett* **1993**, (12), 885-892.
46. (a) Bell, N. A.; Coates, G. E., Some Amino- and Oxy-Beryllium Hydrides - 2-Dimethylaminoethyl-(Methyl)Aminozinc Hydride Dimer. *J Chem Soc A* **1968**, (4), 823-826; (b) Goeden, G. V.; Caulton, K. G., Soluble Copper Hydrides - Solution Behavior and Reactions Related to Co Hydrogenation. *Journal of the American Chemical Society* **1981**, 103 (24), 7354-7355.
47. De Koning, A. J.; Boersma, J.; Van Der Kerk, G. J. M., Synthesis, Characterization and Properties of Some Organozinc Hydride Complexes. *J Organomet Chem* **1980**, 195 (1), 1-12.

48. Bell, N. A.; Moseley, P. T.; Shearer, H. M. M.; Spencer, C. B., Terminal Zinc-Hydrogen Bonding - X-Ray and Neutron-Diffraction Studies of 2-Dimethylaminoethyl(Methyl)Aminozinc Hydride Dimer. *J Chem Soc Chem Comm* **1980**, (8), 359-360.
49. (a) Corriu, R. J. P.; Guerin, C.; Henner, B.; Wang, Q. J., Pentacoordinate Hydridosilicates - Synthesis and Some Aspects of Their Reactivity. *Organometallics* **1991**, 10 (7), 2297-2303; (b) Corriu, R. J. P.; Guerin, C.; Henner, B. J. L.; Wang, Q. J., Pentacoordinate Dihydridosilicates - Synthesis, Structure, and Aspects of Their Reactivity. *Organometallics* **1991**, 10 (10), 3574-3581.
50. Noyori, R.; Tomino, I.; Tanimoto, Y.; Nishizawa, M., Rational Designing of Efficient Chiral Reducing Agents - Highly Enantioselective Reduction of Aromatic Ketones by Binaphthol-Modified Lithium Aluminum-Hydride Reagents. *Journal of the American Chemical Society* **1984**, 106 (22), 6709-6716.
51. Mimoun, H.; de Saint Laumer, J. Y.; Giannini, L.; Scopelliti, R.; Floriani, C., Enantioselective reduction of ketones by polymethylhydrosiloxane in the presence of chiral zinc catalysts. *Journal of the American Chemical Society* **1999**, 121 (26), 6158-6166.
52. Owens, G. S.; Aries, J.; Abu-Omar, M. M., Rhenium oxo complexes in catalytic oxidations. *Catal Today* **2000**, 55 (4), 317-363.
53. Thiel, W. R., On the way to a new class of catalysts - High-valent transition-metal complexes that catalyze reductions. *Angewandte Chemie-International Edition* **2003**, 42 (44), 5390-5392.
54. Kennedy-Smith, J. J.; Nolin, K. A.; Gunterman, H. P.; Toste, F. D., Reversing the role of the metal-oxygen π -bond. Chemoselective catalytic reductions with a rhenium(V)-dioxo complex. *Journal of the American Chemical Society* **2003**, 125 (14), 4056-4057.
55. Nolin, K. A.; Ahn, R. W.; Toste, F. D., Enantioselective reduction of imines catalyzed by a rhenium(V)-oxo complex. *Journal of the American Chemical Society* **2005**, 127 (36), 12462-12463.

56. Rappe, A. K.; Goddard, W. A., Olefin Metathesis - a Mechanistic Study of High-Valent Group-6 Catalysts. *Journal of the American Chemical Society* **1982**, *104* (2), 448-456.
57. Collman, J. P.; Slaughter, L. M.; Eberspacher, T. A.; Strassner, T.; Brauman, J. I., Mechanism of dihydrogen cleavage by high-valent metal oxo compounds: Experimental and computational studies. *Inorganic Chemistry* **2001**, *40* (24), 6272-6280.
58. (a) Ison, E. A.; Cessarich, J. E.; Du, G. D.; Fanwick, P. E.; Abu-Omar, M. M., Synthesis of cationic oxorhenium salen complexes via mu-oxo abstraction and their activity in catalytic reductions. *Inorganic Chemistry* **2006**, *45* (6), 2385-2387; (b) Fernandes, A. C.; Romao, C. C., A novel method for the reduction of imines using the system silane/MoO₂Cl₂. *Tetrahedron Lett* **2005**, *46* (51), 8881-8883; (c) Reis, P. M.; Royo, B., Perrhenic acid as catalyst for hydrosilylation of aldehydes and ketones and dehydrogenative silylation of alcohols. *Catal Commun* **2007**, *8* (7), 1057-1059.
59. Chung, L. W.; Lee, H. G.; Lin, Z. Y.; Wu, Y. D., Computational study on the reaction mechanism of hydrosilylation of carbonyls catalyzed by high-valent rhenium(V)-di-oxo complexes. *J Org Chem* **2006**, *71* (16), 6000-6009.
60. Rappe, A. K.; Goddard, W. A., Hydrocarbon Oxidation by High-Valent Group-6 Oxides. *Journal of the American Chemical Society* **1982**, *104* (12), 3287-3294.
61. (a) Ison, E. A.; Corbin, R. A.; Abu-Omar, M. M., Hydrogen production from hydrolytic oxidation of organosilanes using a cationic oxorhenium catalyst. *Journal of the American Chemical Society* **2005**, *127* (34), 11938-11939; (b) Ison, E. A.; Trivedi, E. R.; Corbin, R. A.; Abu-Omar, M. M., Mechanism for reduction catalysis by metal oxo: Hydrosilation of organic carbonyl groups catalyzed by a rhenium(V) oxo complex. *Journal of the American Chemical Society* **2005**, *127* (44), 15374-15375.
62. Du, G. D.; Abu-Omar, M. M., Catalytic hydrosilylation of carbonyl compounds with cationic oxorhenium(V) salen. *Organometallics* **2006**, *25* (20), 4920-4923.
63. Chen, P., Electrospray ionization tandem mass spectrometry in high-throughput screening of homogeneous catalysts. *Angewandte Chemie-International Edition* **2003**, *42* (25), 2832-2847.

64. Du, G.; Fanwick, P. E.; Abu-Omar, M. M., Cationic oxorhenium chiral salen complexes for asymmetric hydrosilylation and kinetic resolution of alcohols. *Inorg Chim Acta* **2008**, *361* (11), 3184-3192.
65. Dong, H. L.; Berke, H., A Convenient and Efficient Rhenium-Catalyzed Hydrosilylation of Ketones and Aldehydes. *Adv Synth Catal* **2009**, *351* (11-12), 1783-1788.
66. Fernandes, A. C.; Fernandes, R.; Romao, C. C.; Royo, B., [MoO₂Cl₂] as catalyst for hydrosilylation of aldehydes and ketones. *Chem Commun* **2005**, (2), 213-214.
67. Arzoumanian, H.; Krentzien, H.; Corao, C.; Lopez, R.; Agrifoglio, G., Reactions of Chlorosilanes with Dioxomolybdenum(VI) Complexes. *Polyhedron* **1995**, *14* (20-21), 2887-2891.
68. Costa, P. J.; Romao, C. C.; Fernandes, A. C.; Royo, B.; Reis, P. M.; Calhorda, M. J., Catalyzing aldehyde hydrosilylation with a molybdenum(VI) complex: A density functional theory study. *Chem-Eur J* **2007**, *13* (14), 3934-3941.
69. da Costa, A. P.; Reis, P. M.; Gamelas, C.; Romao, C. C.; Royo, B., Dioxomolybdenum(VI) and -tungsten(VI) BINOL and alkoxide complexes: Synthesis and catalysis in sulfoxidation, olefin epoxidation and hydrosilylation of carbonyl groups. *Inorg Chim Acta* **2008**, *361* (7), 1915-1921.
70. Ortiz, C. G.; Abboud, K. A.; Cameron, T. M.; Boncella, J. M., The synthesis of Mo(IV) arene complexes by the hydrogenation of Mo(IV) olefin complexes. *Chem Commun* **2001**, (03), 247-248.
71. Luo, X. L.; Crabtree, R. H., Homogeneous Catalysis of Silane Alcoholysis Via Nucleophilic-Attack by the Alcohol on an Ir(η^2 -HSiR₃) Intermediate Catalyzed by [IrH₂S₂(PPh₃)₂]SbF₆ (S=Solvent). *Journal of the American Chemical Society* **1989**, *111* (7), 2527-2535.
72. Chang, S.; Scharrer, E.; Brookhart, M., Catalytic silane alcoholysis based on the C₅H₅(CO)(PPh₃)Fe⁺ moiety. NMR spectroscopic identification of key intermediates. *J Mol Catal a-Chem* **1998**, *130* (1-2), 107-119.

73. Fang, X. G.; Huhmann-Vincent, J.; Scott, B. L.; Kubas, G. J., H₂ binding to and silane alcoholysis on an electrophilic Mn(I) fragment with tied-back phosphite ligands. X-ray structure of a Mn-CH₂Cl₂ complex. *J Organomet Chem* **2000**, 609 (1-2), 95-103.
74. (a) Belkova, N. V.; Shubina, E. S.; Epstein, L. M., Diverse world of unconventional hydrogen bonds. *Accounts Chem Res* **2005**, 38 (8), 624-631; (b) Belkova, N. V.; Dub, P. A.; Baya, M.; Houghton, J., Kinetics and thermodynamics of proton transfer to Cp*Ru(dppe)H: Via dihydrogen bonding and (η^2 -H₂)-complex to the dihydride. *Inorg Chim Acta* **2007**, 360 (1), 149-162.
75. Brunner, H.; Miehl, W., Asymmetrical Catalysts .22. Enantioselective Hydrosilylation of Ketones with Cu(I)-Catalysts. *J Organomet Chem* **1984**, 275 (2), C17-C21.
76. (a) Mahoney, W. S.; Brestensky, D. M.; Stryker, J. M., Selective Hydride-Mediated Conjugate Reduction of α,β -Unsaturated Carbonyl-Compounds Using [(Ph₃P)CuH]₆. *Journal of the American Chemical Society* **1988**, 110 (1), 291-293; (b) Mahoney, W. S.; Stryker, J. M., Hydride-Mediated Homogeneous Catalysis - Catalytic Reduction of α,β -Unsaturated Ketones Using [(Ph₃P)CuH]₆ and H₂. *Journal of the American Chemical Society* **1989**, 111 (24), 8818-8823; (c) Mahoney, W. S.; Brestensky, D. M.; Stryker, J. M., Selective Hydride-Mediated Conjugate Reduction of α,β -Unsaturated Carbonyl-Compounds Using [(Ph₃P)CuH]₆. *Journal of the American Chemical Society* **1988**, 110 (1), 291-293.
77. (a) Chen, J. X.; Daeuble, J. F.; Stryker, J. M., Phosphine effects in the copper(I) hydride-catalyzed hydrogenation of ketones and regioselective 1,2-reduction of α,β -unsaturated ketones and aldehydes. Hydrogenation of decalin and steroidal ketones and enones. *Tetrahedron* **2000**, 56 (18), 2789-2798; (b) Llamas, T.; Arrayas, R. G.; Carretero, J. C., Catalytic asymmetric conjugate reduction of β,β -disubstituted α,β -unsaturated sulfones. *Angewandte Chemie-International Edition* **2007**, 46 (18), 3329-3332; (c) Appella, D. H.; Moritani, Y.; Shintani, R.; Ferreira, E. M.; Buchwald, S. L., Asymmetric conjugate reduction of α,β -unsaturated esters using a chiral phosphine-copper catalyst. *Journal of the American Chemical Society* **1999**, 121 (40), 9473-9474.

78. Lipshutz, B. H.; Chrisman, W.; Noson, K., Hydrosilylation of aldehydes and ketones catalyzed by $[\text{Ph}_3\text{P}(\text{CuH})]_6$. *J Organomet Chem* **2001**, 624 (1-2), 367-371.
79. Brestensky, D. M.; Huseland, D. E.; Mcgettigan, C.; Stryker, J. M., Simplified, One-Pot Procedure for the Synthesis of $[(\text{Ph}_3\text{p})\text{CuH}]_6$, a Stable Copper Hydride for Conjugate Reductions. *Tetrahedron Lett* **1988**, 29 (31), 3749-3752.
80. (a) Lee, D. W.; Yun, J., Direct synthesis of Stryker's reagent from a Cu(II) salt. *Tetrahedron Lett* **2005**, 46 (12), 2037-2039; (b) Lee, D.; Yun, J., Copper-catalyzed asymmetric hydrosilylation of ketones using air and moisture stable precatalyst $\text{Cu}(\text{OAc})_2 \cdot \text{H}_2\text{O}$. *Tetrahedron Lett* **2004**, 45 (28), 5415-5417.
81. Mori, A.; Fujita, A.; Kajiro, H.; Nishihara, Y.; Hiyama, T., Conjugate reduction of α,β -unsaturated ketones with hydrosilane mediated by copper(I) salt. *Tetrahedron* **1999**, 55 (15), 4573-4582.
82. (a) Lipshutz, B. H.; Servesko, J. M.; Petersen, T. B.; Papa, P. P.; Lover, A. A., Asymmetric 1,4-reductions of hindered beta-substituted cycloalkenones using catalytic SEGPHOS-ligated CuH. *Org Lett* **2004**, 6 (8), 1273-1275; (b) Lipshutz, B. H.; Shimizu, H., Copper(I)-catalyzed asymmetric hydrosilylations of imines at ambient temperatures. *Angewandte Chemie-International Edition* **2004**, 43 (17), 2228-2230.
83. Lipshutz, B. H.; Chrisman, W.; Noson, K.; Papa, P.; Sclafani, J. A.; Vivian, R. W.; Keith, J. M., Copper hydride-catalyzed tandem 1,4-reduction/alkylation reactions. *Tetrahedron* **2000**, 56 (18), 2779-2788.
84. (a) Ito, H.; Ishizuka, T.; Arimoto, K.; Miura, K.; Hosomi, A., Studies on organosilicon chemistry. 138. Generation of a reducing reagent from copper(I) salt and hydrosilane. New practical method for conjugate reduction. *Tetrahedron Lett* **1997**, 38 (51), 8887-8890; (b) Lipshutz, B. H.; Noson, K.; Chrisman, W.; Lower, A., Asymmetric hydrosilylation of aryl ketones catalyzed by copper hydride complexed by nonracemic biphenyl bis-phosphine ligands. *Journal of the American Chemical Society* **2003**, 125 (29), 8779-8789.
85. Lipshutz, B. H.; Ung, C. S.; Sengupta, S., 1,4-Reductions of α,β -unsaturated ketones and aldehydes via *in situ* generated hydridocuprates. *Synlett* **1989**, 64-66.

86. Lipshutz, B. H.; Caires, C. C.; Kuipers, P.; Chrisman, W., Tweaking copper hydride (CuH) for synthetic gain. A practical, one-pot conversion of dialkyl ketones to reduced trialkylsilyl ether derivatives. *Org Lett* **2003**, 5 (17), 3085-3088.
87. Ito, H.; Yamanaka, H.; Ishizuka, T.; Tateiwa, J.; Hosomi, A., New reactivity of a reducing reagent generated from a copper(I) salt and a hydrosilane: Selective reduction of ketones and olefins conjugated with an aromatic group. *Synlett* **2000**, (4), 479-482.
88. (a) Lipshutz, B. H.; Lee, C. T.; Servesko, J. M., Asymmetric CuH-catalyzed hydrosilylations en route to the C-9 epimer of amphidinoketide I. *Org Lett* **2007**, 9 (23), 4713-4716; (b) Lipshutz, B. H.; Tanaka, N.; Taft, B. R.; Lee, C. T., Chiral silanes via asymmetric hydrosilylation with catalytic CuH. *Org Lett* **2006**, 8 (10), 1963-1966; (c) Lipshutz, B. H.; Frieman, B. A.; Tomaso, A. E., Copper-in-charcoal (Cu/C): Heterogeneous, copper-catalyzed asymmetric hydrosilylations. *Angewandte Chemie-International Edition* **2006**, 45 (8), 1259-1264; (d) Diez-Gonzalez, S.; Scott, N. M.; Nolan, S. P., Cationic copper(I) complexes as efficient precatalysts for the hydrosilylation of carbonyl compounds. *Organometallics* **2006**, 25 (9), 2355-2358; (e) Lipshutz, B. H.; Frieman, B. A.; Unger, J. B.; Nihan, D. M., Thermally accelerated asymmetric hydrosilylations using ligated copper hydride. *Can J Chem* **2005**, 83 (6), 606-614; (f) Lipshutz, B. H.; Frieman, B. A., CuH in a bottle: A convenient reagent for asymmetric hydrosilylations. *Angewandte Chemie-International Edition* **2005**, 44 (39), 6345-6348.
89. Parks, D. J.; Piers, W. E., Tris(pentafluorophenyl)boron-catalyzed hydrosilation of aromatic aldehydes, ketones, and esters. *Journal of the American Chemical Society* **1996**, 118 (39), 9440-9441.
90. Parks, D. J.; Blackwell, J. M.; Piers, W. E., Studies on the mechanism of B(C₆F₅)₃-catalyzed hydrosilation of carbonyl functions. *J Org Chem* **2000**, 65 (10), 3090-3098.
91. (a) Reetz, M. T.; Hullmann, M.; Massa, W.; Berger, S.; Rademacher, P.; Heymanns, P., Structure and Electronic Nature of the Benzaldehyde-Boron Trifluoride Adduct. *Journal of the American Chemical Society* **1986**, 108 (9), 2405-2408; (b) Corey, E. J.; Loh, T. P.; Sarshar, S.; Azimioara, M., The Structure of the 2-Methylacrolein

Boron-Trifluoride Complex in the Crystalline Phase and in Solution. *Tetrahedron Lett* **1992**, 33 (46), 6945-6948.

92. (a) Danopoulos, A. A.; Galsworthy, J. R.; Green, M. L. H.; Cafferkey, S.; Doerr, L. H.; Hursthouse, M. B., Equilibria in the $B(C_6F_5)_3-H_2O$ system: synthesis and crystal structures of $B(C_6F_5)_3 \cdot H_2O$ and the anions $[HOB(C_6F_5)_3]^-$ and $[(F_5C_6)_3B(\mu-OH)B(C_6F_5)_3]^-$. *Chem Commun* **1998**, (22), 2529-2530; (b) Blackwell, J. M.; Foster, K. L.; Beck, V. H.; Piers, W. E., $B(C_6F_5)_3$ -catalyzed silylation of alcohols: A mild, general method for synthesis of silyl ethers. *J Org Chem* **1999**, 64 (13), 4887-4892.

93. Li, L. T.; Marks, T. J., New organo-Lewis acids. Tris (beta-perfluoronaphthyl)borane (PNB) as a highly active cocatalyst for metallocene-mediated Ziegler-Natta alpha-olefin polymerization. *Organometallics* **1998**, 17 (18), 3996-4003.

94. Doyle, M. P.; West, C. T.; Donnelly, S. J.; Mcosker, C. C., Silane Reductions in Acidic Media .8. Boron-Trifluoride Catalyzed Organosilane Reductions, Selectivity and Mechanism. *J Organomet Chem* **1976**, 117 (2), 129-140.

95. Fry, J. L.; Orfanopoulos, M.; Adlington, M. G.; Dittman, W. R.; Silverman, S. B., Reduction of Aldehydes and Ketones to Alcohols and Hydrocarbons through Use of Organosilane-Boron Trifluoride System. *J Org Chem* **1978**, 43 (2), 374-375.

96. Ishihara, K.; Hanaki, N.; Funahashi, M.; Miyata, M.; Yamamoto, H., Tris(Pentafluorophenyl)Boron as an Efficient, Air-Stable, and Water Tolerant Lewis-Acid Catalyst. *B Chem Soc Jpn* **1995**, 68 (6), 1721-1730.

97. Lambert, J. B.; Zhang, S. Z.; Ciro, S. M., Silyl Cations in the Solid and in Solution. *Organometallics* **1994**, 13 (6), 2430-2443.

98. Lambert, J. B.; Zhao, Y.; Wu, H. W., β -Silyl and β -Germyl Carbocations Stable at Room Temperature. *J Org Chem* **1999**, 64 (8), 2729-2736.

99. Harrison, D. J.; McDonald, R.; Rosenberg, L., Borane-catalyzed hydrosilylation of thiobenzophenone: A new route to silicon-sulfur bond formation. *Organometallics* **2005**, 24 (7), 1398-1400.

100. (a) Harrison, D. J.; Edwards, D. R.; McDonald, R.; Rosenberg, L., Toward selective functionalisation of oligosilanes: borane-catalysed dehydrogenative coupling of silanes with thiols. *Dalton T* **2008**, (26), 3401-3411; (b) Skjel, M. K.; Houghton, A. Y.;

- Kirby, A. E.; Harrison, D. J.; McDonald, R.; Rosenberg, L., Silane-Controlled Diastereoselectivity in the Tris(pentafluorophenyl)borane-Catalyzed Reduction of α -Diketones to Silyl-Protected 1,2-Diols. *Org Lett* **2010**, *12* (2), 376-379.
101. Chandrasekhar, S.; Reddy, C. R.; Babu, B. N., Rapid defunctionalization of carbonyl group to methylene with polymethylhydrosiloxane- $B(C_6F_5)_3$. *J Org Chem* **2002**, *67* (25), 9080-9082.
102. Roesler, R.; Har, B. J. N.; Piers, W. E., Synthesis and characterization of (perfluoroaryl)borane-functionalized carbosilane dendrimers and their use as Lewis acid catalysts for the hydrosilation of acetophenone. *Organometallics* **2002**, *21* (21), 4300-4302.
103. Blackwell, J. M.; Sonmor, E. R.; Scoccitti, T.; Piers, W. E., $B(C_6F_5)_3$ -catalyzed hydrosilation of imines via silyliminium intermediates. *Org Lett* **2000**, *2* (24), 3921-3923.
104. Blackwell, J. M.; Piers, W. E.; Parvez, M.; McDonald, R., Solution and solid-state characteristics of imine adducts with tris(pentafluorophenyl)borane. *Organometallics* **2002**, *21* (7), 1400-1407.
105. Oestreich, M., Chirality transfer from silicon to carbon. *Chem-Eur J* **2006**, *12* (1), 30-37.
106. Hog, D. T.; Oestreich, M., $B(C_6F_5)_3$ -Catalyzed Reduction of Ketones and Imines Using Silicon-Stereogenic Silanes: Stereoinduction by Single-Point Binding. *Eur J Org Chem* **2009**, (29), 5047-5056.
107. Brown, H. C.; Schlesinger, H. I.; Burg, A. B., Hydrides of Boron. XI. The Reaction of Diborane with Organic Compounds Containing a Carbonyl Group. *Journal of the American Chemical Society* **1939**, *61* (3), 673-680.
108. (a) Brown, H. C.; Rao, B. C. S., Selective Reductions with Diborane, an Acidic-Type Reducing Agent. *J Org Chem* **1957**, *22* (9), 1135-1136; (b) Brown, H. C.; Rao, B. C. S., Hydroboration .3. The Reduction of Organic Compounds by Diborane, an Acid-Type Reducing Agent. *Journal of the American Chemical Society* **1960**, *82* (3), 681-686.
109. Männig, D.; Nöth, H., Catalytic Hydroboration with Rhodium Complexes. *Angew Chem Int Edit* **1985**, *24* (10), 878-879.

110. (a) Evans, D. A.; Bartroli, J.; Godel, T., Acyclic Diastereoselection in the Hydroboration Process - Documented Cases of 1,3-Asymmetric Induction. *Tetrahedron Lett* **1982**, 23 (44), 4577-4580; (b) Evans, D. A.; Fu, G. C.; Hoveyda, A. H., Rhodium(I)-Catalyzed Hydroboration of Olefins - the Documentation of Regiochemical and Stereochemical Control in Cyclic and Acyclic Systems. *Journal of the American Chemical Society* **1988**, 110 (20), 6917-6918; (c) Burgess, K.; Ohlmeyer, M. J., Diastereocontrol in Rhodium-Catalyzed Hydroboration of Chiral Acyclic Allylic Alcohol Derivatives. *Tetrahedron Lett* **1989**, 30 (4), 395-398; (d) Evans, D. A.; Fu, G. C., The Rhodium-Catalyzed Hydroboration of Olefins - a Mechanistic Investigation. *J Org Chem* **1990**, 55 (8), 2280-2282; (e) Evans, D. A.; Fu, G. C., Amide-Directed, Iridium-Catalyzed Hydroboration of Olefins - Documentation of Regiochemical and Stereochemical Control in Cyclic and Acyclic Systems. *Journal of the American Chemical Society* **1991**, 113 (10), 4042-4043; (f) Matsumoto, Y.; Hayashi, T., Asymmetric Double Hydroboration of 1,3-Dienes Catalyzed by Chiral Phosphine-Rhodium Complexes. *Tetrahedron Lett* **1991**, 32 (28), 3387-3390; (g) Evans, D. A.; Fu, G. C.; Hoveyda, A. H., Rhodium(I)-Catalyzed and Iridium(I)-Catalyzed Hydroboration Reactions - Scope and Synthetic Applications. *Journal of the American Chemical Society* **1992**, 114 (17), 6671-6679; (h) Evans, D. A.; Muci, A. R.; Sturmer, R., Samarium(III)-Catalyzed Hydroboration of Olefins with Catecholborane - a General-Approach to the Synthesis of Boronate Esters. *J Org Chem* **1993**, 58 (20), 5307-5309; (i) Pereira, S.; Srebnik, M., A study of hydroboration of alkenes and alkynes with pinacolborane catalyzed by transition metals. *Tetrahedron Lett* **1996**, 37 (19), 3283-3286; (j) Fernandez, E.; Hooper, M. W.; Knight, F. I.; Brown, J. M., Catalytic asymmetric hydroboration-amination. *Chem Commun* **1997**, (2), 173-174; (k) Segarra, A. M.; Guerrero, R.; Claver, C.; Fernandez, E., An unprecedented recyclable catalyst system for asymmetric hydroboration. *Chem Commun* **2001**, (18), 1808-1809; (l) Daura-Oller, E.; Segarra, A. M.; Poblet, J. M.; Claver, C.; Fernandez, E.; Bo, C., On the origin of regio- and stereoselectivity in the rhodium-catalyzed vinylarenes hydroboration reaction. *J Org Chem* **2004**, 69 (8), 2669-2680; (m) Segarra, A. M.; Daura-Oller, E.; Claver, C.; Poblet, J. M.; Bo, C.; Fernandez, E., In quest of factors that control the enantioselective catalytic Markovnikov hydroboration/oxidation of vinylarenes. *Chem-*

Eur J **2004**, *10* (24), 6456-6467; (n) Lillo, V.; Fernandez, E., Heterofunctional control of regio- and enantioselectivity in rhodium-catalysed hydroboration of allylic systems. *Tetrahedron-Asymmetr* **2006**, *17* (3), 315-319.

111. Koren-Selfridge, L.; Londino, H. N.; Vellucci, J. K.; Simmons, B. J.; Casey, C. P.; Clark, T. B., A Boron-Substituted Analogue of the Shvo Hydrogenation Catalyst: Catalytic Hydroboration of Aldehydes, Imines, and Ketones. *Organometallics* **2009**, *28* (7), 2085-2090.

112. Blum, Y.; Czarkie, D.; Rahamim, Y.; Shvo, Y., (Cyclopentadienone)Ruthenium Carbonyl-Complexes - a New Class of Homogeneous Hydrogenation Catalysts. *Organometallics* **1985**, *4* (8), 1459-1461.

113. Menashe, N.; Shvo, Y., Catalytic Disproportionation of Aldehydes with Ruthenium Complexes. *Organometallics* **1991**, *10* (11), 3885-3891.

114. Menashe, N.; Salant, E.; Shvo, Y., Efficient catalytic reduction of ketones with formic acid and ruthenium complexes. *J Organomet Chem* **1996**, *514* (1-2), 97-102.

115. (a) Casey, C. P.; Singer, S. W.; Powell, D. R.; Hayashi, R. K.; Kavana, M., Hydrogen transfer to carbonyls and imines from a hydroxycyclopentadienyl ruthenium hydride: Evidence for concerted hydride and proton transfer. *Journal of the American Chemical Society* **2001**, *123* (6), 1090-1100; (b) Casey, C. P.; Bikzhanova, G. A.; Cui, Q.; Guzei, I. A., Reduction of Imines by hydroxycyclopentadienyl ruthenium hydride: Intramolecular trapping evidence for hydride and proton transfer outside the coordination sphere of the metal. *Journal of the American Chemical Society* **2005**, *127* (40), 14062-14071; (c) Casey, C. P.; Johnson, J. B., Isomerization and deuterium scrambling evidence for a change in the rate-limiting step during imine hydrogenation by Shvo's hydroxycyclopentadienyl ruthenium hydride. *Journal of the American Chemical Society* **2005**, *127* (6), 1883-1894; (d) Casey, C. P.; Johnson, J. B.; Singer, S. W.; Cui, Q., Hydrogen elimination from a hydroxycyclopentadienyl ruthenium(II) hydride: Study of hydrogen activation in a ligand-metal bifunctional hydrogenation catalyst. *Journal of the American Chemical Society* **2005**, *127* (9), 3100-3109; (e) Samec, J. S. M.; Ell, A. H.; Aberg, J. B.; Privalov, T.; Eriksson, L.; Backvall, J. E., Mechanistic study of hydrogen transfer to imines from a hydroxycyclopentadienyl ruthenium hydride. Experimental

support for a mechanism involving coordination of imine to ruthenium prior to hydrogen transfer. *Journal of the American Chemical Society* **2006**, *128* (44), 14293-14305; (f) Casey, C. P.; Clark, T. B.; Guzei, I. A., Intramolecular trapping of an intermediate in the reduction of Imines by a hydroxycyclopentadienyl ruthenium hydride: Support for a concerted outer sphere mechanism. *Journal of the American Chemical Society* **2007**, *129* (38), 11821-11827; (g) Casey, C. P.; Beetner, S. E.; Johnson, J. B., Spectroscopic determination of hydrogenation rates and intermediates during carbonyl hydrogenation catalyzed by Shvo's hydroxycyclopentadienyl diruthenium hydride agrees with kinetic modeling based on independently measured rates of elementary reactions. *Journal of the American Chemical Society* **2008**, *130* (7), 2285-2295.

116. Koren-Selfridge, L.; Query, I. P.; Hanson, J. A.; Isley, N. A.; Guzei, I. A.; Clark, T. B., Synthesis of Ruthenium Boryl Analogues of the Shvo Metal-Ligand Bifunctional Catalyst. *Organometallics* **2010**, *29* (17), 3896-3900.

117. (a) Wirtz, K.; Bonhoeffer, K. F., *Z physik Chem* **1936**, *177A*, 1; (b) Wirtz, K., The interexchange of heavy hydrogen atoms between hydrogen and ammonia. *Naturwissenschaften* **1935**, *23*, 721-722; (c) Wirtz, K., The exchange equation between deuterium and ammonia. *Z Phys Chem B-Chem E* **1935**, *30* (4), 289-297; (d) Wirtz, K., On the evaluation of the equilibrium of exchange reactions with deuterium with the involvement of a molecule with large numbers of atoms. *Z Phys Chem B-Chem E* **1936**, *34* (1/2), 121-140; (e) Wirtz, K., Remarks on identifying the deuterium content of hydrogen compounds after Farka's micro heat conductivity method. *Z Phys Chem B-Chem E* **1936**, *32* (4), 334-340; (f) Wirtz, K., The equilibrium constants of the exchange reactions $\text{HCl} + \text{HD} = \text{DCl} + \text{H}_2$ and $\text{HBr} + \text{HD} = \text{DBr} + \text{H}_2$. *Z Phys Chem B-Chem E* **1936**, *17* (4), 309-318; (g) Wirtz, K., Equilibrium of exchange reactions with deuterium. *Phys Z* **1936**, *37*, 165-165; (h) Wirtz, K., The exchange equilibrium of hydrogen isotopes between water and polyatomic molecules. *Z Elektrochem Angew P* **1937**, *43*, 662-662.

118. Abe, S., *Sci Papers Inst Phys Chem Research (Tokyo)* **1941**, *38*, 287.

119. Claeys, Y.; Dayton, J. C.; Wilmarth, W. K., The Hydrogen Exchange of Alkali Amides and Hydroxide with Deuterium Gas. *J Chem Phys* **1950**, *18*, 759.

120. Wilmarth, W. K.; Dayton, J. C.; Flournoy, J. M., The Mechanism of Exchange of Hydrogen Gas and Aqueous Alkali. *Journal of the American Chemical Society* **1953**, 75 (18), 4549-4553.
121. Wilmarth, W. K.; Dayton, J. C., The Mechanism of the Exchange of Hydrogen Gas with Solutions of Potassium Amide in Liquid Ammonia. *Journal of the American Chemical Society* **1953**, 75 (18), 4553-4556.
122. Ipatieff, V. N.; Schmerling, L., Effect of Hydrogen on Action of Aluminum Chloride on Alkanes. *Ind Eng Chem* **1948**, 40 (12), 2354-2360.
123. (a) Walling, C.; Bollyky, L., Base Catalyzed Homogeneous Hydrogenation. *Journal of the American Chemical Society* **1961**, 83 (13), 2968-2969; (b) Walling, C.; Bollyky, L., Homogeneous Hydrogenation in Absence of Transition-Metal Catalysts. *Journal of the American Chemical Society* **1964**, 86 (18), 3750-3752.
124. Miller, S. L.; Rittenberg, D., The Catalysis of the H₂-D₂O Exchange by Aqueous Buffer Solutions. *Journal of the American Chemical Society* **1958**, 80 (1), 64-65.
125. Berkessel, A.; Schubert, T. J. S.; Muller, T. N., Hydrogenation without a transition-metal catalyst: On the mechanism of the base-catalyzed hydrogenation of ketones. *Journal of the American Chemical Society* **2002**, 124 (29), 8693-8698.
126. (a) Yamakawa, M.; Ito, H.; Noyori, R., The metal-ligand bifunctional catalysis: A theoretical study on the ruthenium(II)-catalyzed hydrogen transfer between alcohols and carbonyl compounds. *Journal of the American Chemical Society* **2000**, 122 (7), 1466-1478; (b) Noyori, R.; Ohkuma, T., Asymmetric catalysis by architectural and functional molecular engineering: Practical chemo- and stereoselective hydrogenation of ketones. *Angewandte Chemie-International Edition* **2001**, 40 (1), 40-73; (c) Noyori, R.; Yamakawa, M.; Hashiguchi, S., Metal-ligand bifunctional catalysis: A nonclassical mechanism for asymmetric hydrogen transfer between alcohols and carbonyl compounds. *J Org Chem* **2001**, 66 (24), 7931-7944.
127. Koster, R., Neue Preparative Moglichkeiten in Der Bor-Chemie Und Silicium-Chemie. *Angewandte Chemie-International Edition* **1956**, 68 (11), 383-383.
128. Dewitt, E. J.; Trapasso, L. E.; Ramp, F. L., Homogeneous Hydrogenation Catalyzed by Boranes. *Journal of the American Chemical Society* **1961**, 83 (22), 4672.

129. (a) Yalpani, M.; Lunow, T.; Köster, R., Reduction of Polycyclic Arenes by B₁₀-Boranes. 2. Borane Catalyzed Hydrogenation of Naphthalenes to Tetralins. *Chem Ber* **1989**, *122* (4), 687-693; (b) Yalpani, M.; Koster, R., Partial Hydrogenation - from Anthracene to Coronene. *Chem Ber* **1990**, *123* (4), 719-724; (c) Haenel, M. W.; Narangerel, J.; Richter, U. B.; Rufinska, A., The first liquefaction of high-rank bituminous coals by preceding hydrogenation with homogeneous borane or iodine catalysts. *Angewandte Chemie-International Edition* **2006**, *45* (7), 1061-1066; (d) Köster, R.; Bruno, G., *Justus Liebigs Ann. Chem.* **1961**, *644*, 1-22; (e) Ramp, F. L.; Dewitt, E. J.; Trapasso, L. E., Homogeneous Hydrogenation Catalyzed by Boranes. *J Org Chem* **1962**, *27* (12), 4368-4372.
130. (a) Siskin, M., Strong Acid Chemistry. II. Catalytic-Hydrogenation of Aromatics in Hydrogen Fluoride-Tantalum Pentafluoride and Related Strong Acid Systems. *Journal of the American Chemical Society* **1974**, *96* (11), 3641-3641; (b) Siskin, M.; Porcelli, J., Strong Acid Chemistry. I. Reactions of Aromatics in Hydrogen Fluoride-Tantalum Pentafluoride (HF-TaF₅) Acid System. *Journal of the American Chemical Society* **1974**, *96* (11), 3640-3641.
131. Wristers, J., Strong Acid-Catalyzed Hydrogenation of Aromatics. *Journal of the American Chemical Society* **1975**, *97* (15), 4312-4316.
132. Zirngibl, C.; Hedderich, R.; Thauer, R. K., N₅,N₁₀-Methylenetetrahydromethanopterin Dehydrogenase from *Methanobacterium Thermoautotrophicum* Has Hydrogenase Activity. *Febs Lett* **1990**, *261* (1), 112-116.
133. Teles, J. H.; Brode, S.; Berkessel, A., Hydrogenation without a metal catalyst: An ab initio study on the mechanism of the metal-free hydrogenase from *Methanobacterium thermoautotrophicum*. *Journal of the American Chemical Society* **1998**, *120* (6), 1345-1346.
134. (a) Scott, A. P.; Golding, B. T.; Radom, L., Remarkable cleavage of molecular hydrogen without the use of metallic catalysts: a theoretical investigation. *New J Chem* **1998**, *22* (11), 1171-1173; (b) Cioslowski, J.; Boche, G., Geometry-tunable Lewis acidity of amidinium cations and its relevance to redox reactions of the Thauer metal-free hydrogenase: A theoretical study. *Angew Chem Int Edit* **1997**, *36* (1-2), 107-109.

135. Berkessel, A., Activation of dihydrogen without transition metals. *Curr Opin Chem Biol* **2001**, 5 (5), 486-490.
136. Welch, G. C.; Juan, R. R. S.; Masuda, J. D.; Stephan, D. W., Reversible, metal-free hydrogen activation. *Science* **2006**, 314 (5802), 1124-1126.
137. (a) Li, B. J.; Xu, Z., A Nonmetal Catalyst for Molecular Hydrogen Activation with Comparable Catalytic Hydrogenation Capability to Noble Metal Catalyst. *Journal of the American Chemical Society* **2009**, 131 (45), 16380-16382; (b) Niemeyer, J.; Erker, G., Fullerene-Mediated Activation of Dihydrogen: A New Method of Metal-Free Catalytic Hydrogenation. *Chemcatchem* **2010**, 2 (5), 499-500.
138. Fan, C.; Mercier, L. G.; Piers, W. E.; Tuononen, H. M.; Parvez, M., Dihydrogen Activation by Antiaromatic Pentaarylboroles. *Journal of the American Chemical Society* **2010**, 132 (28), 9604-9606.
139. (a) Dioumaev, V. K.; Bullock, R. M., A recyclable catalyst that precipitates at the end of the reaction. *Nature* **2003**, 424 (6948), 530-532; (b) Dioumaev, V. K.; Bullock, R. M.; Szalda, D. J., W and mo "green" catalysts for ionic hydrosilylation of carbonyl compounds: A solvent-free process with self-separation and efficient recycling of the catalyst. *Abstr Pap Am Chem S* **2003**, 225, U156-U156; (c) Bullock, R. M., Catalytic ionic Hydrogenations. *Chem-Eur J* **2004**, 10 (10), 2366-2374; (d) Voges, M. H.; Bullock, R. M., Catalytic ionic hydrogenations of ketones using molybdenum and tungsten complexes. *J Chem Soc Dalton* **2002**, (5), 759-770.
140. Hille, R., The mononuclear molybdenum enzymes. *Chem Rev* **1996**, 96 (7), 2757-2816.
141. Wigley, D. E., *Organoimido Complexes of the Transition Metals*. John Wiley & Sons, Inc.: 2007; p 239-482.
142. (a) Cundari, T. R., Transition-Metal Imido Complexes. *Journal of the American Chemical Society* **1992**, 114 (20), 7879-7888; (b) Castro, A.; Galakhov, M. V.; Gomez, M.; Gomez-Sal, P.; Martin, A.; Sanchez, F., Chemical behaviour of alkyl imido cyclopentadienyl niobium and tantalum(V) complexes in insertion processes. X-ray crystal structures of $[\text{MCpCl}(\text{NAr})\{\eta^2\text{-C}(\text{Me})=\text{NAr}\}]$ (Ar=2,6-Me₂C₆H₃; M = Nb,

$\text{Cp}=\eta^5\text{-C}_5\text{H}_4\text{SiMe}_3$; $\text{M} = \text{Ta}$, $\text{Cp} = \eta^5\text{-C}_5\text{Me}_5$ and $[\text{Ta}(\eta^5\text{-C}_5\text{Me}_5)\text{Me}(\text{NAr})\{\eta^2\text{-C}(\text{CH}_2\text{CMe}_2\text{Ph})=\text{O}\}]$ ($\text{Ar} = 2,6\text{-Me}_2\text{C}_6\text{H}_3$). *J Organomet Chem* **2000**, 595 (1), 36-53.

143. (a) Khalimon, A. Y.; Simionescu, R.; Kuzmina, L. G.; Howard, J. A. K.; Nikonov, G. I., Agostic NSi-H center dot center dot center dot Mo complexes: From curiosity to catalysis. *Angewandte Chemie-International Edition* **2008**, 47 (40), 7701-7704; (b) Blackmore, I. J.; Semiao, C. J.; Buschhaus, M. S. A.; Patrick, B. O.; Legzdins, P., Investigations directed at catalytic carbon-carbon and carbon-oxygen bond formation via C-H bond activation. *Organometallics* **2007**, 26 (20), 4881-4889; (c) Williams, D. S.; Schofield, M. H.; Schrock, R. R., Synthesis of d^2 Complexes That Contain $[\text{W}(\text{NAr})_2]$ and $[\text{Re}(\text{NAr})_2]$ Cores, SCF- $X\alpha$ -SW Calculations, and a Discussion of the $\text{MCp}_2/\text{M}'(\text{NR})_2$ Isolobal Relationship. *Organometallics* **1993**, 12 (11), 4560-4571.

144. Samec, J. S. M.; Backvall, J.-E.; Andersson, P. G.; Brandt, P., Mechanistic aspects of transition metal-catalyzed hydrogen transfer reactions. *Chemical Society Reviews* **2006**, 35 (3), 237-248.

145. Shin, J. H.; Parkin, G., The Synthesis, Structures and Reactivity of Some Mononuclear and Dinuclear Pentamethylcyclopentadienyl Molybdenum Complexes. *Polyhedron* **1994**, 13 (9), 1489-1493.

146. Sadow, A. D.; Tilley, T. D., Synthesis and characterization of scandium silyl complexes of the type $\text{Cp}^*_2\text{ScSiHRR}$. σ -Bond metathesis reactions and catalytic dehydrogenative silation of hydrocarbons. *Journal of the American Chemical Society* **2005**, 127 (2), 643-656.

147. (a) Watson, P. L., Methane Exchange-Reactions of Lanthanide and Early-Transition-Metal Methyl Complexes. *Journal of the American Chemical Society* **1983**, 105 (21), 6491-6493; (b) Thompson, M. E.; Baxter, S. M.; Bulls, A. R.; Burger, B. J.; Nolan, M. C.; Santarsiero, B. D.; Schaefer, W. P.; Bercaw, J. E., " σ -Bond Metathesis" for C-H Bonds of Hydrocarbons and Sc-R ($\text{R} = \text{H}$, alkyl, aryl) Bonds of Permethylscandocene Derivatives. Evidence for Noninvolvement of the π -System in Electrophilic Activation of Aromatic and Vinylic C-H Bonds. *Journal of the American Chemical Society* **1987**, 109 (1), 203-219; (c) Woo, H. G.; Tilley, T. D., Sigma-Bond Metathesis Reactions of Si-H and M-Si Bonds - New Routes to d^0 Metal Silyl

Complexes. *Journal of the American Chemical Society* **1989**, *111* (10), 3757-3758; (d) Woo, H. G.; Walzer, J. F.; Tilley, T. D., A Sigma-Bond Metathesis Mechanism for Dehydropolymerization of Silanes to Polysilanes by d^0 Metal-Catalysts. *Journal of the American Chemical Society* **1992**, *114* (18), 7047-7055; (e) Woo, H. G.; Heyn, R. H.; Tilley, T. D., Sigma-Bond Metathesis Reactions for d^0 Metal Silicon Bonds That Produce Zirconocene and Hafnocene Hydrosilyl Complexes. *Journal of the American Chemical Society* **1992**, *114* (14), 5698-5707.

148. (a) Hartwig, J. F.; Bhandari, S.; Rablen, P. R., Addition of Catecholborane to a Ruthenium-Alkyl: Evidence for σ -Bond Metathesis with a Low-Valent, Late Transition-Metal. *Journal of the American Chemical Society* **1994**, *116* (5), 1839-1844; (b) Perutz, R. N.; Sabo-Etienne, S., The σ -CAM Mechanism: σ Complexes as the Basis of σ -Bond Metathesis at Late-Transition-Metal Centers. *Angewandte Chemie-International Edition* **2007**, *46* (15), 2578-2592.

149. (a) Perrin, L.; Maron, L.; Eisenstein, O., A DFT study of SiH_4 activation by Cp_2LnH . *Inorganic Chemistry* **2002**, *41* (17), 4355-4362; (b) Perrin, L.; Eisenstein, O.; Maron, L., Chemoselectivity in sigma bond activation by lanthanocene complexes from a DFT perspective: reactions of Cp_2LnR ($\text{R} = \text{CH}_3, \text{H}, \text{SiH}_3$) with SiH_4 and $\text{CH}_3\text{-SiH}_3$. *New J Chem* **2007**, *31* (4), 549-555; (c) Perrin, L.; Maron, L.; Eisenstein, O.; Tilley, T. D., Bond Activations of PhSiH_3 by Cp_2SmH : A Mechanistic Investigation by the DFT Method. *Organometallics* **2009**, *28* (13), 3767-3775.

150. Webster, C. E.; Fan, Y. B.; Hall, M. B.; Kunz, D.; Hartwig, J. F., Experimental and computational evidence for a boron-assisted, σ -bond metathesis pathway for alkane borylation. *Journal of the American Chemical Society* **2003**, *125* (4), 858-859.

151. Chakraborty, S.; Guan, H., First-row transition metal catalyzed reduction of carbonyl functionalities: a mechanistic perspective. *Dalton T* **2010**, *39* (32), 7427-7436.

152. (a) Campos, J.; Esqueda, A. C.; Carmona, E., Cyclometallation and Hydrogen/Deuterium Exchange Reactions of an Arylphosphine Ligand upon Coordination to $\{\text{Ir}(\eta^5\text{-C}_5\text{Me}_5)\}$. *Chem-Eur J* **2010**, *16* (2), 419-422; (b) Atzrodt, J.; Derdau, V.; Fey, T.; Zimmermann, J., The renaissance of H/D exchange. *Angewandte Chemie-International Edition* **2007**, *46* (41), 7744-7765; (c) Corberan, R.; Sanau, M.,

Peris, E., Highly stable Cp*-Ir(III) complexes with N-heterocyclic carbene ligands as C-H activation catalysts for the deuteration of organic molecules. *Journal of the American Chemical Society* **2006**, *128* (12), 3974-3979; (d) Tenn, W. J.; Young, K. J. H.; Bhalla, G.; Oxgaard, J.; Goddard, W. A.; Periana, R. A., CH activation with an O-donor iridium-methoxo complex. *Journal of the American Chemical Society* **2005**, *127* (41), 14172-14173; (e) Feng, Y.; Lail, M.; Barakat, K. A.; Cundari, T. R.; Gunnoe, T. B.; Petersen, J. L., Evidence for the net addition of arene C-H bonds across a Ru(II)-hydroxide bond. *Journal of the American Chemical Society* **2005**, *127* (41), 14174-14175; (f) Yung, C. M.; Skaddan, M. B.; Bergman, R. G., Stoichiometric and catalytic H/D incorporation by cationic iridium complexes: A common monohydrido-iridium intermediate. *Journal of the American Chemical Society* **2004**, *126* (40), 13033-13043; (g) Santos, L. L.; Mereiter, K.; Paneque, M.; Slugovc, C.; Carmona, E., C-H bond activation reactions by Tp(Me₂)Ir(III) centres. Generation of Fischer-type carbenes and development of a catalytic system for H/D exchange. *New J Chem* **2003**, *27* (1), 107-113.

153. Parks, D. J.; Spence, R. E. V. H.; Piers, W. E., Bis(Pentafluorophenyl)Borane - Synthesis, Properties, and Hydroboration Chemistry of a Highly Electrophilic Borane Reagent. *Angew Chem Int Edit* **1995**, *34* (7), 809-811.

154. Baker, R. T.; Calabrese, J. C.; Westcott, S. A., Coinage Metal-Catalyzed Hydroboration of Imines. *J Organomet Chem* **1995**, *498* (2), 109-117.

155. Fisch, H.; Trucks, G. W.; Schlegel, H. B.; Scuseria, G. E.; Robb, M. A.; Cheeseman, J. R.; Montgomery, J. A.; Vreven, T.; Kudin, K. N.; Burant, J. C.; Millam, J. M.; Lyengar, S. S.; Tomasi, J.; Barone, V.; Mennucci, B.; Cossi, M.; Scalmani, G.; Rega, N.; Petersson, G. A.; Nakatsuji, H.; Hada, M.; Ehara, M.; Toyota, K.; Fukuda, R.; Hasegawa, J.; Ishida, M.; Nakajima, T.; Honda, Y.; Kitao, O.; Nakai, H.; Klene, M.; Li, X.; Knox, J. E.; Hratchian, H. P.; Cross, J. B.; Adamo, C.; Jaramillo, J.; Gomperts, R.; Stratmann, R. E.; Yazyev, O.; Austin, A. J.; Cammi, R.; Pomelli, C.; Ochterski, J. W.; Ayala, P. Y.; Morokuma, K.; Voth, G. A.; Salvador, P.; Dannenberg, J. J.; Zakrzewski, V. G.; Dapprich, S.; Daniels, A. D.; Strain, M. C.; Farkas, O.; Malick, D. K.; Rabuck, A. D.; Raghavachari, K.; Foresman, J. B.; Ortiz, J. V.; Cui, Q.; Baboul, A. G.; Clifford, S.; Cioslowski, J.; Stefanov, B. B.; Liu, G.; Liashenko, A.; Piskorz, P.; Komaromi, I.;

Martin, R. L.; Fox, D. J.; Keith, T.; Al-Laham, M. A.; Peng, C. Y.; Nanayakkara, A.; Challacombe, M.; Gill, P. M. W.; Johnson, B.; Chen, W.; Wong, M. W.; Gonzalez, C.; Pople, J. A. Gaussian Inc.: 2003.

156. Becke, A. D., Density-Functional Thermochemistry. 3. The Role of Exact Exchange. *J Chem Phys* **1993**, *98* (7), 5648-5652.

157. Lee, C.; Yang, W.; Parr, R. G., Development of the Colle-Salvetti correlation-energy formula into a functional of the electron density. *Phys Rev B* **1988**, *37* (2), 785.

158. Godbout, N.; Salahub, D. R.; Andzelm, J.; Wimmer, E., Optimization of Gaussian-Type Basis-Sets for Local Spin-Density Functional Calculations. 1. Boron through Neon, Optimization Technique and Validation. *Can J Chem* **1992**, *70* (2), 560-571.

159. Schafer, A.; Huber, C.; Ahlrichs, R., Fully Optimized Contracted Gaussian-Basis Sets of Triple Zeta Valence Quality for Atoms Li to Kr. *J Chem Phys* **1994**, *100* (8), 5829-5835.

160. Gonzalez, C.; Schlegel, H. B., An Improved Algorithm for Reaction-Path Following. *J Chem Phys* **1989**, *90* (4), 2154-2161.

161. Zeiher, E. H. K.; Dewit, D. G.; Caulton, K. G., Mechanistic Features of C-H Activation by $\text{ReH}_7[\text{P}(\text{C}_6\text{H}_{11})_3]_2$. *Journal of the American Chemical Society* **1984**, *106* (23), 7006-7011.

162. Parks, D. J.; Piers, W. E.; Yap, G. P. A., Synthesis, properties, and hydroboration activity of the highly electrophilic borane bis(pentafluorophenyl)borane, $\text{HB}(\text{C}_6\text{F}_5)_2$. *Organometallics* **1998**, *17* (25), 5492-5503.